University of Alberta
Department of Civil Engineering

Structural Engineering Report No. 200

HIGH PERFORMANCE CONCRETE UNDER HIGH SUSTAINED COMPRESSIVE STRESSES

by

Said Iravani

and

James G. MacGregor

June 1994

Structural Engineering Report No. 200

High Performance Concrete under High Sustained Compressive Stresses

by

Said Iravani

and

James G. MacGregor

Department of Civil Engineering

University of Alberta

Edmonton, Alberta

Canada

June, 1994

Abstract

Anton Brandtzaeg[41] noticed the phenomenon of the critical compressive stress through volumetric strain studies in 1928. The critical stress level was found to be 77 to 85 percent of the ultimate compressive stress. At this stress level the volumetric strain began to increase indicating internal microcracking development. Hubert Rüsch[48] reported that conventional concrete loaded at a late age to sustained compressive stresses in excess of approximately 70 to 75 percent of the short time monotonic ultimate strength of concrete at the time of loading may fail under the sustained compressive stresses after a period of several minutes to several months.

The main purpose of this study was to investigate high performance concrete under high sustained compressive stresses. High performance concretes with 56 day compressive strengths of 65 MPa to 75 MPa (without silica fume), 95 MPa to 105 MPa (with and without silica fume), and 120 MPa (with silica fume) were studied. Stress intensities ranged from 70 to 95 percent of the short term ultimate strength. The effects of moment gradient and silica fume were also studied.

Meanwhile, a supplementary test program was carried out on the same series of high performance concrete to study the mechanical properties of high performance concrete.

The sustained compressive strength of high performance concrete was established. The effect of the compressive strength, eccentricity, and silica fume were also established. The long term sustained compressive strength of high performance concrete is between 70% to 75%, 75% to 80%, 85% to 90%, and 85% to 90% of the short term ultimate strength for 65 MPa to 75 MPa, 95 MPa to 105 MPa (without silica fume), 95 MPa to 105 MPa (with silica fume), and 120 MPa concretes, respectively. The long term sustained compressive strength of high performance concrete under small eccentric loads is approximately 5% higher than under the concentric loads. A modification of the ACI 318M equation for the modulus of elasticity of normal weight high performance concrete was recommended.

Acknowledgements

This Structural Engineering Report is a reprint of a M.Sc. thesis by the same name, written by the first author under the supervision of the second author. The first author would like to express his sincere gratitude and appreciation to his research supervisor, University Professor Emeritus James G. MacGregor, for his consistent and brilliant guidance, comments, suggestions, interest, and encouragement throughout this study. Dr. MacGregor's brilliant comments, suggestions, knowledge, and experience are strongly affected this work and is greatly appreciated by the first author.

The authors would like to thank Dr. S.D.B. Alexander. Dr. Alexander worked with the Network of Centres of Excellence on High-performance Concrete, University of Alberta, till July 1993. His assistance and valuable ideas throughout the experimental work especially in design of the sustained load frames and the data acquisition system is appreciated.

The technical assistance of L. Burden and R. Helfrich from the I.F. Morrison Structural Laboratory, University of Alberta, throughout the experimental program is acknowledged. The technical assistance of D. Erikson from the Network of Centers of Excellence on High-performance Concrete, University of Alberta, is also appreciated.

The assistance of Dr. H. Ibrahim, N. Alca, D. Mullin, and summer students C. Jordan and J. Alexander during the experimental work are also acknowledged.

The extensive financial support for this study provided by the federal government of Canada through the Network of Centers of Excellence on High-performance Concrete is highly appreciated. Meanwhile, the two year scholarship provided by the Ministry of Culture and Higher Education of Iran for the first author is also appreciated.

The cement and admixture donations by Inland Cement, Lafarge Canada Inc., Master Builders Technologies Ltd., and W.R. Grace & Co. of Canada are gratefully acknowledged. Meanwhile, the $600 structural steel donation by Supreme Steel Ltd. is also appreciated.

Table of Contents

1. Introduction		1
1.1	General	1
1.2	Objectives and Scope	1
1.3	Thesis Arrangement	2
2. Experimental Program		3
2.1	Introduction	3
2.2	General	3
2.2.1	Overview of Test Program	3
2.2.2	Test Specimens	4
2.2.3	Bearing Blocks	4
2.2.4	Compressive Strength Test Control System	5
2.3	Materials	6
2.3.1	Cement	6
2.3.2	Fine Aggregate	6
2.3.3	Coarse Aggregate	6
2.3.4	Admixture	7
2.3.5	Silica Fume	7
2.4	Concrete Mix Proportions	7
2.5	Batching, Casting, Consolidating, and Curing	8
2.6	Test Program to Determine Mechanical Properties of High Performance Concrete	9
2.6.1	Compressive Strength Gain with Time	9
2.6.2	Effect of Type of Cement on Compressive Strength	9
2.6.3	Effect of Drying on Compressive Strength	10

2.6.4 Effect of the End Blocks of the Testing Machine on Compressive Strength 10

2.6.5 Effect of Size of Specimen on Compressive Strength 10

2.6.6 Modulus of Elasticity and Poisson's Ratio 11

2.6.7 Tensile Splitting Strength 11

2.6.8 Modulus of Rupture 12

2.7 High Performance Concrete under High Sustained Compressive Stresses 12

2.7.1 Test Program 12

2.7.2 Sustained Load Frames 13

2.7.3 Loading Procedure in Sustained Load Frames 14

2.7.4 Measurements 15

3. Mechanical Properties of High Performance Concrete 26

3.1 Introduction 26

3.2 Compressive Strength Gain with Time 26

3.2.1 Literature Review 26

3.2.2 Test Results 27

3.2.3 Discussion of Results 27

3.3 Effect of Type of Cement on the Compressive Strength Gain 28

3.3.1 Literature Review 28

3.3.2 Test Results 28

3.3.3 Discussion of Results 28

3.4 Effect of Drying on the Compressive Strength Gain 29

3.4.1 Literature Review 29

3.4.2 Test Results 30

3.4.3 Discussion of Results 31

3.5	Effect of the Bearing Block of the Testing Machine on Compressive Strength	32
3.5.1	Literature Review	32
3.5.2	Test Results	32
3.5.3	Discussion of Results	33
3.6	Effect of Specimen Size on Compressive Strength	34
3.6.1	Literature Review	34
3.6.2	Test Results	35
3.6.3	Discussion of Results	35
3.7	Modulus of Elasticity	35
3.7.1	Literature Review	35
3.7.2	Test Results	38
3.7.3	Discussion of Results	38
3.8	Poisson's Ratio	41
3.8.1	Literature Review	41
3.8.2	Test Results	41
3.8.3	Discussion of Results	41
3.9	Tensile Splitting Strength	42
3.9.1	Literature Review	42
3.9.2	Test Results	42
3.9.3	Discussion of Results	43
3.10	Modulus of Rupture	43
3.10.1	Literature Review	43
3.10.2	Test Results	43
3.10.3	Discussion of Results	44
3.11	Conclusions	44

4. High performance Concrete under High Sustained Compressive Stresses 69

4.1 Introduction 69

4.2 Literature Review 70

4.3 Compressive Strength History of Concretes Used 74

4.4 Stress-Strain Behavior of Concretes Used 74

4.5 High Performance Concrete under High Sustained Concentric Stresses 75

4.5.1 Test Results 75

4.5.1.1 General 75

4.5.1.2 LH Series Test Results 75

4.5.1.3 UH Series Test Results 76

4.5.1.4 UU Series Test Results 77

4.5.2 Discussion of Results 78

4.6 High Performance Concrete under High Sustained Eccentric Stresses 81

4.6.1 Test Results 81

4.6.1.1 General 81

4.6.1.2 LH Series Test Results 81

4.6.1.3 UH Series Test Results 82

4.6.1.4 UU Series Test Results 83

4.6.2 Discussion of Results 84

4.7 Conclusions 85

5. Summary, Conclusions, and Recommendations 145

5.1 Summary 145

5.2 General Conclusions 146

5.2.1 Mechanical Properties of High Performance Concrete 146

5.2.2 High Performance Concrete under High Sustained Stresses 147

5.3 Recommendations for Further Studies 148

References 150

R.1 Cited References 150

R.2 Additional and Recommended References 156

Appendix A Test Results Used in Modulus of Elasticity Study 157

Appendix B LH Series Monotonic Test Results 162

Appendix C UH Series Monotonic Test Results 179

Appendix D UU Series Monotonic Test Results 190

Appendix E Mechanical Properties of High Performance Concrete (LU Series Test Results) 201

E-3.1 Introduction 201

E-3.2 Compressive Strength Gain with Time 201

E-3.3 Effect of Type of Cement on the Compressive Strength Gain 201

E-3.4 Effect of Drying on the Compressive Strength Gain 201

E-3.5 Effect of Bearing Blocks of the Testing Machine on Compressive Strength 202

E-3.6 Effect of Specimen Size on Compressive Strength 202

E-3.7 Modulus of Elasticity 202

E-3.8 Poisson's Ratio 203

E-3.9 Tensile Splitting Strength 203

E-3.10 Modulus of Rupture 203

Appendix F High performance Concrete under High Sustained Compressive Stresses (LU Series Test Results) 219

F-4.1 Introduction 219

F-4.2 Literature Review 219

F-4.3 Compressive Strength History of Concretes Used 219

F-4.4 Stress-Strain Behavior of Concretes Used 219

F-4.5 High Performance Concrete under High Sustained Concentric Stresses 219

F-4.6 High Performance Concrete under High Sustained Eccentric Stresses 221

Appendix G LU Series Monotonic Test Results 244

Appendix H Strain Study of High Performance Concrete 255

H-1 Introduction 255

H-2 Literature Review 256

H-3 Stress-Strain Behavior of High Performance Concretes 259

H-3.1 Test Results 259

H-3.2 Discussion of Results 259

H-4 Volumetric Strain Study of High Performance Concrete 260

H-4.1 Test Results 260

H-4.2 Discussion of Results 260

H-5 Poisson's Ratio Study of High Performance Concrete 261

H-5.1 Test Results 261

H-5.2 Discussion of Results 262

H-6 Conclusions 262

Appendix I Details of Concrete Cylinder Tests 298

List of Tables

Table 2.3.1	Compositions of Cements Used	16
Table 2.4.A	Concrete Mix Proportions (LH Series)	16
Table 2.4.B	Concrete Mix Proportions (UH Series)	17
Table 2.4.C	Concrete Mix Proportions (LU Series)	17
Table 2.4.D	Concrete Mix Proportions (UU Series)	18
Table 2.4.E	Concrete Mix Proportions (Supplementary Series)	18
Table 3.2.2.A	Compressive Strength Gain with Time (LH Series)	46
Table 3.2.2.B	Compressive Strength Gain with Time (UH Series)	46
Table 3.2.2.C	Compressive Strength Gain with Time (UU Series)	47
Table 3.3.2.A	Effect of Type of Cement on the Compressive Strength Gain (LH Series)	47
Table 3.3.2.B	Effect of Type of Cement on the Compressive Strength Gain (UH Series)	48
Table 3.3.2.C	Effect of Type of Cement on the Compressive Strength Gain (UU Series)	48
Table 3.4.2.A	Effect of Drying on the Compressive Strength Gain (LH Series)	49
Table 3.4.2.B	Effect of Drying on the Compressive Strength Gain (UH Series)	49
Table 3.4.2.C	Effect of Drying on the Compressive Strength Gain (UU Series)	50
Table 3.4.2.D	Comparison of 147-day and 28-day Compressive Strength	50
Table 3.4.2.E	Comparison of 147-day Compressive Strengths	50
Table 3.5.2.A	Compressive Strength Results with Different Bearing Blocks	51
Table 3.5.2.B	Comparison of the Bearing Blocks of the Testing Machine	51
Table 3.6.2.A	Compressive Strength Results with Different Specimen Sizes	52
Table 3.6.2.B	Comparison of 100 mm and 150 mm Cylinders	53
Table 3.7.2	Modulus of Elasticity and Poisson's Ratio Test Results	54

Table 3.7.3	Recommended Coarse Aggregate Coefficient	55
Table 3.9.2	Tensile Splitting Strength Test Results	56
Table 3.10.2	Modulus of Rupture Test Results	56
Table 4.3.A	Compressive Strength History (LH Series)	87
Table 4.3.B	Compressive Strength History (UH Series)	87
Table 4.3.C	Compressive Strength History (UU Series)	88
Table 4.5.1.1	Compressive Strength of Monotonic Concentric Specimens	88
Table 4.5.1.2	Summary of LH Concentric Series Strain Study	89
Table 4.5.1.3	Summary of UH Concentric Series Strain Study	89
Table 4.5.1.4	Summary of UU Concentric Series Strain Study	90
Table 4.6.1	Summary of Eccentric Series Extreme Fiber Strain Study	90
Table A-3.7.3	Specified Modulus of Elasticity Test Results	157
Table E-3.2	Compressive Strength Gain with Time (LU Series)	204
Table E-3.3	Effect of Type of Cement on the Compressive Strength Gain (LU Series)	204
Table E-3.4.A	Effect of Drying on the Compressive Strength Gain (LU Series)	205
Table E-3.4.B	Comparison of 147-day and 28-day Compressive Strength	205
Table E-3.4.C	Comparison of 147-day Compressive Strengths	205
Table E-3.5.A	Compressive Strength Results with Different Bearing Blocks	206
Table E-3.5.B	Comparison of the Bearing Blocks of the Testing Machine	206
Table E-3.6.A	Compressive Strength Results with Different Specimen Sizes	206
Table E-3.6.B	Comparison of 100 mm and 150 mm Cylinders	206
Table E-3.7.A	Modulus of Elasticity and Poisson's Ratio Test Results	207
Table E-3.7.B	Recommended Coarse Aggregate Coefficient	207
Table E-3.9	Tensile Splitting Strength Test Results	207
Table E-3.10	Modulus of Rupture Test Results	207

Table F-4.3	Compressive Strength History (LU Series)	223
Table F-4.5.A	Compressive Strength of Monotonic Concentric Specimens	223
Table F-4.5.B	Summary of LU Concentric Series Strain Study	224
Table F-4.6	Summary of LU Eccentric Series Extreme Fiber Strain Study	224
Table H-4.2.A	Critical Stress Results (LH Series)	265
Table H-4.2.B	Critical Stress Results (UH Series)	265
Table H-4.2.C	Critical Stress Results (LU Series)	266
Table H-4.2.D	Critical Stress Results (UU Series)	266
Table I-3.2.2.A	Compressive Strength Gain with Time (LH Series)	299
Table I-3.2.2.B	Compressive Strength Gain with Time (UH Series)	300
Table I-3.2.2.C	Compressive Strength Gain with Time (UU Series)	301
Table I-3.3.2.A	Effect of Type of Cement on the Compressive Strength Gain (LH Series)	302
Table I-3.3.2.B	Effect of Type of Cement on the Compressive Strength Gain (UH Series)	303
Table I-3.3.2.C	Effect of Type of Cement on the Compressive Strength Gain (UU Series)	304
Table I-3.4.2.A	Effect of Drying on the Compressive Strength Gain (LH4 Series)	305
Table I-3.4.2.B	Effect of Drying on the Compressive Strength Gain (UH4 Series)	306
Table I-3.4.2.C	Effect of Drying on the Compressive Strength Gain (UU4 Series)	307
Table I-4.3.A	Compressive Strength History (LH1 Series)	308
Table I-4.3.B	Compressive Strength History (UH1 Series)	309
Table I-4.3.C	Compressive Strength History (UU1 Series)	310
Table I-E-3.2	Compressive Strength Gain with Time (LU Series)	311
Table I-E-3.3	Effect of Type of Cement on the Compressive Strength Gain (LU Series)	312
Table I-E-3.4	Effect of Drying on the Compressive Strength Gain (LU4 Series)	313

Table I-F-4.3 Compressive Strength History (LU1 Series) 314

List of Figures

Figure 2.2.3.A	The Ball Seat Bearing Blocks	19
Figure 2.2.3.B	The Spherical Seat Bearing Block	20
Figure 2.3.2	Sieve Analysis of Fine Aggregate	21
Figure 2.3.3	Sieve Analysis of Coarse Aggregate	22
Figure 2.7.2.A	Simplified Drawing of the Sustained Load Frame	23
Figure 2.7.2.B	The Six Sustained Load Frames	24
Figure 2.7.2.C	The Eccentric Sustained Load Frames	25
Figure 3.2.2	Compressive Strength Gain with Time	57
Figure 3.3.2.A	Effect of Type of Cement on Compressive Strength	58
Figure 3.3.2.B	Effect of Type of Cement (LH Series)	59
Figure 3.3.2.C	Effect of Type of Cement (UH Series)	60
Figure 3.3.2.D	Effect of Type of Cement (UU Series)	61
Figure 3.4.2	Effect of Drying on Compressive Strength Gain	62
Figure 3.7.2	Static Modulus of Elasticity Test Results	63
Figure 3.7.3.A	Comparison of Modulus of Elasticity Test Results	64
Figure 3.7.3.B	Effect of Time on Modulus of Elasticity	65
Figure 3.7.3.C	Effect of Coarse Aggregate on Modulus of Elasticity	66
Figure 3.9.3	Tensile Splitting Strength Test Results	67
Figure 3.10.3	Modulus of Rupture Test Results	68
Figure 4.3.A	Compressive Strength History (Ratio of 28-Day Strength)	91
Figure 4.3.B	Compressive Strength History (Ratio of 56-Day Strength)	92
Figure 4.4.A	Stress-Strain Curves of Monotonic Concentric Specimens	93
Figure 4.4.B	Stress - Strain Relationship - LH Series	94
Figure 4.4.C	Stress - Strain Relationship - UH Series	95

Figure 4.4.D	Stress - Strain Relationship - UU Series	96
Figure 4.5.1.2.A	Stress-Strain-Time Relationship - LHC95 Specimen	97
Figure 4.5.1.2.B	Stress-Strain-Time Relationship - LHC90 Specimen	98
Figure 4.5.1.2.C	Stress-Strain-Time Relationship - LHC85 Specimen	99
Figure 4.5.1.2.D	Stress-Strain-Time Relationship - LHC80 Specimen	100
Figure 4.5.1.2.E	Stress-Strain-Time Relationship - LHC75 Specimen	101
Figure 4.5.1.2.F	Stress-Strain-Time Relationship - LHC75(70) Specimen	102
Figure 4.5.1.2.G	Stress-Strain-Time Relationship - LHC70(70) Specimen	103
Figure 4.5.1.3.A	Stress-Strain-Time Relationship - UHC95 Specimen	104
Figure 4.5.1.3.B	Stress-Strain-Time Relationship - UHC90 Specimen	105
Figure 4.5.1.3.C	Stress-Strain-Time Relationship - UHC85 Specimen	106
Figure 4.5.1.3.D	Stress-Strain-Time Relationship - UHC80 Specimen	107
Figure 4.5.1.3.E	Stress-Strain-Time Relationship - UHC75 Specimen	108
Figure 4.5.1.3.F	Stress-Strain-Time Relationship - UHC70 Specimen	109
Figure 4.5.1.4.A	Stress-Strain-Time Relationship - UUC95 Specimen	110
Figure 4.5.1.4.B	Stress-Strain-Time Relationship - UUC90 Specimen	111
Figure 4.5.1.4.C	Stress-Strain-Time Relationship - UUC85(70) Specimen	112
Figure 4.5.1.4.D	Stress-Strain-Time Relationship - UUC80(70) Specimen	113
Figure 4.5.1.4.E	Stress-Strain-Time Relationship - UUC75 Specimen	114
Figure 4.5.2.A	Stress-Strain Relationship - LH Concentric Series	115
Figure 4.5.2.B	Stress-Strain Relationship - UH Concentric Series	116
Figure 4.5.2.C	Stress-Strain Relationship - UU Concentric Series	117
Figure 4.5.2.D	Strain-Time Relationship - LH Concentric Series	118
Figure 4.5.2.E	Strain-Time Relationship - UH Concentric Series	119
Figure 4.5.2.F	Strain-Time Relationship - UU Concentric Series	120
Figure 4.5.2.G	Summary of Concentric Test Results	121

Figure 4.6.1.2.A	Load-Strain-Time Relationship - LHE95 Specimen	122
Figure 4.6.1.2.B	Load-Strain-Time Relationship - LHE90 Specimen	123
Figure 4.6.1.2.C	Load-Strain-Time Relationship - LHE85 Specimen	124
Figure 4.6.1.2.D	Load-Strain-Time Relationship - LHE80 Specimen	125
Figure 4.6.1.2.E	Load-Strain-Time Relationship - LHE80(70) Specimen	126
Figure 4.6.1.2.F	Load-Strain-Time Relationship - LHE75(70) Specimen	127
Figure 4.6.1.3.A	Load-Strain-Time Relationship - UHE95 Specimen	128
Figure 4.6.1.3.B	Load-Strain-Time Relationship - UHE90 Specimen	129
Figure 4.6.1.3.C	Load-Strain-Time Relationship - UHE85 Specimen	130
Figure 4.6.1.3.D	Load-Strain-Time Relationship - UHE80 Specimen	131
Figure 4.6.1.3.E	Load-Strain-Time Relationship - UHE75 Specimen	132
Figure 4.6.1.4.A	Load-Strain-Time Relationship - UUE95 Specimen	133
Figure 4.6.1.4.B	Load-Strain-Time Relationship - UUE90 Specimen	134
Figure 4.6.1.4.C	Load-Strain-Time Relationship - UUE85 Specimen	135
Figure 4.6.1.4.D	Load-Strain-Time Relationship - UUE80 Specimen	136
Figure 4.6.1.4.E	Load-Strain-Time Relationship - UUE75 Specimen	137
Figure 4.6.2.A	Stress-Strain Relationship - LH Eccentric Series	138
Figure 4.6.2.B	Stress-Strain Relationship - UH Eccentric Series	139
Figure 4.6.2.C	Stress-Strain Relationship - UU Eccentric Series	140
Figure 4.6.2.D	Strain-Time Relationship - LH Eccentric Series	141
Figure 4.6.2.E	Strain-Time Relationship - UH Eccentric Series	142
Figure 4.6.2.F	Strain-Time Relationship - UU Eccentric Series	143
Figure 4.6.2.G	Summary of Eccentric Test Results	144
Figure B-4.5.A	Stress-Strain-Time Relationship - LHC100A Specimen	163
Figure B-4.5.B	Stress-Strain-Time Relationship - LHC100B Specimen	164
Figure B-4.5.C	Stress-Strain-Time Relationship - LHC100C Specimen	165

Figure B-4.5.D	Stress-Strain-Time Relationship - LHC100D Specimen	166
Figure B-4.5.E	Stress-Strain-Time Relationship - LHC100E Specimen	167
Figure B-4.5.F	Stress-Strain-Time Relationship - LHC100A(70) Specimen	168
Figure B-4.5.G	Stress-Strain-Time Relationship - LHC100B(70) Specimen	169
Figure B-4.5.H	Stress-Strain-Time Relationship - LHC100C(70) Specimen	170
Figure B-4.6.A	Load-Strain-Time Relationship - LHE100A Specimen	171
Figure B-4.6.B	Load-Strain-Time Relationship - LHE100B Specimen	172
Figure B-4.6.C	Load-Strain-Time Relationship - LHE100C Specimen	173
Figure B-4.6.D	Load-Strain-Time Relationship - LHE100D Specimen	174
Figure B-4.6.E	Load-Strain-Time Relationship - LHE100E Specimen	175
Figure B-4.6.F	Load-Strain-Time Relationship - LHE100A(70) Specimen	176
Figure B-4.6.G	Load-Strain-Time Relationship - LHE100B(70) Specimen	177
Figure B-4.6.H	Load-Strain-Time Relationship - LHE100C(70) Specimen	178
Figure C-4.5.A	Stress-Strain-Time Relationship - UHC100A Specimen	180
Figure C-4.5.B	Stress-Strain-Time Relationship - UHC100B Specimen	181
Figure C-4.5.C	Stress-Strain-Time Relationship - UHC100C Specimen	182
Figure C-4.5.D	Stress-Strain-Time Relationship - UHC100D Specimen	183
Figure C-4.5.E	Stress-Strain-Time Relationship - UHC100E Specimen	184
Figure C-4.6.A	Load-Strain-Time Relationship - UHE100A Specimen	185
Figure C-4.6.B	Load-Strain-Time Relationship - UHE100B Specimen	186
Figure C-4.6.C	Load-Strain-Time Relationship - UHE100C Specimen	187
Figure C-4.6.D	Load-Strain-Time Relationship - UHE100D Specimen	188
Figure C-4.6.E	Load-Strain-Time Relationship - UHE100E Specimen	189
Figure D-4.5.A	Stress-Strain-Time Relationship - UUC100A Specimen	191
Figure D-4.5.B	Stress-Strain-Time Relationship - UUC100B Specimen	192
Figure D-4.5.C	Stress-Strain-Time Relationship - UUC100C Specimen	193

Figure D-4.5.D	Stress-Strain-Time Relationship - UUC100D Specimen	194
Figure D-4.5.E	Stress-Strain-Time Relationship - UUC100E Specimen	195
Figure D-4.6.A	Load-Strain-Time Relationship - UUE100A Specimen	196
Figure D-4.6.B	Load-Strain-Time Relationship - UUE100B Specimen	197
Figure D-4.6.C	Load-Strain-Time Relationship - UUE100C Specimen	198
Figure D-4.6.D	Load-Strain-Time Relationship - UUE100D Specimen	199
Figure D-4.6.E	Load-Strain-Time Relationship - UUE100E Specimen	200
Figure E-3.2	Compressive Strength Gain with Time	208
Figure E-3.3.A	Effect of Type of Cement on Compressive Strength	209
Figure E-3.3.B	Effect of Type of Cement (LU Series)	210
Figure E-3.4	Effect of Drying on Compressive Strength Gain	211
Figure E-3.7.A	Static Modulus of Elasticity Test Results	212
Figure E-3.7.B	Comparison of Modulus of Elasticity Test Results	213
Figure E-3.7.C	Effect of Time on Modulus of Elasticity	214
Figure E-3.7.D	Effect of Coarse Aggregate on Modulus of Elasticity	215
Figure E-3.8	Poisson's Ratio Test Results	216
Figure E-3.9	Tensile Splitting Strength Test Results	217
Figure E-3.10	Modulus of Rupture Test Results	218
Figure F-4.3.A	Compressive Strength History (Ratio of 28-Day Strength)	225
Figure F-4.3.B	Compressive Strength History (Ratio of 56-Day Strength)	226
Figure F-4.4.A	Stress-Strain Curves of Monotonic Concentric Specimens	227
Figure F-4.4.B	Stress - Strain Relationship - LU Series	228
Figure F-4.5.A	Stress-Strain-Time Relationship - LUC95 Specimen	229
Figure F-4.5.B	Stress-Strain-Time Relationship - LUC90 Specimen	230
Figure F-4.5.C	Stress-Strain-Time Relationship - LUC85 Specimen	231
Figure F-4.5.D	Stress-Strain-Time Relationship - LUC80 Specimen	232

Figure F-4.5.E	Stress-Strain-Time Relationship - LUC75 Specimen	233
Figure F-4.5.F	Stress-Strain Relationship - LU Concentric Series	234
Figure F-4.5.G	Strain-Time Relationship - LU Concentric Series	235
Figure F-4.5.H	Summary of Concentric Test Results	236
Figure F-4.6.A	Load-Strain-Time Relationship - LUE95 Specimen	237
Figure F-4.6.B	Load-Strain-Time Relationship - LUE90 Specimen	238
Figure F-4.6.C	Load-Strain-Time Relationship - LUE85 Specimen	239
Figure F-4.6.D	Load-Strain-Time Relationship - LUE80 Specimen	240
Figure F-4.6.E	Stress-Strain Relationship - LU Eccentric Series	241
Figure F-4.6.F	Strain-Time Relationship - LU Eccentric Series	242
Figure F-4.6.G	Summary of Eccentric Test Results	243
Figure G-F-4.5.A	Stress-Strain-Time Relationship - LUC100A Specimen	245
Figure G-F-4.5.B	Stress-Strain-Time Relationship - LUC100B Specimen	246
Figure G-F-4.5.C	Stress-Strain-Time Relationship - LUC100C Specimen	247
Figure G-F-4.5.D	Stress-Strain-Time Relationship - LUC100D Specimen	248
Figure G-F-4.5.E	Stress-Strain-Time Relationship - LUC100E Specimen	249
Figure G-F-4.6.A	Load-Strain-Time Relationship - LUE100A Specimen	250
Figure G-F-4.6.B	Load-Strain-Time Relationship - LUE100B Specimen	251
Figure G-F-4.6.C	Load-Strain-Time Relationship - LUE100C Specimen	252
Figure G-F-4.6.D	Load-Strain-Time Relationship - LUE100D Specimen	253
Figure G-F-4.6.E	Load-Strain-Time Relationship - LUE100E Specimen	254
Figure H-4.1.A	Stress-Strain Relationships - LHC100A Specimen	267
Figure H-4.1.B	Stress-Strain Relationships - LHC100B Specimen	268
Figure H-4.1.C	Stress-Strain Relationships - LHC100C Specimen	269
Figure H-4.1.D	Stress-Strain Relationships - LHC100D Specimen	270
Figure H-4.1.E	Stress-Strain Relationships - LHC100E Specimen	271

Figure H-4.1.F	Stress-Strain Relationships - LHC100A(70) Specimen	272
Figure H-4.1.G	Stress-Strain Relationships - LHC100B(70) Specimen	273
Figure H-4.1.H	Stress-Strain Relationships - LHC100C(70) Specimen	274
Figure H-4.1.I	Stress-Strain Relationships - UHC100A Specimen	275
Figure H-4.1.J	Stress-Strain Relationships - UHC100B Specimen	276
Figure H-4.1.K	Stress-Strain Relationships - UHC100C Specimen	277
Figure H-4.1.L	Stress-Strain Relationships - UHC100D Specimen	278
Figure H-4.1.M	Stress-Strain Relationships - UHC100E Specimen	279
Figure H-4.1.N	Stress-Strain Relationships - LUC100A Specimen	280
Figure H-4.1.O	Stress-Strain Relationships - LUC100B Specimen	281
Figure H-4.1.P	Stress-Strain Relationships - LUC100C Specimen	282
Figure H-4.1.Q	Stress-Strain Relationships - LUC100D Specimen	283
Figure H-4.1.R	Stress-Strain Relationships - LUC100E Specimen	284
Figure H-4.1.S	Stress-Strain Relationships - UUC100A Specimen	285
Figure H-4.1.T	Stress-Strain Relationships - UUC100B Specimen	286
Figure H-4.1.U	Stress-Strain Relationships - UUC100C Specimen	287
Figure H-4.1.V	Stress-Strain Relationships - UUC100D Specimen	288
Figure H-4.1.W	Stress-Strain Relationships - UUC100E Specimen	289
Figure H-4.2.A	Summary of Volumetric Strain Study - LH Series	290
Figure H-4.2.B	Summary of Volumetric Strain Study - UH Series	291
Figure H-4.2.C	Summary of Volumetric Strain Study - LU Series	292
Figure H-4.2.D	Summary of Volumetric Strain Study - UU Series	293
Figure H-5.1.A	Poisson's Ratio Study - LH Series	294
Figure H-5.1.B	Poisson's Ratio Study - UH Series	295
Figure H-5.1.C	Poisson's Ratio Study - LU Series	296
Figure H-5.1.D	Poisson's Ratio Study - UU Series	297

List of Symbols

A	=	cross sectional area of cylinder
C_{ca}	=	coarse aggregate coefficient
E_c	=	static modulus of elasticity
f_c	=	ultimate compressive stress (strength) of cylinder
f_{ct}	=	t-day ultimate compressive stress (strength) of cylinder
f'_c	=	specified compressive strength of concrete
f'_{ct}	=	t-day specified compressive strength of concrete
f'_r	=	modulus of rupture of concrete
f'_{sp}	=	tensile splitting strength of concrete
f_y	=	specified yield strength of steel
P_c	=	ultimate compressive load on cylinder
R.H.	=	relative humidity
S_i	=	specimen no. i
S_{n-1}	=	sample standard deviation

1. Introduction

1.1 General

High performance concrete is defined as concrete which meets special performance and uniformity requirements that cannot always be achieved routinely by using only conventional materials and normal mixing, placing, and curing practices. The requirements may involve one or some of the following properties:

1. High 28 day compressive strength.
2. High one day compressive strength.
3. High modulus of elasticity.
4. Low creep.
5. High durability to chemicals.
6. High freeze - thaw durability.
7. Self leveling, flowing concrete.
8. Enhancement of placement and compacting without segregation.
9. Toughness.
10. Volumetric stability.
11. High durability in severe environment.

Concrete is usually used to resist compressive stresses. A major application of high performance concrete with high compressive strength will be in compression members like columns, arches, domes, shells, rigid frames for tunnels, and long span bridges (to decrease the weight to compressive strength capacity ratio). High performance concrete may also be used from the standpoint of weight reduction or architectural aspects.

High performance concrete is a new material and there is relatively limited available information about its properties. The results of old researches on conventional concrete are no longer applicable. An extended comprehensive knowledge of the fundamental properties of high performance concrete is necessary. The mechanical properties of high performance concrete and its behavior under high sustained compressive stresses are among those fundamental properties.

1.2 Objectives and Scope

The main objective of this study is to investigate high performance concrete under high sustained compressive stresses. Four series of high performance concrete were tested under high sustained compressive stresses. The specimens were subjected to 3 month long term sustained loads. The primary parameter was the compressive strength of the high

performance concrete. The other significant parameters were stress intensity, moment gradient, and the presence of silica fume as supplementary cementitious material and filler. High performance concretes with 56 day compressive strengths of 65 MPa to 75 MPa (without silica fume), 95 MPa to 105 MPa (with and without silica fume), and 120 MPa (with silica fume) were used.

Concurrently, a supplementary test program was carried out on the same series of high performance concretes to study their mechanical properties. This experimental program included the study of the following objectives:

1. Compressive strength gain with time.
2. Effect of type of cement on compressive strength.
3. Effect of drying on compressive strength.
4. Effect of the bearing blocks of the testing machine on the compressive strength.
5. Effect of the size of specimen on the compressive strength.
6. Modulus of elasticity.
7. Poisson's ratio.
8. Tensile splitting strength.
9. Modulus of rupture.

1.3 Report Arrangement

The experimental program is explained in Chapter 2. Details of test specimens, materials, concrete grades, casting, curing, and the sustained load frames are also given in Chapter 2. For each of the mechanical properties of high performance concrete studied, the literature review, test results, and discussion of results are presented in Chapter 3. Conclusions concerning the mechanical properties of high performance concrete are presented at the end of Chapter 3. The study of high performance concrete under high sustained compressive stresses is presented in Chapter 4. The literature review, stress - strain relationship, the compressive strength history of concretes used in this test series, details of test results, and discussion of results for both concentric and eccentric tests are all presented in Chapter 4. Conclusions concerning the sustained compressive strength are presented at the end of Chapter 4. A summary, general conclusions, and recommendations for further studies are presented in Chapter 5.

The data from three of these four series are presented in the main body of the report. The data from the fourth series are presented in Appendixes E and F. A strain study of high performance concrete for predicting its long term sustained compressive strength is presented in Appendix H.

2. Experimental Program

2.1 Introduction

The experimental program was carried out to study four series of high performance concretes. Twenty batches of concrete were cast, four batches for each series and four extra batches. The concretes were chosen to cover the range of high performance concrete available in industry. The experimental program consisted of two parts:

1. Four series of high performance concrete were tested under high sustained compressive stresses. The primary parameter was the compressive strength of the high performance concrete. Among other variables, two high performance concretes with the same compressive strength range were used to compare the performance of high performance concretes with and without silica fume under high sustained compressive stresses.

2. A supplementary test program was carried out on the same four series of high performance concrete and four extra batches to study the mechanical properties of high performance concrete. High performance concrete is a new material and there is relatively limited available information about its properties. This supplementary test program was done to develop information about mechanical properties of high performance concrete and also present a relatively complete characterization of the concretes used in the study of high performance concrete under high sustained compressive stresses.

2.2 General

2.2.1 Overview of Test Program

Four series of high performance concrete, classified based on their compressive strength, were used. Four batches of concrete were cast for each series to provide the necessary specimens. An additional four batches of concrete were cast to provide more test specimens for study the mechanical properties of high performance concrete. The experimental program can be considered as two main test series:

A. Supplementary test series:

Series of tests were carried out to study the mechanical properties of high performance concretes used at the University of Alberta node of "The Network of Centers of Excellence on High-performance Concrete". This study covered the following properties:

A.1 Compressive strength gain with time

A.2 Effect of type of cement on compressive strength

A.3 Effect of drying on compressive strength

A.4 Effect of the bearing blocks of the testing machine on compressive strength

A.5 Effect of the size of specimen on compressive strength

A.6 Modulus of elasticity

A.7 Poisson's ratio

A.8 Tensile splitting strength

A.9 Modulus of rupture

B. Sustained load test series:

Four series of tests were carried out to study high performance concrete under high sustained compressive stresses. Two groups of test were conducted for each series:

B.1 Sustained concentric compressive load tests

B.2 Sustained eccentric compressive load tests (Eccentricity / Diameter = 0.1)

2.2.2 Test Specimens

Standards, specifications, and recommended practices[3,5,7,28] still consider 150 mm by 300 mm cylinder as the standard compressive strength test specimen for concrete. In spite of this, almost all commercial tests on high performance concrete in Canada are done on 100 mm by 200 mm cylinders. In this study, all tests were done on 100 mm by 200 mm cylinders through this study except the following:

a. 150 mm by 300 mm cylinders were used to study tensile splitting strength.

b. 150 mm by 300 mm and 100 mm by 200 mm cylinders were used to study the effect of size of specimen on compressive strength.

c. 150 mm by 150 mm by 550 mm beams were used to study the modulus of rupture.

Capping is not a suitable end preparation for concrete with compressive strength more than about 70 MPa. End preparation of all specimens was done by grinding to maintain uniform end condition, regardless of the age or the compressive strength. The real dimensions of the specimens were taken into consideration in calculations. Each dimension was considered as the average of three measurements each having an accuracy of ±0.05 mm.

2.2.3 Bearing Blocks

Two kind of bearing blocks were used to load the cylinders in this study, a ball seat bearing block (Figure 2.2.3.A) and an ASTM C 39[30] standard spherical seat bearing block (Figure 2.2.3.B). Each ball seat bearing block was made from two cylindrical pieces of heat treated D-2 Tool Steel (125 mm diameter and 63.5 mm thick) with f_y=2000 MPa. A 31.75

mm diameter ball bearing was used between the pair of platens. The oiled ball bearing fitted into a 15.88+0.05 mm depression, 11.113 ± 0.025 mm deep. The position of the ball bearing was machined with an accuracy of ±0.05 mm. Circular alignment marks were also marked with an accuracy of ±0.05 mm. The ASTM standard spherical seat bearing block of the test machine had 165 mm diameter platens and a 102 mm diameter spherical seat.

The ball seat bearing blocks were required to maintain the desired eccentricity for the monotonic and sustained eccentric compressive loadings in the sustained eccentric compressive load test series. The same kind of bearing blocks were used for monotonic and sustained concentric compressive loading in the sustained concentric load test series to provide the same end condition throughout and to make the results comparable. The ball seat bearing blocks were included as a variable in the supplementary test program to see their effect on the compressive strength of high performance concrete. Ball seat bearing blocks were used for all compressive strength tests to decrease the end restraints on the specimen and to maintain a stress field closer to a uniform uniaxial compression stress field. The standard spherical seat bearing block was used in the following cases:

a. Half of the specimens tested to study the effect of the end blocks of the testing machine on compressive strength
b. Specimens tested to study the effect of the size of specimen on compressive strength

2.2.4 Compressive Strength Test Control System

Three different control systems can be used to test normal strength concrete specimens:

a. Constant load rate control
b. Constant displacement rate control
c. Constant stroke of testing machine rate control

High performance concrete frequently has an unstable and uncontrollable failure. The reasons for violent uncontrollable failure after the peak load can be as follows[4]:

a. The rate of load increase is kept constant.
b. The testing machine stiffness is lower than the specimen stiffness, though the displacement rate is kept constant.
c. The elastic strain energy in the specimen is larger than the total fracture energy of the specimen.

Unstable failure of specimen in the cases (a) and (b) can be controlled if a stiff testing machine is used at a constant displacement rate. If a parameter which increases

monotonically during the course of the fracture progress is adopted as the feedback control signal to a stiff closed-loop servo-controlled testing machine, the unstable failure of specimens can be prevented in all the cases.

All specimens were tested using a 2600 kN electro-hydraulic closed-loop rock mechanics test system MTS 815. The stiffness of the load frame of MTS 815 is 10.5×10^9 N/m. By comparison, the axial stiffness of a 100 mm by 200 mm cylinder of 100 MPa concrete is 1.96×10^9 N/m and a 150 mm by 300 mm cylinder is 2.95×10^9 N/m. Tests were controlled using the differential signal between a load signal and a displacement signal as the feedback control signal to the closed-loop of servo-controlled testing machine. Above mentioned feedback system has been demonstrated to provide a stable and controllable procedure for testing specimens of high performance concrete in compression[4]. The feedback control signal to the closed-loop of the servo-controlled testing machine was chosen so that the stroke rate was 12 microstrain per second on average for 100 mm by 200 mm specimens and 18 microstrain per second for 150 mm by 300 mm specimens to satisfy the loading rate requirements of CAN/CSA-A23.2-9C[5] and ASTM C 39[30].

2.3 Materials

2.3.1 Cement

Normal portland cement CAN/CSA-A23.1-M90 Type 10 (ASTM Type I) and high early strength portland cement CAN/CSA-A23.1-M90 Type 30 (ASTM Type III), supplied by Lafarge Canada Inc. and Inland Cement, were used. The compositions of these cements provided by the suppliers are presented in Table 2.3.1 .

2.3.2 Fine Aggregate

Commercial locally available washed sand was used. Based on petrograghic analysis, it was composed of 21.7% high quartzite sandstone, 63.0% quartzite, 4.9% sandstone, 1.5% trap (basalt), and 1.9% granite. These "good" rocks formed 93% of the whole sand. The remaining 7% was composed of chert, weathered granite, siliceous ironstone, and soft sandstone. The fineness modulus, specific gravity, and absorption were 2.55, 2.60, and 0.013 respectively. The sieve analysis of the sand used is shown in Figure 2.3.2 .

2.3.3 Coarse Aggregate

Commercial locally available, washed, crushed coarse aggregate with the nominal maximum aggregate size of 14.0 mm was used. Based on petrographic analysis, it was composed of 62.6% high quartzite sandstone, 14.1% quartzite, 10.6% hard sandstone, 5.6% trap (basalt), 4.0% rhyolite, and 0.1% granite. These "good" rocks formed 97% of the whole

coarse aggregate. The remaining 3% was composed of hard chert, medium sandstone, medium limestone, weathered chert, silicious clay ironstone, and clay ironstone. Specific gravity and absorption were 2.60 and 0.016 respectively. The sieve analysis of the coarse aggregate is shown in Figure 2.3.3 .

2.3.4 Admixture

A poly-naphthaline sulfate based superplasticizer (SPN), produced by CONCHEM and supplied by W.R. Grace & Co. of Canada Ltd. was used. It contained 68.75% water.

2.3.5 Silica Fume

Silica fume is a by-product of the melting process used to produce silicon metal and ferrosilicon alloys. The main characteristics of silica fume are its high content of amorphous SiO_2 ranging from 85 to 98% with a mean particle size of 0.1-0.2 microns and its spherical shape. Silica fume acts both as a filler and as a pozzolan. Liquid silica fume (Force 10000 supplied by W.R. Grace & Co. of Canada Ltd.) was used in mixtures containing silica fume. The silica fume mixture was 49% solid with a specific gravity of 1.364 .

2.4 Concrete Mix Proportions

Basically, four different concrete mixes were used. They are classified based on their nominal 56 day compressive strength with the curing regime of three weeks at 100% relative humidity (R.H.) and then 50% R.H. as follows (The first letter stands for lower or upper bound on strength, the second letter stands for whether the concrete is high strength concrete (without silica fume) or ultra high strength concrete (with silica fume)):

a. LH : **L**ower bound of **H**igh strength concrete with a compressive strength of 65-75 MPa (without silica fume)

b. UH : **U**pper bound of **H**igh strength concrete with a compressive strength of 95-105 MPa (without silica fume)

c. LU : **L**ower bound of **U**ltra high strength concrete with a compressive strength of 95-105 MPa (with silica fume)

d. UU : **U**pper bound of **U**ltra high strength concrete available with local materials, with a compressive strength of +120 MPa (with silica fume)

Four batches of concrete were cast for each mix to provide the necessary specimens. Mix proportions are presented in Tables 2.4.A through 2.4.D. Three of the four batches contained Type 10 cement, the other batch had Type 30 cement. An additional four batches of concrete were cast for other studies related to objectives of this study. Those batches are

named S1 through S4. Their mix proportions are presented in Table 2.4.E and the related test results in Chapter 3. Air content was not measured. It has been assumed to be 2% based on previous experiences at the laboratory with the same materials.

2.5 Batching, Casting, Consolidating, and Curing

A horizontal rotary-drum (Eirich, Counter-current Rapid Mixer DE18) with 0.2 cubic meter capacity was used. The following batching procedure was used in order to make uniform mixtures. Fine aggregate, coarse aggregate, and cement were put in the mixer and mixed for at least five minutes. If the mixture contained silica fume, liquid silica fume was added at this time. Then, 2/3 of the mixing water and superplasticizer were added and mixed for three to seven minutes. The remaining 1/3 of mixing water and superplasticizer were added gradually.

100 mm by 200 mm and 150 mm by 300 mm cylinders were cast in reusable plastic molds and 150 mm by 150 mm by 550 mm beams were cast in steel molds. All molds were oiled prior to placing the concrete. Concrete was placed in cylinder molds in two layers and was consolidated on a ASTM C 192[31] and CAN/CSA-A23.2-3C [5] standard vibrating table in two intervals of vibration. In the first interval, the molds were filled with concrete up to the top and vibrated until the surface became flat. Then, more concrete was added to fill the molds again. The molds were then vibrated until the concrete surface became smooth. Beams were cast in one layer and consolidated using a pencil vibrator. The placing and consolidating of the concrete from one batch were always done in less than fifteen minutes.

All specimens were cured under polyethylene sheets for 24 hours in the laboratory environment. The specimens were then removed from the molds and transferred to tubs of saturated lime water in order to be in 100% relative humidity.

According to MacGregor[1], concrete is sensitive to humidity and temperature changes. For this reason, a study of the time dependent properties of concrete needs controlled curing conditions to make the studies repeatable and comparable. 100% R.H. and 23 ± 2 °C are considered as the standard moist curing condition for concrete specimens by ASTM C 192[31]. 50% R.H. and 23 ± 2 °C are recommended by ASTM E 171[32] as a standard atmosphere for conditioning and testing of materials known to be sensitive to variations in temperature or relative humidity. ASTM E 171[32] reports that the Coordination Committee on Atmospheric Conditioning for Testing of the International Organization for Standardization (ISO), recommends that the following standard atmospheres be used for testing materials that are used in conditions approximating ambient atmospheres:

a. 20 ± 2 °C and 65% ± 5% R.H.

b. 23 ± 2 °C and 50% ± 5% R.H.

c. 27 ± 2 °C and 65% ± 5% R.H.

Based on all of these, two curing regimes were chosen. A saturated lime water bath was used to provide 100% R.H. and 23 ± 2 °C as the moist curing regime. A controlled environment room was used to provide 50 ± 3% R.H. and 23 ± 2 °C as the air dry curing condition and the testing environment for the sustained load tests. Humidity was maintained by a Herrmidifier 707TW humidifier in the controlled environment room.

2.6 Test Program to Determine Mechanical Properties of High Performance Concrete

2.6.1 Compressive Strength Gain with Time

Two batches of concrete were cast for each series (batches 2 and 4). 100 mm by 200 mm cylinder specimens, cured continuously at 100% R.H., were tested using a 2600 kN electro-hydraulic closed-loop rock mechanics test system MTS 815. Tests were conducted up to 21 weeks (5 months) at the ages of 1, 3, 7, 28, 56, 91, and 147 days. Two specimens were tested at each age. If their compressive strength differed more than 5%, a third specimen was tested. The results are reported as the average of the all specimens tested. Ball seat bearing blocks were used. The end preparation of all specimens were done by grinding to maintain uniform end conditions regardless of the compressive strength or the age. The real dimensions of the test specimens and the maximum applied load were measured.

2.6.2 Effect of Type of Cement on Compressive Strength

The same size of batches of concrete were cast with exactly the same mix proportions to investigate the effect of type of cement on compressive strength of high performance concrete. Batches of concrete were cast at 1/2 hour intervals or less for each series (batches 2 and 3 of each series). 100 mm by 200 mm cylinder specimens, cured continuously at 100% R.H., were tested using a 2600 kN electro-hydraulic closed-loop rock mechanics test system MTS 815. Tests were conducted up to 21 weeks (5 months) at the ages of 1, 3, 7, 28, 56, 91, and 147 days. Two specimens were tested at each age. If their compressive strength differed more than 5%, a third specimen was tested. The results are reported as the average of the all specimens tested. Ball seat bearing blocks were used. The end preparation of all specimens were done by grinding to maintain uniform end conditions regardless of the compressive strength or the age. The real dimensions of the test specimens and the maximum applied load were measured.

2.6.3 Effect of Drying on Compressive Strength

Three different curing regimes were used to investigate the effect of drying on compressive strength gain of high performance concrete as follows:

a. Continuously at 100% R.H.

b. Three weeks at 100% R.H., then at 50% R.H.

c. Seven weeks at 100% R.H., then at 50% R.H.

One batch of concrete was cast for each series (batch 4). 100 mm by 200 mm cylinder specimens were tested using a 2600 kN electro-hydraulic closed-loop rock mechanics test system MTS 815. Tests were conducted up to 21 weeks (5 months) at the ages of 1, 3, 7, 28, 56, 91, and 147 days. Two specimens were tested at each age for each curing regime. If their compressive strength differed more than 5%, a third specimen was tested for each curing regime. The results are reported as the average of the all specimens tested. Ball seat bearing blocks were used. The end preparation of all specimens were done by grinding to maintain uniform end conditions regardless of the compressive strength or the age. The real dimensions of the test specimens and the maximum applied load were measured.

2.6.4 Effect of the End Blocks of the Testing Machine on Compressive Strength

Five 100 mm by 200 mm cylinder specimens from batch 4 of each series, cured continuously at 100% R.H., were tested using each type of end block using a 2600 kN electro-hydraulic closed-loop rock mechanics test system MTS 815 at the age of 56 days. The end preparation of all specimens were done by grinding to maintain uniform end conditions regardless of the compressive strength or the age. The real dimensions of the test specimens and the maximum applied load were measured.

2.6.5 Effect of Size of Specimen on Compressive Strength

Five 150 mm by 300 mm and five 100 mm by 200 mm cylinder specimens from batch 4 of each series, cured continuously at 100% R.H., were tested using a 2600 kN electro-hydraulic closed-loop rock mechanics test system MTS 815 at the age of 56 days. Meanwhile, three 150 mm by 300 mm and three 100 mm by 200 mm cylinder specimens, cured continuously at 100% R.H., were tested using the MTS 815 from batch S3 at the ages of 7, 28, 56, and 91 days and batch S4 at the ages of 28, 56 days. The ASTM standard spherical seat bearing blocks were used. The end preparation of all specimens were done

by grinding to maintain uniform end conditions regardless of the compressive strength or the age. The real dimensions of the test specimens and the maximum applied load were measured.

2.6.6 Modulus of Elasticity and Poisson's Ratio

100 mm by 200 mm cylinder specimens from batches LH1, UH1, LU1, and UU1, cured three weeks at 100% R.H. and then at 50% R.H., were tested in the 2600 kN electro-hydraulic closed-loop rock mechanics test system MTS 815 based on ASTM C 469[33] at the age of 56 days. The modulus of elasticity and Poisson's ratio were measured at 40% of ultimate, to be in the elastic range. Ball seat bearing blocks were used at both ends of each specimen. The end preparation of all specimens were done by grinding and the real dimensions of specimens were taken into consideration in calculation.

A high speed Fluke data acquisition system was used to collect the necessary data including load and strains continuously. Strains were measured using electrical resistance strain gages mounted at the mid-height of specimens at least ten days after transferring them from 100% R.H. to 50% R.H. so as to have a reasonably dry surface and at least ten days before loading to satisfy the required curing period for the epoxy adhesive. The strain gage area was cleaned by sand paper. Gages were mounted at mid-height of specified specimens by using Armstrong Epoxy Resin A-12. Axial strain was based on the average of two strain gages mounted on the opposite faces of specimen. Lateral strain was based on one strain gage for LH and UH series and average of two for LU and UU series. Three different brands of strain gages were used through experimental program as follows:

1. Test series LH :
BALDWIN SR-4 TYPE FAE-100N-12-50L (25.40 mm length)

2. Test series UH :
KYOWA TYPE KC-70-A1-11 (67.00 mm length)

3. Test series LU and UU :
SHOWA TYPE N11-FA-60-120-11 (60.00 mm length)

2.6.7 Tensile Splitting Strength

150 mm by 300 mm cylinder specimens from batch 2 of each series and batches S1 and S2, all cured continuously at 100% R.H., were tested at the age of 56 days using a 1350 kN Baldwin hydraulic testing machine. Tests were carried out according to ASTM C 496[34]

and CAN/CSA-A23.2-8C[5]. The real dimensions of the test specimen, the maximum applied load, and the estimated proportion of coarse aggregate fractured during the test were recorded.

2.6.8 Modulus of Rupture

150 mm by 150 mm by 550 mm beam specimens from batch 2 of each series and batches S1 and S2, all cured continuously at 100% R.H., were tested at the age of 56 days using a 1000 kN electro-hydraulic closed-loop material testing system MTS 810. Tests were carried out according to ASTM C 78[35] and CAN/CSA-A23.2-13C[5]. Loads were applied at the third points of a 456 mm span. The real dimensions of the test specimen and the maximum applied load were measured.

2.7 High Performance Concrete under High Sustained Compressive Stresses

2.7.1 Test Program

100 mm by 200 mm cylinder specimens from batches LH1, UH1, LU1, and UU1, cured 3 weeks at 100% R.H. and then at 50% R.H., were used for this study. The end preparation of all specimens were done by grinding to maintain uniform end conditions regardless of the compressive strength or the age. Four series of tests were carried out to study high performance concrete under high sustained compressive stresses. Two groups of test were conducted for each series :

- Sustained concentric compressive load tests
- Sustained eccentric compressive load tests (Eccentricity / Diameter = 0.10)

The eccentricity was chosen as 10 percent of the diameter to maintain small eccentricity inside the elastic Kern of the section (The elastic Kern of the section is at eccentricity/diameter = 0.125); but as it will be reported in Chapter 4, inelastic non linear stress - strain relationship caused tension strains on one side of some specimens.

Sturman et al [2] have suggested that a rectangular prism is the most suitable specimen for eccentric compressive tests because cylinders have a small area in the extreme fiber zone. The author believes a cylinder is an adequate test specimen for eccentric compressive tests because the effect of the small bearing area in the extreme fiber zone of cylindrical elements can be taken into consideration in studies conducted to investigate the behavior of structural elements under axial loads and moment gradient. Therefore, cylinders were used for both the concentric and eccentric sustained compressive load tests.

Ball seat bearing blocks were used to maintain the desired eccentricity for monotonic and sustained eccentric compressive load tests. The same kind of bearing blocks were used for monotonic and sustained concentric load tests to provide the same end condition and make the results comparable.

Five concentric and five eccentric specimens were tested monotonically in compression. Monotonic tests were done with the 2600 kN electro-hydraulic closed-loop rock mechanics test system MTS 815 with the procedure explained in section 2.2.4. Based on the average of the ultimate strengths, additional specimens were loaded under different percentages of the ultimate load, corrected, if necessary, for differences in dimensions. In a typical series, concentrically loaded specimens were tested at 95%, 90%, 85%, 80%, 75%, and 70% and eccentrically loaded specimens at 95%, 90%, 85%, 80%,and 75% of the short time ultimate compressive strength. Specimens under very high percentages of the short time ultimate compressive strength, such as 95% and 90%, were tested using the electro-hydraulic closed-loop rock mechanics test system MTS 815 . Specimens tested under lower percentages of the ultimate were tested in the six load frames (see Section 2.7.2), three used for concentric loading and the other three for eccentric loading. The frames were located in the controlled environment room with $50 \pm 3\%$ R.H. and 23 ± 2 °C to satisfy the standard environment requirements of ASTM E 171[32] for conditioning and testing of materials known to be sensitive to variations in temperature or relative humidity.

If a specimen in a load frame failed within the first two weeks (between ages 56 and 70 days), an additional specimen was placed in the load frame at the age of 70 days under different percentage of the ultimate compressive strength based on the average of three specimens tested monotonically with the 2600 kN MTS 815 at a standard loading rate at the age of 70 days. The sustained load period for the replacement cylinders was 90 days (three months).

2.7.2 Sustained Load Frames

A simplified drawing of load frames is shown in Figure 2.7.2.A. Pictures of the test room and load frames are shown in Figures 2.7.2.B and 2.7.2.C. The nominal capacity of the load frames is 1200 kN. Plates A, B, C, and D (63.5 mm thick) were made from steel with f_y=350 MPa and designed based on deflection criteria to minimize dishing of the plates. Load cells were made from 4340 steel with f_y=883 MPa and had a sensitivity of ±0.5 kN. Up to nine springs could be used. The springs were designed to be able to carry up to 140 kN each. The arrangement of the springs was based on symmetry and load criteria. Springs were always under more than 100 kN load to minimize the load drop-off in the load frames due to creep of the specimen. Four turned, ground, and polished steel shafts (25 mm diameter

with f_y=350 MPa) are used to guide suspended plate B. These passed through low friction holes containing press fit Oilight bearings (#SS 3240-40) in plate B and were restrained by plate A and the main body of the frame at the top and bottom respectively. Load rods were threaded throughout their length. They were made from steel with f_y=883 MPa. Low friction surfaces on parts where threaded load rods passed through holes in plates were provided by press fit Oilight bearings (#SS 4864-40) in the holes and turned, ground, and polished steel sleeves on the load rods.

Plate A sits on four 76 mm by 76 mm by 6 mm angles, braced with four 610 mm by 305 mm by 6 mm plates around plate A. Part E, made from four 76 mm by 76 mm by 6 mm angles and horizontally braced with a 585 mm by 585 mm by 6 mm plate, is used as the bracing system for the bottom of the load frame. The concentric load frames needed more lateral stiffness than the eccentric frames due to the higher loads. The possible lateral movement of plate D in these load frames was restrained with four 76 mm by 76 mm by 6 mm angles, braced with four 525 mm by 190 mm by 13 mm plates at the top and four 525 mm by 255 mm by 6 mm plates above plate A,. These details have been omitted from Figure 2.7.2.A for clarity.

The ball seat bearing blocks are described in Section 2.2.3. Due to the behavior of the ball seat bearing blocks, any misalignment of the load frame can not affect the alignment of the specimen or the level of load.

2.7.3 Loading Procedure in Sustained Load Frames

The loading procedure of sustained load frames is as follows:

1. Turn the nuts above plate A and below plate B to touch plates A and B respectively.
2. Turn the nuts above plate D to be loose.
3. Provide sufficient space for specimen by turning the nuts below plate D.
4. Fix the position of specimen between the ball seat bearing blocks by turning the nuts below plate D .
5. Align the specimen accurately by light tapping with a plastic hammer.
6. Turn the nuts above plate D to touch the plate.
7. Turn the nuts above plate A to be loose.
8. Position the hydraulic jacks between plates B and C.
9. Load the system with a hand oil pump up to 10 kN below target load.
10. Turn the nuts below plate B to touch the plate
11. Apply the remaining 10 kN to the system by tightening the nuts below plate B.
12. Release the hydraulic jacks.

13. At intervals, readjust the load by loading the system with a hand oil pump and hydraulic jacks and tightening the nuts below plate B. The load was adjusted when the drop in load approached 5% for LH series and 2.5% for other series.

2.7.4 Measurements

The real dimensions of specimens were taken into consideration in calculations. Each dimension was considered as the average of three measurements with the accuracy of ±0.05 mm. Strains were measured using electrical resistance strain gages mounted at the mid-height of specimens. Two electrical resistance strain gages were mounted longitudinally on the opposite faces of each specimen tested under monotonic or sustained eccentric compressive load. For specimens tested under monotonic or sustained concentric compressive loads, axial strain was based on average of two longitudinal strain gages mounted on the opposite faces of the specimen and lateral strain was based on one transverse strain gage for LH and UH series and average of two for LU and UU series. The type of electrical resistance strain gages used and the method of application are described in Section 2.6.6.

A high speed Fluke data acquisition system was used to collect data continuously for specimens tested in the 2600 kN electro-hydraulic closed-loop rock mechanics test system MTS 815. Data including time, load, and output of strain gages were collected every 15 seconds up to 30 minutes after loading, then every 5 minutes for those specimens tested by MTS 815. A package of data acquisition system (a Campbell Scientific, Inc. CR10 with a Campbell Scientific, Inc. AM416 Relay Multiplexer) and related softwares, supplied by Campbell Scientific Canada Corp., was used to collect data including time, load, and output of strain gages from the six sustained load frames. Data from the six load frames were automatically collected based on whichever of the following criteria occurred first:

a. Every 24 hour
b. Every 100 microstrain change in any strain gage output
c. Every 1 kN change in the load

Table 2.3.1 - Compositions of Cements Used

Cement	C_3S(%)	C_2S(%)	C_3A(%)	C_4AF(%)	Fineness (cm^2/g)
Inland Type 10	49.0	22.0	8.6	8.9	4180
Lafarge Type 10	55.6	18.0	5.8	9.0	4150
Lafarge Type 30	55.0	16.2	7.1	7.8	5510

Table 2.4.A - Concrete Mix Proportions (LH series)

Batch	LH1	LH2	LH3	LH4
W/C	0.40	0.40	0.40	0.40
Water+(kg/m^3)	150.0	150.0	150.0	150.0
Cement (kg/m^3)	375.0 (TYPE 10)	375.0 (TYPE 10)	375.0 (TYPE 30)	375.0 (TYPE 10)
Coarse Aggregate*(kg/m^3)	1100.0	1100.0	1100.0	1100.0
Fine Aggregate*(kg/m^3)	741.5	741.5	741.5	741.5
SPN (l/m^3)**	7.52	7.52	7.52	7.52
Air (assumed)	2%	2%	2%	2%
Yield (m^3)	0.106	0.120	0.120	0.127

+ Including water content of SPN.
* Based on dry weight.
** Superplasticizer, see section 2.3.4.

Table 2.4.B - Concrete Mix Proportions (UH Series)

Batch	UH1	UH2	UH3	UH4
W/C	0.245	0.245	0.245	0.245
Water^{+}(kg/m^3)	135.0	135.0	135.0	135.0
Cement(kg/m^3)	550.0 (TYPE 10)	550.0 (TYPE 10)	550.0 (TYPE 30)	550.0 (TYPE 10)
Coarse Aggregate*(kg/m^3)	1100.0	1100.0	1100.0	1100.0
Fine Aggregate*(kg/m^3)	628.7	628.7	628.7	628.7
SPN(l/m^3)**	18.1	18.1	18.1	18.1
Air (Assumed)	2%	2%	2%	2%
Yield (m^3)	0.120	0.120	0.120	0.120

Table 2.4.C - Concrete Mix Proportions (LU Series)

Batch	LU1	LU2	LU3	LU4
W/(C+S.F.)	0.265	0.265	0.265	0.265
Water^{+}(kg/m^3)	131.2	131.2	131.2	131.2
Cement(kg/m^3)	450.0 (TYPE 10)	450.0 (TYPE 10)	450.0 (TYPE 30)	450.0 (TYPE 10)
Silica Fume(Solid)(kg/m^3)	45.0	45.0	45.0	45.0
Coarse Aggregate*(kg/m^3)	1100.0	1100.0	1100.0	1100.0
Fine Aggregate*(kg/m^3)	669.3	669.3	669.3	669.3
SPN(l/m^3)**	14.9	14.9	14.9	14.9
Air (assumed)	2%	2%	2%	2%
Yield (m^3)	0.095	0.115	0.115	0.127

+ Including water content of SPN and silica fume.
* Based on dry weight.
** Superplasticizer, see section 2.3.4.

Table 2.4.D - Concrete Mix Proportions (UU Series)

Batch	UU1	UU2	UU3	UU4
W/(C+S.F.)	0.21	0.23	0.23	0.21
Water^{+}(kg/m^3)	126.0	126.5	126.5	115.5
Cement(kg/m^3)	546.0 (TYPE 10)	500.0 (TYPE 10)	500.0 (TYPE 30)	500.0 (TYPE 10)
Silica Fume(Solid)(kg/m^3)	54.0	50.0	50.0	50.0
Coarse Aggregate*(kg/m^3)	1100.0	1100.0	1100.0	1100.0
Fine Aggregate*(kg/m^3)	591.1	633.8	633.8	662.4
SPN(l/m^3)**	18.1	16.6	16.1	16.6
Air (assumed)	2%	2%	2%	2%
Yield (m^3)	0.100	0.120	0.120	0.127

Table 2.4.E - Concrete Mix Proportions (Supplementary Series)

Batch	S1	S2	S3	S4
W/C or W/(C+S.F.)	0.25	0.236	0.3375	0.3375
Water^{+}(kg/m^3)	131.3	129.8	135.0	135.0
Cement(kg/m^3)	500.0 (TYPE 10)	500.0 (TYPE 10)	400.0 (TYPE 10)	400.0 (TYPE 10)
Silica Fume(Solid)(kg/m^3)	25.0	50.0	-	-
Coarse Aggregate*(kg/m^3)	1100.0	1100.0	1100.0	1100.0
Fine Aggregate*(kg/m^3)	651.7	633.8	759.0	759.0
SPN(l/m^3)**	15.8	16.6	9.6	9.6
Air (assumed)	2%	2%	2%	2%
Yield (m^3)	0.150	0.150	0.190	0.190

+ Including water content of SPN and silica fume.
* Based on dry weight.
** Superplasticizer, see section 2.3.4.

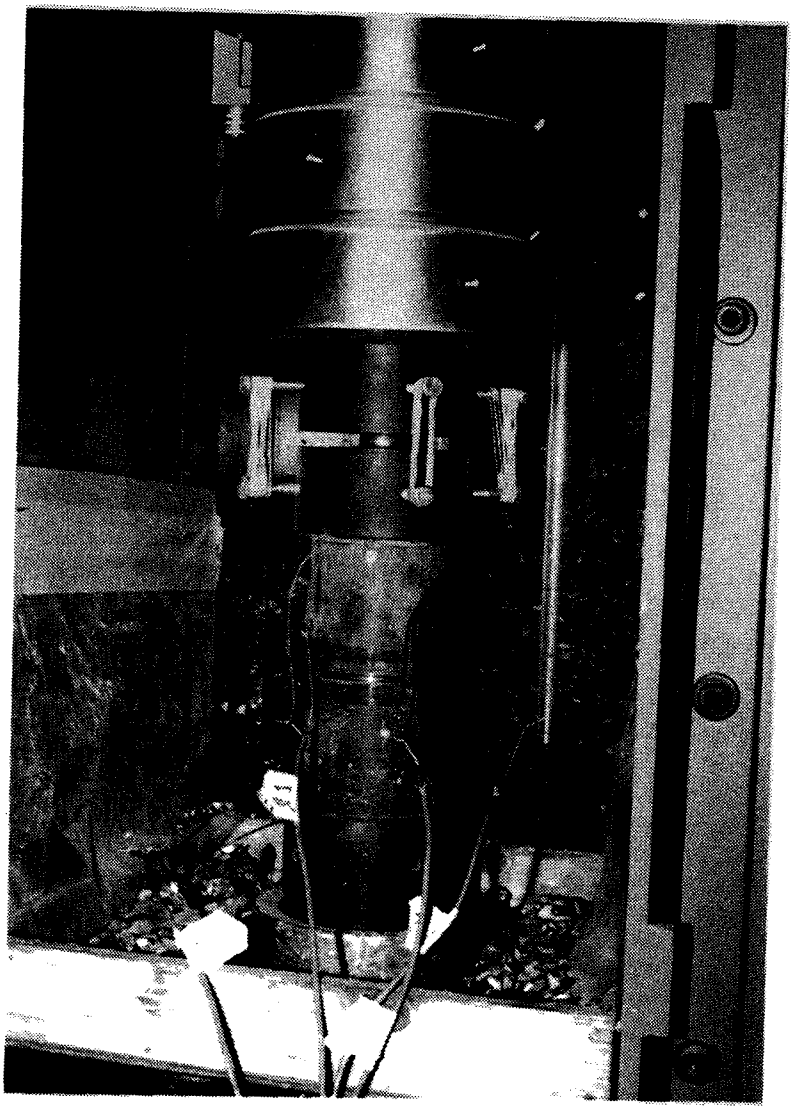

Figure 2.2.3.A - The Ball Seat Bearing Blocks

Figure 2.2.3.B - The Spherical Seat Bearing Block

Sieve	% Passing
10 mm	100
5 mm	94.1
2.5 mm	78.8
1.25	69.9
0.630 mm	63.2
0.315 mm	32.0
0.160 mm	6.9
0.080 mm	1.4

Fineness Modulus = 2.55

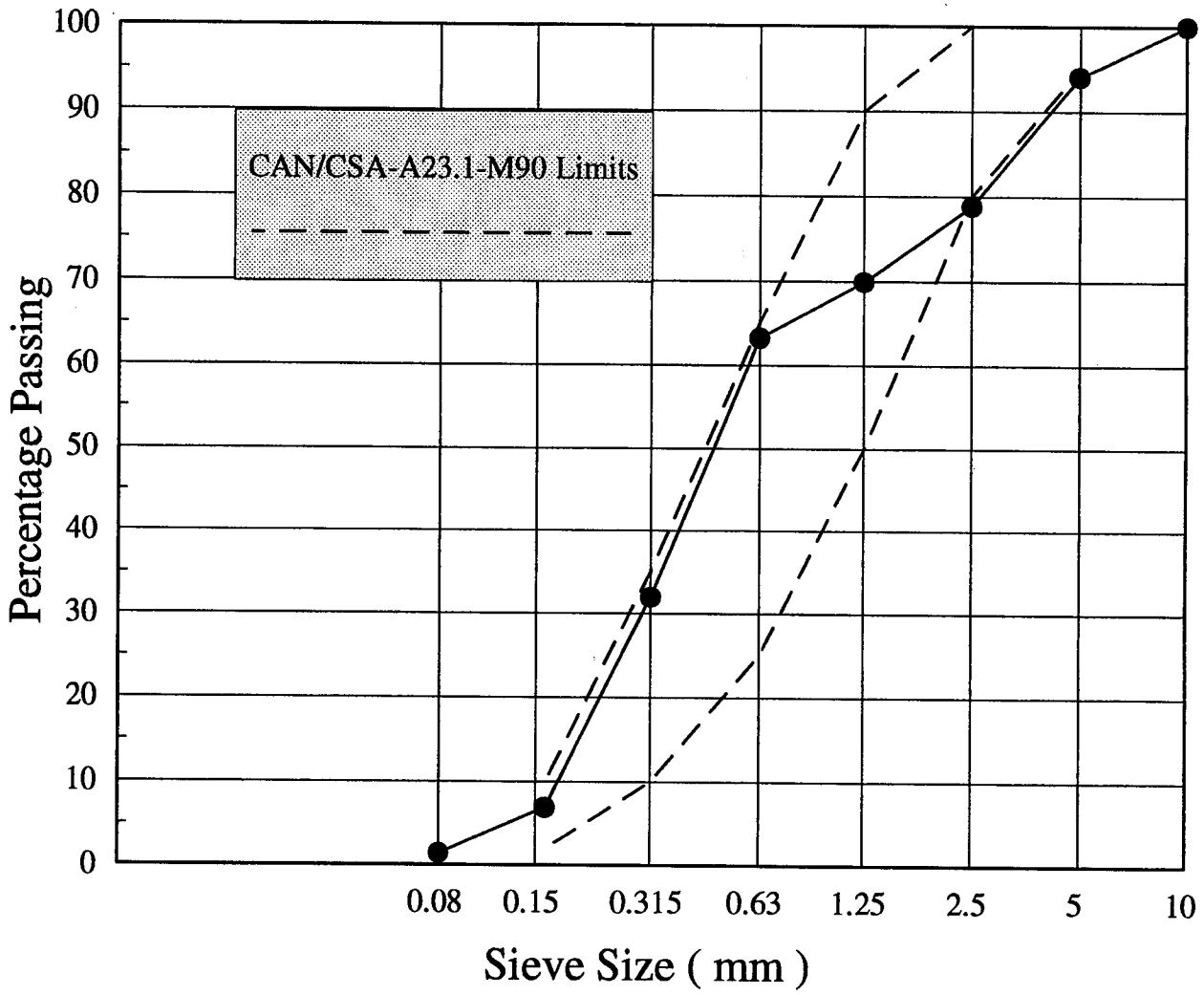

Figure 2.3.2 - Sieve Analysis of Fine Aggregate

Sieve	% Passing
20 mm	100.0
14 mm	97.5
10 mm	60.5
5 mm	2.2
2.5 mm	0.5
1.25 mm	0.4
0.630 mm	0.3
0.315 mm	0.2
0.160 mm	0.0

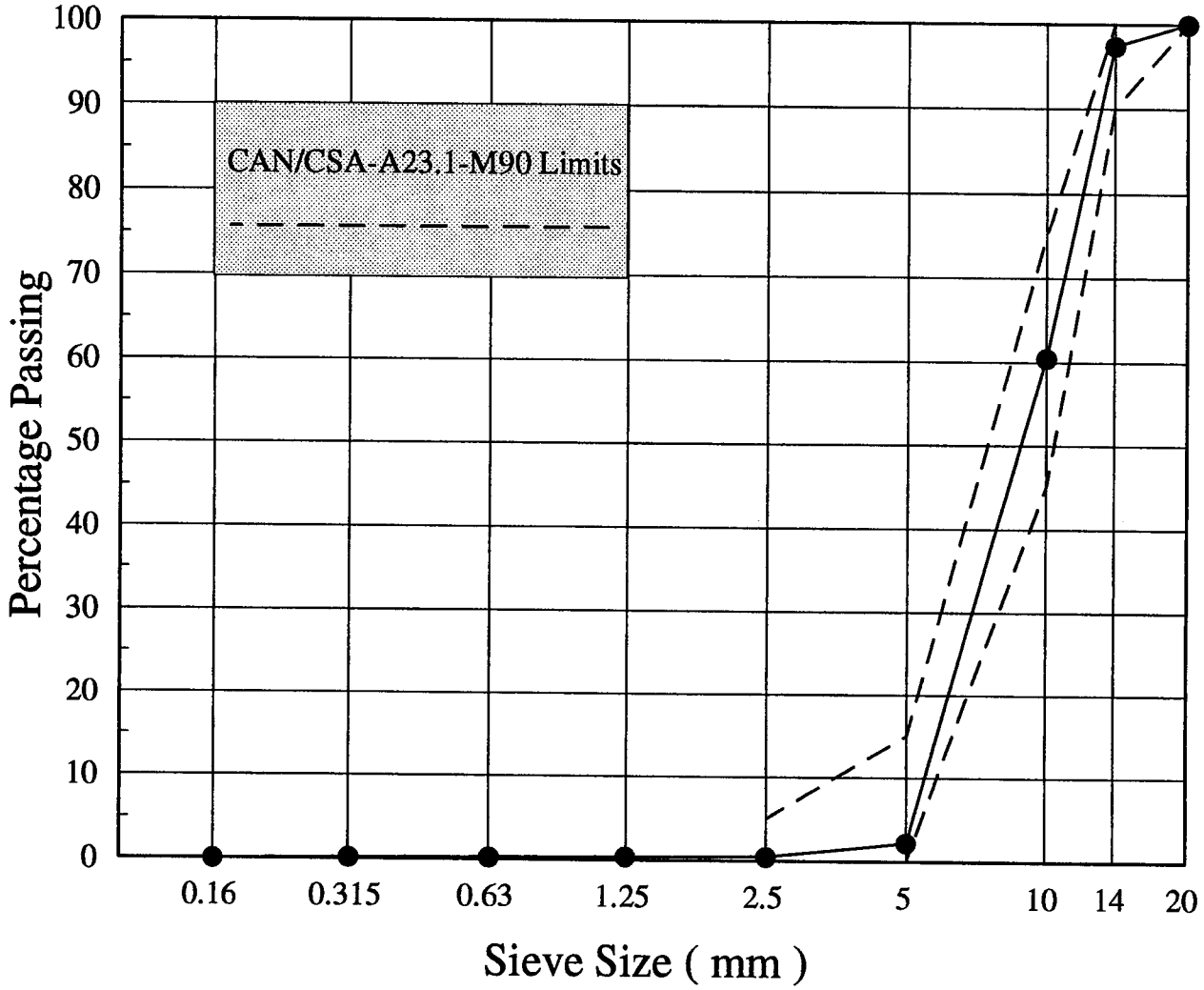

Figure 2.3.3 - Sieve Analysis of Coarse Aggregate

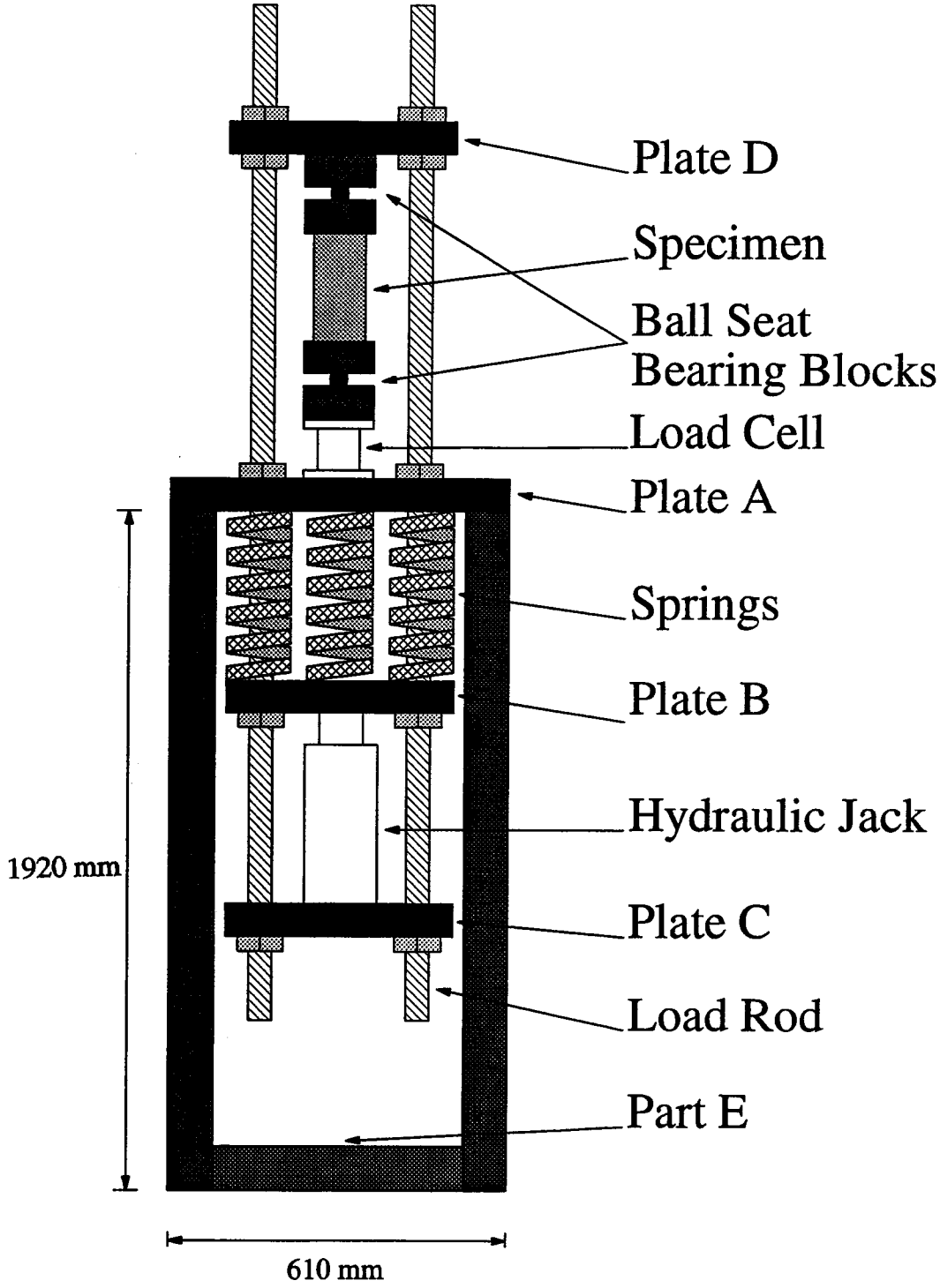

Figure 2.7.2.A - Simplified Drawing of the Sustained Load Frame

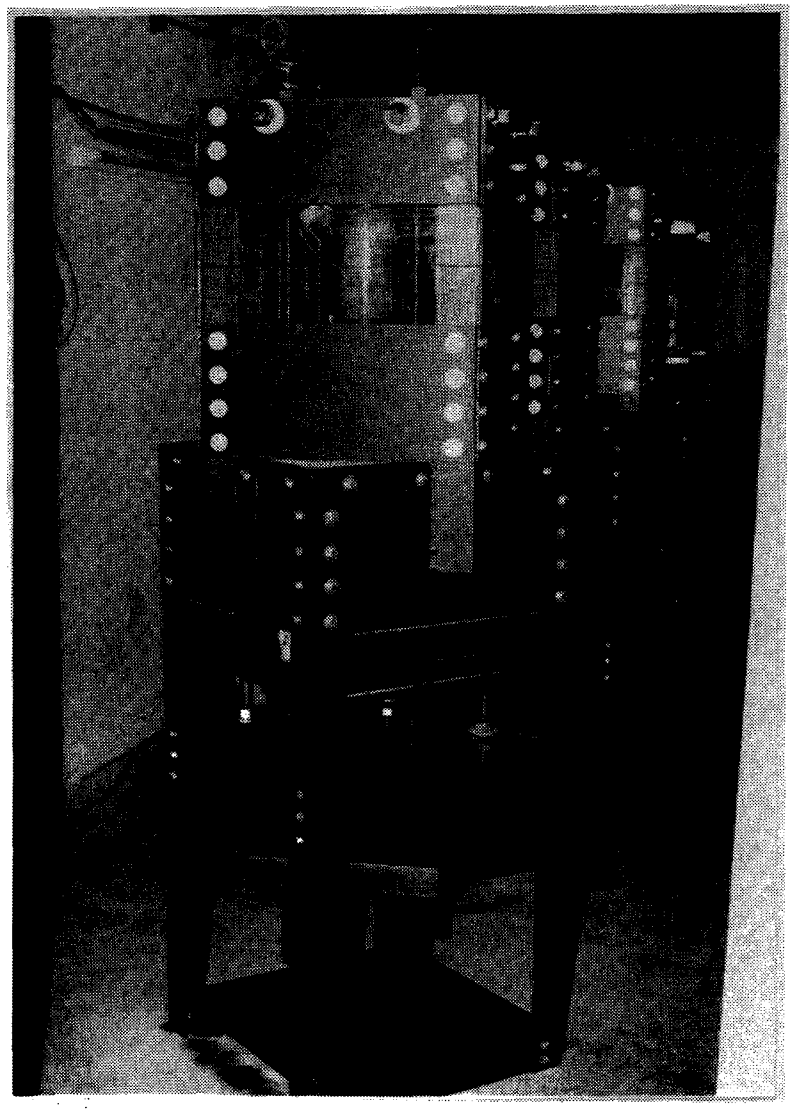

Figure 2.7.2.B - The Six Sustained Load Frames

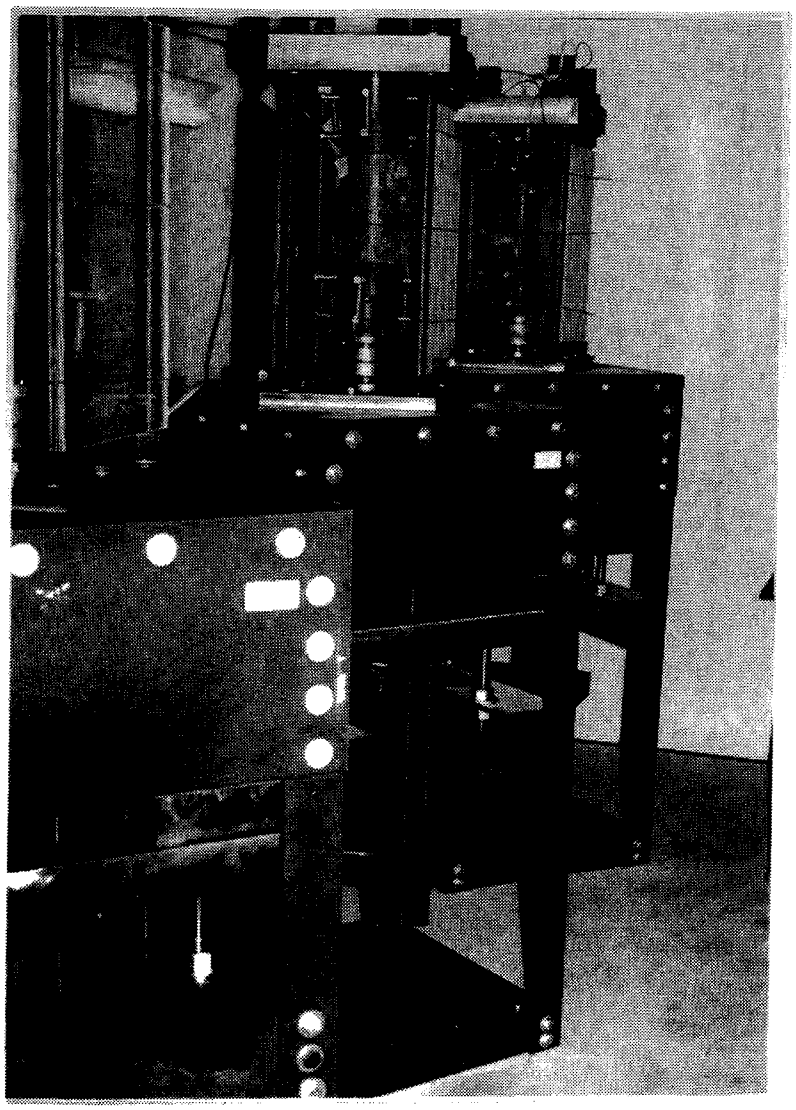

Figure 2.7.2.C - The Eccentric Sustained Load Frames

3. Mechanical Properties of High Performance Concrete

3.1 Introduction

High performance concrete is a new material and there is relatively limited available information about its properties. A supplementary test program was carried out to develop information about mechanical properties of high performance concrete and also present a relatively complete characterization of the concretes used in the study of high performance concrete under high sustained compressive stresses. This study gives information pertaining the following objectives:

1. Compressive strength gain with time.
2. Effect of type of cement on compressive strength.
3. Effect of drying on compressive strength.
4. Effect of the bearing blocks of the testing machine on compressive strength.
5. Effect of the size of specimen on compressive strength.
6. Modulus of elasticity.
7. Poisson's ratio.
8. Tensile splitting strength.
9. Modulus of rupture.

The results of the supplementary test program are presented in this chapter. A short literature review of previous studies are presented at the start of each section. The results are discussed, explained, and compared with standards and recommended practices and specifications. Based on the current study and previous studies, general conclusions are presented at the end of this chapter.

3.2 Compressive Strength Gain with Time

3.2.1 Literature Review

The compressive strength is the most common parameter used to characterize concrete. The compressive strength depends on geometry, size, age, curing regime etc. The in-situ strength of concrete can also be different from that of laboratory specimens for various reasons including consolidation and curing.

FIP/CEB Bulletin d'Information No. 197[8] summarized the results of different studies about the compressive strength gain with time. It is reported that "the relative increase in the short term strength of a high strength concrete after 28 days is generally lower than for a normal grade concrete. This is due to the lack of available free water for further hydration combined with a possible limitation from the capacity of the aggregate". It is also reported that high strength concrete containing silica fume generally has lower relative strength gain after 28 days than concrete without silica fume.

ACI 363R-84[7] concludes that high strength concrete shows a higher rate of strength gain at early ages as compared to lower strength concrete but at later ages the difference is not significant.

3.2.2 Test Results

The test results for LH, UH, and UU series are presented in Tables 3.2.2.A through C. The test results for LU series are presented in Appendix E. The reported results are the average compressive strength of the specimens tested for each series. The compressive strength of individual specimens are reported in Appendix I, Tables I-3.2.2.A through C. All results are based on moist cured specimens. The compressive strength gain, expressed as the percentage of the 28 day compressive strength, is shown in the same tables and Figure 3.2.2. The results shown in Figure 3.2.2 are based on the average of the two batches presented in Tables 3.2.2.A through C for each series.

3.2.3 Discussion of Results

The ratios of 7-day to 28-day compressive strength for LH and UH series are 0.85 to 0.88 which are compatible with the 0.8 to 0.9 range reported by ACI 363R-84[7] based on studies done by Parrott[21]. The ratios of 7-day to 91-day compressive strength for LH and UH series are 0.75 to 0.79 which are higher than the 0.65 to 0.73 reported by ACI 363R-84[7] based on studies done by Carrasquillo et al[12].

The UU series gained its major compressive strength between 7-day and 28-days as can be concluded from Figure 3.2.2 and the ratios of 7-day to 28-day and 147-day to 28-day compressive strength from Tables 3.2.2.A through C. The UU series, an ultra high strength silica fume high performance concrete, gained less strength after 28 days as predicted[8]. This observation is in complete agreement with studies by Sarkar et al[23]. They report that, due to low water to cementitious materials ratio, all ultra fine silica fume particles are not consumed. The low water to cementitious materials ratio alters the hydration rate. It effectively delays the dissolution of silica fume particles. In such a situation, the silica fume dissolution process is much slower than reported by several researchers. Its consumption

is completed with 28 days. Sarkar et al[23] also reported that superplasticizer is useful not only in dispersing cement particles but also in giving a uniform distribution of ultra fine silica fume particles.

3.3 Effect of Type of Cement on the Compressive Strength Gain

3.3.1 Literature Review

The choice of the proper type of cement for high performance concrete is one of the most important factors among materials selection. The strength development in high performance concrete requires portland cement with the optimum quality from the standpoint of uniformity, strength, and workability. Based on a report by the Chicago Committee on High Rise Buildings[14], for mixes with f'_{c28} = 62 to 72 MPa with a 76 mm ± 13 mm slump, Type I (Type 10) cement develops the highest and Type III (Type 30) cement develops the lowest compressive strength at all ages among Type I, II, and III cements.

3.3.2 Test Results

One of the four batches in each series was made with Type 30 cement, the other three with Type 10. The test results for LH, UH, and UU series are presented in Tables 3.3.2.A through C and Figure 3.3.2.A. The test results for LU series are presented in Appendix E. The reported results are the average compressive strength of the specimens tested for each series. The compressive strength of individual specimens are reported in Appendix I, Tables I-3.3.2.A through C. All results are based on moist cured specimens. The compressive strength gain, expressed as the percentage of the 28 day compressive strength, is also shown in the same tables and Figure 3.3.2.B through D.

3.3.3 Discussion of Results

In the study done by the Chicago Committee on High Rise Buildings[14], a constant slump was maintained for mixes with the different types of cement. Due to the higher fineness of Type III cement, the mixture with Type III cement required more water to provide the same workability as the mixture with Type I cement. Therefore, due to the increase of water to cementitious materials ratio, the compressive strength decreases. It should be mentioned that the mixtures used in that study contained 12% fly ash.

The high performance concrete mixtures with Type 30 cements in this test series show higher compressive strength for the LH and UH series as it can be concluded from Figure 3.3.2.A. The mix proportions were maintained constant for each series in this study. As a result, the mixtures with Type 30 cement had less workability. Type 30 cement can have better performance than Type 10 cement as the fine filler to produce dense and strong high

performance concrete in the absence of sufficient water and supplementary cementitious materials. It should be mentioned that the total amount of cement may not hydrate in high performance concretes with low water to cementitious materials ratios. The extra amount of cement acts as a fine filler to produce dense concrete while superplasticizer provides the necessary workability and helps the uniform distribution of these fine particles. Based on above discussion, it seems that the mixtures with Type 30 cement develop higher compressive strength for high performance concretes with the same mix proportions.

The ultra high strength concrete mixture with Type 30 cement and silica fume (UU) developed lower compressive strength after early ages than the mixtures with Type 10 cement as can be concluded from Figure 3.3.2.A. This can be explained by the effect of the presence of the ultra fine particles of silica fume that can be a better filler to produce dense concrete and higher demand of water by Type 30 cement.

Figure 3.3.2.B through D show the compressive strength gain of mixes as a function of time, normalized based on their compressive strength at the age of 28 days. The rate of compressive strength gain of mixture UU3 with Type 30 cement is higher after 28 days in spite of its lower compressive strength. As reported by Sarkar et al[23], the dissolution process of silica fume takes more time (nearly 7 days) in high performance concrete mixtures with low water to cementitious materials ratios, than in high performance concrete mixtures with higher water to cementitious materials ratios. Due to the higher fineness of Type 30 cement, there are more cement particles in a mixture with Type 30 cement for the same cement factor. As a result, a silica fume high performance concrete with Type 30 cement and a low water to cementitious materials ratio tends to have more delay in dissolution of ultra fine silica fume particles compared to the same mixture with Type 10 cement. Therefore the silica fume high performance concrete mixture with Type 30 cement can have higher rate of compressive strength gain after the age of 28 days.

3.4 Effect of Drying on the Compressive Strength Gain

3.4.1 Literature Review

The effect of drying, or in other words, the effect of the curing regime of concrete specimens on the compressive strength gain as a function of time has always been an important concern. The service environment of the structure is different from the laboratory environment condition. As a result, studies on dry and moist cured specimens are necessary.

According to Parrott[21], high strength concrete specimens (with 28-day cube compressive strengths of 80 to 100 MPa) moist cured for 7, 14, and 28 days, followed by exposure to air at a relative humidity of 65% had 90 day cube strengths of 90, 95, and 100% respectively, of those of control specimens which were continuously moist cured.

Carrasquillo et al[12] studied two different curing regimes. They compared moist cured high strength concrete (f'_{c28} = 70.4 MPa) specimens to specimens which were moist cured for seven days and then air dried at 50% R.H. till the age of 28 days. The air dried specimens showed an average strength reduction of 10% relative to continuously moist cured specimens. They also compared moist cured high strength concrete (f'_{c28} = 70.4 MPa) specimens with specimens moist cured for twenty eight days and then air dried at 50% R.H. till the age of 95 days. The air dried specimens showed an average reduction of 4% relative to continuously moist cured specimens.

Aitcin et al[24], studied air cured, sealed, and moist cured specimens. The air cured specimens were cured continuously in air after casting. As expected, the moist cured specimens gave higher compressive strengths than the sealed specimens, which in turn, gave higher compressive strengths than the air cured specimens. The air cured specimens had compressive strengths of about 80% of moist cured specimens and 84% of sealed specimens. The largest difference between moist cured and sealed specimens occurred for the 120 MPa high performance concrete. The 13% difference was considered to be the result of the very low water to cementitious materials ratios (W/C=0.25).

According to Asselanis et al[16], for a high performance concrete with a 28 day compressive strength of 98.8 MPa, specimens moist cured for seven days and continuously moist cured specimens had approximately the same compressive strength at 28 days but had compressive strengths 16% higher than specimens which were cured continuously in air after casting. They also reported that specimens moist cured for twenty eight days had 8% and 22% higher compressive strengths at 56 days compared to continuously moist cured specimens and continuously air cured specimens respectively.

According to Burg et al[13], continuously moist cured specimens generally had higher or equal compressive strength at the age of 426 days than specimens which were moist cured for twenty eight days and then air dried at 50% R.H.. It should be mentioned that concretes studied by them showed some compressive strength loss at late ages.

3.4.2 Test Results

The test results for LH, UH, and UU series are presented in Tables 3.4.2.A through C. The test results for LU series are presented in Appendix E. The reported results are the average compressive strength of the specimens tested for each series. The compressive

strength of individual specimens are reported in Appendix I, Tables I-3.4.2.A through C. The compressive strength gain is shown in Figure 3.4.2 as a function of age for the three different curing regimes. The ratio of 147 day compressive strength to the 28 day compressive strength of moist cured specimen, for specimen with the three curing regimes under study, are presented in Table 3.4.2.D. The ratio of 147 day compressive strength of specimens moist cured for 3 and 7 weeks to the 147 days compressive strength of moist cured specimens are presented in Table 3.4.2.E.

3.4.3 Discussion of Results

Many studies on conventional concrete show that the compressive strength of continuously moist cured specimens is lower than that those allowed to dry after a sufficient period of moist curing. In all three series plotted in Figure 3.4.2 the compressive strength of the continuously moist cured specimens was lower than that of those allowed to dry after a period of moist curing. The compressive strength gain of LH and UH series between the ages of 28 and 147 days are 9% for continuously moist cured specimens and between 32% to 37% for 3 and 7 weeks moist cured specimens. For LH and UH series, the compressive strength of specimens moist cured for 3 and 7 weeks are 21% to 26% higher than the continuously moist cured specimens at the age of 147 days. Meanwhile, the compressive strength of specimens moist cured for 3 and 7 weeks are very close at the age of 147 days for LH and UH series. As a result, it can be concluded that 3 weeks moist curing will be enough for high performance concretes like LH and UH series and also will cause higher rate of strength gain. This conclusion is in reasonable agreement with studies done by Parrott[21] and Asselanis et al[16].

The compressive strength gains of UU series between the ages of 28 and 147 days are 16% for continuously moist cured specimens (compared to 9% for LH and UH series), 24% for 3 weeks moist cured specimens (compared to 32% to 35% for LH and UH series), and 36% for 7 weeks moist cured specimens (compared to 35% to 37% for LH and UH series). The compressive strength of 3 and 7 weeks moist cured specimens are only 7% and 17% higher than the continuously moist cured specimens at the age of 147 days (compared to 35% to 37% for LH and UH series). The higher compressive strength of 3 weeks moist cured specimens compared to continuously moist cured specimens at the age of 147 days suggests that 3 weeks moist curing can be enough for high performance concretes like UU series. The higher compressive strength of specimens moist cured for 7 weeks and also the higher rate of strength gain of continuously moist cured specimens and 7 weeks moist cured specimens imply that for silica fume ultra high strength concrete with a very low water to cementitious materials ratios, the hydration of cement and dissolution of silica fume can

continue until late ages if the necessary water will be available. The behavior of UU series is in complete agreement with results of studies by Sarkar et al[23] and Aitcin et al[24]. It can be explained by the high rate of compressive strength gain of ultra high strength silica fume concrete with a low water to cementitious materials ratio in the presence of sufficient moisture between the ages of 7 and 28 days due to late dissolution of the ultra fine particles of silica fume.

3.5 Effect of the Bearing Blocks of the Testing Machine on Compressive Strength

3.5.1 Literature Review

It was necessary to load the specimens using the ball seat bearing blocks in the sustained load tests. The effect of these on compressive strength was studied. A spherically seated bearing block on one end is suggested by many studies including references 7, 26, and 39 to insure a central and uniformly distributed load on specimen. A spherical seat bearing block on one end simulates a semi-fixed end condition and a fixed seat bearing block on the other side simulates a fixed end condition. Ball seat bearing blocks at both ends simulate a hinged-hinged end condition. With a reasonable alignment, the ball seat bearing blocks can also provide a central and uniformly distributed load on specimen.

According to Lessard et al[25], the diameter of the spherical seat can affect the compressive strength test results. Sigvaldason[39] and Cole[40] reported that use of proper platen size is critical if strengths are to be maximized and variations reduced. They also suggested that the upper platen must have a spherical seat bearing block able to rotate and achieve full contact with the specimen under initial load and perform in a fixed mode when approaching the ultimate load.

According to ACI 363R-84[7], the diameters of the platen and spherical bearing socket are critically important. Ideally, the platen and spherical bearing block diameters should be approximately the same as the bearing surface of the specimen. Bearing surfaces larger than the specimen will be restrained (due to size effects) against lateral expansion, will probably not expand as rapidly as the specimen, and will consequently create confining stresses in the specimen end. Bearing surfaces smaller in diameter than the specimen may result in portions of the specimens remaining unloaded. Spherical seating blocks smaller in diameter than the specimen may result in bending of the platen around the socket with a consequent nonuniform distribution of stresses. This tendency decreases as the thickness of the platen outside the spherical head increases.

3.5.2 Test Results

The test results for LH, UH, and UU series are presented in Table 3.5.2.A. The test results for LU series are presented in Appendix E. The mean values of the compressive strength of specimens tested by both of the end conditions and the ratio of the compressive strength with ball seat bearing blocks to the compressive strength with spherical seat bearing blocks are presented in Table 3.5.2.B.

3.5.3 Discussion of Results

Ball seat bearing blocks simulate a hinged-hinged end condition for a specimen. As a result, due to less rotational end restraint compared to a spherical seat bearing block in one side and fixed bearing block in the other side, ball seat bearing blocks can provide a better central uniform load on specimen if the specimen is well aligned. With a poorly aligned test set up, the stress distribution is more uniform with a spherical seat bearing block in one side and fixed bearing block in the other side than a set of ball seat bearing blocks.

According to Sigvaldason[39], when both sides of the specimen are effectively pinned, the load is applied in a straight line between the pins, irrespective of the location of the specimen in the testing machine. Consequently, in non homogeneous and/or misaligned specimens, elements within the specimens strain at different rates in order to maintain the centroid of resistance at every cross section co-linear with the line of action of the applied load. According to him, when one end of the specimen is effectively pinned, whilst the other end is effectively fixed, any non uniformity or misalignment will cause differential straining of opposite sides of the specimen. This results in bending of the specimen, which produces a lateral movement of the pinned end relative to the fixed end, so inducing a lateral reaction from the machine. Thus, the loading system for this case can be represented by a cantilever loaded simultaneously by an axial load and laterally at its free end. He also reported that when both ends of the specimen are effectively fixed, no tilting of the ends of the specimen during loading is possible. Thus, the specimen is deformed uniformly throughout, the centroid of action of the machine being co-linear with the centroid of resistance of the uniformly deformed specimen.

The disadvantage of the hinged-hinged end condition is instability of the test after the peak load. As a result, if the behavior of descending branch is a concern, the ball seat bearing blocks are not suitable bearing blocks. The ball seat bearing blocks can also provide a desired eccentricity if required. As a result, due to suitable central uniform uniaxial load distribution and the ability of providing desired required eccentricity, ball seat bearing blocks were used in this study. The results of this study suggest that high performance concrete

specimens tested with ball seat bearing blocks have lower compressive strengths than high performance concrete specimens tested with standard spherical seat bearing blocks by up to 7 percent.

It seems unlikely that the 125 mm diameter bearing block with a thickness of 63.5 mm from D-2 tool steel with f_y=2000 MPa will deform significantly under levels of load used in this study. The possible lower compressive strength of specimens tested using the ball seat bearing blocks is probably explained by the hinged-hinged behavior of the ball seat bearing blocks. This behavior provides less end restraint and less chance of stress redistribution upon a localized crack development.

3.6 Effect of Specimen Size on Compressive Strength

3.6.1 Literature Review

The compressive strength of concrete is probably the most important property of concrete. It is generally considered as the measure of quality of concrete and it is the prime parameter in design of concrete and reinforced concrete. Standards, specifications, and recommended practices[3,5,7,28] still consider 150 mm by 300 mm cylinder as the standard compressive strength test specimen for concrete. In spite of this, almost all commercial test on high performance concrete are done on 100 mm by 200 mm cylinders.

ACI 211.4R-93[3] suggests that the specimen size used by the concrete producer to determine mixture proportions should be compatible with the load capacity of the testing machine and consistent with the cylinder size specified by the designer for acceptance. No guidance is given as to what "compatible" and "consistent" mean. They also state that the measurements of strength using 150mm by 300 mm cylinder are not interchangeable with those obtained when using 100 mm by 200 mm.

According to Carrasquillo et al[12], the average ratio of compressive strength of 150 mm by 300 mm to 100 mm by 200 mm cylinders in their study was 0.90 regardless of strength and test age. Cook[15] reported approximately 5% higher compressive strength for 100 mm by 200 mm cylinders compared to 150 mm by 300 mm cylinders. Burg et al[13] reported approximately 1% higher compressive strength for 100 mm by 200 mm cylinders compared to 150 mm by 300 mm cylinders. According to ACI 363R-84[7] and Lessard et al[25], the compressive strength results can also be different if we use the same spherical seat bearing blocks for testing 100 mm by 200 mm cylinders and 150 mm by 300 mm cylinders as it is discussed in section 3.5.1. Lessard et al[25] reported an average of 4% higher compressive strength for 100 mm by 200 mm cylinders compared to 150 mm by 300 mm when 102 mm and 152 mm diameter spherical seats were used for 100 mm by 200 mm and 150 mm by

300 mm respectively. They reported an average of 20% higher compressive strength for 100 mm by 200 mm cylinders compared to 150 mm by 300 mm when 102 mm diameter spherical seat were used for both 100 mm by 200 mm and 150 mm by 300 mm cylinders. Baalbaki et al[13] suggested the following equation based on their studies and those by Lessard et al[25]:

$$f'_{c150} = 0.93 f'_{c100} + 1.1 \qquad (MPa) \qquad (3.6.1.A)$$

3.6.2 Test Results

The test results for LH, UH, UU, S3, and S4 series are presented in Table 3.6.2.A. The test results for LU series are presented in Appendix E. The mean values of the compressive strength of 100 mm by 200 mm and 150 mm by 300 mm cylinders and the ratio of the compressive strength of 150 mm by 300 mm to 100 mm by 200 mm cylinders are presented in Table 3.6.2.B. The average ratio of the compressive strength of 150 mm by 300 mm to 100 mm by 200 mm cylinders is 0.95 with the sample standard deviation (S_{n-1}) of 0.035.

3.6.3 Discussion of Results

Different ratios of the compressive strength of 150 mm by 300 mm to 100 mm by 200 mm cylinders are reported by different researchers. The size of the spherical seat of the bearing block of the test machine, the stiffness of the test machine, and the quality of consolidation can affect this ratio. Among these parameters, it seems that the stiffness of the test machine has the most important effect. Results of tests using very stiff test machine shows 1% or less difference between the compressive strength of 100 mm by 200 mm and 150 mm 300 mm cylinders[13].

3.7 Modulus of Elasticity

3.7.1 Literature Review

The modulus of elasticity of concrete is one of the most important mechanical properties of concrete. The modulus of elasticity of concrete is closely related to the properties of the cement paste, the stiffness of the selected aggregates, and also the method of determining the modulus[8]. Since most national standards express the modulus of elasticity as a function of the compressive strength determined with compression tests, these expressions will only be correct if the most common mixture designs and materials are selected. Concrete mixtures for high performance concrete are based on supplementary cementitious materials, chemical admixtures, a low water to cementitious materials ratio

and carefully selected aggregates. The influences of these characteristics on the modulus of elasticity are considerable and the validity of well known expressions for the modulus of elasticity must be re-examined.

Pauw[10] recommended the following equation for the modulus of elasticity of concrete in 1960:

$$E_c = 0.043\, W_c^{1.5} \sqrt{f'_c} \qquad 2.5\,MPa < f'_c < 40\,MPa \qquad (3.7.1.A)$$

$$W_c = 1500\ to\ 2500\ kg/m^3$$

In which E_c= the static modulus of elasticity of concrete (MPa); W_c= air dry weight of the concrete at time of test in kg/m^3; f'_c= the cylinder compressive strength of concrete at the time of test in MPa. Equation 3.7.1.A is the current ACI 318M-89[17] equation for modulus of elasticity of concrete which for normal density concrete reduces to:

$$E_c = 4700\sqrt{f'_c} \qquad (3.2.1.B)$$

ACI 363R-84[7] recommends another equation for E_c, originally suggested by Carrasquillo et al[12], based on test data from Pauw[10], Kaar et al, Perenchio et al[19], and their own data:

$$E_c = 3300\sqrt{f'_c} + 6900 \qquad 21\,MPa < f'_c < 83\,MPa \qquad (3.7.1.C)$$

According to Asselanis et al[16], the curing condition can affect the modulus of elasticity of high performance concrete. They reported significantly lower values for modulus of elasticity of specimens with less than 7 days moist curing. Based on that study, they considered that 7 days moist curing can be enough and will make concrete sufficiently impervious. Burg et al[13] reported slightly higher values of modulus of elasticity at the age of 91 days for continuously moist cured specimens compared to specimens moist cured for four weeks and then air dried at 50% R.H.. They also reported an average of 3400 MPa higher values (7 to 10 percent higher) for modulus of elasticity of 100 mm by 200 mm cylinders compared to 150 mm by 300 mm cylinders. This difference may be at least partially due to test method, but falls within the range of precision of ASTM C 469[13]. In contrast with the study done by Burg et al[13], Baalbaki et al[9] reported that the modulus of elasticity measured using 100 mm by 200 mm high performance concrete specimens were only 95% of the results from 150 mm by 300 mm cylinders. The results of the study by Burg et al[13] suggest that supplementary cementitious materials (like silica fume and fly ash) and chemical admixtures can affect the modulus of elasticity of high performance concrete. Jerath et al[36] also reported that superplasticizer can affect the modulus of elasticity of concrete. Previous

research works also suggest that the modulus of elasticity of high performance concrete will increase with time[9,11,13,14,15,16,20,27]. According to Parrott[20], increases in modulus of elasticity with age for a given concrete depend mainly upon continued hydration of the cement and the associated reduction in the porosity of the cement paste. It should be mentioned that the continued reduction of porosity of the cement paste in high performance concrete which is very dense can be questionable. Hwee et al[37] reported approximately no increase in modulus of elasticity of high strength concrete with time between 14 and 88 days in spite of an increase in the compressive strength in a study with a simulated field curing condition of 7 days curing with wet burlap. Test data from these studies show lower rate of increase of modulus of elasticity with time for high performance concretes containing supplementary cementitious materials.

The coarse aggregate used in making high performance concrete can have very significant effect on the modulus of elasticity of high performance concrete[9,11,12,18,20,27]. The difference between the modulii of elasticity of high performance concretes with the same mixture design and with approximately the same compressive strength, but with different coarse aggregates, can be as high as 18000 MPa[9]. Parrott[20] recommends the following equation for modulus of elasticity of concrete:

$$E_{28} = C_o + 0.2 f_{28} \qquad 20\,MPa < f_{28} < 70\,MPa \qquad (3.7.1.D)$$

In which E_{28}= 28 day modulus of elasticity, f_{28}= 28 day cube strength, and C_o is a factor closely related to the modulus of elasticity of the aggregate. He also recommends the following equation for modulus of elasticity of concrete at age t days:

$$E_t = E_{28}(0.4 + 0.6 f_t / f_{28}) \qquad (3.7.1.E)$$

In which f_t= the cube strength at age t days. Alexander[18] recommends the following method of predicting the modulus of elasticity of concrete for two levels of importance of the modulus of elasticity:

- Level 1: The modulus of elasticity does not have a significant effect on application. He recommends a single value equal to 30000 MPa for grades of concrete between 20 MPa and 60 MPa regardless of other factors.

- Level 2: The modulus of elasticity has a significant effect on application. He recommends Equation 3.7.1.D and classifies South African coarse aggregates in two groups as follows:

-Group 1: Aggregates with low to medium values of elastic modulus (C_o ranges from 10000 MPa to 19000 MPa with the mean value of 15000 MPa)

-Group 2: Aggregates with medium to high values of elastic modulus (C_o ranges from 20000 MPa to 30000 MPa with the mean value of 25000 MPa)

The recommended C_o values by Alexander[18] are based on the following relation between C_o and E_a (aggregate elastic modulus) based on the results of tests conducted in the U.K.:

$$C_o = 0.4E_a \qquad (3.7.1.F)$$

3.7.2 Test Results

Test results for LH, UH, and UU series including the compressive strength, the strain at the maximum stress, and the measured static modulus of elasticity and the Poisson's ratio at 40% of the ultimate stress based on ASTM C 469-87a[33] are presented in Table 3.7.2. The test results for LU series are presented in Appendix E. The following equation gives the best fit line for the relation between the measured static modulus of elasticity and square root of the compressive strength of high performance concretes used in this study:

$$E_c = 3422\sqrt{f'_c} \qquad 55MPa < f'_c < 125MPa \qquad (3.7.2)$$

The measured static modulus of elasticity of high performance concretes tested in this study are compared to the ACI 318M-89[17] equation, the ACI 363R-84[7] equation, the CAN3-A23.3-M84[28] equation, and Equation (3.7.2) in Figure 3.7.2. The ACI 318M-89[17], the ACI 363R-84[7], and the CAN3-A23.3-M84[28] equations significantly overestimate the static modulus of elasticity of high performance concretes tested in this study.

3.7.3 Discussion of the Results

The static modulus of elasticity of high performance concrete can be affected by following parameters:

1. Curing regime
2. Chemical admixtures
3. Supplementary cementitious materials
4. Specimen size
5. Age of concrete
6. Coarse aggregate used

Based on studies by Asselanis et al[16] and Burg et al[13], seven days moist curing can be considered as a satisfactory curing regime. Chemical admixtures are a necessary part of most high performance concretes and as a result their effect is always present. On the other hand, their effects are negligible compared to the magnitude of the effects of the other parameters. Based on results of the study by Burg et al[13], concrete mixtures with supplementary cementitious materials have higher modulus of elasticity at the age of 28 days but the rate of increase with time is less compared to the rate of increase of the compressive strength. The overall effect is less than 3% on average and it can be assumed negligible compared to effect of other parameters. The effect of specimen size can be +5% as reported by Burg et al[13] or -5% as reported by Baalbaki et al[9]. The current ACI 363R-84[7] recommended equation also based on test results with both sizes of cylinders and is based on test results at the ages of 28 and 53 days. Based on results of previous studies[9,11,13,14,15,16,20,27], the modulus of elasticity of high performance concrete increases with time. The static modulus of elasticity of concretes with supplementary cementitious materials has less increase with time.

According to Hurd et al[38], the slabs in a structure will frequently be under much higher loads during construction than their design loads. Meanwhile, based on a study with a field simulated curing condition of 7 days curing with wet burlap, Hwee et al[37] reported approximately no increase in modulus of elasticity of high strength concrete with time in spite of an increase of the compressive strength. As a result, it can be concluded that the increase in the static modulus of elasticity at late ages can not be useful from the standpoint of crack or deflection control.

Studies of the effect of coarse aggregate used to make high performance concrete on the modulus of elasticity[9,11,12,18,20,27] have shown that this effect can be as high as 18000 MPa (about 50%). As a result, the kind of coarse aggregate is considered as the most significant parameter but it is obvious that other parameters have lesser effects.

Figure 3.7.3.A shows test results of current study and selected test results from references 9, 11, 12, 13, 14, 15, 16, 19, and 27. The criteria for selecting these test data are as follows:

1. Tests done on specimens before the age of 28 days are not considered as test on mature concrete and as a result these test data are not used in this study. Only data from tests done on specimens between the ages 28 to 56 days are used.
2. Only tests done on specimens with at least 7 days moist curing are used.
3. Tests on both 100 mm by 200 mm and 150 mm by 300 mm cylinders are used interchangably.

4. Test data include results from studies with and without supplementary cementitious materials and different chemical admixtures.

5. Test data include results from studies with different kinds of coarse aggregate.

The data from this study appear to fall near the lower boundary of the data plotted. Figure 3.7.3.A also shows lines representing ACI 318M-89[17] equation (Equation 3.7.1.B), ACI 363R-84[7] recommended equation (Equation 3.7.1.C), Equation (3.7.2) based on results of this study, and the following lines:

A. Line representing 70% of the ACI 318M-89[17] equation predicted values.

B. Line representing 115% of the ACI 363R-84[7] recommended equation values.

C. Line representing 85% of the ACI 363R-84[7] recommended equation values.

Most test results fall between lines representing the ACI 318M-89[17] equation and 70% of the ACI 318M-89[17] equation. Similar observations can be made for lines representing ±15% of the ACI 363R-84[7] recommended equation. In other words, the static modulus of elasticity of high performance concrete falls in a band with the ACI 318M-89[17] equation and 70% of the ACI 318M-89[17] equation predicted values as limits. It can also be represented by ACI 363R-84[7] recommended equation with a ±15% tolerance.

Figure 3.7.3.B shows the same test data and also test data from the same references and this study, from tests on specimens older than 56 days. As it can be seen, there is an increase in modulus of elasticity due to increasing age. These test data from older concrete may be the reason that some researchers claim that the ACI 318M-89[17] equation underestimates the static modulus of elasticity.

A summary of information about the test data used in Figure 3.7.3.A including the compressive strength, the measured static modulus of elasticity, the ACI 318M-89[17] equation predicted value, the ratio of measured to predicted static modulus of elasticity, the kind of coarse aggregate, and the reference are presented in Appendix A, Table A-3.7.3.

As a result of this study, the following modified ACI 318M-89[17] equation is proposed for estimating the static modulus of elasticity of high performance concrete:

$$E_c = 4700\, C_{ca} \sqrt{f'_c} \qquad 55\,MPa < f'_c < 125\,MPa \qquad (3.7.3)$$

Where C_{ca} is an empirical coarse aggregate coefficient. The recommended coarse aggregate coefficients, based on current available test data, are shown in Table 3.7.3. It should be mentioned that due to the low correlation between current available test data on diabase and sandstone coarse aggregates, care should be taken in using the current recommended coarse aggregate coefficient for these kind of coarse aggregates. Figure

3.7.3.C shows the test data from Figure 3.7.3.A after normalizing with coarse aggregate coefficients. Figure 3.7.3.C also shows Equation 3.7.3 and as it can be seen the fluctuation is in reasonable limits.

3.8 Poisson's Ratio

3.8.1 Literature Review

Experimental data on values of Poisson's ratio for high performance concrete are very limited. Carrasquillo et al[12] reported values of Poisson's ratio between 0.20 and 0.25 for high performance concrete regardless of the compressive strength and kind of coarse aggregate. Perenchio et al[19] also reported values of Poisson's ratio between 0.20 and 0.28 for high performance concrete regardless of the compressive strength and kind of coarse aggregate, but it seems that in their study the Poisson's ratio tended to decrease with increase of water to cement ratio for mixtures with the same kind of coarse aggregates. Based on tests on high performance plain concrete columns, Ibrahim et al[38] reported Poisson's ratio about 0.18 on average for 40% of the ultimate stress.

3.8.2 Test Results

Test results for LH, UH, and UU series including the compressive strength, the strain at the maximum stress, and the measured static modulus of elasticity and the Poisson's ratio at 40% of the ultimate stress based on ASTM C 469-87a[33] are presented in Table 3.7.2. The test results for LU series are presented in Appendix E. The values of Poisson's ratio for high performance concretes used in this study mainly varies between 0.15 and 0.20.

3.8.3 Discussion of Results

The values of Poisson's ratio of high performance concretes used in this study mainly range from 0.15 to 0.20 with an average of 0.17 and sample standard deviation (S_{n-1}) of 0.025. Most reported values for Poisson's ratio of high performance concrete by other researchers[12,19] are higher than this. Based on test results from the current study and references 12 and 19 for high performance concretes with compressive strengths ranging from 55 MPa to 125 MPa, the average value for the Poisson's ratio is 0.20 with a sample standard deviation (S_{n-1}) of 0.03. The static modulus of elasticity of high performance concretes used in this study are low and also close to the lower bound of values for static modulus of elasticity of high performance concrete. As a result, it seems that the high performance concretes used in this study tend to have high longitudinal deformation and low lateral deformation compared to other studies.

3.9 Tensile Splitting Strength

3.9.1 Literature Review

The tensile strength of concrete is neglected in computations of the flexural strength of reinforced and prestressed concrete structures[8,17,28] but in general, it is an important characteristic for the development of cracking and therefore, for the prediction of deformations and the durability of concrete. Other characteristics such as bond and development length of reinforcement and the concrete contribution to the shear and torsion capacity are closely related to the tensile strength of concrete. The tensile strength generally increases with the compressive strength. The following equation is recommended by ACI 363R-84[7] for the prediction of the tensile splitting strength f'_{sp} of normal weight concrete, based on a study by Carrasquillo et al[12]:

$$f'_{sp} = 0.59\sqrt{f'_c} \qquad 21\,MPa < f'_c < 83\,MPa \tag{3.9.1}$$

This equation is based on moist cured specimens tested at the ages of 7, 28, and 95 days. Burg et al[13] reported that moist cured specimens have higher tensile splitting strength than air dry specimens. Their moist cured specimens tested at the age of 91 days, had tensile splitting strength in the range from +10% to -10% of ACI 363R-84[7] recommended equation predicted values. Leming[27] reported values for tensile splitting strength of high strength concrete in the range from 60% to 75% of those predicted by the ACI 363R-84[7] equation. He stated that he did not know the reasons for the difference.

3.9.2 Test Results

The test results for LH, UH, UU, S1, and S2 series are presented in Table 3.9.2. The test results for LU series are presented in Appendix E. The moist cured specimens were tested at the age of 56 days. The equation of the fit line for the results of this study is as follows:

$$f'_{sp} = 0.56\sqrt{f'_c} \qquad 50\,MPa < f'_c < 100\,MPa \tag{3.9.2}$$

3.9.3 Discussion of Results

Test results of this study, the study by Burg et al[13], and the ACI 363R-84[7] recommended equation are shown in Figure 3.9.3. As it can be seen from Figure 3.9.3, test results of this study and the study by Burg et al[13] mainly are in the range of ±10% of ACI 363R-84[7] recommended equation. Based on results of this study and the study by Burg et al[13], the

validity of the equation recommended by ACI 363R-84[7] can be extended for high performance concretes with or without supplementary cementitious materials with a compressive strength up to 120 MPa at the age of 28 days.

3.10 Modulus of Rupture

3.10.1 Literature Review

The flexural tensile strength or the modulus of rupture is important in predicting flexural cracking. The tensile strength generally increases with the compressive strength. The following equation is recommended by ACI 363R-84[7] for the prediction of the flexural tensile strength or modulus of rupture, f'_r, of normal weight concrete based on a study by Carrasquillo et al[12]:

$$f'_r = 0.94\sqrt{f'_c} \qquad 21\,MPa < f'_c < 83\,MPa \qquad (3.10.1)$$

This equation is based on moist cured specimens tested at the ages of seven, twenty eight, and ninety five days. Burg et al[13] reported that moist cured specimens have higher flexural tensile strength or modulus of rupture than air dry specimens. Their moist cured specimens tested at the age of 91 days, had the modulus of rupture in the range from +10% to -10% of ACI 363R-84[7] recommended equation predicted values. Ezeldin et al[29] also reported values mainly falling in the range of ±10% of the ACI 363R-84[7] recommended equation. Leming[27] reported values for modulus of rupture of high strength concrete in the range from 70% to 129% of values predicted by the ACI 363R-84[7] recommended equation.

3.10.2 Test Results

The test results for LH, UH, UU, S1, and S2 series are presented in Table 3.10.2. Additional tests currently underway for LU series will be presented in Structural Engineering Report No. 200. The moist cured specimens were tested at the age of 56 days. The equation of the fit line for the results of this study is as follows:

$$f'_r = 0.97\sqrt{f'_c} \qquad 50\,MPa < f'_c < 100\,MPa \qquad (3.10.2)$$

3.10.3 Discussion of Results

Test results of this study, the study by Burg et al[13], the study by Ezeldin et al[29], and the ACI 363R-84[7] recommended equation are shown in Figure 3.10.3. As it can be seen from Figure 3.10.3, test results of this study, the study by Burg et al[13], and the study by Ezeldin et al[29] are mainly in the range of ±10% of ACI 363R-84[7] recommended equation.

Based on results of these studies, the validity of the equation recommended by ACI 363R-84[7] can be extended for high performance concretes with or without supplementary cementitious materials with a compressive strength up to 120 MPa at the age of 28 days.

3.11 Conclusions

Based on results of current study and previous studies mentioned in literature, the following conclusions can be drawn for the mechanical properties of high performance concrete especially similar to those used in the current study:

1. For high performance concretes without silica fume, the ratio of compressive strength gain before 28-day increases, and the ratio of compressive strength gain after 28-day decreases, as the 28 day compressive strength of high performance concrete increases.

2. In the tests reported here, the ratio of 7 day to 28 day compressive strengths were 0.85, 0.87, and 0.76 for 65 MPa to 75 MPa, 95 MPa to 105 MPa, 120 MPa concretes respectively. These ratios suggest that a significant strength gain happens between 7 days and 28 days for the ultra high strength silica fume high performance concrete.

3. For high performance concretes without silica fume, the mix with Type 30 cement develop higher compressive strength than mix with Type 10 cement for the same mix design.

4. For ultra high strength silica fume high performance concrete, the mix with Type 30 cement developed lower compressive strength than mixture with Type 10 cement for the same mix design, but for the mix with Type 30 cement, the strength gain with time continues in presence of water.

5. Drying after moist curing increases the compressive strength gain of high performance concrete. It can be concluded that 3-week is a suitable and sufficient moist curing period.

6. High performance concrete specimens tested with ball seat bearing blocks appear to have up to 7 percent less compressive strength than high performance concrete specimens tested with standard spherical seat bearing blocks. The available data is not sufficient to present a general conclusion.

7. The ratio of the compressive strength of moist cured 100 mm by 200 mm to 150 mm by 300 mm high performance concrete cylinders used in this study, tested using 2600 kN electro-hydraulic closed-loop rock mechanics test system MTS 815 with a 102 mm diameter spherical seat bearing block, is 0.95. This machine has an axial stiffness about six times that of a 100 mm by 200 mm 80 MPa concrete cylinder.

8. Age of the high performance concrete, size of the test specimen, chemical admixtures, supplementary cementitious materials, curing regime, and the kind of coarse aggregate all can affect the static modulus of elasticity of high performance concrete. Among these, the kind of coarse aggregate has the major effect. Most test results in North America for specimens tested between ages of 28 days and 56 days fall in a band between 1.0 and 0.70 times the values predicted by the ACI 318M-89[17] equation.

9. Equation 3.7.3 is proposed for estimating the static modulus of elasticity of high performance concrete:

$$E_c = 4700\, C_{ca} \sqrt{f'_c} \qquad 55\,MPa < f'_c < 125\,MPa \tag{3.7.3}$$

Where C_{ca} is an empirical coarse aggregate coefficient. The recommended coarse aggregate coefficients, based on the current available test data, are shown in Table 3.7.3. It should be mentioned that due to low correlation between current available test data on diabase and sandstone coarse aggregate, care should be taken in using the current recommended coarse aggregate coefficient for these kind of coarse aggregates.

10. The values of Poisson's ratio of high performance concretes used in this study range from 0.15 to 0.20 with an average of 0.17. Most reported values for Poisson's ratio of high performance concrete by other researchers[12,19] are higher than measured values in this study. Based on test results from current study and references 12 and 19, the average value for the Poisson's ratio is 0.20 for high performance concretes with the compressive strengths ranging from 55 MPa to 125 MPa.

11. The results of this study are in complete agreement with ACI 363R-84[7] recommended equation for estimating the tensile splitting strength and modulus of rupture. Based on results of the current study, the study by Burg et al[13], and the study by Ezeldin et al[29], the validity of equations recommended by ACI 363R-84[7] can be extended for high performance concretes with or without supplementary cementitious materials and with the compressive strength up to 120 MPa at the age of 28 days.

Table 3.2.2.A - Compressive Strength Gain with Time (LH Series)

Age (Days)	LH2 (MPa)	f_{ct}/f_{c28} (LH2)	LH4 (MPa)	f_{ct}/f_{c28} (LH4)	f_{ct}/f_{c28} (LH2+LH4)/2
1	24.0	0.47	24.5	0.48	0.47
3	37.5	0.73	39.7	0.78	0.75
7	43.8	0.85	43.4	0.85	0.85
28	51.5*	1.00	51.0*	1.00	1.00
56	56.1	1.09	55.3	1.08	1.09
91	58.2	1.13	56.9	1.12	1.12
147	58.3	1.13	55.4	1.09	1.11

* Δf_{c28} = 0.5 MPa

Table 3.2.2.B - Compressive Strength Gain with Time (UH Series)

Age (Days)	UH2 (MPa)	f_{ct}/f_{c28} (UH2)	UH4 (MPa)	f_{ct}/f_{c28} (UH4)	f_{ct}/f_{c28} (UH2+UH4)/2
1	55.6	0.79	54.1	0.78	0.78
3	57.5	0.81	55.2	0.80	0.80
7	62.1	0.88	59.2	0.86	0.87
28	70.8*	1.00	69.2*	1.00	1.00
56	75.7	1.07	71.5	1.03	1.05
91	78.9	1.11	72.5	1.05	1.08
147	79.8	1.13	75.3	1.09	1.11

* Δf_{c28} = 1.6 MPa

Table 3.2.2.C - Compressive Strength Gain with Time (UU Series)

Age (Days)	UU2 (MPa)	f_{ct}/f_{c28} (UU2)	UU4 (MPa)	f_{ct}/f_{c28} (UU4)	f_{ct}/f_{c28} (UU2+UU4)/2
1	55.3	0.58	56.8	0.57	0.58
3	66.9	0.70	64.1	0.64	0.67
7	73.1	0.77	75.0	0.75	0.76
28	95.3*	1.00	99.6*	1.00	1.00
56	95.6	1.00	102.9	1.03	1.02
91	98.5	1.03	108.1	1.09	1.06
147	98.2	1.03	115.9	1.16	1.10

* Δf_{c28} = 4.3 MPa

Table 3.3.2.A - Effect of Type of Cement on the Compressive Strength Gain (LH Series)

Age (Days)	LH2 (MPa)	f_{ct}/f_{c28} (LH2)	LH3 (MPa)	f_{ct}/f_{c28} (LH3)
1	24.0	0.47	39.3	0.63
3	37.5	0.73	48.4	0.78
7	43.8	0.85	51.0	0.82
28	51.5	1.00	61.9	1.00
56	56.1	1.09	65.1	1.05
91	58.2	1.13	65.7	1.06
147	58.3	1.13	68.3	1.10

Table 3.3.2.B - Effect of Type of Cement on the Compressive Strength Gain (UH Series)

Age (Days)	UH2 (MPa)	f_{ct}/f_{c28} (UH2)	UH3 (MPa)	f_{ct}/f_{c28} (UH3)
1	55.6	0.79	61.0	0.79
3	57.5	0.81	65.0	0.84
7	62.1	0.88	71.8	0.93
28	70.8	1.00	77.0	1.00
56	75.7	1.07	87.1	1.13
91	78.9	1.11	87.2	1.13
147	79.8	1.13	84.9**	1.10

** The compressive strength at the age of 273 days was 90.2 MPa

Table 3.3.2.C - Effect of Type of Cement on the Compressive Strength Gain (UU Series)

Age (Days)	UU2 (MPa)	f_{ct}/f_{c28} (UU2)	UU3 (MPa)	f_{ct}/f_{c28} (UU3)
1	55.3	0.58	60.7	0.72
3	66.9	0.70	66.9	0.79
7	73.1	0.77	76.0	0.90
28	95.3	1.00	84.2	1.00
56	95.6	1.00	93.0	1.10
91	98.5	1.03	94.8	1.13
147	98.2	1.03	93.9	1.12

Table 3.4.2.A - Effect of Drying on the Compressive Strength Gain (LH Series)

Age (Days)	LH4 Continuously Moist	LH4 3 Weeks Moist	LH4 7 Weeks Moist
1	24.5	-	-
3	39.7	-	-
7	43.4	-	-
28	51.0	57.2	-
56	55.3	66.0	64.1
91	56.9	66.9	67.3
147	55.4	67.2	69.8

Table 3.4.2.B - Effect of Drying on the Compressive Strength Gain (UH Series)

Age (Days)	UH4 Continuously Moist	UH4 3 Weeks Moist	UH4 7 Weeks Moist
1	54.1	-	-
3	55.2	-	-
7	59.2	-	-
28	69.2	80.8	-
56	71.5	88.6	85.9
91	72.5	89.0	87.3
147	75.3	93.6	93.1

Table 3.4.2.C - Effect of Drying on the Compressive Strength Gain (UU Series)

Age (Days)	UU4 Continuously Moist	UU4 3 Weeks Moist	UU4 7 Weeks Moist
1	56.8	-	-
3	64.1	-	-
7	75.0	-	-
28	99.6	109.5	-
56	102.9	118.9	110.6
91	108.1	119.4	127.4
147	115.9	123.7	135.4

Table 3.4.2.D - Comparison of 147-day and 28-day Compressive Strength

Concrete Series	$\frac{f_{c147(moist)}}{f_{c28(moist)}}$	$\frac{f_{c147(3\ weeks\ moist)}}{f_{c28(moist)}}$	$\frac{f_{c147(7\ weeks\ moist)}}{f_{c28(moist)}}$
LH	1.09	1.32	1.37
UH	1.09	1.35	1.35
UU	1.16	1.25	1.36

Table 3.4.2.E - Comparison of 147-day Compressive Strengths

Concrete Series	$\frac{f_{c147(3\ weeks\ moist)}}{f_{c147(moist)}}$	$\frac{f_{c147(7\ weeks\ moist)}}{f_{c147(moist)}}$
LH	1.21	1.26
UH	1.24	1.24
UU	1.07	1.17

Table 3.5.2.A - Compressive Strength Results with Different Bearing Blocks

Concrete Series	Bearing Block	Compressive Strength (MPa)						
		S_1	S_2	S_3	S_4	S_5	Mean	S_{n-1}
LH	Ball Seat	55.1	53.8	57.8	54.2	55.7	55.3	1.574
LH	Spherical Seat	56.8	55.2	55.9	54.2	54.6	55.3	1.038
UH	Ball Seat	71.1	71.7	69.3	73.9	71.6	71.5	1.644
UH	Spherical Seat	79.1	74.6	77.9	77.6	75.6	77.0	1.823
UU	Ball Seat	97.2	104.0	98.3	106.9	108.2	102.9	4.974
UU	Spherical Seat	111.2	110.3	110.4	110.8	111.9	110.9	0.653

Table 3.5.2.B - Comparison of the Bearing Blocks of the Testing Machine

Concrete	$f_{c(Ball\ Seat)}$ (MPa)	$f_{c(Spherical\ Seat)}$ (MPa)	$\frac{f_{c(Ball\ Seat)}}{f_{c(Spherical\ Seat)}}$
LH	55.3	55.3	1.00
UH	71.5	77.0	0.93
UU	102.9	110.9	0.93

Table 3.6.2.A - Compressive Strength Results with Different Specimen Sizes

Concrete Series	Size of the Cylinder	Compressive Strength (MPa)						
		S_1	S_2	S_3	S_4	S_5	Mean	S_{n-1}
LH	150 mm	54.2	55.0	56.4	57.5	54.7	55.6	1.358
LH	100 mm	56.8	55.2	55.9	54.2	54.6	55.3	1.038
UH	150 mm	72.9	72.9	70.3	68.8	72.0	71.3	1.731
UH	100 mm	79.1	74.6	77.9	77.6	75.6	77.0	1.823
UU	150 mm	102.3	100.4	101.0	100.9	99.3	100.8	1.085
UU	100 mm	111.2	110.3	110.4	110.8	111.9	110.9	0.653
S3	150 mm (7-day)	51.5	54.0	53.0	-	-	52.8	1.258
S3	100 mm (7-day)	54.1	56.5	55.3	-	-	55.3	1.200
S3	150 mm (28-day)	63.7	63.0	61.7	-	-	62.8	1.015
S3	100 mm (28-day)	63.2	65.4	66.0	-	-	64.9	1.474
S3	150 mm (56-day)	64.7	64.9	64.0	-	-	64.5	0.473
S3	100 mm (56-day)	64.1	68.0	63.8	-	-	65.3	2.343
S3	150 mm (91-day)	65.6	65.7	67.3	-	-	66.2	0.954
S3	100 mm (91-day)	74.5	70.9	72.0	-	-	72.5	1.845
S4	150 mm (28-day)	54.7	56.4	54.3	-	-	55.1	1.115
S4	100 mm (28-day)	58.0	60.3	60.9	-	-	59.7	1.531
S4	150 mm (56-day)	58.1	61.1	60.9	-	-	60.0	1.677
S4	100 mm (56-day)	64.2	66.0	64.0	-	-	64.1	1.102

Table 3.6.2.B - Comparison of 100 mm and 150 mm Cylinders

Concrete	$f_{c(150mm)}$ (MPa)	$f_{c(100mm)}$ (MPa)	$\frac{f_{c(150mm)}}{f_{c(100mm)}}$
LH	55.6	55.3	1.01
UH	71.3	77.0	0.93
UU	100.8	110.9	0.91
S3 (7-day)	52.8	55.3	0.95
S3 (28-day)	62.8	64.9	0.97
S3 (56-day)	64.5	65.3	0.99
S3 (91-day)	66.2	72.5	0.91
S4 (28-day)	55.1	59.7	0.92
S4 (56-day)	60.0	64.7	0.93

Table 3.7.2 - Modulus of Elasticity and Poisson's Ratio Test Results

Concrete	Compressive Strength (MPa)	Strain at Maximum Stress (microstrain)	Modulus of Elasticity (MPa)	Poisson's Ratio
LH	64.3	2839	29446	0.15
LH	65.3	3070	29528	0.16
LH	66.0	3679	24615	0.11
LH	66.2	3481	29672	0.20
LH	66.3	2997	28517	0.15
LH	66.4	2968	31908	0.19
LH	66.4	3139	27195	0.14
LH	67.1	2981	28933	0.16
UH	90.9	3196	31479	0.19
UH	94.2	3337	32094	0.15
UH	95.9	3641	31900	0.18
UH	97.5	3514	32456	0.19
UH	97.9	3754	30293	0.16
UU	106.1	2883	35151	0.16
UU	115.5	2901	38816	0.20
UU	119.7	3319	36163	0.19
UU	120.6	3442	37181	0.19
UU	121.6	2938	37188	0.20
UU	125.0	3086	37922	0.19

Table 3.7.3 - Recommended Coarse Aggregate Coefficients

Kind of Coarse Aggregate	Recommended C_{ca}	Coefficient of Variation
Sandstone Gravel[+]	0.72	0.068
Siliceous Gravel[**]	0.76	-
Limestone	0.92	0.093
Dolomite	0.92	0.087
Quartzites	0.97	0.055
Granite	0.82	0.072
Trap Rock	0.97	0.018
Diabase[*]	0.90	0.119
Sandstone[*]	0.61	0.143

+ Gravels with dominant sandstone rock.

* Poorly Correlated, more documentation needed.

** Limited available test data, more documentation needed.

Table 3.9.2 - Tensile Splitting Strength Test Results

Concrete	f_{c28} (MPa)	f_{c56} (MPa)	S_1 (MPa)	S_2 (MPa)	S_3 (MPa)	Mean (MPa)	S_{n-1}	Fractured Coarse Aggregate
LH	51.5	56.1	4.05	4.35	4.15	4.20	0.15	95%
UH	70.8	75.7	4.85	5.45	5.05	5.10	0.31	99%
UU	95.3	95.6	5.00	5.95	5.10	5.35	0.52	99%
S1	82.8	86.8	5.50	5.50	4.60	5.20	0.52	100%
S2	94.9	97.3	5.60	5.25	5.25	5.35	0.20	99%

Table 3.10.2 - Modulus of Rupture Test Results

Concrete	f_{c28} (MPa)	f_{c56} (MPa)	S_1 (MPa)	S_2 (MPa)	S_3 (MPa)	Mean (MPa)	S_{n-1}
LH	51.5	56.1	7.15	7.35	7.10	7.20	0.13
UH	70.8	75.7	8.25	8.40	8.80	8.5	0.28
UU	95.3	95.6	9.55	9.45	9.45	9.50	0.06
S1	82.8	86.8	9.15	9.05	8.90	9.05	0.13
S2	94.9	97.3	9.55	9.70	9.20	9.50	0.26

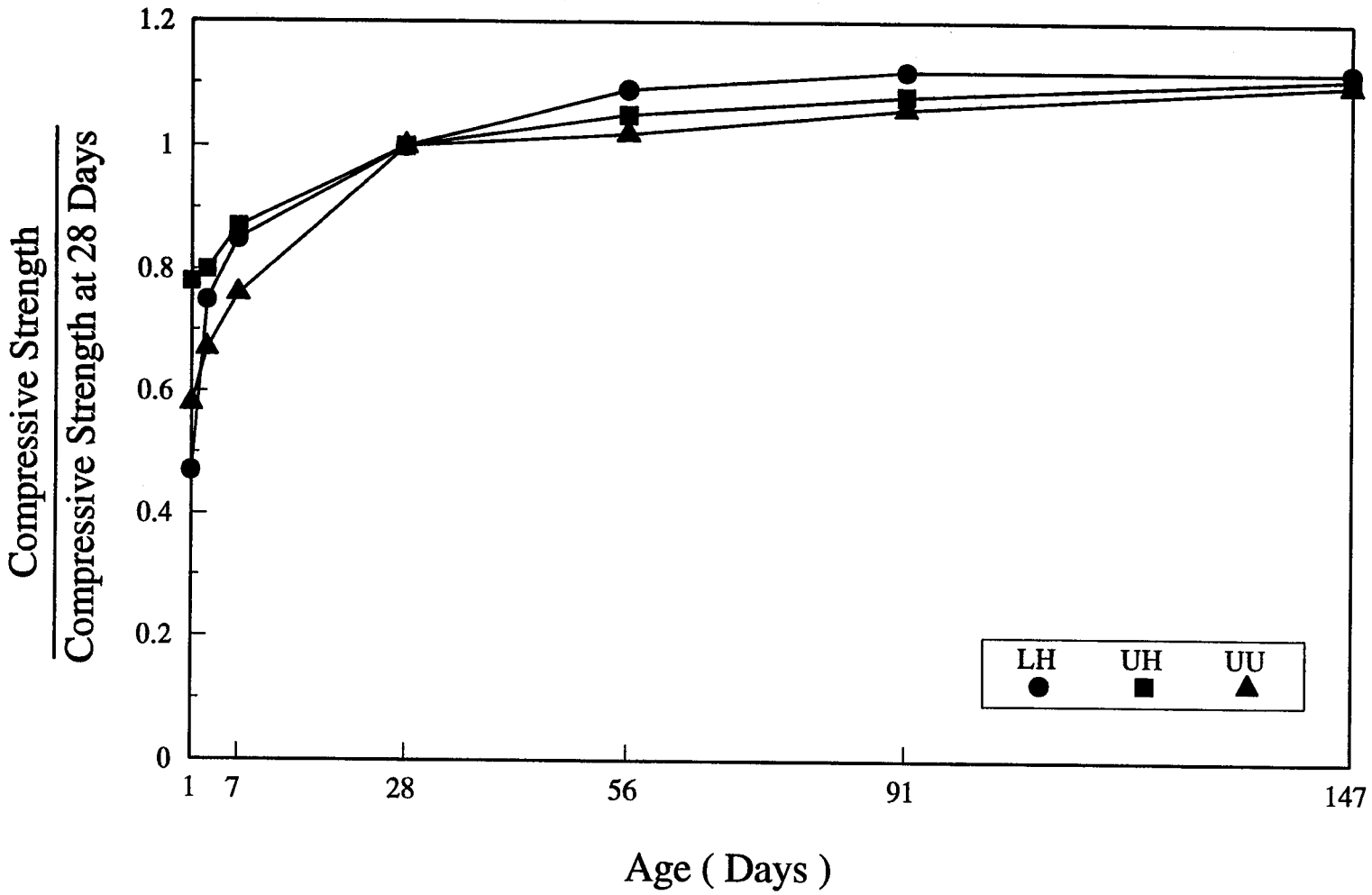

Figure 3.2.2 - Compressive Strength Gain with Time

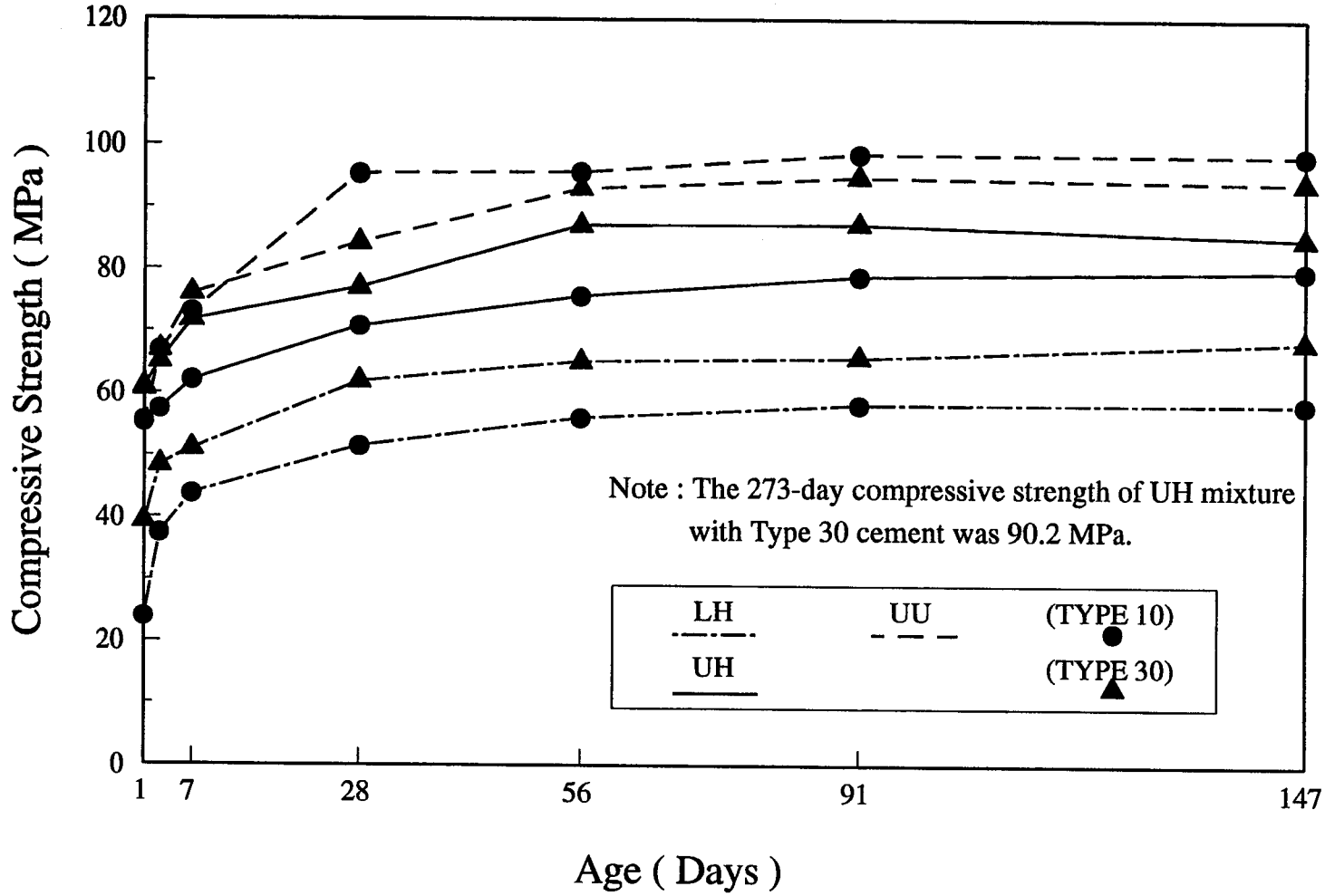

Figure 3.3.2.A - Effect of Type of Cement on Compressive Strength

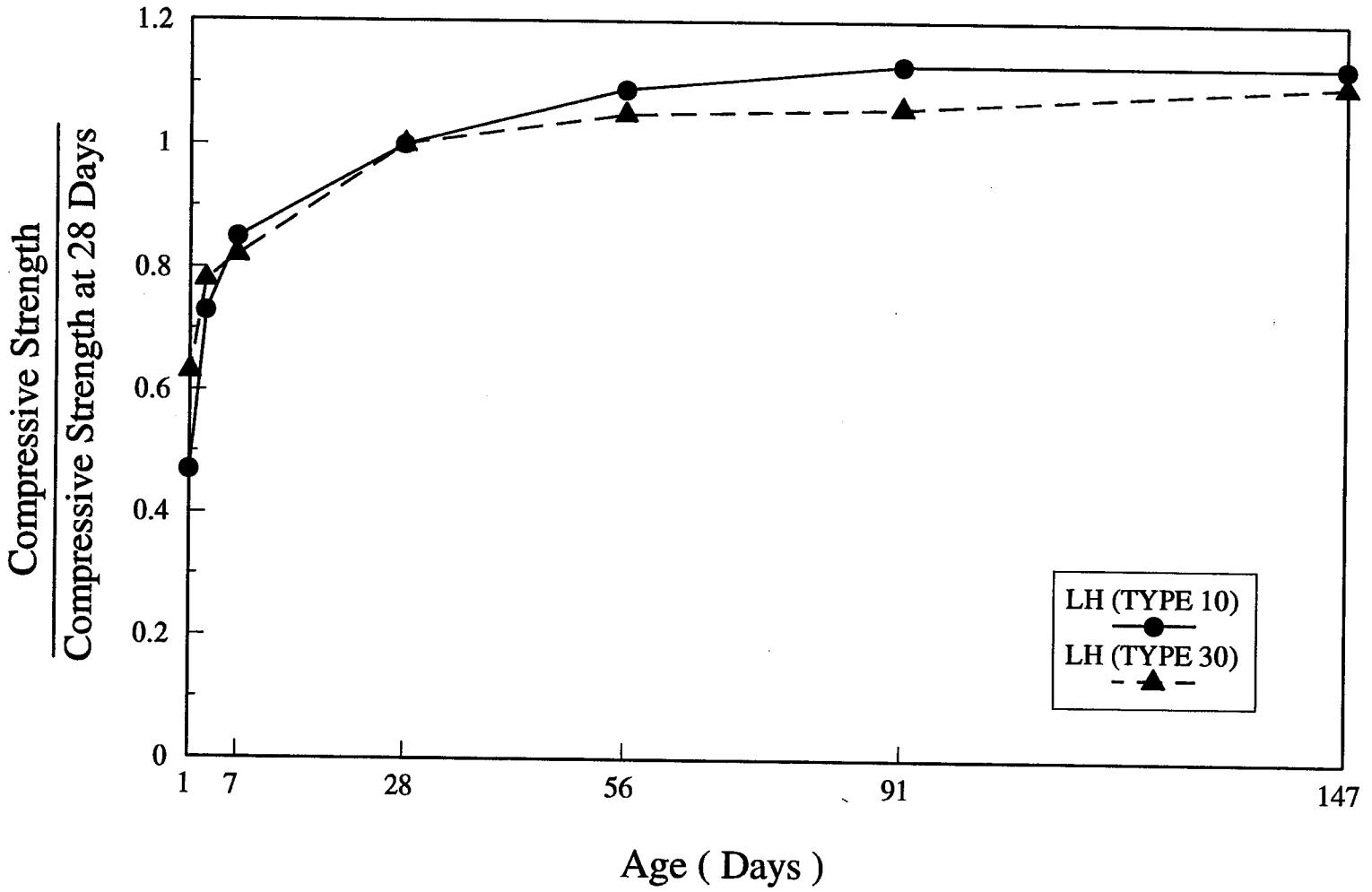

Figure 3.3.2.B - Effect of Type of Cement (LH Series)

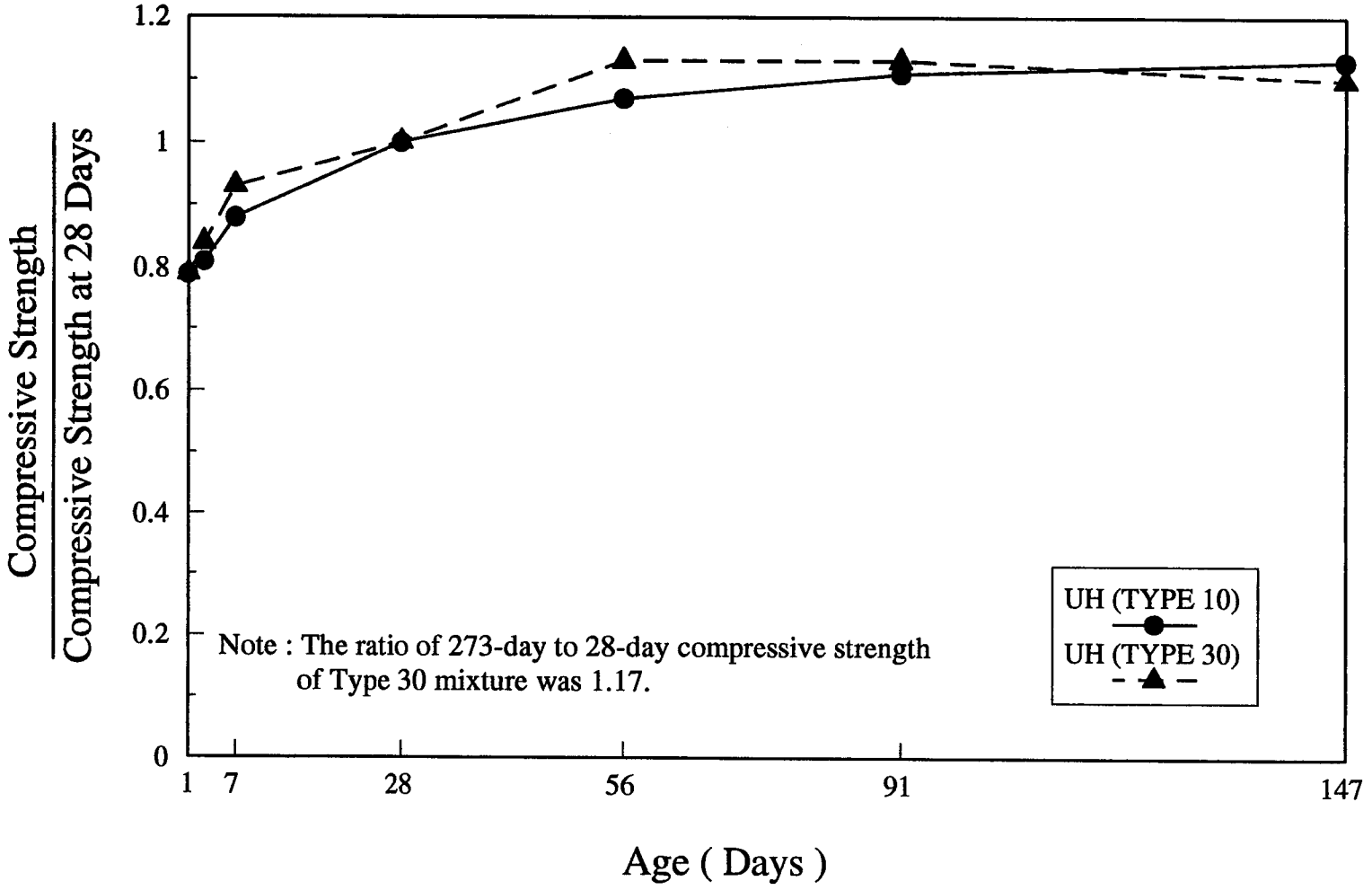

Figure 3.3.2.C - Effect of Type of Cement (UH Series)

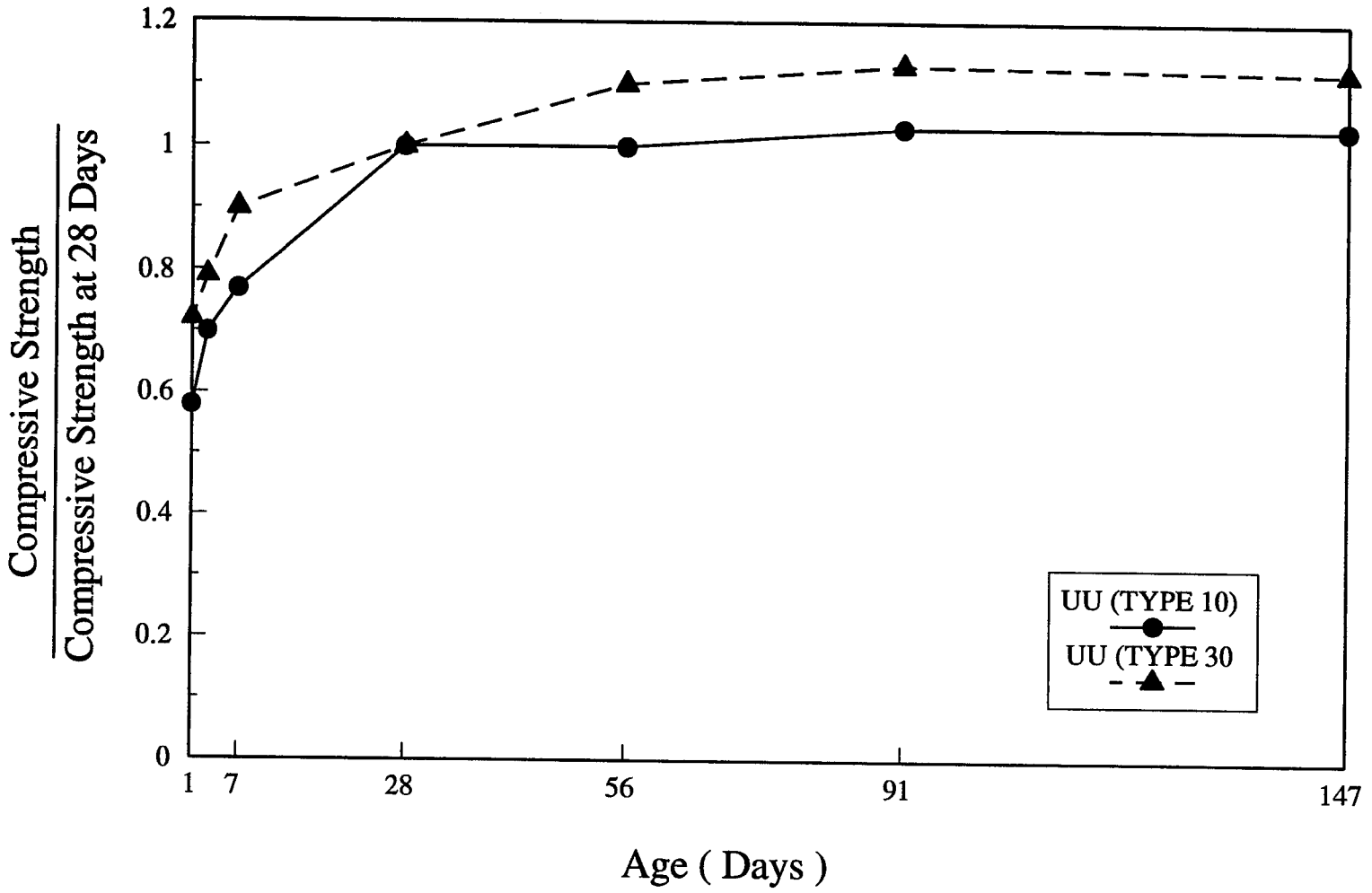

Figure 3.3.2.D - Effect of Type of Cement (UU Series)

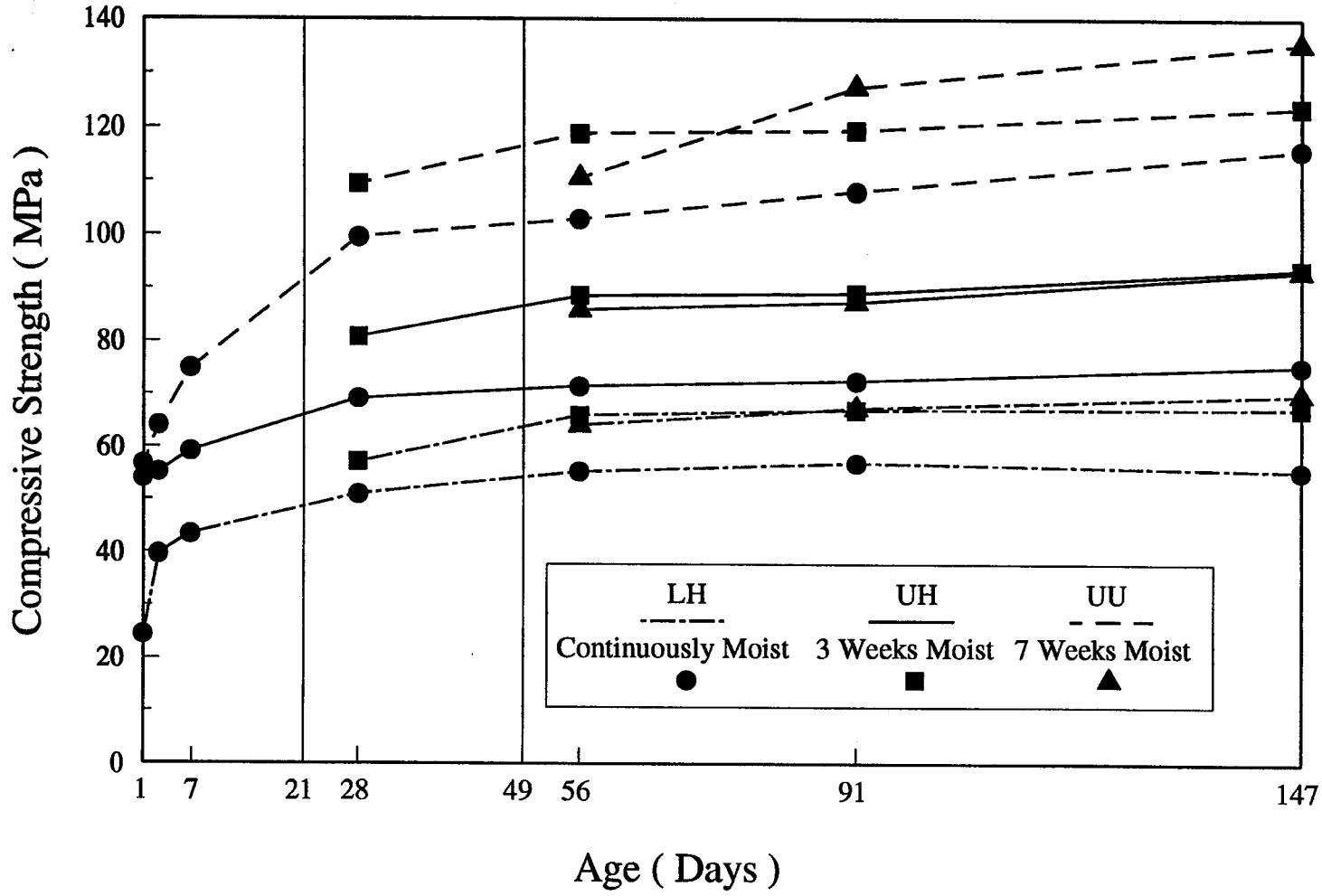

Figure 3.4.2 - Effect of Drying on Compressive Strength Gain

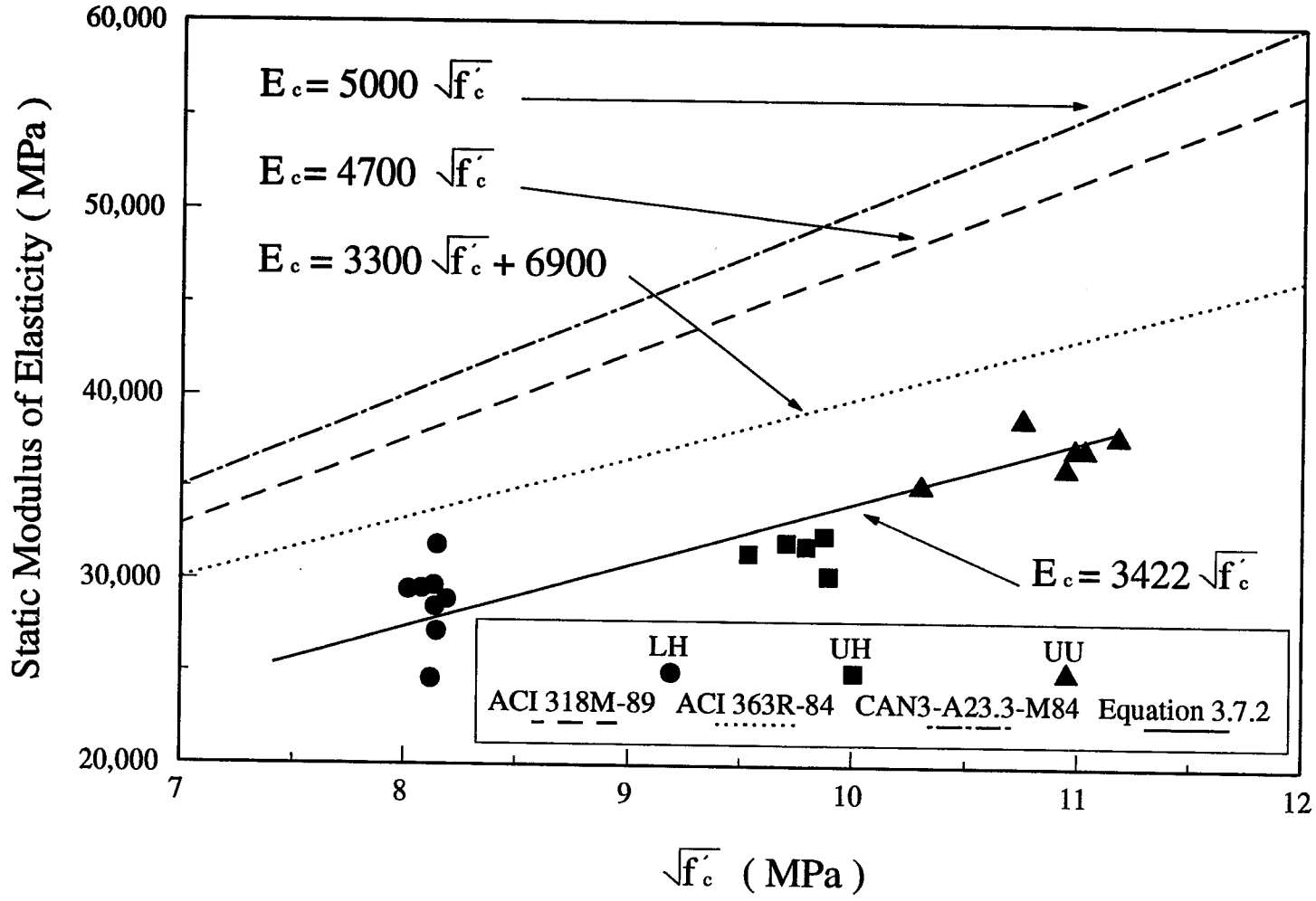

Figure 3.7.2 - Static Modulus of Elasticity Test Results

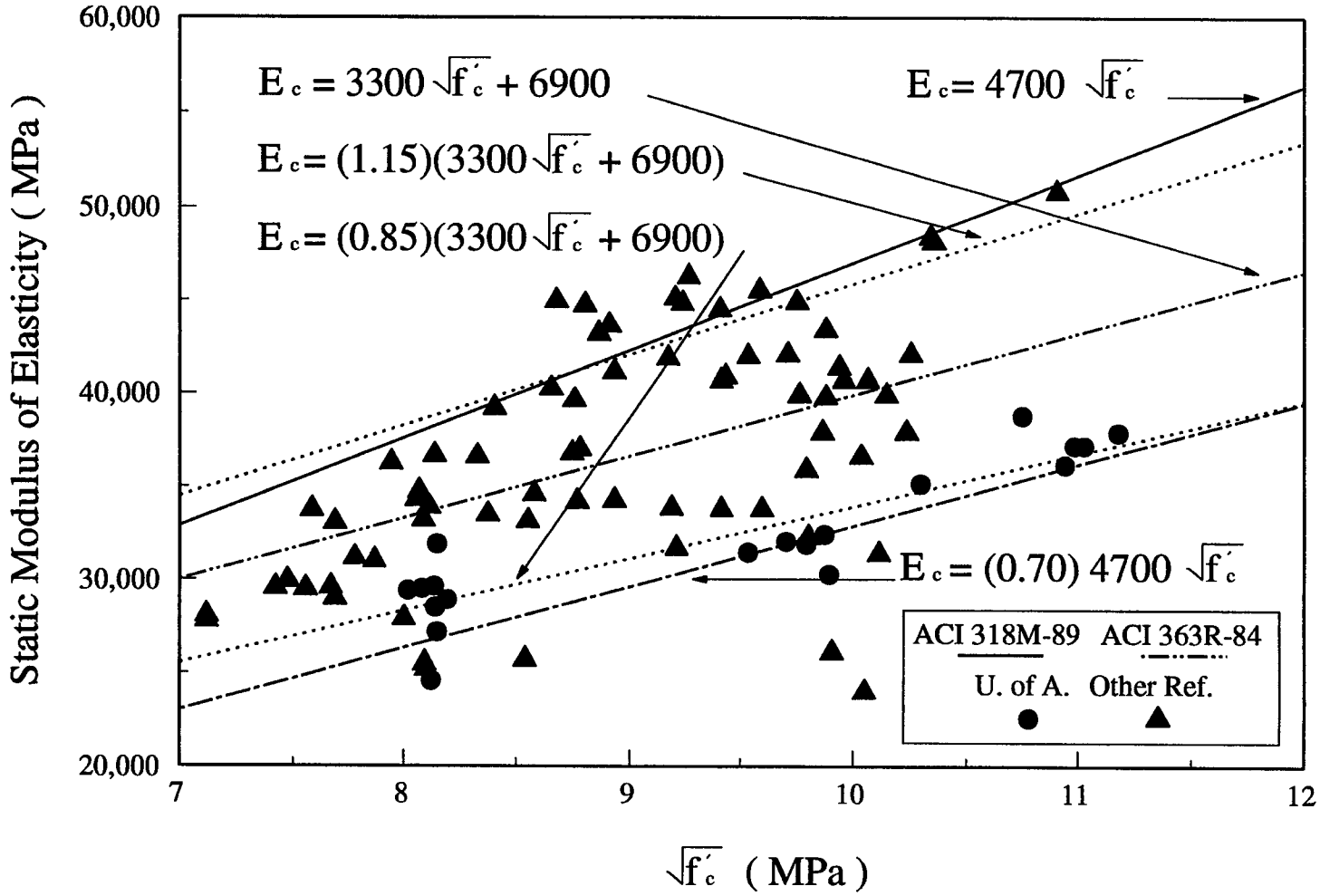

Figure 3.7.3.A - Comparison of Modulus of Elasticity Test Results

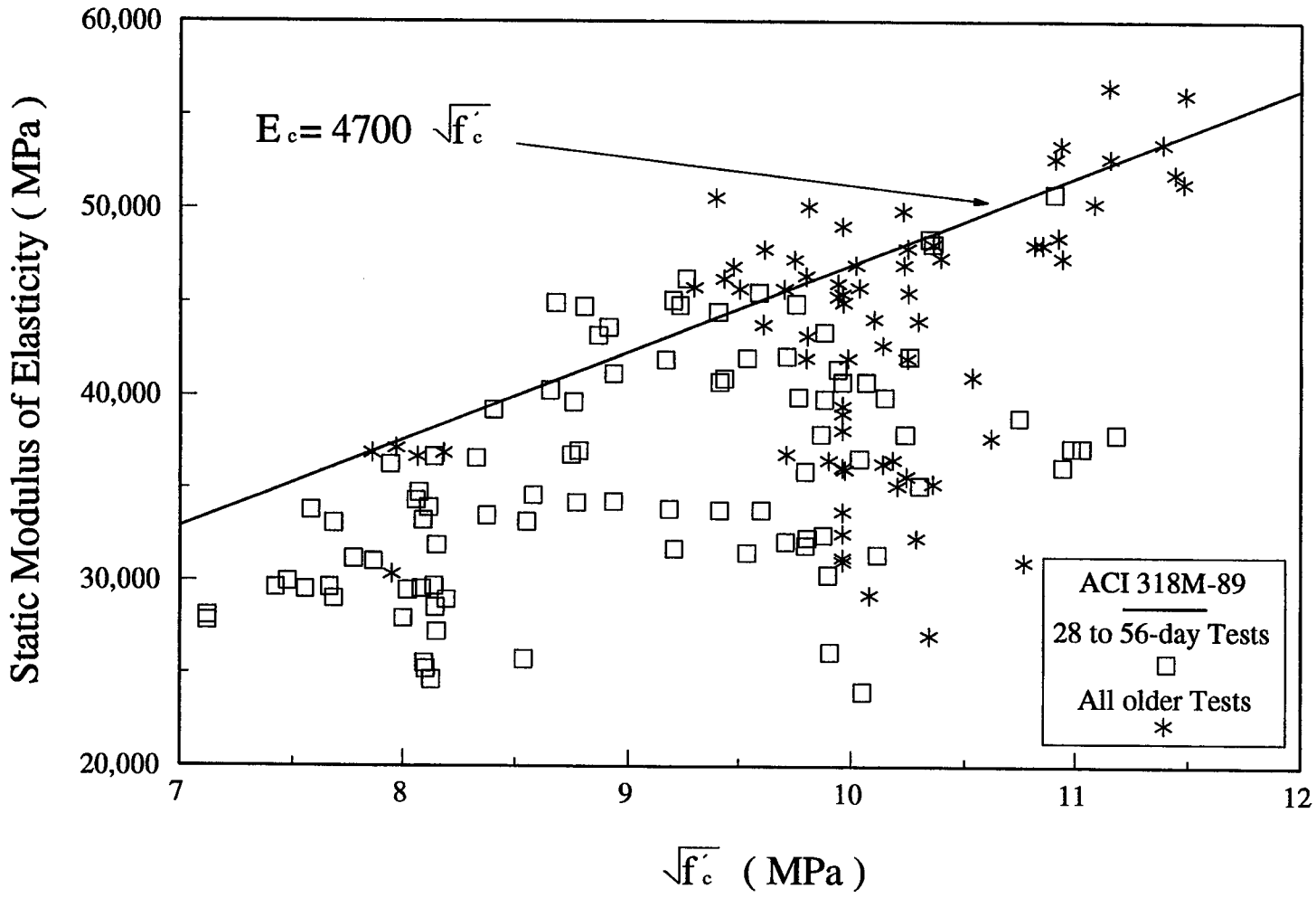

Figure 3.7.3.B - Effect of Time on Modulus of Elasticity

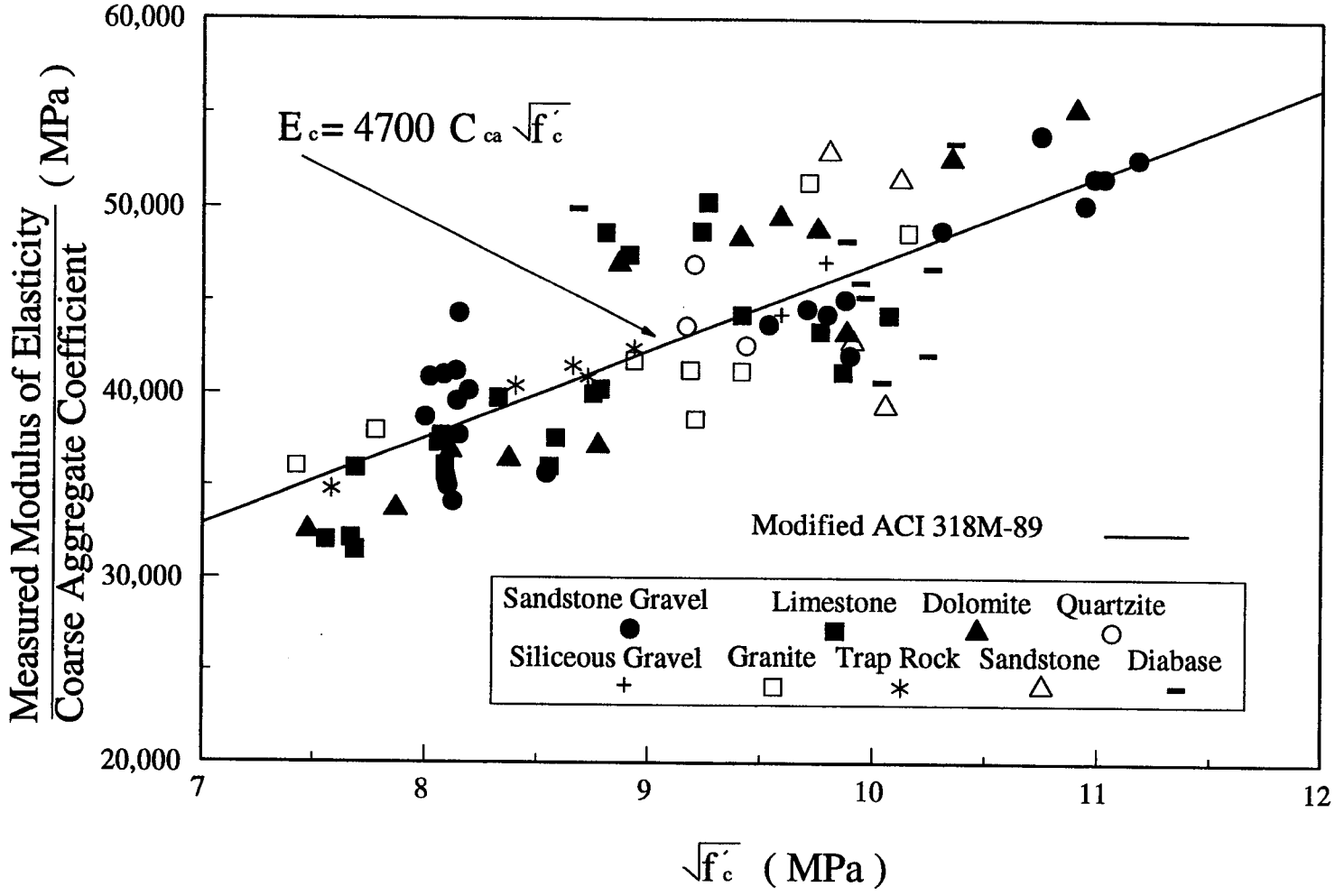

Figure 3.7.3.C - Effect of Coarse Aggregate on Modulus of Elasticity

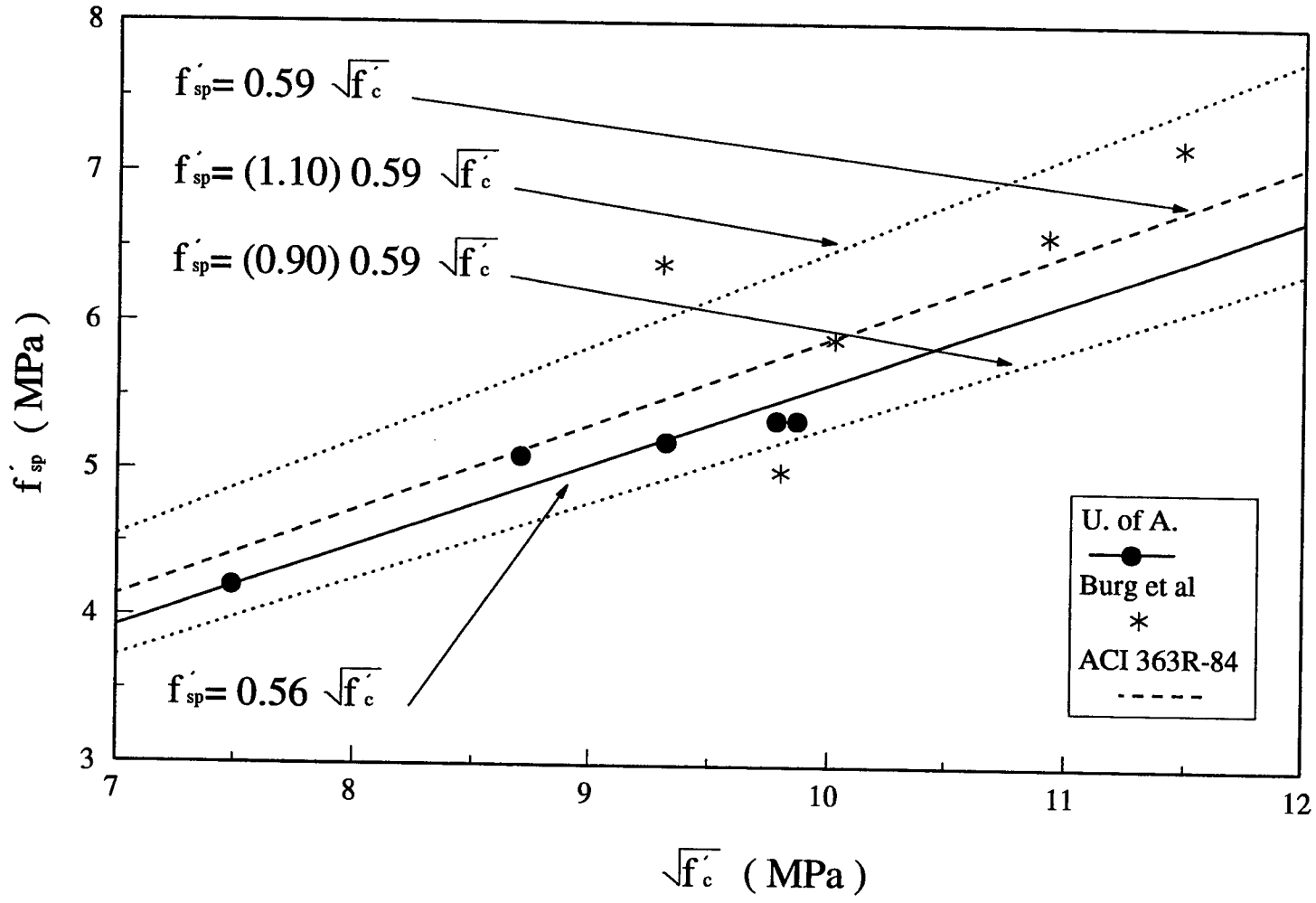

Figure 3.9.3 - Tensile Splitting Strength Test Results

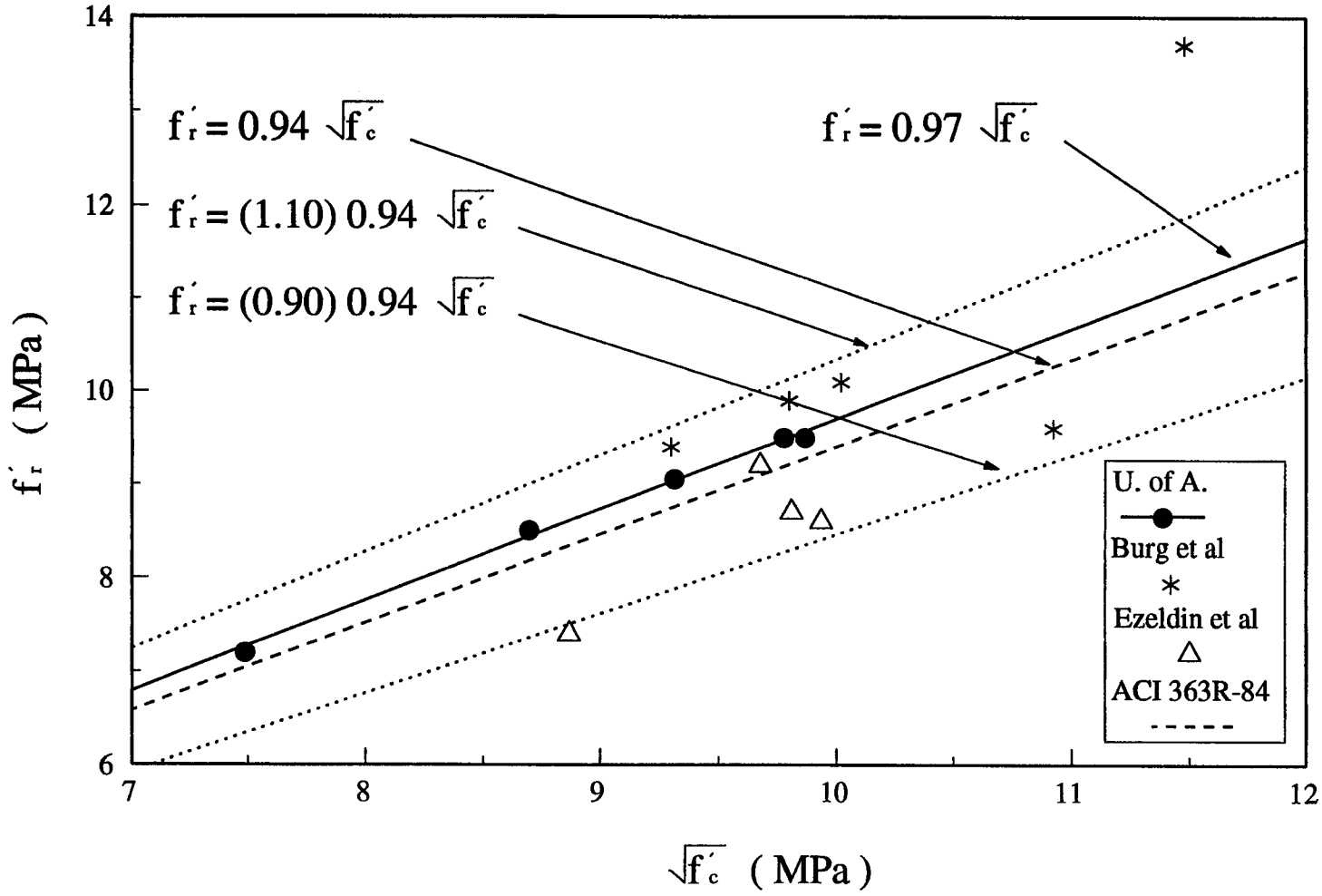

Figure 3.10.3 - Modulus of Rupture Test Results

4. High Performance Concrete under High Sustained Compressive Stresses

4.1 Introduction

The design of concrete and reinforced concrete structures is based on the short time compressive stress-strain relationship of concrete. The loading of the actual structures generally takes place in a more unfavorable manner. In fact, the load is applied relatively quickly and is then held constant. Conventional concrete loaded at a late age to sustained compressive stresses in excess of approximately 70 to 75 percent of the short time monotonic ultimate strength of concrete at the time of loading may fail under the sustained compressive stresses after a period of several minutes to several months. It means that the margin of safety for a plain concrete determinate structure may be less than what is assumed based on short term monotonic ultimate compressive strength of concrete.

Numerous studies were done to investigate the sustained compressive strength of conventional concrete in this century. These studies can be divided to three major groups:

a. Prediction of sustained compressive strength of concrete based on investigation of characteristics of the short time monotonic compressive strength test. In these methods, the sustained compressive strength has been predicted based on a study of the strain characteristics, internal changes that happen within the concrete microstructure, stress-strain curve characteristics, log stress - log strain curve characteristics, and ultrasonic velocity tests on the specimen. The study of the strain characteristics may include volumetric strain study, critical strain level, and critical Poisson's ratio value.

b. Prediction of the long term sustained compressive strength of concrete based on short term experiments on specimens subjected to sustained compressive stresses. In this method, specimens have been loaded for a short period under sustained compressive stresses ranging from several hours to several days. Then, the long term compressive strength has been predicted by extrapolation of the stress - log of time or strain - log of time relationships.

c. Study of the long term sustained compressive strength of concrete with long term sustained compressive stress experiments on specimens. In this method, specimens have been subjected to sustained compressive loads for periods ranging from several months to several years. The long term sustained compressive

strength or the long term true ultimate compressive strength of concrete is defined based on the level of stress as the percentage of the short term ultimate compressive stress that a specimen can be subjected to for a sustained period without failure. Characteristic of stress, strain, and time relationships are used in establishing this.

Information about the behavior of high performance concrete under high sustained compressive stresses is very limited. Study on microcrack systems in concrete cylinders indicates the sustained compressive strength of high performance concrete is in the order of 90 percent of the short term monotonic strength at the age of loading. Sixty day sustained load study on 60 MPa high strength concrete indicates that the sustained compressive strength of high performance concrete is in the order of 80 to 85 percent of the short term monotonic strength at the age of loading.

A test program was carried out to study practical high performance concretes under high sustained compressive stresses. The specimens were subjected to long term (3 months) sustained stresses. The test program can be classified as a group three test. The primary parameter was the compressive strength of the high performance concrete. The other significant parameters were the level of sustained compressive stress as the percentage of the ultimate short term monotonic compressive strength, moment gradient, or in other words eccentricity, and the presence of silica fume as supplementary cementitious material and filler. Two high performance concretes with the same compressive strength range were used to compare the performance of high performance concretes with and without silica fume under high sustained compressive stresses.

The results for LH, UH, and UU series are presented in this Chapter. The results for LU series are presented in Appendix F. Literature review of previous studies is presented. A short report on the compressive strength gain history of concretes used and also the stress - strain relationship of the specimens tested monotonically are presented. Results of sustained concentric and eccentric compressive load tests are presented, explained, discussed, and compared with previous works. The results of sustained concentric and eccentric compressive load tests are also compared to each other. General conclusions are presented at the end of this Chapter based on results of the current study and previous studies.

4.2 Literature Review

When concrete is subjected to sustained compressive stresses, microcracks initiated prior to and during initial load application propagate during time. New cracks are also initiate and propagate under sustained compressive loads. On the other hand, creep deformation caused by sustained load may have positive effect and may increase the

compressive strength of concrete. As reported by Smadi et al[52] from other studies, the increase of compressive strength of concrete can be due to closure of microcracks as the results of autogenous healing, post compacting of concrete as the result of load, forced hydration of cement as the result of pressure in possible free water in concrete, and an increase in secondary bonding strength between gel particles of cement paste because of a decrease in the inter-particle distances resulting from consolidation. It is believed by different researchers including Ngab et al[51], Shah et al[49], and stockl[50] that the compressive strength of concrete may increase under sustained stresses which are less than the critical sustained stress intensity. The overall effect depends on the sustained stress intensity. At high sustained stresses above the critical intensity that can be considered as the safe long term sustained compressive strength, the process of crack development is stronger than these positive effects and causes a decrease in the load carrying capacity of the concrete and leads the specimen toward failure under sustained compressive stress. As reported by Smadi et al[52] from other studies, the reduction in strength under high sustained stresses above critical sustained stress intensity appears to be dominated by crack propagation. Crack development reaches such a stage that the crack system is unstable and the release of strain energy is sufficient to make the cracks self propagating until complete disruption and failure of the specimen.

Anton Brandtzaeg[41] was the first researcher to notice the phenomenon of the critical compressive stress through volumetric strain studies in 1928. According to those studies, the critical compressive stress was found to be 77 to 85 percent of the ultimate compressive stress based on volumetric strain study. At this stress level the volumetric strain began to increase indicating internal microcracking.

The study by Richart et al[42] was the first long term sustained load study to recognize that the long term compressive strength of concrete under sustained stresses would be less than the short term monotonic compressive strength. Their experimental study at the University of Illinois was on reinforced concrete columns under sustained compressive stresses with intensity ranging from 70 to 95 percent of the ultimate. All reinforced concrete columns under sustained load with the intensity of 95 percent and some of those under 90 percent failed and it was concluded that the sustained strength of reinforced concrete should be about 90 percent of the ultimate.

Based on a short term sustained compressive stress study by Shank[43], the sustained compressive strength of concrete should be about 85 percent of the ultimate compressive strength. The specimen under 91.8 percent failed in less than 30 minutes and the specimen

under 90.5 percent failed in less than 7 hours. It is mentioned that for the third batch of concrete the sustained compressive strength was 85 percent but the author did not mention the duration of the test.

According to Price[44] and based on extrapolation of a 4 hour short term sustained compressive stress study, the long term sustained compressive strength of concrete should be around 70 percent of the short term monotonic ultimate strength.

Viest et al[45] studied conventional 150 mm by 150 mm by 500 mm reinforced concrete columns under long term sustained eccentric compressive stresses. The concrete grade ranged from 10.8 MPa to 39.2 MPa. The initial eccentricity was between 76 mm and 141 mm from tension rebars. The duration of tests were approximately 1.5 years. The specimens were tested at different ages ranging from 28 days to 9 months. The long term sustained strength was 86.6 percent on average for moderate eccentricities and 93.3 percent on average for small eccentricities. The overall average of the sustained strength of conventional eccentrically loaded reinforced concrete columns was 89 percent.

According to Rüsch et al[46] and based on tests on 150 mm by 150 mm by 600 mm prisms, the long term sustained compressive strength of conventional concrete should be about 70 percent of the ultimate short term monotonic compressive strength of cubes.

Rüsch[48] also summarized the studies at the Technical University of Munich. Based on test specimens loaded at the age of 56 days for up to 2 years, the long term sustained compressive strength of conventional concrete should be about 75 percent of the ultimate short term monotonic compressive strength of cubes at the age of 56 days. The specimens under 80 percent of the ultimate failed in less than 7 days. If the sustained compressive stress is taken as the average stress in the concrete compression zone at ultimate strength over the compressive strength of concrete at the failure time, the sustained compressive strength of conventional concrete decreases as the eccentricity increases. The sustained compressive strength decreases from 0.78 to 0.63 as the ratio of eccentricity to depth of the section increases from 0 to 0.10.

According to Sell[47] and based on extrapolation of a 7 days short term sustained compressive stress study on conventional concrete specimens with a 56 day cube compressive strength of 40 MPa, loaded at different ages ranging from 20 days to 448 days, the long term sustained compressive strength should be about 70 percent of the ultimate short term monotonic compressive strength of the cube. He reported failures from 66 to 76 percent of the ultimate. Based on tests results with eccentricities within the elastic Kern of

the section, he also concluded that the long term sustained compressive strength could be relatively independent of eccentricity. He also reported transverse tension strains in excess of 3500 microstrain under sustained concentric stresses.

In a 4 hour short term sustained load study by Shah et al[49] on conventional concrete, specimens under 80 and 90 percent sustained concentric compressive stresses of the short time ultimate strength failed while the specimen under the 70 percent of the short time ultimate stress did not fail. Based on these tests, the sustained compressive strength can be within 70 to 80 percent of the ultimate short time strength.

Based on a 660 day long term sustained load study on reinforced concrete beams by Iyengar et al[53], the true ultimate flexural strength or the sustained flexural strength of the reinforced concrete beams used in that experiment is about 75 percent of the ultimate flexural strength.

Stockl[50] reported the results of 15 years of study on concrete under sustained stresses that originally started by Professor H. Rüsch at the Technical University of Munich. He reported results for concretes with 28 day cylinder compressive strength up to 50 MPa. Failures of specimens loaded to 70 to 75 percent of the ultimate short term strength are reported even for 50 MPa concrete. Specimens loaded at the age of 28 days had failures after 70 days but specimens loaded at the age of 16 months had failures before 70 days. He concluded that the long term sustained compressive strength could be around 80 percent of the ultimate short term compressive strength regardless of the compressive strength of concrete and the eccentricity of load on specimen. It should be mentioned that he reported failures of 41 MPa concrete, loaded at the age of 56 days, under 64.3 percent of the ultimate. He also reported transverse strain in excess of 3500 microstrain under sustained compressive concentric stresses.

According to Ngab et al[51], while 39 MPa conventional concrete specimens, loaded at the age of 30 days, failed under 65 percent of the ultimate short term strength, 62 MPa high strength concrete, loaded at the age of 30 days, did not fail under 85 percent of the ultimate during the 60 day sustained load period.

Smadi et al[52] studied three grade of concretes, loaded at the age of 28 days, under long term sustained compressive concentric stresses with a duration of 60 days. None of the four 20 to 25 MPa concrete specimens, loaded under 75 percent of the ultimate, failed during the 60 day loading period. Two of the four 35 to 40 MPa concrete specimens, loaded under 75 percent of the ultimate, did not fail during the 60 day experiment, while the other two specimens failed after 49 days under sustained loads. Two of the four 60 to 70 MPa concrete specimens, loaded under 80 percent of the ultimate, did not fail during the 60 day experiment,

while the other two specimens failed after 14 days under sustained loads. Meanwhile, none of the four 60 to 70 MPa concrete specimens, loaded under 70 percent of the ultimate, failed during the 60 day experiment. It should be mentioned that Smadi et al[52] did not test any specimens under 75 percent of the ultimate for the 60 to 70 MPa concrete. Based on their studies and those by Ngab et al[51], they concluded that the sustained compressive concentric strength of conventional and high strength concrete should be in neighborhood of 75 and 80 percent, respectively.

4.3 Compressive Strength History of Concretes Used

The test results for LH1, UH1, and UU1 series are presented in Tables 4.3.A through C. The test results for LU1 series are presented in Appendix F. The reported results are the average compressive strength of specimens tested for each series. The compressive strength of individual specimens are reported in Appendix I, Tables I-4.3.A through C. All specimens were cured 3 weeks at 100% R.H. and then at 50% R.H.. The compressive strength gain as the percentage of the 28 day compressive strength is presented in the same tables and in Figure 4.3.A. Due to start of the study of these high performance concretes under sustained compressive stresses at the age of 56 days, the compressive strength gain as the percentage of the 56 day compressive strength is also presented in the same tables and in Figure 4.3.B.

4.4 Stress - Strain Behavior of Concretes Used

The test results for LH, UH, and UU series are presented in Figure 4.4.A. The test results for LU series are presented in Appendix F. The strain results are based on data from electrical resistance strain gages. Details of experimental program are presented in section 2.6.6. Due to the behavior of the ball seat bearing blocks and the nature of electrical resistance strain gages, data about the descending branches are not available.

The relation between stress, as a percentage of the ultimate stress, and strain are presented in Figures 4.4.B through D for LH, UH, and UU series, respectively. It is clear that the ascending branch of stress - strain curves have a steeper slope and is more nearly linear over a greater range as the compressive strength of concrete increases. As can be seen from Figures 4.4.B through 4.4.D, the stress - strain curves are deviated from straight line at about 65 to 70, 75 to 80, and above 85 percent of the ultimate stress for LH, UH, and UU series, respectively. These can be considered as the approximate start of unstable self propagating crack development in the system. The average strain at the ultimate stress is greater for UH series than for LH and UU series.

4.5 High Performance Concrete under High Sustained Concentric Stresses

4.5.1 Test Results

4.5.1.1 General

The experimental results of the specimens tested concentrically for LH, UH, and UU series are presented in this section. The experimental results of the specimens tested concentrically for LU series are presented in Appendix F. Each specimen is represented by an abbreviation such as LHC75(70). The first two characters represent the concrete series to which the specimen belongs (See Section 2.4). The third character stands for concentric, C, and eccentric, E, specimens. The first number represents the stress intensity or load intensity on the specimen as a percent of the short time strength at the time of loading. The possible next character distinguishes the specimens with the same intensity. If the specimen is loaded at the age of 70 days instead of 56 days, the age appears in parentheses. The compressive strength of monotonic concentric specimens tested are presented in Table 4.5.1.1.

The creep strain is calculated by deducting the initial strain measured just after the application of the load from the total strain. The shrinkage strain of specimens is neglected in calculations. As reported by Smadi et al[52] from other studies, superposition of shrinkage and creep strains is not valid due to being from dependent phenomena. Meanwhile the creep strain is much larger than the shrinkage strain at high stress intensities. As a result, neglecting shrinkage strain does not affect the results significantly. The creep coefficient is defined as the ratio of calculated creep strain over the initial strain. The specific creep is defined as the ratio of creep strain over the stress on specimen.

4.5.1.2 LH Series Test Results

The experimental results for monotonic concentric tests are presented in Figures B-4.5.A through H of Appendix B. The experimental results for sustained concentric tests are presented in Figures 4.5.1.2.A through G. The stress is shown (right-hand scale) as the ratio of the ultimate strength of the specimen for monotonic specimens and as the ratio of the average ultimate stress of monotonic specimens for sustained specimens. Stress, longitudinal strain, and transverse strain are shown as a function of time. The ultimate compressive stress and the cross sectional area of the specimen are also presented in each figure.

Specimens LHC95 and LHC90 were tested in MTS 815 test machine and the other sustained specimens were tested in the sustained load frames. Specimens LHC95 and LHC90 failed after being under sustained concentric stresses of 95 and 90 percent of the ultimate for 4 and 33 minutes respectively (See Figures 4.5.1.2.A and B). The specimens in the three sustained concentric load frames were subjected to sustained concentric stresses of 85, 80, and 75 percent of the ultimate at the age of 56 days. Specimens LHC85, LHC80, and LHC75 failed after being under sustained concentric stresses of 85, 80, and 75 percent of the ultimate for 4 hours and 21 minutes; 3 days, 5 hours, and 41 minutes; and 33 days and 13 minutes respectively (See Figures 4.5.1.2.C through E). Due to failure of the test specimens in two of three sustained concentric load frames within the first two weeks of loading, two additional specimens were subjected to sustained concentric stresses of 75 and 70 percent of the ultimate at the age of 70 days. Specimen LHC75(70) specimen also failed after being under sustained concentric stress of 75 percent of the ultimate for 13 days and 22 hours and 29 minutes (See Figure 4.5.1.2.F). Specimen LHC70(70) did not fail during the 3 month sustained load test (See Figure 4.5.1.2.G). As can be seen, the transverse strains were generally less than 4500 microstrain until near the failures. This was not true for LHC75(70) and LHC70(70). An examination of the specimens did not show vertical cracking.

For all sustained specimens, the total strain, the initial strain, the creep strain, the creep coefficient, the specific creep, and time after loading are presented in Table 4.5.1.2 for the time of failure or the end of the test. The initial recovery is also presented in the same table for those specimens which did not fail during the 3 month test.

4.5.1.3 UH Series Test Results

The experimental results for monotonic concentric tests are presented in Figures C-4.5.A through E of Appendix C. The experimental results for sustained concentric tests are presented in Figures 4.5.1.3.A through F. The stress is shown (right-hand scale) as the ratio of the ultimate strength of the specimen for monotonic specimens and as the ratio of the average ultimate stress of monotonic specimens for sustained specimens. Stress, longitudinal strain, and transverse strain are shown as a function of time. The ultimate compressive stress and the cross sectional area of the specimen are also presented in each figure.

Specimens UHC95, UHC90, and UHC85 were tested in MTS 815 test machine and the other sustained specimens were tested in the sustained load frames. Specimens UHC95 and UHC90 failed after being under sustained concentric stresses of 95 and 90 percent of the ultimate for 8 minutes and 4 hours and 56 minutes respectively (See Figures 4.5.1.3.A and B). Specimen UHC85 was loaded to 85 percent of the ultimate stress for 11 days, 7

hours, and 53 minutes. Due to a sudden oil pressure change in the other hydraulic testing machine which share the same hydraulic pump as the MTS 815, the load on the specimen increased and it failed under 94 percent of the ultimate stress after 3 hours and 9 minutes at the increased stress (See Figure 4.5.1.3.C). The total longitudinal strain was 6484 microstrain when the stress intensity started to increase and 6759 microstrain at failure. The specimens in the three sustained concentric load frames were subjected to sustained concentric stresses of 80, 75, and 70 percent of the ultimate at the age of 56 days. Specimen UHC80 failed after being under sustained concentric stress of 80 percent of the ultimate for 19 days, 2 hours, and 40 minutes (See Figure 4.5.1.3.D). The specimens UHC75 and UHC70 did not fail during the 3 month sustained load test (See Figures 4.5.1.3.E and F). As can be seen, the transverse strains were generally less than 3500 microstrain until near the failures.

For all sustained specimens, the total strain, the initial strain, the creep strain, the creep coefficient, the specific creep, and time after loading are presented in Table 4.5.1.3 for the time of failure or the end of the test. The initial recovery is also presented in the same table for those specimens which did not fail during the 3 month test.

4.5.1.4 UU Series Test Results

The experimental results for monotonic concentric tests are presented in Figures D-4.5.A through E of Appendix D. The experimental results for sustained concentric tests are presented in Figures 4.5.1.4.A through E. The stress is shown (right-hand scale) as the ratio of the ultimate strength of the specimen for monotonic specimens and as the ratio of the average ultimate stress of monotonic specimens for sustained specimens. Stress, longitudinal strain, and transverse strain are shown as a function of time. The ultimate compressive stress and the cross sectional area of the specimen are also presented in each figure.

Specimens UUC95 and UUC90 were tested in MTS 815 test machine and the other sustained specimens were tested in the sustained load frames. Specimen UUC95 failed just after reaching the 95 percent of the ultimate stress (See Figure 4.5.1.4.A). Due to fluctuation in ultimate strength of ultra high strength concrete, this may have been the ultimate compressive strength of the specimen. Specimen UUC90 failed after being under sustained concentric stress of 90 percent of the ultimate for 5 hours and 52 minutes (See Figure 4.5.1.4.B). The specimens in the three sustained concentric load frames were subjected to sustained concentric stresses of 85, 80, and 75 percent of the ultimate. Specimens UUC85(70), UUC80(70), and UUC75 did not fail during the 3 month sustained load test (See Figure 4.5.1.4.C through E). As can be seen, the transverse strains were generally less than 1000 microstrain until near the failures.

For all sustained specimens, the total strain, the initial strain, the creep strain, the creep coefficient, the specific creep, and time after loading are presented in Table 4.5.1.4 for the time of failure or the end of the test. The initial recovery is also presented in the same table for those specimens which did not fail during the 3 month test.

4.5.2 Discussion of Results

The stress - strain relationships are summarized in Figures 4.5.2.A through C for LH, UH, and UU concentric series respectively; and the strain - log of time relationships are also summarized in Figures 4.5.2.D through F for LH, UH, and UU concentric series respectively. Vertical marks (]) at the end of the curves indicate failure and arrows indicate no failure.

The general behavior of specimens tested under high sustained concentric stresses consisted of three stages. The first stage is similar to the general creep behavior where the strain rate is high after application of the load. The period under which the first stage takes place increases as the stress intensity decreases. For no silica fume high strength concrete, this period is longer as the compressive strength of concrete increases. For silica fume ultra high strength concrete, the period of high creep strain is shorter than for both grades of high strength concrete studied. The second stage is represented by a slow or even constant strain rate. This stage existed in all specimens tested. In general, for the same stress intensity, the length of stage two increases as the compressive strength increases. The major difference between specimens which failed under sustained compressive stresses and those which did not is in the third stage. In this stage, the strain rate increases sharply and leads the specimen to failure for those specimens under sustained stresses above the sustained compressive strength. The length of the period during which the last stage takes place increases as the stress intensity decreases. It is sometimes difficult to observe the last stage at stress intensities close to the ultimate stress. The last stage is completely different for those specimens which did not fail under sustained compressive stresses. For these specimens, the third stage is represented by decrease in strain rate or in other words a change of curvature of the strain - log of time curves.

For stress intensities above the sustained compressive strength, the total strain increases as the stress intensity decreases. For no silica fume high strength concrete, the total strain increases as the compressive strength of concrete increases; but the total strain of silica fume ultra high strength concrete is much less than no silica fume high strength concretes. For stress intensities above the sustained compressive strength, the creep strain, the creep coefficient, and the specific creep increase as the stress intensity decreases; but they decrease as the compressive strength of high performance concrete increases. The period under sustained compressive stress up to failure increases as the stress intensity decreases and the

compressive strength of high performance concrete increases. The initial strain recovery is larger for the silica fume ultra high strength concrete than for both grades of high strength concrete studied. It seems that the initial strain recovery is not sensitive to the compressive strength of high strength concrete.

The results of concentric specimens tested in this study are summarized in Figure 4.5.2.G. Results are presented as stress intensity versus the short time ultimate compressive strength at the time of loading. As can be seen from Figure 4.5.2.G, the highest stress intensities that the specimens did not fail during the three month sustained compressive concentric study were 70, 75, and 85 percent of the ultimate short term compressive strength for LH, UH, and UU series respectively. As can be seen from Figures 4.5.2.D through F, in spite of the strain increase for those specimens that did not fail, their strain - log of time curves have a convex curvature (in contrast with the concave curvature of those that failed). In addition, the total strain, the creep strain, the creep coefficient, and the specific creep of LHC70(70), UHC75, and UUC85(70) specimens which did not fail are less than those values for LHC75(70), UHC80, and UUC90 specimens which did fail, respectively. As the result, it can be suggested that the sustained compressive concentric strength of concrete is 70 to 75, 75 to 80, and 85 to 90 percent of the short term ultimate compressive strength for 65 MPa to 75 MPa, 95 MPa to 105 MPa, and 120 MPa high performance concretes, respectively. Meanwhile, it can be suggested that the sustained compressive strength of high performance concrete improves as the compressive strength of concrete at the time of loading increases.

The long term sustained compressive strength of conventional plain concrete should be in vicinity of 70 percent of the short term monotonic ultimate strength regardless of possible eccentricity and age at the time of loading[46,48,50,51,52]. Based on a microcracking study on high strength concrete subjected to short term loading, Carrasquillo et al[54] predict that high strength concrete can be loaded to a higher stress - strength ratio without initiating a self propagating mechanism leading to disruptive failure. In other words their study indicates that the sustained strength of high strength concrete is a higher percentage of the short term strength. Due to the compatibility of the compressive strength of LH series at the ages of 28 days and 56 days, the LH series results can be compared with some of the previous studies.

Stockl[50] plotted two hundred and four failures of specimens under sustained loads as the stress intensity versus time regardless of eccentricity and whether there is a failure under lower stress intensity for the same batch. Based on a curve fitted to this data, he concluded that the long term sustained compressive strength should be around 80 percent of the short term compressive strength regardless of the compressive strength of concrete and the

possible eccentricity of load on the specimen. The presence of data for failures under higher stress intensities than the minimum stress intensity failure is questionable for the regression to establish such a curve fit. Meanwhile, he reported failures within 70 to 75, and 64 percent of the short term ultimate strength for 50 MPa and 40 MPa concretes respectively. As the results, it can be concluded that the long term sustained strength of concrete should be in vicinity of 65 to 75 percent of the ultimate.

The studies by Ngab et al[51] and Smadi et al[52] were done at Cornell University with the same facility and materials. Therefore, the results from both studies can be combined. Based on the study by Ngab et al[51], the 39 MPa conventional concrete specimens failed under 65 percent of the ultimate while based on the study by Smadi et al[52], the 20 to 25 MPa conventional concrete specimens did not fail under 75 percent of the ultimate. As the result, it can be concluded that the long term sustained compressive strength of conventional concrete should be in vicinity of 65 to 75 percent of the short term ultimate strength. Based on the study by Ngab et al[51], the 62 MPa high strength concrete did not fail under 85 percent of the ultimate, while based on the study by Smadi et al[52], two of the four 60 to 70 MPa high strength concrete specimens failed under 80 percent of the ultimate. It should be mentioned that Smadi et al[52] did not test 60 to 70 MPa concrete under 75 percent of the ultimate. As the result, it can be concluded that the long term sustained compressive strength should be in vicinity of 75 to 85 percent of the short term ultimate strength for the Lower bound of High strength concrete.

The higher long term sustained compressive strength of their high strength concrete compared to the LH series can be due to usage of limestone coarse aggregate which has a much better performance in most aspects of concrete related to strain behavior; but the following issues are questionable about both Ngab et al[51] and Smadi et al[52] studies:

a. The sustained load frames used to study conventional and high strength concrete were different (helical springs and spring loading system with lever arm respectively).

b. The load frames used for conventional concrete had the fixed end conditions while the load frames used for high strength concrete had the ball seat bearing blocks.

c. The sitting of the two capped specimens at the top of each other caused an undefined end condition and as a result an undefined stress field on one end of each specimen.

d. The tests were carried out in the laboratory environment instead of 50% R.H. As shown by many studies including the current study, the rate of strength gain of high strength concrete can be higher in a drier environment after a sufficient moist curing period.

e. The strain - log of time curve representing 80 percent stress intensity has a sharp concave curvature. It implies possible failure at later ages.

f. The adequacy of the 60 day sustained load period can be questionable.

4.6 High Performance Concrete under High Sustained Eccentric Stresses

4.6.1 Test Results

4.6.1.1 General

The experimental results of the specimens tested eccentrically for LH, UH, and UU series are presented in this section. The experimental results of the specimens tested eccentrically for LU series are presented in Appendix F. Each specimen is represented by an abbreviation such as LHE80(70). The first two characters represent the concrete series to which the specimen belongs (See Section 2.4). The third character stands for concentric, C, and eccentric, E, specimens. The first number represents the stress intensity or load intensity on the specimen as a percent of the short time strength at the time of loading. The possible next character distinguishes the specimens with the same intensity. If the specimen is loaded at the age of 70 days instead of 56 days, the age appears in parentheses. The creep strain and the creep coefficient are calculated as explained in section 4.5.1.1.

4.6.1.2 LH Series Test Results

The experimental results for monotonic eccentric tests are presented in Figures B-4.6.A through H of Appendix B. The experimental results for sustained eccentric tests are presented in Figures 4.6.1.2.A through F. The load is shown (right-hand scale) as the ratio of the ultimate load of the specimen for monotonic specimens and as the ratio of the average ultimate load of monotonic specimens, after necessary adjustment for possible diameter differences, for sustained specimens. Load, longitudinal strain in extreme fiber, and longitudinal strain in the opposite side are shown as a function of time. The ultimate load and the cross sectional area of the specimen are also presented in each figure.

Specimen LHE95 was tested in MTS 815 test machine and the other sustained specimens were tested in the sustained load frames. Specimen LHE95 failed after being under sustained eccentric stress of 95 percent of the ultimate for 4 minutes (See Figure 4.6.1.2.A). The specimens in the three sustained eccentric load frames were subjected to sustained eccentric stresses of 90, 85, and 80 percent of the ultimate at the age of 56 days. Specimen LHE90 failed approximately 10 minutes after loading. The data acquisition system was on manual control. As the result, there is no available strain data after end of loading process (See Figure 4.6.1.2.B). Specimens LHE85, and LHE80 failed after being

under sustained eccentric stresses of 85 and 80 percent of the ultimate for 2 hours and 29 minutes and 15 days, 5 hours, and 21 minutes respectively (See Figures 4.6.1.2.C and D). Due to failure of the test specimens in two of the three sustained eccentric load frames within the first two weeks of loading, two additional specimens were subjected to sustained eccentric stresses of 80 and 75 percent of the ultimate at the age of 70 days. Specimen LHE80(70) specimen also failed after being under sustained eccentric stress of 80 percent of the ultimate for 7 days and 1 hour and 45 minutes (See Figure 4.6.1.2.E). The specimen LHE75(70) did not fail during the 3 month sustained load test (See Figure 4.6.1.2.F). The longitudinal strain in the opposite side was always in tension at failure. As it can be seen, the longitudinal strain in the opposite side was generally less than 1000 microstrain until near the failure.

For sustained specimens that did not fail, the total strain, the initial strain, the creep strain, the creep coefficient, the initial recovery, and time after loading are presented in Table 4.6.1 for the end of the test.

4.6.1.3 UH Series Test Results

The experimental results for monotonic eccentric tests are presented in Figures C-4.6.A through E of Appendix C. The experimental results for sustained eccentric tests are presented in Figures 4.6.1.3.A through E. The load is shown (right-hand scale) as the ratio of the ultimate load of the specimen for monotonic specimens and as the ratio of the average ultimate load of monotonic specimens, after necessary adjustment for possible diameter differences, for sustained specimens. Load, longitudinal strain in extreme fiber, and longitudinal strain in the opposite side are shown as a function of time. The ultimate load and the cross sectional area of the specimen are also presented in each figure.

Specimens UHE95 and UHE90 were tested in MTS 815 test machine and the other sustained specimens were tested in the sustained load frames. Specimens UHE95 and UHE90 failed after being under sustained eccentric stresses of 95 and 90 percent of the ultimate for 15 minutes and 9 hours and 43 minutes respectively (See Figures 4.6.1.3.A and B). The specimens in the three sustained eccentric load frames were subjected to sustained eccentric stresses of 85, 80, and 75 percent of the ultimate at the age of 56 days. Specimen UHE85 failed after being under sustained eccentric stresses of 85 percent of the ultimate for 19 days, 2 hours, and 47 minutes (See Figure 4.6.1.3.C). Specimens UHE80 and UHE75 did not fail during the 3 month sustained load test (See Figure 4.6.1.3.D and E). As it can be seen, the longitudinal strain in the opposite side was generally less than 1000 microstrain until near failure.

For sustained specimens that did not fail, the total strain, the initial strain, the creep strain, the creep coefficient, the initial recovery, and time after loading are presented in Table 4.6.1 for the end of the test.

4.6.1.4 UU Series Test Results

The experimental results for monotonic eccentric tests are presented in Figures D-4.6.A through E of Appendix D. The experimental results for sustained eccentric tests are presented in Figures 4.6.1.4.A through E. The load is shown as (right-hand scale) the ratio of the ultimate load of the specimen for monotonic specimens and as the ratio of the average ultimate load of monotonic specimens, after necessary adjustment for possible diameter differences, for sustained specimens. Load, longitudinal strain in extreme fiber, and longitudinal strain in the opposite side are shown as a function of time. The ultimate load and the cross sectional area of the specimen are also presented in each figure.

Specimens UUE95 and UUE90 were tested in MTS 815 test machine and the other sustained specimens were tested in the sustained load frames. Specimens UUE95 and UUE90 both failed after being under sustained eccentric stresses of 93 and 90 percent of the ultimate for 2 minutes (See Figures 4.6.1.4.A and B). The specimens in the three sustained eccentric load frames were subjected to sustained eccentric stresses of 85, 80, and 75 percent of the ultimate at the age of 56 days. Specimens UUE85, UUE80, and UUE75 did not fail during the 3 month sustained load test (See Figures 4.6.1.4.C through E). As it can be seen, the longitudinal strain in the opposite side was generally less than 1000 microstrain until near failure.

For sustained specimens that did not fail, the total strain, the initial strain, the creep strain, the creep coefficient, the initial recovery, and time after loading are presented in Table 4.6.1 for the end of the test.

4.6.2 Discussion of Results

The load - extreme fiber strain relationships are summarized in Figures 4.6.2.A through C for LH, UH, and UU eccentric series respectively; and the extreme fiber strain - log of time relationships are also summarized in Figures 4.6.2.D through F for LH, UH, and UU series respectively. Vertical marks (]) at the end of the curves indicate failure and arrows indicate no failure.

The general behavior of specimens tested under high sustained eccentric loads consisted of three stages as did the concentric specimens. The first two stages are similar to those for specimens tested under high sustained concentric stresses. The third stage is also similar for those specimens that did not fail under sustained loads; but for those

specimens which failed, the third stage is different. The strain rate increases sharply and leads to crushing of the concrete in extreme fiber zone and wide tension crack development in the opposite side. Due to the strain gradient, stress redistribution on the cross section, and loss of part of the cross section in both sides, the specimen still carries the load. However, the higher percentage of the load on the remaining cross section after stress redistribution leads the specimen toward failure. The strain drop in the extreme fiber and sudden tension strain increase in the opposite side support the above discussion.

The results of eccentric specimens tested in this study are summarized in Figure 4.6.2.G. Results are presented as load intensity versus the short time ultimate compressive strength at the time of loading. As can be seen from Figure 4.6.2.G, the highest load intensities that the specimens did not fail during the three month sustained compressive eccentric study were 75, 80, and 85 percent of the ultimate short term compressive strength for LH, UH, and UU series respectively. As can be seen from Figures 4.6.2.D through F, in spite of the strain increase for those specimens that did not fail, their strain - log of time curves have a convex curvature (in contrast with the concave curvature of those that failed). As the result, it can be suggested that the sustained compressive strength of high performance concrete under small eccentricities is 75 to 80, 80 to 85, and 85 to 90 percent of the short term ultimate compressive strength for 65 MPa to 75 MPa, 95 MPa to 105 MPa, and 120 MPa concretes, respectively.

Based on the results of current study, it can be suggested that moment gradient, or eccentricity, slightly improves the sustained compressive strength of high performance concrete. The long term sustained compressive strength of high performance concrete under small eccentric loads was approximately 5 percent higher than under the concentric loads.

Based on a study of microcracking in conventional concrete, Sturman et al[2] reported that the most highly strained area is also the most highly cracked area for the eccentric specimen. It is also reported that even though the average strain in that area is approximately the same as the strain in the companion concentric specimen, the cracking in this area is only about half of the average cracking in the companion concentric specimen.

Sturman et al[2] reported that at strains about 1700 microstrain, development of mortar cracking is pronounced in the concentric specimens, while its increase is more gradual in the eccentric specimens. He also reported that at strains above 1700 microstrain, there is more mortar cracking in the concentric specimens than in eccentric specimens.

Meanwhile, Carrasquillo et al[54] reported that the behavior and failure of high strength concrete is governed by combined cracks (combination of bond and mortar cracks) with at least two bond cracks and two mortar cracks, with bond cracks connected by at least one mortar crack.

Based on results of studies by Sturman et al[2] and Carrasquillo et al[54], it can be suggested that less microcracking especially less mortar cracks in eccentric specimens compared to concentric specimens as the result of moment gradient and less mortar cracks as the result of the stronger paste are the possible reasons for the higher sustained compressive strength of high performance concrete under eccentric loads.

4.7 Conclusions

Based on results of the current study and previous studies mentioned in the literature, the following conclusions can be drawn for high performance concrete under high sustained compressive stresses:

1. The long term sustained compressive strength of high performance concrete increases as the compressive strength of concrete increases. The long term sustained compressive strength of high performance concrete is between 70 to 75, 75 to 80, and 85 to 90 percent of the short term ultimate strength for 65 MPa to 75 MPa, 95 MPa to 105 MPa, and 120 MPa concretes, respectively.

2. Small eccentricities slightly improve the long term sustained compressive strength of high performance concrete. The long term sustained compressive strength of high performance concrete under eccentric loads at or near the Kern point was approximately 5 percent higher than under the concentric loads.

3. In specimens subjected to stress intensities above the sustained compressive strength, the total strain at failure increases as the stress intensity decreases. For no silica fume high strength high performance concretes, the total strain at failure increases as the compressive strength of concrete increases. The total strain at failure of silica fume ultra high strength high performance concrete is much less than that of no silica fume high strength high performance concrete.

4. In specimens subjected to stress intensities above the sustained compressive strength, the creep strain, the creep coefficient, and the specific creep increase as the stress intensity decreases.

5. The period under sustained compressive stresses until failure generally increases as the stress intensity decreases. The period under sustained compressive stresses until failure generally increases as the compressive strength of high performance concrete increases.

6. The initial strain recovery of silica fume ultra high strength high performance concrete is higher than for no silica fume high strength high performance concrete.

Table 4.3.A - Compressive Strength History (LH Series)

Age (Days)	LH1 (MPa)	f_{ct}/f_{c28}	f_{ct}/f_{c56}
1	27.5	0.48	0.42
3	38.3	0.67	0.58
7	42.6	0.74	0.65
28	57.5	1.00	0.88
56	65.5	1.12	1.00
70	66.0	1.15	1.01
160	69.2	1.20	1.06

Table 4.3.B - Compressive Strength History (UH Series)

Age (Days)	UH1 (MPa)	f_{ct}/f_{c28}	f_{ct}/f_{c56}
1	49.7	0.59	0.52
3	59.5	0.70	0.62
7	65.7	0.78	0.69
28	84.5	1.00	0.89
56	95.3	1.13	1.00
146	101.8	1.20	1.07

Table 4.3.C - Compressive Strength History (UU Series)

Age (Days)	UU1 (MPa)	f_{ct}/f_{c28}	f_{ct}/f_{c56}
1	60.2	0.54	0.50
3	71.5	0.64	0.59
7	80.0	0.72	0.66
28	111.4	1.00	0.92
56	120.5	1.08	1.00
70	119.8	1.08	0.99
160	136.4	1.22	1.13

Table 4.5.1.1 - Compressive Strength of Monotonic Concentric Specimens

Concrete Series	Age (Days)	S_1 (MPa)	S_2 (MPa)	S_3 (MPa)	S_4 (MPa)	S_5 (MPa)	Mean (MPa)	S_{n-1}
LH1	56	65.5	64.1	65.9	65.8	66.0	65.5	0.78
LH1	70	66.7	66.2	65.1	-	-	66.0	0.82
UH1	56	97.5	90.9	95.9	97.9	94.2	95.3	2.85
UU1	56	115.5	125.0	121.6	119.7	120.6	120.5	3.43
UU1	70	120.5	118.0	120.8	-	-	119.8	1.54

Table 4.5.1.2 - Summary of LH Concentric Series Strain Study

Specimen	Total Strain μmm/mm	Initial Strain μmm/mm	Creep Strain μmm/mm	Creep Coeff.	Specific Creep 10^{-6}/MPa	Time Min.	Initial Recovery μmm/mm
LHC95	2999	2793	206	0.074	3.3	2	-
LHC90	4010	2535	1475	0.582	25.0	33	-
LHC85	4321	3170	1151	0.363	20.7	261	-
LHC80	5782	2735	3047	1.114	54.7	4661	-
LHC75	6698	1832	4866	2.656	99.1	47533	-
LHC75(70)	7303	2310	4993	2.161	100.9	20069	-
LHC70(70)	6392	1874	4518	2.411	97.8	129600	1584

Table 4.5.1.3 - Summary of UH Concentric Series Strain Study

Specimen	Total Strain μmm/mm	Initial Strain μmm/mm	Creep Strain μmm/mm	Creep Coeff.	Specific Creep 10^{-6}/MPa	Time Min.	Initial Recovery μmm/mm
UHC95	3635	3227	408	0.126	4.5	7	-
UHC90	4507	2950	1557	0.528	18.2	296	-
UHC85	-	2759	-	-	-	-	-
UHC80	5984	2415	3569	1.478	46.8	27520	-
UHC75	6258	2316	3942	1.702	55.2	129600	1777
UHC70	5296	2140	3156	1.475	47.3	129600	1552

Table 4.5.1.4 - Summary of UU Concentric Series Strain Study

Specimen	Total Strain μmm/mm	Initial Strain μmm/mm	Creep Strain μmm/mm	Creep Coeff.	Specific Creep 10^{-6}/MPa	Time Min.	Initial Recovery μmm/mm
UUC95	3064	3064	0	0	0	0	-
UUC90	3438	2919	519	0.178	4.8	352	-
UUC85(70)	4106	2524	1582	0.627	15.5	129600	2319
UUC80(70)	4047	2557	1490	0.583	15.5	129600	1883
UUC75	3750	2458	1992	0.526	14.3	129600	2048

Table 4.6.1 - Summary of Eccentric Series Extreme Fiber Strain Study

Specimen	Total Strain μmm/mm	Initial Strain μmm/mm	Creep Strain μmm/mm	Creep Coeff.	Time Min.	Initial Recovery μmm/mm
LHE75(70)	7798	2893	4905	1.695	129600	2281
UHE80	8503	3140	5363	1.708	129600	2200
UHE75	7191	2899	4292	1.481	129600	2312
UUE85	5117	3553	1564	0.440	129600	2737
UUE80	5131	3229	1902	0.589	129600	2433
UUE75	4668	3048	1620	0.531	129600	2328

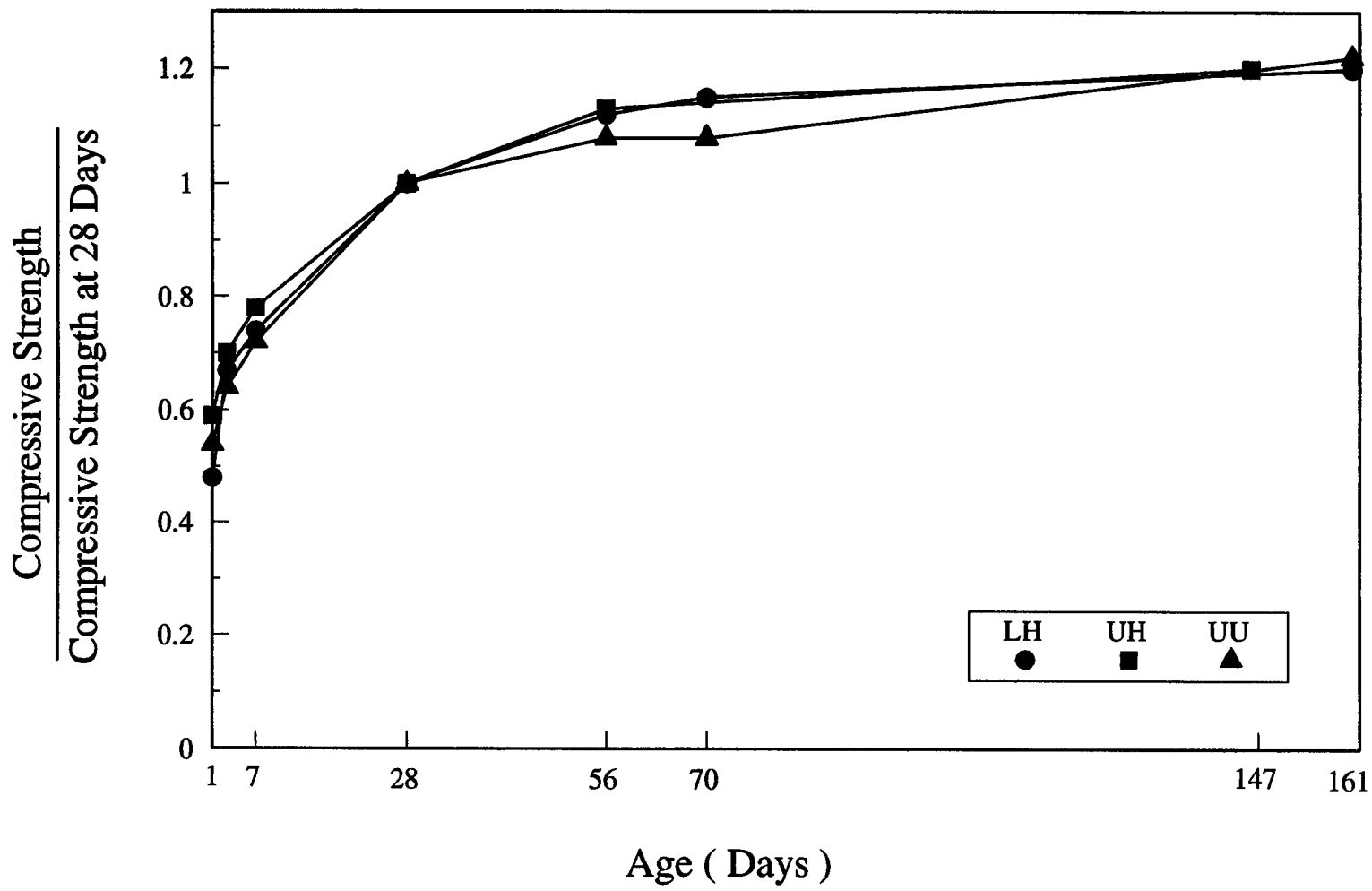

Figure 4.3.A - Compressive Strength History (Ratio of 28-Day Strength)

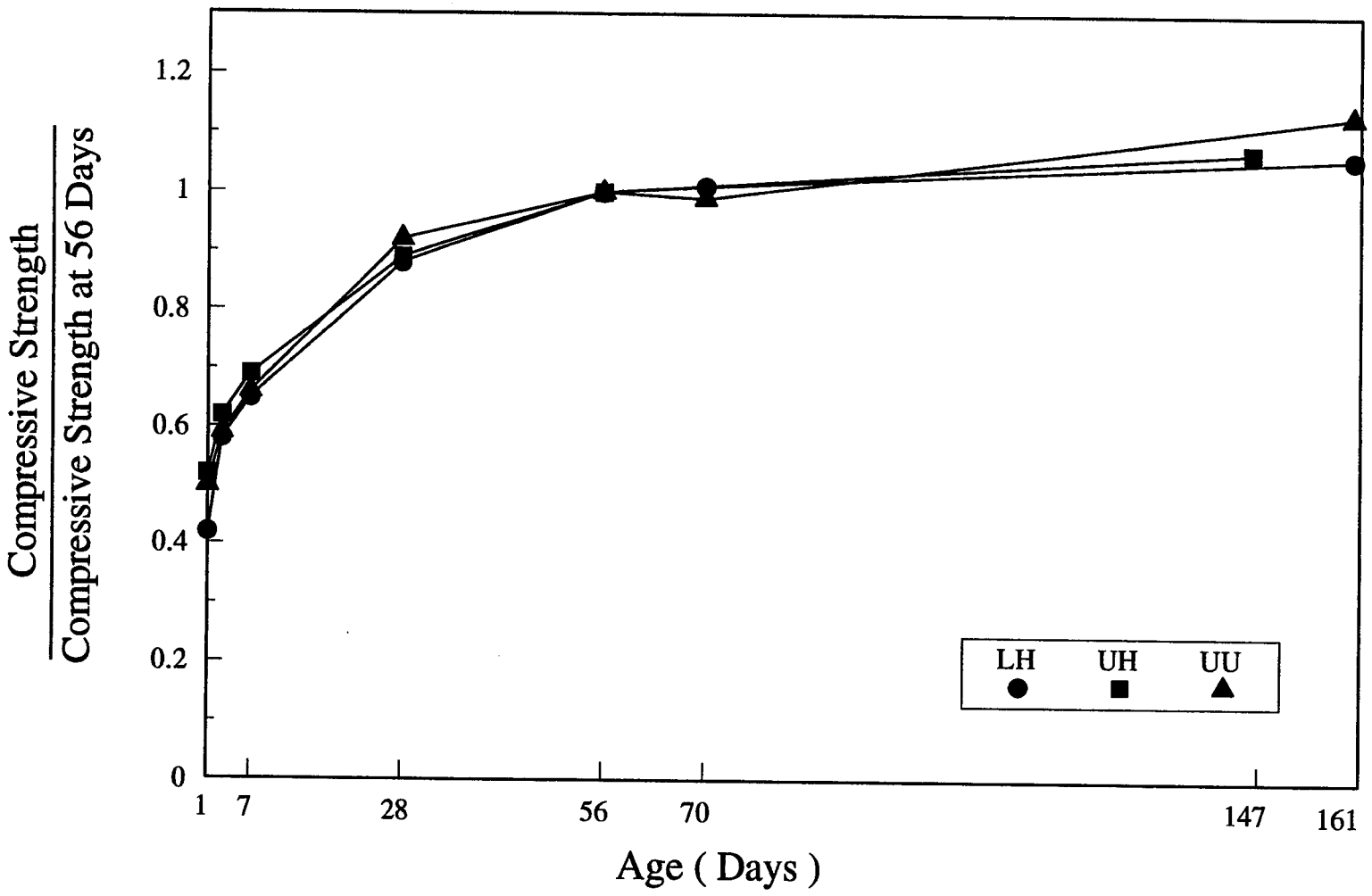

Figure 4.3.B - Compressive Strength History (Ratio of 56-Day Strength)

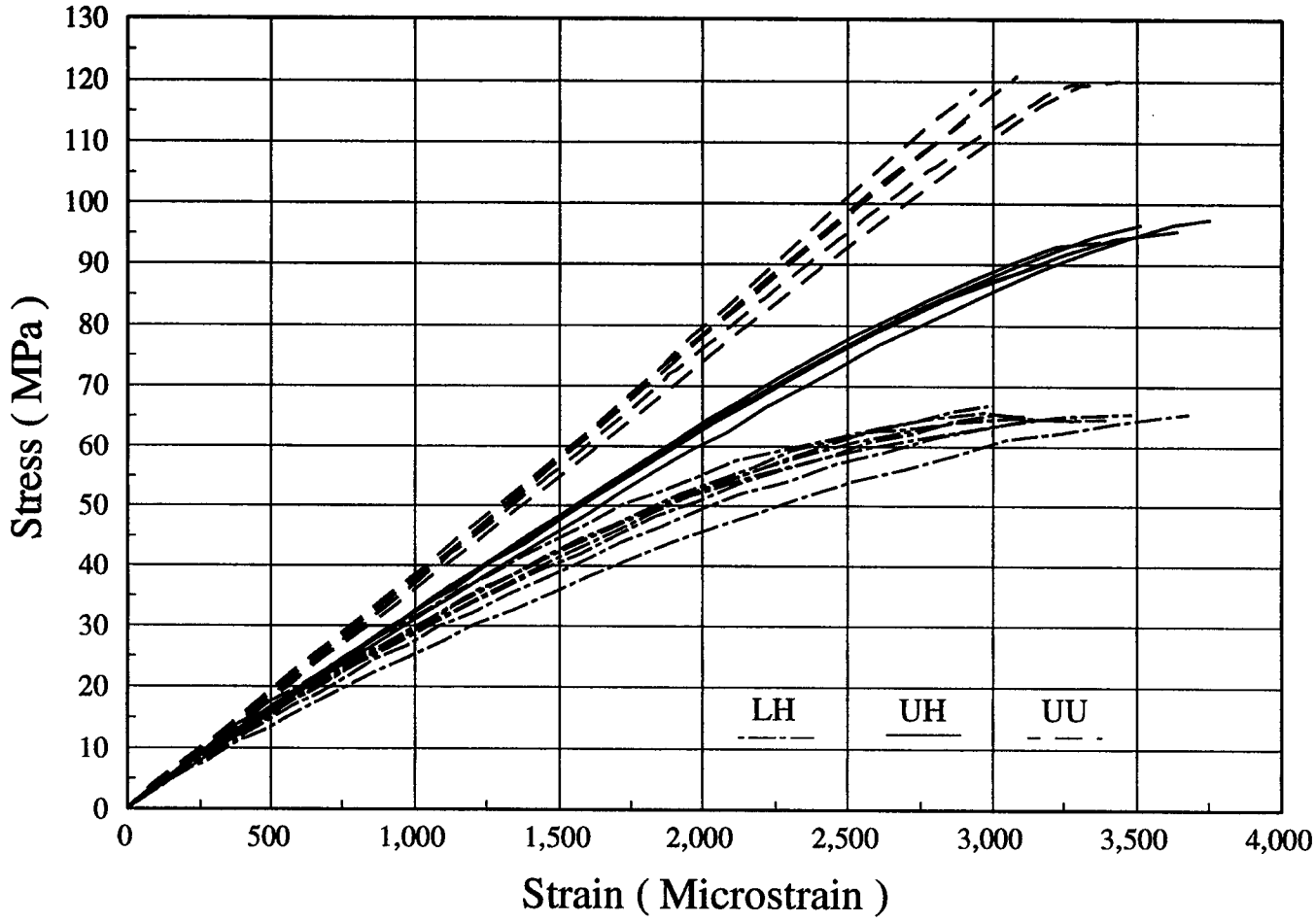

Figure 4.4.A - Stress-Strain Curves of Monotonic Concentric Specimens

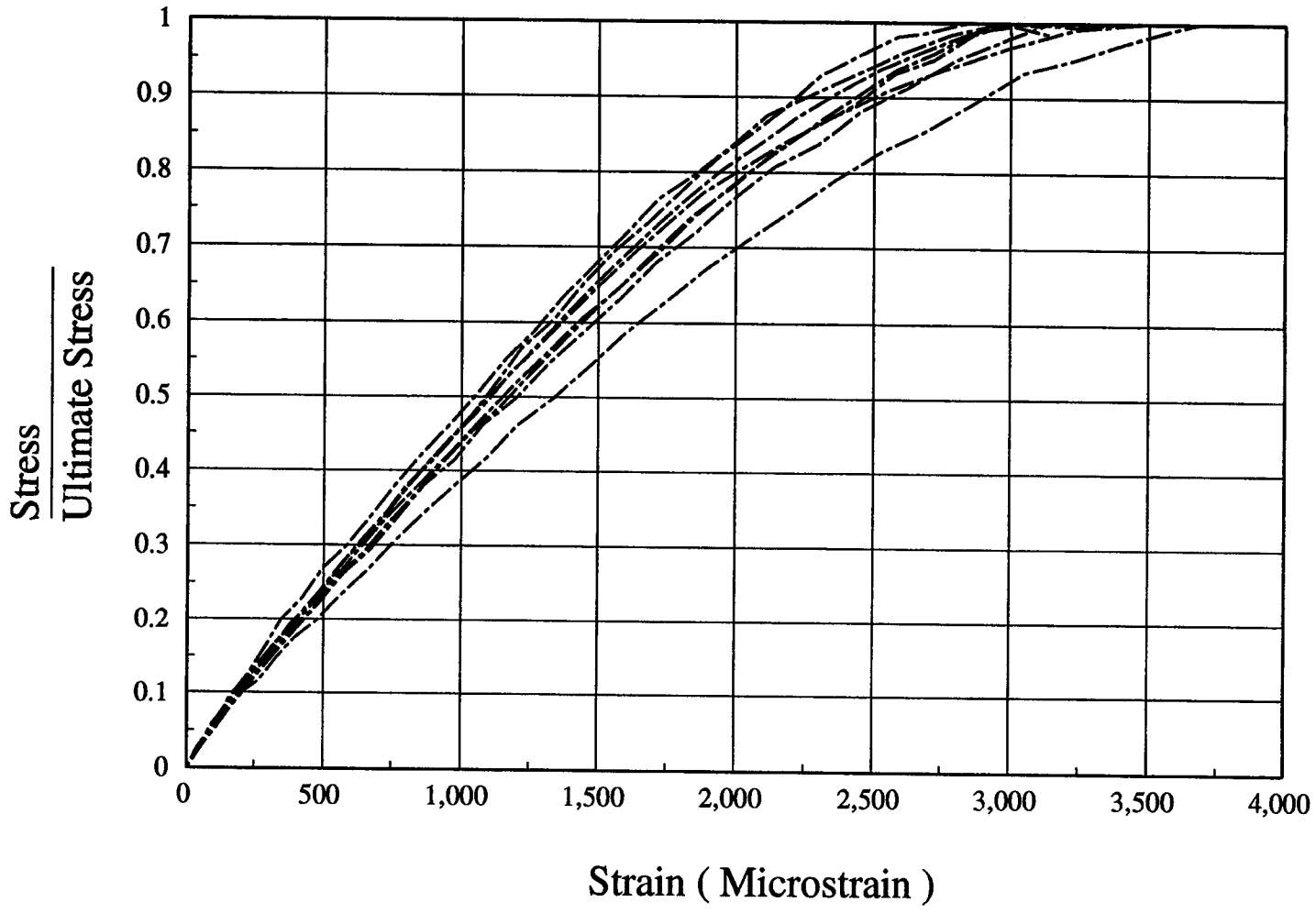

Figure 4.4.B - Stress - Strain Relationship - LH Series

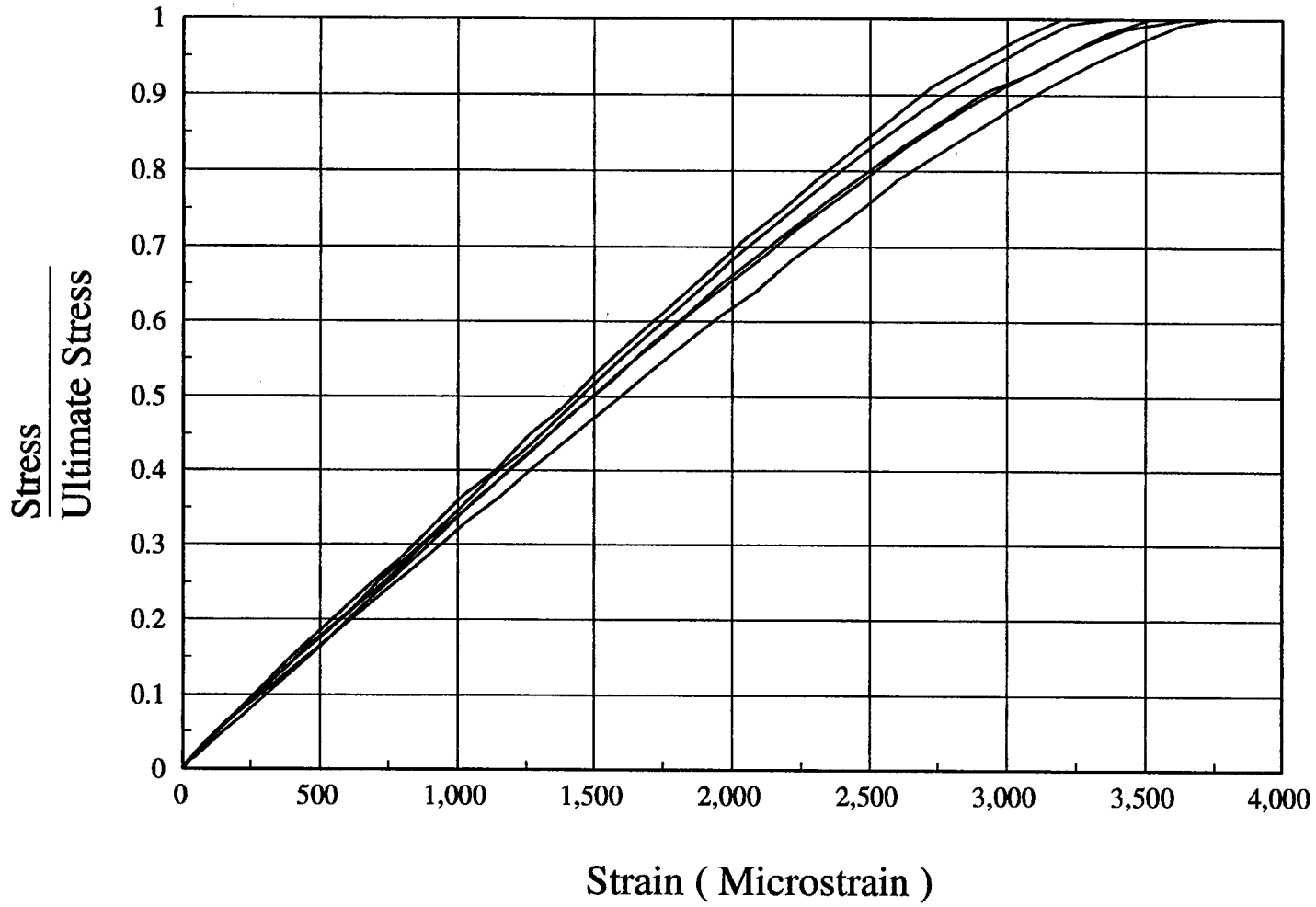

Figure 4.4.C - Stress - Strain Relationship - UH Series

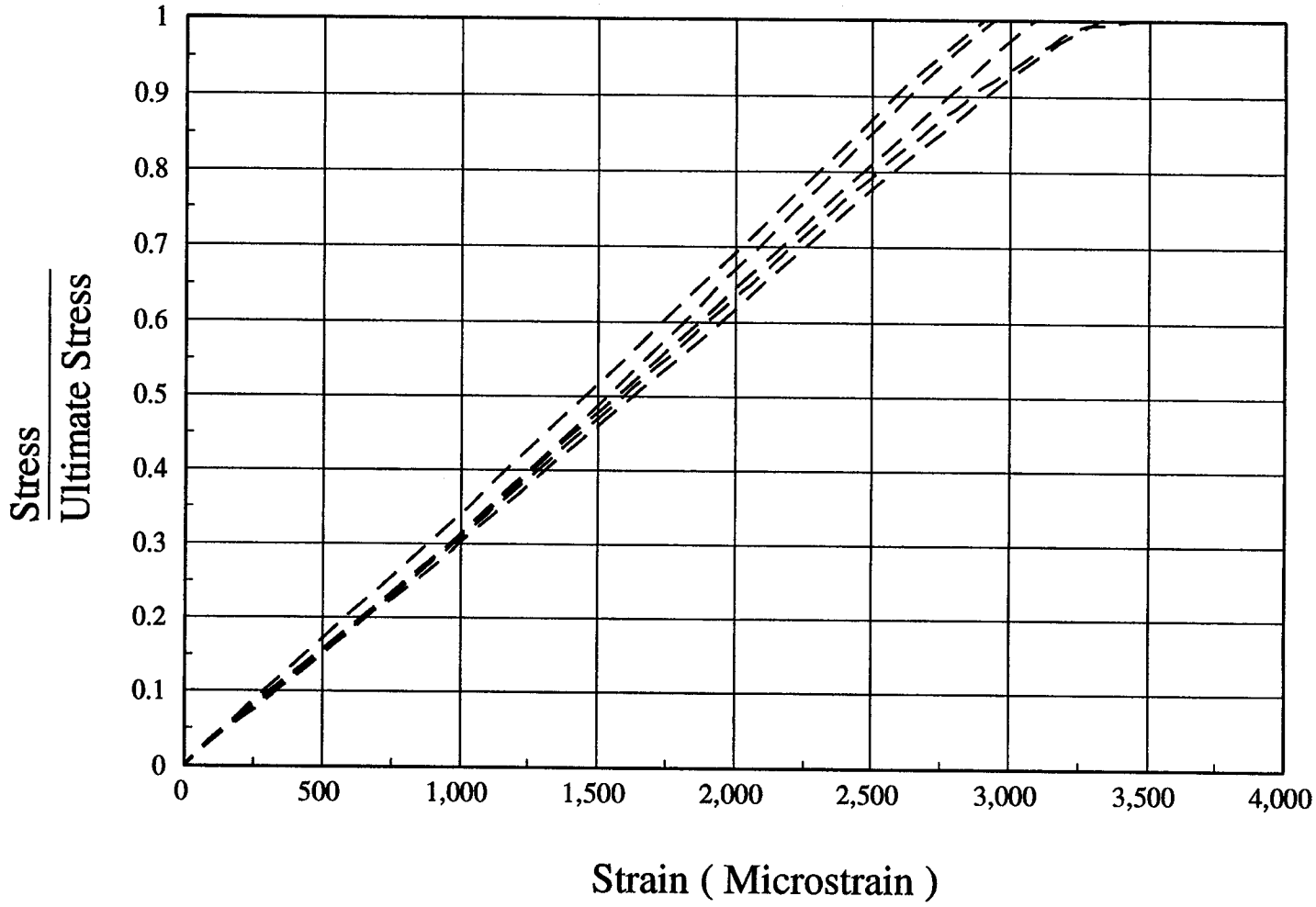

Figure 4.4.D - Stress - Strain Relationship - UU Series

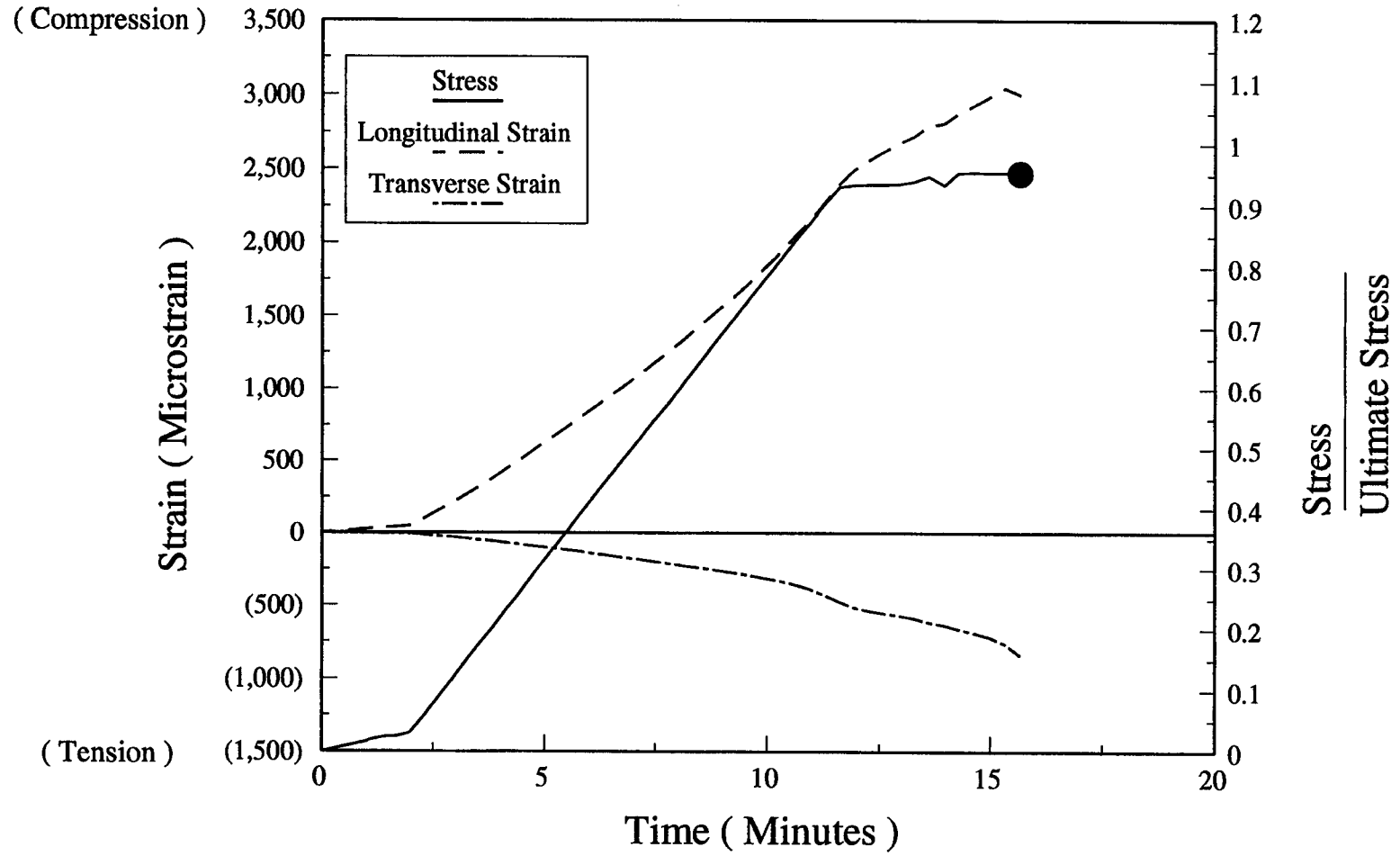

f_c= 65.5 MPa A = 7763 mm^2

Figure 4.5.1.2.A - Stress-Strain-Time Relationship - LHC95 Specimen

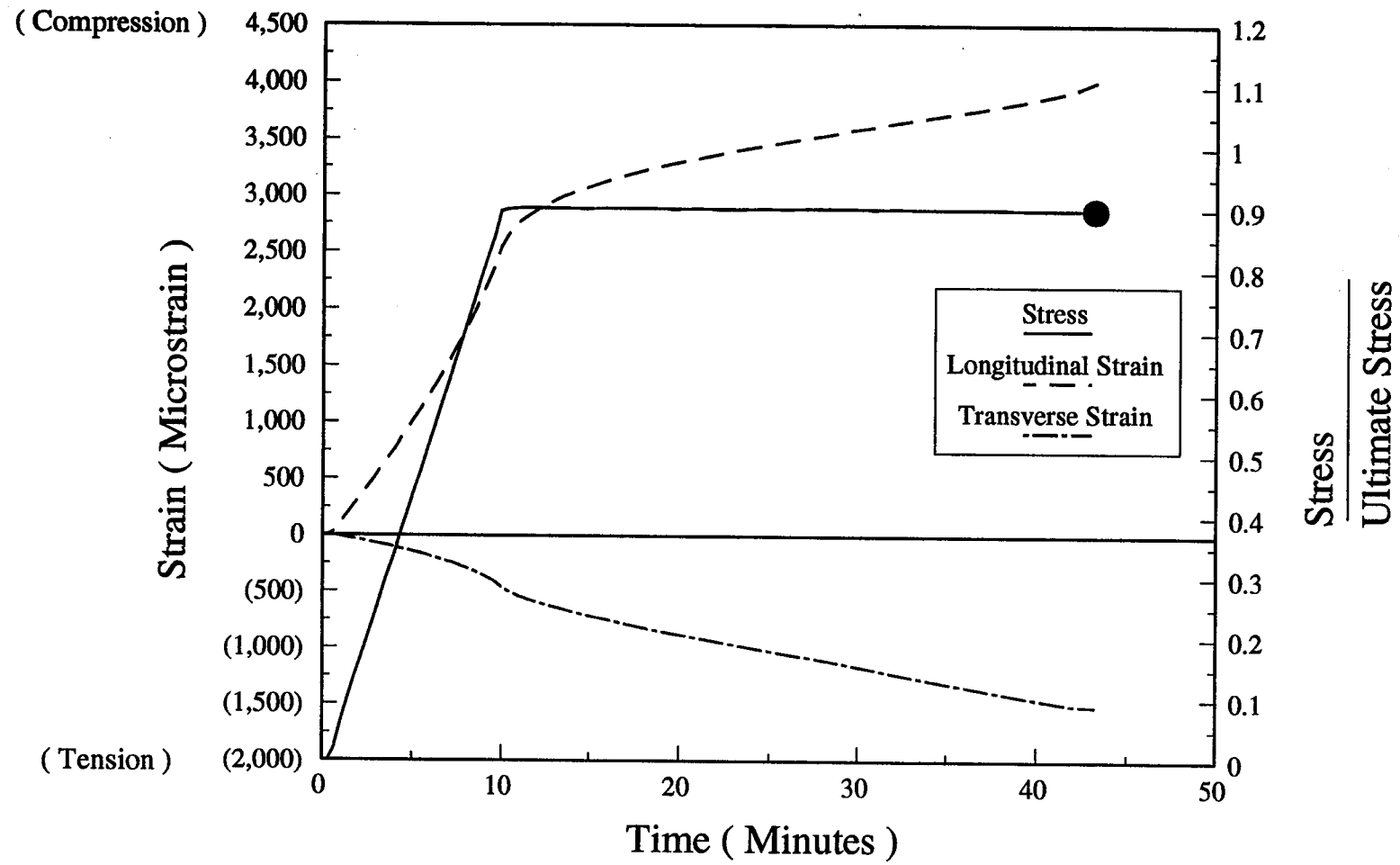

$f_c = 65.5$ MPa $\qquad A = 7810\ mm^2$

Figure 4.5.1.2.B - Stress-Strain-Time Relationship - LHC90 Specimen

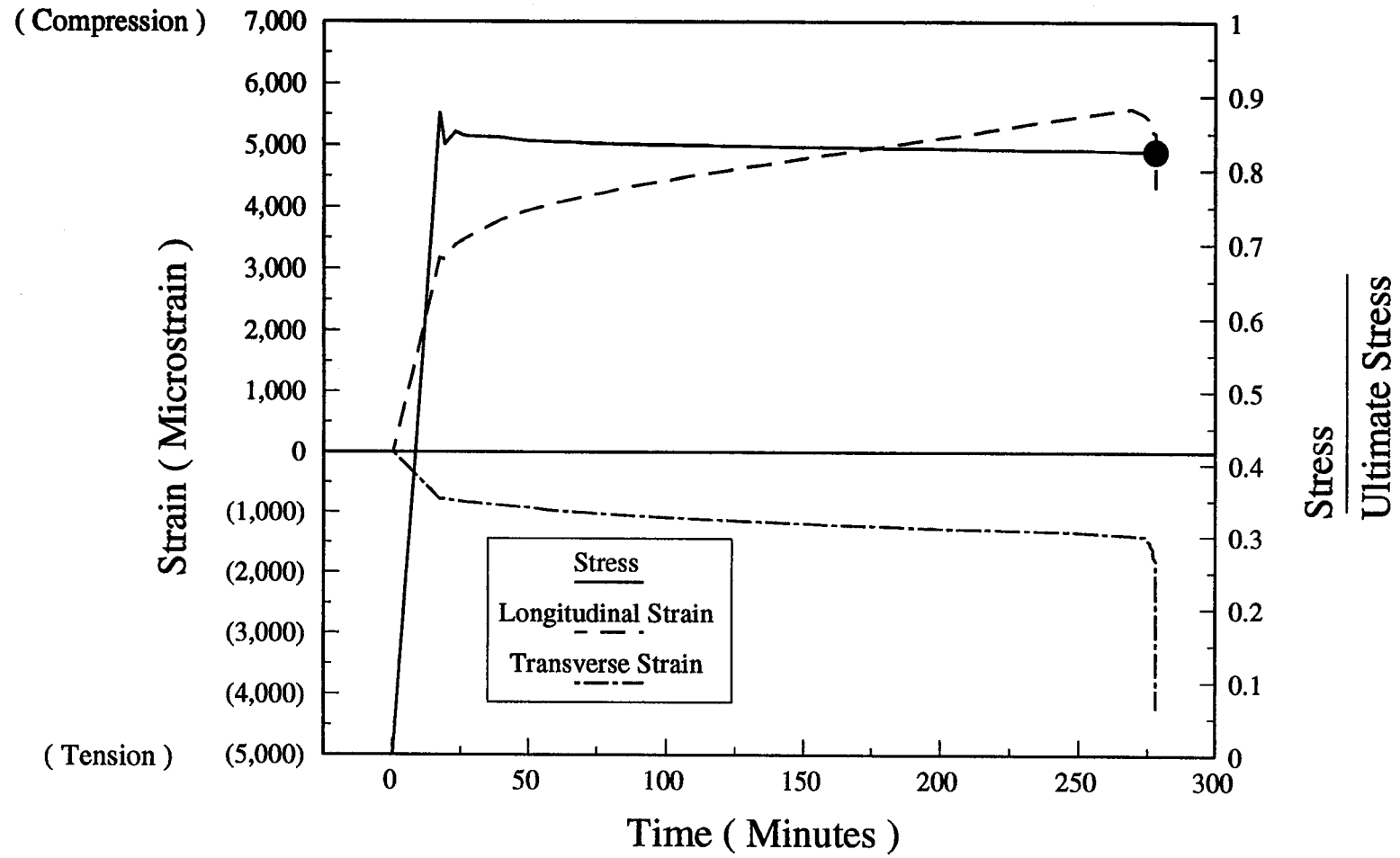

$f_c = 65.5$ MPa $\qquad A = 8110\ mm^2$

Figure 4.5.1.2.C - Stress-Strain-Time Relationship - LHC85 Specimen

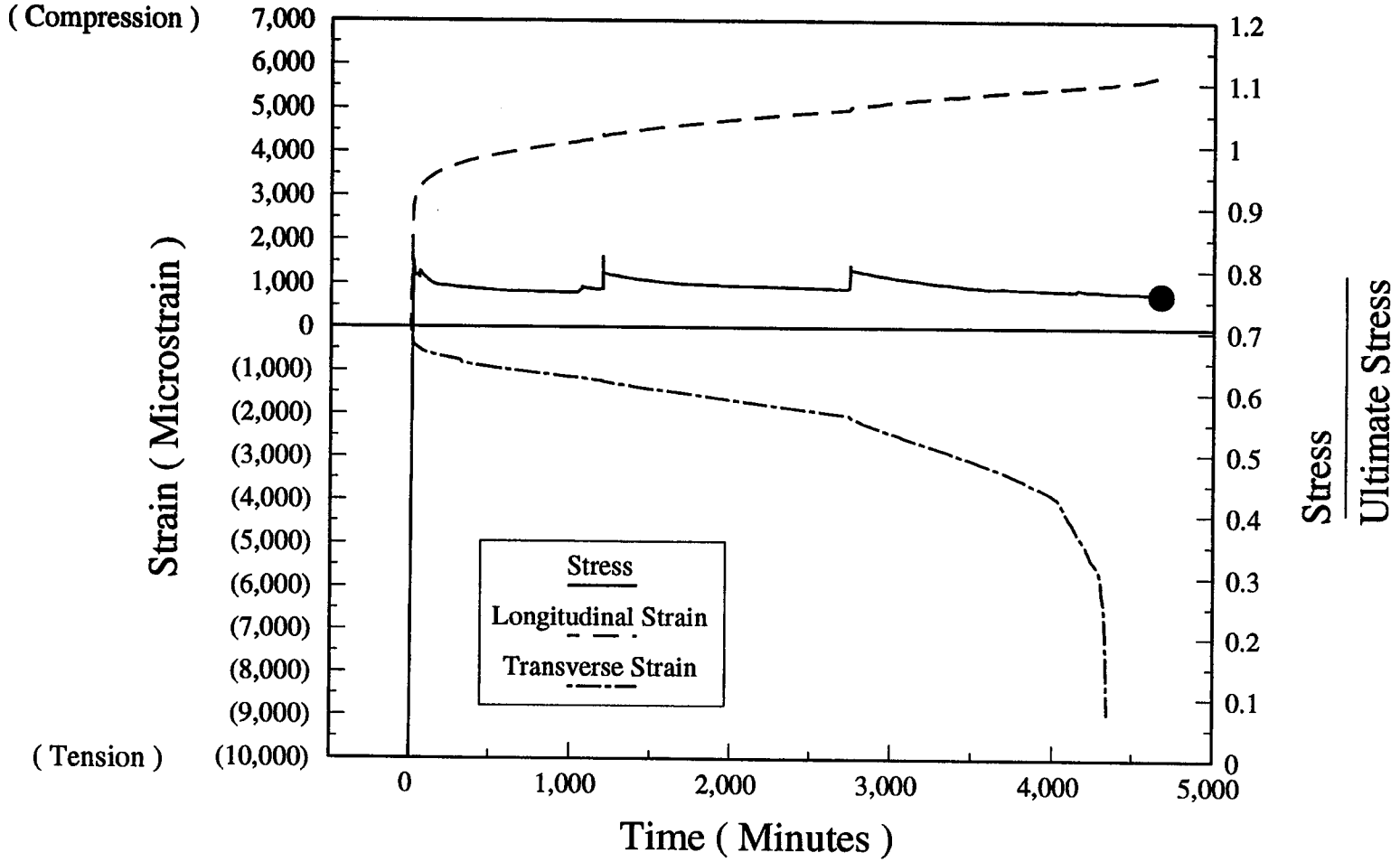

$f_c = 65.5$ MPa $\qquad A = 7781\ mm^2$

Figure 4.5.1.2.D - Stress-Strain-Time Relationship - LHC80 Specimen

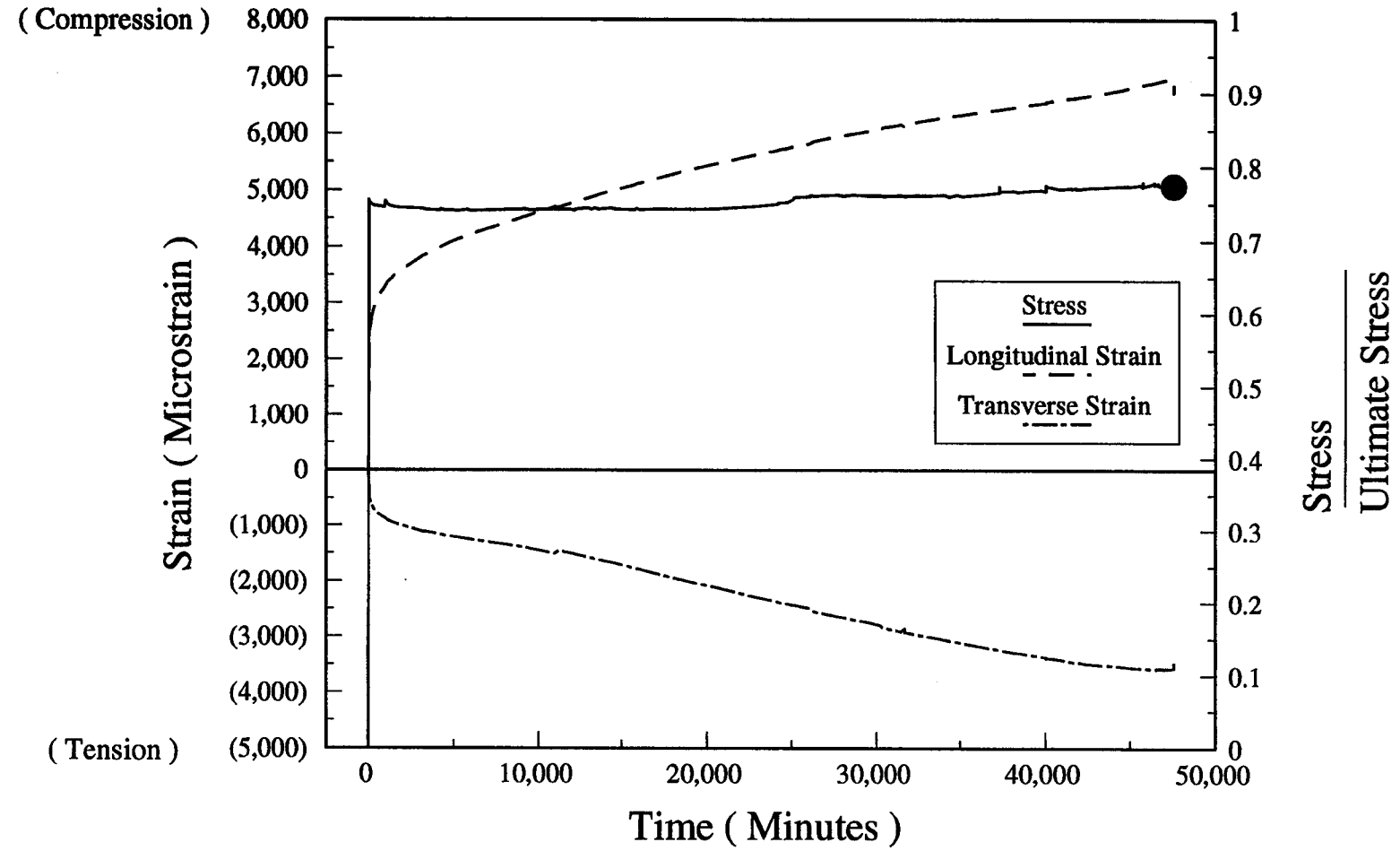

$f_c = 65.5$ MPa $\qquad A = 8089\ mm^2$

Figure 4.5.1.2.E - Stress-Strain-Time Relationship - LHC75 Specimen

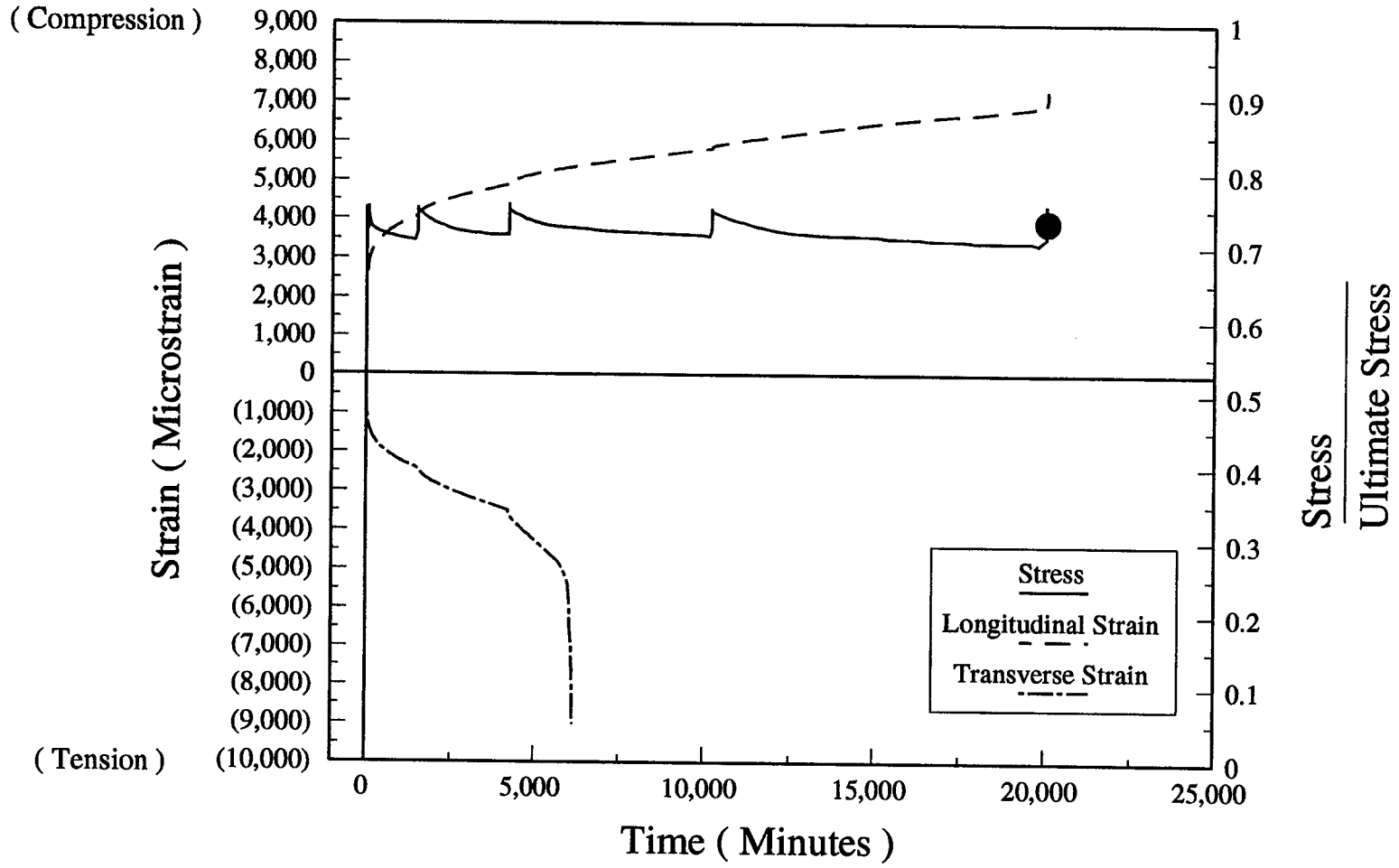

$f_c = 66.0$ MPa $\qquad A = 7804\ mm^2$

Figure 4.5.1.2.F - Stress-Strain-Time Relationship - LHC75(70) Specimen

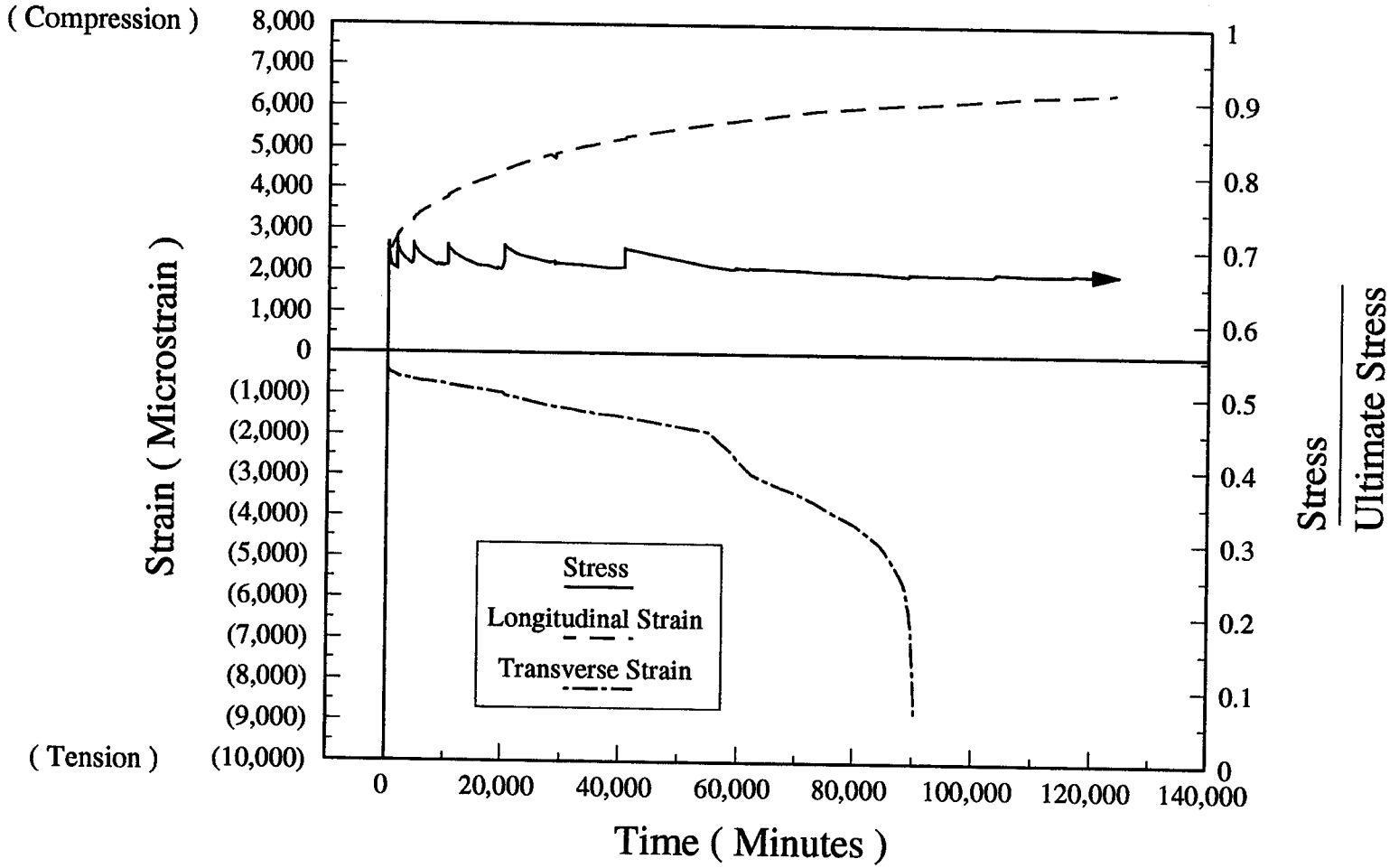

$f_c = 66.0$ MPa $\qquad A = 8129\ mm^2$

Figure 4.5.1.2.G - Stress-Strain-Time Relationship - LHC70(70) Specimen

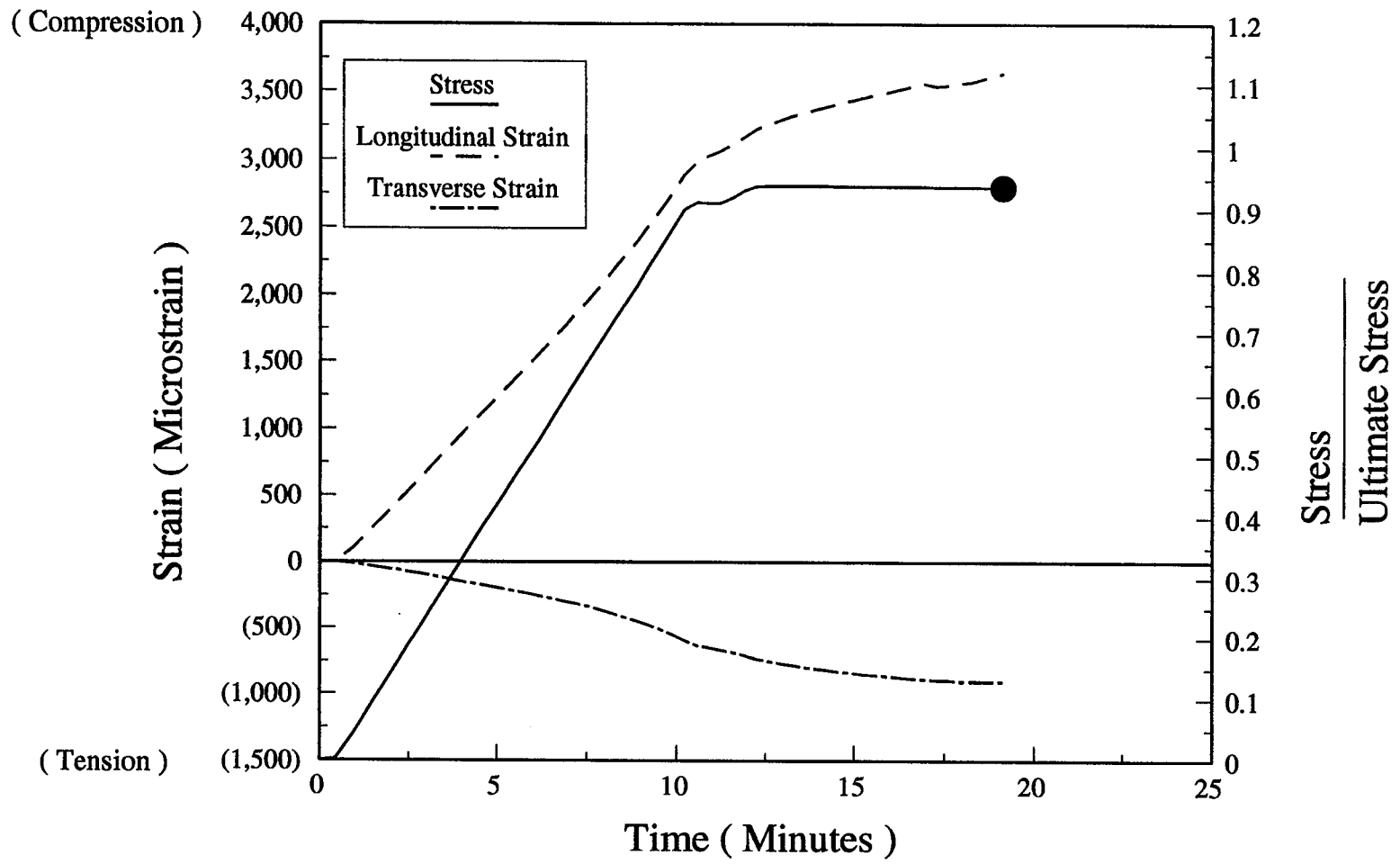

f_c= 95.3 MPa A = 8166 mm^2

Figure 4.5.1.3.A - Stress-Strain-Time Relationship - UHC95 Specimen

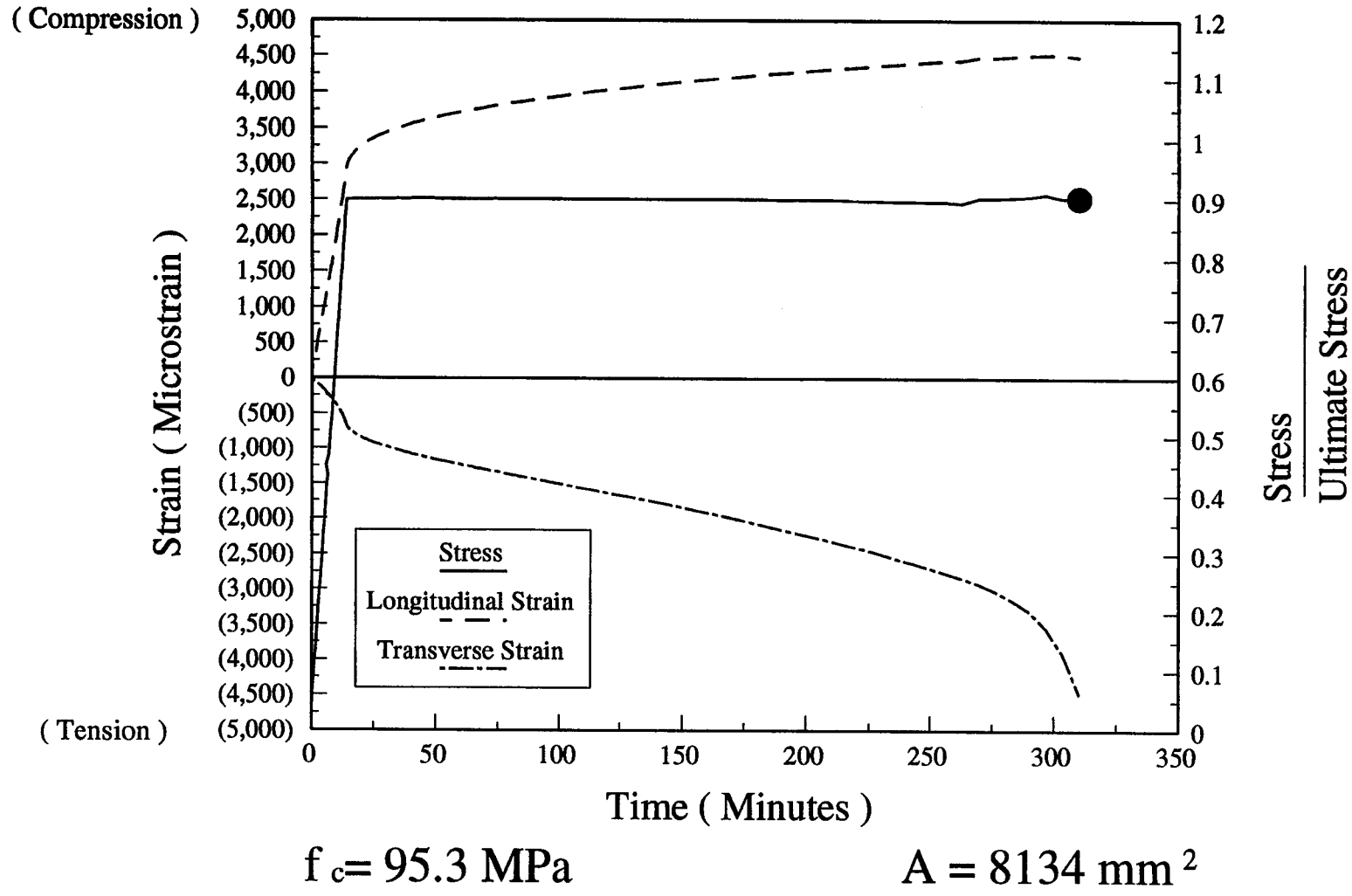

Figure 4.5.1.3.B - Stress-Strain-Time Relationship - UHC90 Specimen

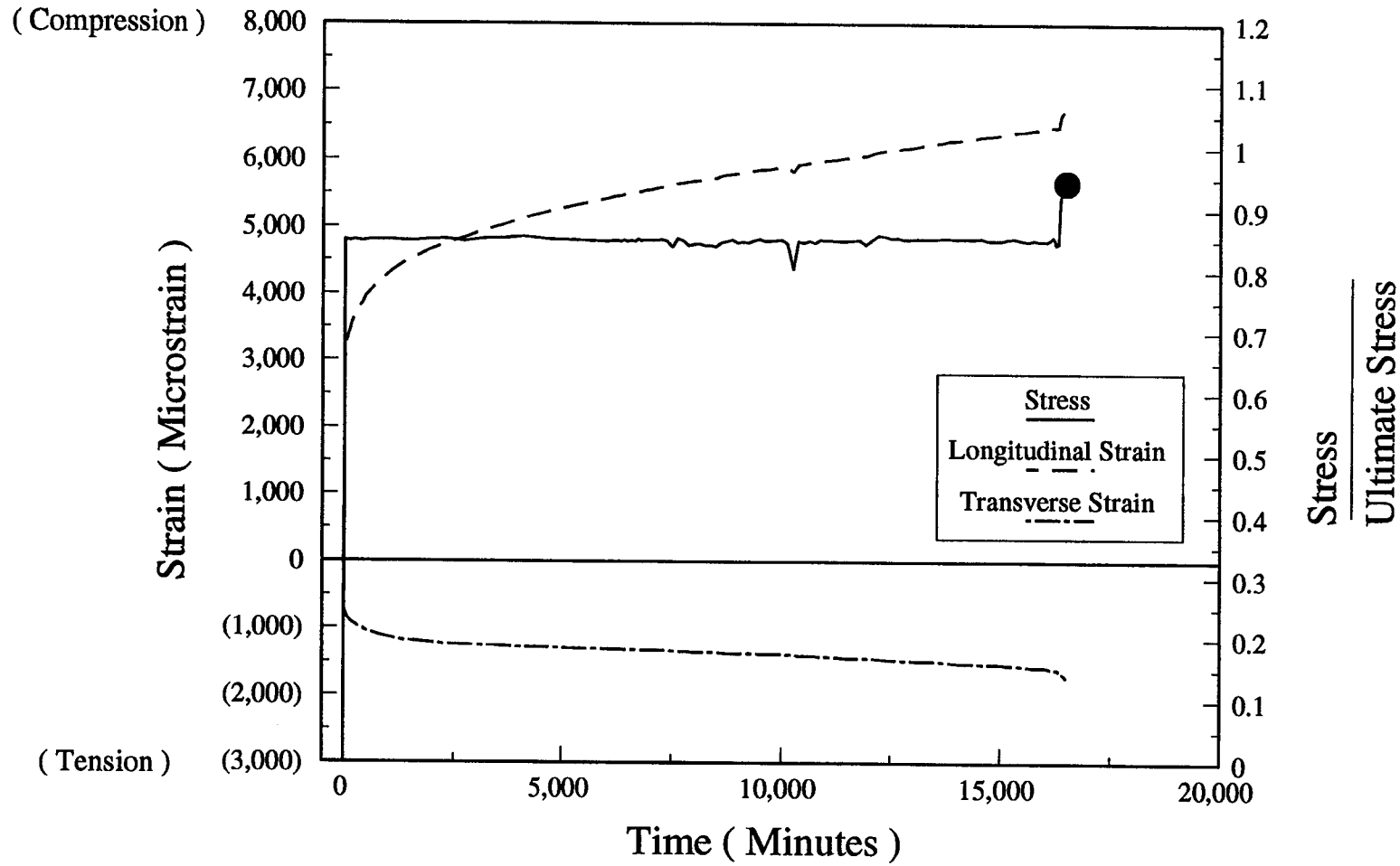

$f_c = 95.3$ MPa $\qquad A = 7755\ mm^2$

Figure 4.5.1.3.C - Stress-Strain-Time Relationship - UHC85 Specimen

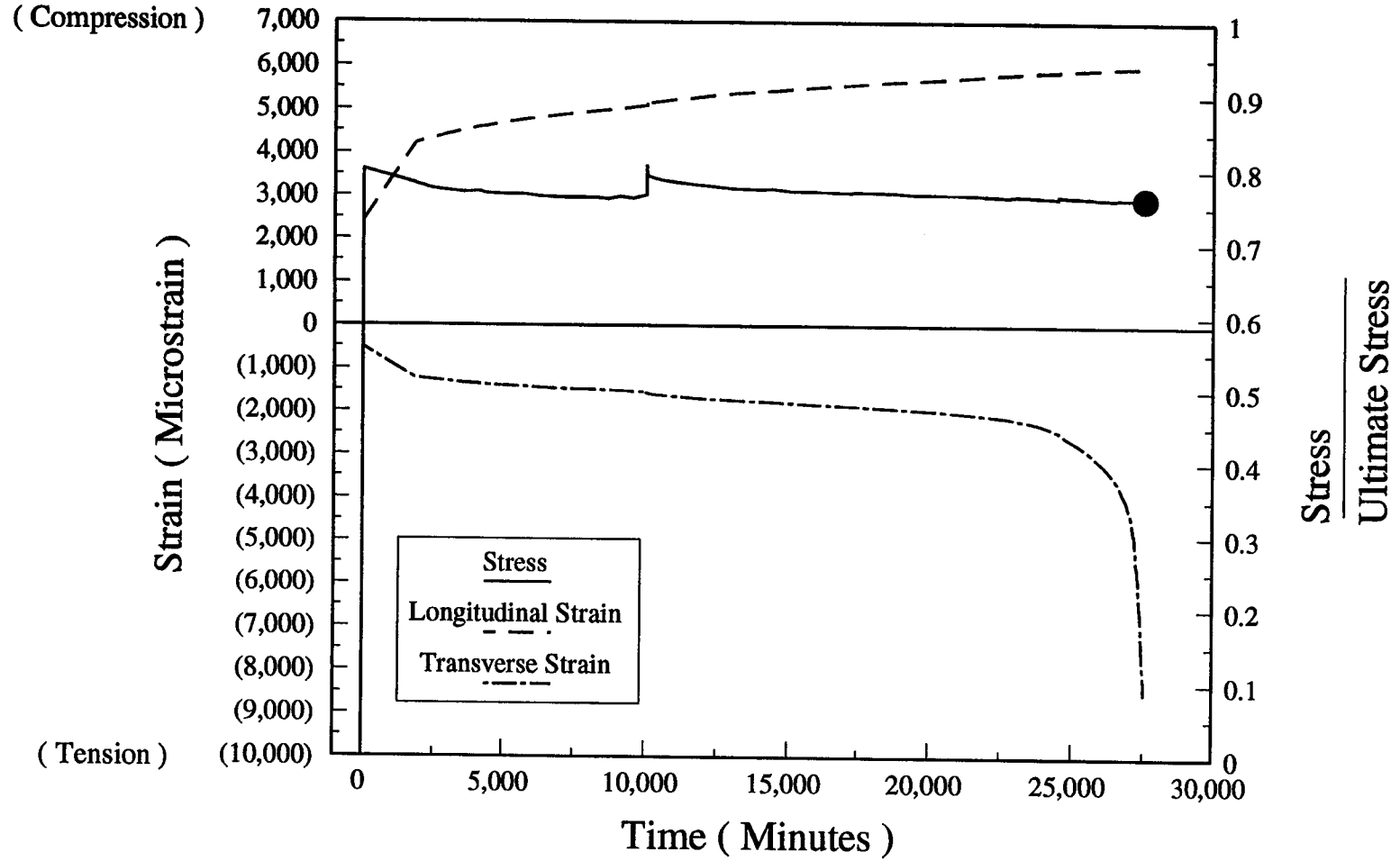

$f_c = 95.3$ MPa $\qquad A = 8115\ mm^2$

Figure 4.5.1.3.D - Stress-Strain-Time Relationship - UHC80 Specimen

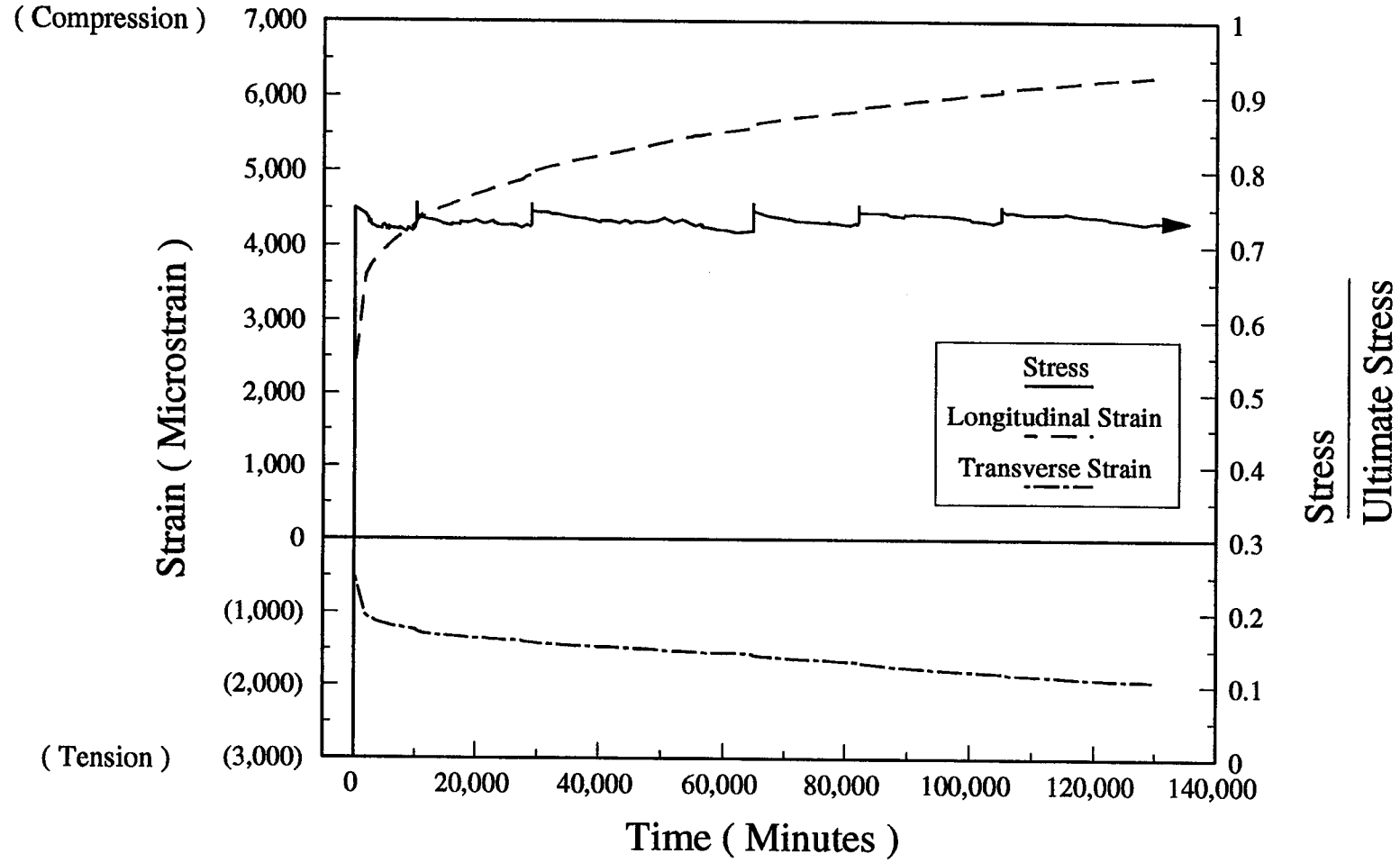

$f_c = 95.3$ MPa $\qquad A = 8179\ mm^2$

Figure 4.5.1.3.E - Stress-Strain-Time Relationship - UHC75 Specimen

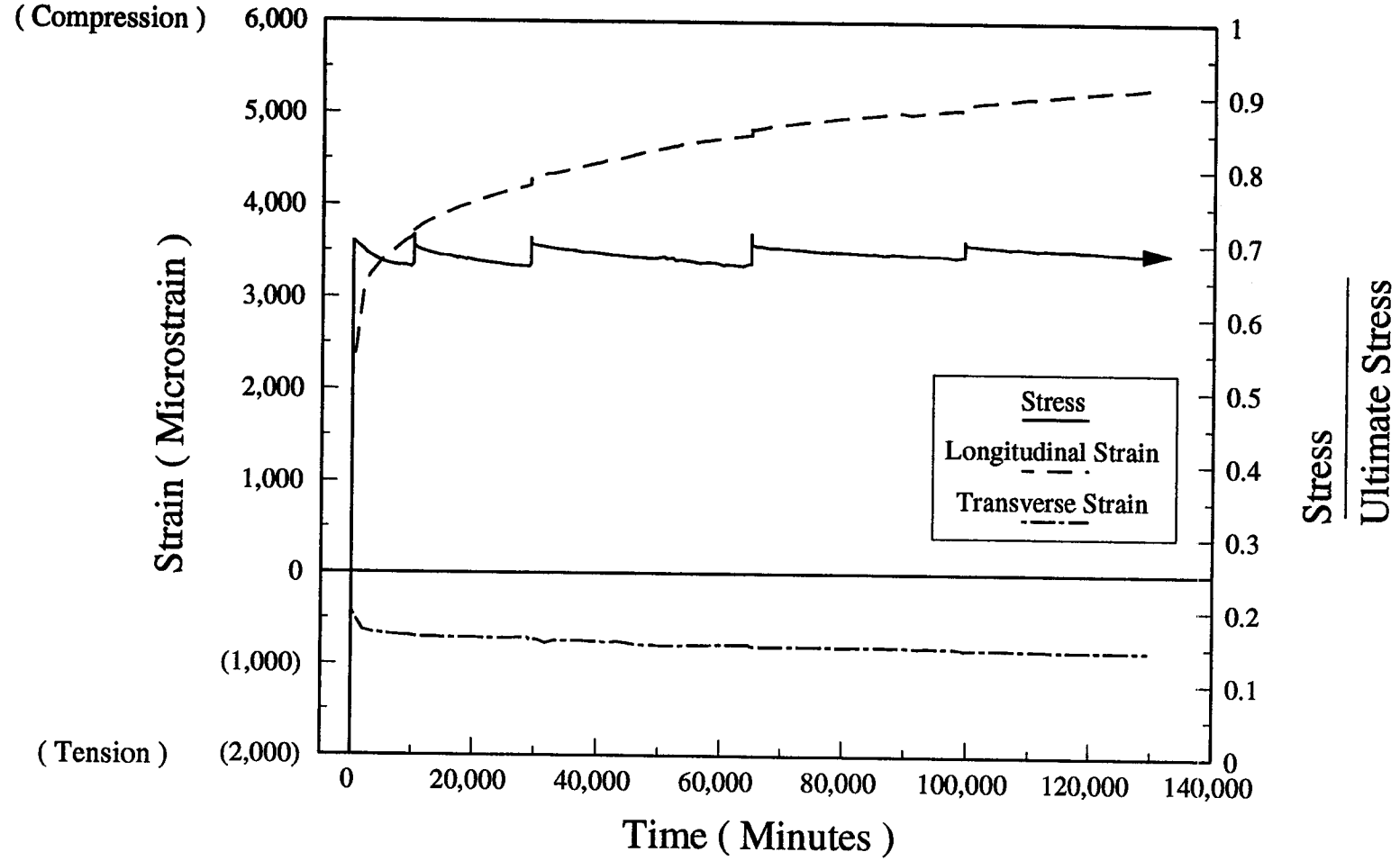

$f_c = 95.3$ MPa $\qquad A = 7781\ mm^2$

Figure 4.5.1.3.F - Stress-Strain-Time Relationship - UHC70 Specimen

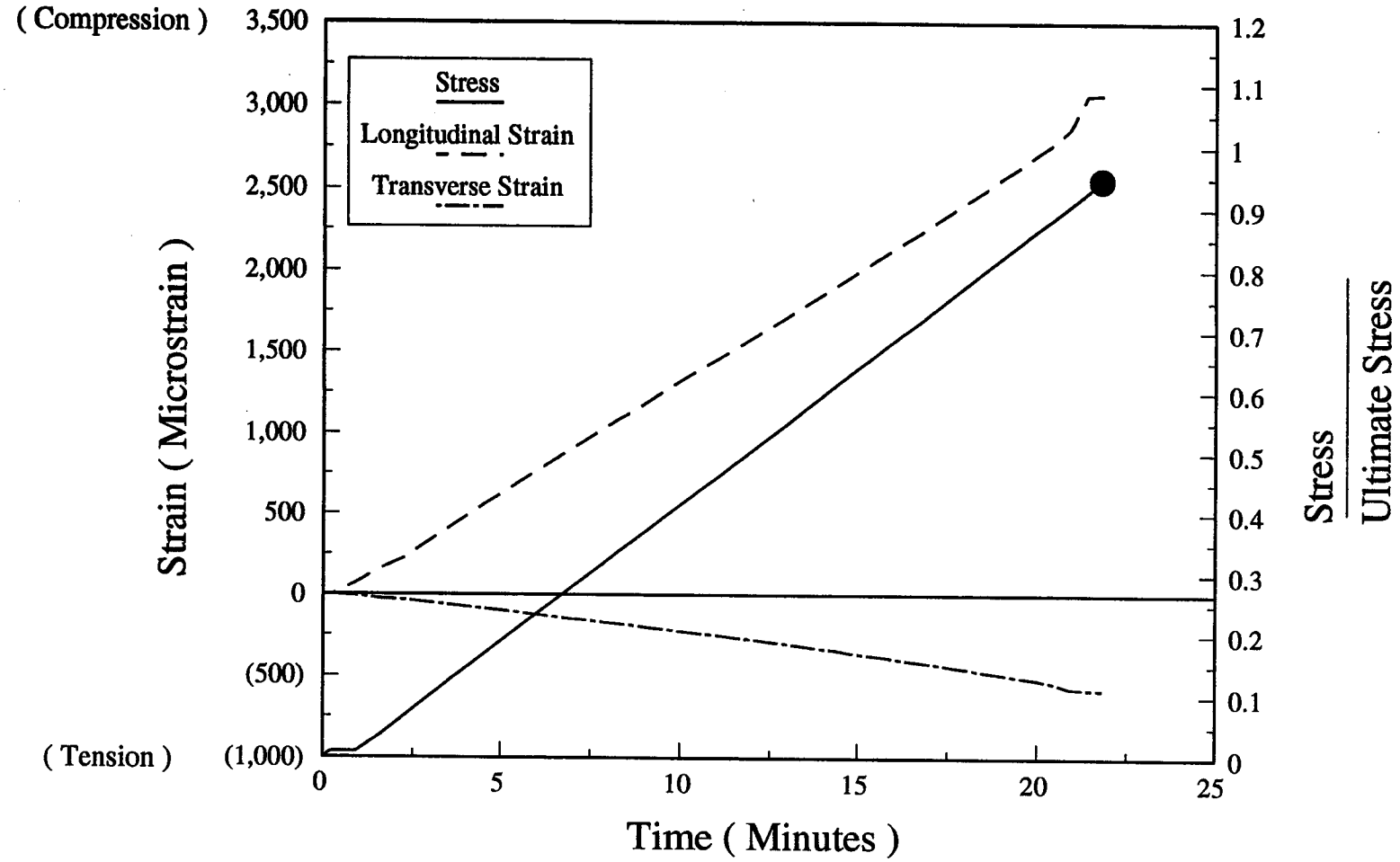

f_c= 120.5 MPa A = 7693 mm^2

Figure 4.5.1.4.A - Stress-Strain-Time Relationship - UUC95 Specimen

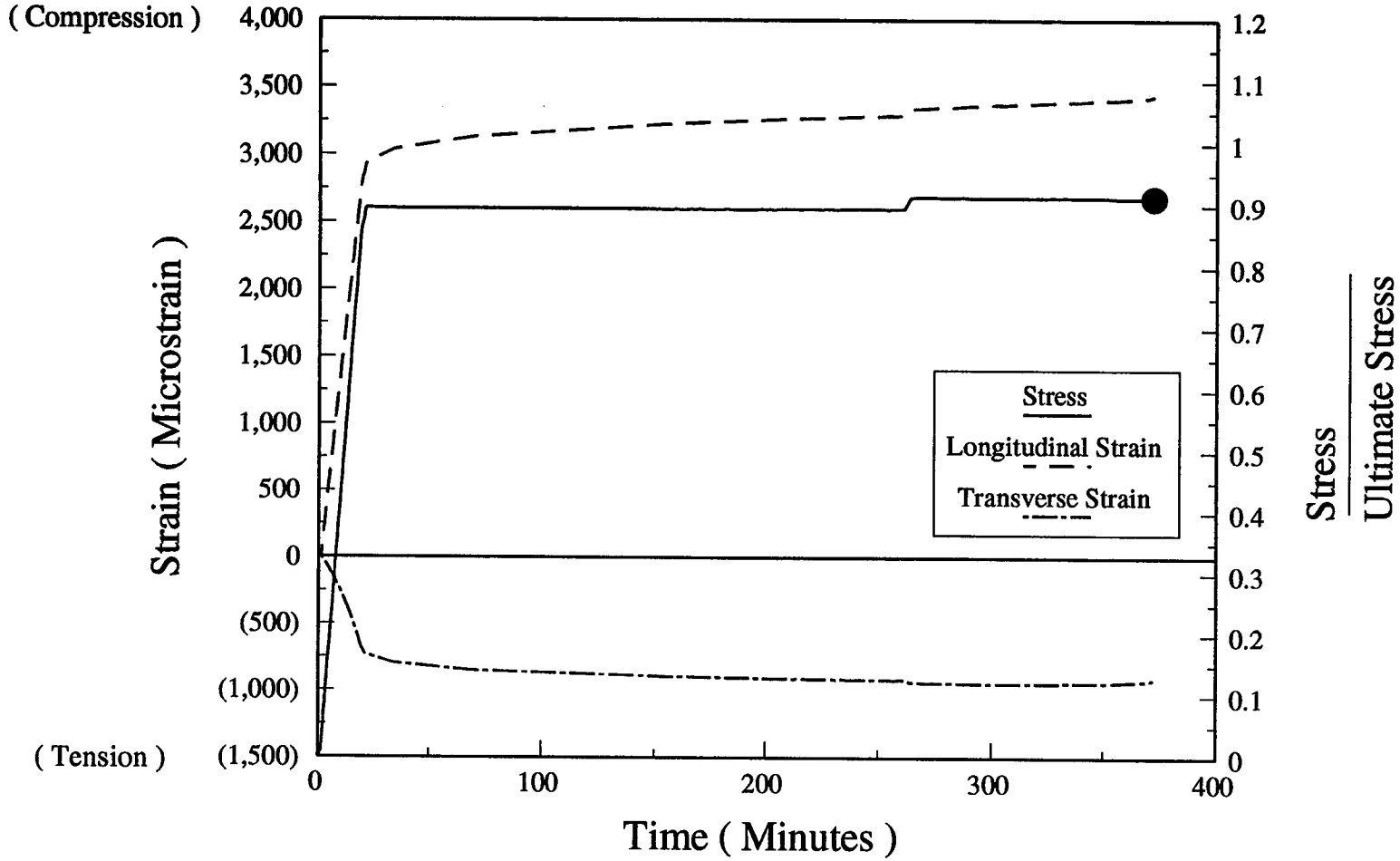

f_c= 120.5 MPa A = 8244 mm^2

Figure 4.5.1.4.B - Stress-Strain-Time Relationship - UUC90 Specimen

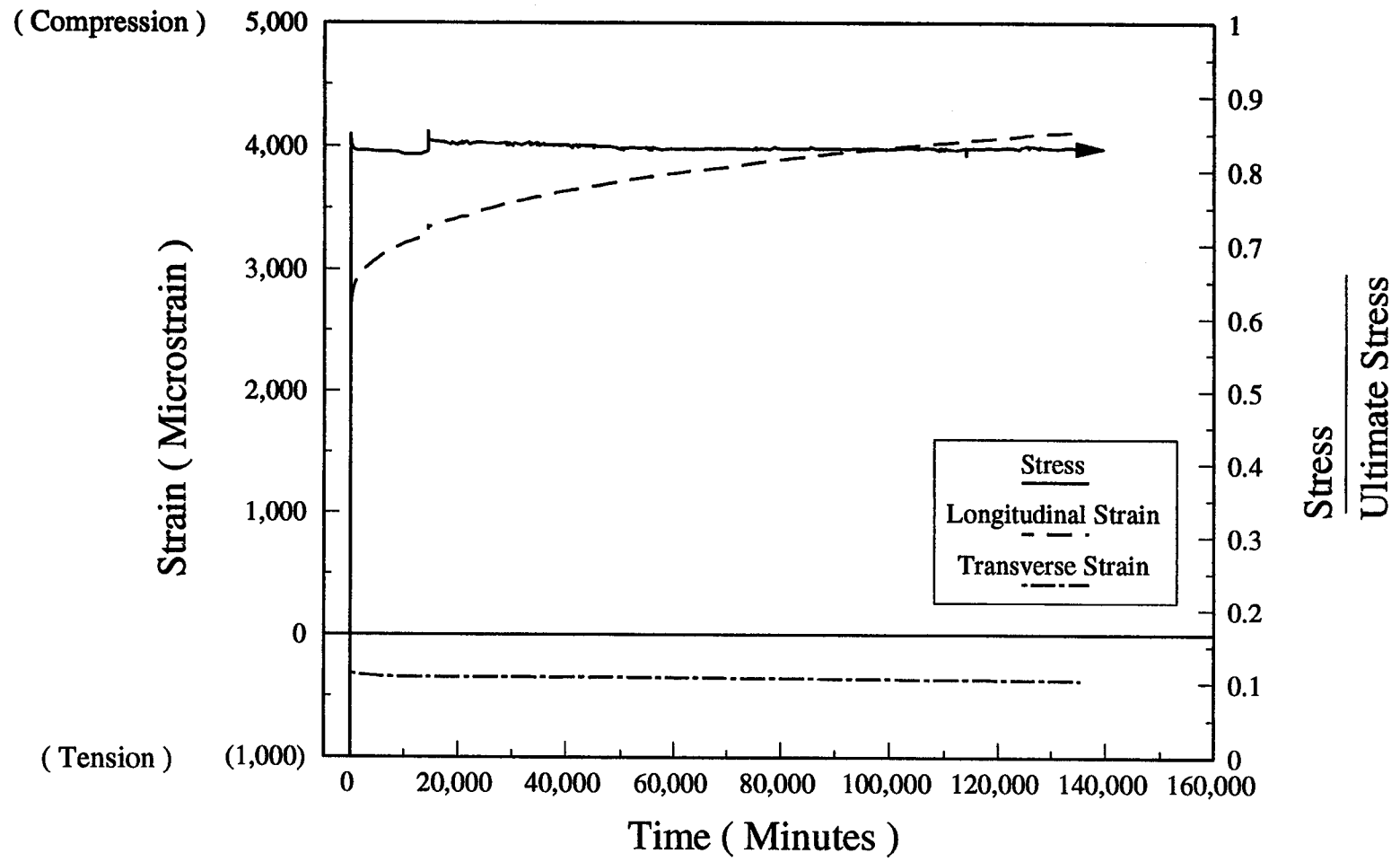

f_c= 119.8 MPa A = 7917 mm^2

Figure 4.5.1.4.C - Stress-Strain-Time Relationship - UUC85(70) Specimen

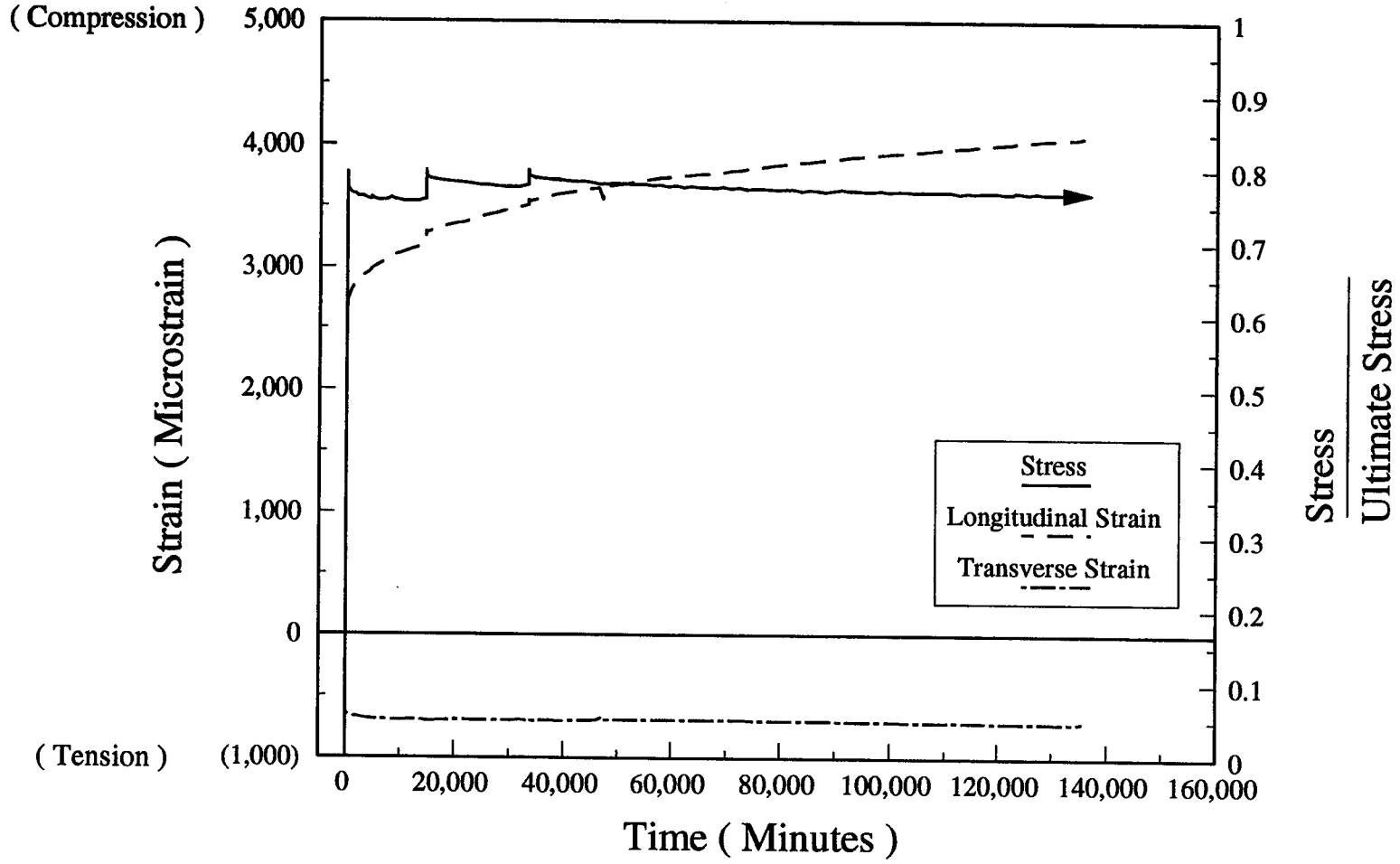

f_c = 119.8 MPa A = 7643 mm^2

Figure 4.5.1.4.D - Stress-Strain-Time Relationship - UUC80(70) Specimen

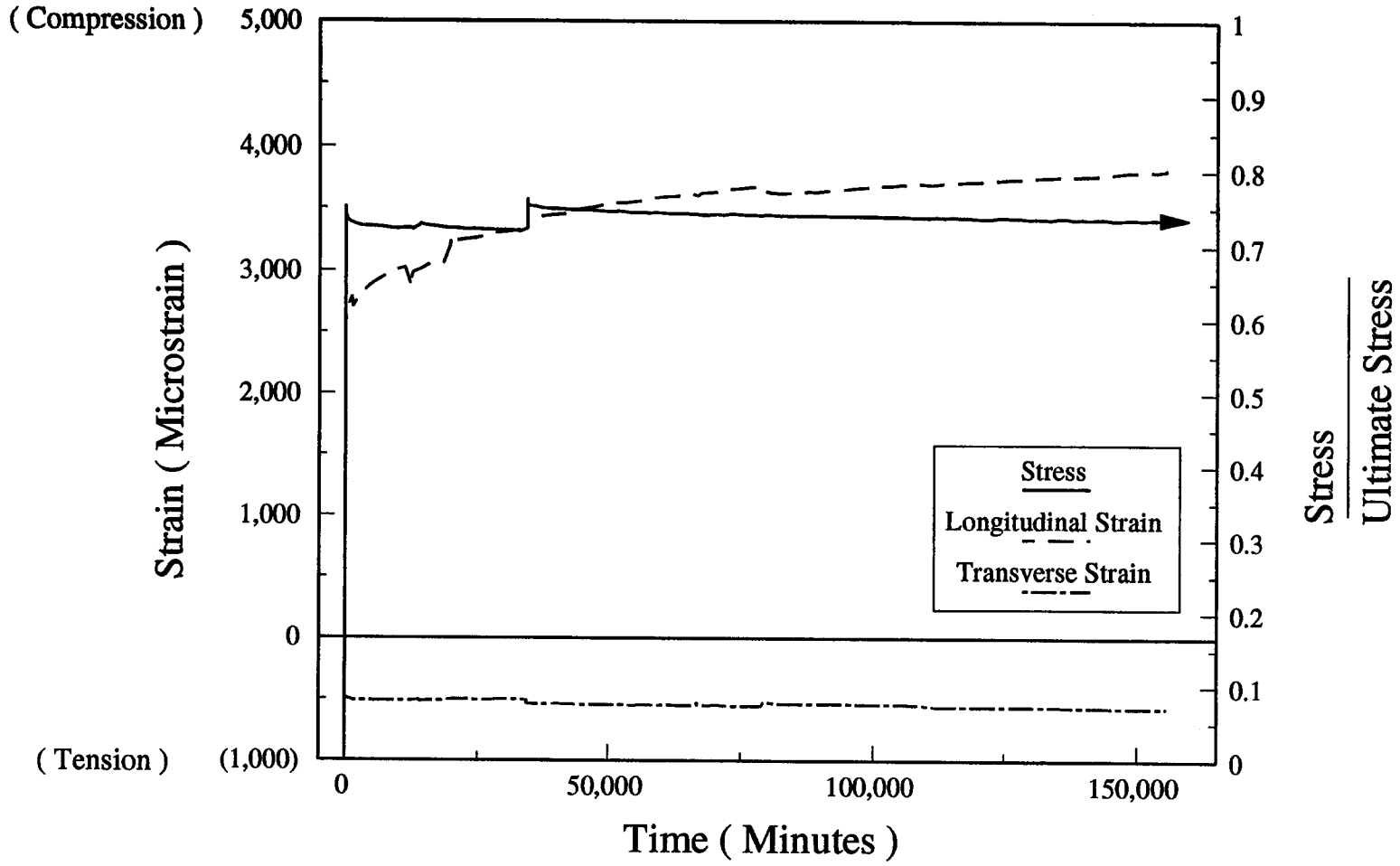

f_c = 120.5 MPa A = 8139 mm^2

Figure 4.5.1.4.E - Stress-Strain-Time Relationship - UUC75 Specimen

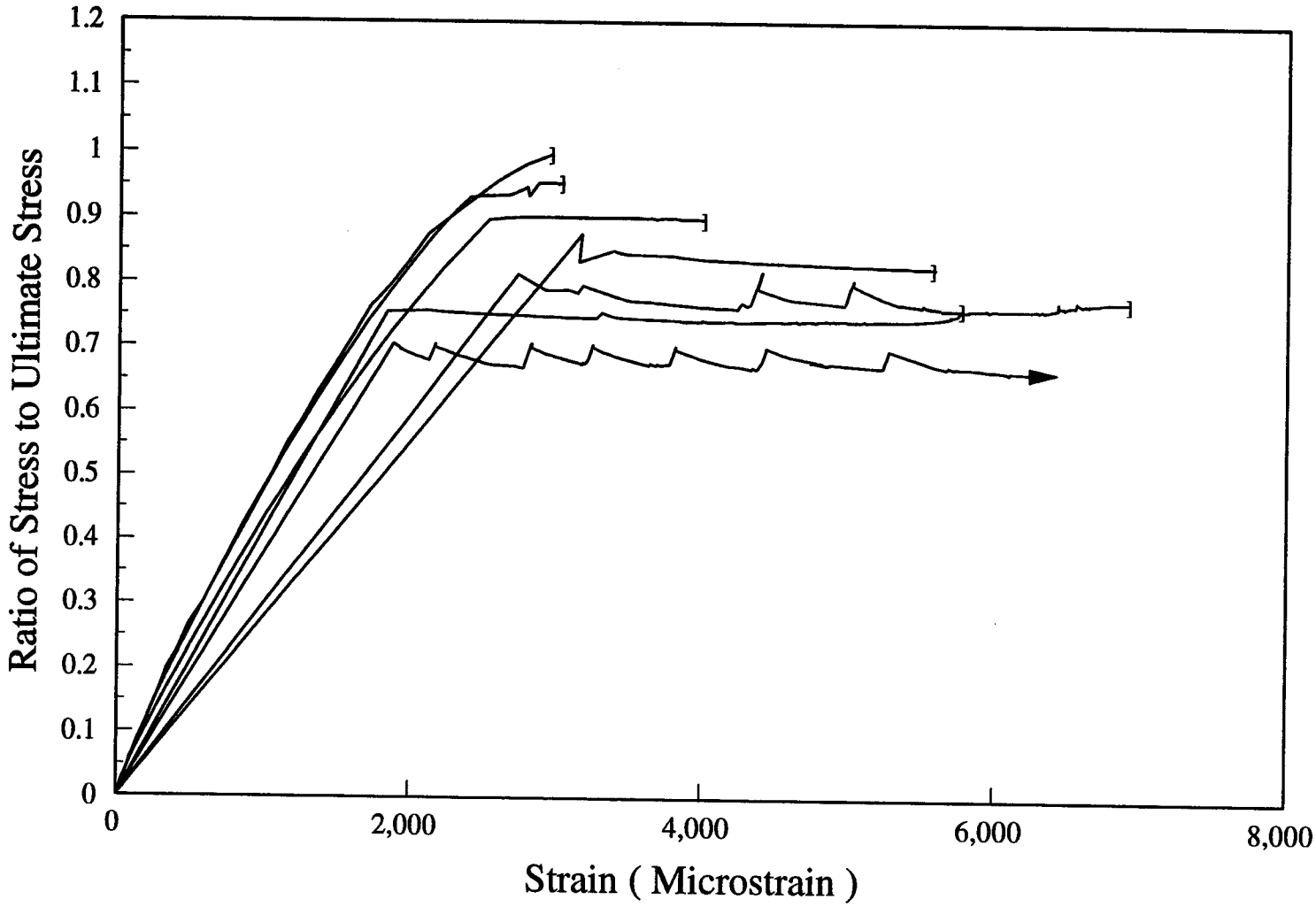

Figure 4.5.2.A - Stress-Strain Relationship - LH Concentric Series

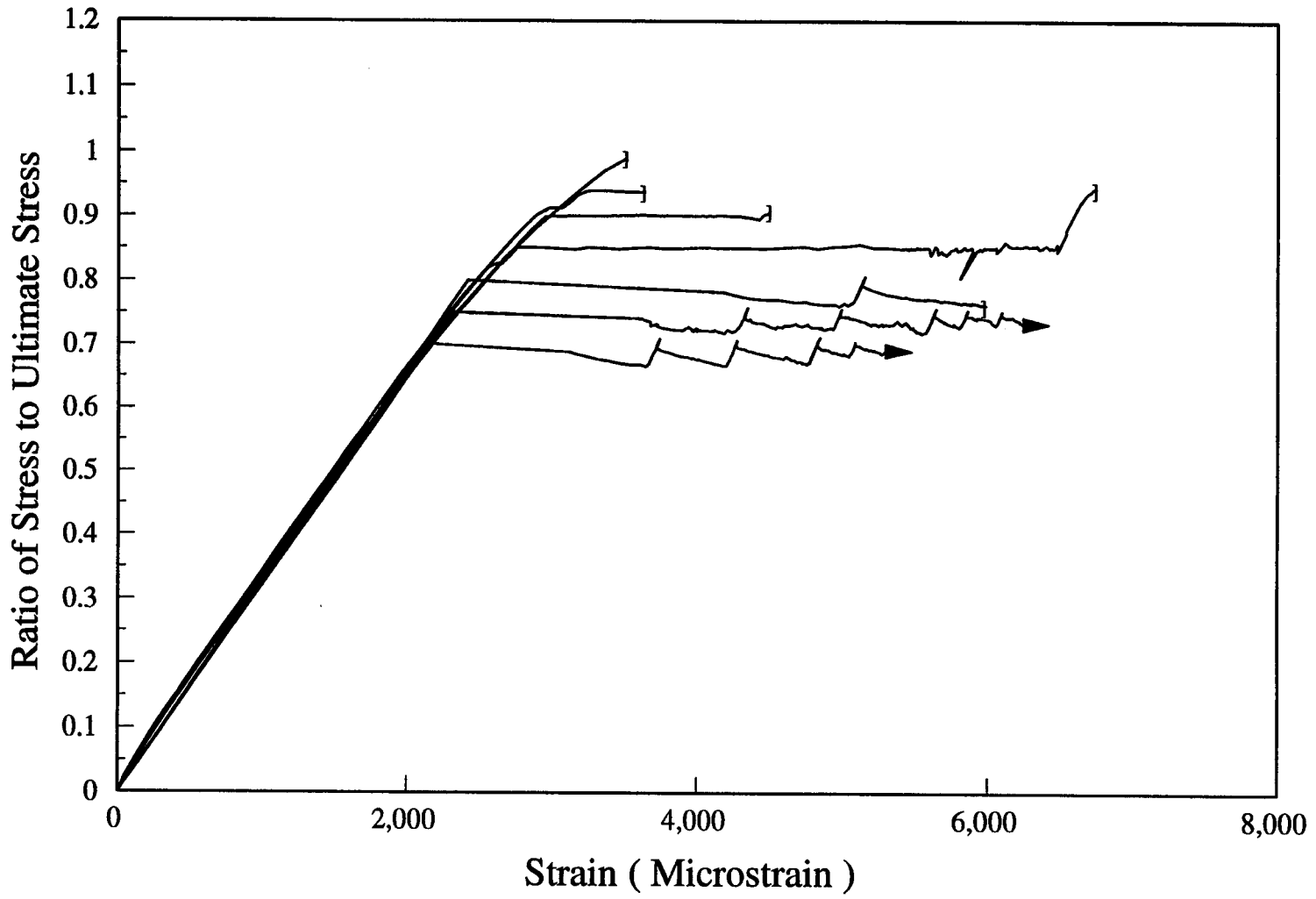

Figure 4.5.2.B - Stress-Strain Relationship - UH Concentric Series

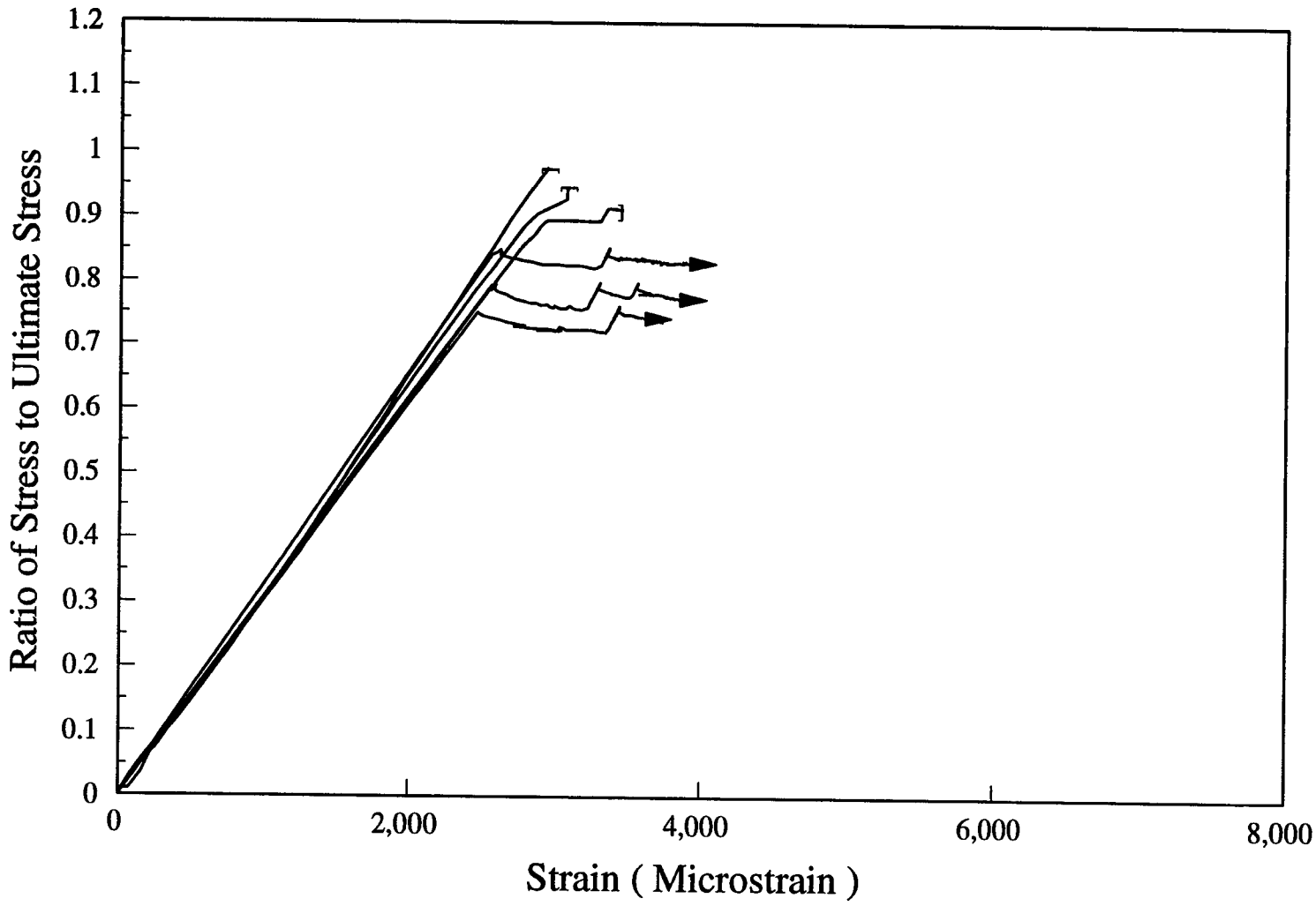

Figure 4.5.2.C - Stress-Strain Relationship - UU Concentric Series

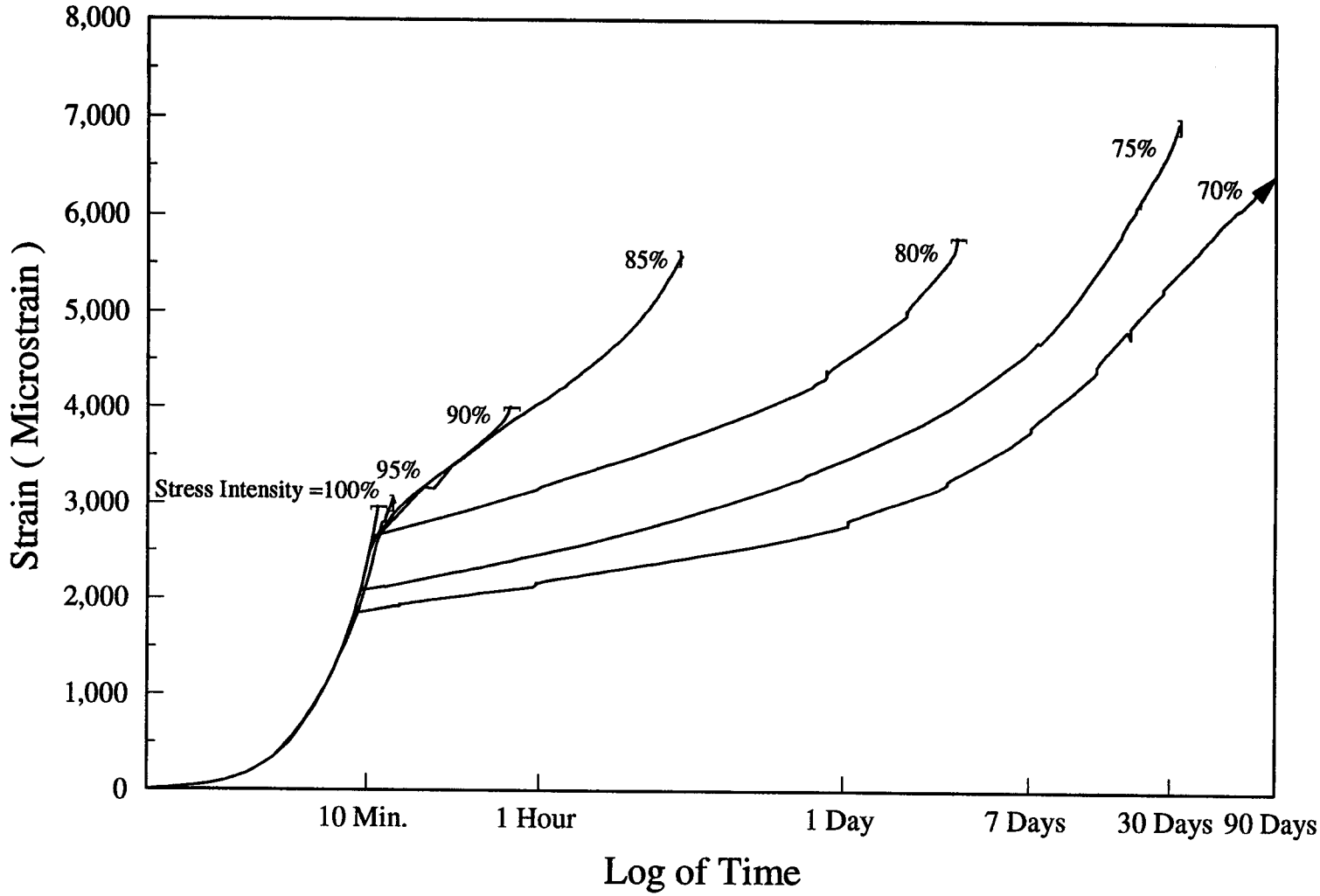

Figure 4.5.2.D - Strain-Time Relationship - LH Concentric Series

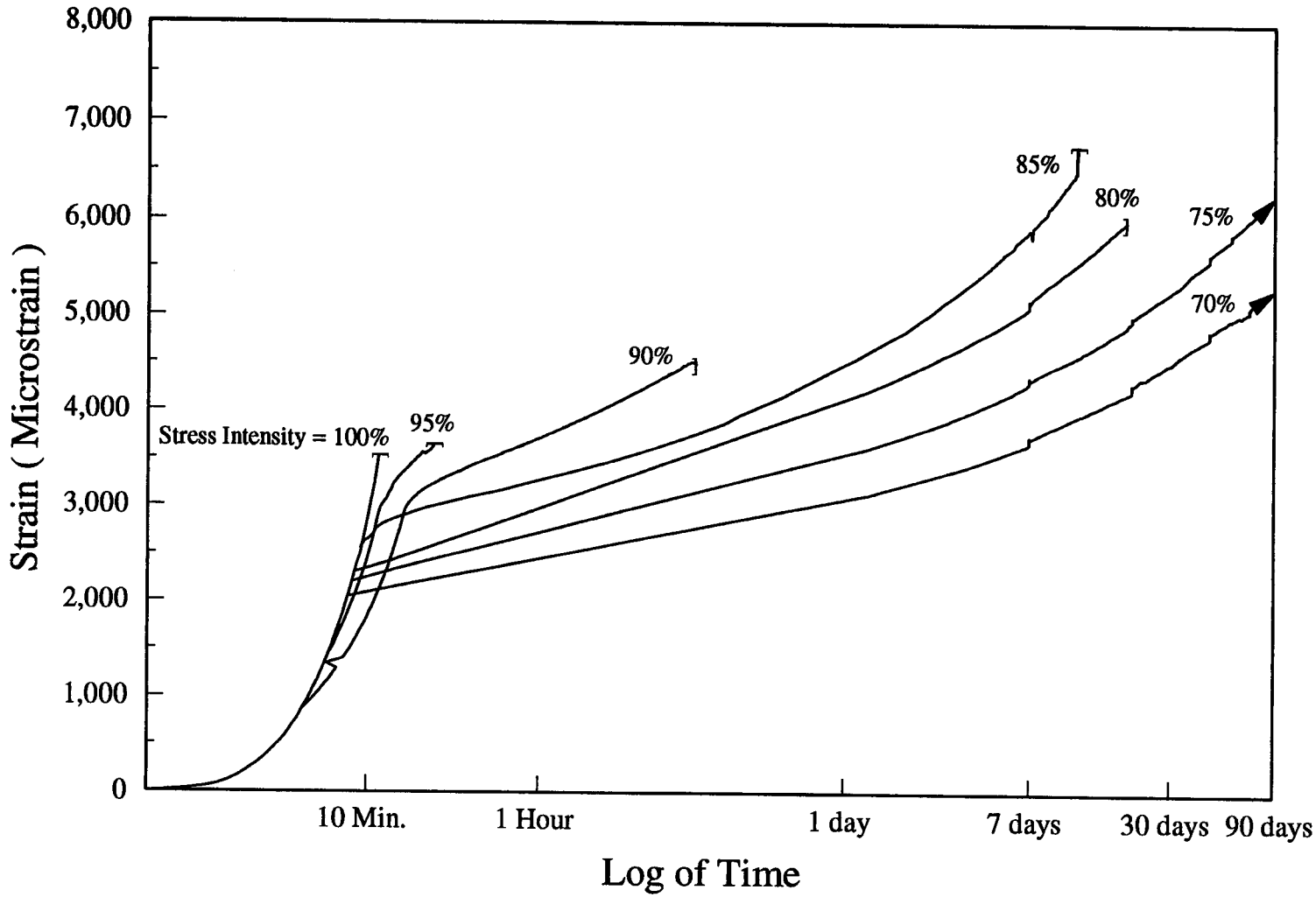

Figure 4.5.2.E - Strain-Time Relationship - UH Concentric Series

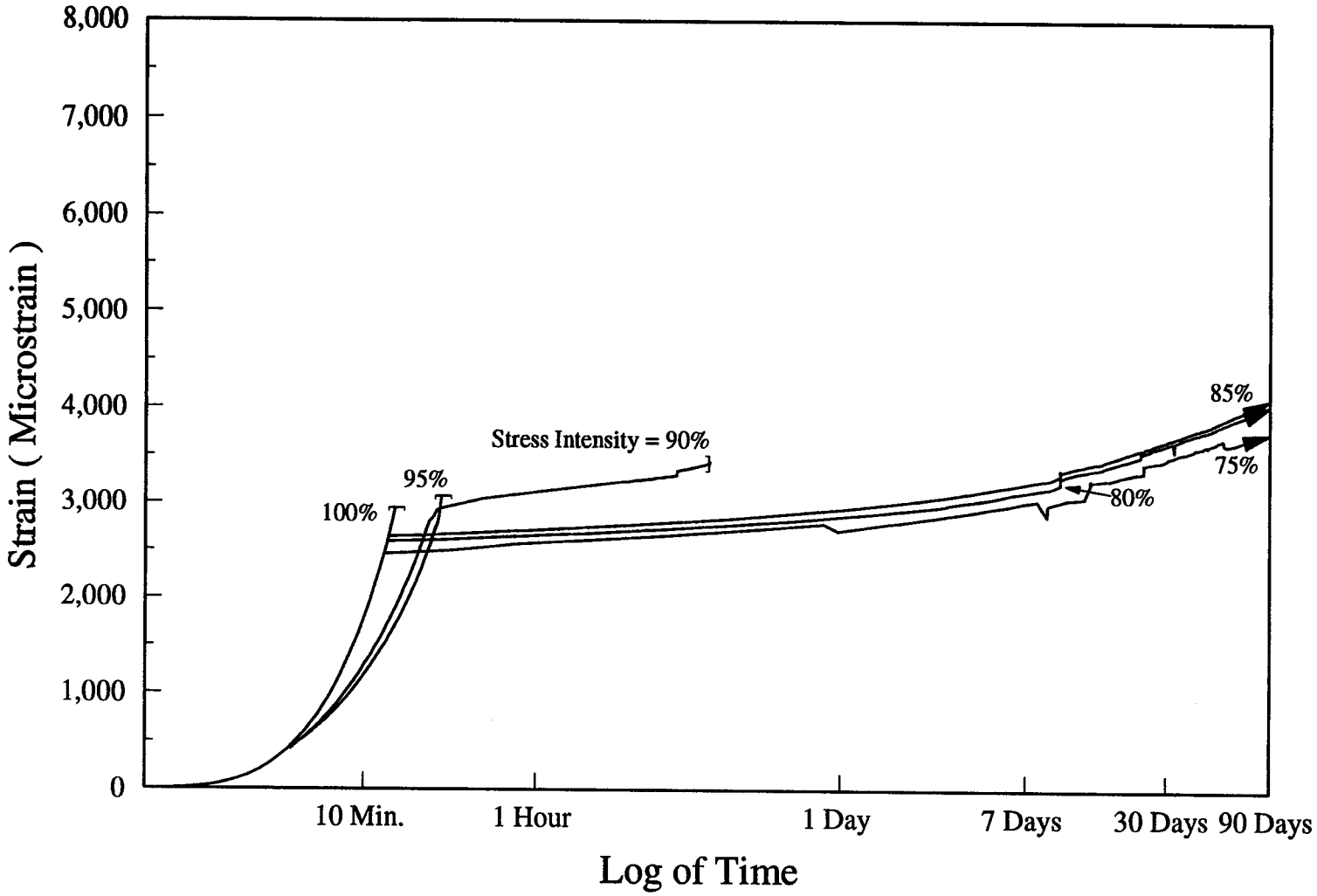

Figure 4.5.2.F - Strain-Time Relationship - UU Concentric Series

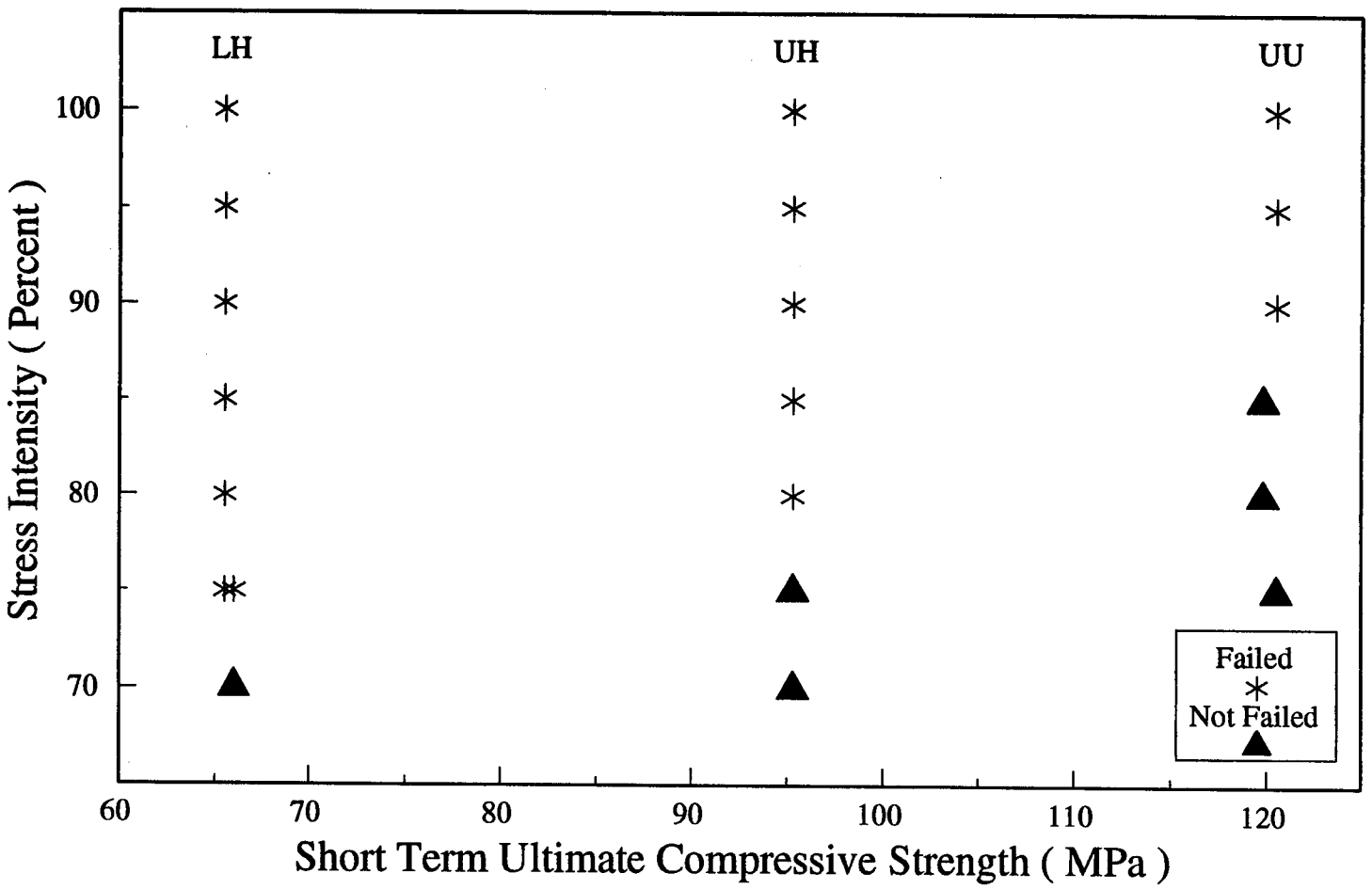

Figure 4.5.2.G - Summary of Concentric Test Results

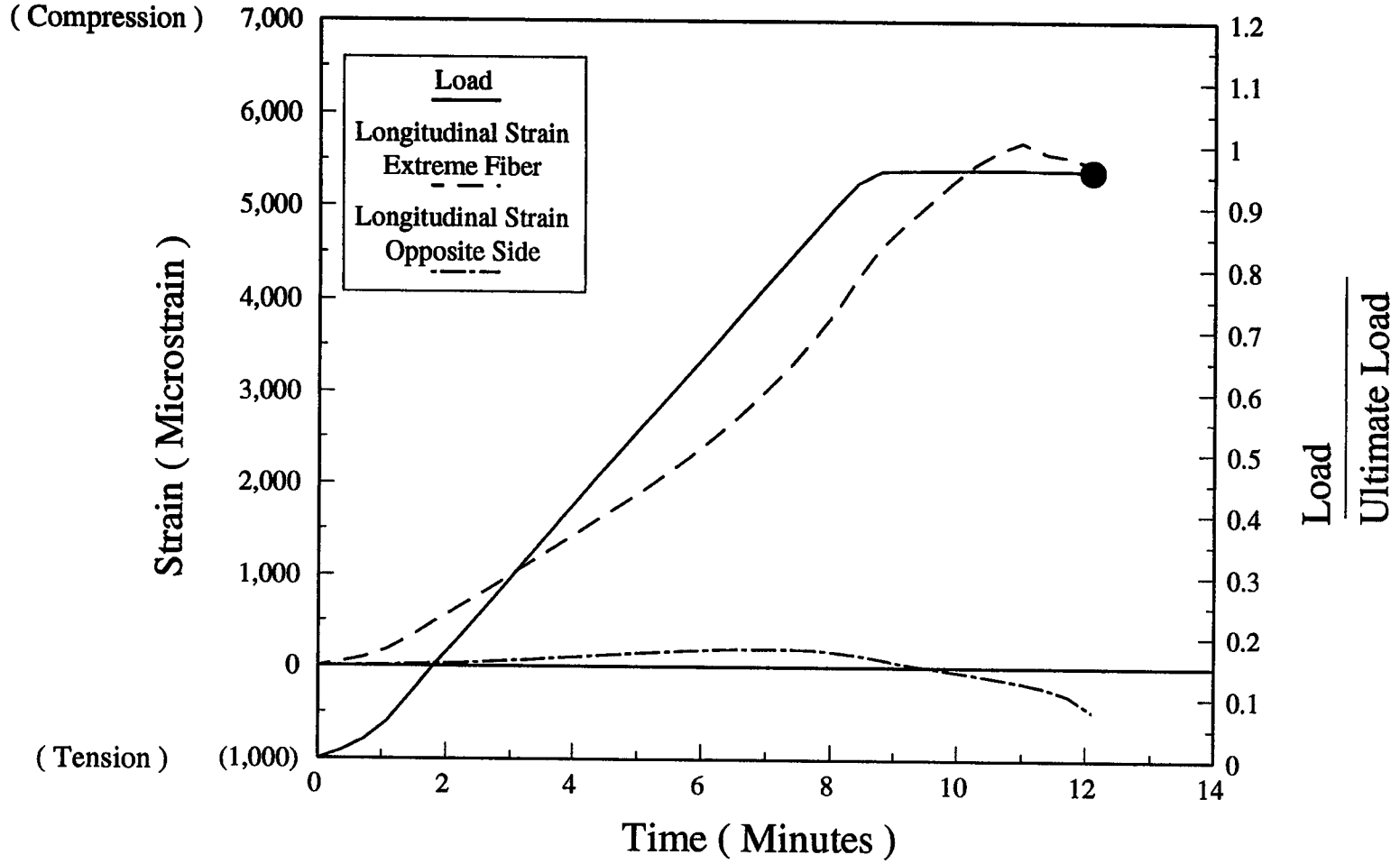

$P_c = 397.5$ kN $\qquad A = 8102$ mm^2

Figure 4.6.1.2.A - Load-Strain-Time Relationship - LHE95 Specimen

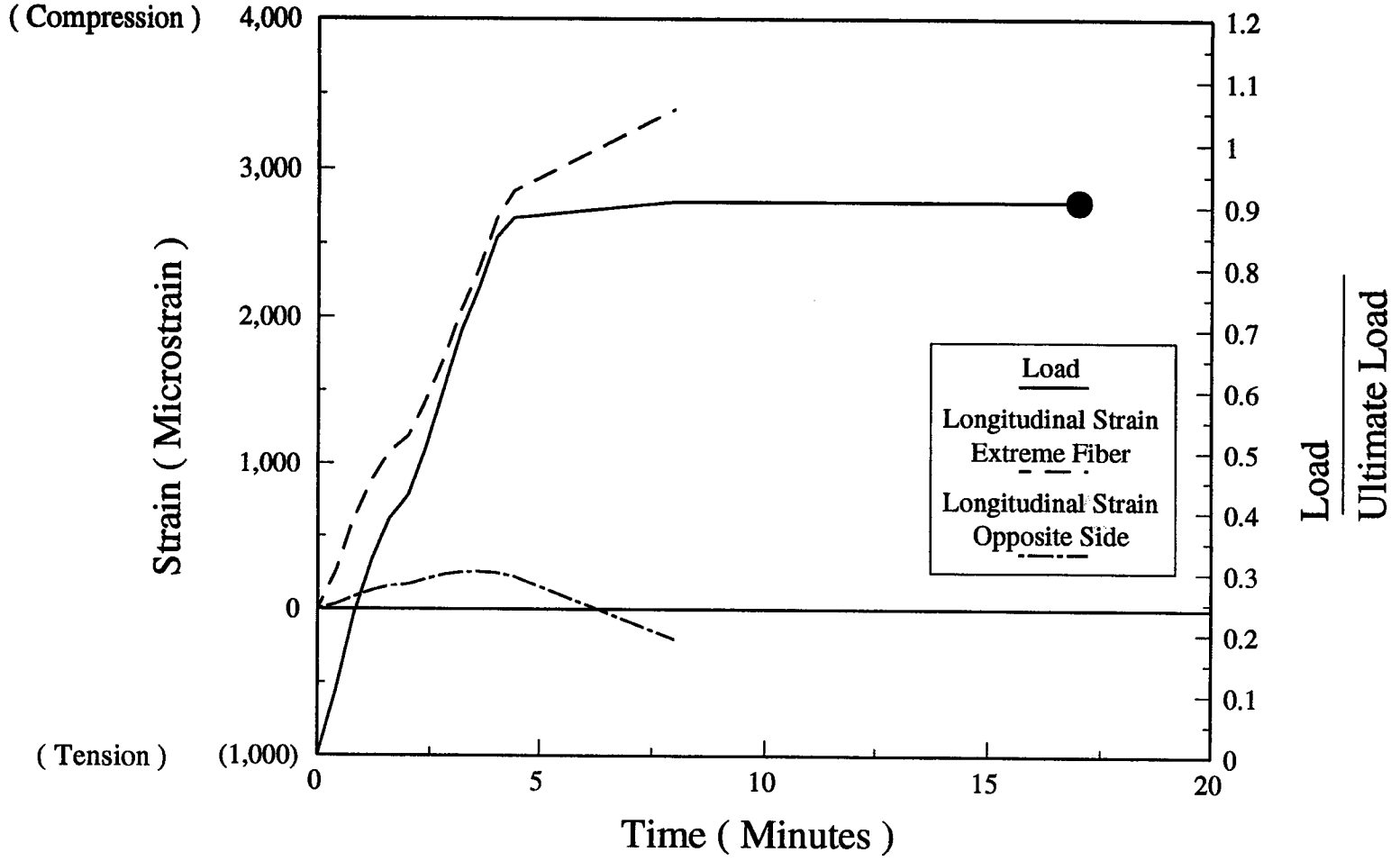

$P_c = 379.8$ kN $\qquad A = 7742$ mm^2

Figure 4.6.1.2.B - Load-Strain-Time Relationship - LHE90 Specimen

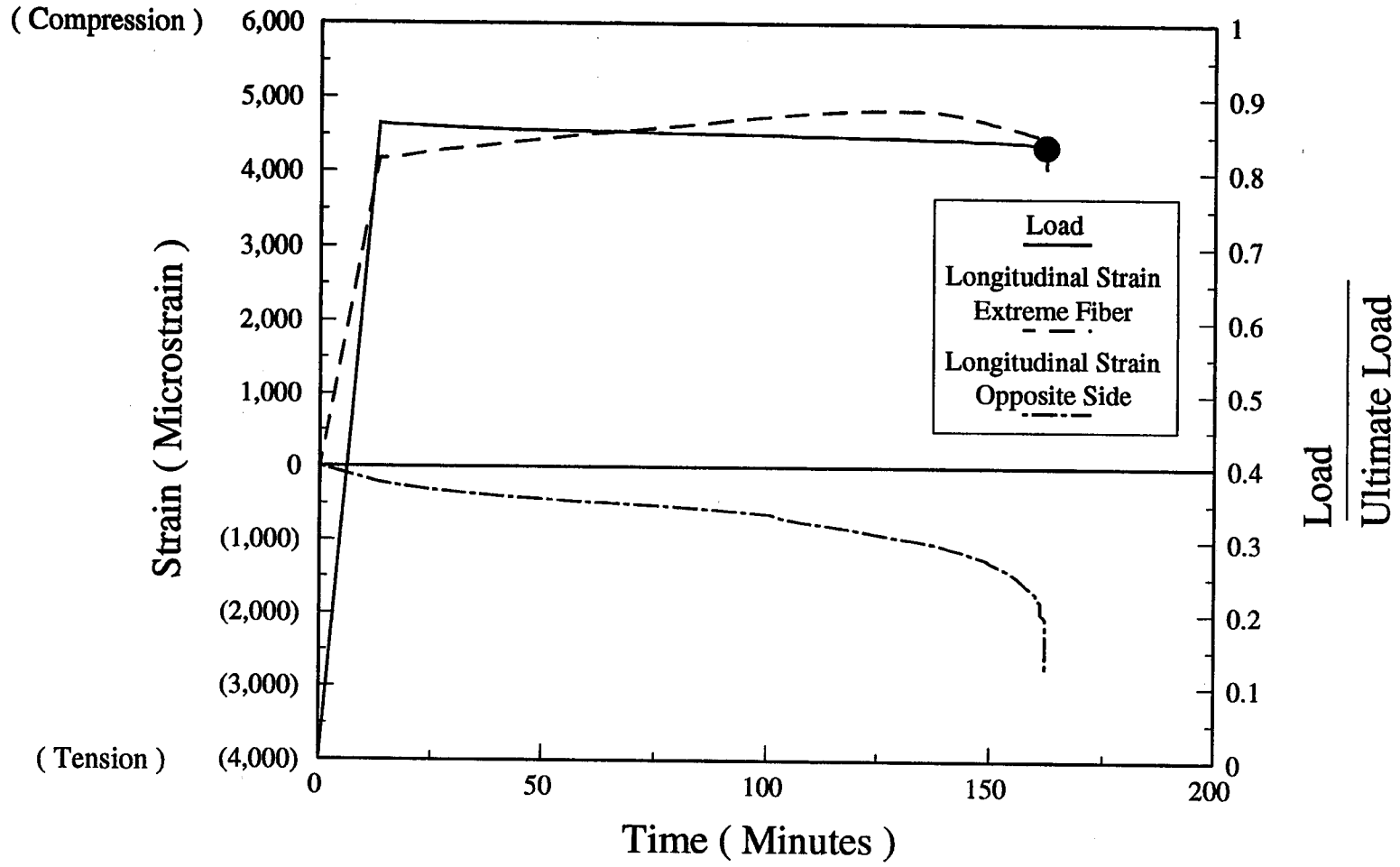

$P_c = 396.4$ kN $\qquad A = 8081$ mm^2

Figure 4.6.1.2.C - Load-Strain-Time Relationship - LHE85 Specimen

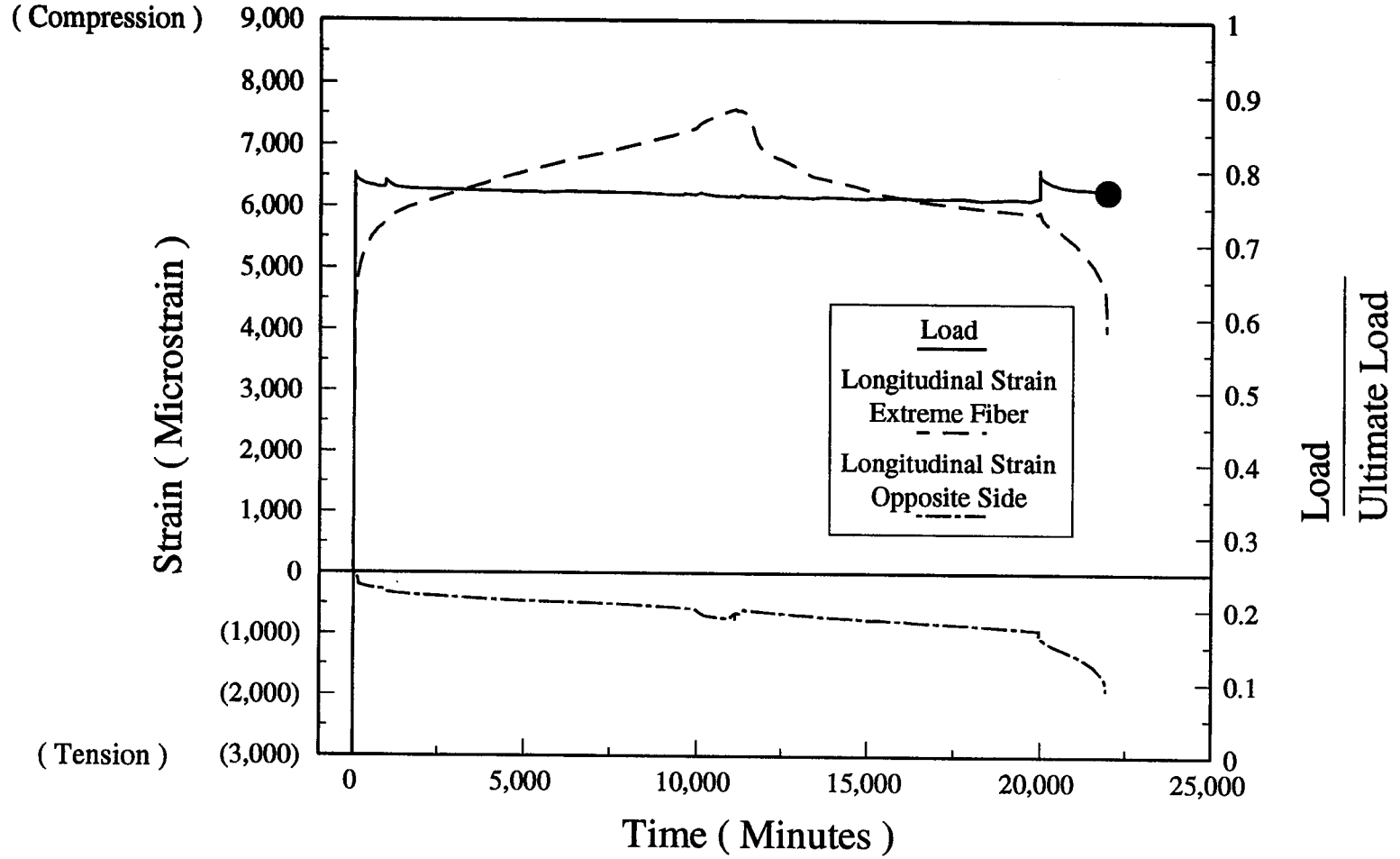

$P_c = 395.4$ kN $\qquad A = 8060$ mm^2

Figure 4.6.1.2.D - Load-Strain-Time Relationship - LHE80 Specimen

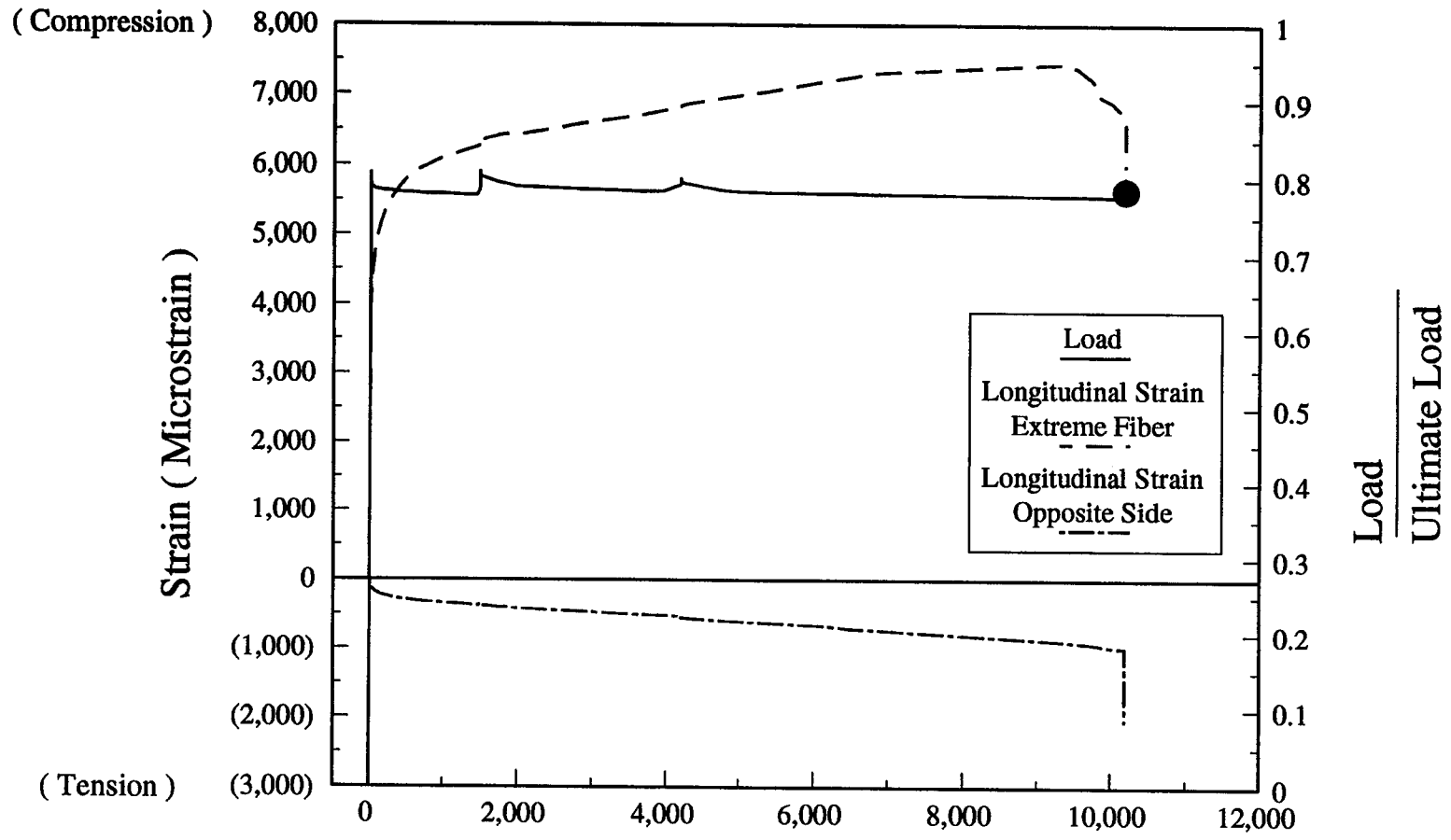

$P_c = 410.4$ kN $\qquad A = 8078$ mm^2

Figure 4.6.1.2.E - Load-Strain-Time Relationship - LHE80(70) Specimen

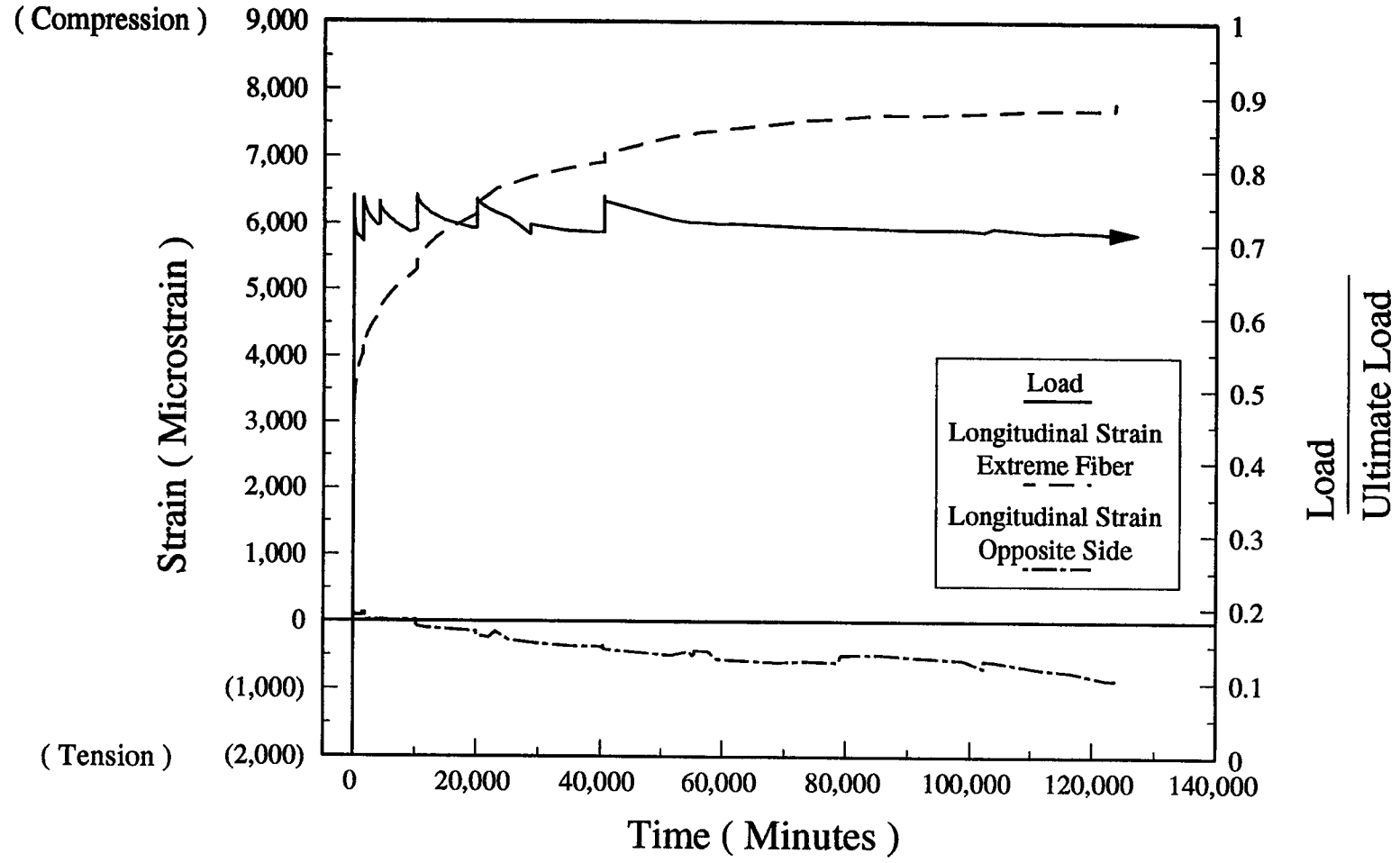

$P_c = 410.4$ kN $\qquad A = 8099$ mm^2

Figure 4.6.1.2.F - Load-Strain-Time Relationship - LHE75(70) Specimen

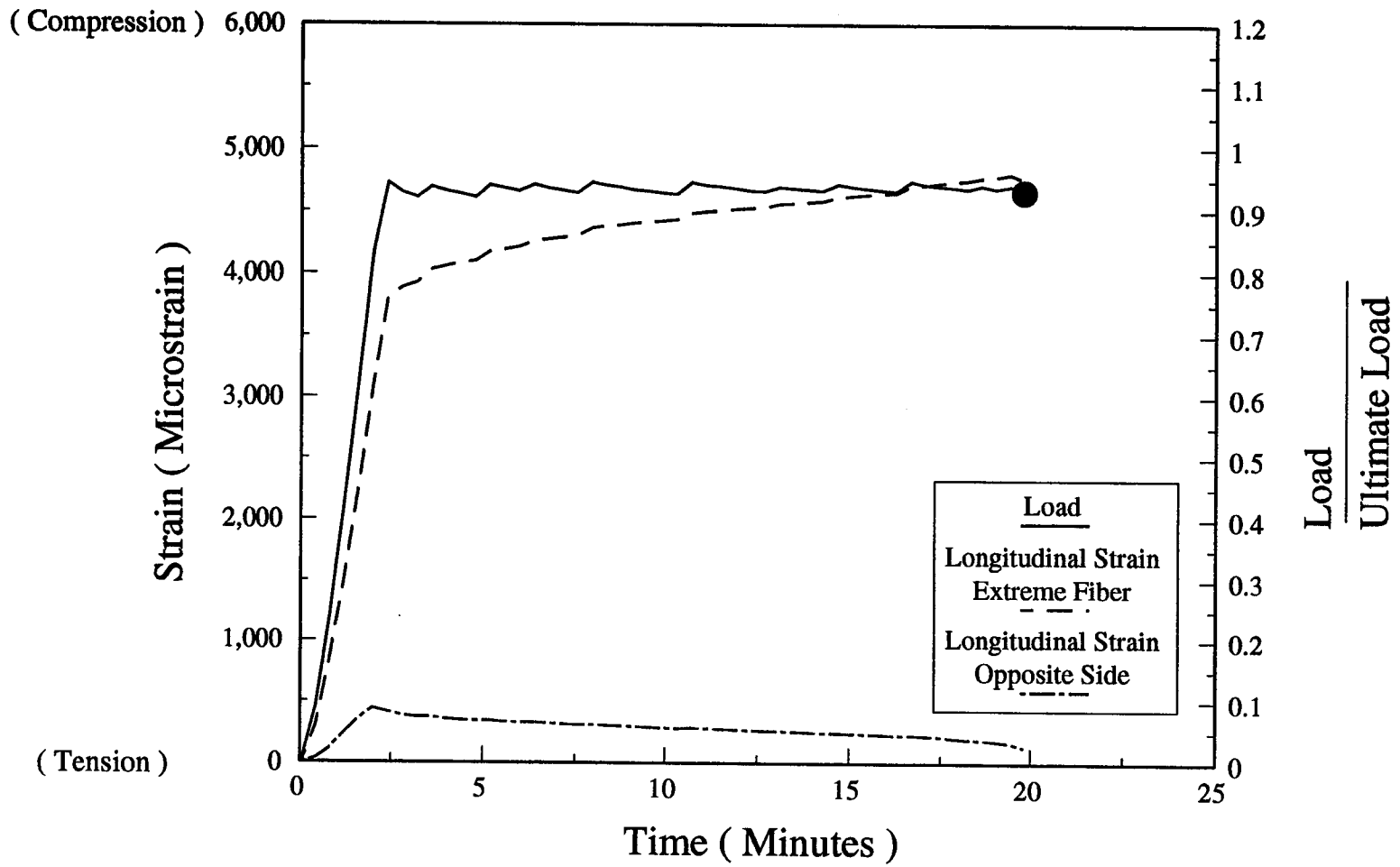

$P_c = 535.1$ kN $\qquad A = 7693$ mm^2

Figure 4.6.1.3.A - Load-Strain-Time Relationship - UHE95 Specimen

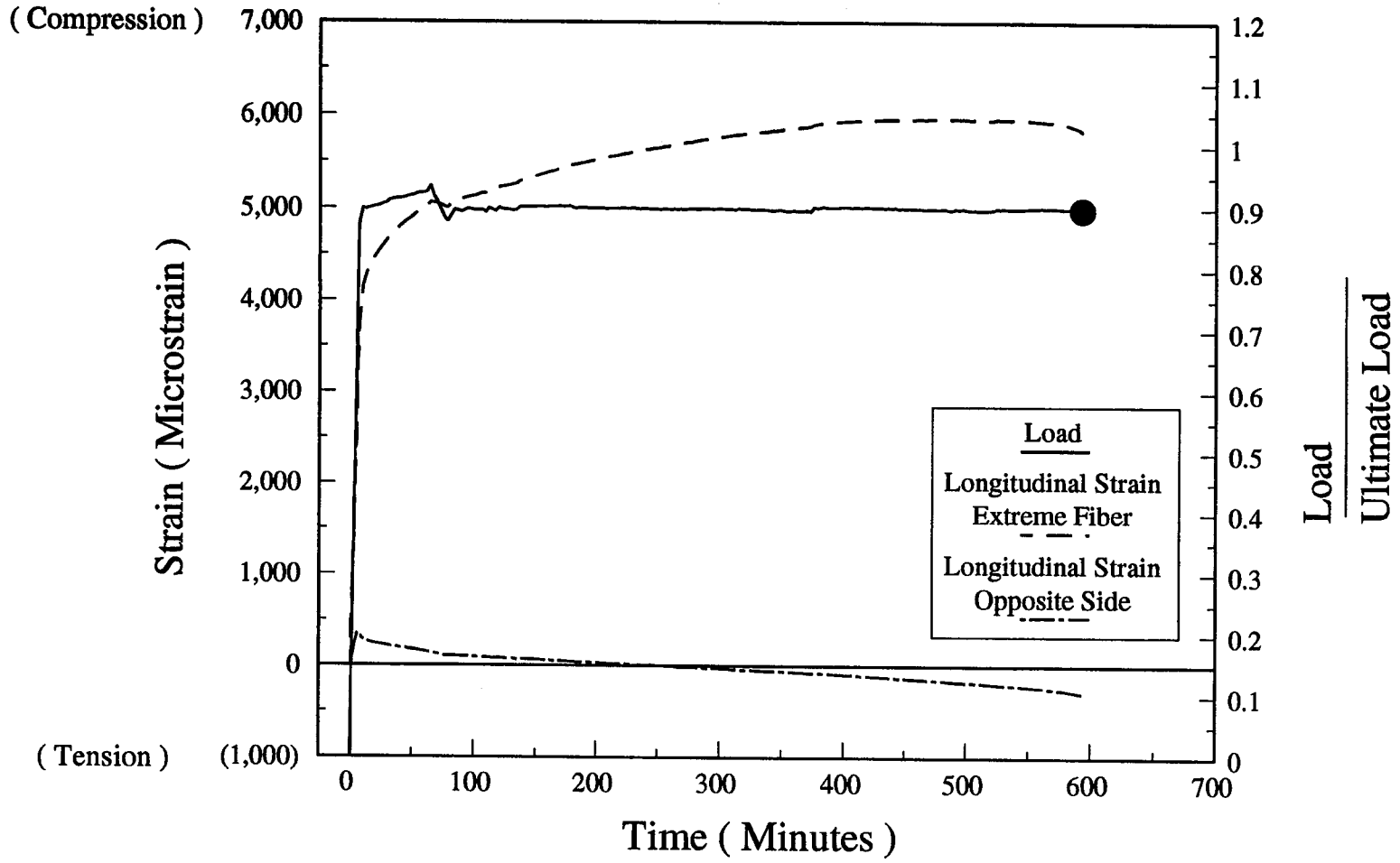

$P_c = 543.7$ kN $\qquad A = 7817$ mm^2

Figure 4.6.1.3.B - Load-Strain-Time Relationship - UHE90 Specimen

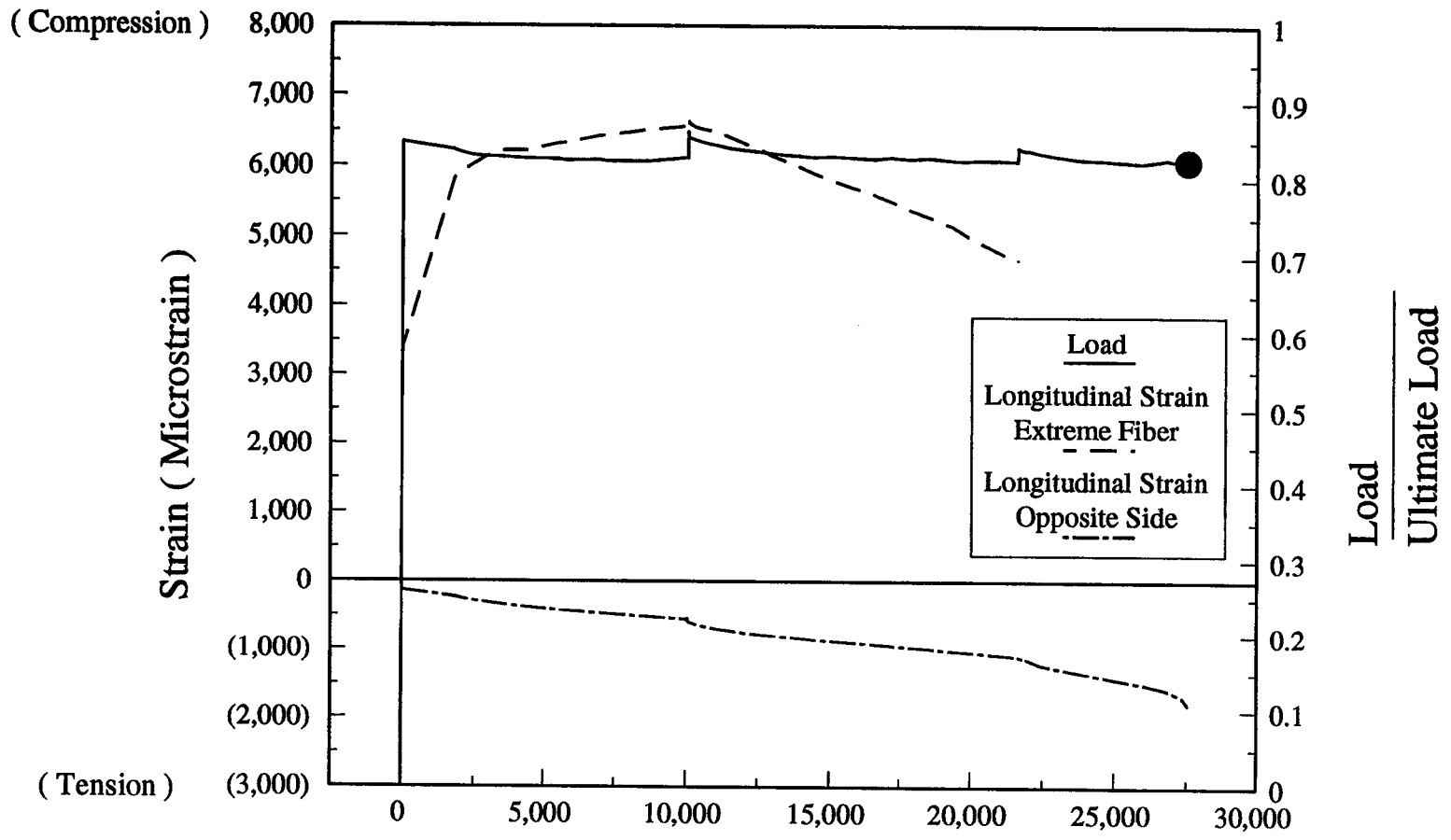

$P_c = 561.6$ kN $\qquad A = 8075$ mm^2

Figure 4.6.1.3.C - Load-Strain-Time Relationship - UHE85 Specimen

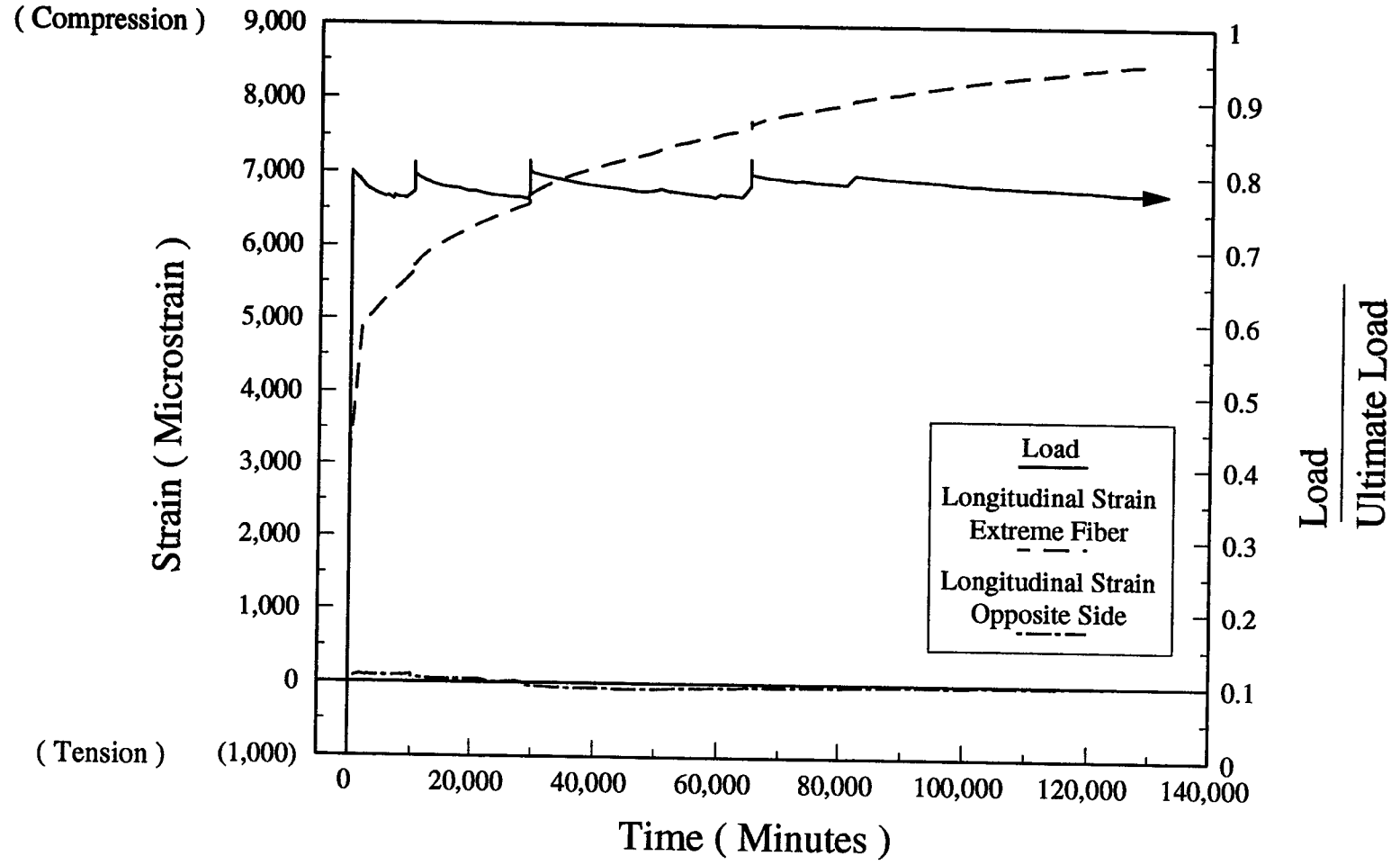

$P_c = 561.1$ kN $\qquad A = 8067$ mm^2

Figure 4.6.1.3.D - Load-Strain-Time Relationship - UHE80 Specimen

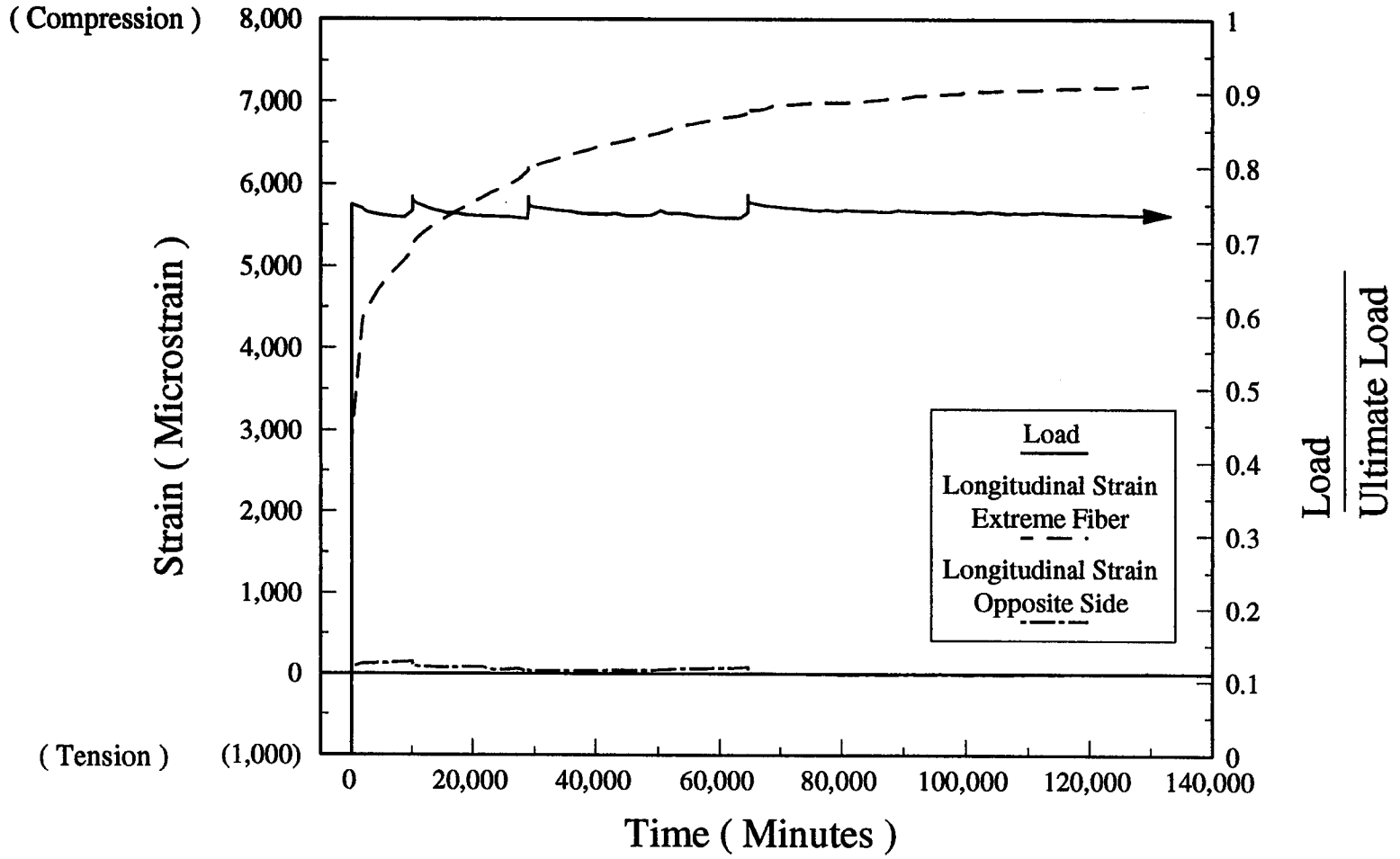

$P_c = 563.7$ kN $\qquad A = 8105$ mm^2

Figure 4.6.1.3.E - Load-Strain-Time Relationship - UHE75 Specimen

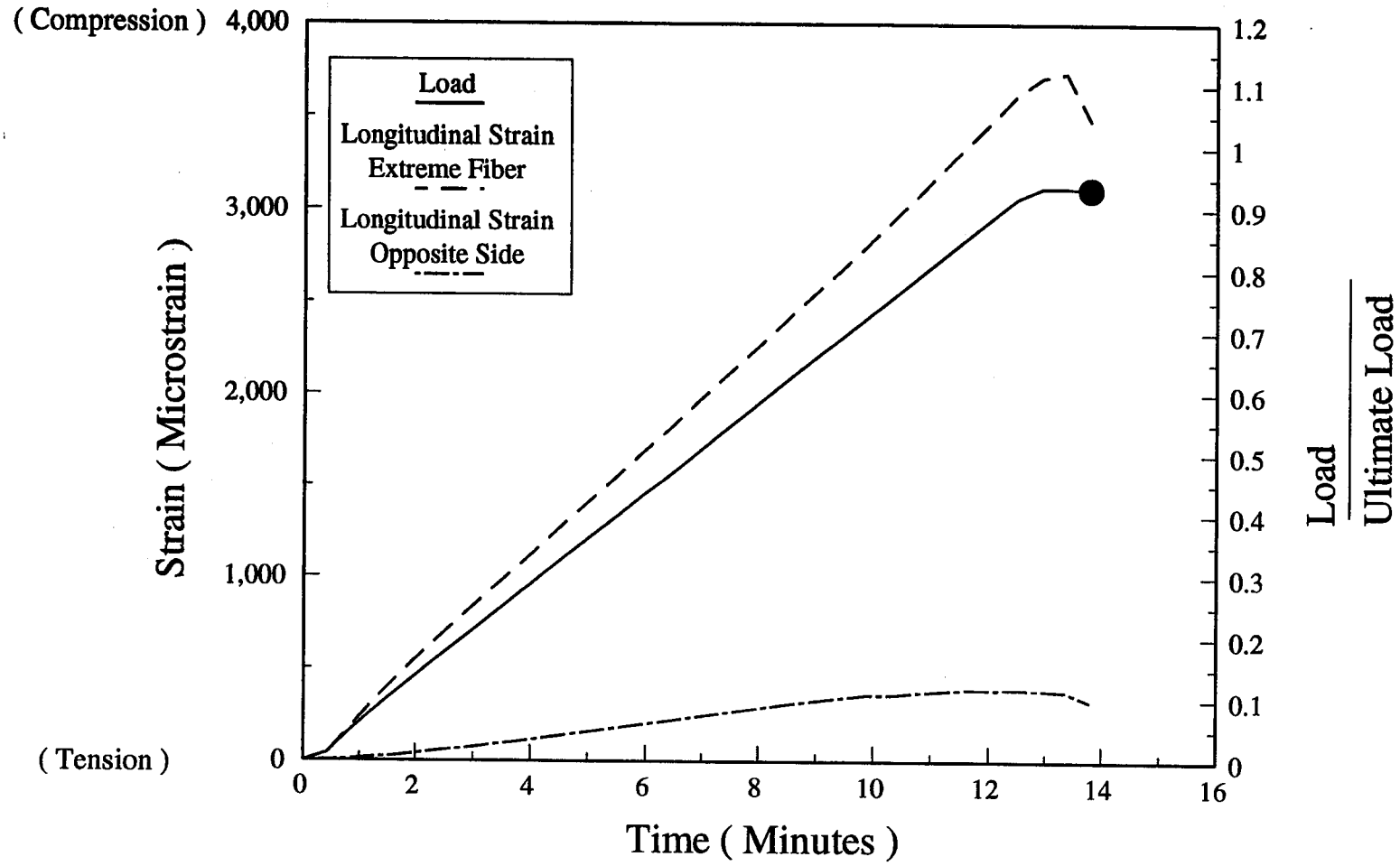

$P_c = 651.6$ kN $\qquad A = 7701$ mm^2

Figure 4.6.1.4.A - Load-Strain-Time Relationship - UUE95 Specimen

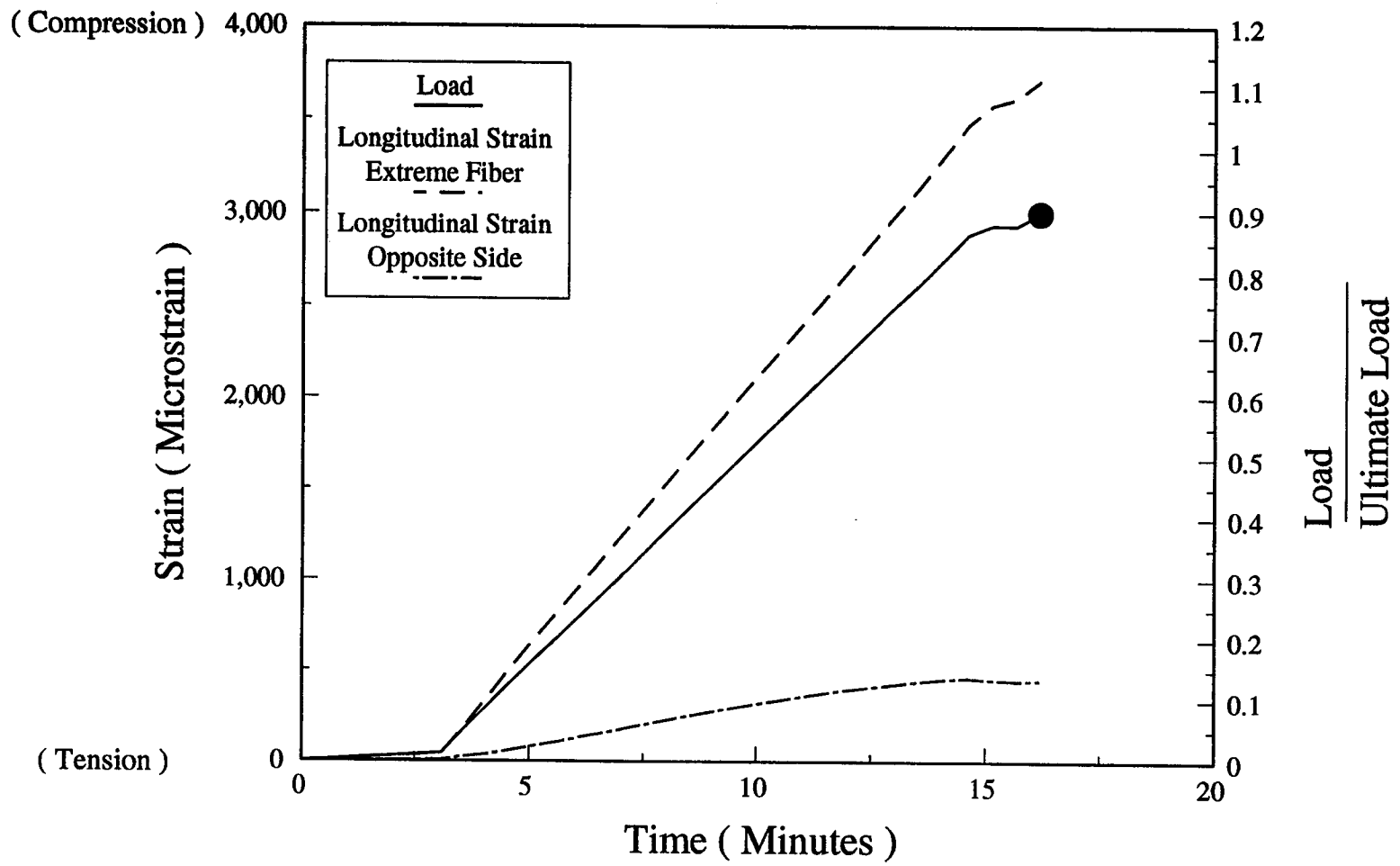

$P_c = 672.2$ kN $\qquad A = 7799$ mm^2

Figure 4.6.1.4.B - Load-Strain-Time Relationship - UUE90 Specimen

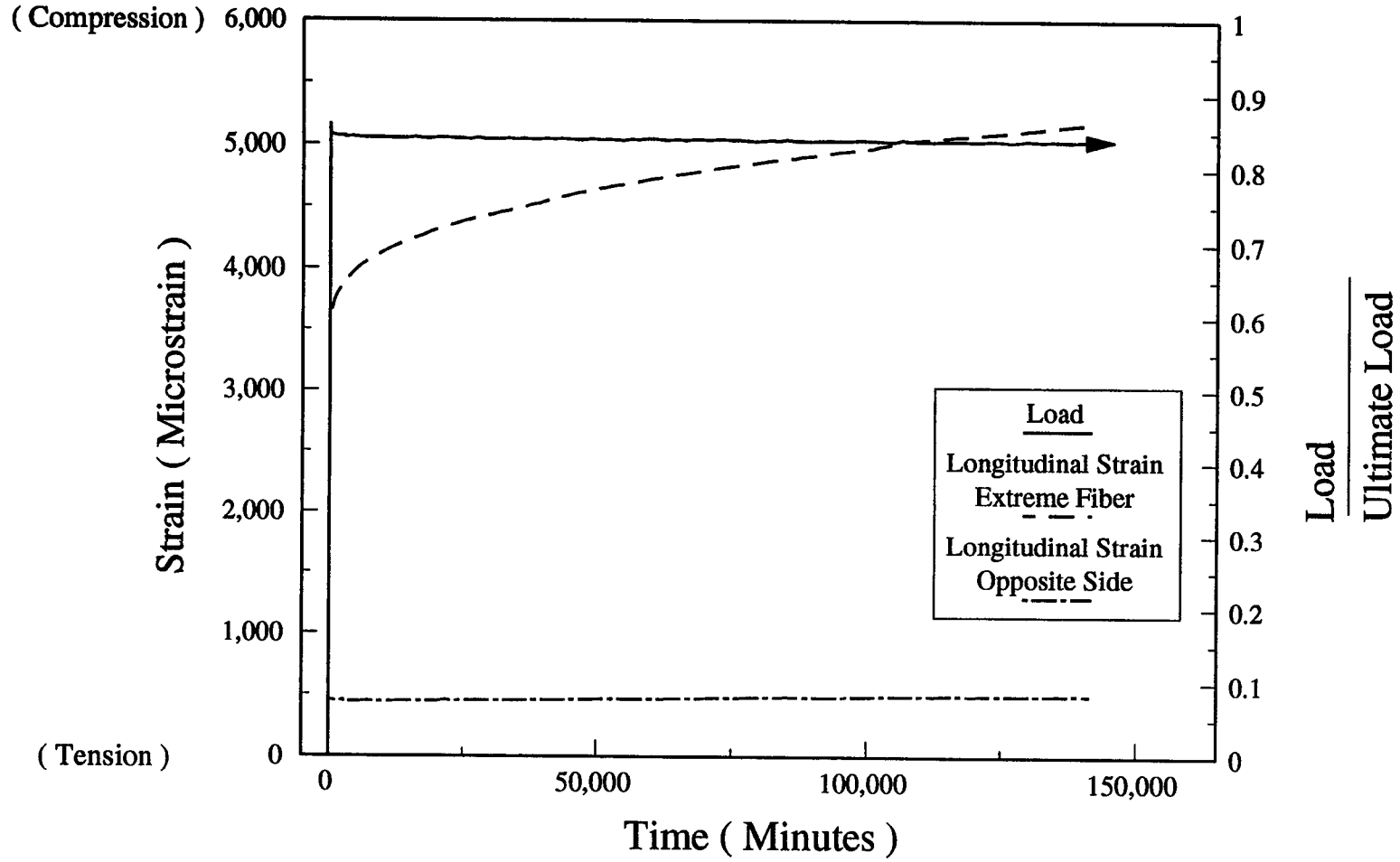

$P_c = 683.1$ kN $\qquad A = 8072$ mm^2

Figure 4.6.1.4.C - Load-Strain-Time Relationship - UUE85 Specimen

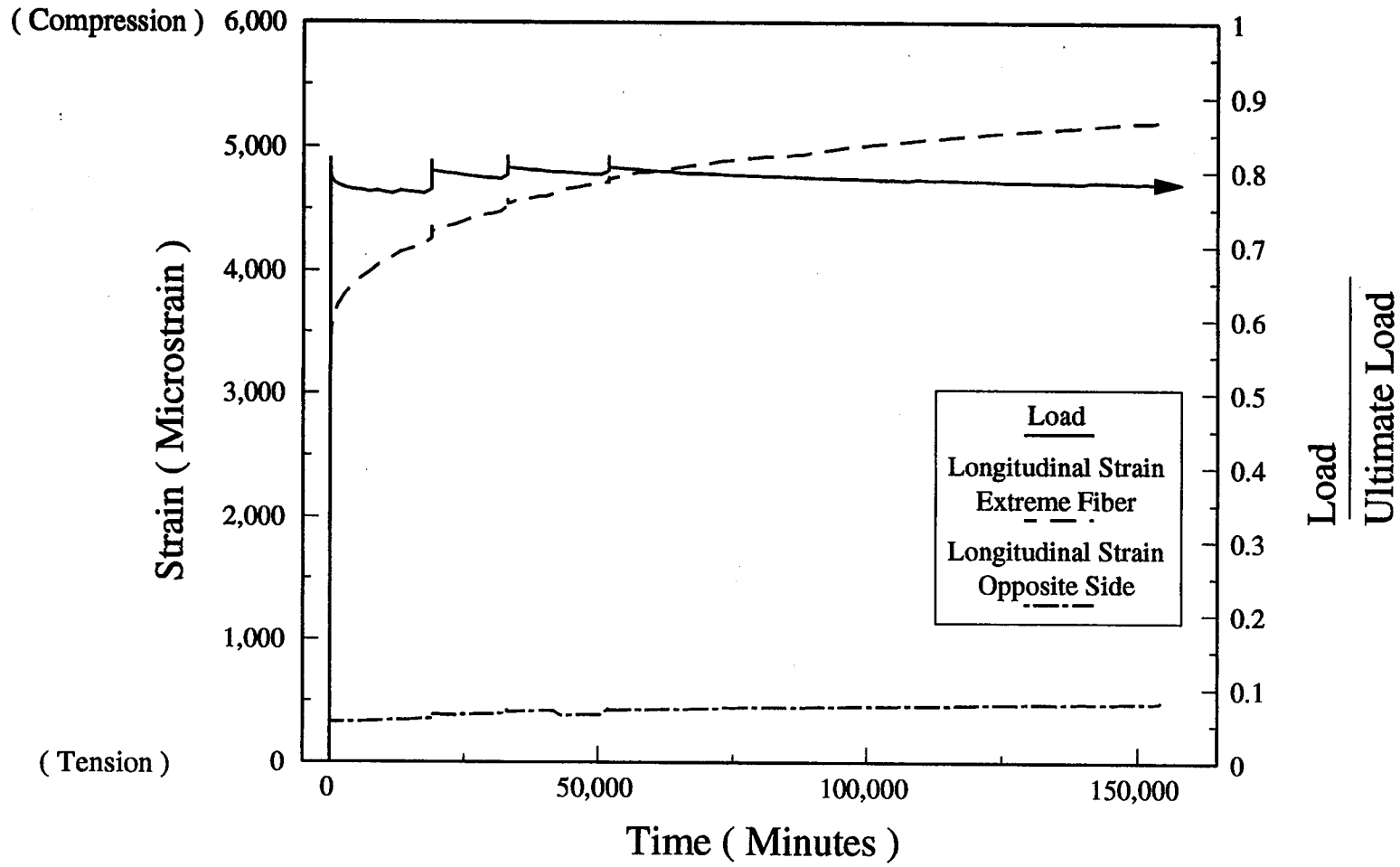

$P_c = 675.0$ kN $\qquad A = 7830$ mm^2

Figure 4.6.1.4.D - Load-Strain-Time Relationship - UUE80 Specimen

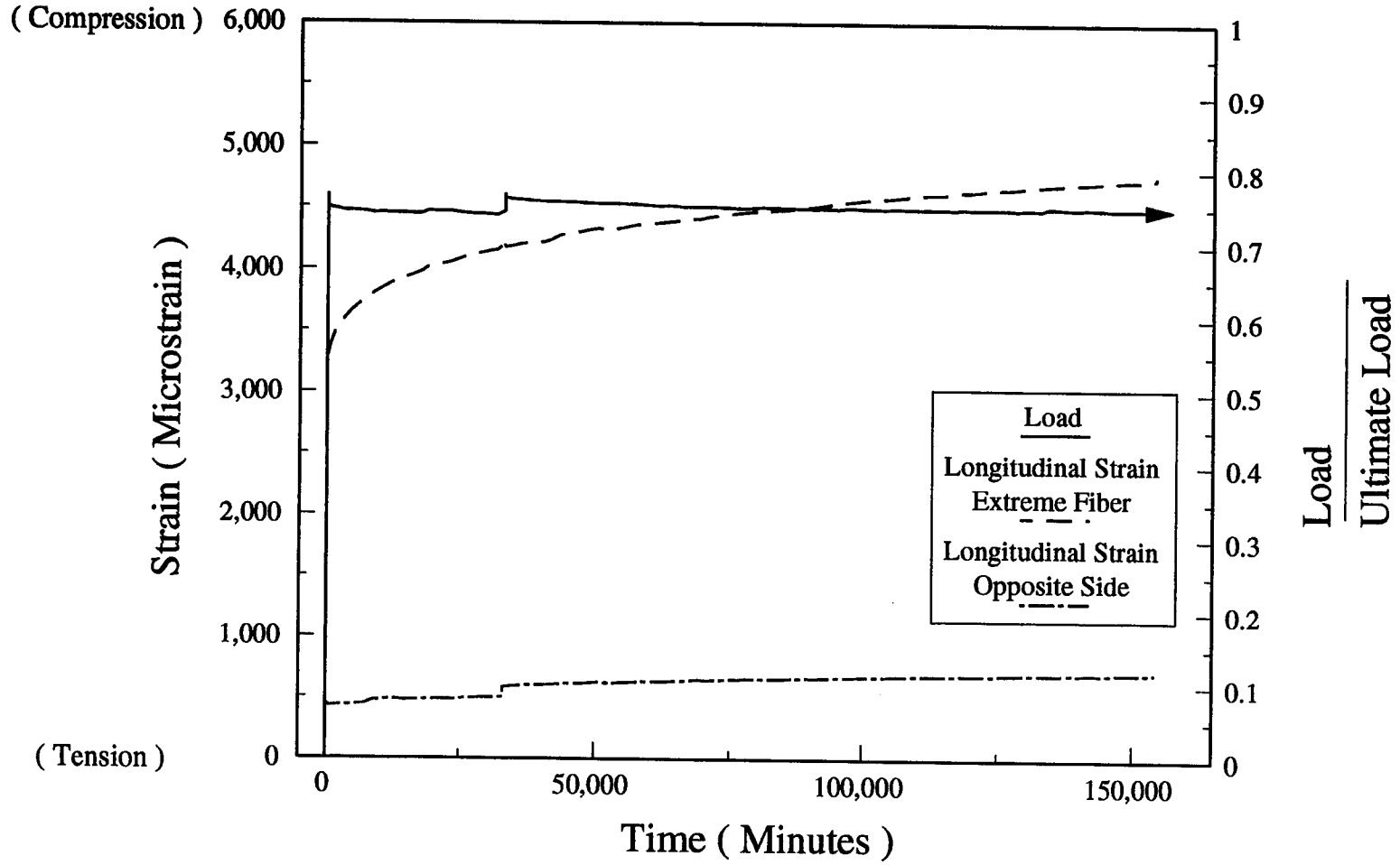

$P_c = 696.3$ kN $\qquad A = 8075$ mm^2

Figure 4.6.1.4.E - Load-Strain-Time Relationship - UUE75 Specimen

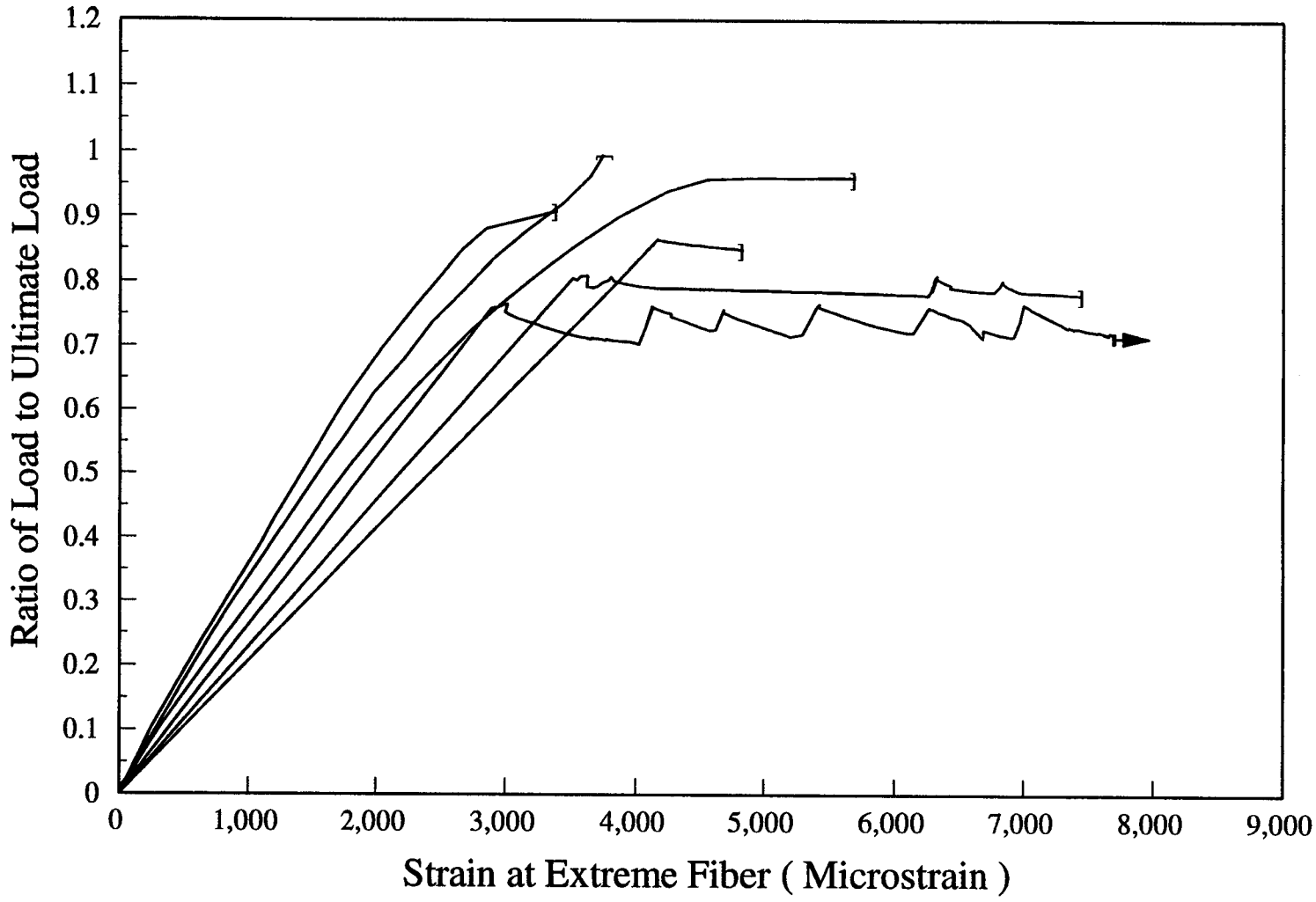

Figure 4.6.2.A - Stress-Strain Relationship - LH Eccentric Series

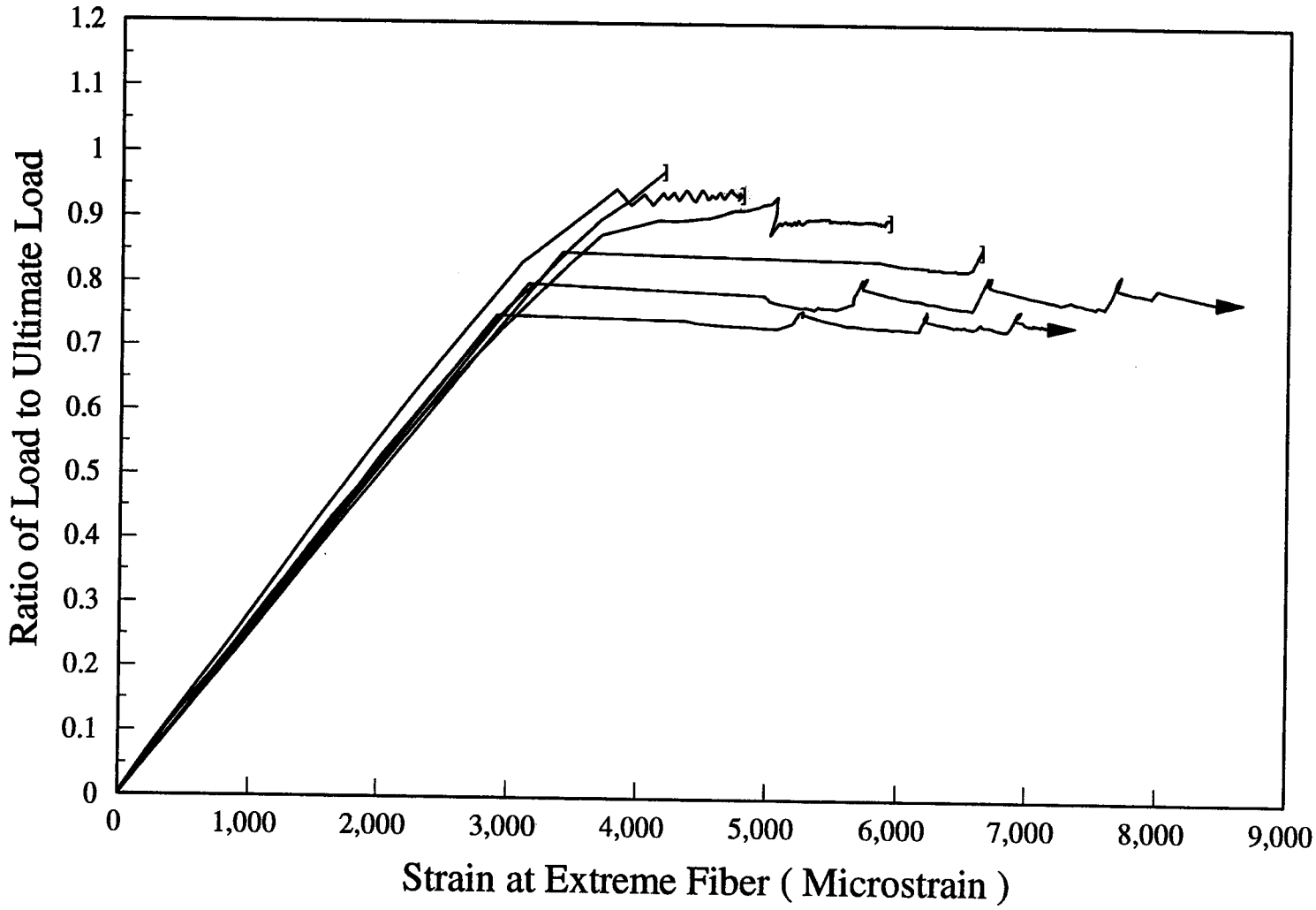

Figure 4.6.2.B - Stress-Strain Relationship - UH Eccentric Series

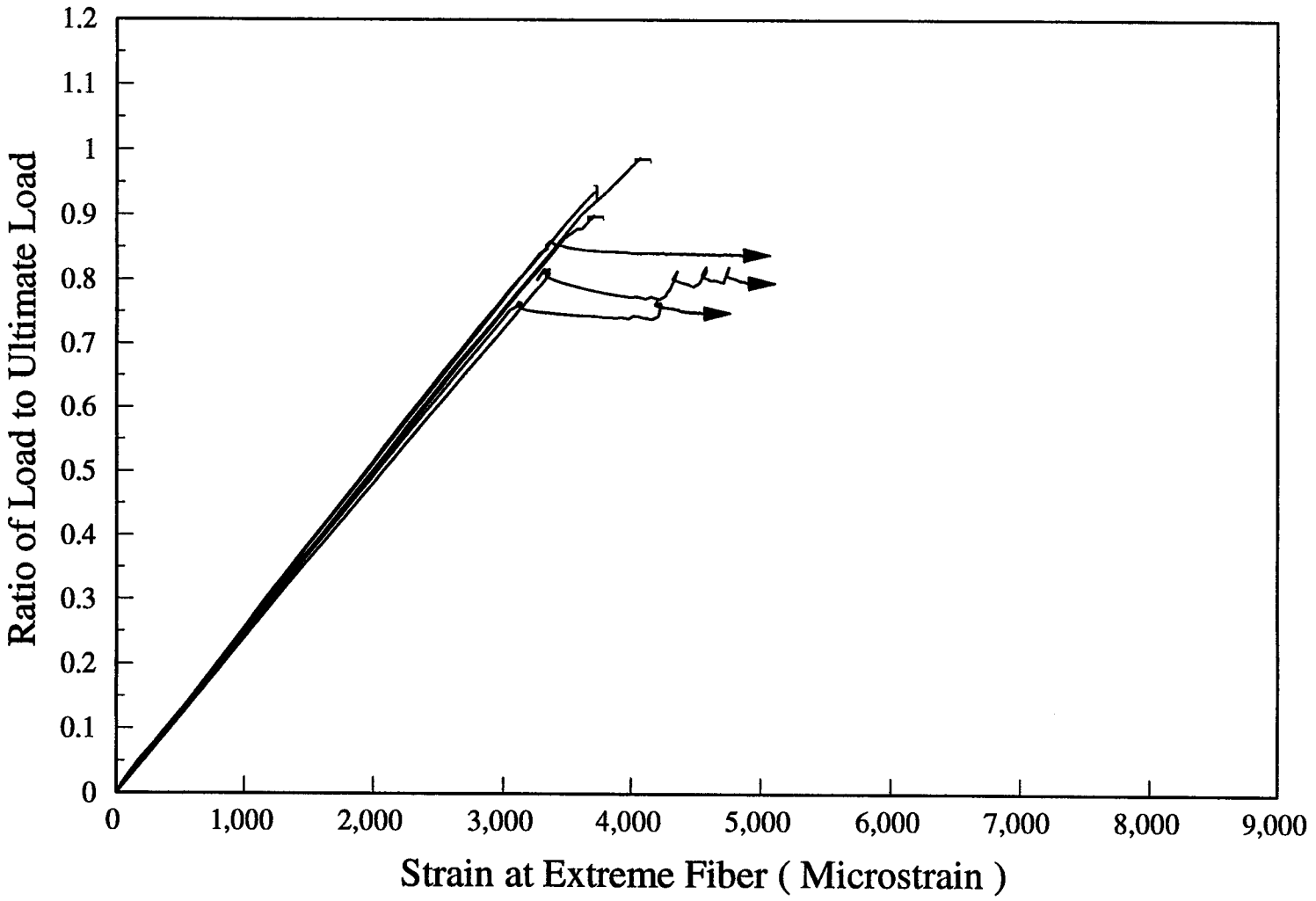

Figure 4.6.2.C - Stress-Strain Relationship - UU Eccentric Series

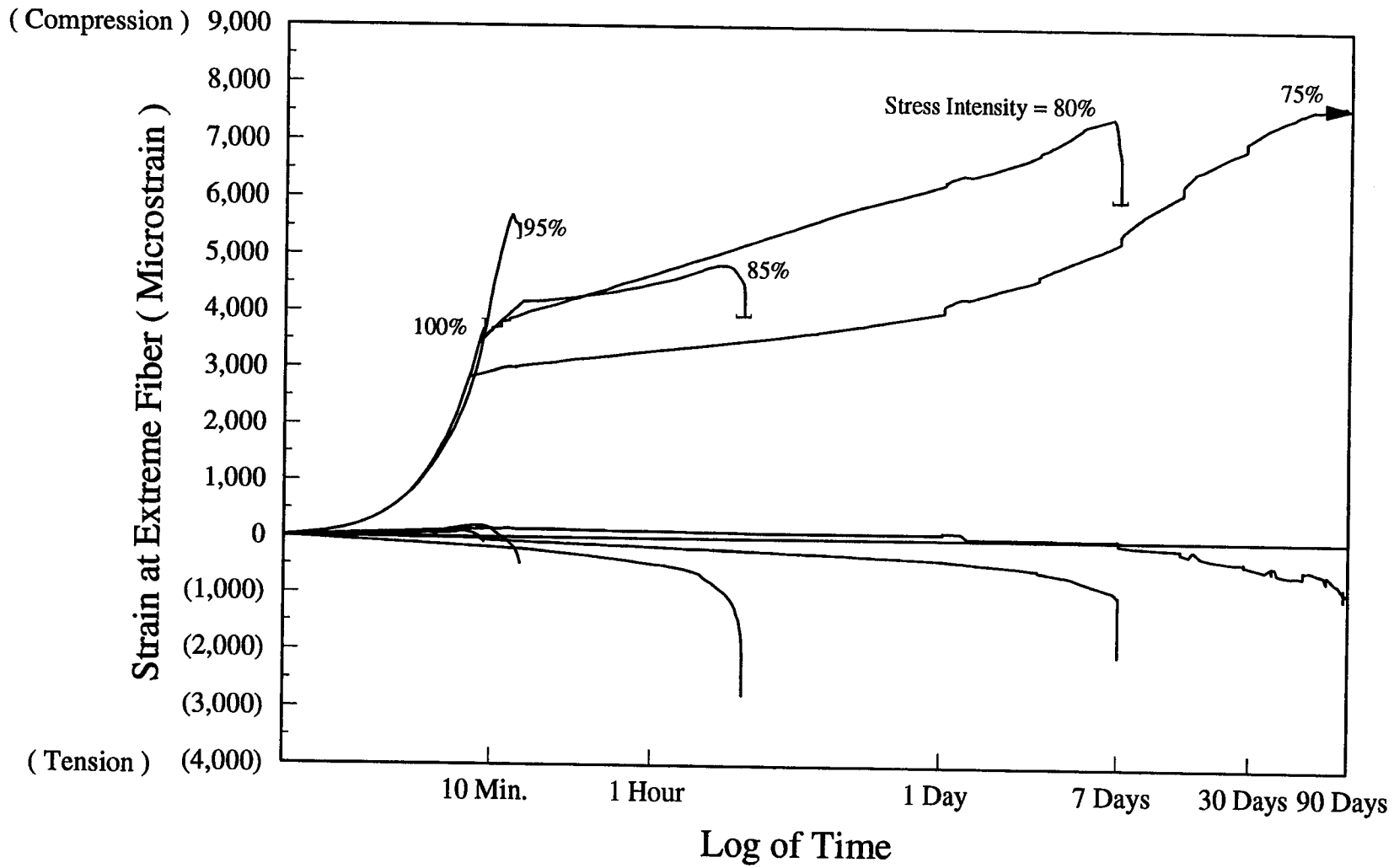

Figure 4.6.2.D - Strain-Time Relationship - LH Eccentric Series

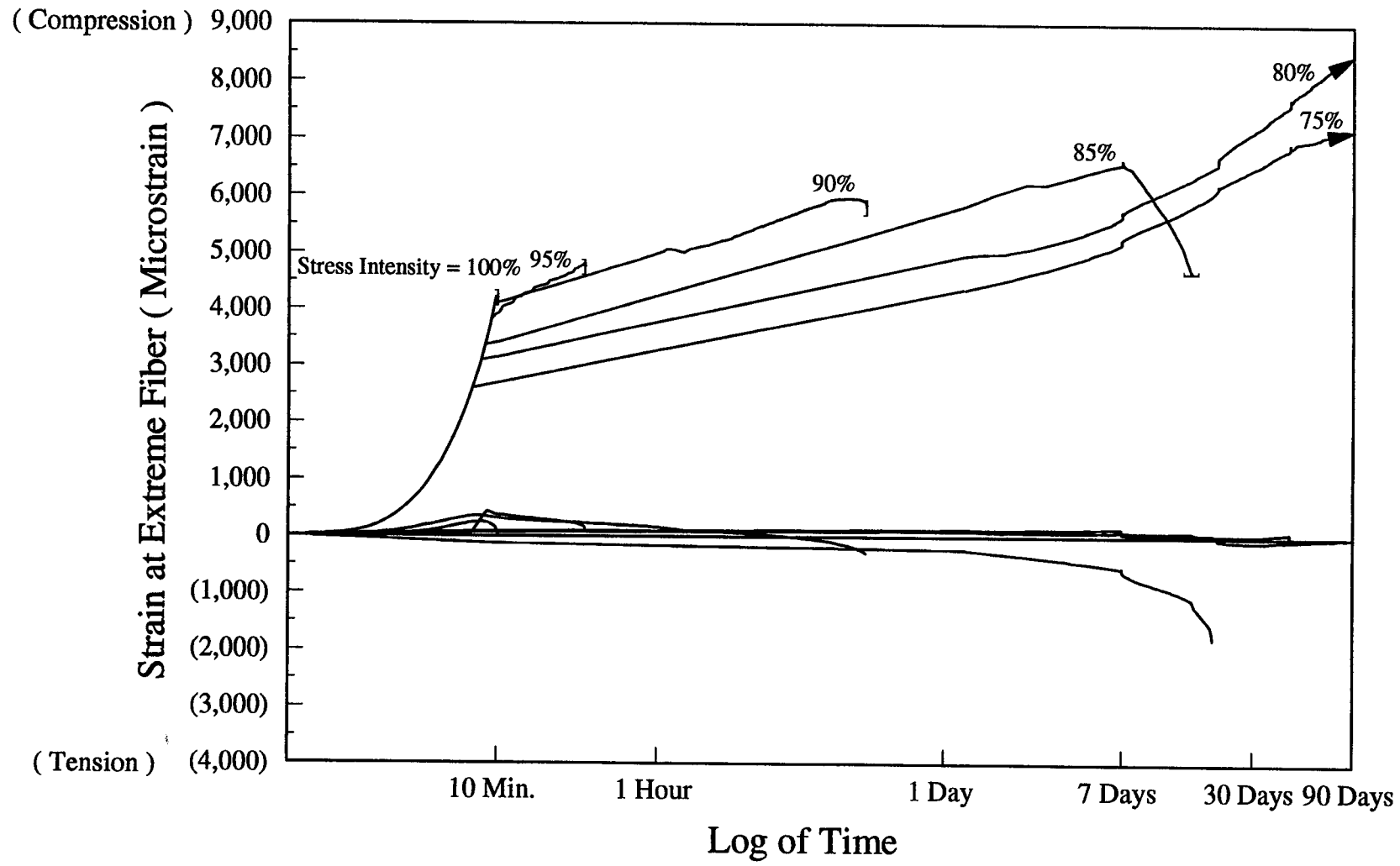

Figure 4.6.2.E - Strain-Time Relationship - UH Eccentric Series

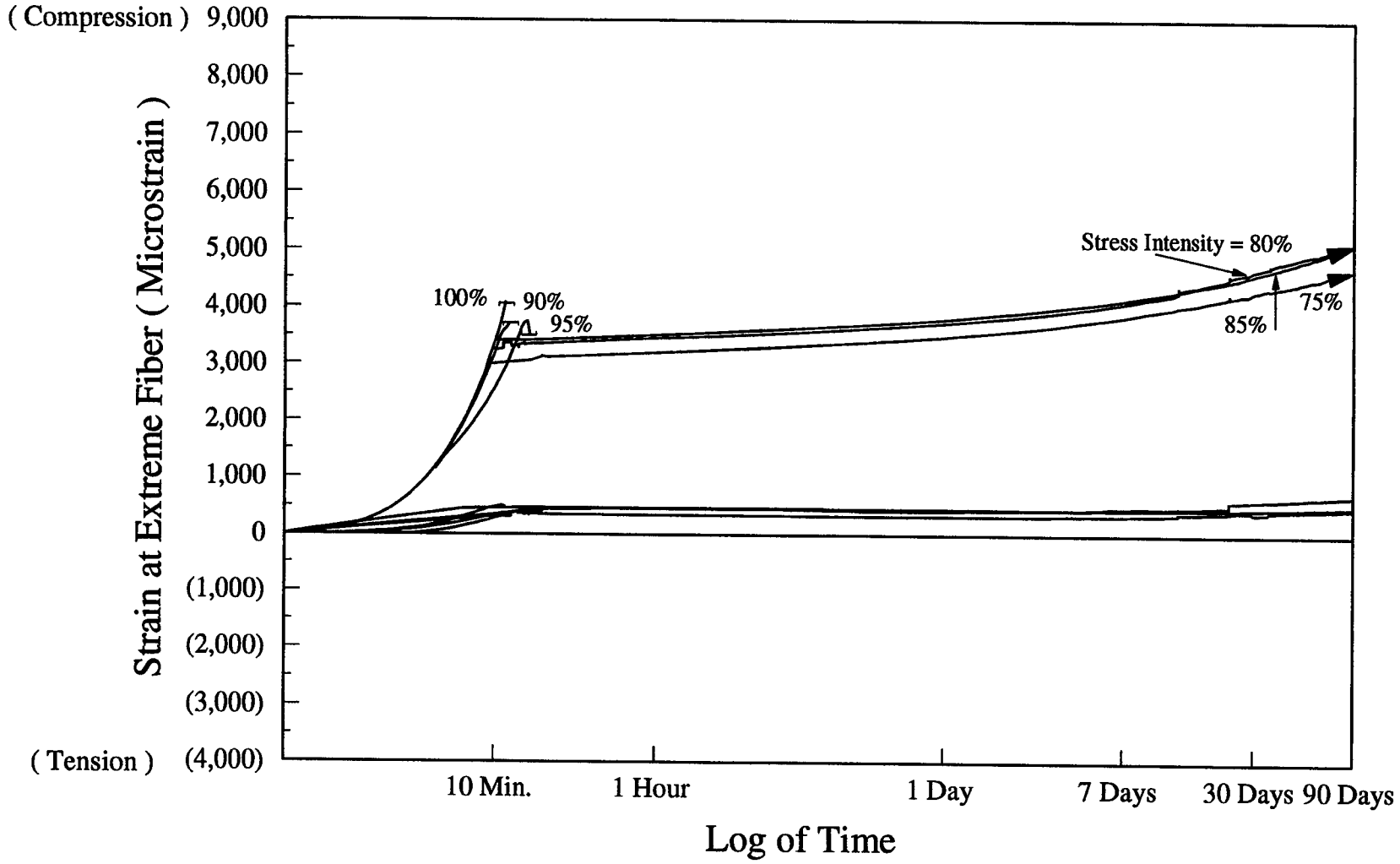

Figure 4.6.2.F - Strain-Time Relationship - UU Eccentric Series

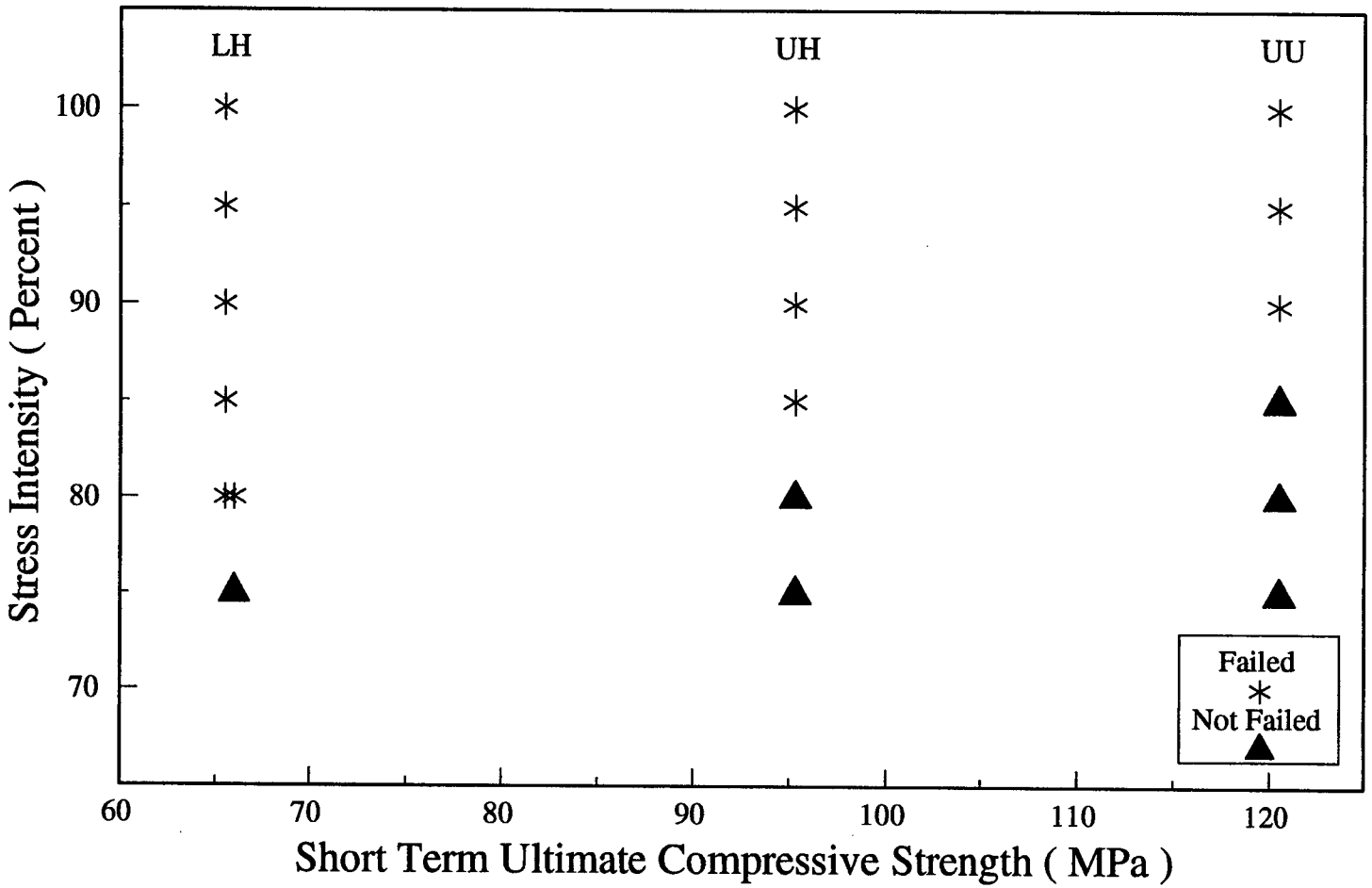

Figure 4.6.2.G - Summary of Eccentric Test Results

5. Summary, Conclusions, and Recommendations

5.1 Summary

The main objective of this study was to investigate high performance concrete under high sustained compressive stresses. Four series of high performance concretes were tested under high sustained compressive stresses. The specimens were subjected to sustained loads for periods up to three months. The primary parameter was the compressive strength of high performance concrete. The other significant parameters were the stress intensity, the moment gradient, and the presence of silica fume as supplementary cementitious material and filler. High performance concretes with 56 day compressive strengths of 65 MPa to 75 MPa (without silica fume), 95 MPa to 105 MPa (with and without silica fume), and 120 MPa (with silica fume) were used. The experimental program was explained in Chapter 2. The load, longitudinal strain, transverse strain, and time until failure were measured. The literature review, test results, and discussion of results were presented in Chapter 4. The stress - strain and strain - log of time relationships were studied. The sustained compressive strength of high performance concrete was established.

A supplementary test program was carried out on the same four series of high performance concretes to study their mechanical properties. This experimental program included the study of following objectives:

1. Compressive strength gain with time.
2. Effect of type of cement on compressive strength.
3. Effect of drying on compressive strength.
4. Effect of the bearing blocks of the testing machine on the compressive strength.
5. Effect of the size of specimen on the compressive strength.
6. Modulus of elasticity.
7. Poisson's ratio.
8. Tensile splitting strength.
9. Modulus of rupture.

The experimental program of the supplementary study was presented in Chapter 2. For each objective of the supplementary study, the literature review, test results, and discussion of results were presented in Chapter 3. A modification of the ACI 318M equation for the modulus of elasticity of normal weight high performance concrete was recommended.

5.2 General Conclusions

Based on results of the current study and previous studies mentioned in literature, the following conclusions can be drawn for high performance concrete especially for those used in the current study:

5.2.1 Mechanical Properties of High Performance Concrete

The following conclusions are drawn based on the study of mechanical properties of high performance concrete:

1. For high performance concretes without silica fume, the ratio of compressive strength gain before 28-day increases, and the ratio of compressive strength gain after 28-day decreases, as the 28 day compressive strength of high performance concrete increases.

2. In the tests reported here, the ratio of 7 day to 28 day compressive strengths were 0.85, 0.87, and 0.76 for 65 MPa to 75 MPa, 95 MPa to 105 MPa, 120 MPa concretes respectively. These ratios suggest that a significant strength gain happens between 7 days and 28 days for the ultra high strength silica fume high performance concrete.

3. For high performance concretes without silica fume, the mix with Type 30 cement develop higher compressive strength than mix with Type 10 cement for the same mix design.

4. For ultra high strength silica fume high performance concrete, the mix with Type 30 cement developed lower compressive strength than mixture with Type 10 cement for the same mix design, but for the mix with Type 30 cement, the strength gain with time continues in presence of water.

5. Drying after moist curing increases the compressive strength gain of high performance concrete. It can be concluded that 3-week is a suitable and sufficient moist curing period.

6. High performance concrete specimens tested with ball seat bearing blocks appear to have up to 7 percent less compressive strength than high performance concrete specimens tested with standard spherical seat bearing blocks. The available data is not sufficient to present a general conclusion.

7. The ratio of the compressive strength of moist cured 100 mm by 200 mm to 150 mm by 300 mm high performance concrete cylinders used in this study, tested using 2600 kN electro-hydraulic closed-loop rock mechanics test system MTS 815 with a 102 mm diameter spherical seat bearing block, is 0.95. This machine has an axial stiffness about six times that of a 100 mm by 200 mm 80 MPa concrete cylinder.

8. Age of the high performance concrete, size of the test specimen, chemical admixtures, supplementary cementitious materials, curing regime, and the kind of coarse aggregate all can affect the static modulus of elasticity of high performance concrete. Among these, the kind of coarse aggregate has the major effect. Most test results in North America for specimens tested between ages of 28 days and 56 days fall in a band between 1.0 and 0.70 times the values predicted by the ACI 318M-89[17] equation.

9. Equation 3.7.3 is proposed for estimating the static modulus of elasticity of high performance concrete:

$$E_c = 4700\, C_{ca} \sqrt{f'_c} \qquad 55\,MPa < f'_c < 125\,MPa \qquad (3.7.3)$$

Where C_{ca} is an empirical coarse aggregate coefficient. The recommended coarse aggregate coefficients, based on the current available test data, are shown in Table 3.7.3. It should be mentioned that due to low correlation between current available test data on diabase and sandstone coarse aggregate, care should be taken in using the current recommended coarse aggregate coefficient for these kind of coarse aggregates.

10. The values of Poisson's ratio of high performance concretes used in this study range from 0.15 to 0.20 with an average of 0.17. Most reported values for Poisson's ratio of high performance concrete by other researchers[12,19] are higher than measured values in this study. Based on test results from current study and references 12 and 19, the average value for the Poisson's ratio is 0.20 for high performance concretes with the compressive strengths ranging from 55 MPa to 125 MPa.

11. The results of this study are in complete agreement with ACI 363R-84[7] recommended equation for estimating the tensile splitting strength and modulus of rupture. Based on results of the current study, the study by Burg et al[13], and the study by Ezeldin et al[29], the validity of equations recommended by ACI 363R-84[7] can be extended for high performance concretes with or without supplementary cementitious materials and with the compressive strength up to 120 MPa at the age of 28 days.

5.2.2 High Performance Concrete under High Sustained Compressive Stresses

The following conclusions are also drawn based on the study of high performance concrete under high sustained compressive stresses:

1. The long term sustained compressive strength of high performance concrete increases as the compressive strength of concrete increases. The long term sustained compressive strength of high performance concrete is between 70 to 75, 75 to 80, and 85 to 90 percent of the short term ultimate strength for 65 MPa to 75 MPa, 95 MPa to 105 MPa, and 120 MPa concretes, respectively.

2. Small eccentricities slightly improve the long term sustained compressive strength of high performance concrete. The long term sustained compressive strength of high performance concrete under eccentric loads at or near the Kern point was approximately 5 percent higher than under the concentric loads.

3. In specimens subjected to stress intensities above the sustained compressive strength, the total strain at failure increases as the stress intensity decreases. For no silica fume high strength high performance concretes, the total strain at failure increases as the compressive strength of concrete increases. The total strain at failure of silica fume ultra high strength high performance concrete is much less than that of no silica fume high strength high performance concrete.

4. In specimens subjected to stress intensities above the sustained compressive strength, the creep strain, the creep coefficient, and the specific creep increase as the stress intensity decreases.

5. The period under sustained compressive stresses until failure generally increases as the stress intensity decreases. The period under sustained compressive stresses until failure generally increases as the compressive strength of high performance concrete increases.

6. The initial strain recovery of silica fume ultra high strength high performance concrete is higher than for no silica fume high strength high performance concrete.

5.3 Recommendations for Further Studies

Based on results of the current study on high performance concrete and previous studies on both conventional and high performance concrete, the following recommendations are suggested for further studies:

1. More studies on all objectives covered in the current study are recommended to improve the statistical significance of the results of the current study. These studies can be carried out with using the same material used in the current study or with using different kinds of cement, fly ash, silica fume, fibers, and coarse aggregates. An identical experimental program is recommended substituting the coarse aggregate used in these tests with a stiff coarse aggregate like dolomite or trap rock.

2. More studies on the effect of the bearing blocks of the testing machine on the compressive strength are necessary.

3. An extended study on the modulus of elasticity and Poisson's ratio of concretes with 28 day compressive strength of 10 to 130 MPa is recommended with different kind of

coarse aggregates from all around the North America. Such a study can extend the range of validity of the recommended modified ACI 318M equation for modulus of elasticity and would provide sufficient data about Poisson's ratio.

4. Analytical and experimental study on high performance concrete members and also indeterminate structural systems under high sustained compressive stresses is necessary to establish the true capacity of these members and the effect of load transfer from concrete to steel on the likelihood of failure of the concrete under high sustained stresses.

References

The References listed were the latest at the time this document was Written. Since some of these references are revised frequently, generally in minor details only, the user of this document should check directly with the sponsoring group if it is desired to refer to the latest revision. The ACI, ASTM, and CSA publications may be obtained from the following addresses respectively:

American Concrete Institute
P.O. Box 19150
Detroit, MI, U.S.A. 48219-0150

American Society for Testing and Materials
1916 Race Street
Philadelphia, PA, U.S.A. 19103

Canadian Standard Association
178 Rexdale Boulevard
Rexdale, Ontario, Canada M9W 1R3

R.1 Cited References

1. James G. MacGregor, "REINFORCED CONCRETE, Mechanics and Design", Second Edition, Prentice-Hall, Englewood Cliffs, NJ 07632 U.S.A., 1992, 848 pp.

2. Gerald M. Sturman, Surendra P. Shah, and George Winter, "Effects of Flexural Strain Gradients on Microcracking and Stress-Strain Behavior of Concrete", American Concrete Institute, ACI Journal, Proceedings, Vol. 62, July 1965, pp. 805-821.

3. ACI 211.4R.93, "Guide for Selecting Proportions for High-Strength Concrete with Portland Cement and Fly Ash", American Concrete Institute, ACI Manual of Concrete Practice, Part 1, 1994.

4. K. Rokugo, S. Ohno, and W. Koyanagi, "Automatical Measuring System of Load-Displacement Curves Including Post-Failure Region of Concrete Specimens", Fracture Toughness and Fracture Energy of Concrete, Edited by F.H. Witmann, Elsevier Science Publishers B.V., Amsterdam Netherlands, 1986, pp. 403-411.

5. CAN/CSA-A23.2-M90, "Methods of Test for Concrete", Canadian Standard Association, Toronto Ontario Canada, March 1990.

6. CAN/CSA-A23.1-M90, "Concrete Materials and Methods of Concrete Construction", Canadian Standard Association, Toronto Ontario Canada, March 1990.

7. ACI 363R-84, "State-of-the-Art Report on High-Strength Concrete", American Concrete Institute, ACI Manual of Concrete Practice, Part 1, 1993.

8. "High Strength Concrete, State of the Art Report", FIP/CEB Bulletin d'Information NO. 197, August 1990.

9. Walid Baalbaki, Moussa Baalbaki, Brahim Benmokrane, and Pierre-Claude Aitcin, "Influence of Specimen Size on Compressive Strength and Elastic Modulus of High-Performance Concrete", American Society for Testing and Materials, Cement, Concrete, and Aggregates, Vol. 14, No. 2, Winter 1992, pp. 113-117.

10. Adrian Pauw, "Static Modulus of Elasticity of Concrete as affected by Density", American Concrete Institute, ACI Journal, Proceedings, Vol. 57, December 1960, pp. 679-688.

11. P-C Aitcin and P.K. Mehta, "Effect of Coarse-Aggregate Characteristics on Mechanical Properties of High-Strength Concrete", American Concrete Institute, ACI Materials Journal, Proceedings, Vol. 87, March-April 1990, pp. 103-107.

12. Ramon L. Carrasquillo, Arthur H. Nilson, and Floyd O. Slate, "Properties of High Strength Concrete Subject to Short-Term Loads", American Concrete Institute, ACI Journal, Proceedings, Vol. 78, May-June 1981, pp. 171-178.

13. R.G. Burg and B.W. Ost, "Engineering Properties of Commercially Available High-Strength Concretes", Portland Cement Association, Skokie, Illinois, U.S.A., 1992, Research and Development Bulletin No. RD104T, 55 pp.

14. "High-Strength Concrete in Chicago High-Rise Buildings", Chicago Committee on High-Rise Buildings, Task Force Report No. 5, February 1977, 63 pp.

15. James E. Cook, "10,000 psi Concrete", American Concrete Institute, Concrete International, Vol. 10, No. 10, October 1989, pp. 67-75.

16. Jon G. Asselanis, Pierre-Claude Aitcin, and P.K. Mehta, "Effect of Curing Conditions on the Compressive Strength and Elastic Modulus of Very High-Strength Concrete", American Society for Testing and Materials, Cement, Concrete, and Aggregates, Vol. 11, No. 1, Summer 1989, pp. 80-83.

17. ACI 318M-89 (Revised 1992), "Building Code Requirements for Reinforced Concrete", American Concrete Institute, ACI Manual of Concrete Practice, Part 3, 1993.

18. M.G. Alexander, "Prediction of Elastic Modulus for Design of Concrete Structures", The South African Institution of Civil Engineers, The Civil Engineer in South Africa, Vol. 27, No. 6, June 1985, PP. 313-324.

19. William F. Perenchio and Paul Klieger, "Some Physical Properties of High Strength Concrete", Portland Cement Association, Skokie, Illinois, U.S.A., 1978, Research and Development Bulletin No. RD056.01T, 7 pp.

20. L.J. Parrott, "Simplified Methods of Predicting the Deformation of Structural Concrete", Cement and Concrete Association, United Kingdom, Development Report No. 3, October 1979, 11 pp.

21. L.J. Parrott, "The production & Properties of High-Strength Concrete", Concrete, Vol. 3, No. 11, Nov. 1969, pp. 443-448.

22. M.K. Hurd and P.D. Courtois, "Method of Shoring and Reshoring in Multistory Buildings", (Unpublished Paper).

23. S.L. Sarkar and P.-C. Aitcin, "Dissolution Rate of Silica Fume in Very High Strength Concrete", Cement and Concrete Research, 1987, Vol. 17, pp. 591-601.

24. Pierre-Claude Aitcin, Buquan Miao, William D. Cook, and Denis Mitchell, "Effects of Cylinder Size and Curing on the Compressive Strength of High Performance Concretes", Accepted by American Concrete Institute, It will be published in ACI Materials Journal.

25. Michel Lessard, Omar Chaallal, and Pierre-Claude Aitcin, "Testing High Strength Concrete Compressive Strength", American Concrete Institute, ACI Materials Journal, Proceedings, Vol. 90, July-August 1993, pp. 303-308.

26. "Significance of Tests and Properties of Concrete and Concrete Aggregates", American Society for Testing and Materials, ASTM Special Technical Publication No. 169, 1955, Page 84.

27. Michael L. Leming, "Comparison of Mechanical Properties of High-Strength Concrete Made with Different Raw Materials", Transportation Research Board, National Research Council, Washington, D.C., 1990, Transportation Research Record No. 1284, pp. 23-30.

28. CAN3-A23.3-M84, "Design of Concrete Structures for Buildings", Canadian Standard Association, Toronto Ontario Canada, December 1984.

29. A. Samer Ezeldin and Pierre-Claude Aitcin, "Effect of Coarse Aggregate on the Behavior of Normal and High-Strength Concretes", American Society for Testing and Materials, Cement, Concrete, and Aggregates, Vol. 13, No. 2, Winter 1991, pp. 121-124.

30. ASTM C 39-86, "Standard Test Method for Compressive Strength of Cylindrical Concrete Specimens", American Society for Testing and Materials, 1993.

31. ASTM C 192-90a, "Standard Practice for Making and Curing Concrete Test Specimens in the Laboratory", American Society for Testing and Materials, 1993.

32. ASTM E 171-87, "Standard Specification for Standard Atmospheres for Conditioning and Testing Materials", American Society for Testing and Materials, 1993.

33. ASTM C 469-87a, "Standard Test Method for Static Modulus of Elasticity and Poisson's Ratio of Concrete in Compression", American Society for Testing and Materials, 1993.

34. ASTM C 496-90, "Standard Test Method for Splitting Tensile Strength of Cylindrical Compressive Specimens", American Society for Testing and Materials, 1993.

35. ASTM C 78-84, "Standard Test Method for Flexural Strength of Concrete (Using Simple Beam with Third-Point Loading)", American Society for Testing and Materials, 1993.

36. Sukhvarsh Jerath and Lindsay C. Yamane, "Mechanical Properties and Workability of Superplasticized Concrete", American Society for Testing and Materials, Cement, Concrete, and Aggregates, Vol. 9, No. 1, Summer 1987, pp. 12-19.

37. Yau Seng Hwee and B. Vijaya Rangan, "Studies on Commercial High-Strength Concretes", American Concrete Institute, ACI Materials Journal, Proceedings, Vol. 87, September-October 1990, pp. 440-445.

38. Hisham Ibrahim and James G. MacGregor, "Flexural Behavior of High-Strength Concrete Columns", Structural Engineering Report No. 196, Department of Civil Engineering, University of Alberta, Edmonton, Canada, March 1994, 197 pp.

39. O.T. Sigvaldason, "The Influence of Testing Machine Characteristics upon the Cube and Cylinder Strength of Concrete", Magazine of Concrete Research (London), Vol. 18, No. 57, December 1966, pp. 197-206.

40. D.G. Cole, "Some Mechanical Aspects of Compression Testing Machines", Magazine of Concrete Research (London), Vol. 19, No. 61, December 1967, pp. 247-251.

41. F.E. Richart, A. Brandtzaeg, and R.L. Brown, "A Study of the Failure of Concrete under Combined Compressive Stresses", Bulletin No. 185, University of Illinois, Engineering Experimental Station, Urbana, Illinois, November 1928.

42. F.E. Richart and R.L. Brown, "An Investigation of Reinforced Concrete Columns", Bulletin No. 267, University of Illinois, Engineering Experimental Station, Urbana, Illinois, June 1934.

43. J.R. Shank, "Plastic Flow of Concrete at High Overload", American Concrete Institute, ACI Journal, Proceedings, Vol. 45, February 1949, pp. 493-498.

44. W.H. Price, "Factors Influencing Concrete Strength", American Concrete Institute, ACI Journal, Proceedings, Vol. 47, February 1951, pp. 417-432.

45. I.M. Viest, R.C. Elstner, and E. Hognestad, "Sustained Load Strength of Eccentrically Loaded Short Reinforced Concrete Columns", American Concrete Institute, ACI Journal, Proceedings, Vol. 52, March 1956, pp. 755-727.

46. H. Rüsch and C. Rasch, "Investigation into the Strength of Concrete under Sustained Load", RILEM Symposium on the Influence of Time upon Strength and Deformation of Concrete, Munich, November 1958.

47. R. Sell, "Investigations into the Strength of Concrete under Sustained Load", RILEM Bulletin No. 5, December 1959, pp. 5-13.

48. H. Rüsch, "Researches Toward a General Flexural Theory for Structural Concrete", American Concrete Institute, ACI Journal, Proceedings, Vol. 57, July 1960, pp. 1-28.

49. S.P. Shah and S. Chandra, "Fracture of Concrete Subjected to Cyclic and Sustained Loading", American Concrete Institute, ACI Journal, Proceedings, Vol. 67, October 1970, pp. 816-825.

50. S. Stokl, "Strength of Concrete under Uniaxial Sustained Loading", American Concrete Institute, ACI Special Publication, Concrete for Nuclear Reactors, SP-34, Vol. 1, 1972, pp. 313-326.

51. A.S. Ngab, A.H. Nilson, and F.O. Slate, "Shrinkage and Creep of High Strength Concrete", American Concrete Institute, ACI Journal, Proceedings, Vol. 78, July-August 1981, pp. 255-261.

52. M.M. Smadi, F.O. Slate, and A.H. Nilson, "Time-Dependent Behavior of High-Strength Concrete under High Sustained Compressive Stresses", Research Report No. 82-16, Department of Structural Engineering, Cornell University, Ithaca, November 1982, 264 pp.

53. K.T.S.R. Iyengar, P. Desayi, and C.S. Viswanatha, "A New Approach for the Prediction of 'True Ultimate Strength' of Reinforced Concrete Flexural Members", Southampton Civil Engineering Materials Conference: Structure, Solid Mechanics and Engineering Design, Proceedings, Jhon-Wiley & Sons, New York, U.S.A., 1971, pp. 1313-1319.

54. Ramon L. Carrasquillo, Arthur H. Nilson, and Floyd O. Slate, "Microcracking and Behavior of High Strength Concrete Subject to Short-Term Loading", American Concrete Institute, ACI Journal, Proceedings, Vol. 78, May-June 1981, pp. 179-186.

55. Surendra P. Shah and Sushil Chandra, "Critical Stress, Volume Change, and Microcracking of Concrete", American Concrete Institute, ACI Journal, Proceedings, Vol. 65, September 1968, pp. 770-781.

56. Lajos Beres, "Investigation on Structural Loosening of Compressed Concrete", RILEM Bulletin No. 36, September 1967, pp. 185-190.

57. R. K. Dhir and C.M. Sangha, "A Study of the Relationships between Time, Strength, Deformation and Fracture of Plain Concrete", Magazine of Concrete Research (London), Vol. 24, No. 81, December 1972, pp. 197-208.

58. L. Berntsson, B. Hedberg, and R. Malinowski, "Triaxial Deformations by Uniaxial Compressive Load on Heat-Cured and High-Strength Concrete", Proceedings, Southampton Civil Engineering Materials Conference: Structure, Solid Mechanics and Engineering Design, Editor: M. Te'eni, Jhon-Wiley & Sons, 1971, PP. 799-813.

59. K. Newman and J. B. Newman, "Failure Theories and Design Criteria for Plain Concrete", Proceedings, Southampton Civil Engineering Materials Conference: Structure, Solid Mechanics and Engineering Design, Editor: M. Te'eni, Jhon-Wiley & Sons, 1971, PP. 963-995.

60. Prakash Desayi and B. R. R. Sen, "An Investigation into the Prediction of Creep and the True Ultimate Strength of Concrete, Part 2", Indian Concrete Journal, Vol. 40, No. 6, June 1966, PP. 248-256.

61. Prakash Desayi and C. S. Viswanatha, "True Ultimate Strength of Plain Concrete", RILEM Bulletin No. 36, September 1967, pp. 163-173.

62. K. M. Alexander, J. Wardlaw, and D. J. Gilbert, "Aggregate-Cement Bond, Cement Paste Bond, Cement Paste Strength and the Strength of Concrete", The Structure of Concrete and its Behavior under Load: Proceedings of an International Conference, London, 1965. Cement and Concrete Association, 1968, pp. 59-81.

R.2 Additional and Recommended References

R.2.1. ACI 116R-85, "Cement and Concrete Terminology", American Concrete Institute, ACI Manual of Concrete Practice, Part 1, 1993.

R.2.2. Gajanan M. Sabnis, Harry G. Harris, Richard N. White, and M. Saeed Mirza, "Structural Modeling & Experimental Techniques", Prentice-Hall, Englewood Cliffs, NJ 07632 U.S.A., 1983, 585 pp.

R.2.3. James W. Dally and William F. Riley, "Experimental Stress Analysis, Second Edition", McGraw-Hill, New York, U.S.A., 1978, 571 pp.

R.2.4. Arthur P. Boresi and Omar M. Sidebottom, "Advanced Mechanics of Materials, Fourth Edition", Jhon-Wiley & Sons, New York, U.S.A., 1985, 763 pp.

R.2.5. Kenneth S. Edwards, Jr. and Robert B. McKee, "Fundamentals of Mechanical Component Design", McGraw-Hill, New York, U.S.A., 1991, 689 pp.

R.2.6. Timoshenko, Woinowsky, and Krieger, "Theory of Plates and Shells, Second Edition", McGraw-Hill, New York, U.S.A., 1959, 580 pp.

R.2.7. Gregory E. Small and Sidney H. Simmonds, "Spreadsheet Solution of Elastic Plate Bending Problems", Structural Report No. 149, Department of Civil Engineering, University of Alberta, Edmonton, Canada, July 1987, 71 pp.

R.2.8. R.J. Roark, "Formulas for Stress and Strain, Fifth Edition", McGraw-Hill, New York, U.S.A., 1975, 624 pp.

R.2.9. "Metals Handbook, Volume 11, Nondestructive Inspection and Quality Control, 8th Edition", American Society for Testing and Materials, 1976, 446 pp.

Appendix A - Test Results used in Modulus of Elasticity Study

Table A-3.7.3 - Specified Modulus of Elasticity Test Results

Ref. #	f_c (MPa)	$E_{c(Measured)}$ (MPa)	$E_{c(Calculated)}$ (MPa) (ACI 318M-89)*	Kind of Coarse Aggregate	$\frac{E_{c(Measured)}}{E_{c(Calculated)}}$
U of A+	64.3	29446	37688	Sandstone Gravel	0.78
U of A+	65.3	29528	37980	Sandstone Gravel	0.78
U of A+	66.0	24615	38183	Sandstone Gravel	0.64
U of A+	66.2	29672	38241	Sandstone Gravel	0.78
U of A+	66.3	28517	38270	Sandstone Gravel	0.75
U of A+	66.4	31908	38299	Sandstone Gravel	0.83
U of A+	66.4	27195	38299	Sandstone Gravel	0.71
U of A+	67.1	28933	38500	Sandstone Gravel	0.75
U of A+	90.9	31479	44811	Sandstone Gravel	0.70
U of A+	94.2	32094	45617	Sandstone Gravel	0.70
U of A+	95.9	31900	46026	Sandstone Gravel	0.69
U of A+	97.5	32456	46409	Sandstone Gravel	0.70
U of A+	97.9	30293	46504	Sandstone Gravel	0.65
U of A+	102.4	31448	47561	Sandstone Gravel	0.66
U of A+	103.5	30065	47815	Sandstone Gravel	0.63
U of A+	105.1	31683	48184	Sandstone Gravel	0.66
U of A+	106.2	32333	48435	Sandstone Gravel	0.67
U of A+	106.5	34353	48503	Sandstone Gravel	0.71
U of A+	106.1	35151	48412	Sandstone Gravel	0.73
U of A+	115.5	38816	50511	Sandstone Gravel	0.77

Table A-3.7.3 - Continued

Ref. #	f_c (MPa)	$E_{c(Measured)}$ (MPa)	$E_{c(Calculated)}$ (MPa) (ACI 318M-89)*	Kind of Coarse Aggregate	$\frac{E_{c(Measured)}}{E_{c(Calculated)}}$
U of A+	119.7	36163	51422	Sandstone Gravel	0.70
U of A+	120.6	37181	51614	Sandstone Gravel	0.72
U of A+	121.6	37188	51828	Sandstone Gravel	0.72
U of A+	125.0	37922	52548	Sandstone Gravel	0.72
12	64.0	27900	37600	Sandstone Gravel	0.74
12	65.6	25200	38067	Sandstone Gravel	0.66
12	65.5	25500	38038	Sandstone Gravel	0.67
12	72.9	25700	40129	Sandstone Gravel	0.64
11	92.1	33800	45105	Siliceous Gravel	0.75
11	95.9	35900	46026	Siliceous Gravel	0.78
12	73.6	34600	40322	Limestone	0.86
12	69.3	36600	39126	Limestone	0.94
12	76.5	36800	41108	Limestone	0.90
12	58.8	29600	36040	Limestone	0.82
12	57.1	29500	35515	Limestone	0.83
12	59.1	29000	36132	Limestone	0.80
15	79.4	43645	41880	Limestone	1.04
15	77.5	44749	41376	Limestone	1.08
15	85.3	44818	43408	Limestone	1.03
15	85.8	46265	43535	Limestone	1.06
11	97.3	37900	46361	Limestone	0.82

Table A-3.7.3 - Continued

Ref. #	f_c (MPa)	$E_{c(Measured)}$ (MPa)	$E_{c(Calculated)}$ (MPa) (ACI 318M-89)*	Kind of Coarse Aggregate	$\frac{E_{c(Measured)}}{E_{c(Calculated)}}$
11	101.3	40700	47305	Limestone	0.86
9	95.3	39900	45882	Limestone	0.87
27	64.9	34335	37863	Limestone	0.91
19	77.1	37024	41269	Limestone	0.90
19	73.1	33163	40184	Limestone	0.83
19	65.4	33232	38009	Limestone	0.87
19	65.1	34749	37922	Limestone	0.92
19	59.1	33094	36132	Limestone	0.92
9	88.6	40700	44240	Limestone	0.92
13	78.6	43200	41669	Dolimite	1.04
13	88.5	44500	44215	Dolimite	1.01
13	91.9	45500	45056	Dolimite	1.01
13	118.9	50800	51249	Dolimite	0.99
13	107.0	48400	48617	Dolimite	1.00
19	76.9	34197	41216	Dolimite	0.83
19	70.1	33508	39351	Dolimite	0.85
19	65.8	33922	38125	Dolimite	0.89
19	61.9	31026	36978	Dolimite	0.84
19	55.9	29923	35140	Dolimite	0.85
9	97.6	39800	46433	Dolimite	0.86
9	95.1	44900	45834	Dolimite	0.98

Table A-3.7.3 - Continued

Ref. #	f_c (MPa)	$E_{c(Measured)}$ (MPa)	$E_{c(Calculated)}$ (MPa) (ACI 318M-89)*	Kind of Coarse Aggregate	$\frac{E_{c(Measured)}}{E_{c(Calculated)}}$
9	90.9	42000	44811	Quartzites	0.94
9	89.0	40900	44340	Quartzites	0.92
9	84.7	45100	43255	Quartzites	1.04
9	84.1	41900	43102	Quartzites	0.97
11	84.8	31700	43281	Granite	0.73
11	88.6	33800	44240	Granite	0.76
9	103	39900	47700	Granite	0.84
27	79.8	34266	41986	Granite	0.82
27	84.4	33853	43179	Granite	0.78
27	55.1	29578	34888	Granite	0.85
27	60.5	31164	36557	Granite	0.85
9	94.3	42100	45641	Granite	0.92
19	79.8	41161	41986	Trap Rock	0.98
19	76.1	39644	41001	Trap Rock	0.97
19	74.9	40265	40676	Trap Rock	0.99
19	70.6	39231	39491	Trap Rock	0.99
19	66.2	36680	38241	Trap Rock	0.96
19	57.5	33784	35640	Trap Rock	0.95
11	100.7	36600	47164	Diabase	0.78
11	104.8	37900	48115	Diabase	0.79
16	99.2	40700	46812	Diabase	0.87

Table A-3.7.3 - Continued

Ref. #	f_c (MPa)	$E_{c(Measured)}$ (MPa)	$E_{c(Calculated)}$ (MPa) (ACI 318M-89)*	Kind of Coarse Aggregate	$\frac{E_{c(Measured)}}{E_{c(Calculated)}}$
16	98.8	41400	46717	Diabase	0.89
16	105.2	42100	48207	Diabase	0.87
16	97.6	43400	46433	Diabase	0.93
27	75.3	44953	40785	Diabase	1.10
27	107.3	48125	48685	Diabase	0.99
9	101.0	24000	47234	Sandstone	0.51
9	102.3	31400	47537	Sandstone	0.66
9	98.1	26100	46551	Sandstone	0.56
9	96.1	32300	46074	Sandstone	0.70

+ Data from the current study.

* $E_c = 4700\sqrt{f'_c}$

Appendix B. LH Series Monotonic Test Results

The experimental results for short term monotonic concentric tests are presented in Figures B-4.5.A through H of this appendix. The details of experimental results for sustained concentric tests and also the discussion of results are presented in sections 4.5.1.2 and 4.5.2.

The experimental results for short term monotonic eccentric tests are presented in Figures B-4.6.A through H of this appendix. The details of experimental results for sustained eccentric tests and also the discussion of results are presented in sections 4.6.1.2 and 4.6.2.

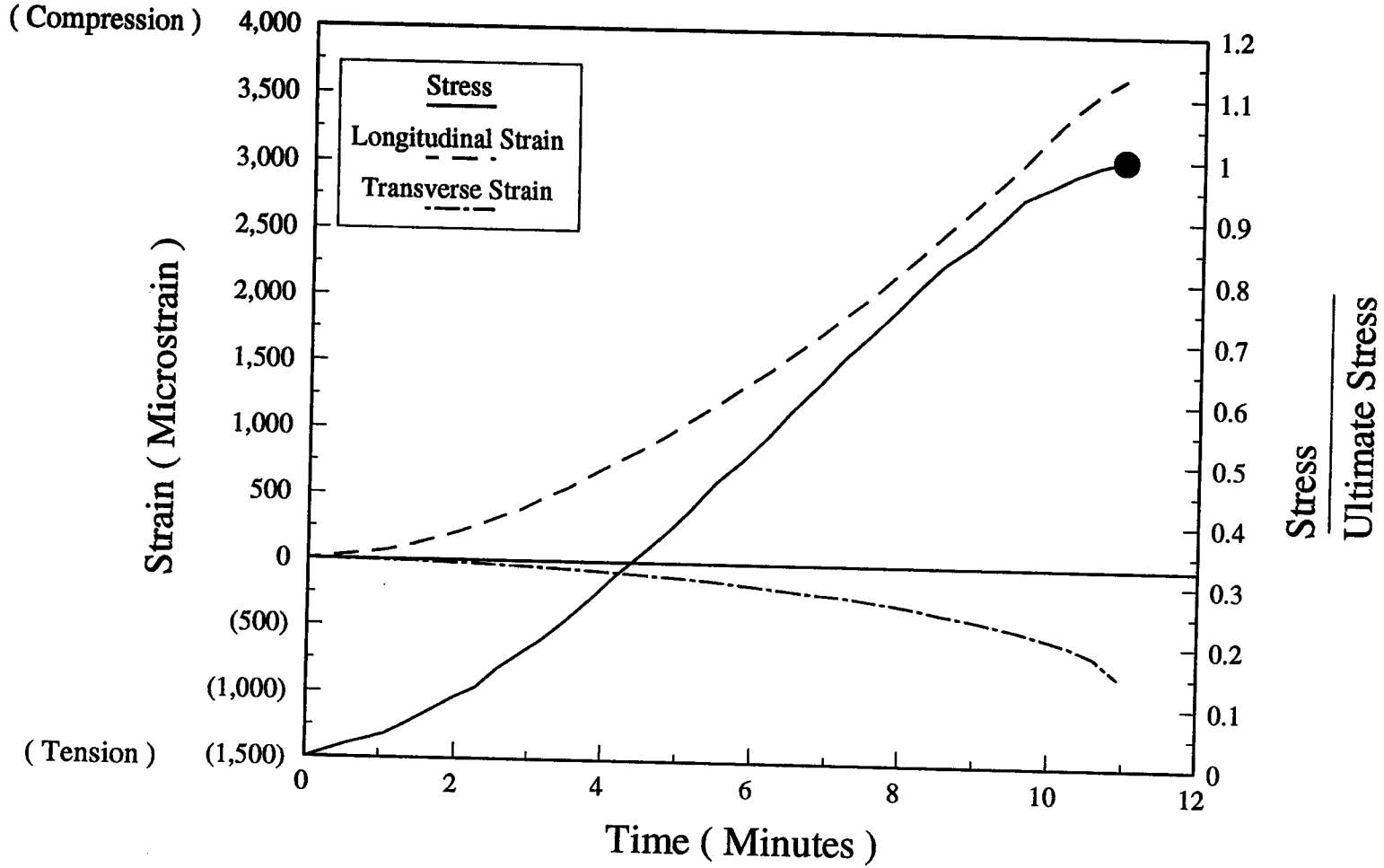

f_c= 66.0 MPa

A = 7867 mm^2

Figure B-4.5.A - Stress-Strain-Time Relationship - LHC100A Specimen

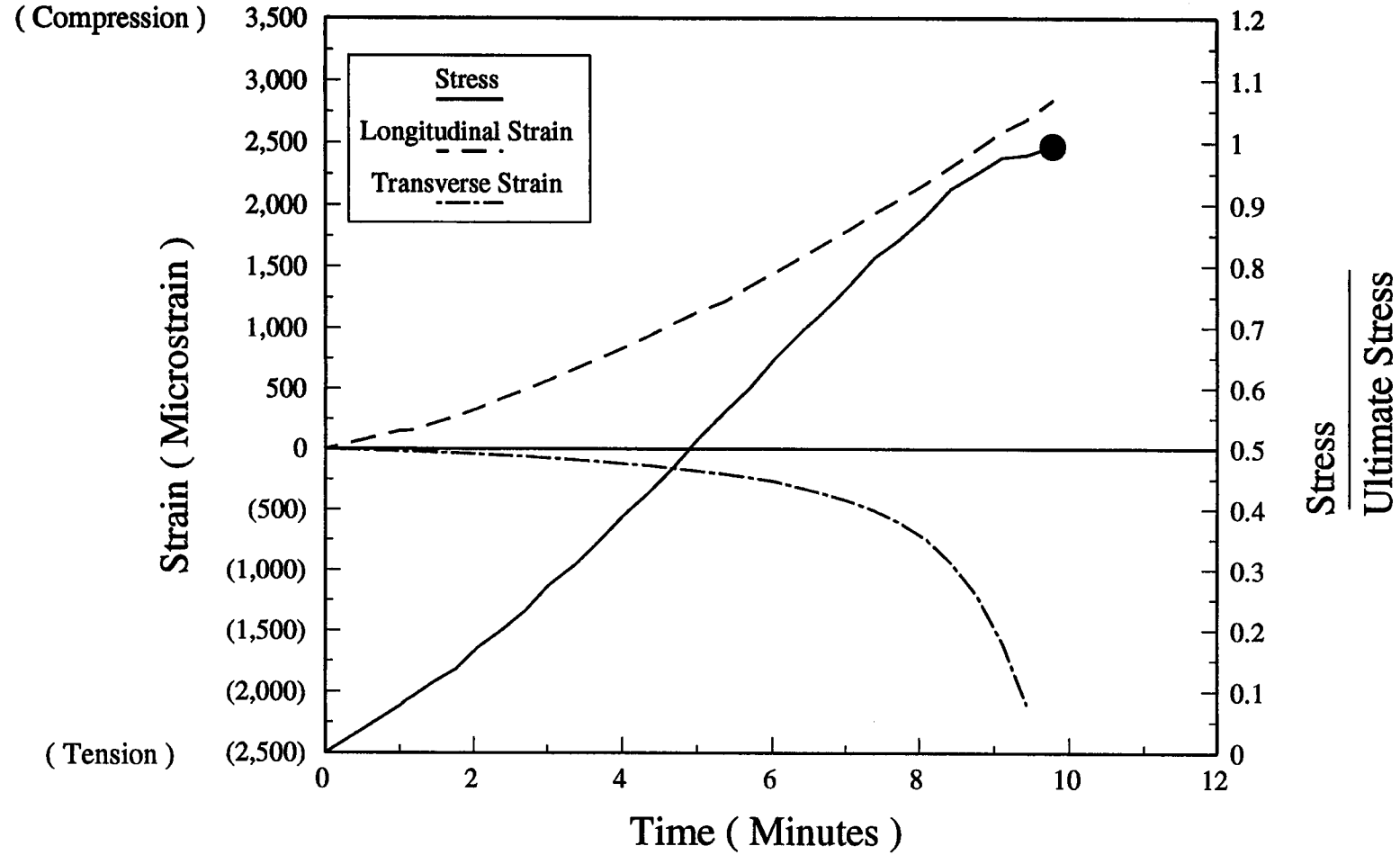

$f_c = 64.3$ MPa $\qquad A = 8134\ mm^2$

Figure B-4.5.B - Stress-Strain-Time Relationship - LHC100B Specimen

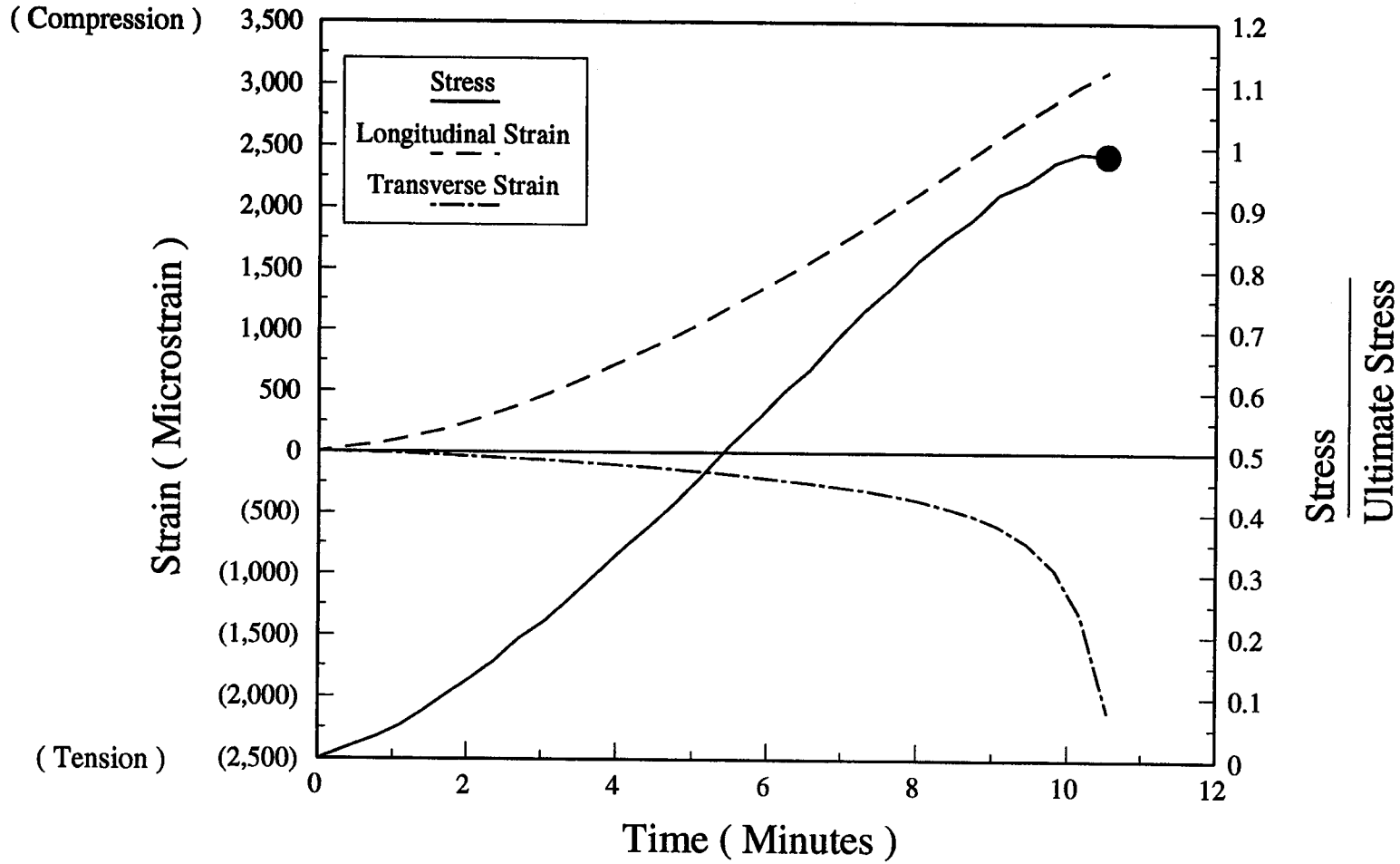

$f_c = 66.3$ MPa $\qquad A = 8599\ mm^2$

Figure B-4.5.C - Stress-Strain-Time Relationship - LHC100C Specimen

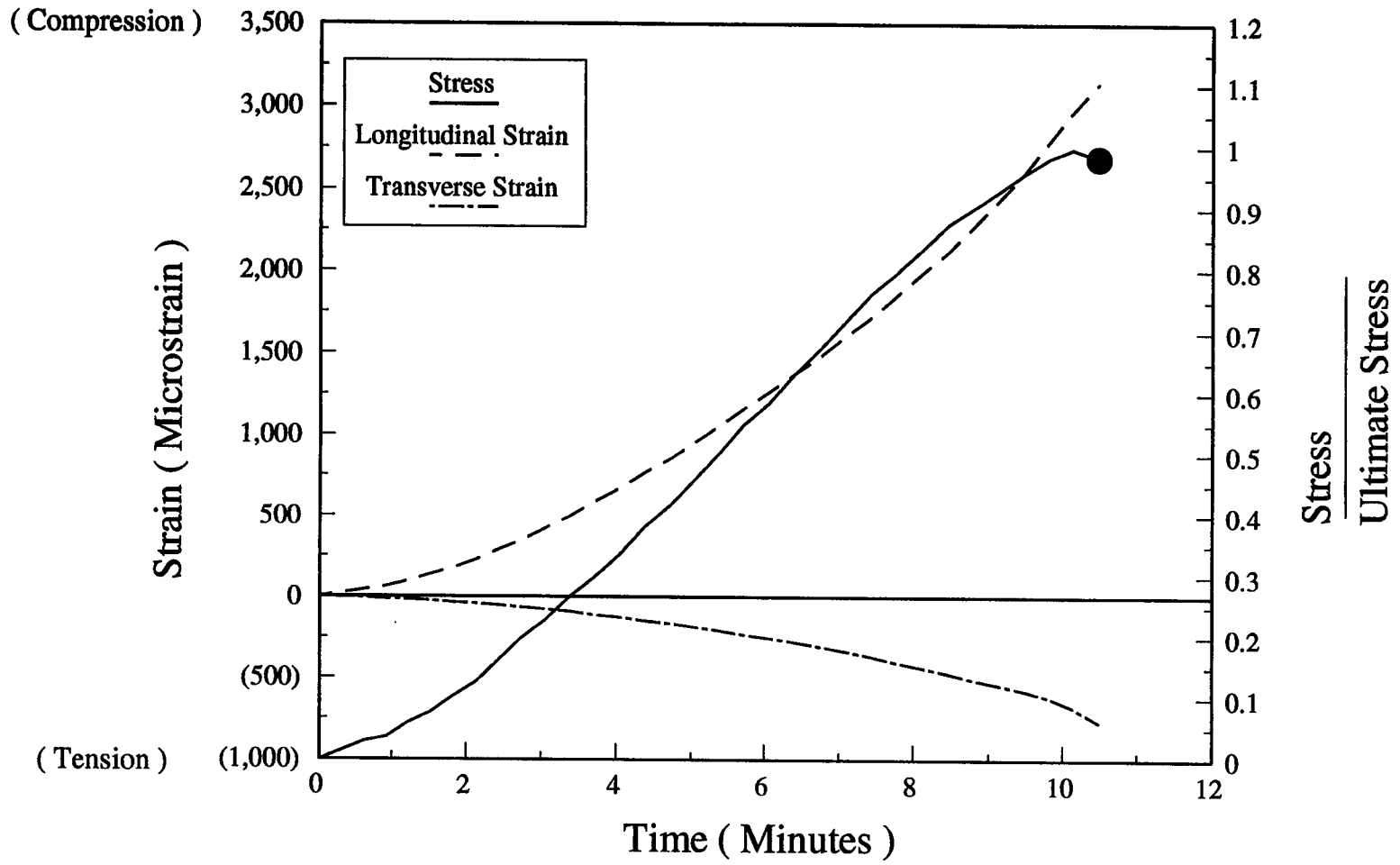

$f_c = 66.4$ MPa $\qquad A = 7755\ mm^2$

Figure B-4.5.D - Stress-Strain-Time Relationship - LHC100D Specimen

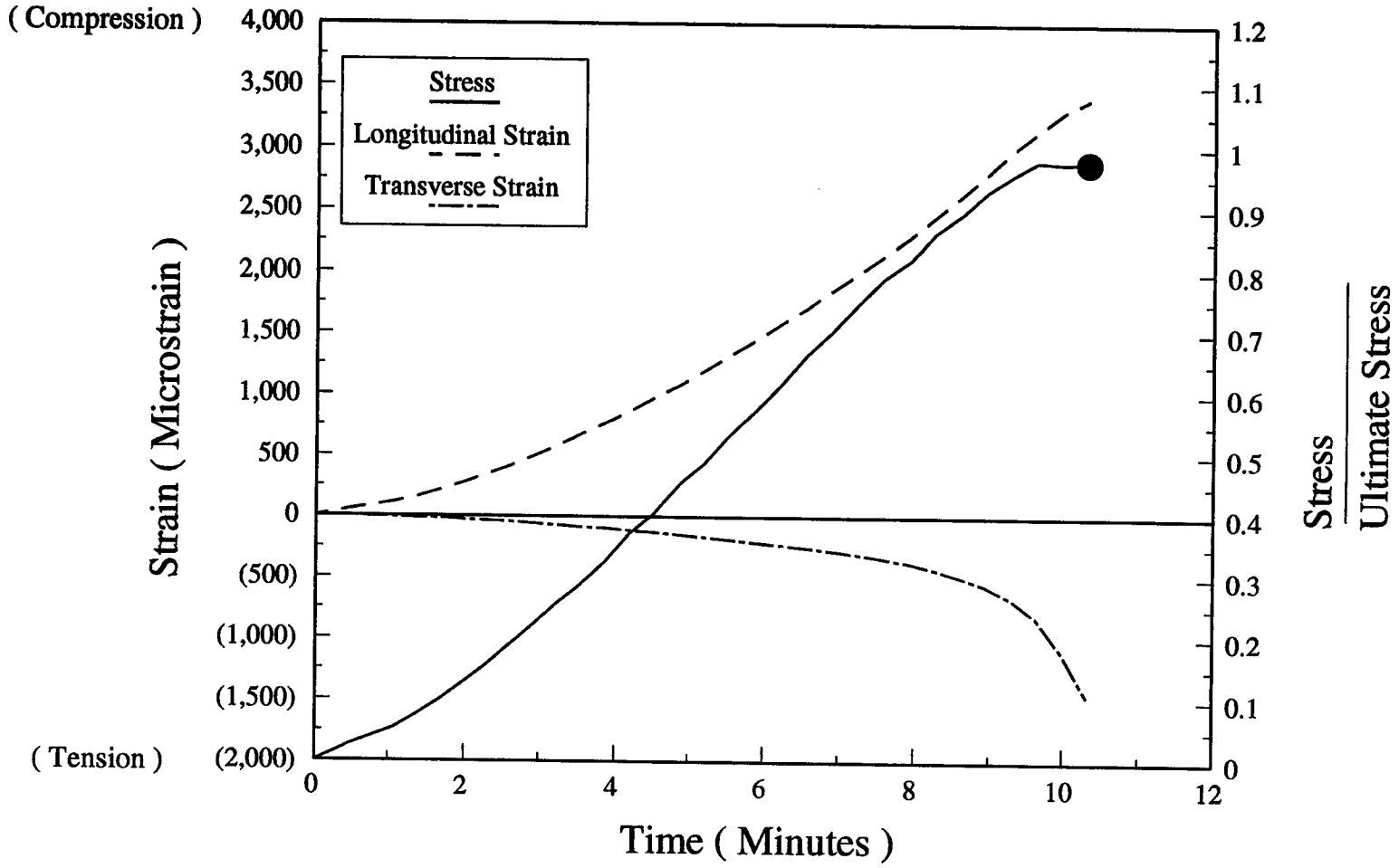

f_c= 66.4 MPa A = 7773 mm^2

Figure B-4.5.E - Stress-Strain-Time Relationship - LHC100E Specimen

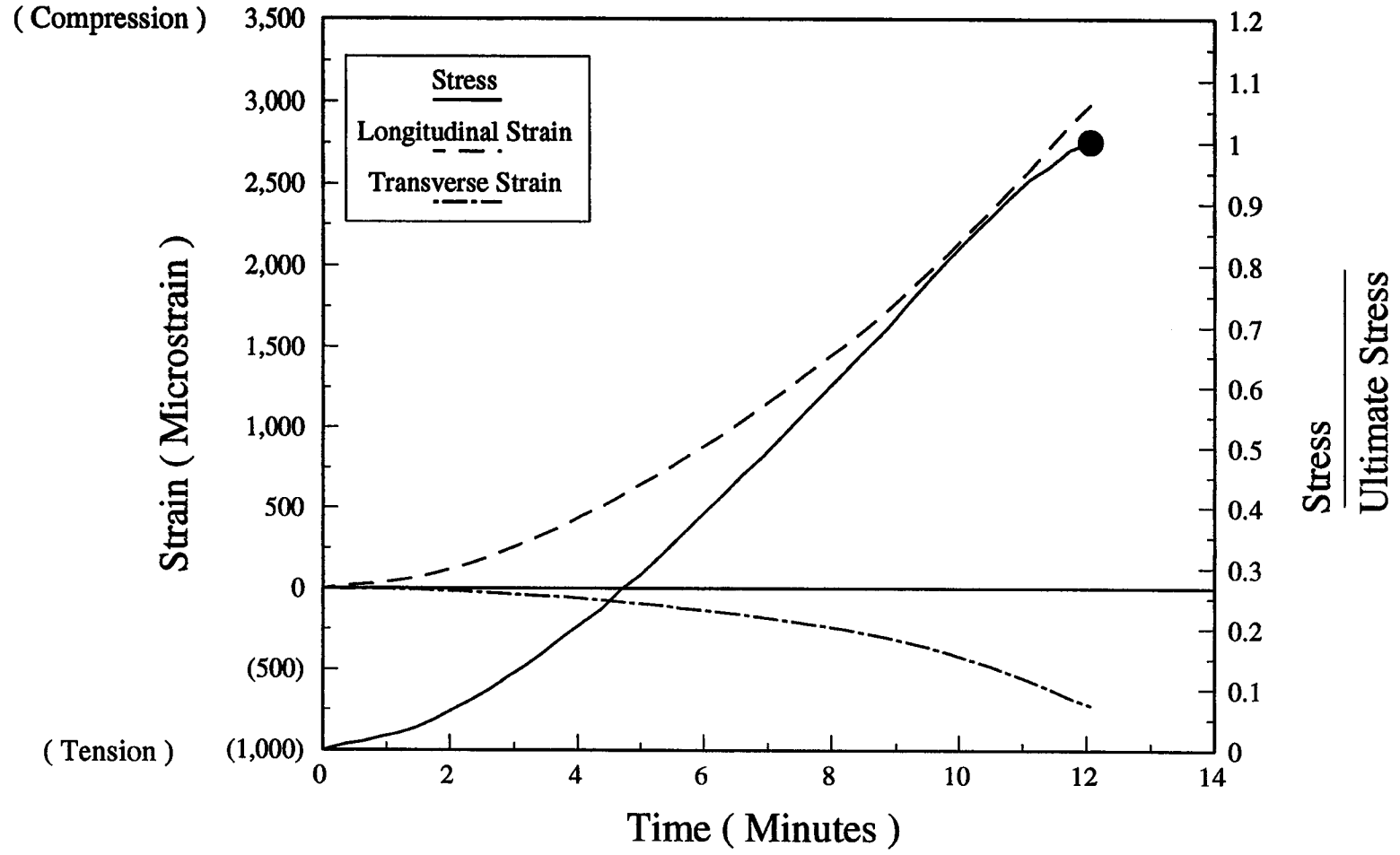

$f_c = 67.1$ MPa $\qquad A = 8103\ mm^2$

Figure B-4.5.F - Stress-Strain-Time Relationship - LHC100A(70) Specimen

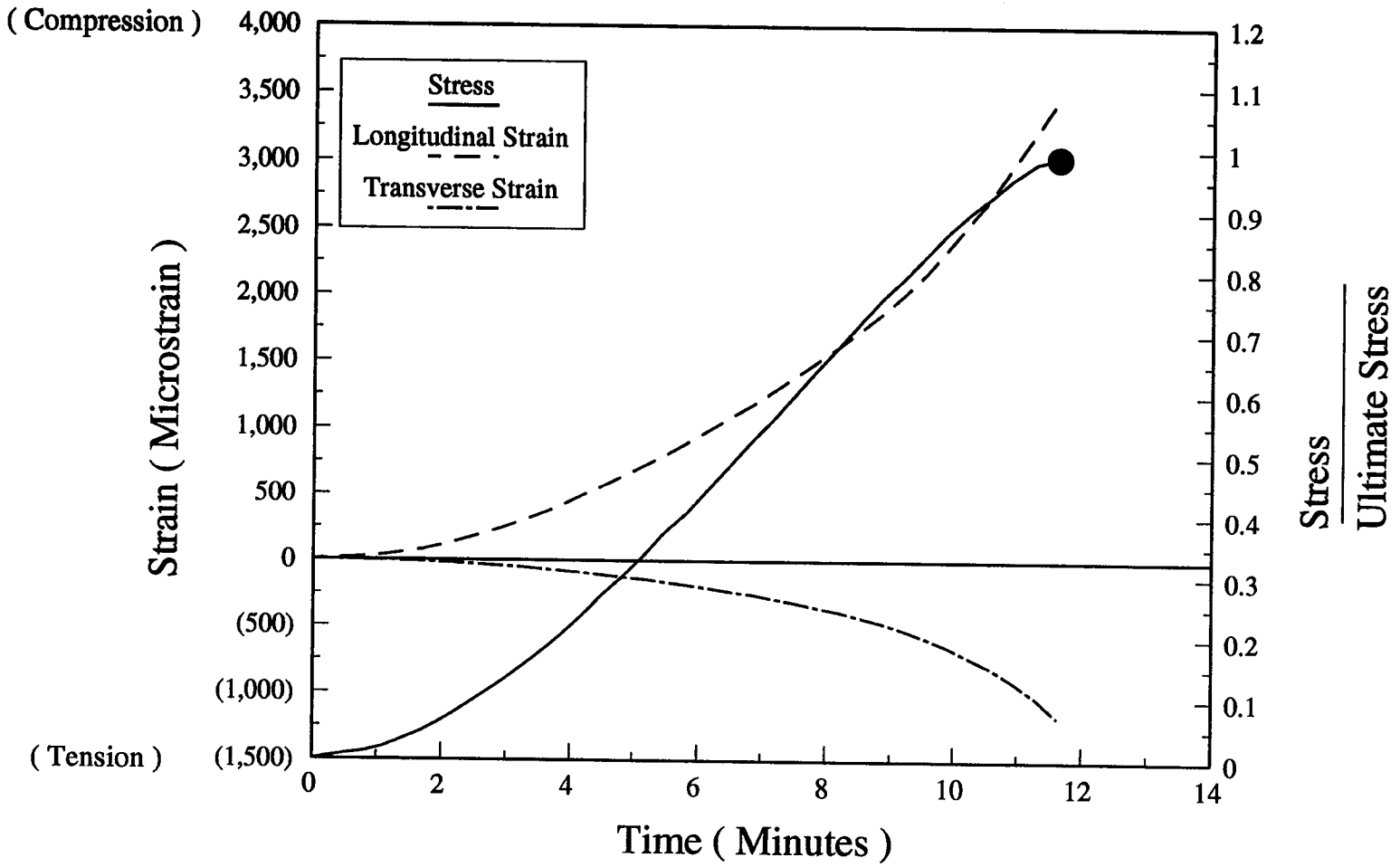

$f_c = 66.2$ MPa $\qquad A = 8476\ mm^2$

Figure B-4.5.G - Stress-Strain-Time Relationship - LHC100B(70) Specimen

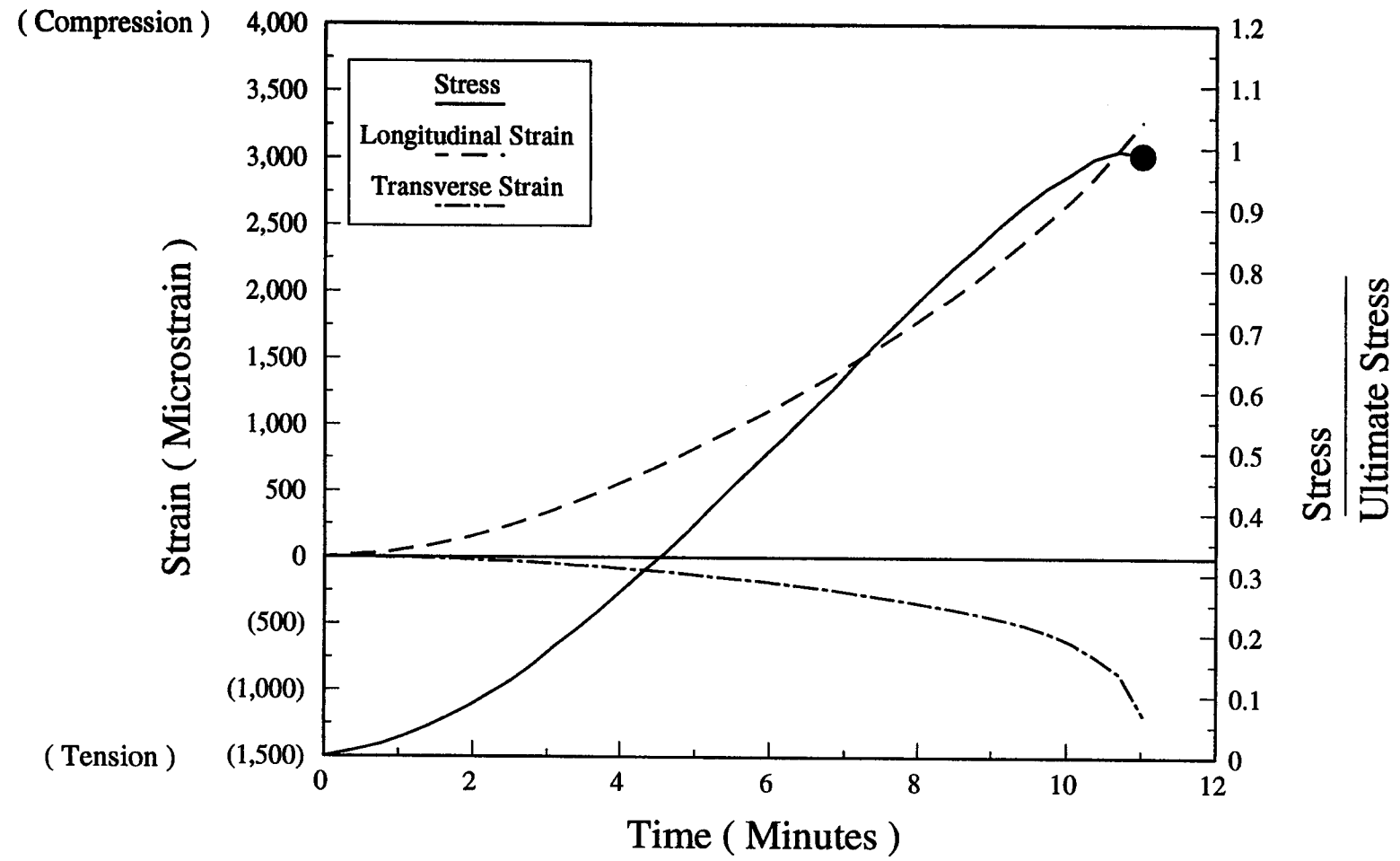

$f_c = 65.3$ MPa $\qquad A = 7776\ mm^2$

Figure B-4.5.H - Stress-Strain-Time Relationship - LHC100C(70) Specimen

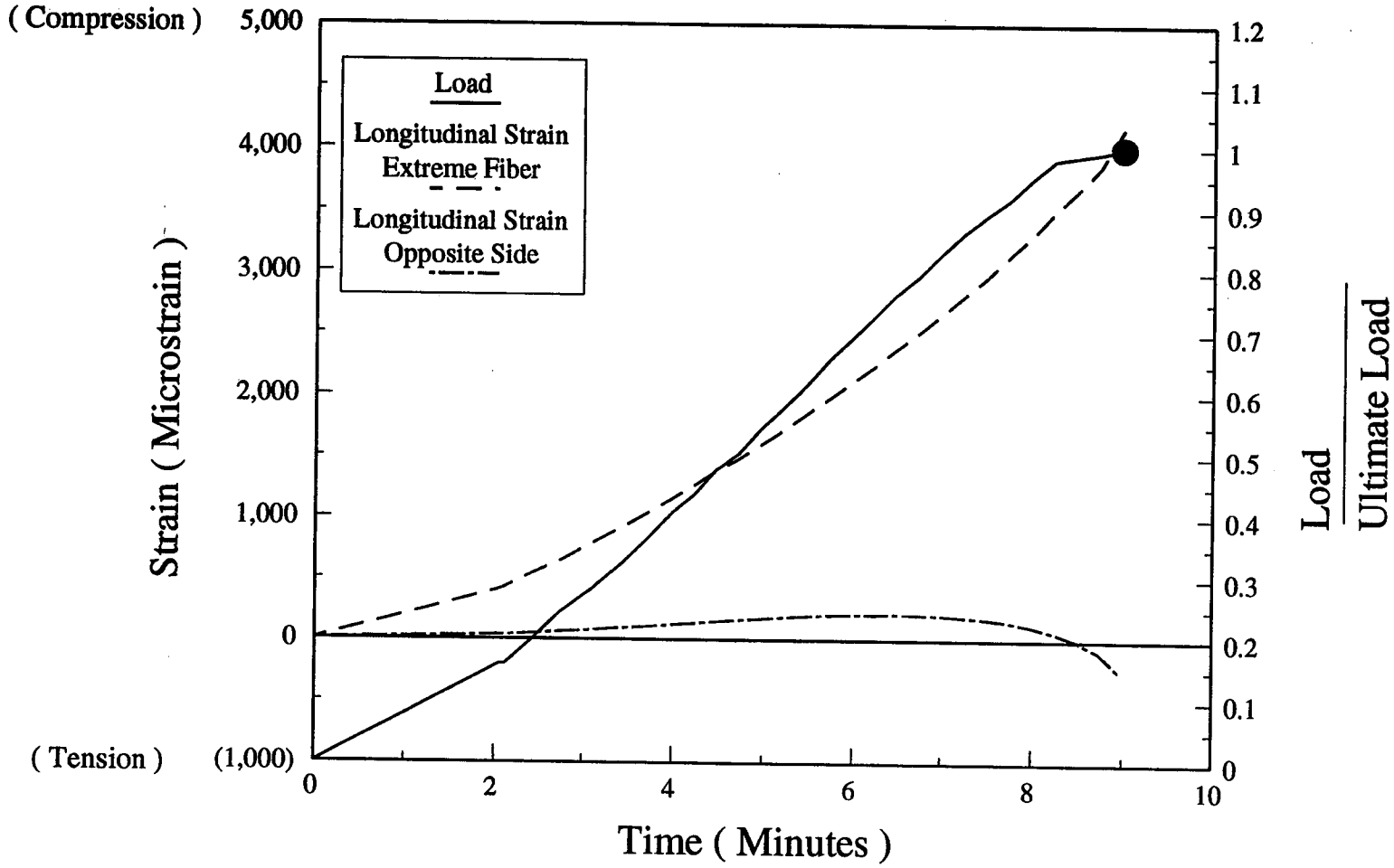

$P_c = 405.0$ kN $\qquad A = 8155$ mm^2

Figure B-4.6.A - Load-Strain-Time Relationship - LHE100A Specimen

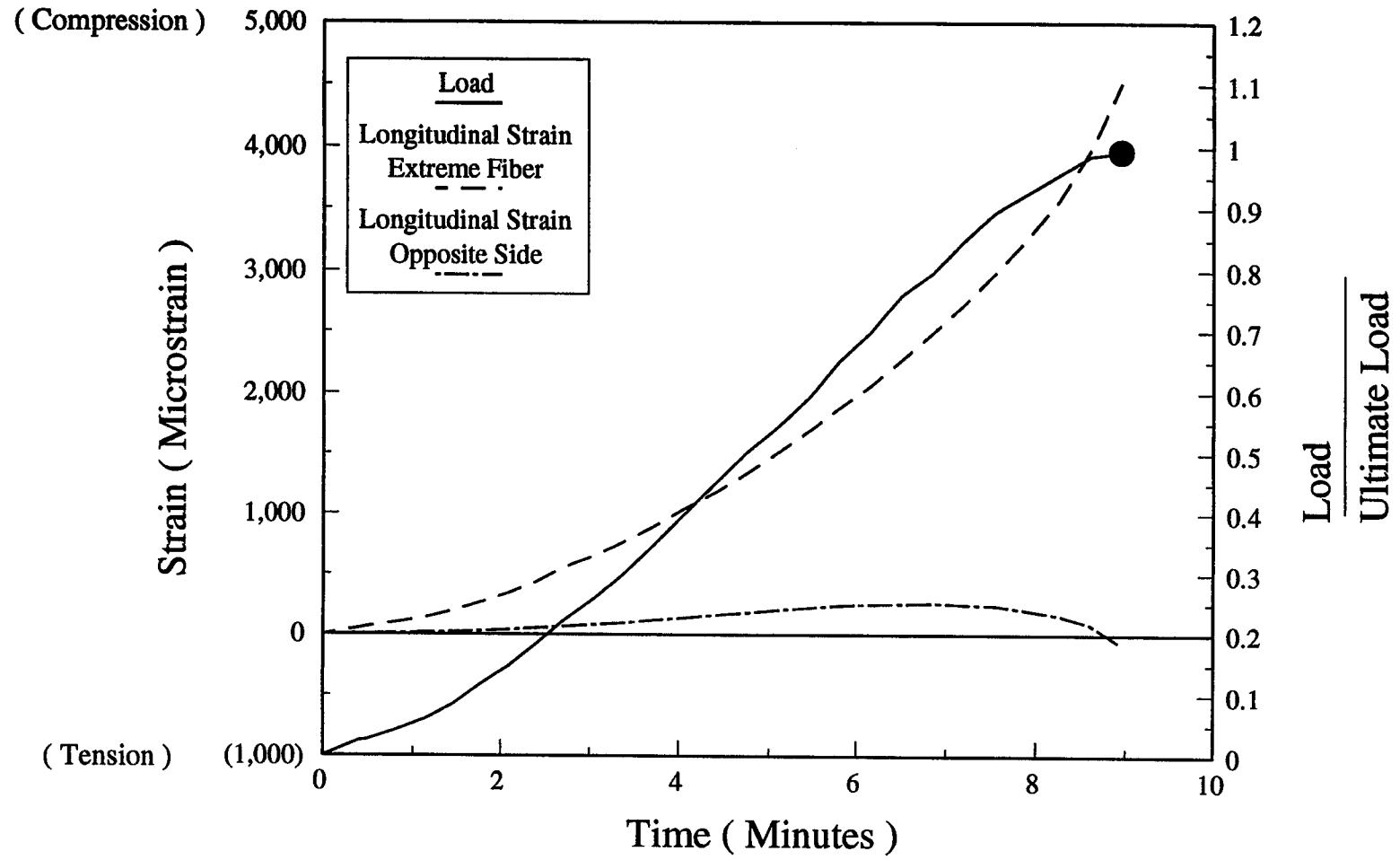

$P_c = 401.0$ kN $\qquad A = 8147$ mm^2

Figure B-4.6.B - Load-Strain-Time Relationship - LHE100B Specimen

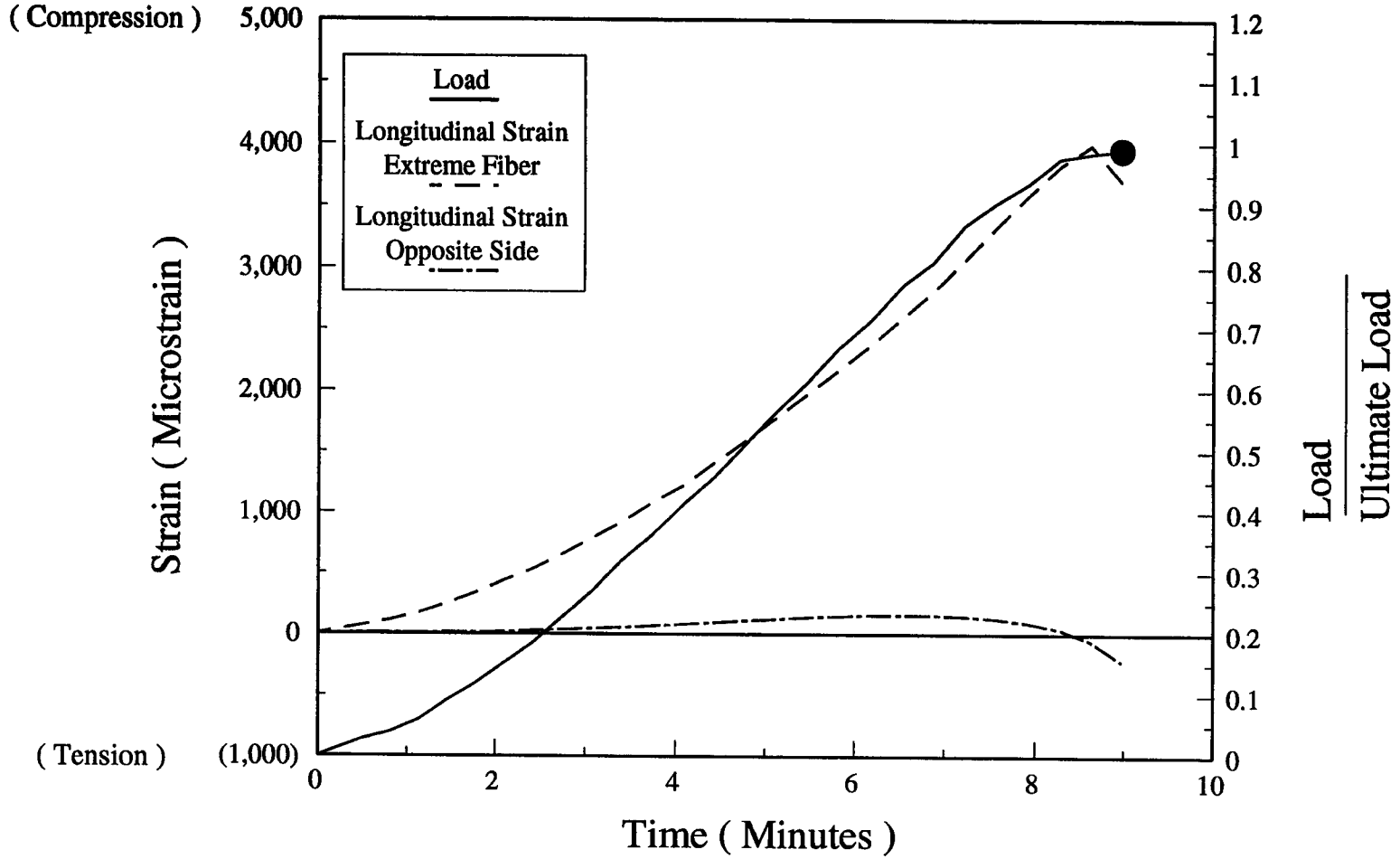

$P_c = 386.0$ kN $\qquad A = 7776$ mm^2

Figure B-4.6.C - Load-Strain-Time Relationship - LHE100C Specimen

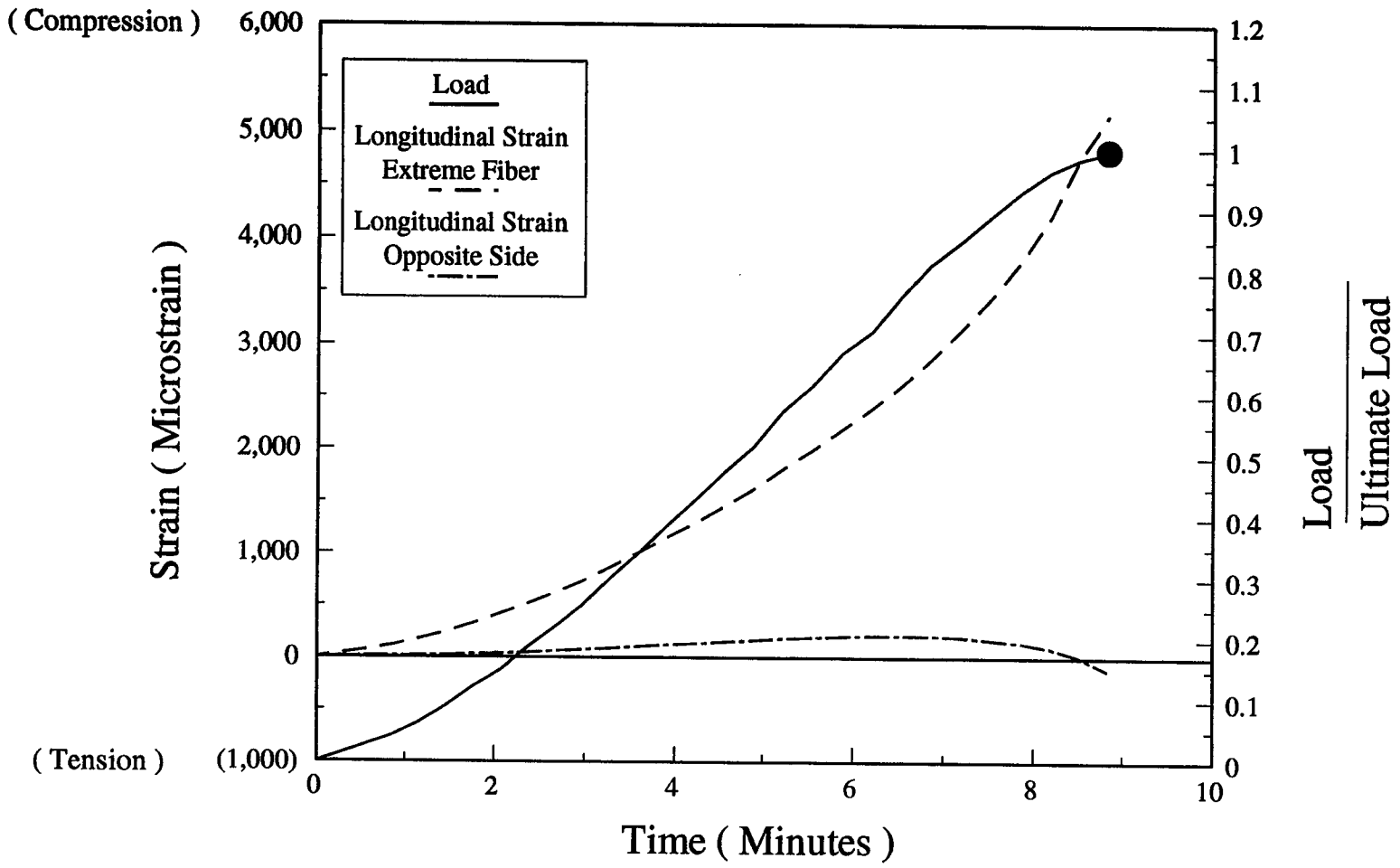

$P_c = 398.0$ kN $A = 8129$ mm^2

Figure B-4.6.D - Load-Strain-Time Relationship - LHE100D Specimen

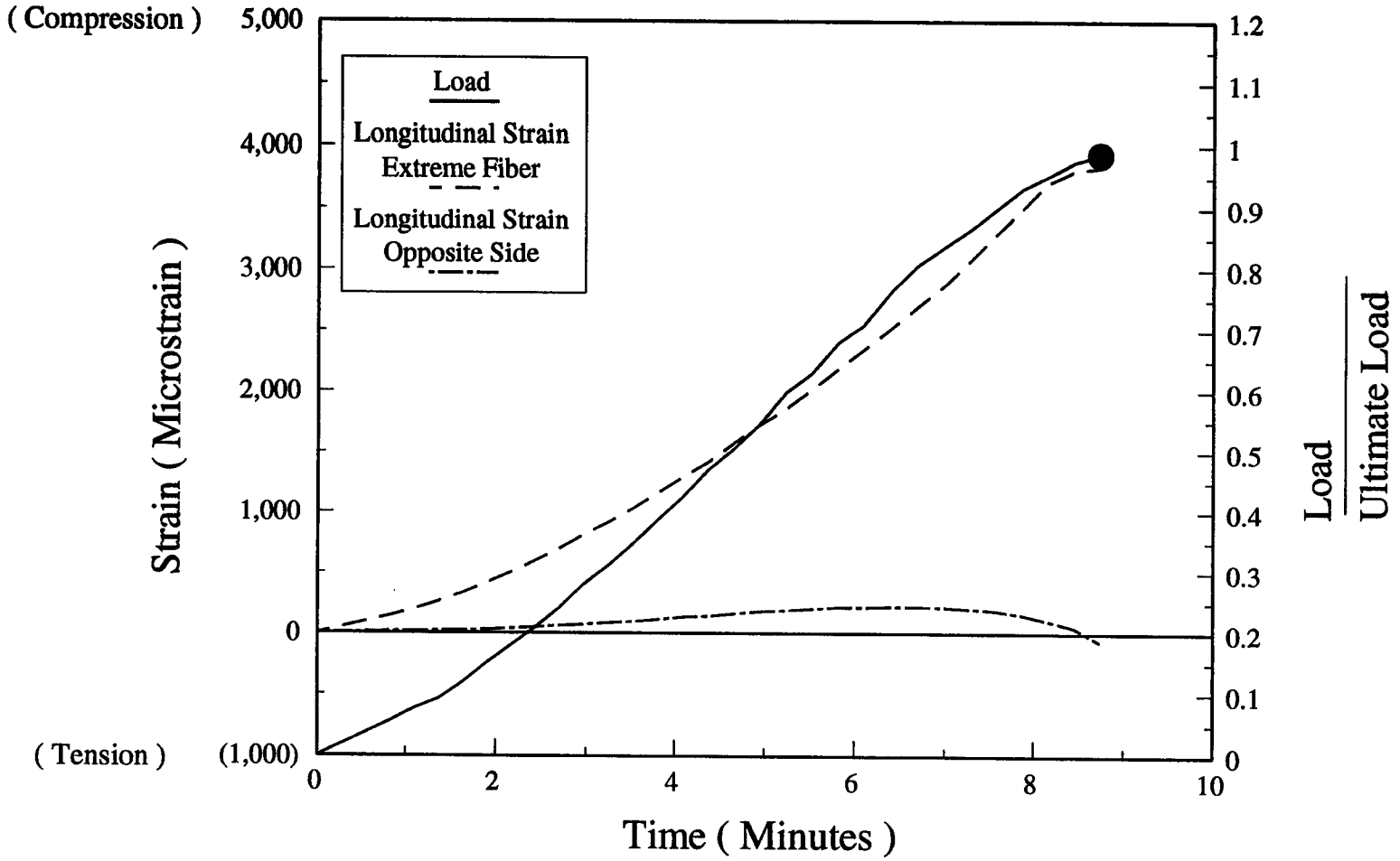

$P_c = 381.0$ kN $\qquad A = 7804$ mm^2

Figure B-4.6.E - Load-Strain-Time Relationship - LHE100E Specimen

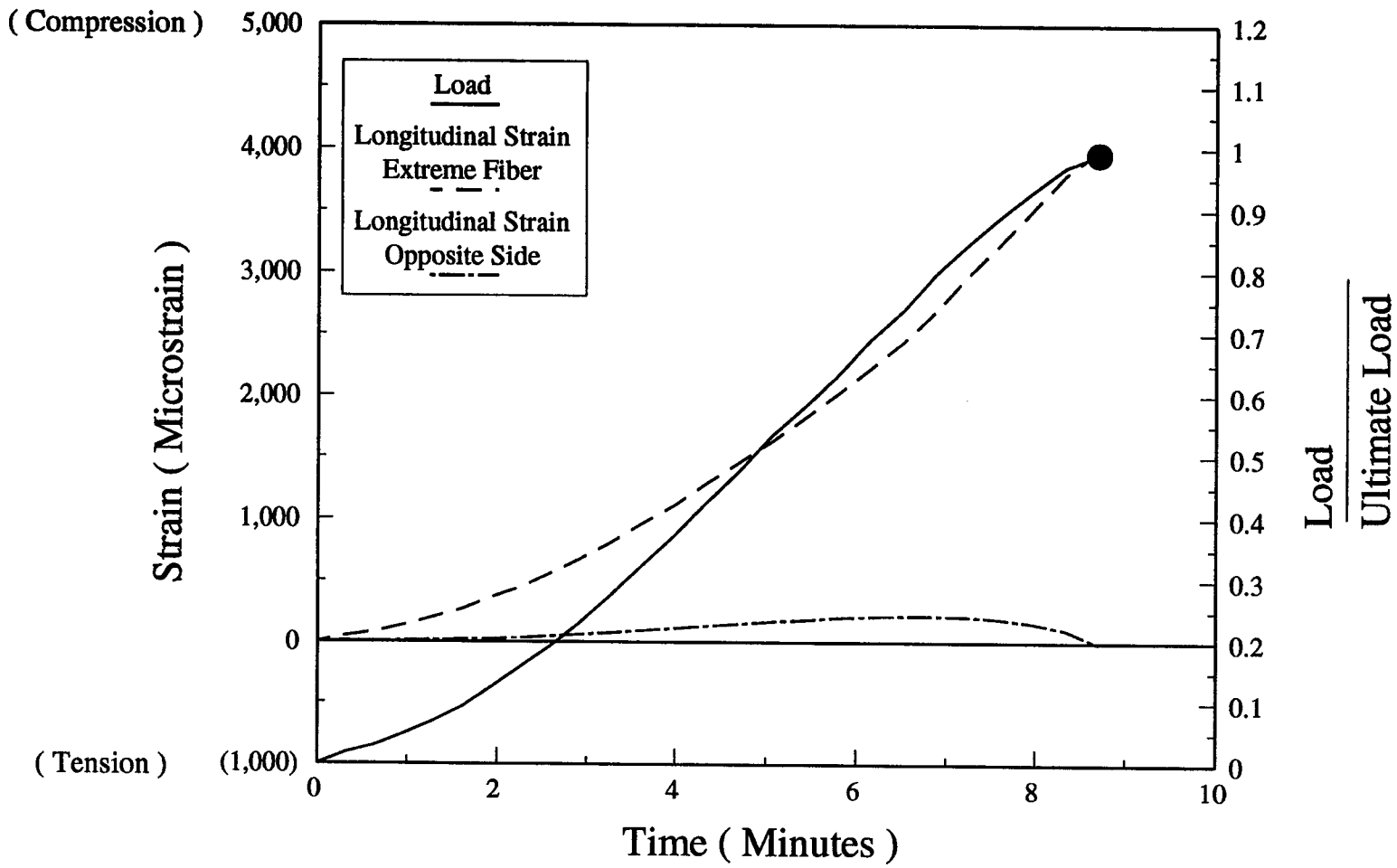

$P_c = 405.0$ kN $\qquad A = 8118$ mm^2

Figure B-4.6.F - Load-Strain-Time Relationship - LHE100A(70) Specimen

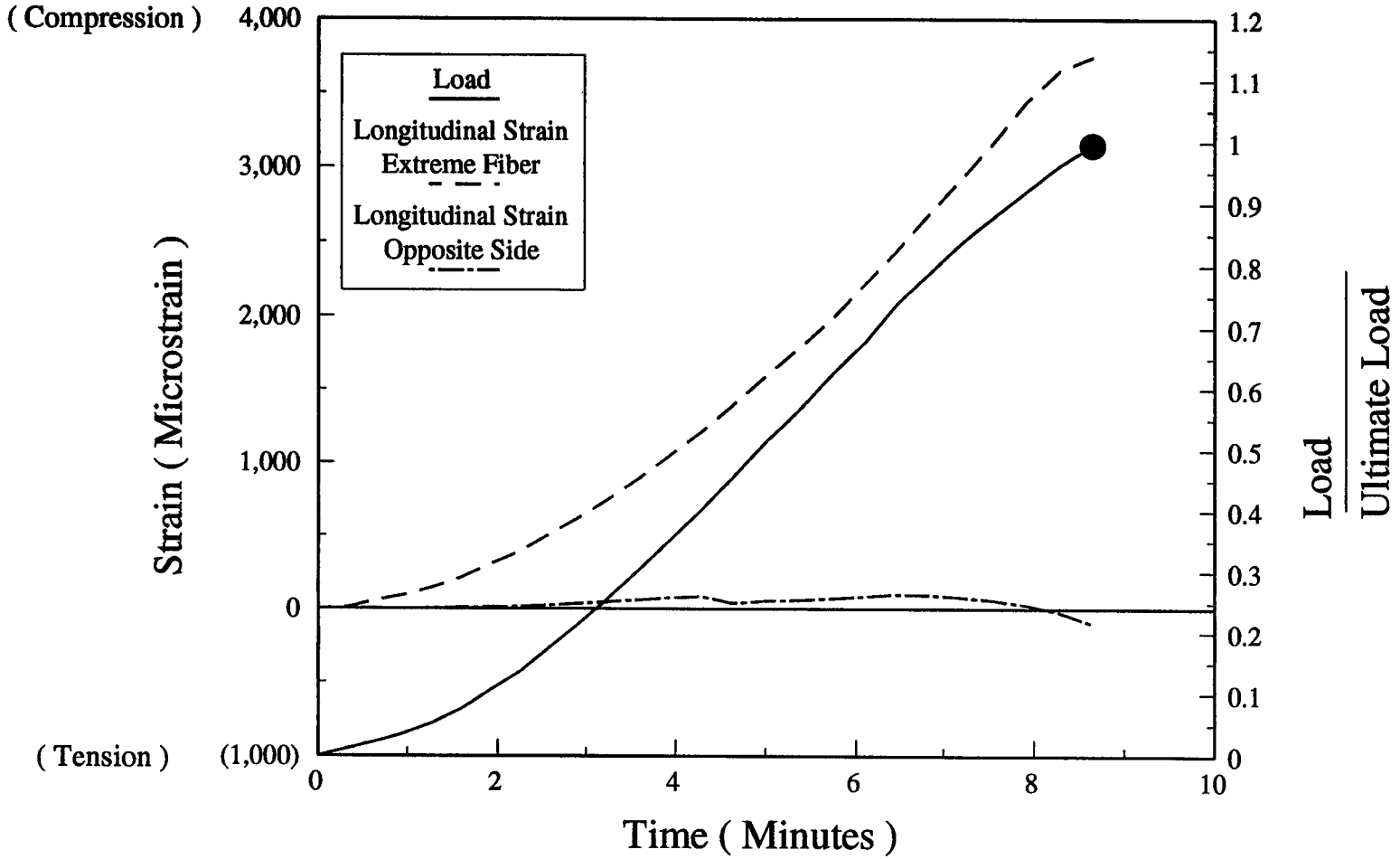

$P_c = 398.0$ kN $\qquad A = 7705$ mm^2

Figure B-4.6.G - Load-Strain-Time Relationship - LHE100B(70) Specimen

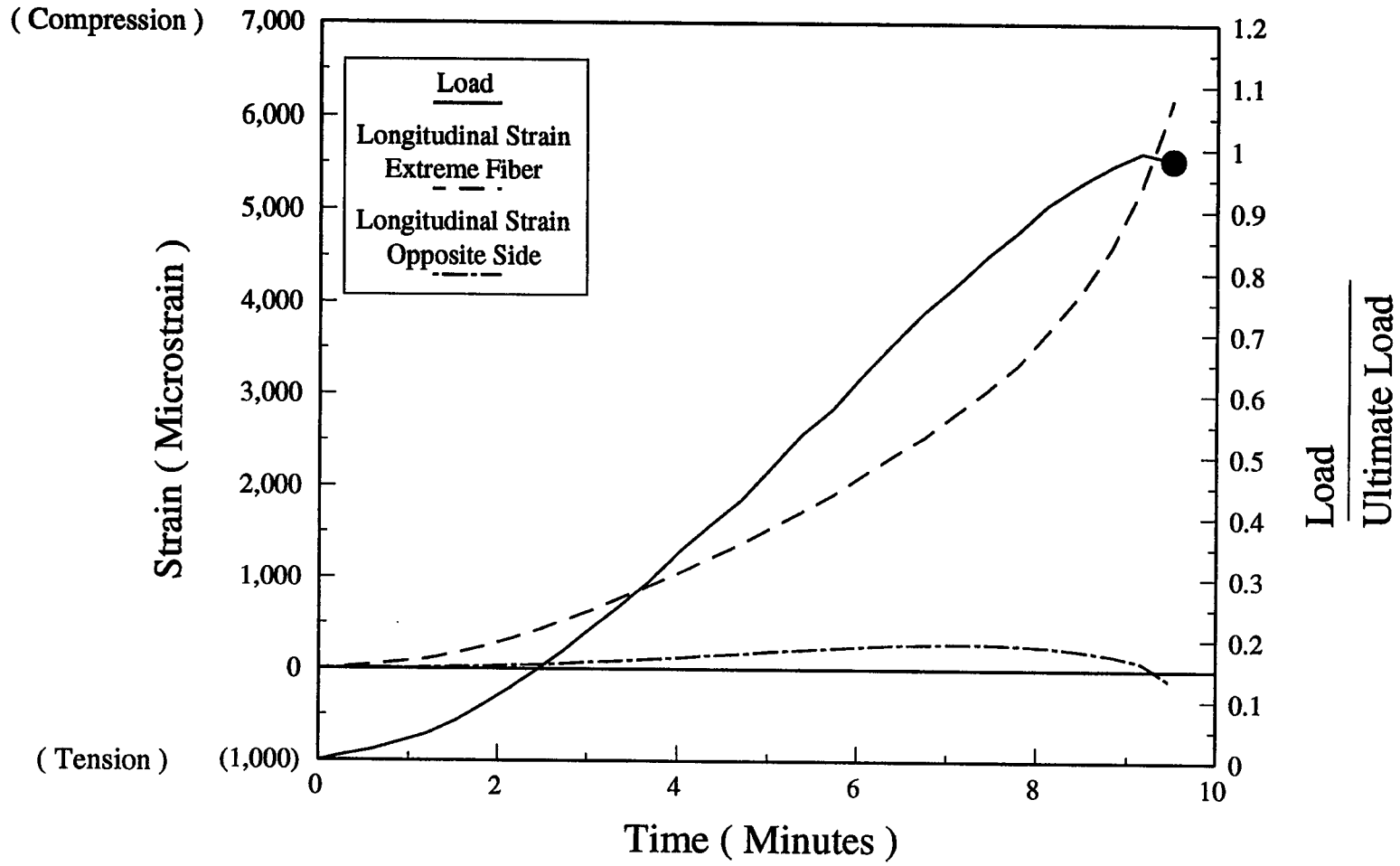

$P_c = 396.0$ kN $A = 7734$ mm^2

Figure B-4.6.H - Load-Strain-Time Relationship - LHE100C(70) Specimen

Appendix C. UH Series Monotonic Test Results

The experimental results for short term monotonic concentric tests are presented in Figures C-4.5.A through E of this appendix. The details of experimental results for sustained concentric tests and also the discussion of results are presented in sections 4.5.1.3 and 4.5.2.

The experimental results for short term monotonic eccentric tests are presented in Figures C-4.6.A through E of this appendix. The details of experimental results for sustained eccentric tests and also the discussion of results are presented in sections 4.6.1.3 and 4.6.2.

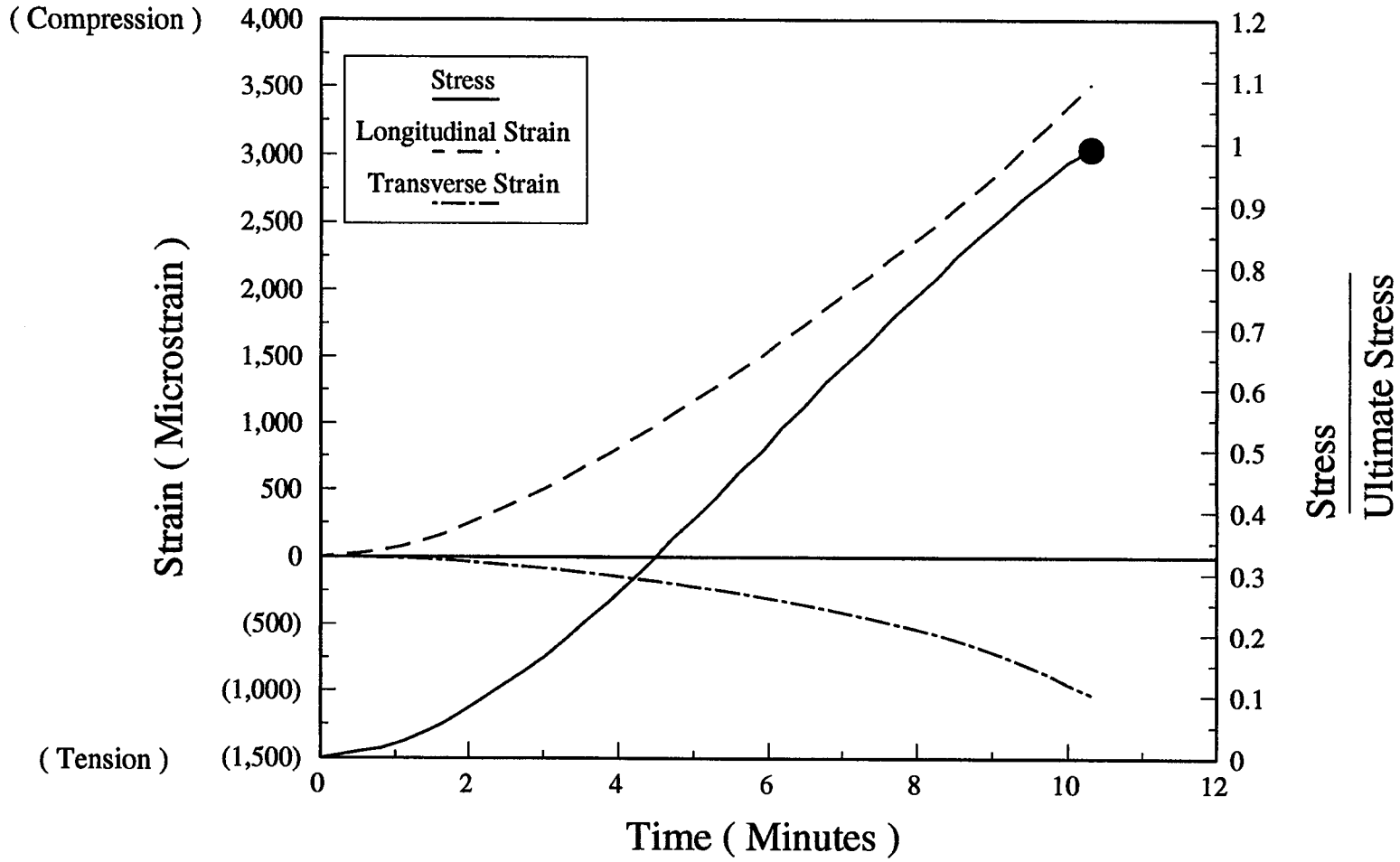

$f_c = 97.5$ MPa $\qquad A = 8017$ mm^2

Figure C-4.5.A - Stress-Strain-Time Relationship - UHC100A Specimen

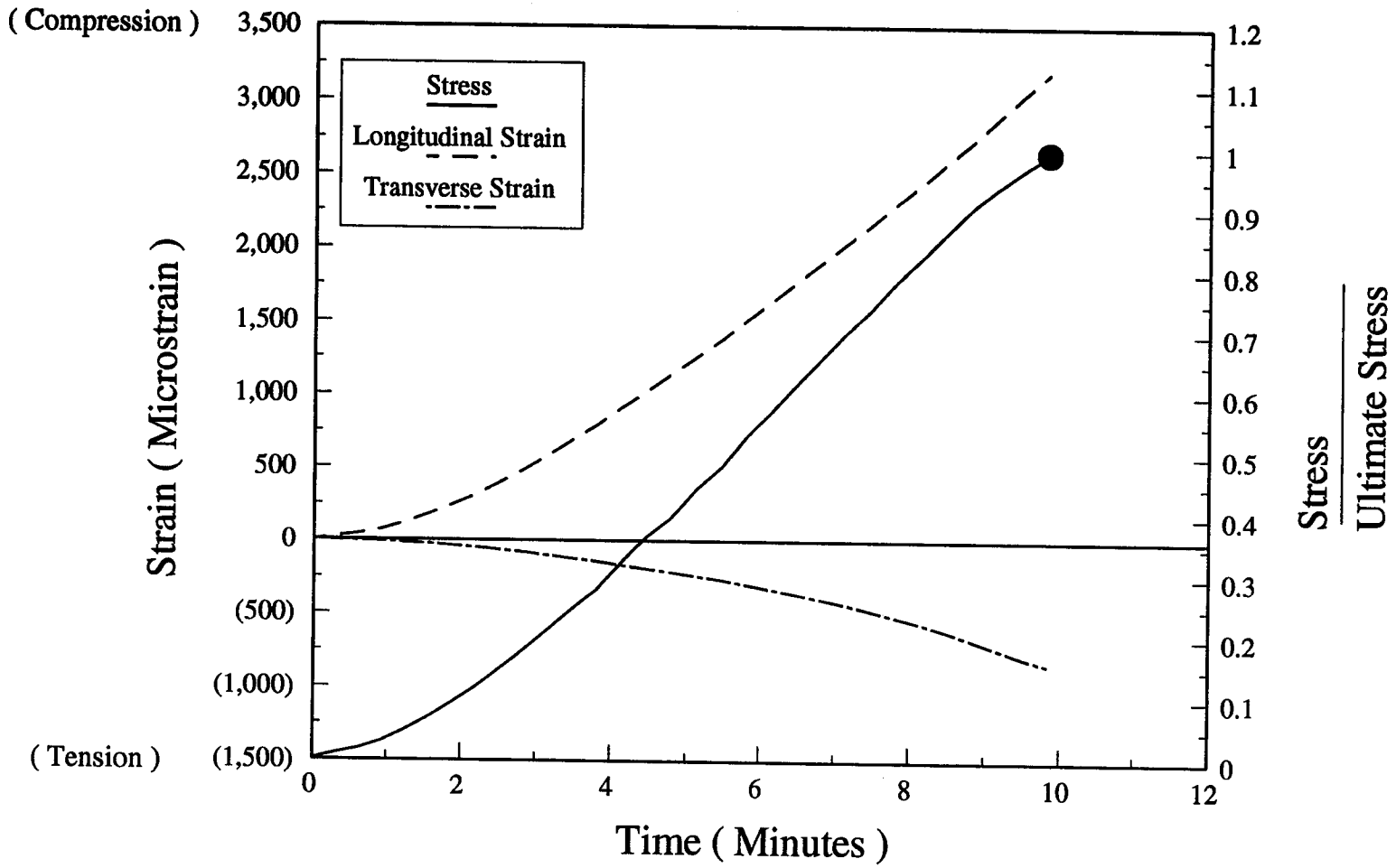

$f_c = 90.9$ MPa $\qquad A = 8152\ mm^2$

Figure C-4.5.B - Stress-Strain-Time Relationship - UHC100B Specimen

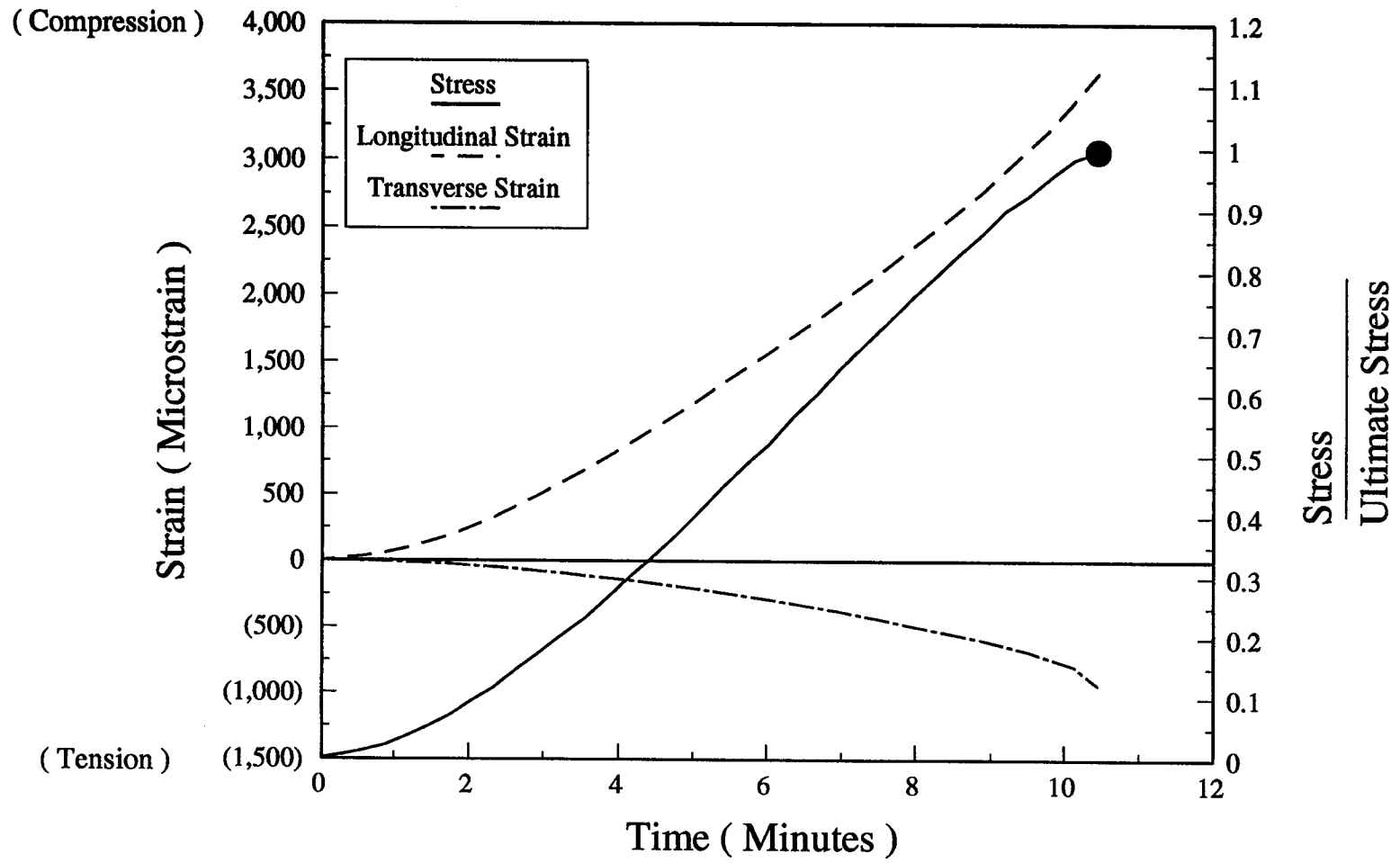

f_c = 95.9 MPa A = 8166 mm^2

Figure C-4.5.C - Stress-Strain-Time Relationship - UHC100C Specimen

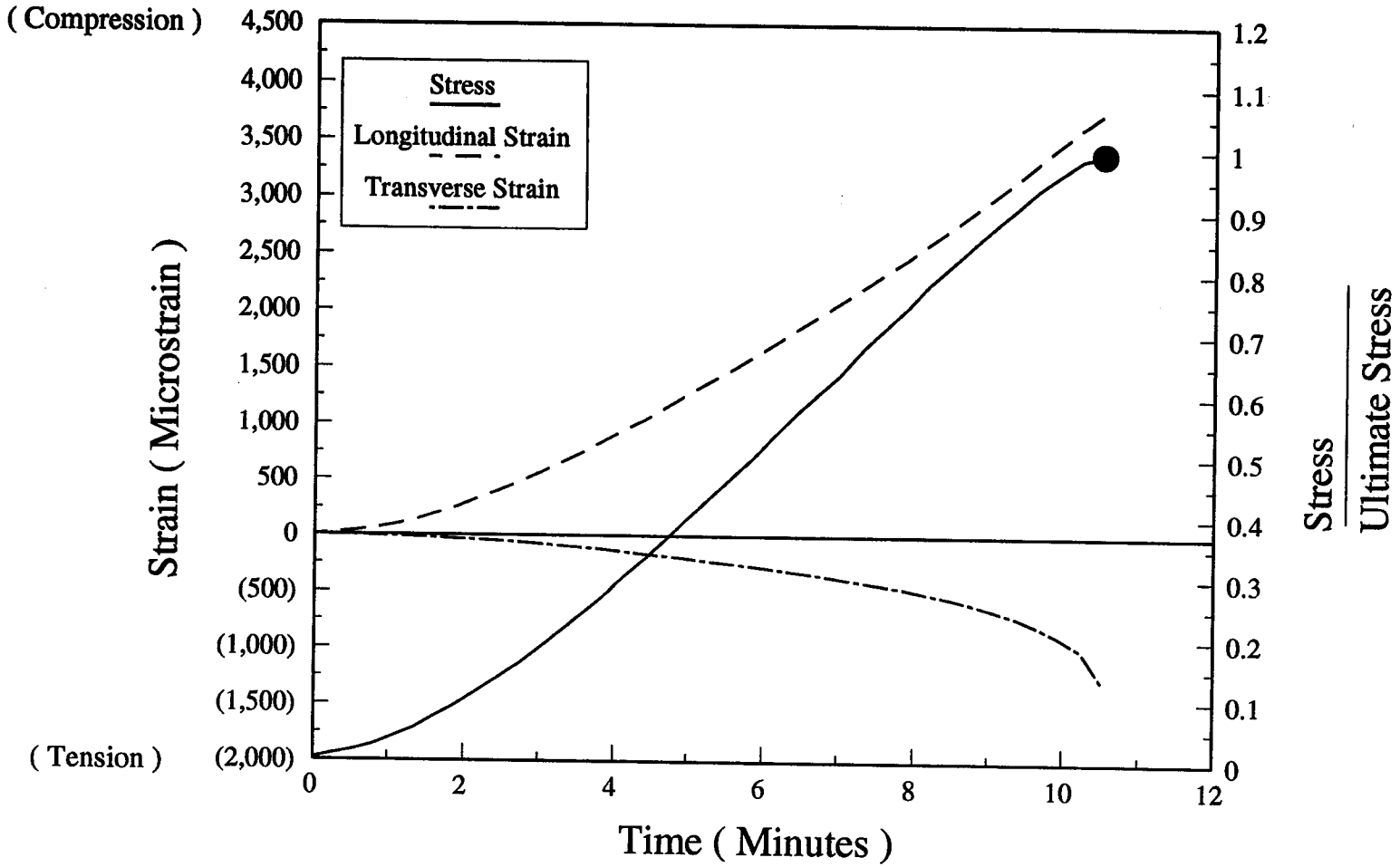

$f_c = 97.9$ MPa $\qquad A = 7812\ mm^2$

Figure C-4.5.D - Stress-Strain-Time Relationship - UHC100D Specimen

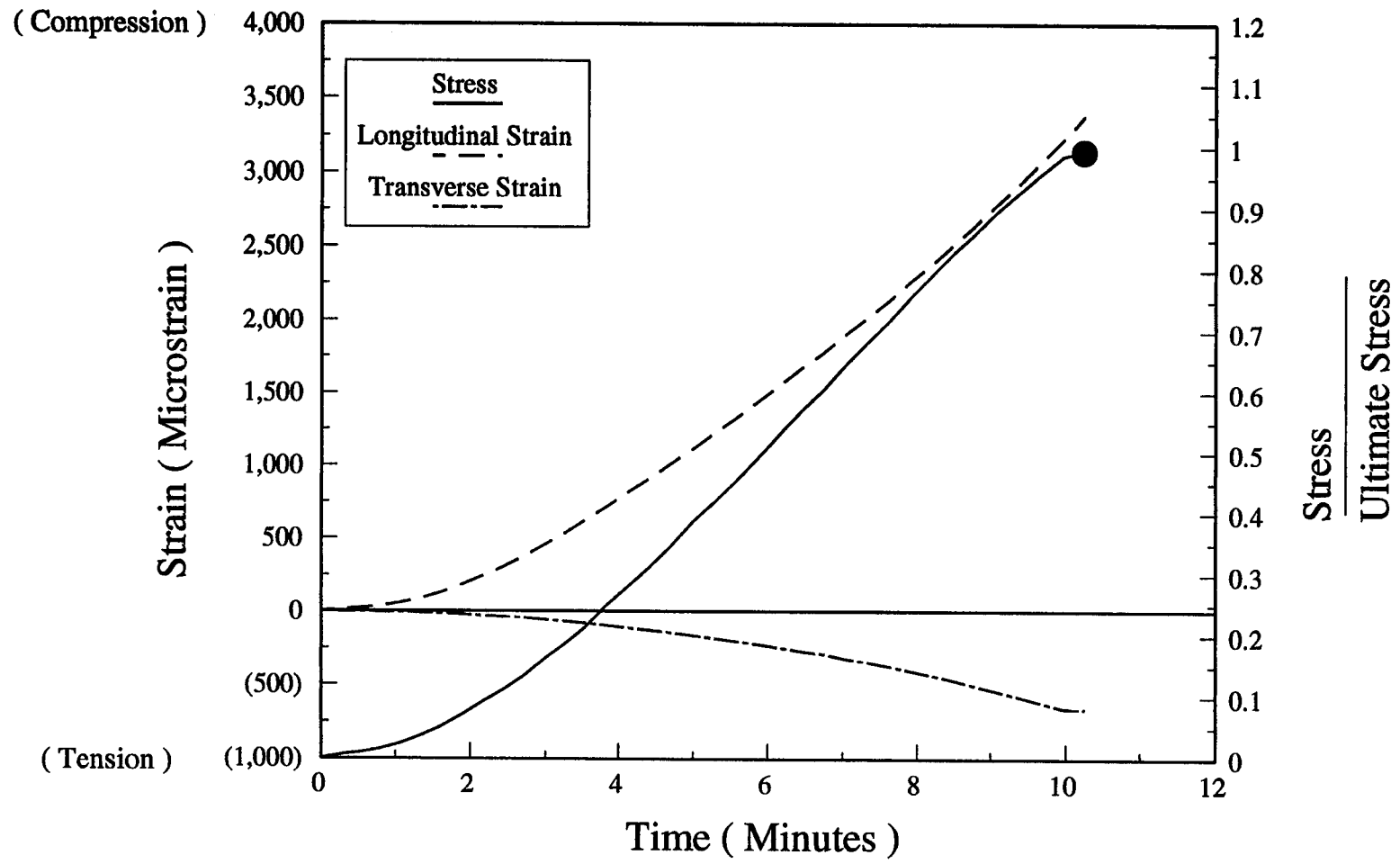

$f_c = 94.2$ MPa $\qquad A = 7721\ mm^2$

Figure C-4.5.E - Stress-Strain-Time Relationship - UHC100E Specimen

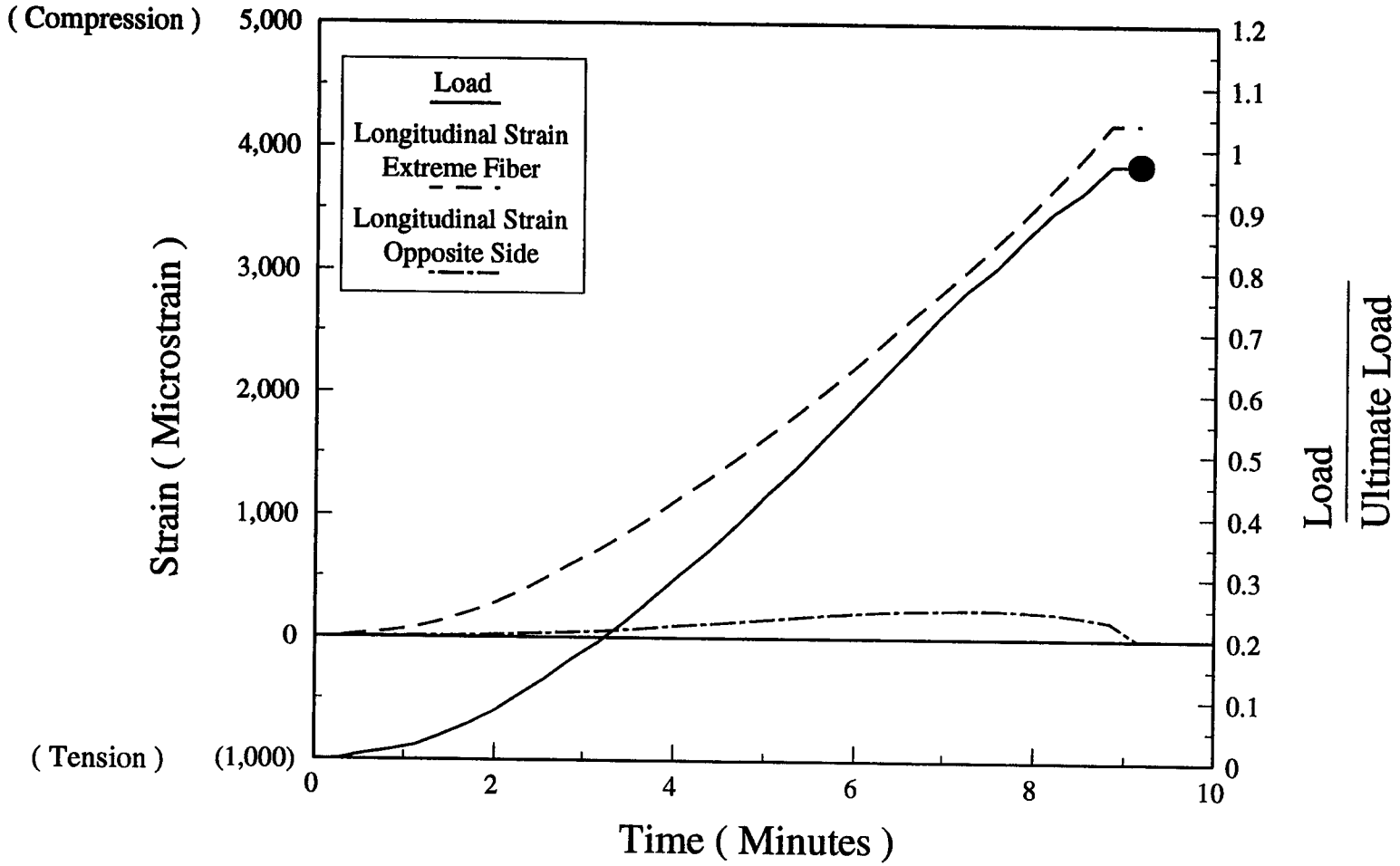

$P_c = 544.0$ kN $\qquad A = 7750$ mm^2

Figure C-4.6.A - Load-Strain-Time Relationship - UHE100A Specimen

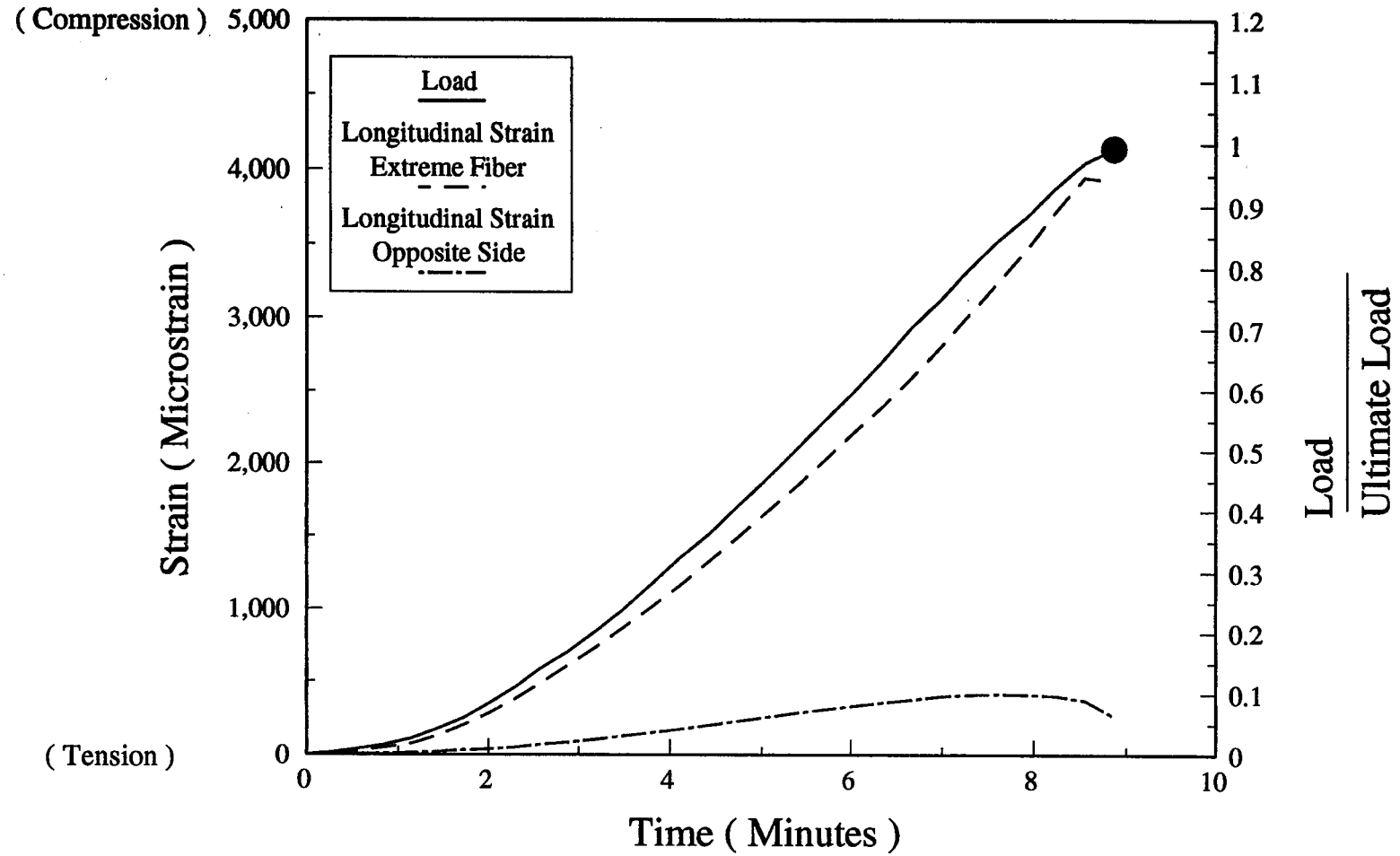

$P_c = 557.0$ kN $\qquad A = 8091$ mm^2

Figure C-4.6.B - Load-Strain-Time Relationship - UHE100B Specimen

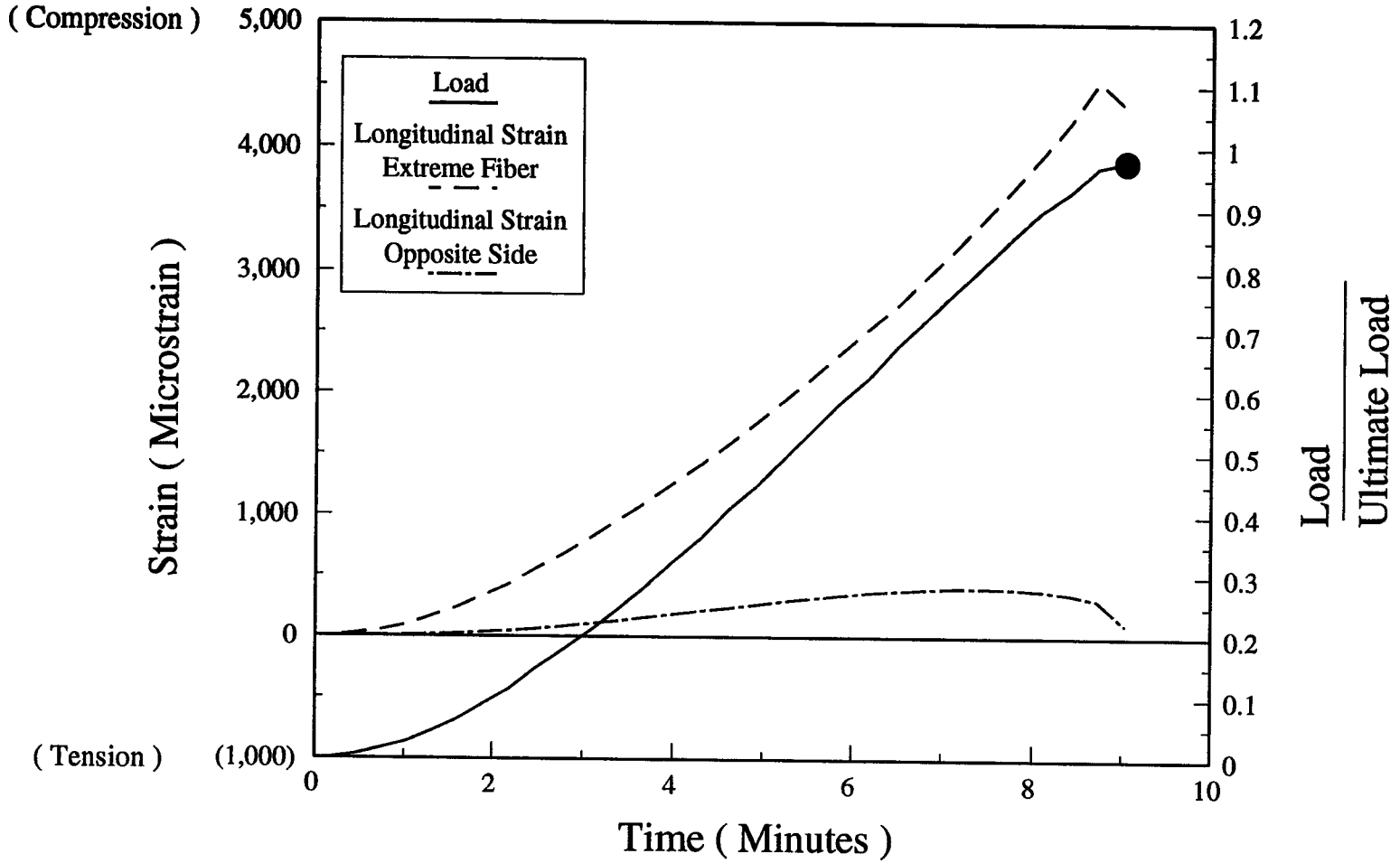

$P_c = 577.0$ kN $\qquad A = 8129$ mm^2

Figure C-4.6.C - Load-Strain-Time Relationship - UHE100C Specimen

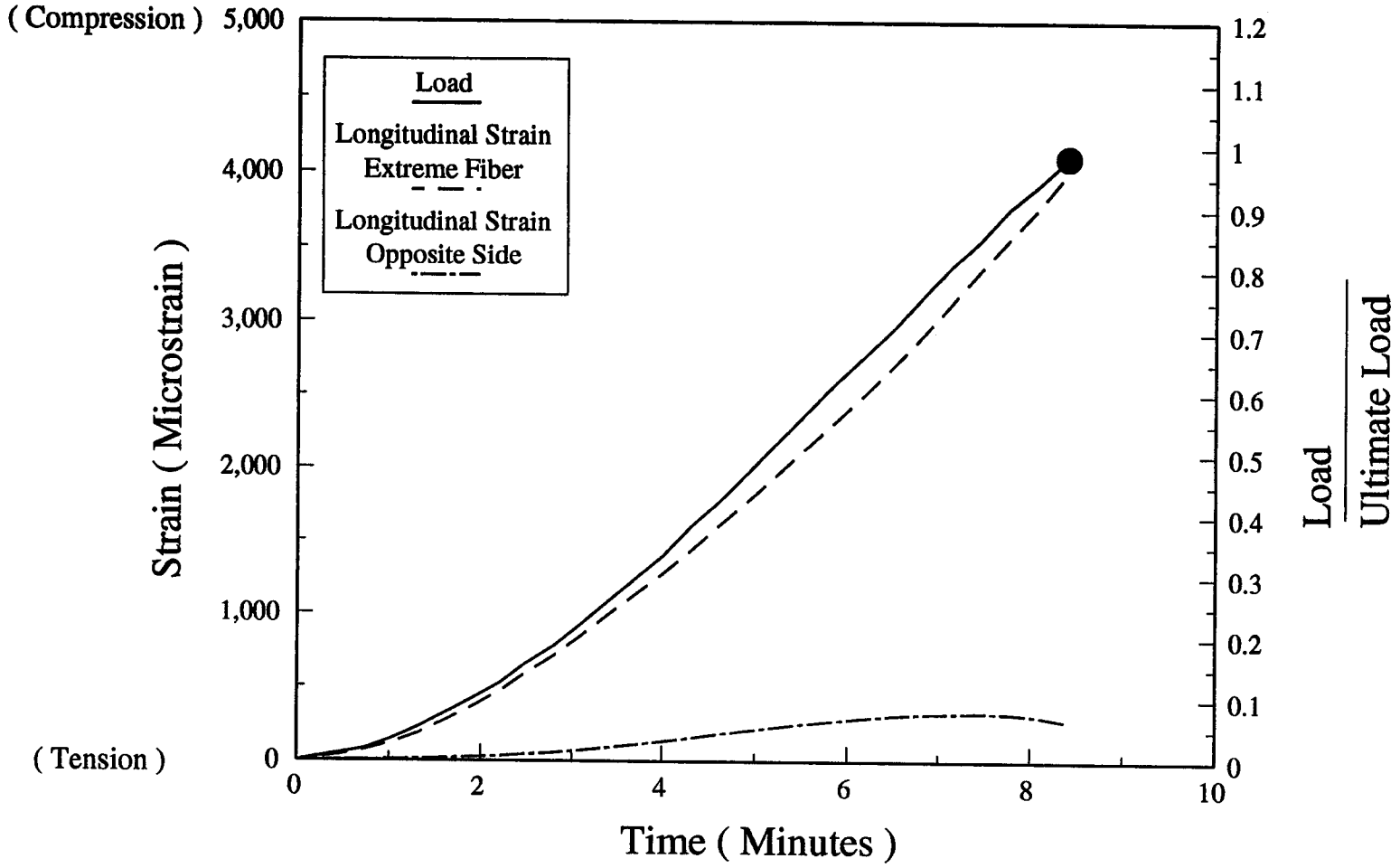

$P_c = 527.0$ kN $\qquad A = 7773$ mm^2

Figure C-4.6.D - Load-Strain-Time Relationship - UHE100D Specimen

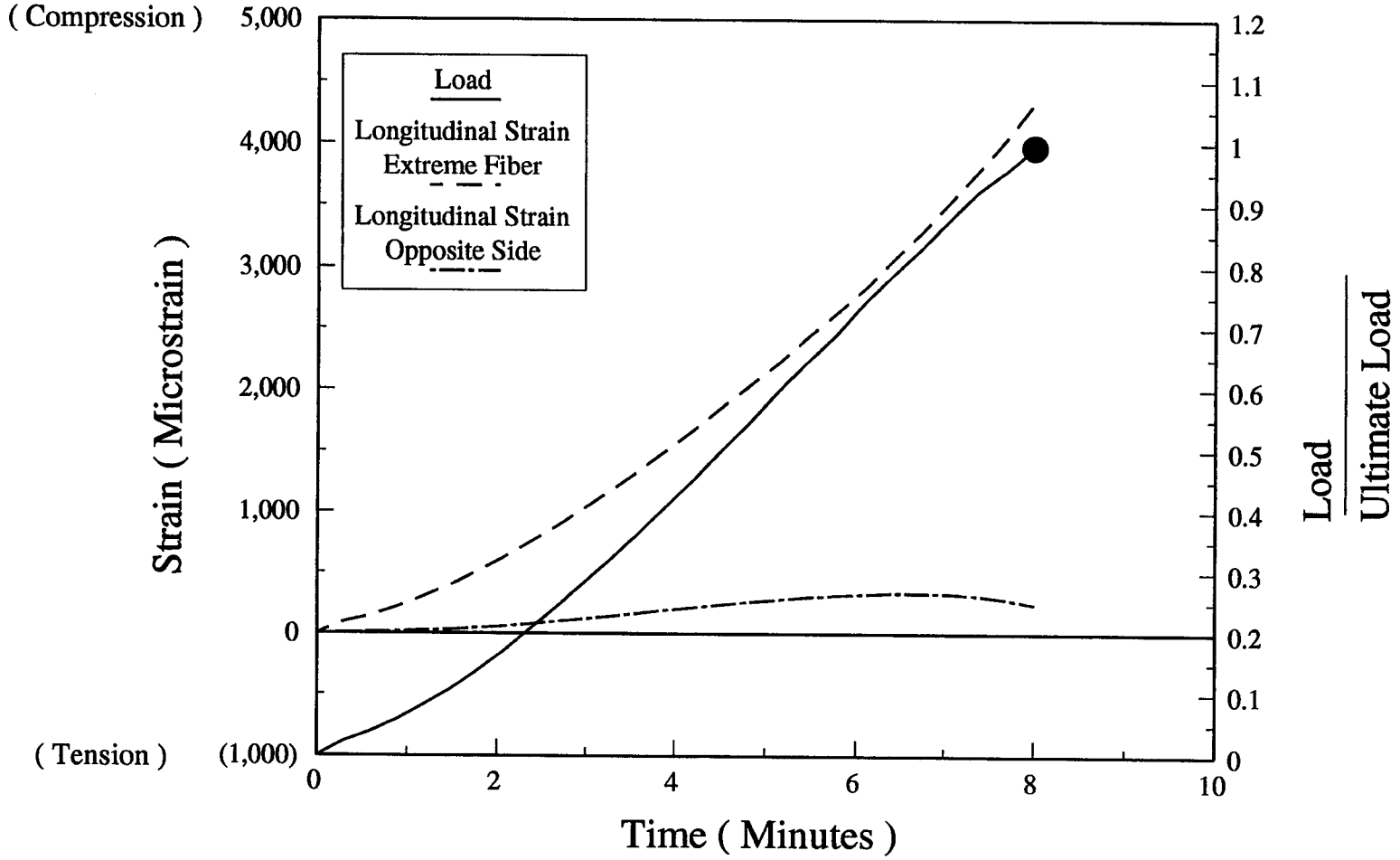

$P_c = 538.0$ kN $\qquad A = 7685$ mm^2

Figure C-4.6.E - Load-Strain-Time Relationship - UHE100E Specimen

Appendix D. UU Series Monotonic Test Results

The experimental results for short term monotonic concentric tests are presented in Figures D-4.5.A through E of this appendix. The details of experimental results for sustained concentric tests and also the discussion of results are presented in sections 4.5.1.4 and 4.5.2.

The experimental results for short term monotonic eccentric tests are presented in Figures D-4.6.A through E of this appendix. The details of experimental results for sustained eccentric tests and also the discussion of results are presented in sections 4.6.1.4 and 4.6.2.

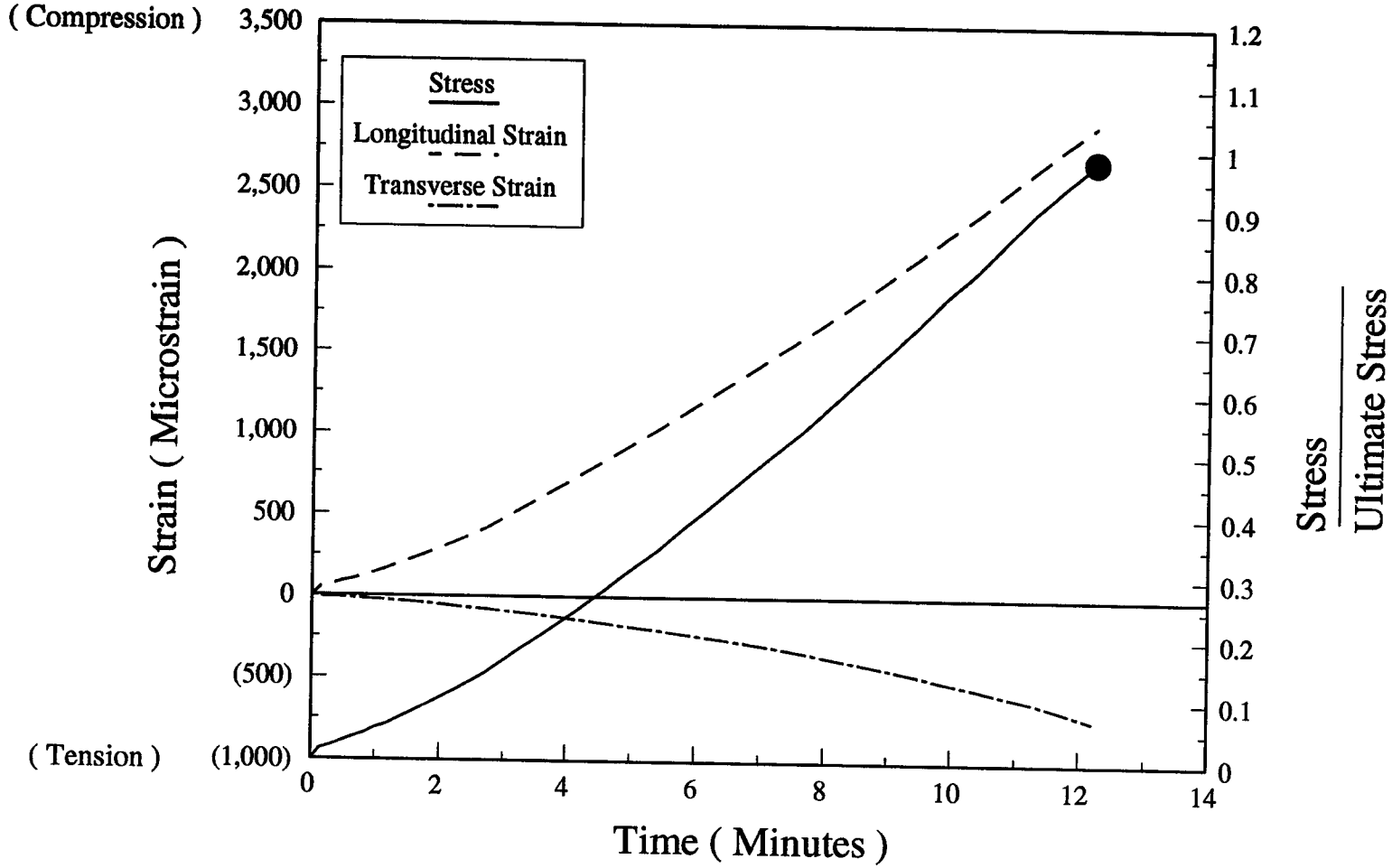

f_c= 115.5 MPa A = 7781 mm^2

Figure D-4.5.A - Stress-Strain-Time Relationship - UUC100A Specimen

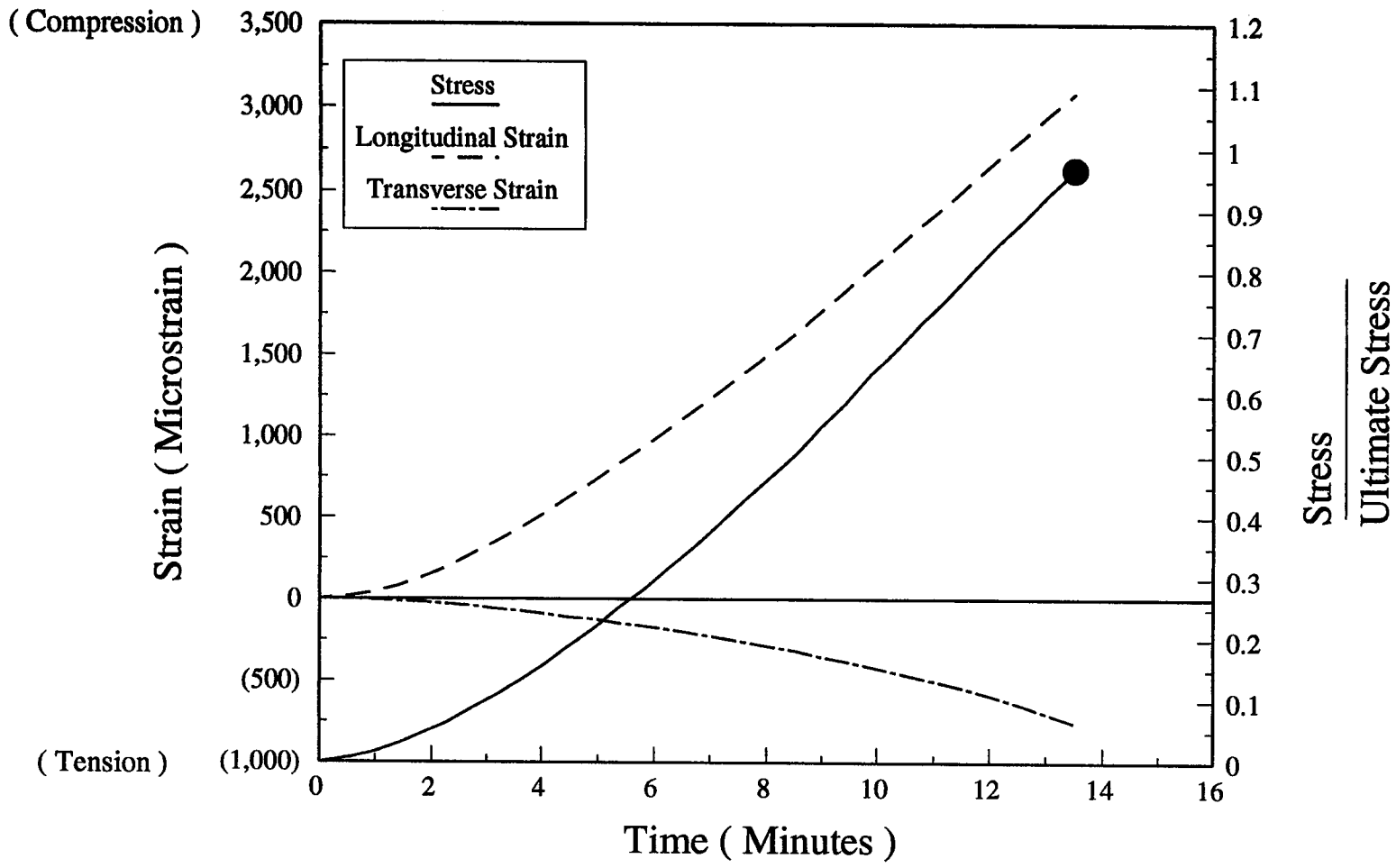

$f_c = 125.0$ MPa $\qquad A = 7833\ mm^2$

Figure D-4.5.B - Stress-Strain-Time Relationship - UUC100B Specimen

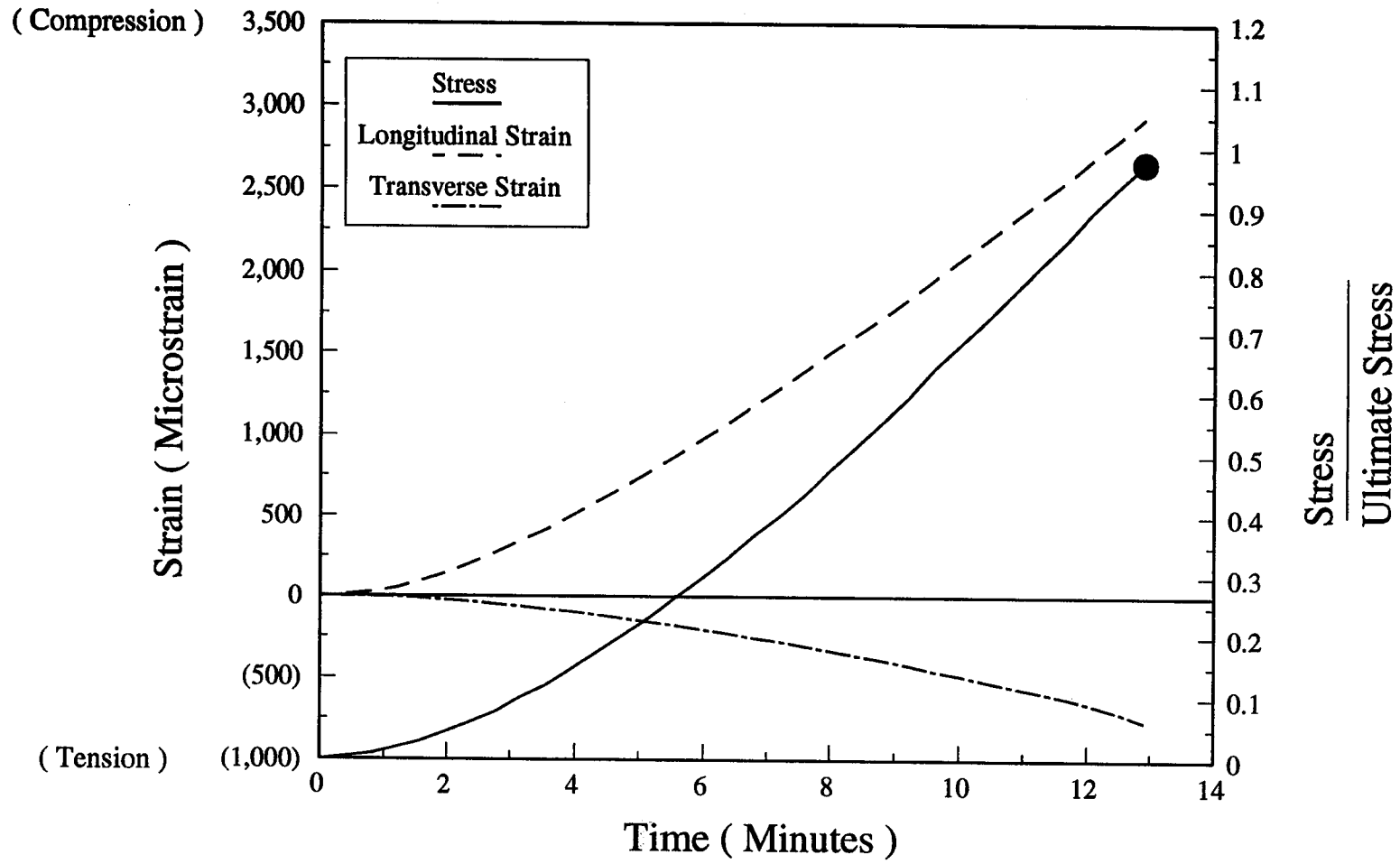

f_c= 121.6 MPa A = 7823 mm^2

Figure D-4.5.C - Stress-Strain-Time Relationship - UUC100C Specimen

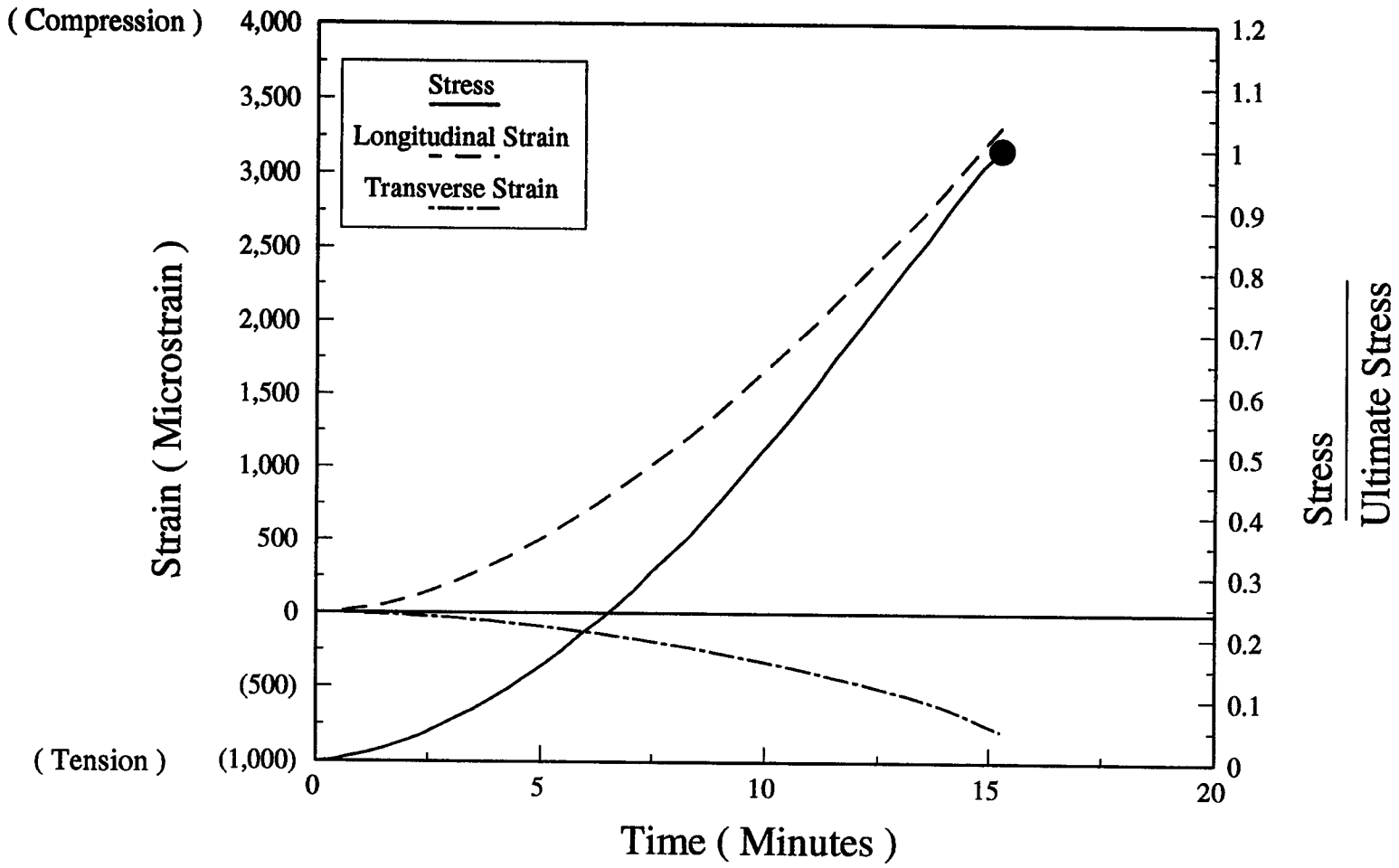

f_c= 119.7 MPa A = 8177 mm^2

Figure D-4.5.D - Stress-Strain-Time Relationship - UUC100D Specimen

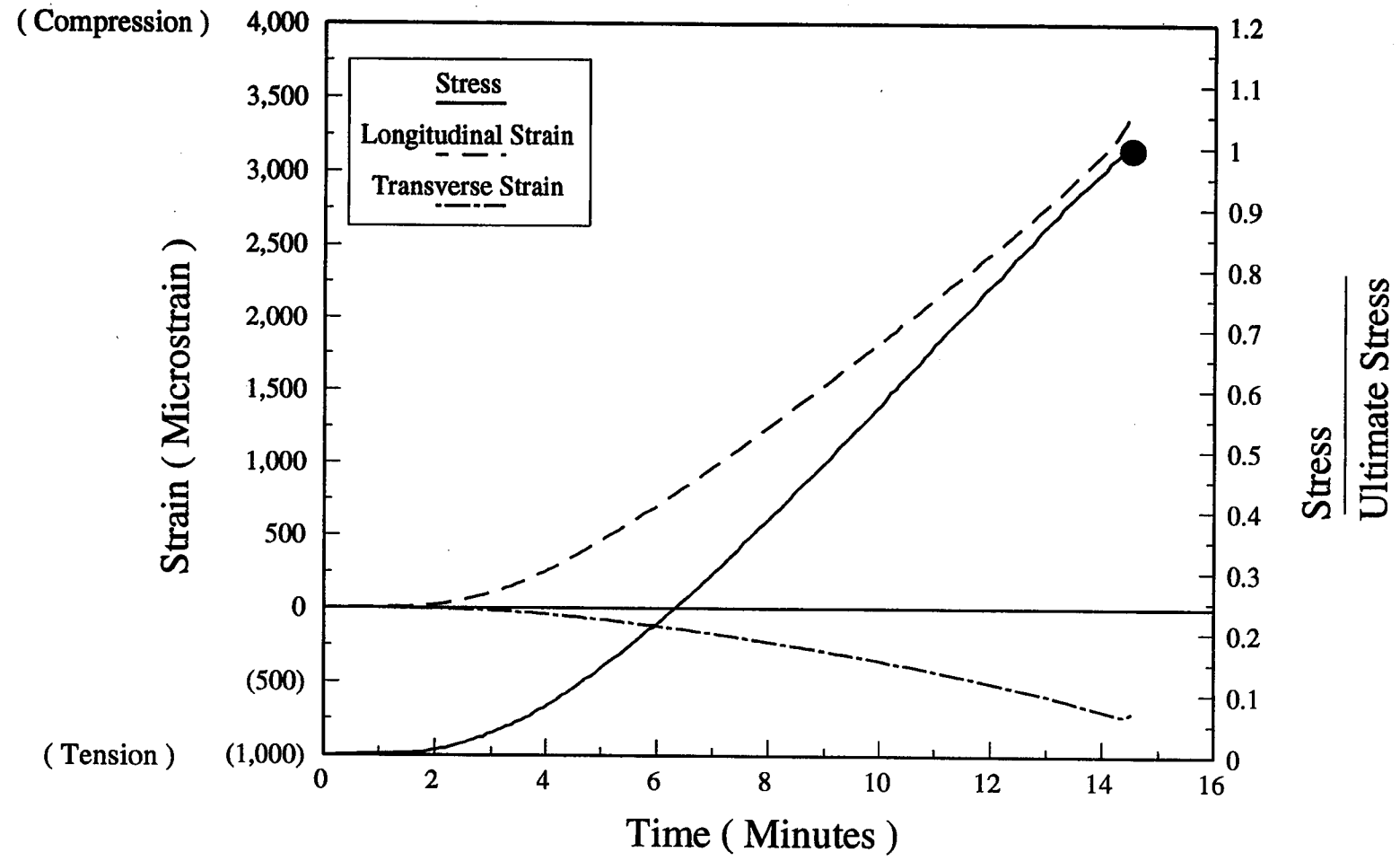

f_c= 120.6 MPa A = 7867 mm^2

Figure D-4.5.E - Stress-Strain-Time Relationship - UUC100E Specimen

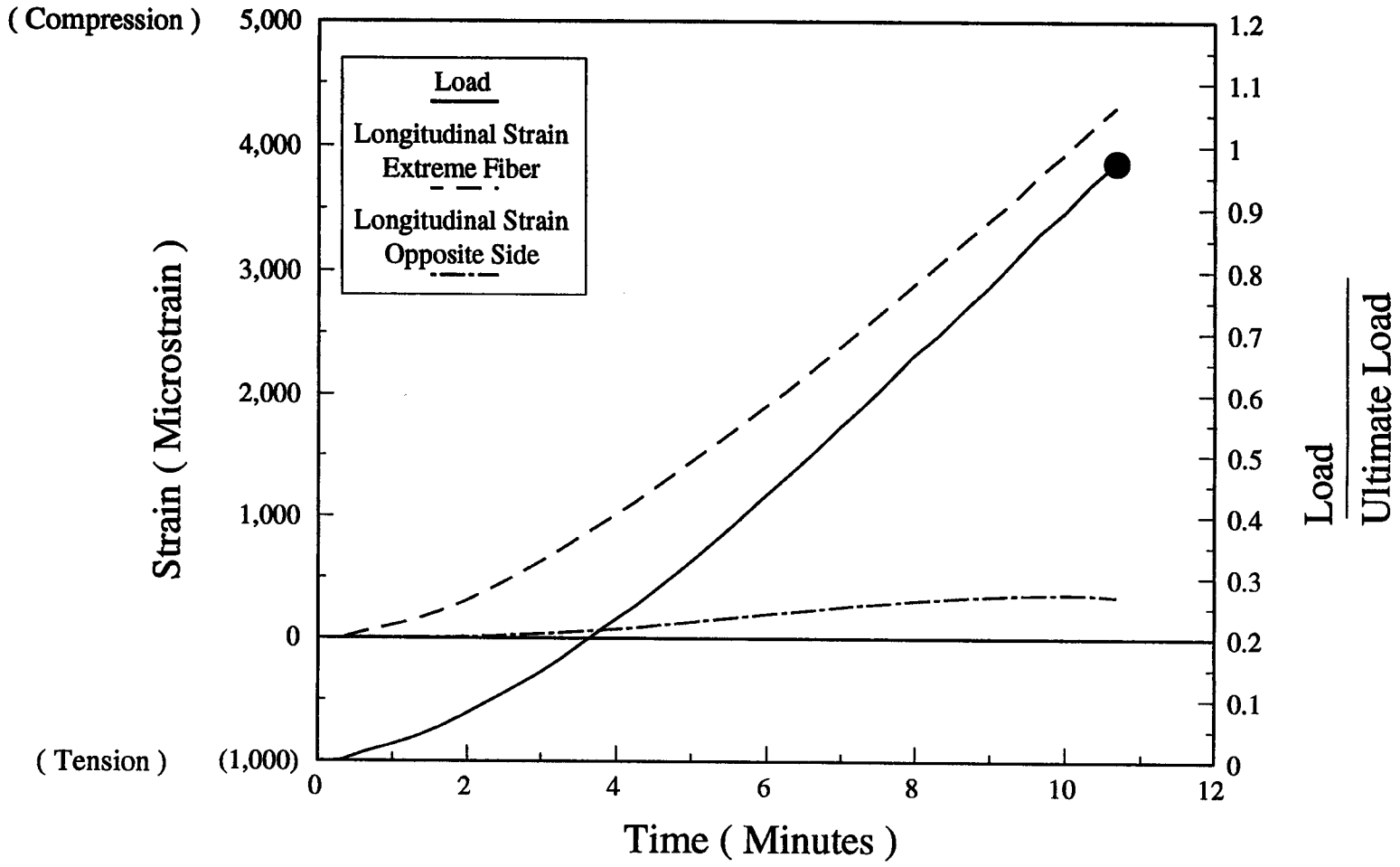

$P_c = 697.0$ kN $\qquad A = 7802$ mm^2

Figure D-4.6.A - Load-Strain-Time Relationship - UUE100A Specimen

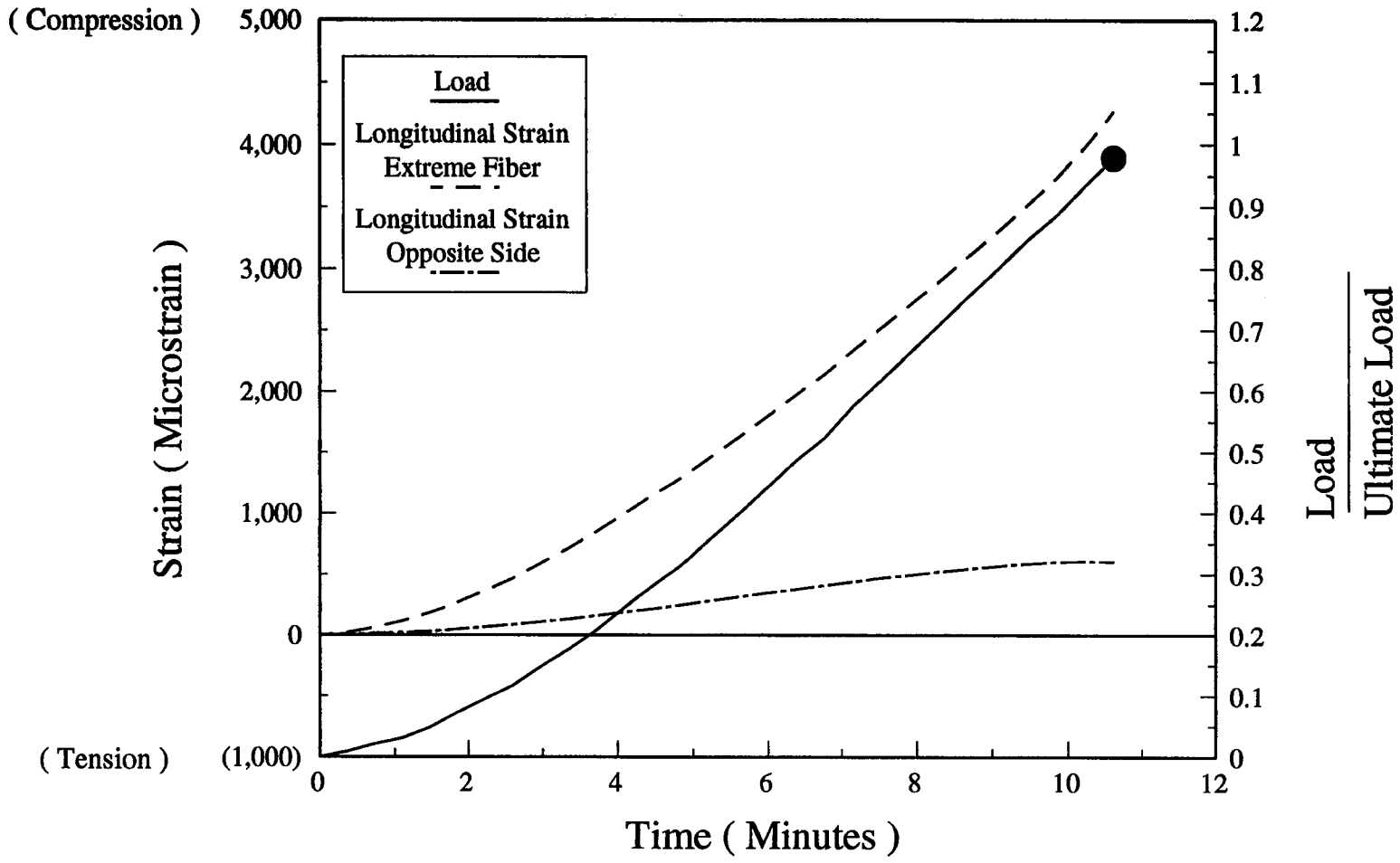

$P_c = 712.0$ kN $\qquad A = 8217$ mm^2

Figure D-4.6.B - Load-Strain-Time Relationship - UUE100B Specimen

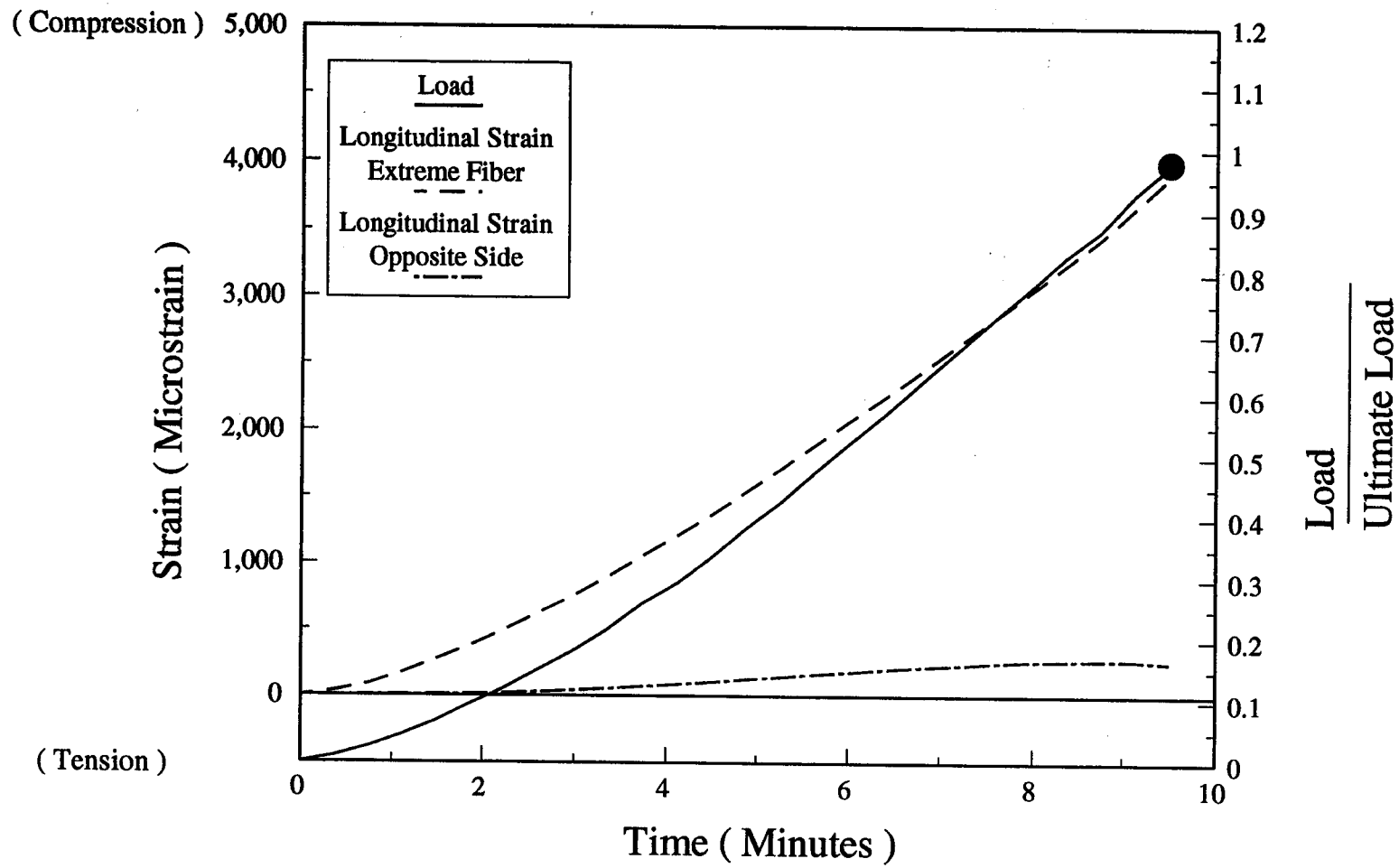

$P_c = 611.0$ kN $\qquad A = 7804$ mm^2

Figure D-4.6.C - Load-Strain-Time Relationship - UUE100C Specimen

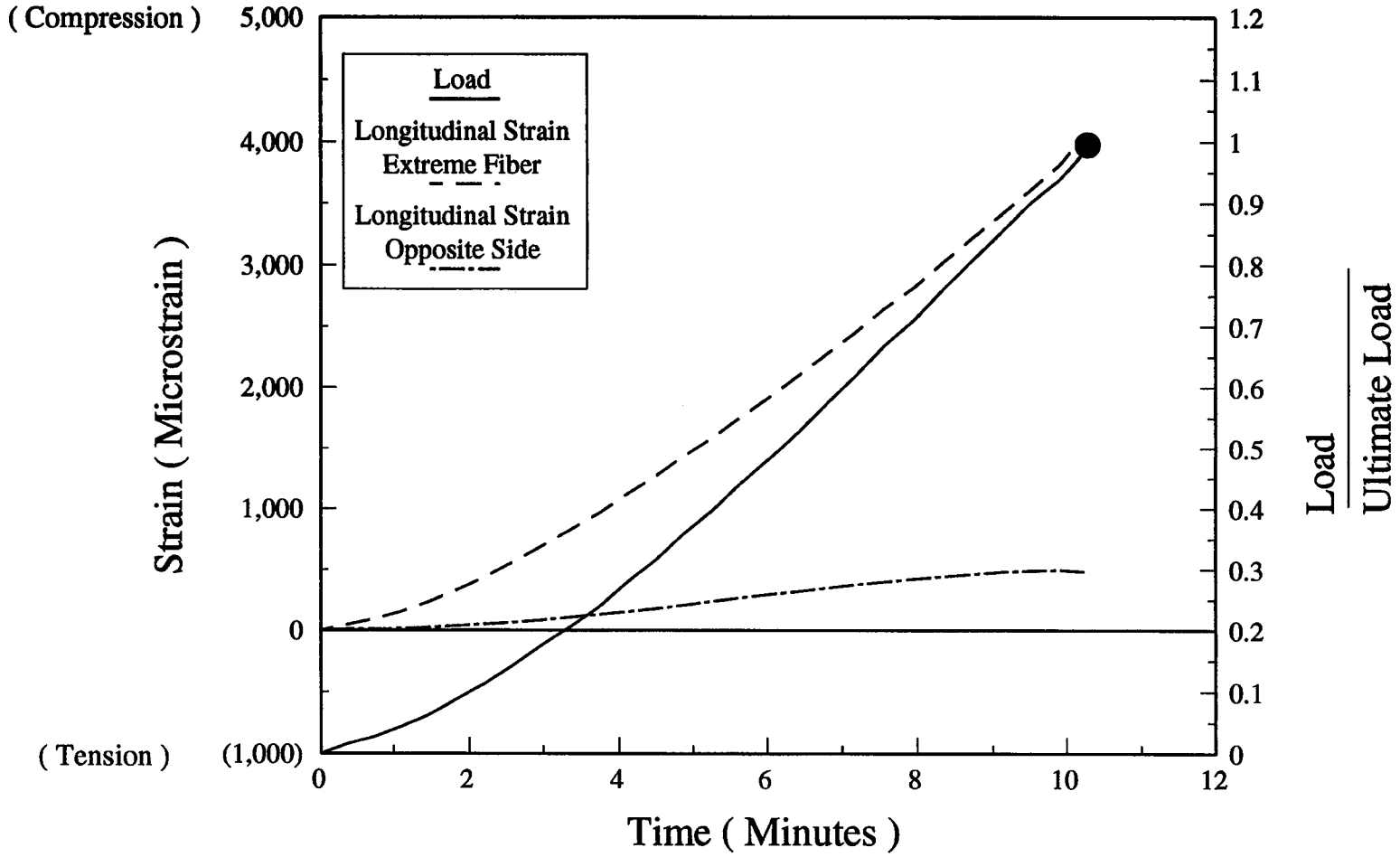

$P_c = 693.0$ kN $\qquad A = 8094$ mm^2

Figure D-4.6.D - Load-Strain-Time Relationship - UUE100D Specimen

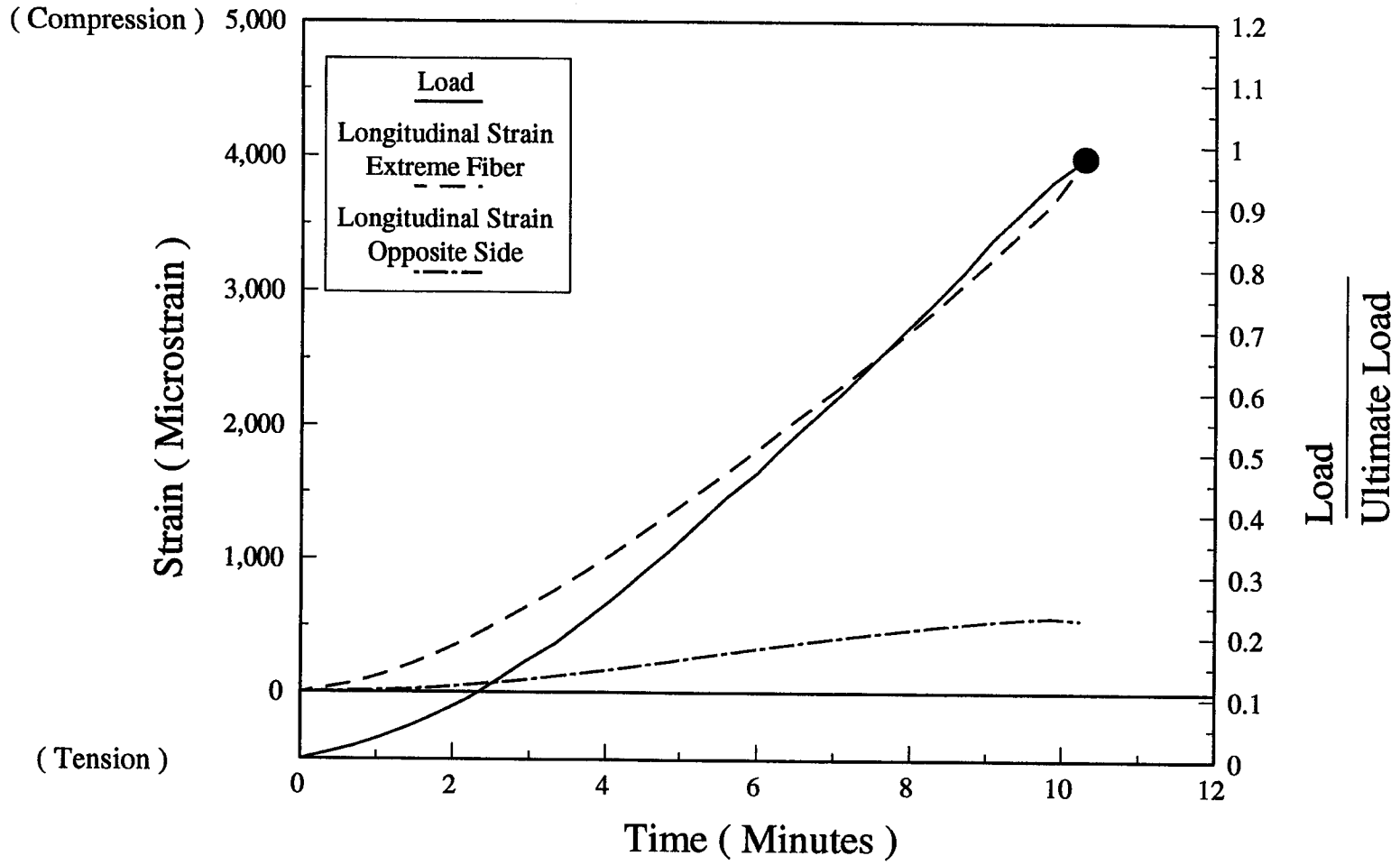

$P_c = 677.0$ kN $\qquad A = 8129$ mm^2

Figure D-4.6.E - Load-Strain-Time Relationship - UUE100E Specimen

Appendix E. Mechanical Properties of High Performance Concrete (LU Series Test Results)

E-3.1 Introduction

The results of the supplementary test program for LH, UH, and UU series are presented in Chapter 3. The results of the supplementary test program for LU series are presented in this appendix.

E-3.2 Compressive Strength Gain with Time

The test results for LU series are presented in Table E-3.2. The reported results are the average compressive strength of the specimens tested for LU series. The compressive strength of individual specimens are reported in Appendix I, Table I-E-3.2. All results are based on moist cured specimens. The compressive strength gain, expressed as the percentage of the 28 day compressive strength, is shown in the same table and Figure E-3.2. The results shown in Figure E-3.2 are based on the average of the two batches presented in Table E-3.2 for LU series.

E-3.3 Effect of Type of Cement on the Compressive Strength Gain

One of the four batches in LU series (LU3) was made with Type 30 cement, the other three with Type 10. The test results for LU series are presented in Table E-3.3 and Figure E-3.3.A. The reported results are the average compressive strength of the specimens tested for LU series. The compressive strength of individual specimens are reported in Appendix I, Table I-E-3.3. All results are based on moist cured specimens. The compressive strength gain, expressed as the percentage of the 28 day compressive strength, is also shown in the same table and Figure E-3.3.B.

E-3.4 Effect of Drying on the Compressive Strength Gain

The test results for LU series are presented in Table E-3.4.A. The reported results are the average compressive strength of the specimens tested for LU series. The compressive strength of individual specimens are reported in Appendix I, Table I-E-3.4. The compressive strength gain is shown in Figure E-3.4 as a function of age for the three different curing regimes. The ratio of 147 day compressive strength to the 28 day compressive strength of moist cured specimen, for specimen with the three curing regimes under study, are presented

in Table E-3.4.B. The ratio of 147 day compressive strength of specimens moist cured for 3 and 7 weeks to the 147 days compressive strength of moist cured specimens are presented in Table E-3.4.C.

E-3.5 Effect of the Bearing Blocks of the Testing Machine on Compressive Strength

The test results for LU series are presented in Table E-3.5.A. The mean values of the compressive strength of specimens tested by both of the end conditions and the ratio of the compressive strength with ball seat bearing blocks to the compressive strength with spherical seat bearing blocks are presented in Table E-3.5.B.

E-3.6 Effect of Specimen Size on Compressive Strength

The test results for LU series are presented in Table E-3.6.A. The mean values of the compressive strength of 100 mm by 200 mm and 150 mm by 300 mm cylinders and the ratio of the compressive strength of 150 mm by 300 mm to 100 mm by 200 mm cylinders are presented in Table E-3.6.B.

E-3.7 Modulus of Elasticity

Test results for LU series including the compressive strength, the strain at the maximum stress, and the measured static modulus of elasticity and the Poisson's ratio at 40% of the ultimate stress based on ASTM C 469-87a[33] are presented in Table E-3.7.A. The following equation gives the best fit line for the relation between the measured static modulus of elasticity and square root of the compressive strength of high performance concretes used in this study (including LU series):

$$E_c = 3375\sqrt{f'_c} \qquad 55MPa < f'_c < 125MPa \qquad (E-3.7.A)$$

The measured static modulus of elasticity of high performance concretes tested in this study are compared to the ACI 318M-89[17] equation, the ACI 363R-84[7] equation, the CAN3-A23.3-M84[28] equation, and Equation (E-3.7.A) in Figure E-3.7.A.

Figure E-3.7.B shows test results of current study (including LU series) and selected test results from references 9, 11, 12, 13, 14, 15, 16, 19, and 27. Figure E-3.7.C shows the same test data and also test data from the same references and this study, from tests on specimens older than 56 days.

As a result of this study, the following modified ACI 318M-89[17] equation is proposed for estimating the static modulus of elasticity of high performance concrete:

$$E_c = 4700\, C_{ca}\sqrt{f'_c} \qquad 55\,MPa < f'_c < 125\,MPa \qquad (3.7.3)$$

Where C_{ca} is an empirical coarse aggregate coefficient. The recommended coarse aggregate coefficient for sandstone gravel, based on current available test data (including LU series), is shown in Table E-3.7.B. Figure E-3.7.D shows the test data from Figure E-3.7.B (including LU series) after normalizing with coarse aggregate coefficients. Figure E-3.7.D also shows Equation 3.7.3 and as can be seen, the fluctuation is in reasonable limits.

E-3.8 Poisson's Ratio

Test results for LU series including the compressive strength, the strain at the maximum stress, and the measured static modulus of elasticity and the Poisson's ratio at 40% of the ultimate stress based on ASTM C 469-87a[33] are presented in Table E-3.7.A. The values of Poisson's ratio for high performance concretes used in this study (including LU series) mainly varies between 0.15 and 0.20. The test results of the current study (LH, UH, LU, and UU series), study by Carrasquillo et al[12], and study by Perenchio et al[19] are presented in Figure E-3.8.

E-3.9 Tensile Splitting Strength

The test results for LU series are presented in Table E-3.9. The moist cured specimens were tested at the age of 56 days. The equation of the fit line for the results of this study (including LU series) is as follows:

$$f'_{sp} = 0.57\sqrt{f'_c} \qquad 50\,MPa < f'_c < 100\,MPa \qquad (E-3.9)$$

E-3.10 Modulus of Rupture

The test results for LU series are presented in Table E-3.10. The moist cured specimens were tested at the age of 56 days. The equation of the fit line for the results of this study (including LU series) is as follows:

$$f'_r = 0.97\sqrt{f'_c} \qquad 50\,MPa < f'_c < 100\,MPa \qquad (E-3.10)$$

Table E-3.2 - Compressive Strength Gain with Time (LU Series)

Age (Days)	LU2 (MPa)	f_{ct}/f_{c28} (LU2)	LU4 (MPa)	f_{ct}/f_{c28} (LU4)	f_{ct}/f_{c28} (LU2+LU4)/2
1	32.7	0.36	31.9	0.36	0.36
3	54.0	0.60	54.0	0.62	0.61
7	70.6	0.78	68.8	0.78	0.78
28	90.0	1.00	87.7	1.00	1.00
56	96.5	1.07	95.3	1.09	1.08
91	104.7	1.16	103.4	1.18	1.17
147	104.9	1.17	103.7	1.18	1.18

* Δf_{c28} = 2.3 MPa

Table E-3.3 - Effect of Type of Cement on the Compressive Strength Gain (LU Series)

Age (Days)	LU2* (MPa)	f_{ct}/f_{c28} (LU2)	LU3+ (MPa)	f_{ct}/f_{c28} (LU3)
1	32.7	0.36	55.5	0.59
3	54.0	0.60	66.5	0.70
7	70.6	0.78	79.6	0.84
28	90.0	1.00	94.6	1.00
56	96.5	1.07	100.1	1.06
91	104.7	1.16	104.3	1.10
147	104.9	1.17	105.4	1.11

* Mix with Type 10
+ Mix with Type 30

Table E-3.4.A - Effect of Drying on the Compressive Strength Gain (LU Series)

Age (Days)	LU4 Continuously Moist	LU4 3 Weeks Moist	LU4 7 Weeks Moist
1	31.9	-	-
3	54.0	-	-
7	68.8	-	-
28	87.7	96.3	-
56	95.3	106.1	104.5
91	103.4	108.3	113.3
147	103.7	114.8	115.8

Table E-3.4.B - Comparison of 147-day and 28-day Compressive Strength

Concrete Series	$\frac{f_{c147(moist)}}{f_{c28(moist)}}$	$\frac{f_{c147(3\ weeks\ moist)}}{f_{c28(moist)}}$	$\frac{f_{c147(7\ weeks\ moist)}}{f_{c28(moist)}}$
LU	1.18	1.31	1.32

Table E-3.4.C - Comparison of 147-day Compressive Strengths

Concrete Series	$\frac{f_{c147(3\ weeks\ moist)}}{f_{c147(moist)}}$	$\frac{f_{c147(7\ weeks\ moist)}}{f_{c147(moist)}}$
LU	1.11	1.12

Table E-3.5.A - Compressive Strength Results with Different Bearing Blocks

Concrete Series	Bearing Block	Compressive Strength (MPa)						S_{n-1}
		S_1	S_2	S_3	S_4	S_5	Mean	
LU	Ball Seat	98.8	95.9	93.8	98.2	89.8	95.3	3.658
LU	Spherical Seat	101.3	96.7	101.9	97.1	99.9	99.4	2.382

Table E-3.5.B - Comparison of the Bearing Blocks of the Testing Machine

Concrete	$f_{c(Ball\ Seat)}$ (MPa)	$f_{c(Spherical\ Seat)}$ (MPa)	$\frac{f_{c(Ball\ Seat)}}{f_{c(Spherical\ Seat)}}$
LU	95.3	99.4	0.96

Table E-3.6.A - Compressive Strength Results with Different Specimen Sizes

Concrete Series	Size of the Cylinder	Compressive Strength (MPa)						S_{n-1}
		S_1	S_2	S_3	S_4	S_5	Mean	
LU	150 mm	94.8	87.6	93.5	92.8	89.5	91.6	2.987
LU	100 mm	101.3	96.7	101.9	97.1	99.9	99.4	2.382

Table E-3.6.B - Comparison of 100 mm and 150 mm Cylinders

Concrete	$f_{c(150mm)}$ (MPa)	$f_{c(100mm)}$ (MPa)	$\frac{f_{c(150mm)}}{f_{c(100mm)}}$
LU	91.6	99.4	0.92

Table E-3.7.A - Modulus of Elasticity and Poisson's Ratio Test Results

Concrete	Compressive Strength (MPa)	Strain at Maximum Stress (microstrain)	Modulus of Elasticity (MPa)	Poisson's Ratio
LU	103.5	3451	30065	0.18
LU	102.4	3324	31448	0.20
LU	105.1	3537	31683	0.18
LU	106.2	3351	32333	0.18
LU	106.5	3276	34353	0.18

Table E-3.7.B - Recommended Coarse Aggregate Coefficients

Kind of Coarse Aggregate	Recommended C_{ca}	Coefficient of Variation
Sandstone Gravel+	0.71	0.066

+ Gravels with dominant sandstone rock.

Table E-3.9 - Tensile Splitting Strength Test Results

Concrete	f_{c28} (MPa)	f_{c56} (MPa)	S_1 (MPa)	S_2 (MPa)	S_3 (MPa)	Mean (MPa)	S_{n-1}	Fractured Coarse Aggregate
LU	90.0	96.5	6.10	5.65	6.35	6.05	0.35	99%

Table E-3.10 - Modulus of Rupture Test Results

Concrete	f_{c28} (MPa)	f_{c56} (MPa)	S_1 (MPa)	S_2 (MPa)	S_3 (MPa)	Mean (MPa)	S_{n-1}
LU	90.0	96.5	9.75	9.65	9.65	9.70	0.08

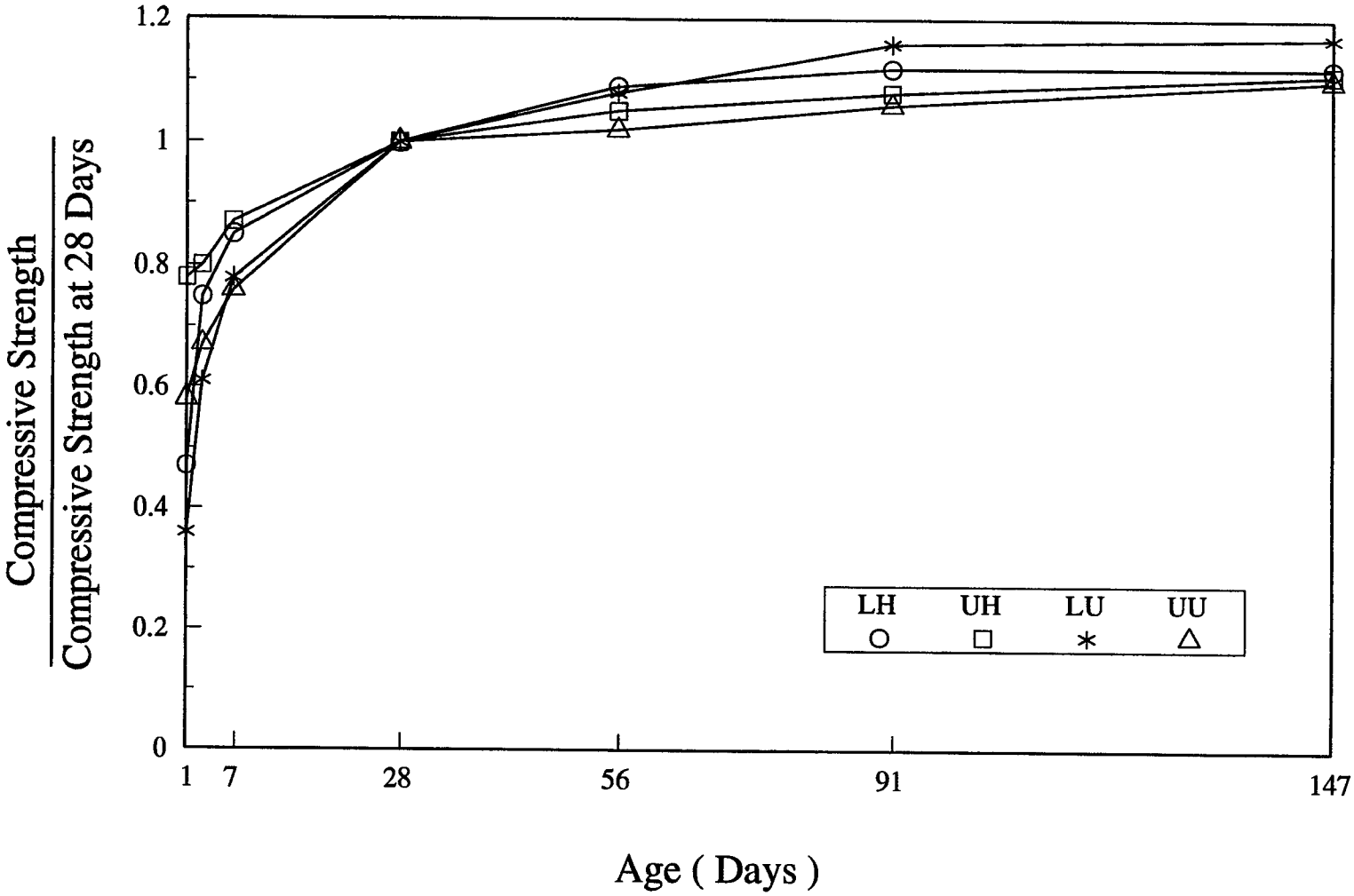

Figure E-3.2 - Compressive Strength Gain with Time

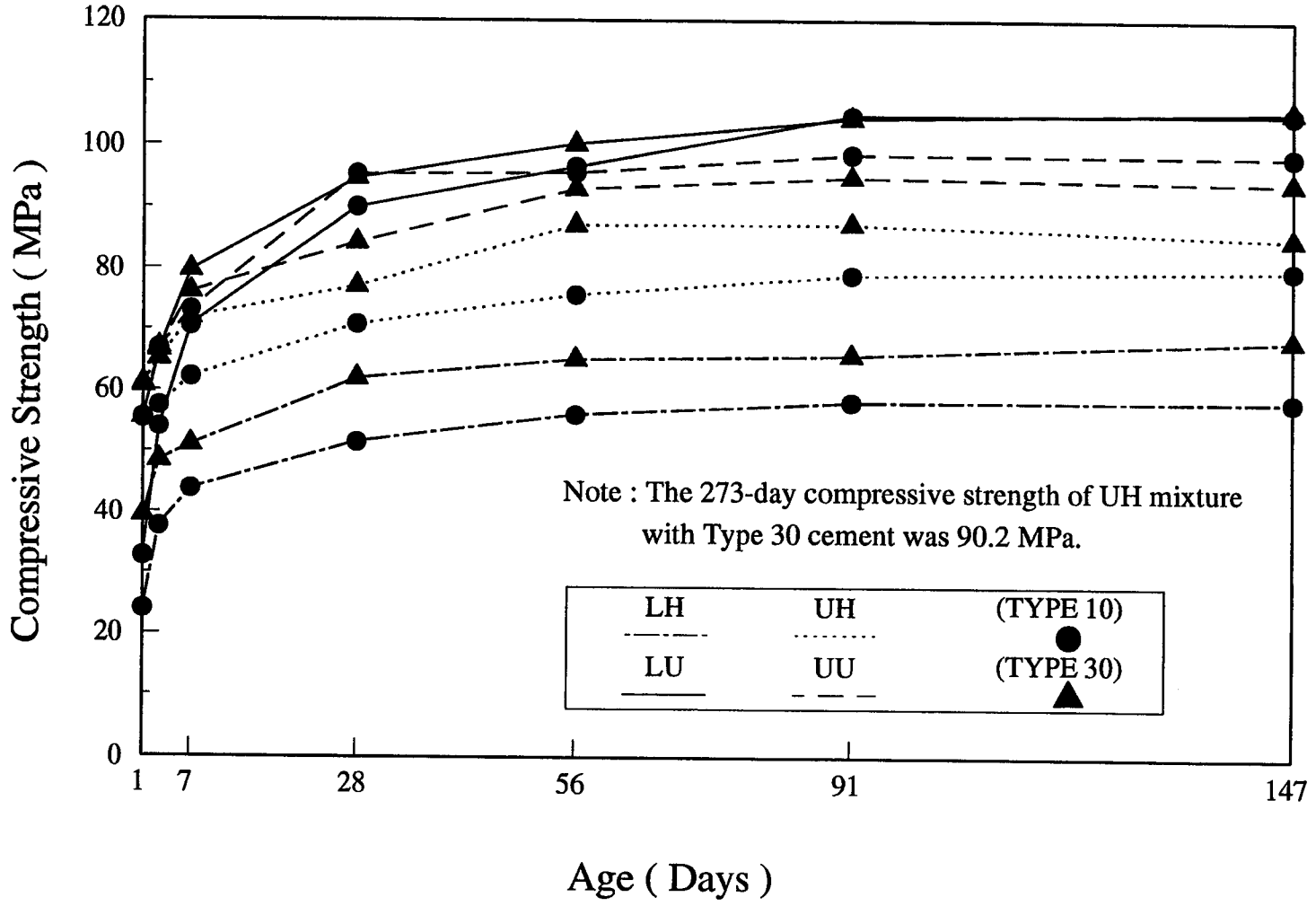

Figure E-3.3.A - Effect of Type of Cement on Compressive Strength

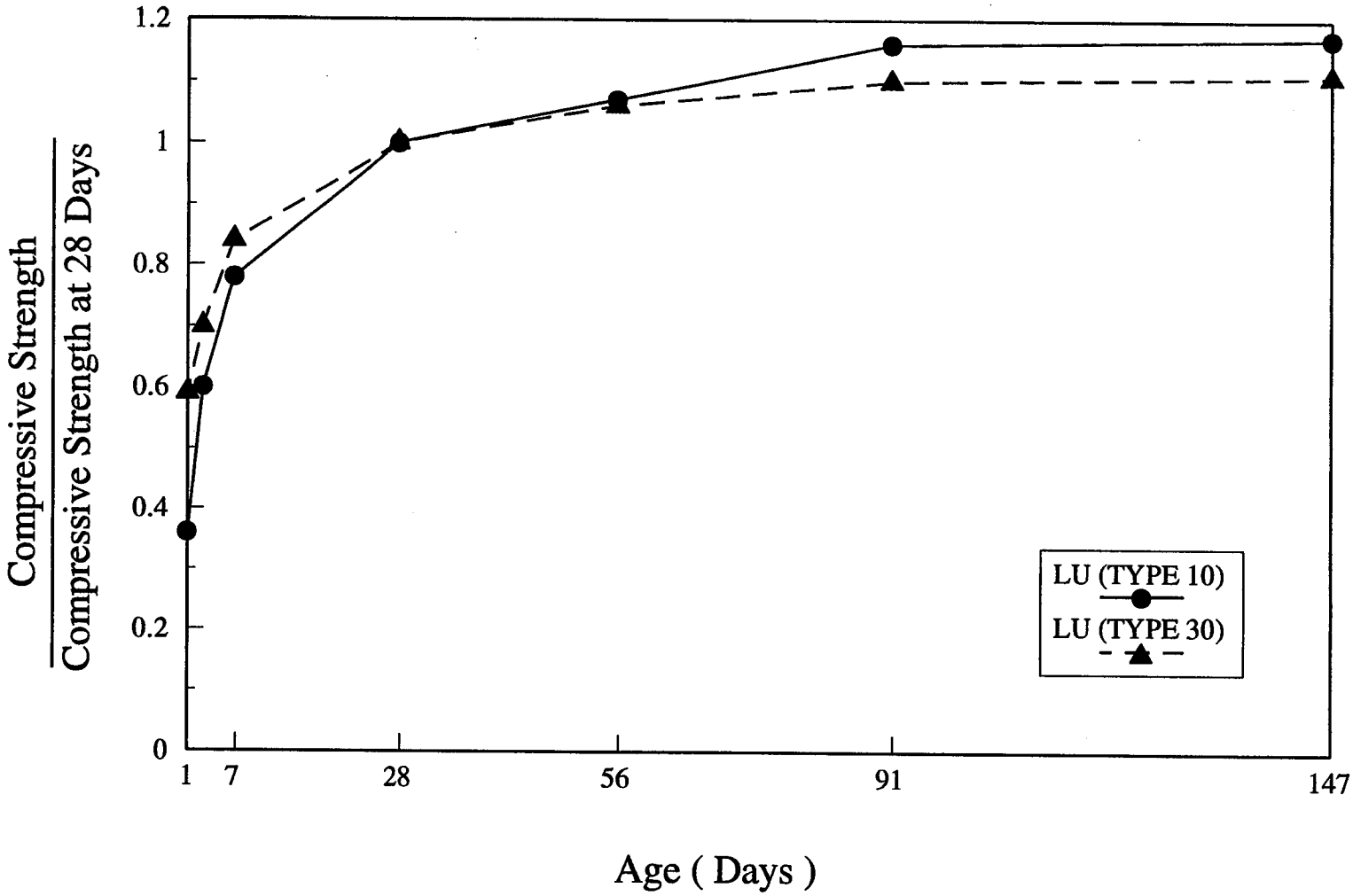

Figure E-3.3.B - Effect of Type of Cement (LU Series)

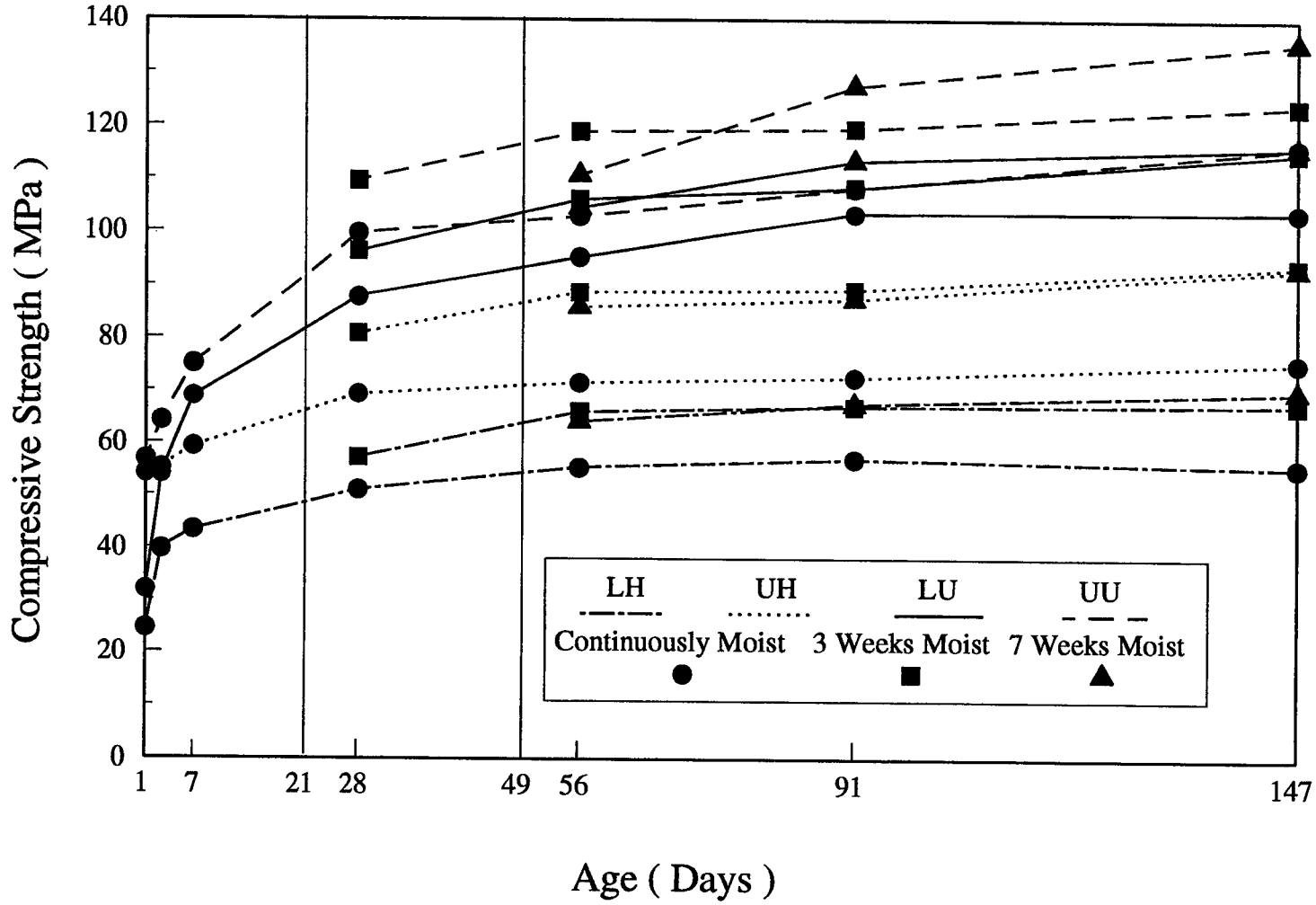

Figure E-3.4 - Effect of Drying on Compressive Strength Gain

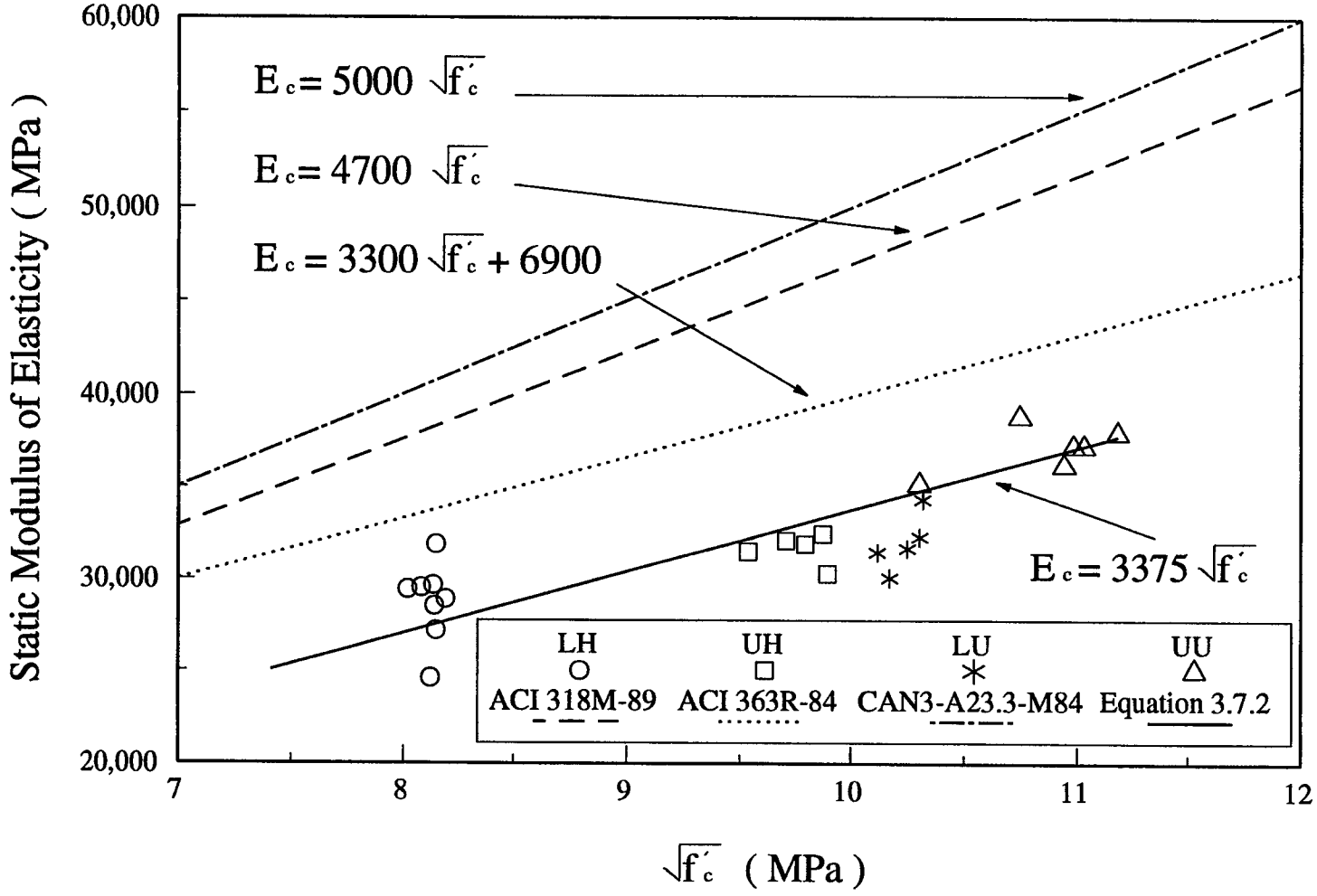

Figure E-3.7.A - Static Modulus of Elasticity Test Results

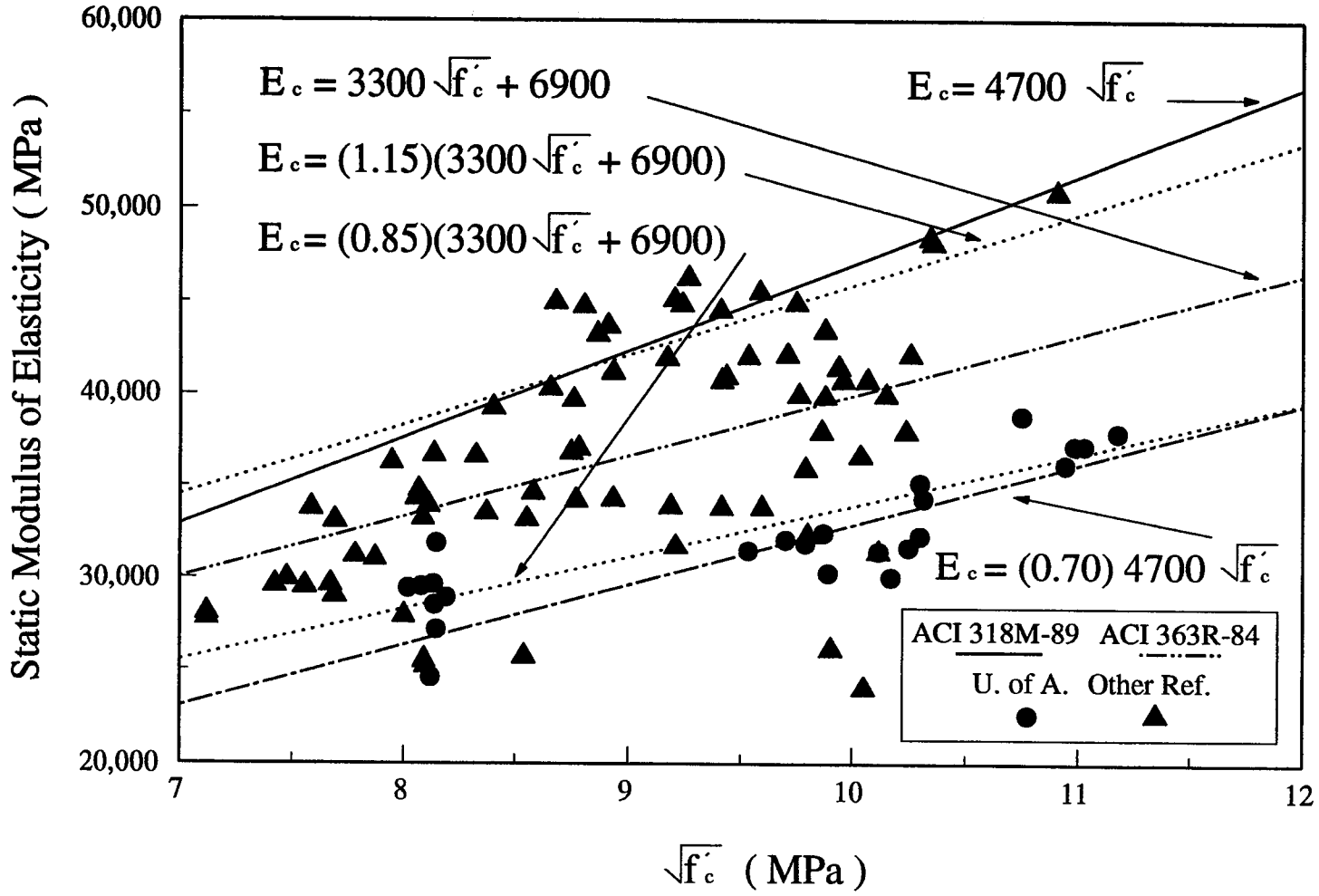

Figure E-3.7.B - Comparison of Modulus of Elasticity Test Results

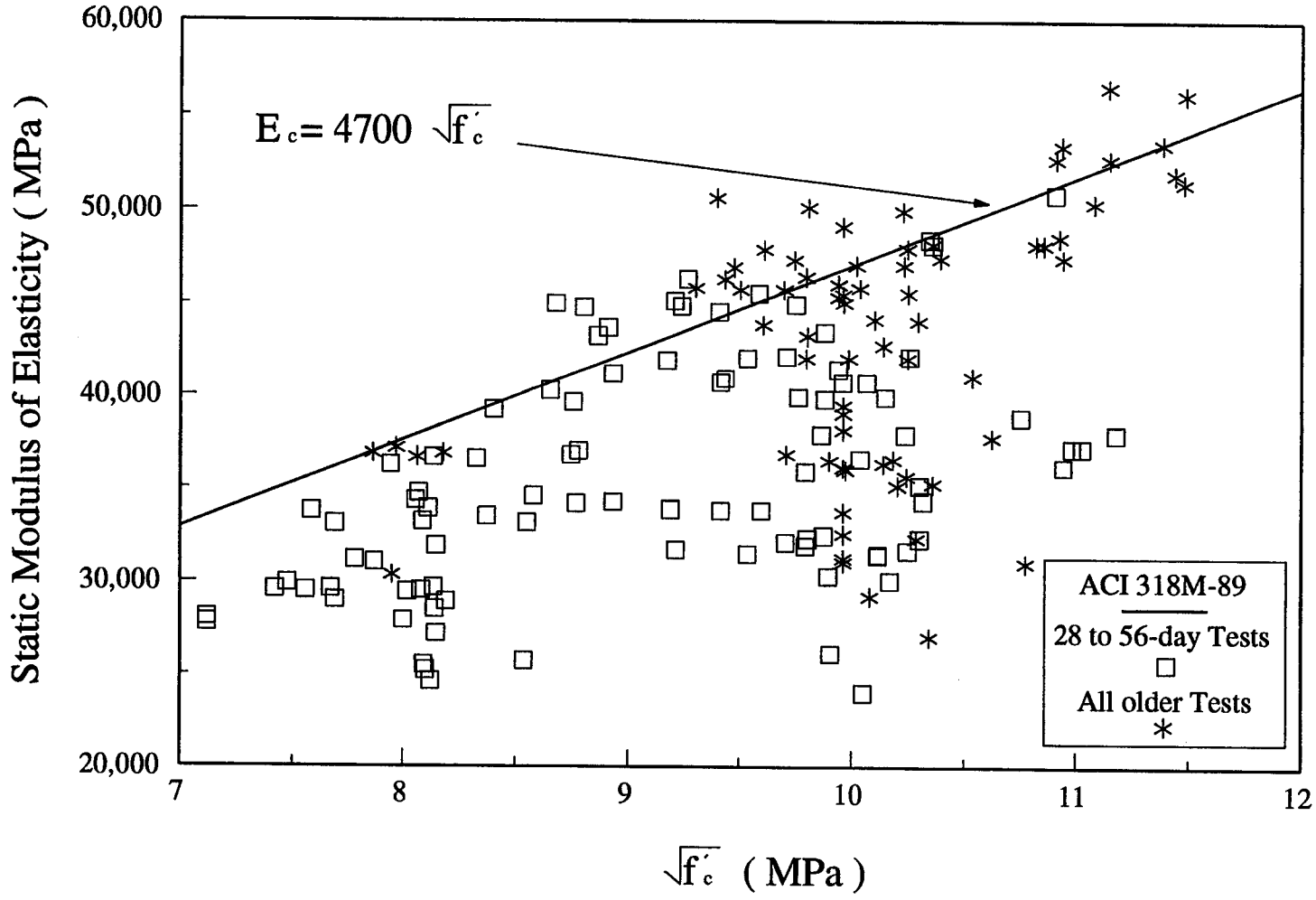

Figure E-3.7.C - Effect of Time on Modulus of Elasticity

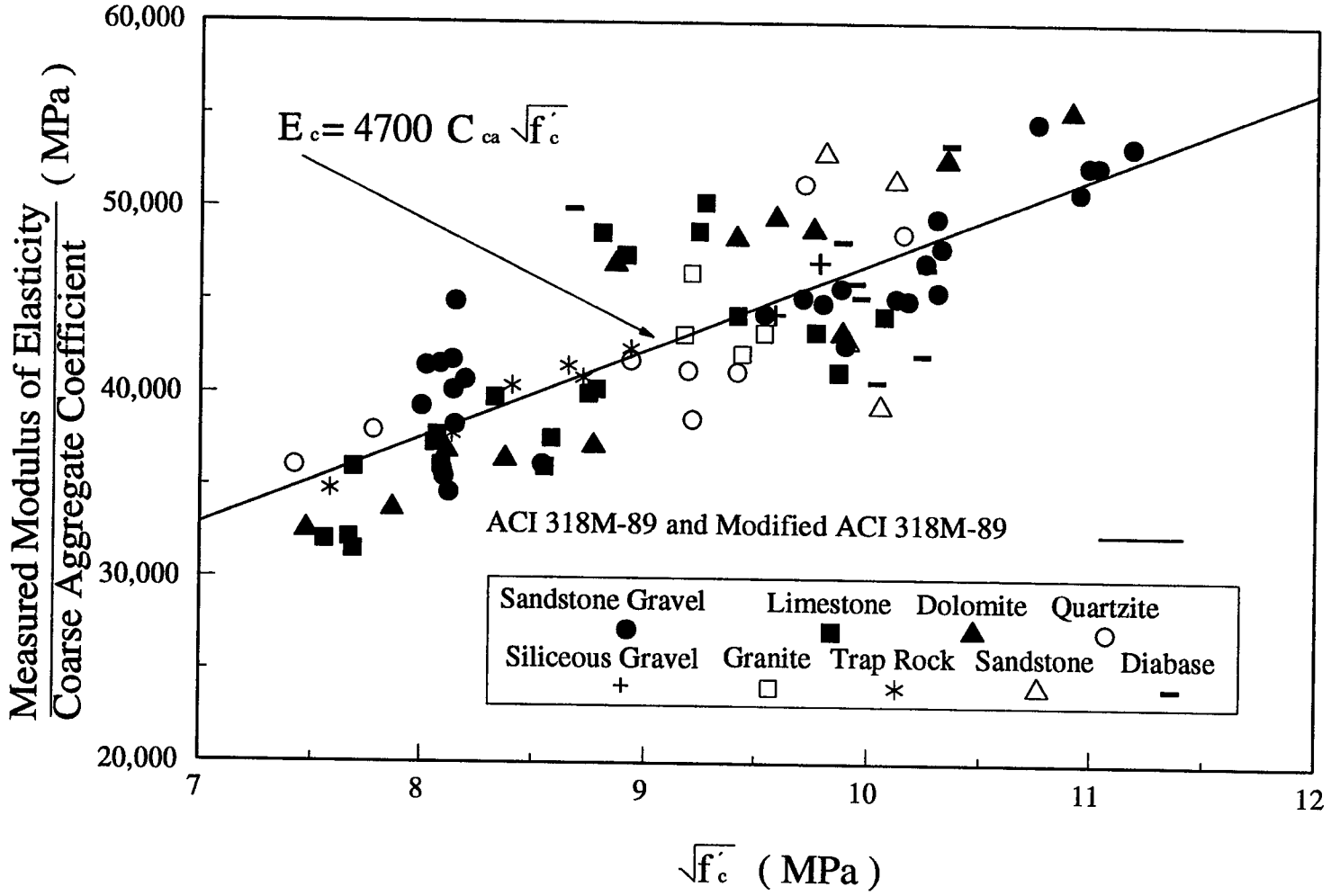

Figure E-3.7.D - Effect of Coarse Aggregate on Modulus of Elasticity

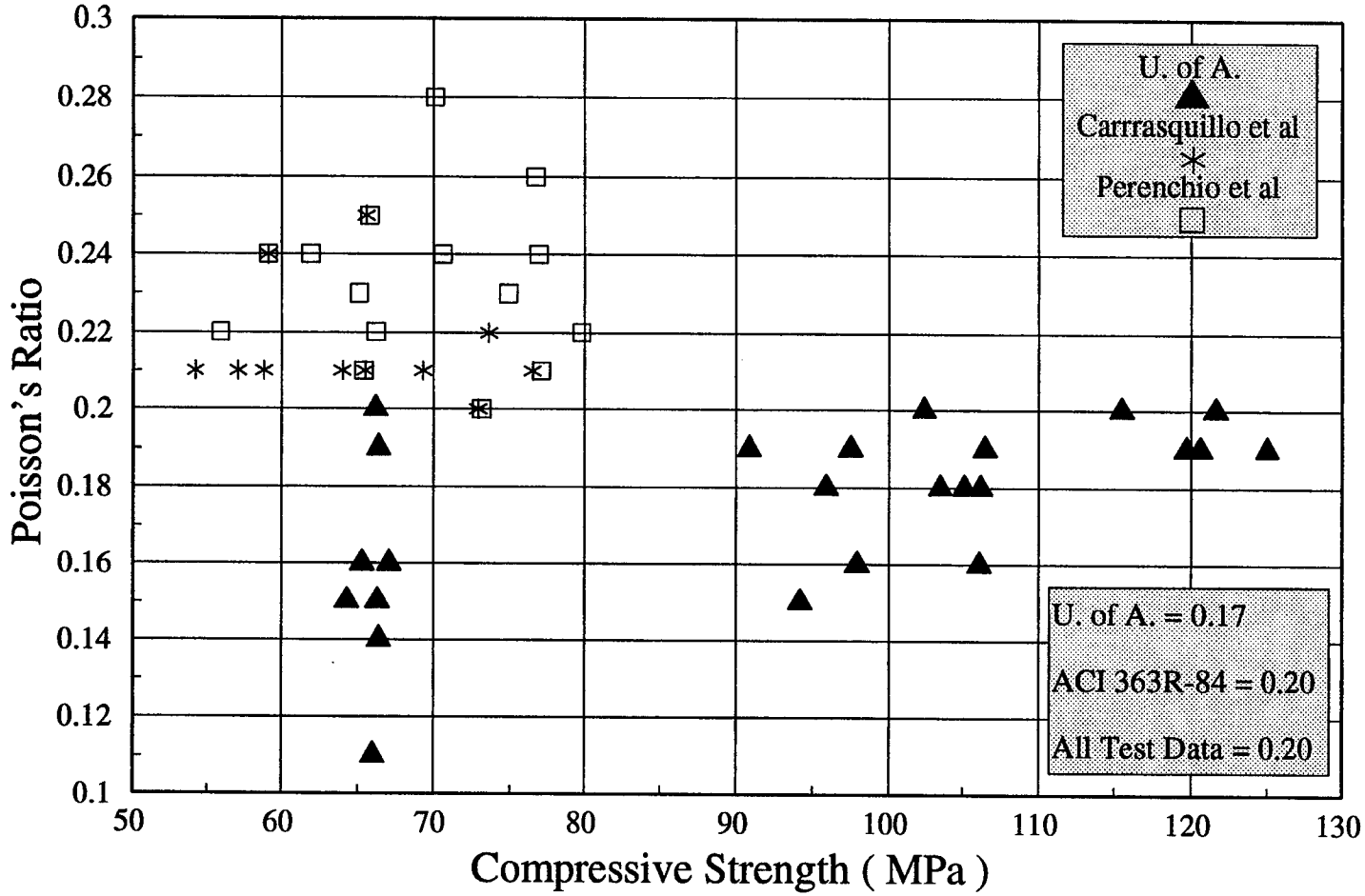

Figure E-3.8 - Poisson's Ratio Test Results

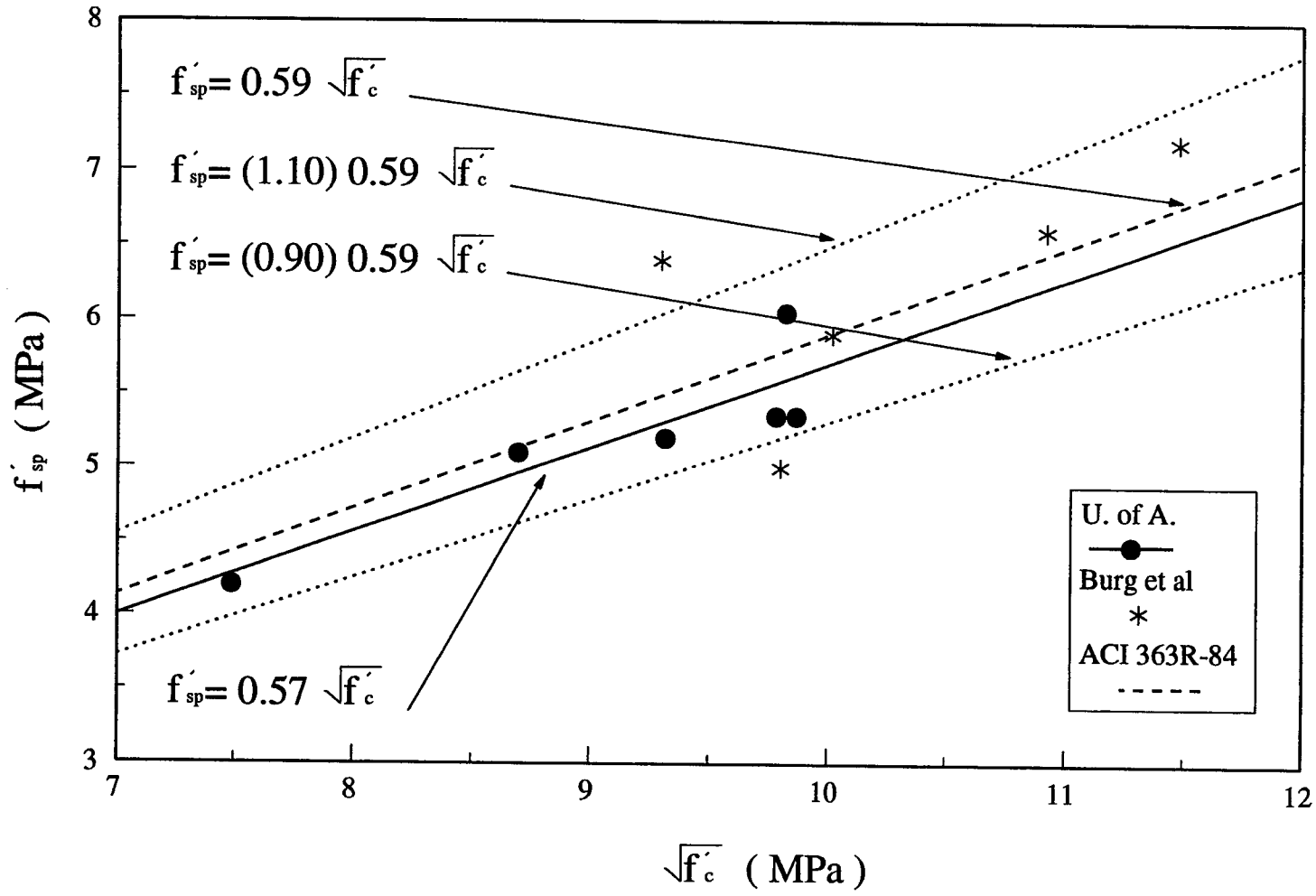

Figure E-3.9 - Tensile Splitting Strength Test Results

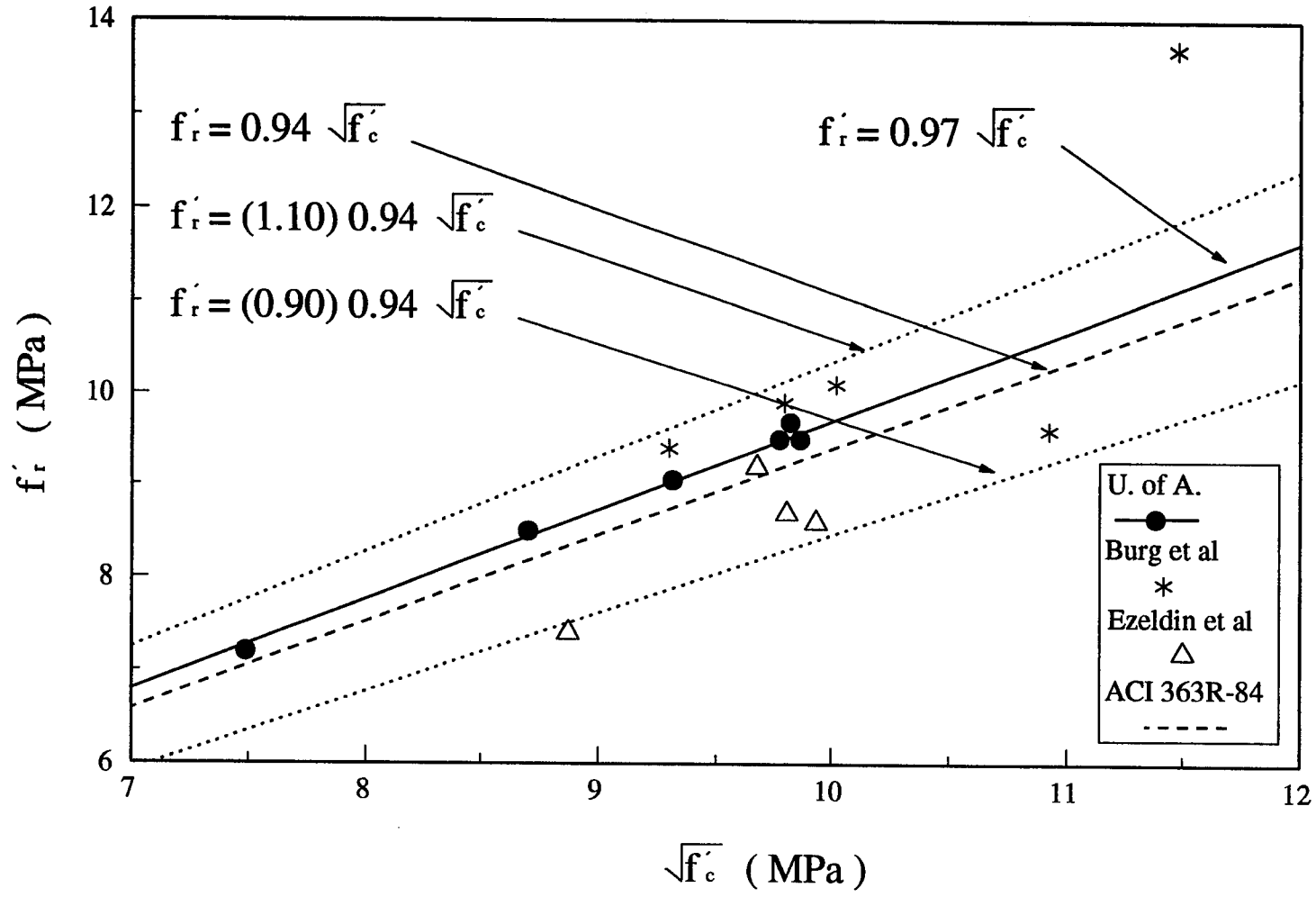

Figure E-3.10 - Modulus of Rupture Test Results

Appendix F. High Performance Concrete under High Sustained Compressive Stresses (LU Series Test Results)

F-4.1 Introduction

The results of the study of high performance concrete under high sustained compressive stresses are presented in Chapter 4 for LH, UH, and UU series. The results are presented in this appendix for LU series.

F-4.2 Literature Review

Literature review of previous studies is presented in section 4.2 of Chapter 4.

F-4.3 Compressive Strength History of Concretes Used

The test results for LU1 series are presented in Table F-4.3. The reported results are the average compressive strength of specimens tested for LU series. The compressive strength of individual specimens are reported in Appendix I, Table I-F-4.3. All specimens were cured 3 weeks at 100% R.H. and then at 50% R.H.. The compressive strength gain as the percentage of the 28 day compressive strength is presented in the same table and in Figure F-4.3.A. Due to start of the study of these high performance concretes under sustained compressive stresses at the age of 56 days, the compressive strength gain as the percentage of the 56 day compressive strength is also presented in the same table and in Figure F-4.3.B.

F-4.4 Stress - Strain Behavior of Concretes Used

The test results for LH, UH, LU, and UU series are presented in Figure F-4.4.A. The relation between stress, as a percentage of the ultimate stress, and strain are presented in Figures F-4.4.B for LU series. As can be seen from Figure F-4.4.B, the stress - strain curves for LU series deviated from straight line above 85 percent of the ultimate stress.

F-4.5 High Performance Concrete under High Sustained Concentric Stresses

The experimental results of the specimens tested concentrically for LU series are presented in this section. Each specimen is represented by an abbreviation such as LHC75(70). The first two characters represent the concrete series to which the specimen belongs (See Section 2.4). The third character stands for concentric, C, and eccentric, E, specimens. The first number represents the stress intensity or load intensity on the specimen as a percent of the short time strength at the time of loading. The possible next character

distinguishes the specimens with the same stress intensity. If the specimen is loaded at the age of 70 days instead of 56 days, the age appears in parentheses. The compressive strength of monotonic concentric specimens tested are presented in Table F-4.5.A.

The experimental results for monotonic concentric tests are presented in Figures G-F-4.5.A through E of Appendix G. The experimental results for sustained concentric tests are presented in Figures F-4.5.A through E. The stress is shown (right-hand scale) as the ratio of the ultimate strength of the specimen for monotonic specimens and as the ratio of the average ultimate stress of monotonic specimens for sustained specimens. Stress, longitudinal strain, and transverse strain are shown as a function of time. The ultimate compressive stress and the cross sectional area of the specimen are also presented in each figure.

Specimens LUC95 and LUC90 were tested in the MTS 815 test machine and the other sustained specimens were tested in the sustained load frames. Specimen LUC95 failed after being under sustained concentric stress of 95 percent of the ultimate for 9 minutes (See Figure F-4.5.A). Specimen LUC90 was loaded to approximately 87 percent of the ultimate stress as the result of an error in calculation. It sustained this stress for 1 day, 3 hours, and 53 minutes. Then, the load on the specimen increased to the proper level and it failed under 90 percent of the ultimate stress after 1 day, 2 hours and 23 minutes at the increased stress (See Figure F-4.5.B). The specimens in the three sustained concentric load frames were subjected to sustained concentric stresses of 85, 80, and 75 percent of the ultimate at the age of 56 days. Specimens LUC85, LUC80, and LUC75 did not fail during the 3 month sustained load test (See Figure F-4.5.C through E). As can be seen, the transverse strains were generally less than 2000 microstrain until near the failures.

For all sustained specimens, the total strain, the initial strain, the creep strain, the creep coefficient, the specific creep, and time after loading are presented in Table F-4.5.B for the time of failure or the end of the test. The initial recovery is also presented in the same table for those specimens which did not fail during the 3 month test.

The stress - strain relationships are summarized in Figure F-4.5.F for LU concentric series and the strain - log of time relationships are also summarized in Figure F-4.5.G for LU series. Vertical marks (]) at the end of the curves indicate failure and arrows indicate no failure. The results of concentric specimens tested in this study are summarized in Figure F-4.5.H. Results are presented as stress intensity versus the short time ultimate compressive strength at the time of loading. As can be seen from Figure F-4.5.H, the highest stress

intensities under which the specimens did not fail during the three month sustained compressive concentric study were 70, 75, 85, and 85 percent of the ultimate short term compressive strength for LH, UH, LU, and UU series, respectively.

F-4.6 High Performance Concrete under High Sustained Eccentric Stresses

The experimental results of the specimens tested eccentrically for LU series are presented in this section. Each specimen is represented by an abbreviation such as LHE80(70). The first two characters represent the concrete series to which the specimen belongs (See Section 2.4). The third character stands for concentric, C, and eccentric, E, specimens. The first number represents the stress intensity or load intensity on the specimen as a percent of the short time strength at the time of loading. The possible next character distinguishes the specimens with the same intensity. If the specimen is loaded at the age of 70 days instead of 56 days, the age appears in parentheses.

The experimental results for monotonic eccentric tests are presented in Figures G-F-4.6.A through E of Appendix G. The experimental results for sustained eccentric tests are presented in Figures F-4.6.A through D. The load is shown (right-hand scale) as the ratio of the ultimate load of the specimen for monotonic specimens and as the ratio of the average ultimate load of monotonic specimens, after necessary adjustment for possible diameter differences, for sustained specimens. Load, longitudinal strain in extreme fiber, and longitudinal strain in the opposite side are shown as a function of time. The ultimate load and the cross sectional area of the specimen are also presented in each figure.

Specimen LUE95 was tested in MTS 815 test machine and the other sustained specimens were tested in the sustained load frames. Specimen LUE95 failed after being under sustained eccentric stress of 95 percent of the ultimate for 3 minutes (See Figure F-4.6.A). The specimens in the three sustained eccentric load frames were subjected to sustained eccentric stresses of 90, 85, and 80 percent of the ultimate at the age of 56 days. Specimens LUE90, LUE85, and LUE80 did not fail during the 3 month sustained load test (See Figures F-4.6.B through D). As it can be seen, the longitudinal strain in the opposite side was generally less than 1000 microstrain compression until near failure.

For sustained specimens that did not fail, the total strain, the initial strain, the creep strain, the creep coefficient, the initial recovery, and time after loading are presented in Table F-4.6 for the end of the test.

The load - extreme fiber strain relationships are summarized in Figure F-4.6.E for LU eccentric series; and the extreme fiber strain - log of time relationships are also summarized in Figure F-4.6.F for LU series. Vertical marks (]) at the end of the curves indicate failure and arrows indicate no failure. The results of eccentric specimens tested in this study are

summarized in Figure F-4.6.G. Results are presented as load intensity versus the short time ultimate compressive strength at the time of loading. As can be seen from Figure F-4.6.G, the highest load intensities that the specimens did not fail during the three month sustained compressive eccentric study were 75, 80, 90, and 85 percent of the ultimate short term compressive strength for LH, UH, LU, and UU series respectively.

Table F-4.3 - Compressive Strength History (LU Series)

Age (Days)	LU1 (MPa)	f_{ct}/f_{c28}	f_{ct}/f_{c56}
1	32.1	0.34	0.30
3	54.9	0.58	0.52
7	68.2	0.72	0.65
28	94.4	1.00	0.90
56	104.7	1.11	1.00
154	112.3	1.19	1.07

Table F-4.5.A - Compressive Strength of Monotonic Concentric Specimens

Concrete Series	Age (Days)	S_1 (MPa)	S_2 (MPa)	S_3 (MPa)	S_4 (MPa)	S_5 (MPa)	Mean (MPa)	S_{n-1}
LU1	56	103.5	102.4	105.1	106.2	106.5	104.7	1.57

Table F-4.5.B - Summary of LU Concentric Series Strain Study

Specimen	Total Strain μmm/mm	Initial Strain μmm/mm	Creep Strain μmm/mm	Creep Coeff.	Specific Creep 10^{-6}/MPa	Time Min.	Initial Recovery μmm/mm
LUC95	3407	3222	185	0.057	1.9	9	-
LUC90	-	-	-	-	-	-	-
LUC85	4981	2683	2298	0.857	25.8	129600	1998
LUC80	5059	2725	2334	0.857	28.0	129600	2125
LUC75	4338	2509	1829	0.729	23.3	129600	1934

Table F-4.6 - Summary of LU Eccentric Series Extreme Fiber Strain Study

Specimen	Total Strain μmm/mm	Initial Strain μmm/mm	Creep Strain μmm/mm	Creep Coeff.	Time Min.	Initial Recovery μmm/mm
LUE90	7130	3836	3294	0.859	129600	2874
LUE85	6497	3692	2805	0.760	129600	2770
LUE80	6287	3486	2801	0.800	129600	2500

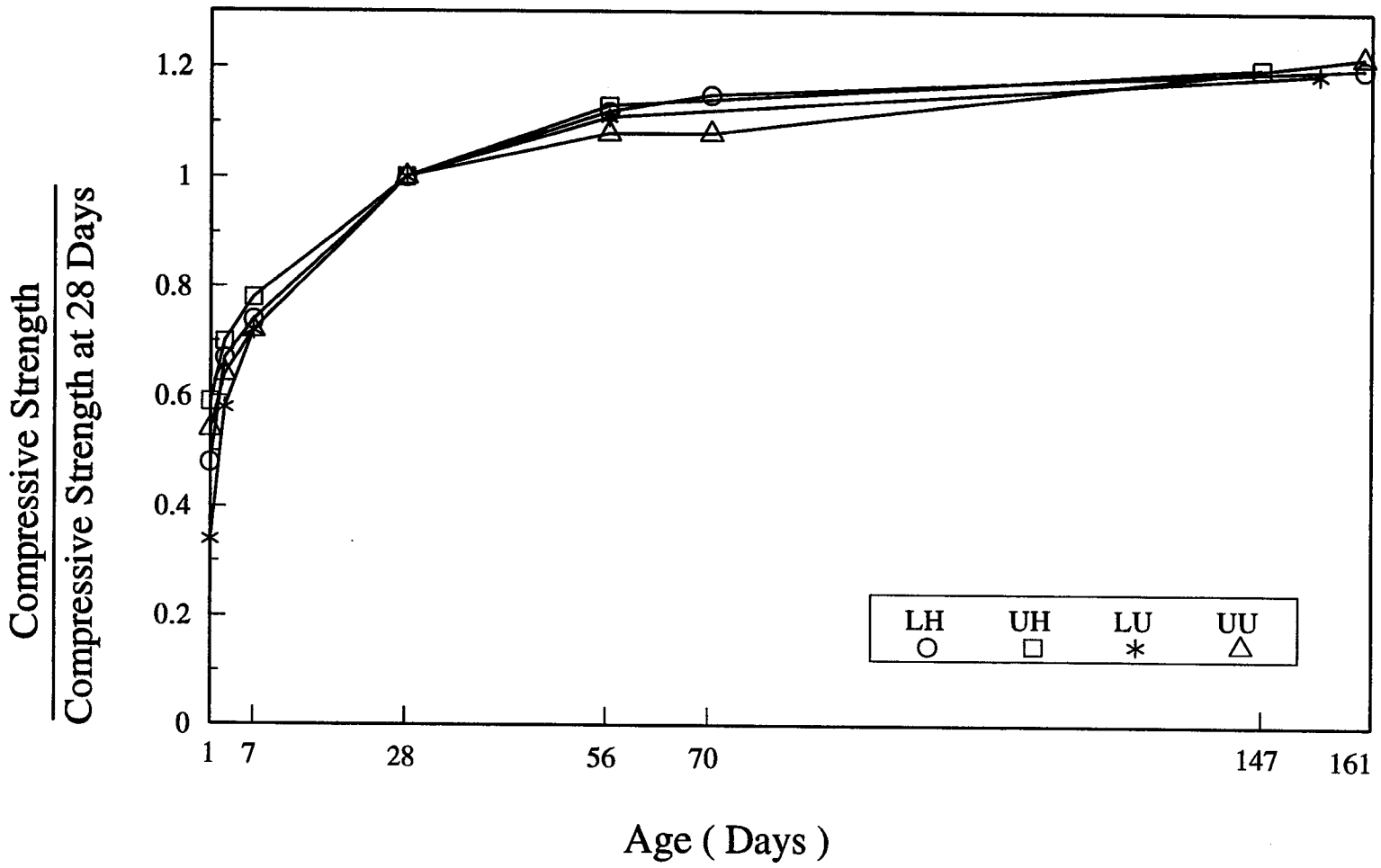

Figure F-4.3.A - Compressive Strength History (Ratio of 28-Day Strength)

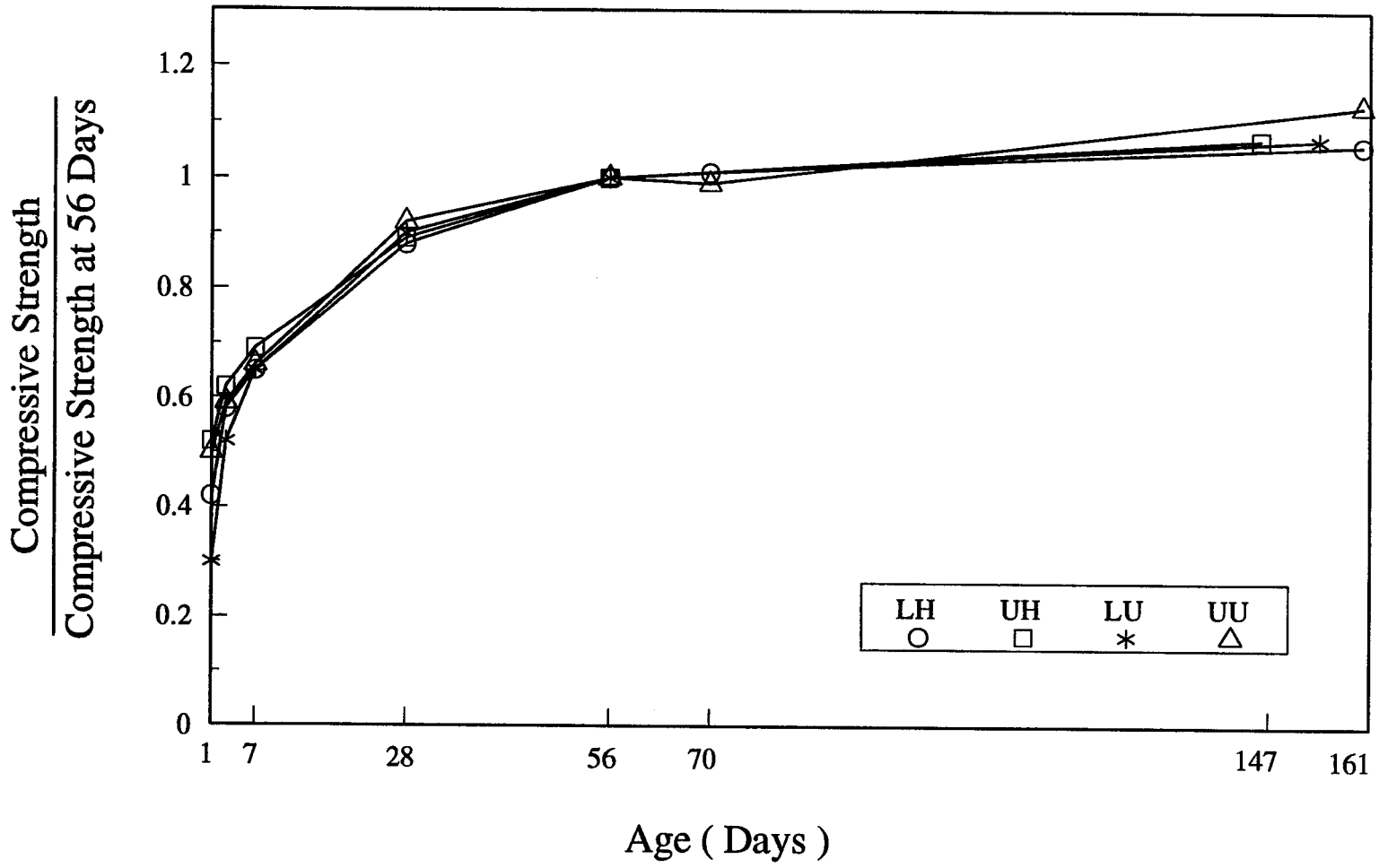

Figure F-4.3.B - Compressive Strength History (Ratio of 56-Day Strength)

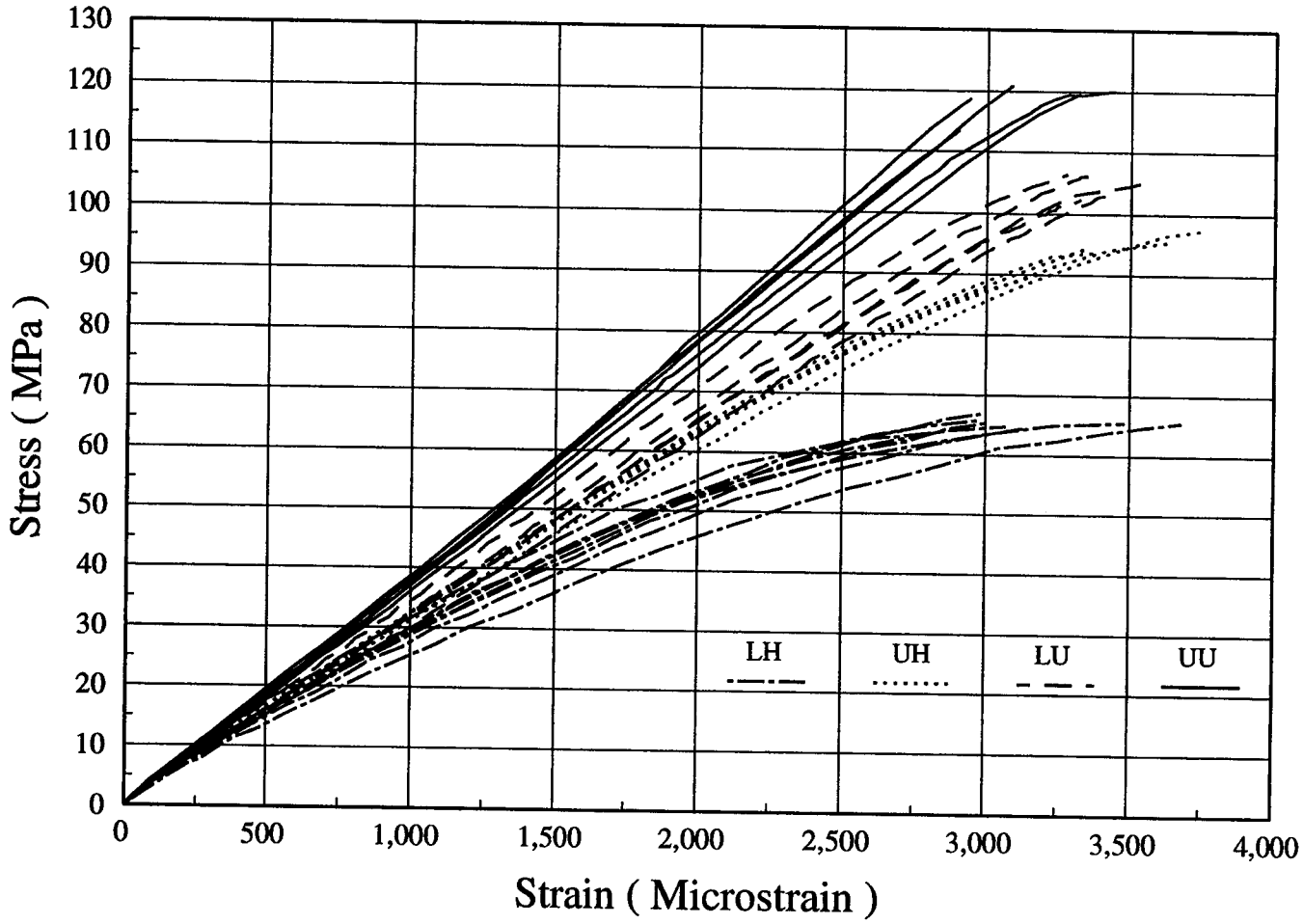

Figure F-4.4.A - Stress-Strain Curves of Monotonic Concentric Specimens

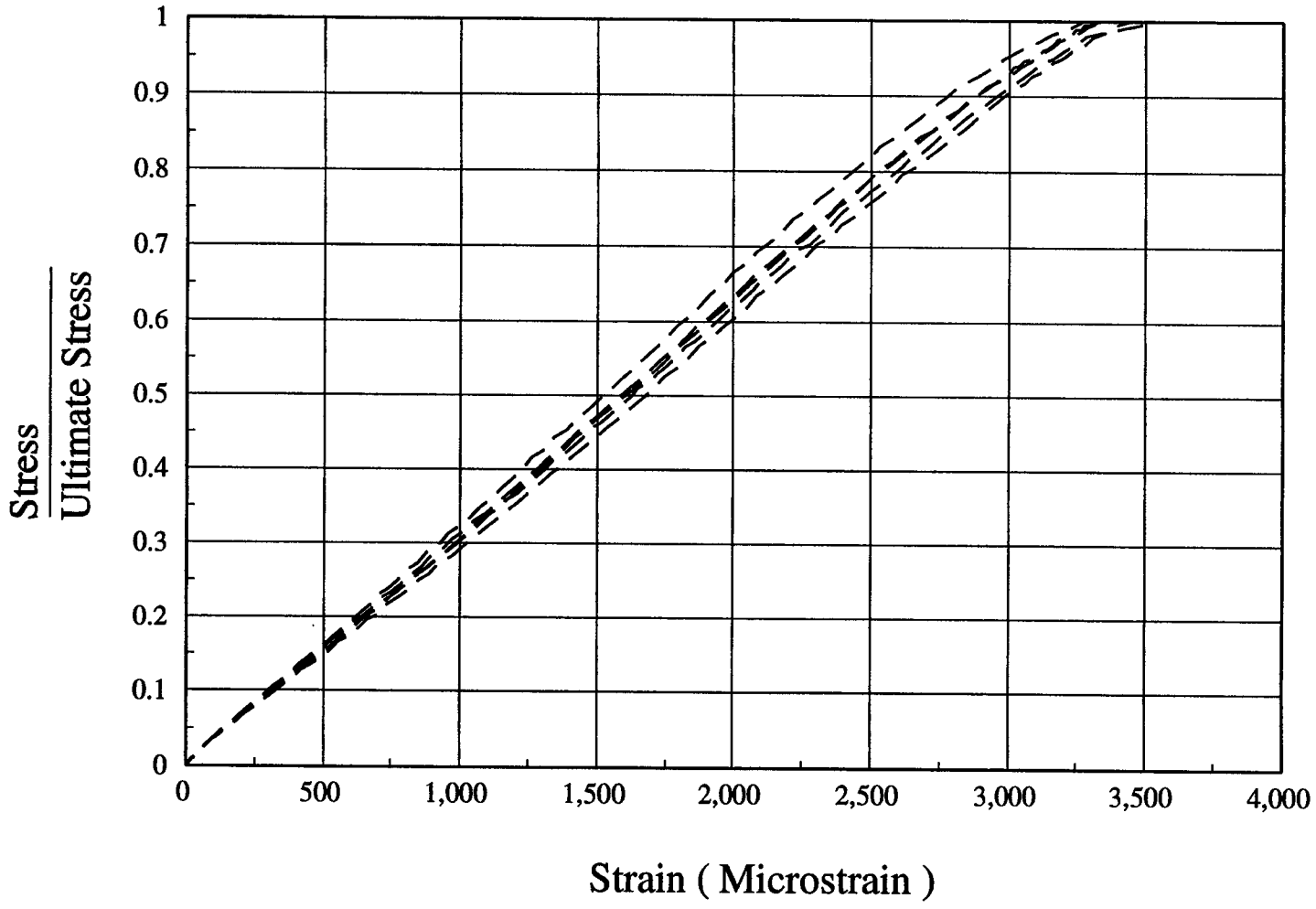

Figure F-4.4.B - Stress - Strain Relationship - LU Series

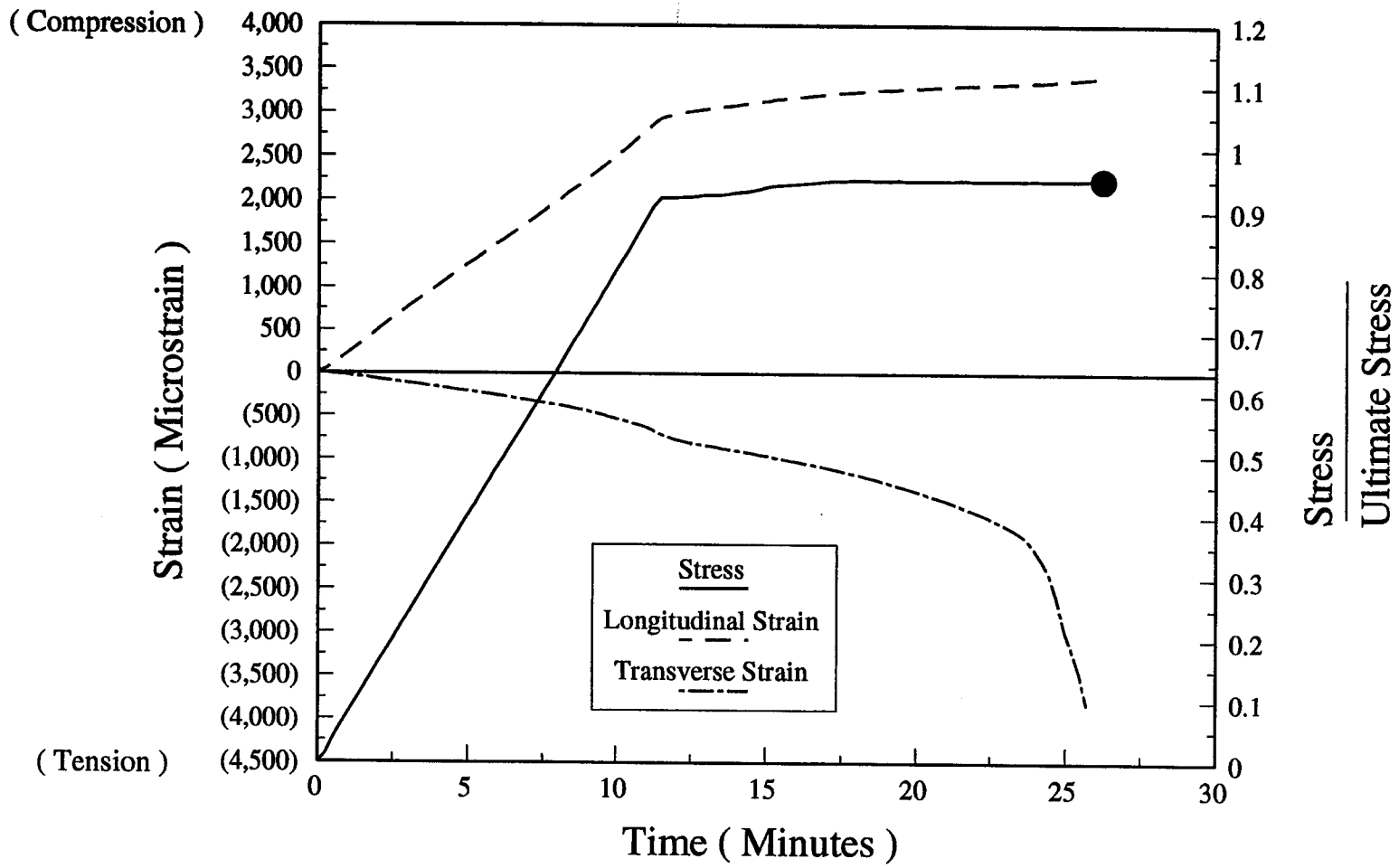

$f_c = 104.7$ MPa $\qquad A = 8316\ mm^2$

Figure F-4.5.A - Stress-Strain-Time Relationship - LUC95 Specimen

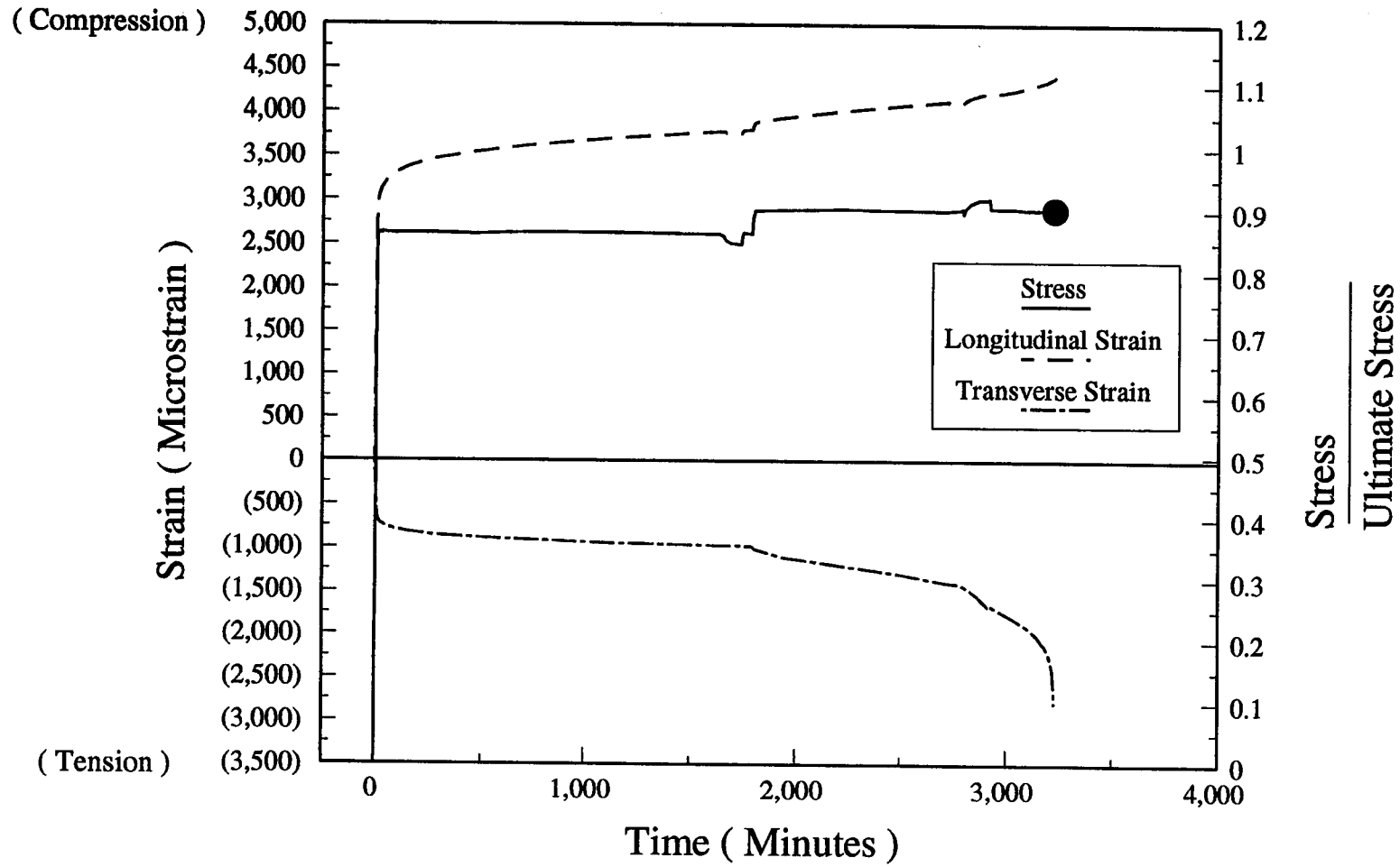

$f_c = 104.7$ MPa $\qquad A = 8028\ mm^2$

Figure F-4.5.B - Stress-Strain-Time Relationship - LUC90 Specimen

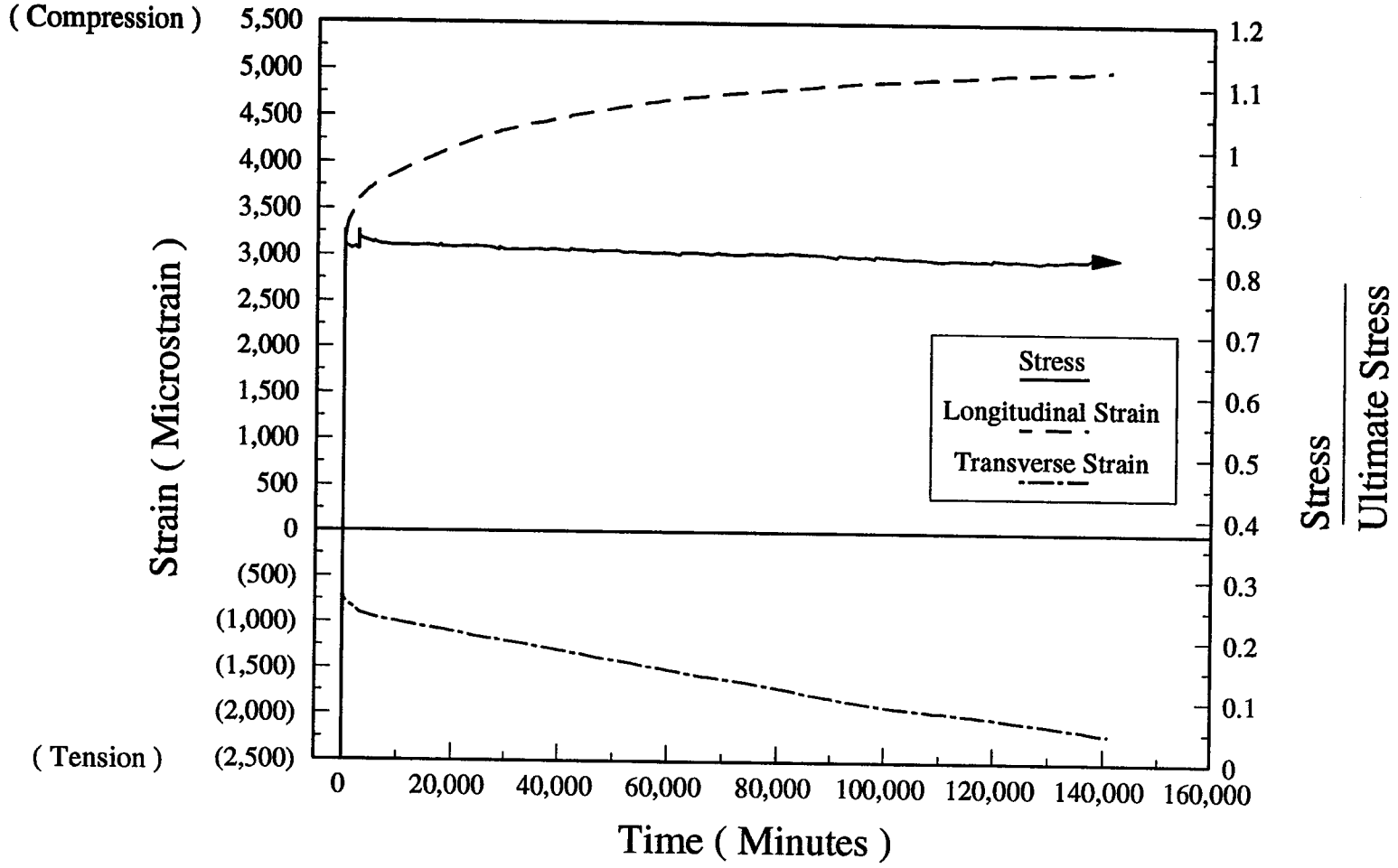

f_c= 104.7 MPa A = 7838 mm^2

Figure F-4.5.C - Stress-Strain-Time Relationship - LUC85 Specimen

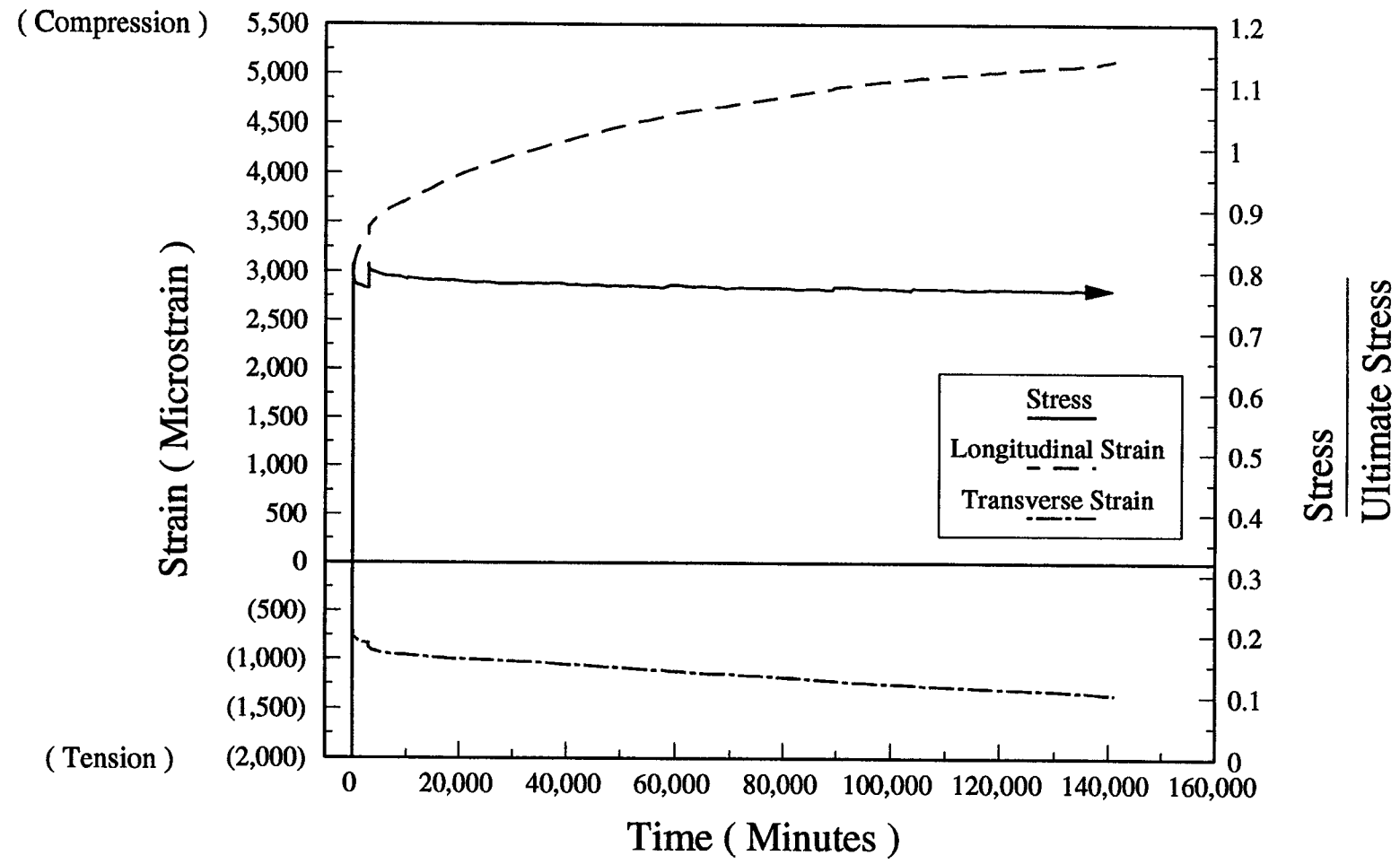

f_c = 104.7 MPa A = 8268 mm^2

Figure F-4.5.D - Stress-Strain-Time Relationship - LUC80 Specimen

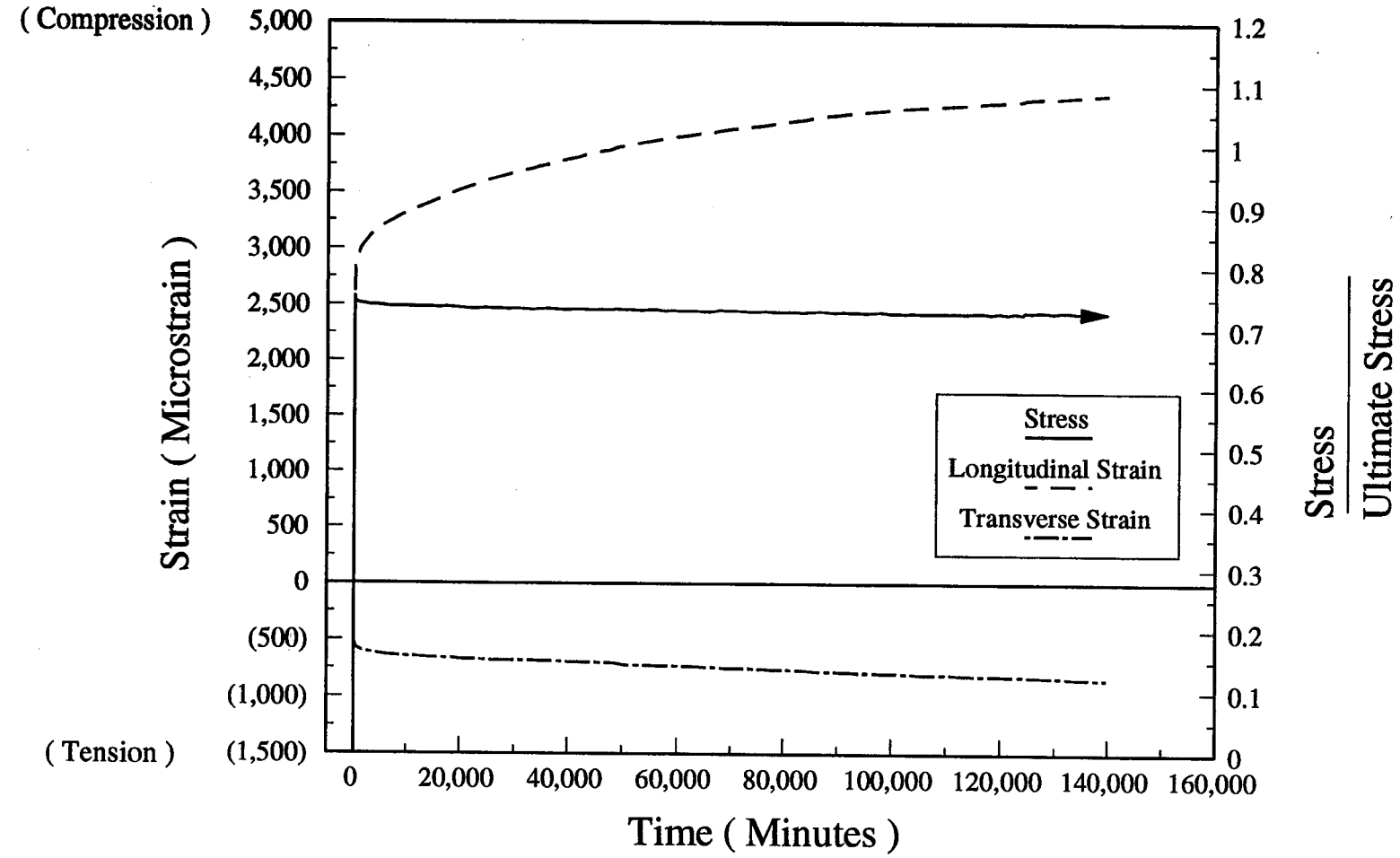

f_c = 104.7 MPa A = 8273 mm^2

Figure F-4.5.E - Stress-Strain-Time Relationship - LUC75 Specimen

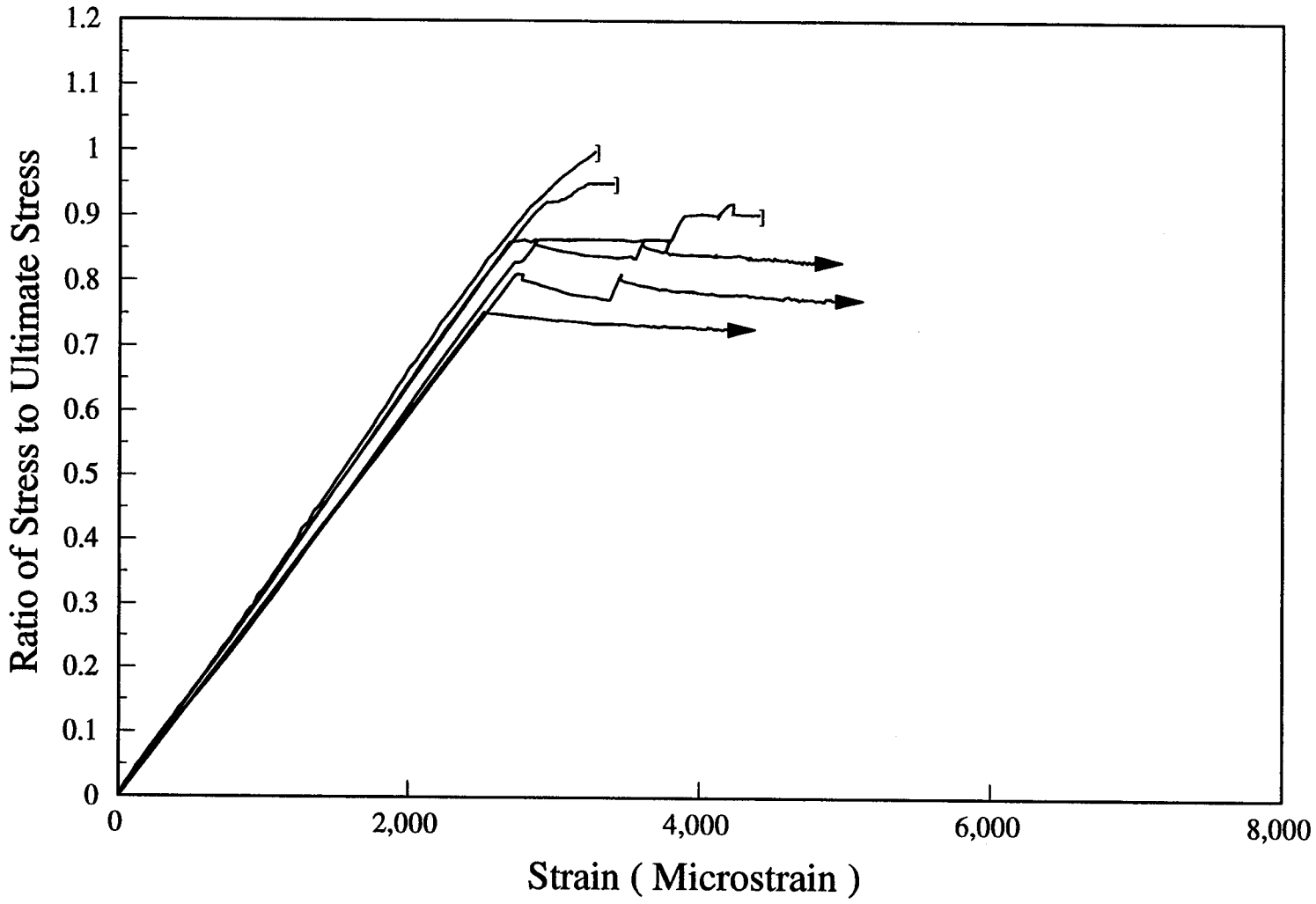

Figure F-4.5.F - Stress-Strain Relationship - LU Concentric Series

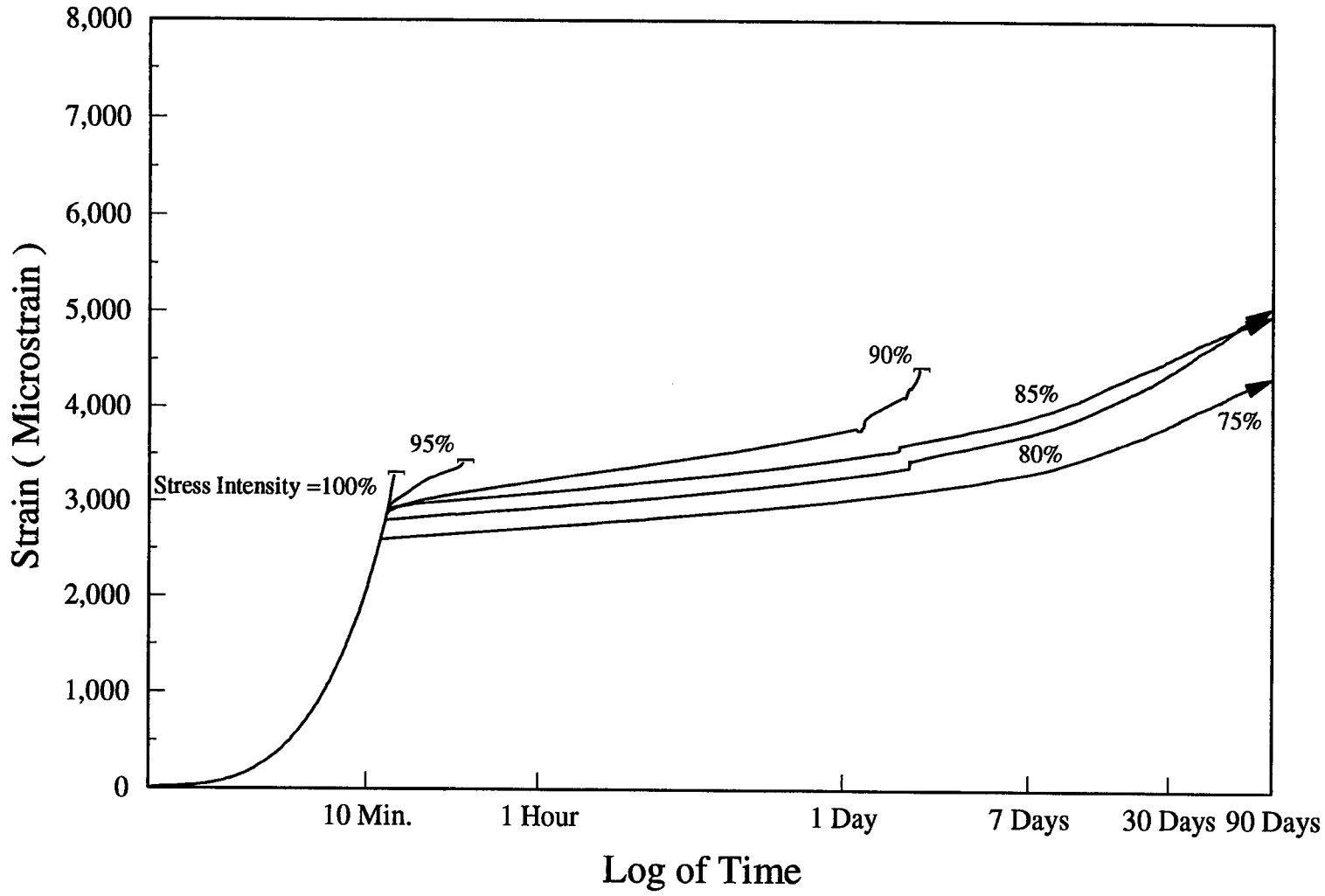

Figure F-4.5.G - Strain-Time Relationship - LU Concentric Series

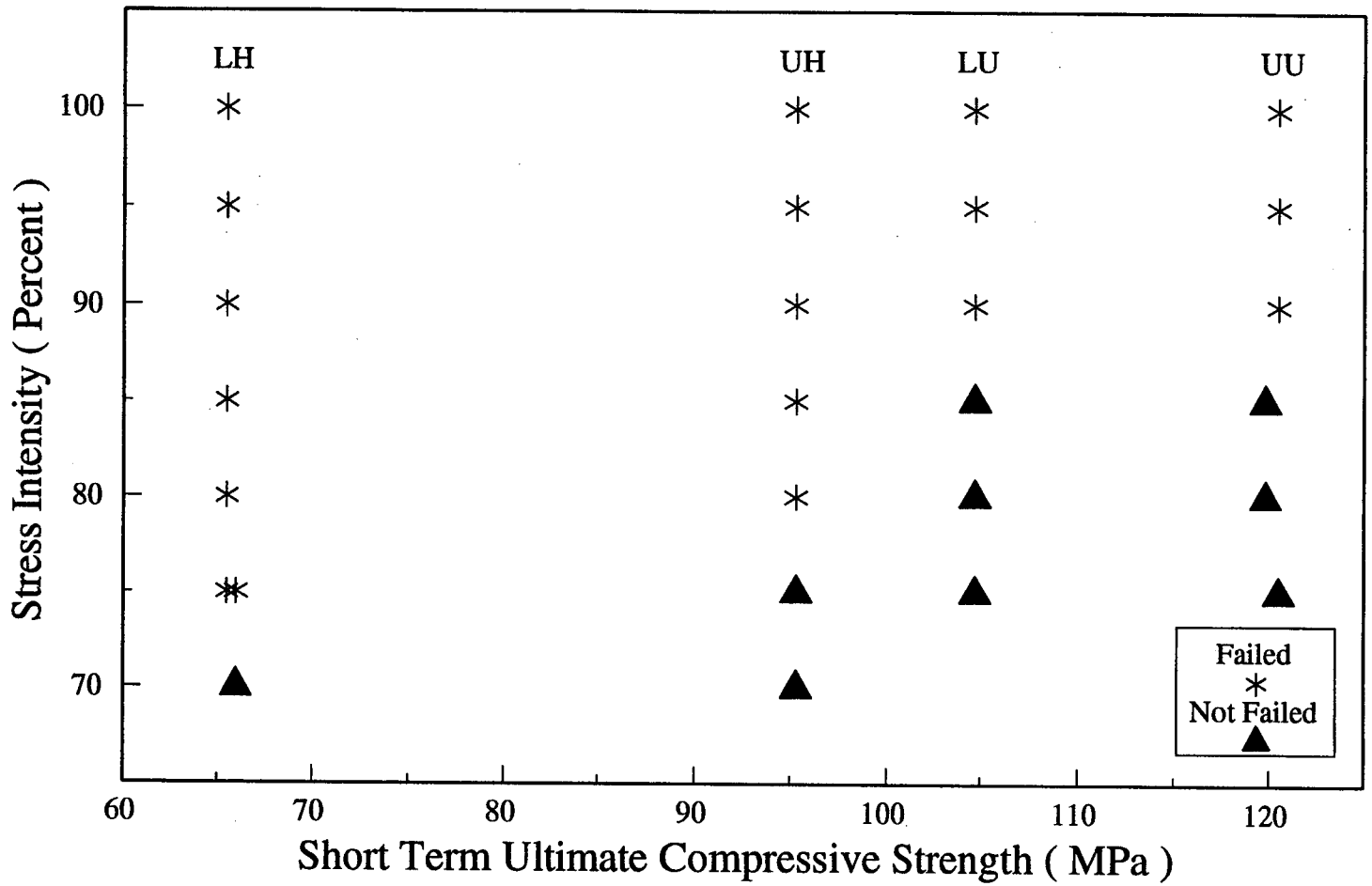

Figure F-4.5.H - Summary of Concentric Test Results

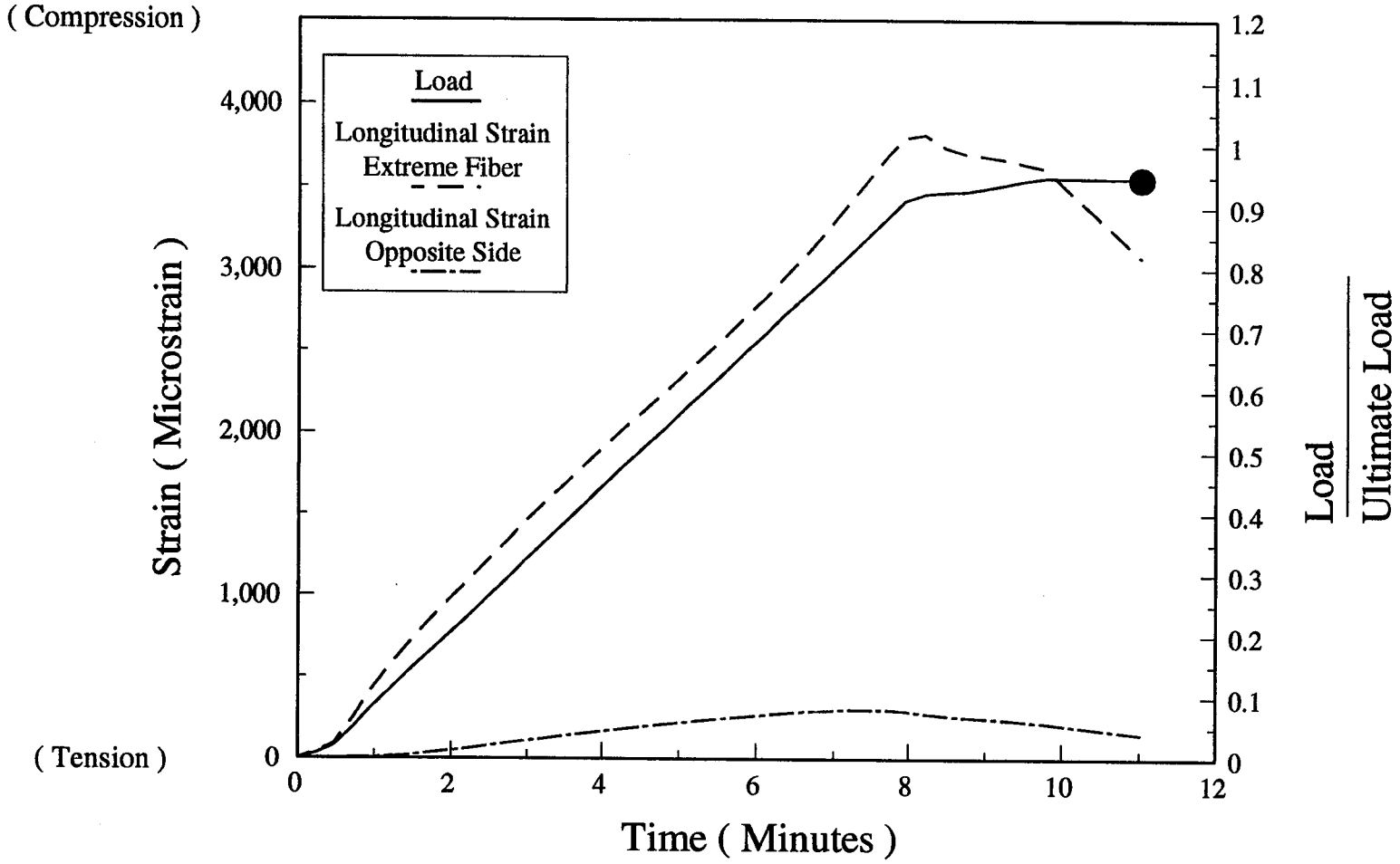

$P_c = 590.5$ kN $\qquad A = 7893$ mm^2

Figure F-4.6.A - Load-Strain-Time Relationship - LUE95 Specimen

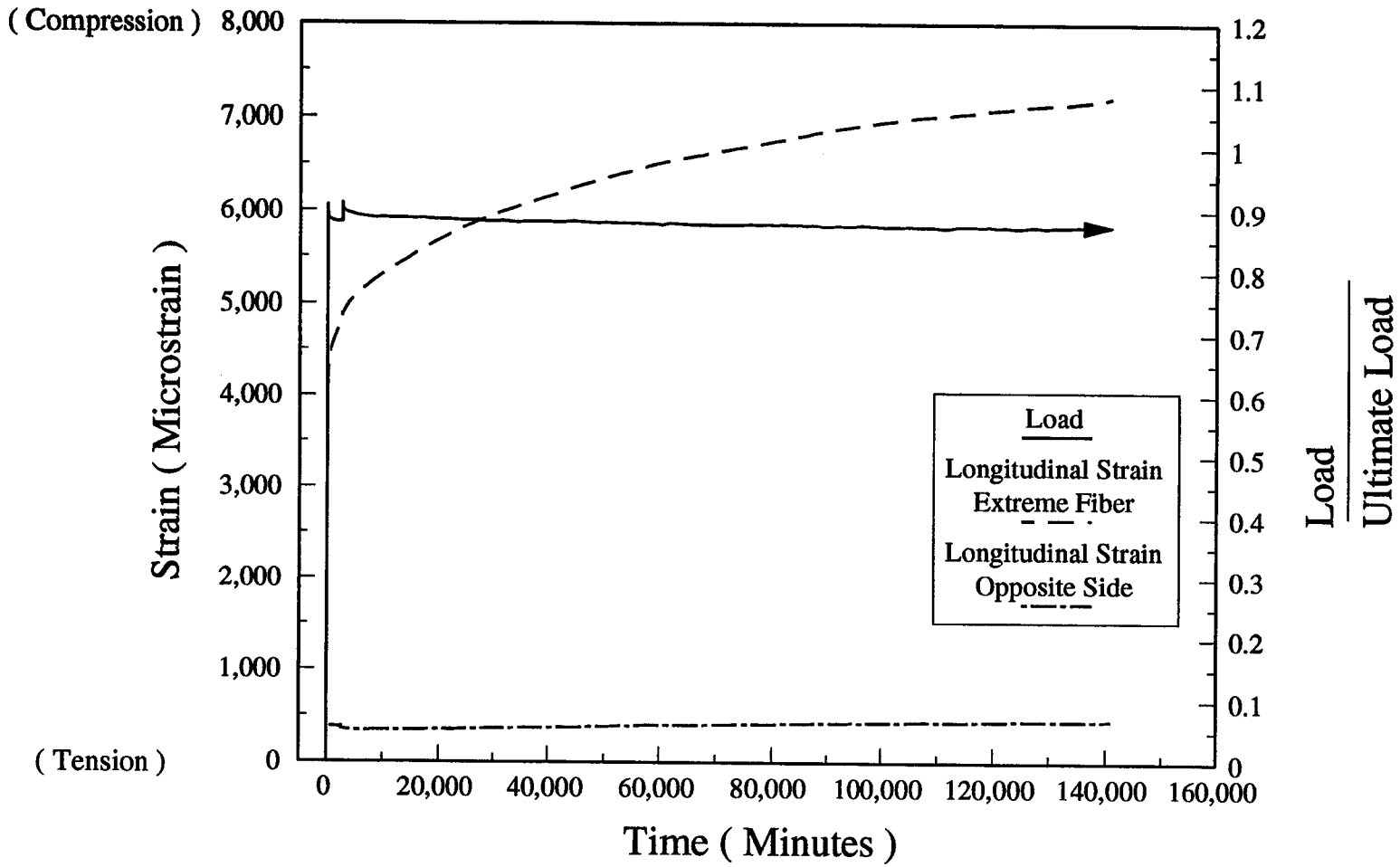

$P_c = 610.0$ kN $\qquad A = 8067$ mm^2

Figure F-4.6.B - Load-Strain-Time Relationship - LUE90 Specimen

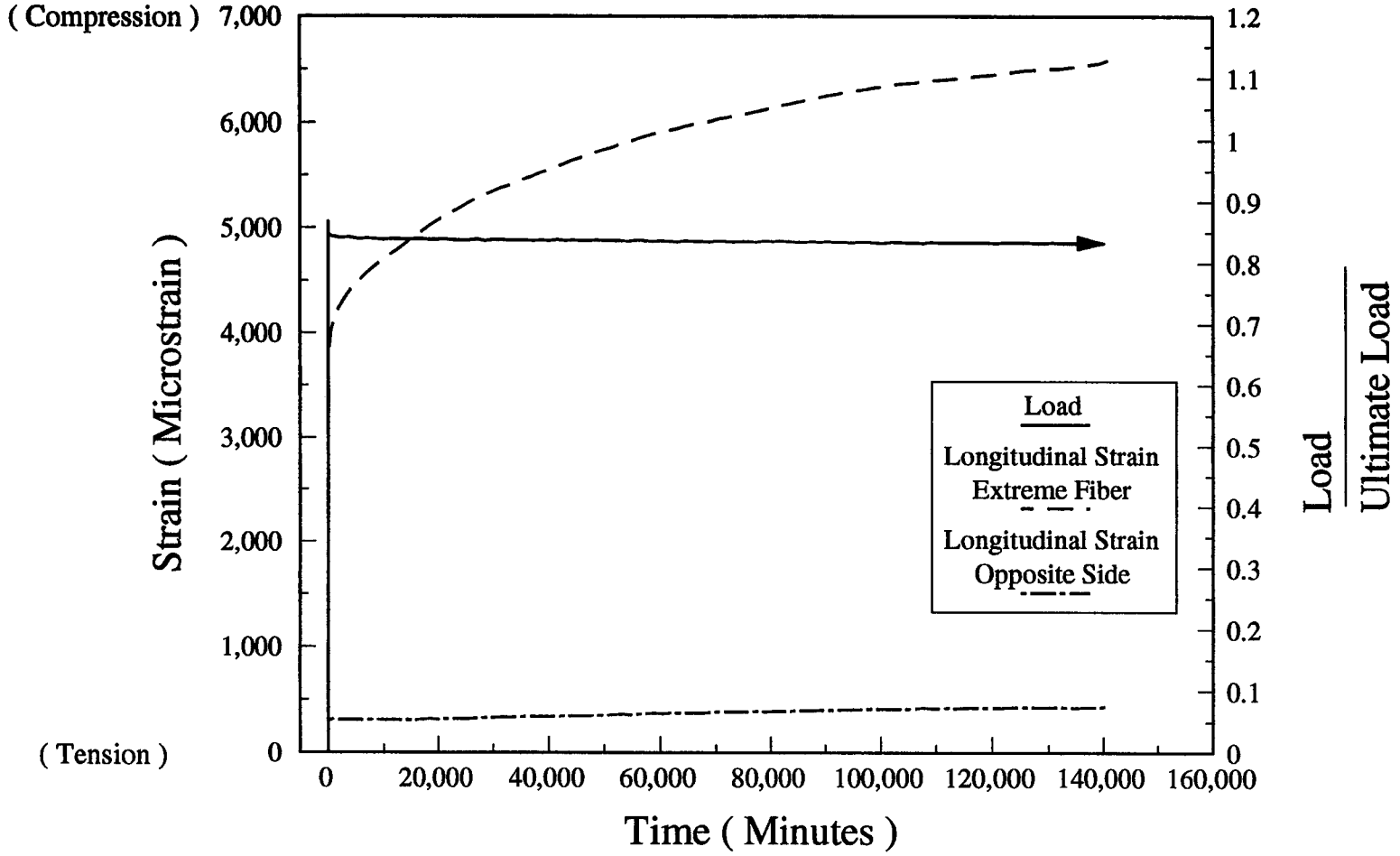

$P_c = 597.6$ kN $\qquad A = 7953$ mm^2

Figure F-4.6.C - Load-Strain-Time Relationship - LUE85 Specimen

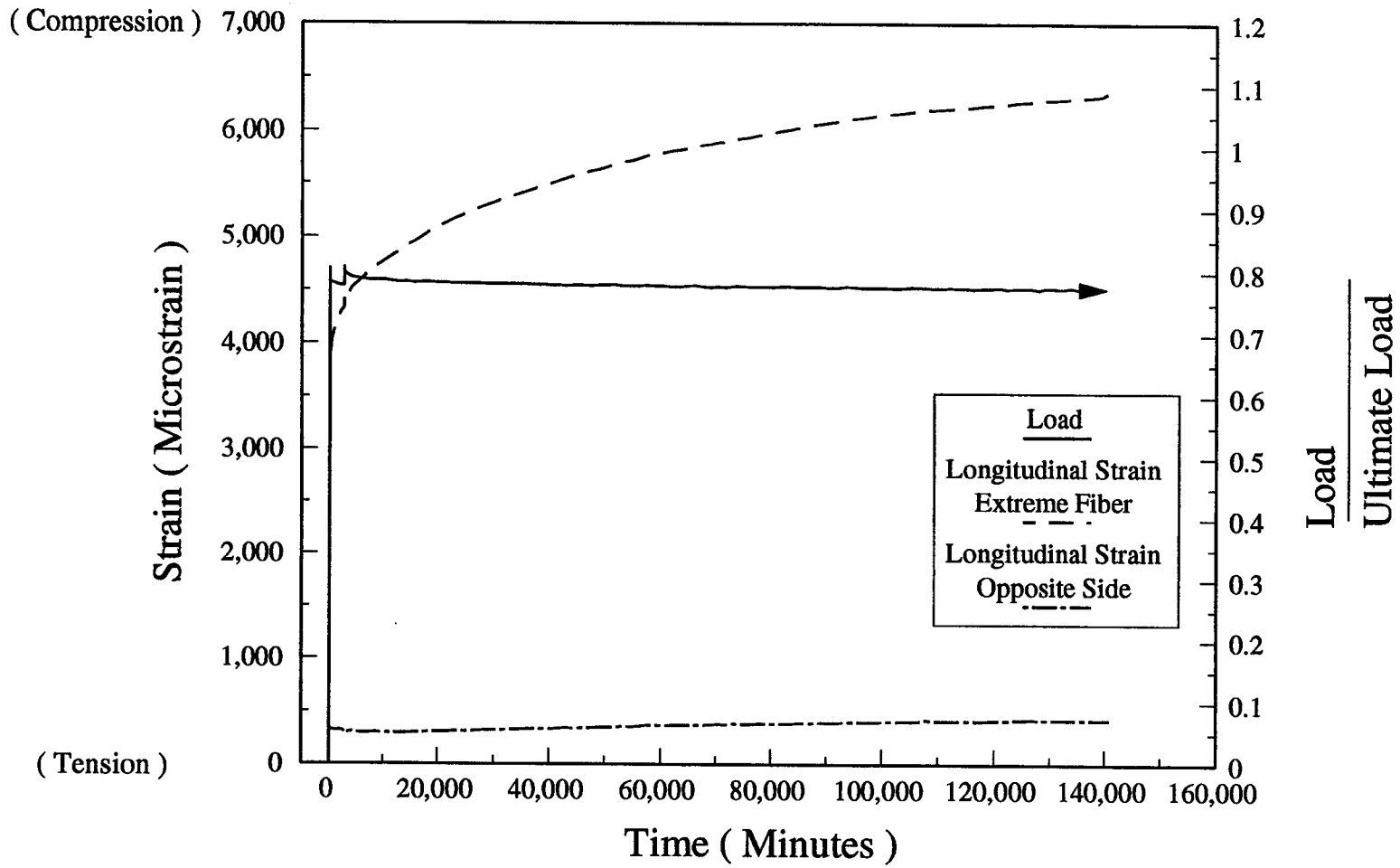

$P_c = 620.0$ kN $\qquad A = 8261$ mm^2

Figure F-4.6.D - Load-Strain-Time Relationship - LUE80 Specimen

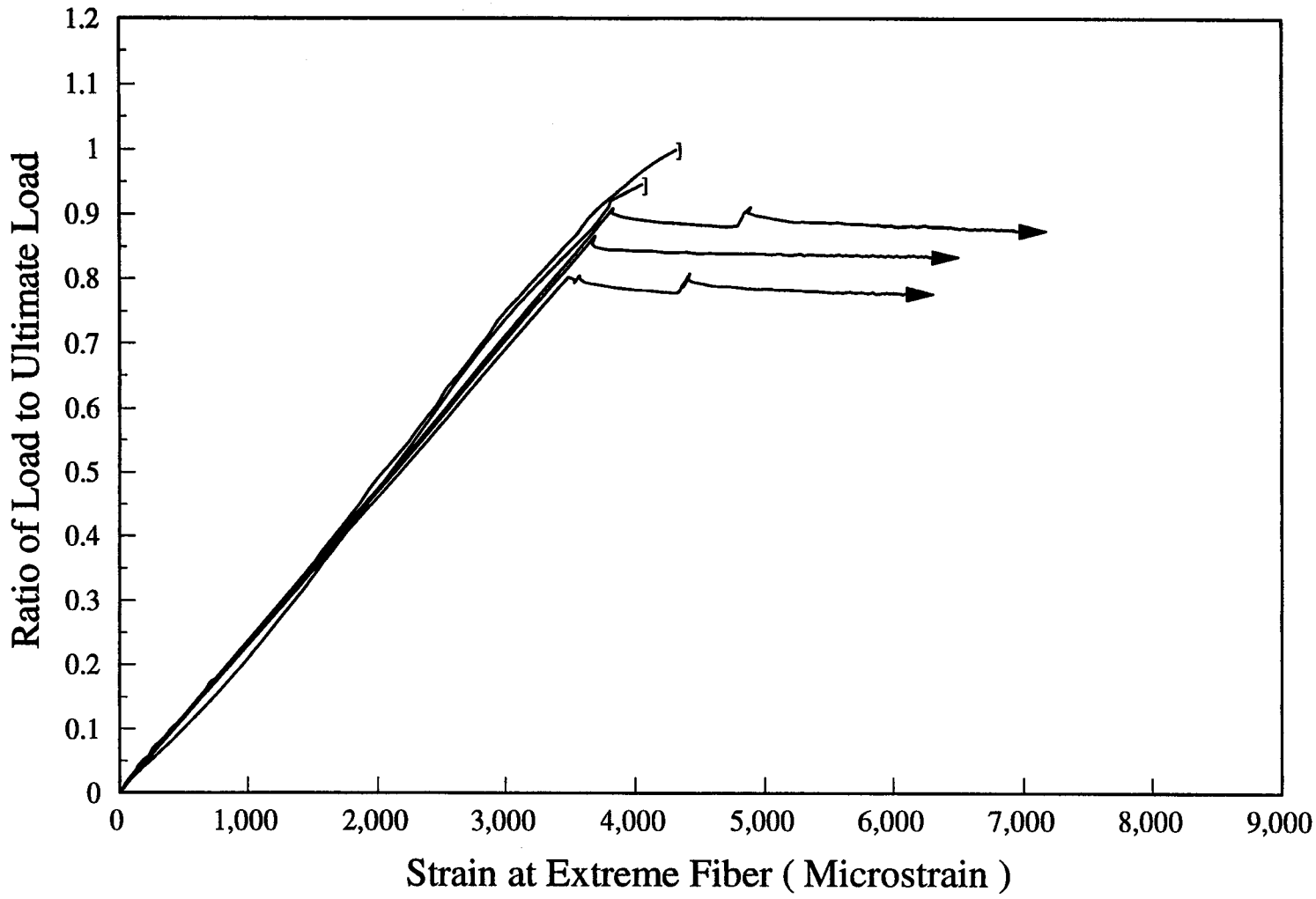

Figure F-4.6.E - Stress-Strain Relationship - LU Eccentric Series

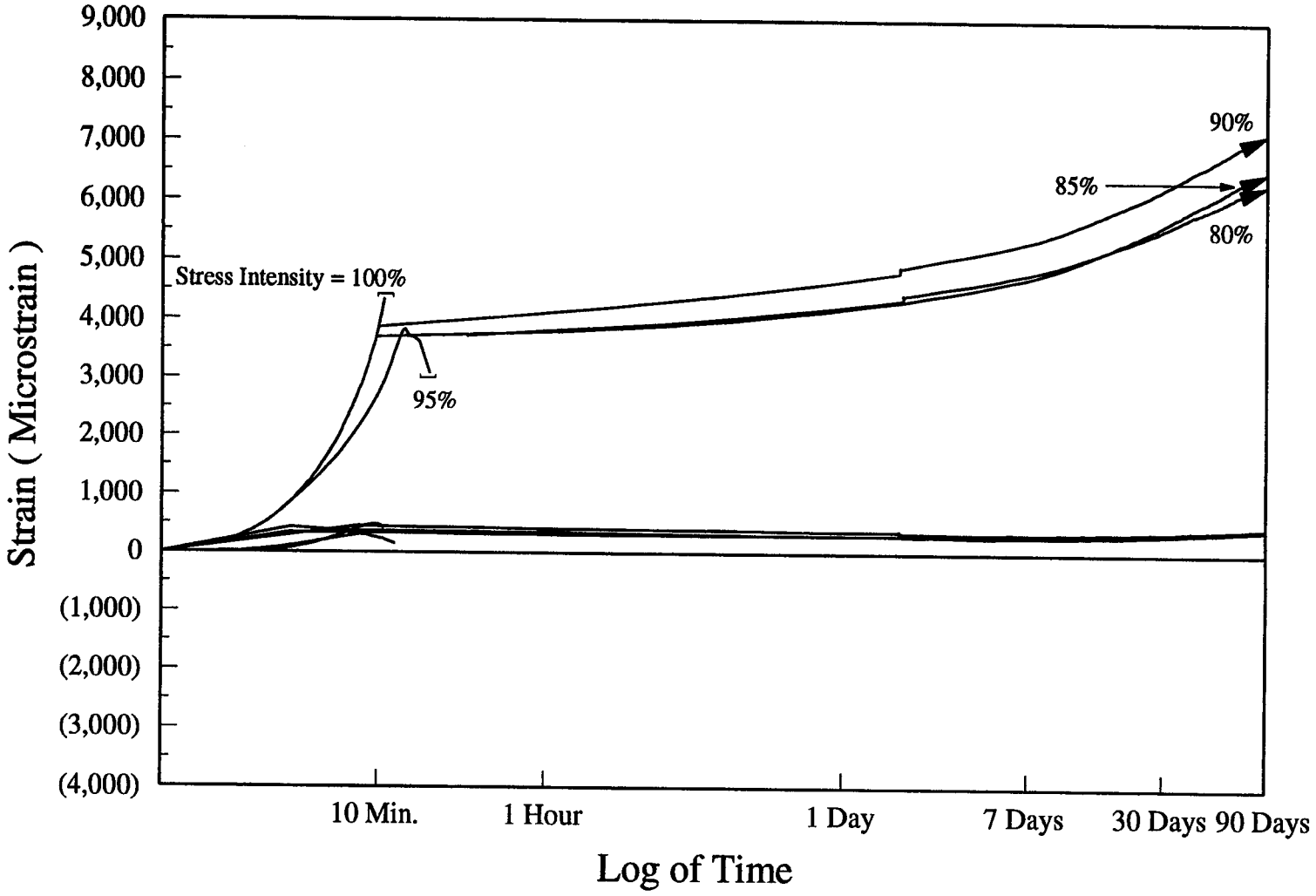

Figure F-4.6.F - Strain-Time Relationship - LU Eccentric Series

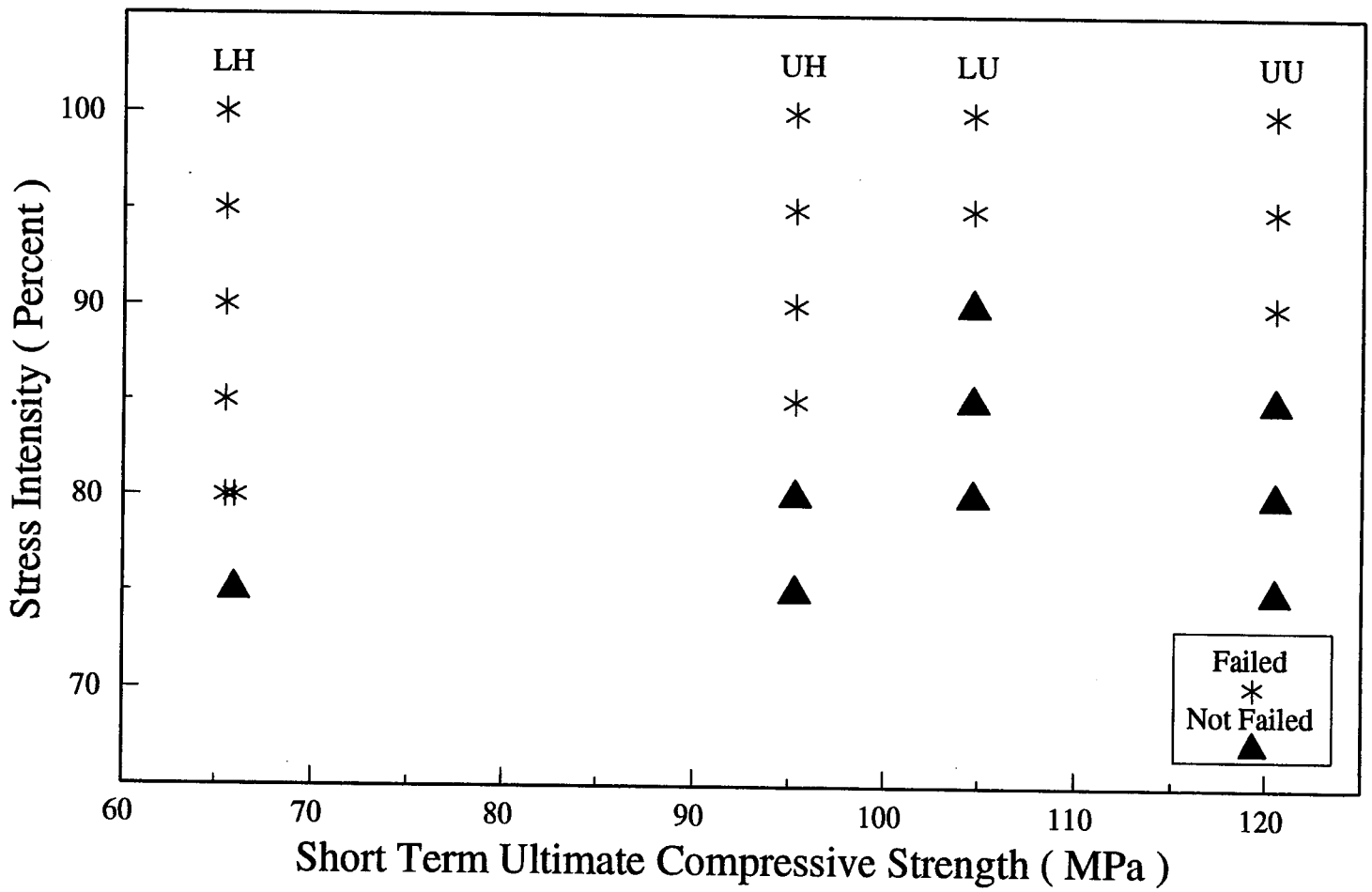

Figure F-4.6.G - Summary of Eccentric Test Results

Appendix G. LU Series Monotonic Test Results

The experimental results for short term monotonic concentric tests are presented in Figures G-F-4.5.A through E of this appendix. The details of experimental results for sustained concentric tests are presented in section F-4.5 of Appendix F.

The experimental results for short term monotonic eccentric tests are presented in Figures G-F-4.6.A through E of this appendix. The details of experimental results for sustained eccentric tests are presented in section F-4.6 of Appendix F.

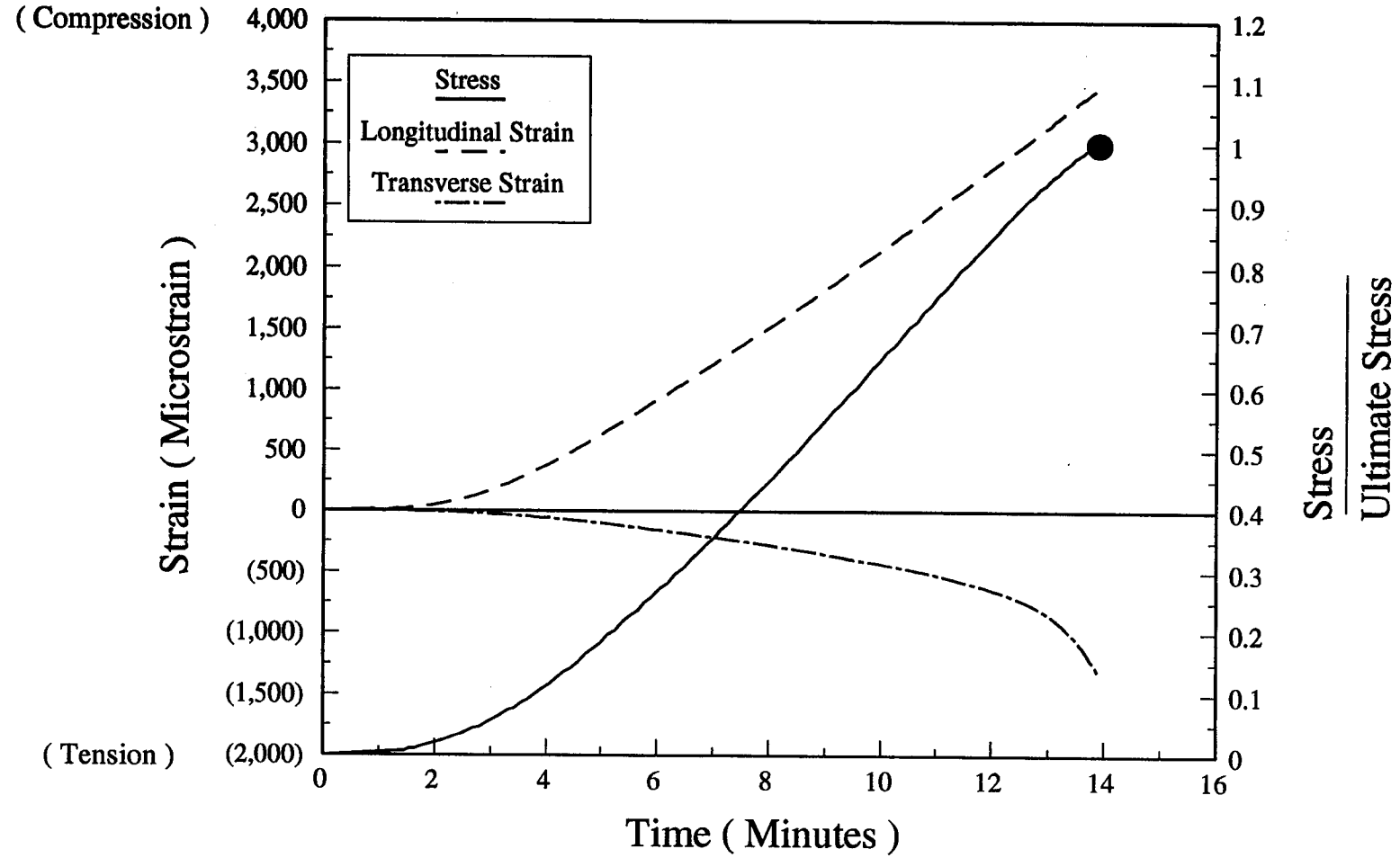

f_c= 103.5 MPa A = 8532 mm^2

Figure G-F-4.5.A - Stress-Strain-Time Relationship - LUC100A Specimen

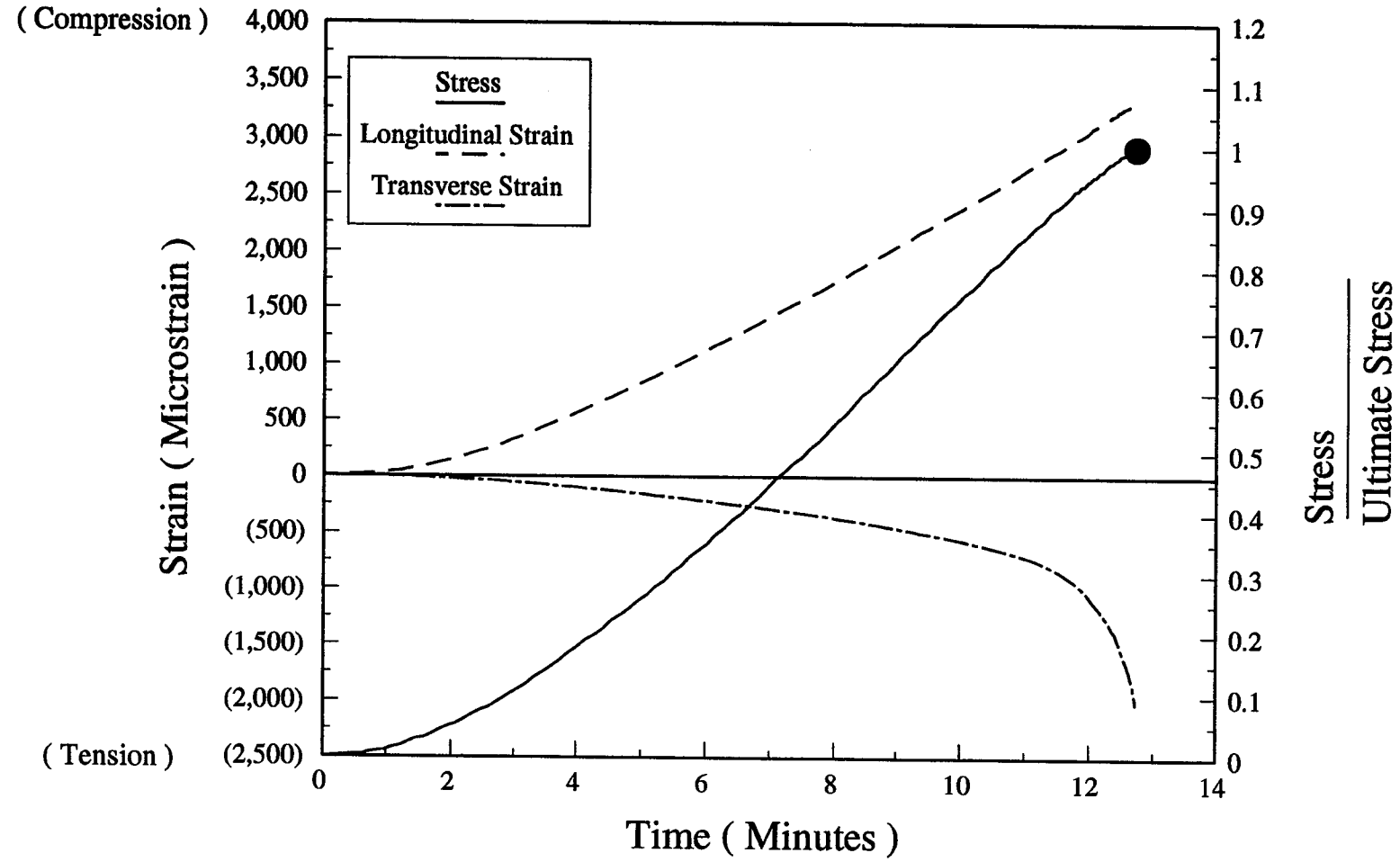

$f_c = 102.4$ MPa $\qquad A = 8321\ mm^2$

Figure G-F-4.5.B - Stress-Strain-Time Relationship - LUC100B Specimen

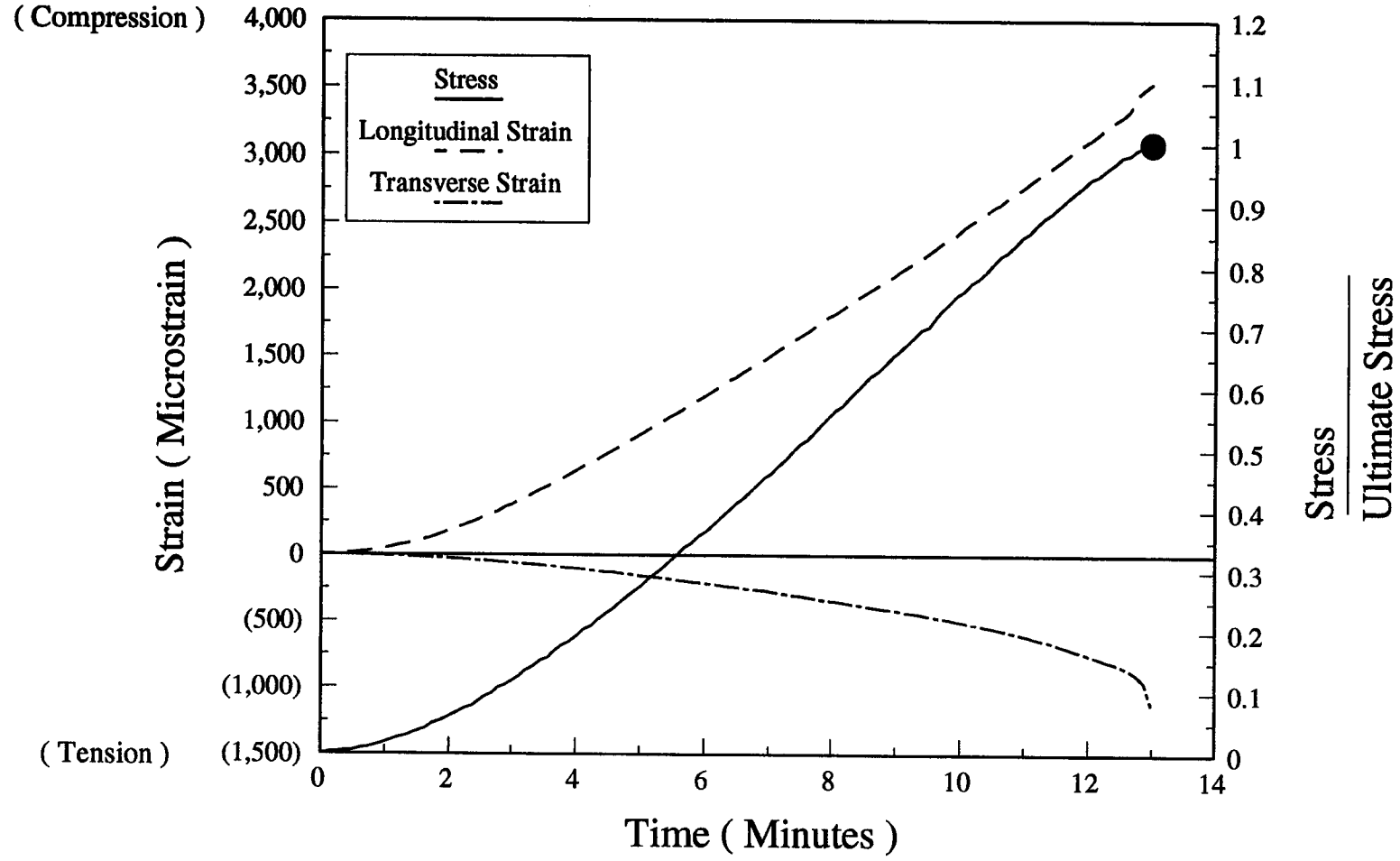

$f_c = 105.1$ MPa $\qquad A = 8180\ mm^2$

Figure G-F-4.5.C - Stress-Strain-Time Relationship - LUC100C Specimen

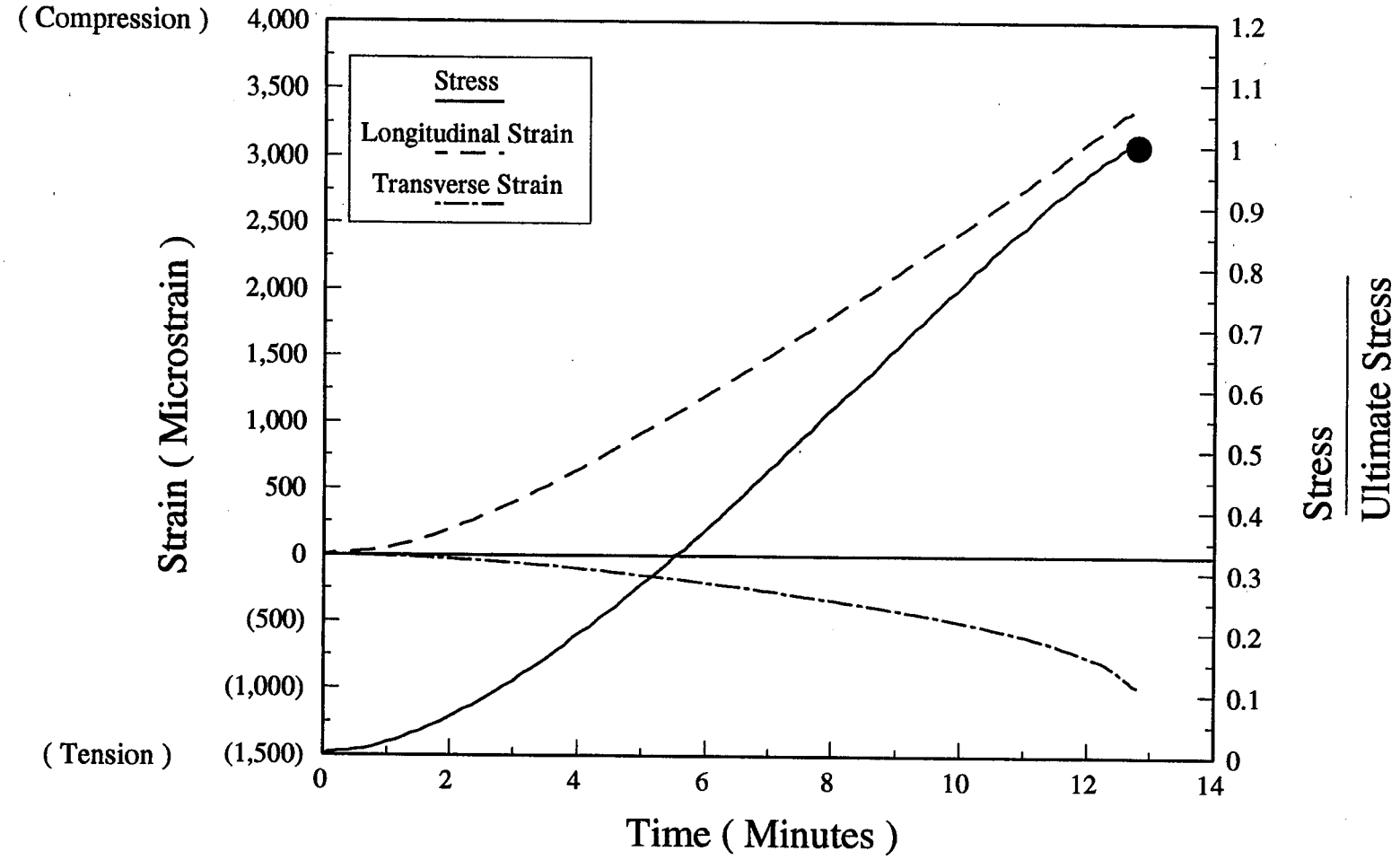

$f_c = 106.2$ MPa $\qquad A = 8123\ mm^2$

Figure G-F-4.5.D - Stress-Strain-Time Relationship - LUC100D Specimen

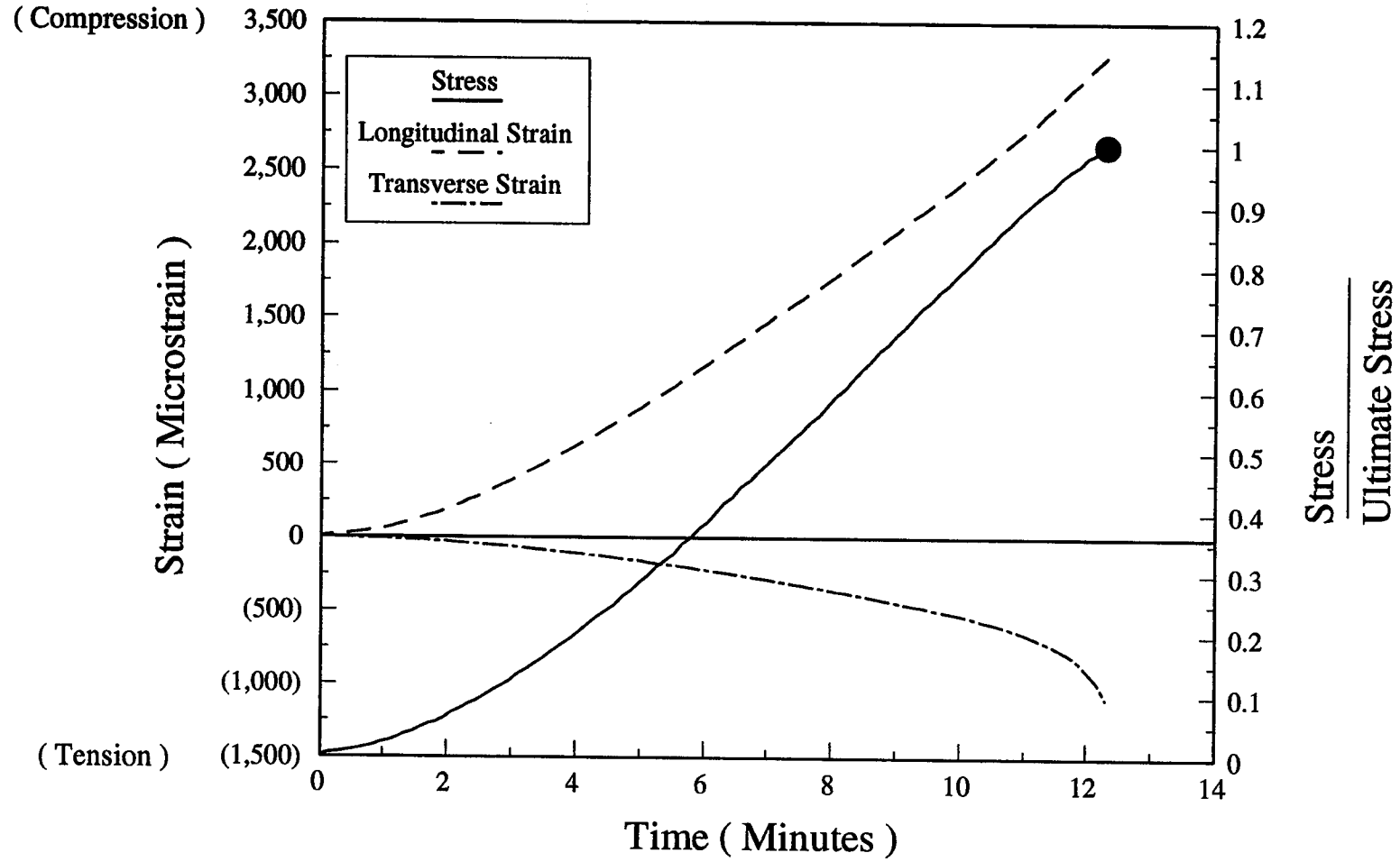

$f_c = 106.5$ MPa $\qquad A = 7710\ mm^2$

Figure G-F-4.5.E - Stress-Strain-Time Relationship - LUC100E Specimen

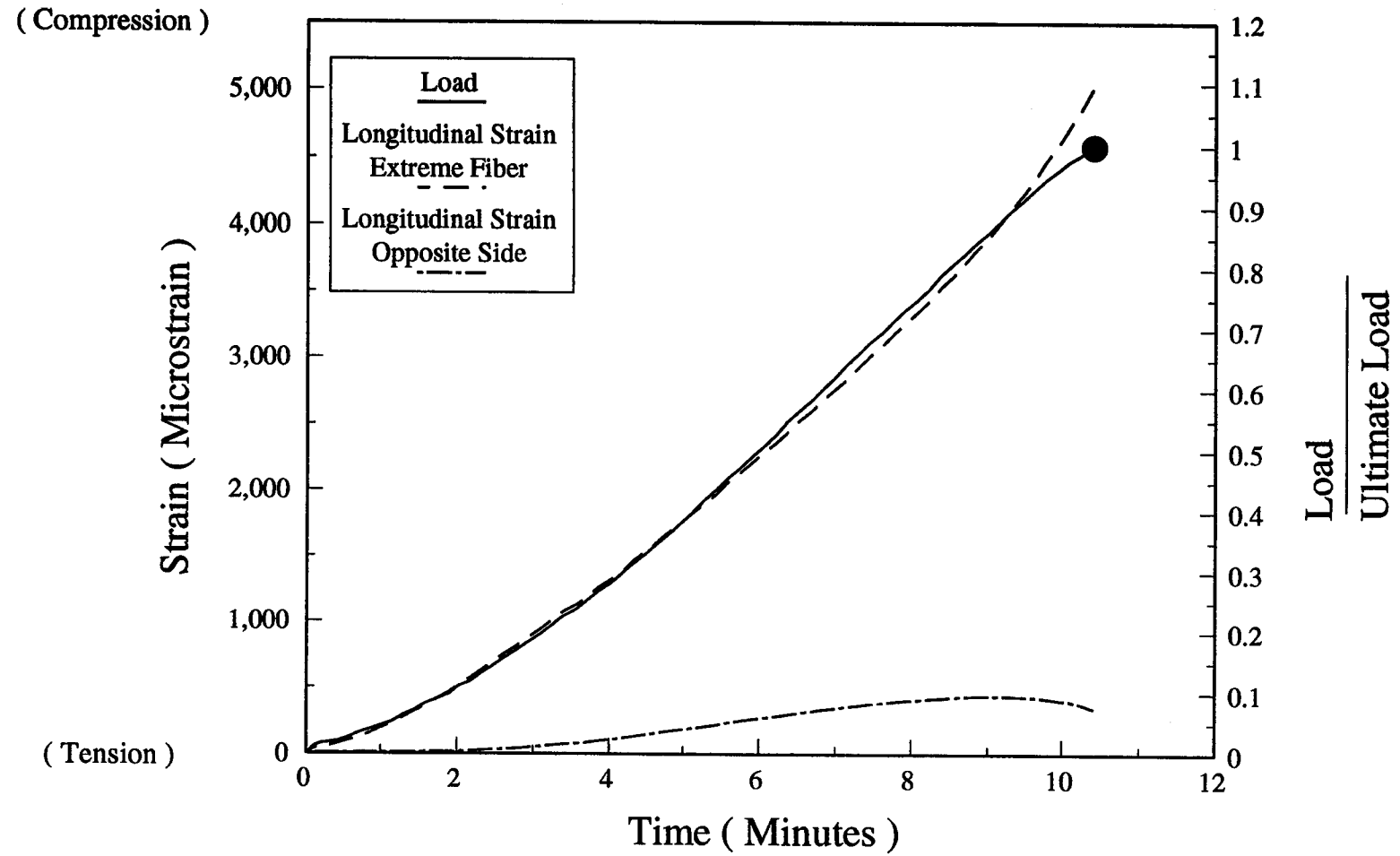

$P_c = 645.0$ kN $\qquad A = 8352$ mm^2

Figure G-F-4.6.A - Load-Strain-Time Relationship - LUE100A Specimen

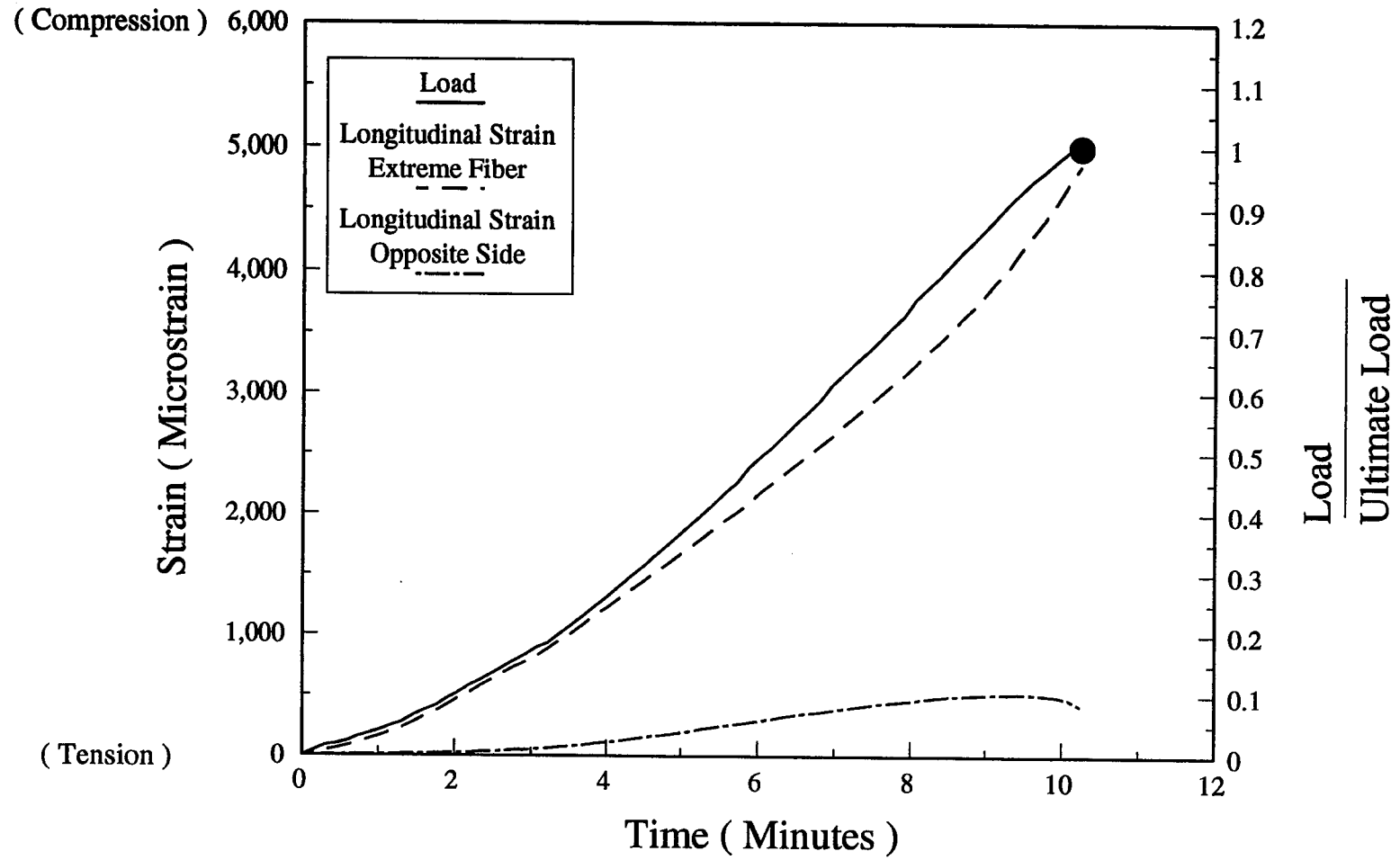

$P_c = 578.0$ kN $\qquad A = 7768$ mm^2

Figure G-F-4.6.B - Load-Strain-Time Relationship - LUE100B Specimen

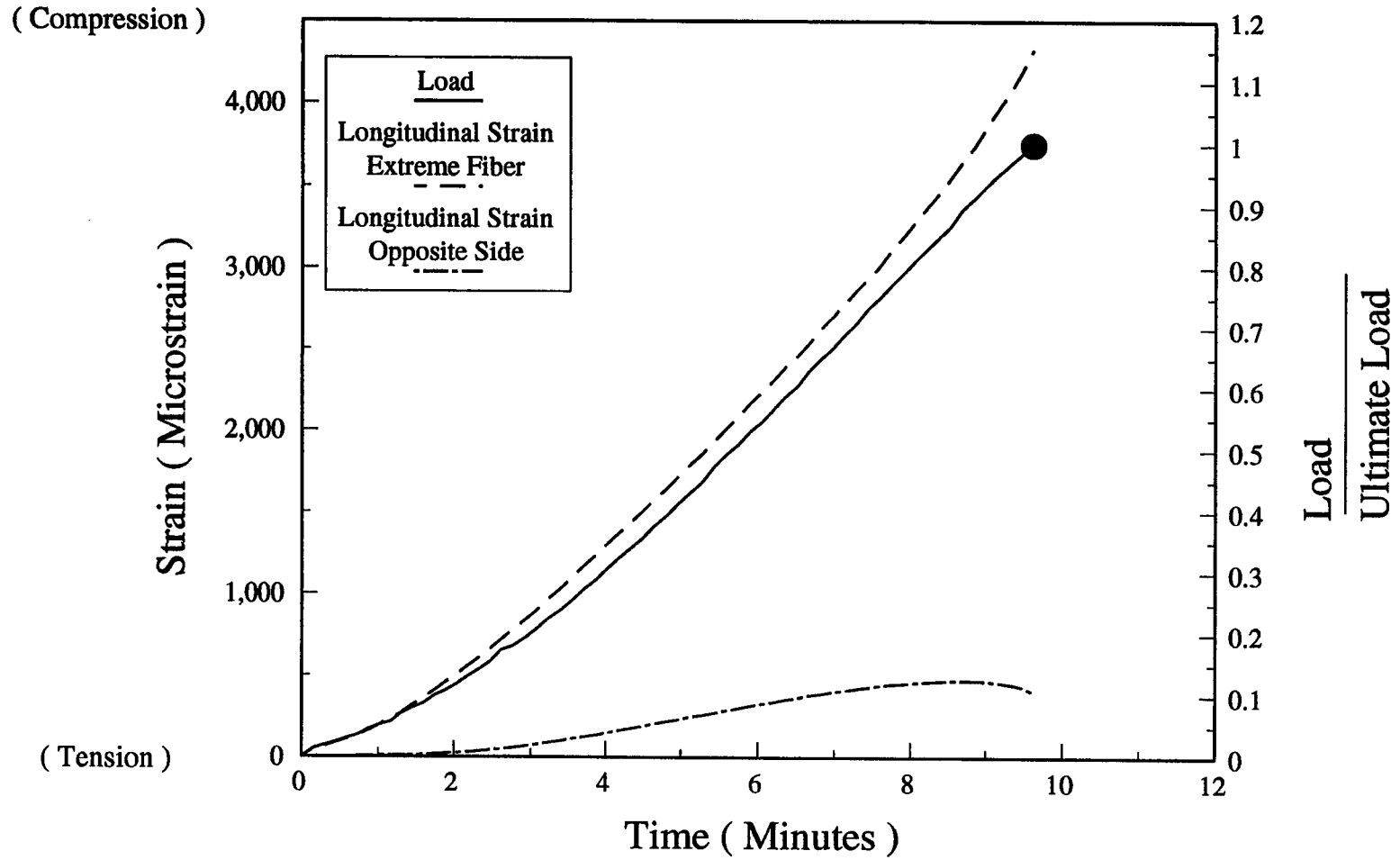

$P_c = 577.0$ kN $\qquad A = 7924$ mm ^{2}

Figure G-F-4.6.C - Load-Strain-Time Relationship - LUE100C Specimen

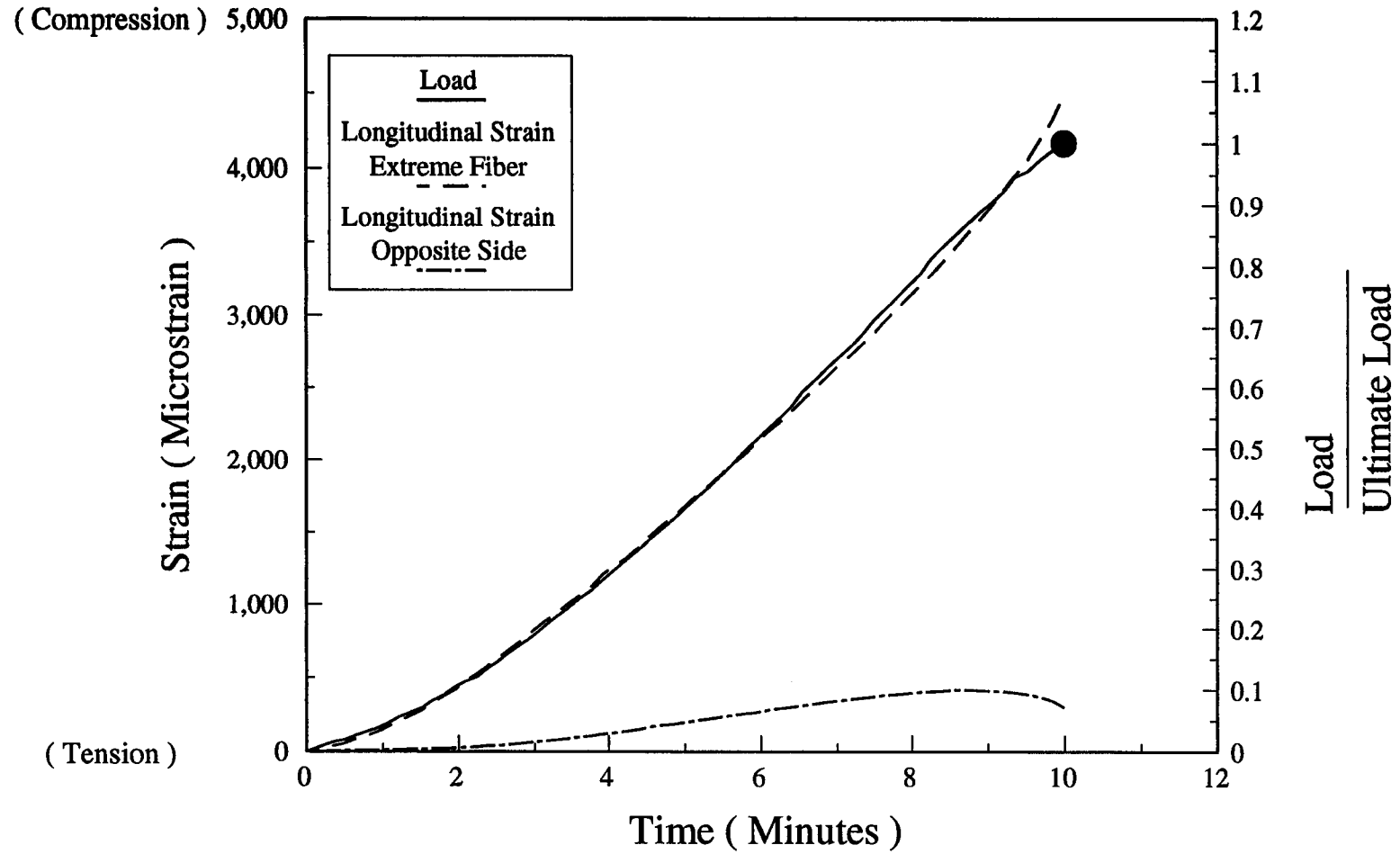

$P_c = 608.0$ kN $\qquad A = 8007$ mm^2

Figure G-F-4.6.D - Load-Strain-Time Relationship - LUE100D Specimen

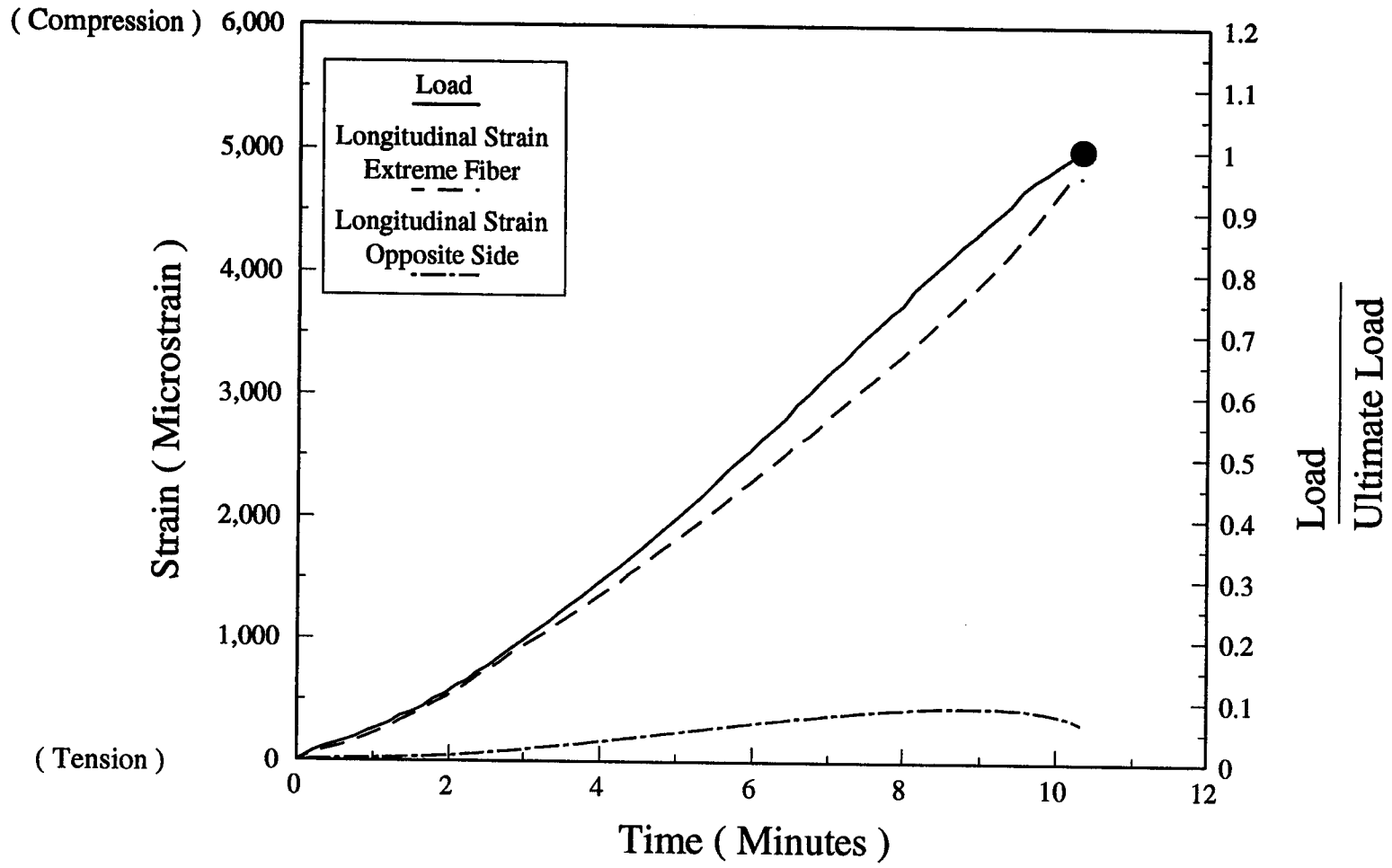

$P_c = 618.0$ kN $\qquad A = 8240$ mm^2

Figure G-F-4.6.E - Load-Strain-Time Relationship - LUE100E Specimen

Appendix H- Strain Study of High Performance Concrete

H-1 Introduction

It is known that the maximum compressive stress that concrete can resist under sustained compressive loading is less than that under short-term, monotonically-increasing loading. Numerous studies have been done to investigate the sustained compressive strength of conventional concrete. A major group of these studies were part of investigations of characteristics of the short term monotonic compressive strength. In these investigations, the sustained compressive strength has been predicted based on study of the strain characteristics, internal changes that happen within the concrete microstructure, stress - strain curve characteristics, log stress - log strain curve characteristics, and ultrasonic velocity tests on the specimen. The study of strain characteristics may include volumetric strain, critical strain level, and critical Poisson's ratio value.

Most of these studies have recognized the presence of a critical stress level above which the concrete begins to deteriorate severely. They indicated that failure will eventually take place if the concrete is subjected to sustained compressive stresses in excess of the critical stress intensity. This stress level has been considered to correspond to the long term sustained compressive strength of concrete.

The behavior of high performance concrete under high sustained compressive stresses is discussed in Chapter 4 and Appendix F. The sustained compressive strength of high performance concrete is established based on long term sustained compressive stress experience on specimens. In these tests, the long term sustained compressive strength of high performance concrete is 70% to 75%, 75% to 80%, 85% to 90%, and 85% to 90% of the short term ultimate compressive strength for 65 MPa to 75 MPa, 95 MPa to 105 MPa (without silica fume), 95 MPa to 105 MPa (with silica fume), and 120 MPa concretes, respectively.

The sustained compressive strength of conventional concrete has been established to be 70 to 75 percent of the short term monotonic ultimate compressive strength based on tests under long term sustained compressive stress[46, 48, 50] while investigations on short term monotonic compressive strength tests give values of the critical stress between 65 to 90 percent of the short term monotonic ultimate compressive strength. As can be seen, the

lower bound of the critical stress observed in short term investigations and the sustained compressive strengths measured in the long term tests show an approximate correlation. In other words, there is an approximate correlation between the critical stress defined based on short term tests and that defined using long term tests.

Short term stress - strain curve characteristics, volumetric strains, and Poisson's ratio changes in the short term monotonic compressive strength tests are presented, explained, and discussed in this Appendix. A Literature review of previous studies on conventional concrete is presented. General conclusions are presented at the end of this appendix based on results of the current study.

H-2 Literature Review

Many investigators have observed changes in some mechanical properties of concrete as load increased monotonically to failure.

Anton Brandtzaeg[41] was the first researcher to notice the phenomenon of the critical compressive stress through volumetric strain studies in 1928. According to those studies, the critical compressive stress was found to be 77 to 85 percent of the ultimate compressive stress based on volumetric strain study. At this stress level the volumetric strain began to increase indicating internal microcracking.

Volumetric strain characteristics, Poisson's ratio, and microcracking of rock, paste, and conventional concrete specimens were studied by Shah et al[55]. The initiation stress was defined as the stress level at which the Poisson's ratio of concrete and mortar specimens started to continuously and significantly increase. The critical stress was defined as the stress level at which the volume of the concrete started to increase rather than continuing to decrease. The following behavior was observed for rock specimens:

1. In a compressive test, the volume of the specimen continues to decrease except at the very end of the test when a slight expansion occurs.

2. There is a slight and continuous increase in the values of Poisson's ratio.

The following conclusions were drawn by Shah et al[55] regarding the mechanical behavior of hardened paste specimens:

1. The volume of the paste specimens continues to decrease throughout a compressive test. The rate of consolidation increases with an increased load.

2. Although variations in Poisson's ratio occurred as a function of the water - cement ratios, in general, Poisson's ratio does not increase continuously with increasing load.

3. The stress - strain curves for paste in uniaxial compression are nonlinear. This nonlinearity appears to increase with an increased amount of water.

The following conclusions were observed for concrete specimens with coarse aggregate to cement ratio varying from 0 (paste) to 5:

1. Poisson's ratio continuously increases above a certain stress. This stress is termed the initiation stress.

2. When the amount of gravel is greater, the relative magnitude of the initiation stress is lower and the final value of Poisson's ratio is higher.

3. Above the critical stress, the volume starts to increase rather than continuing to decrease.

4. Generally, when the amount of gravel is greater, the relative magnitude of the critical stress is lower and the subsequent expansion is more pronounced.

According to their study, the initiation and critical stress were found to be 45 to 75 percent and 84 to 98 percent, respectively of the ultimate short term monotonic compressive strength for conventional concrete.

Based on a study by K. M. Alexander et al[62], Smadi et al[52] reported that the level of the initiation stress (referred to as the discontinuity stress by the original author) is closely associated with bond failure and depending on the type of rock, it might occur at some stage between approximately 45 and 80 percent of the ultimate short term monotonic compressive strength.

A volumetric strain study by Beres[56] indicated that the critical stress varies between 62 and 77 percent of the ultimate short term monotonic compressive strength regardless of the grade of concrete.

Dhir et al[57] defined the critical stress as the stress intensity at which the Poisson's ratio becomes equal to 0.50 (Volumetric strain equals to zero.) instead of the stress intensity at which the rate of change of volumetric strain becomes equal to zero. The critical stress defined in this way varied from 76 to 88 percent of the ultimate short term monotonic compressive strength.

Based on a study by Berntsson et al[58], the critical stress was found to be from 73 to 94 percent of the ultimate short term monotonic compressive strength. Poisson's ratio became equal to 0.50 at stress intensities equal to 85 to 98 percent of the ultimate short term monotonic compressive strength.

Newman et al[59] reported that K. Newman, in trying to establish a definition for the failure of concrete, originally coined the term "discontinuity" for the behavior of brittle materials when fast crack propagation had begun. The discontinuity point was related to the load (or stress) stage at which more severe cracking begins, and at which concrete can no longer withstand the applied load without disruption. At the same time, the stress and strain at discontinuity were defined in terms of the stage at which there is a deviation of the volumetric strain from linearity.

Newman et al[59] defined the discontinuity level as the stress below which concrete can be considered to act in a quasi - elastic manner and suffer no significant deterioration for any given environmental condition, irrespective of the type and pattern of loading. They also mentioned that the stress level at discontinuity, compared with the ultimate strength under short term loading, will depend upon such factors as the structure of concrete, the applied state of stress of strain and the strain rate and pattern of loading. They reported from other studies that the discontinuity point was found to be a higher percentage of ultimate strength for mixes containing rough textured aggregates bonded by a strong paste matrix. They also reported from other studies that as the volume fraction and maximum size of the aggregate is increased, the corresponding increase in local strain concentrations causes a considerable decrease in the average tensile strain at discontinuity.

Desayi et al[60] used log stress - log strain plots of the short term monotonic compressive tests of concrete specimens, tested with constant rate of load increment, to predict the long term sustained compressive strength of conventional concrete. They observed that the plot consisted of three straight lines showing two clear kinks, the first one at about 15 to 25 percent of the ultimate and the second at about 70 to 90 percent of the ultimate compressive stress. They have proposed that the stress intensity corresponding to the second change of slope of the log stress - log strain plot be taken as the true ultimate strength, or in other words, the long term sustained compressive strength of conventional concrete. Based on their approach, the long term sustained compressive strength of conventional concrete was predicted to be 70 to 89 percent of the ultimate short term monotonic compressive strength.

Based on a volumetric strain study and the above mentioned log stress - log strain approach, Desayi et al[61] predicted that the long term sustained compressive strength of conventional concrete should be 77 to 85 percent of the ultimate short term monotonic compressive strength of conventional concrete.

As mentioned in section 2.2.4 and Reference 4, high strength high performance concrete has an unstable and violent uncontrollable failure if the rate of load increase is kept constant. In the study by Desayi et al[60], the magnitude of the second change of slope of log

stress - log strain plot decreased as the compressive strength of concrete increased. As a result, due to unstable failure of specimen and decrease of magnitude of change of slope, the log stress - log strain approach does not appear to be suitable for predicting the long term sustained compressive strength of high strength high performance concretes.

Based on a microcracking study by Carrasquillo et al., Smadi et al[52] predicted the critical stress to be 76 to 90, 84 to 96, and 96 to 100 percent of the ultimate short term monotonic compressive strength for 30 MPa, 55 MPa, and 75 MPa crushed limestone concretes, respectively. For 30 MPa, 50 MPa, and 70 MPa gravel concretes, the critical stress was predicted to be 76 to 91, 83 to 95, and 94 to 100 percent of the ultimate short term monotonic compressive strength, respectively. It should be mentioned that Carrasquillo et al. defined the critical stress as the stage at which progressive crack growth (formation of large cracks) begins.

These short term studies estimated the long term sustained compressive strength of conventional concrete with a considerable fluctuation.

H-3 Stress - Strain Behavior of High Performance Concrete

H-3.1 Test Results

The stress - strain curves of the specimens tested monotonically under uniaxial compression are presented in Figure F-4.4.A for LH, UH, UU, and LU series. The strain results are based on data from electrical resistance strain gages. Due to the behavior of the ball seat bearing blocks and the nature of electrical resistance strain gages, data about the descending branches are not available. The relation between stress, as a percentage of the ultimate stress, and strain are presented in Figures 4.4.B through D and Figure F-4.4.B for LH, UH, UU, and LU series, respectively.

H-3.2 Discussion of Results

It is clear that the ascending branches of the stress - strain curves have a steeper slope and are more nearly linear over a greater range as the compressive strength of concrete increases. As can be seen from Figures 4.4.B through 4.4.D and Figure F-4.4.B, the stress - strain curves deviated from straight line at about 65 to 70, 75 to 80, above 85, and above 85 percent of the ultimate stress for LH, UH, UU, and LU series respectively. These can be considered as the approximate start of unstable self propagating crack development in the system.

As observed in this study, the sustained compressive strength of LH, UH, UU, and LU series were 70 to 75, 75 to 80, 85 to 90, and 85 to 90 percent of the ultimate short term monotonic compressive strength. It should be mentioned that the specimens tested monotonically and tested under sustained compressive stresses had the same test conditions including curing condition, bearing blocks, end preparation, and specimen size. This suggests that if the specimens have the same test condition as of those under sustained compressive stresses, the deviation of stress - strain curve from straight line in a short term test can be an approximate estimate of the sustained compressive strength of high performance concrete. The stress intensity, at which the first deviation of stress - strain curve happens can also be assumed as the discontinuity point for high performance concrete as defined by Newman et al[59].

H-4 Volumetric Strain Study of High Performance Concrete

H-4.1 Test Results

The experimental results of the specimens tested monotonically and concentrically are presented in Figures H-4.1.A through H, I through M, N through R, and S through W for LH, UH, LU, and UU series, respectively. Each specimen is represented by an abbreviation such as LHC75(70). The first two characters represent the concrete series to which the specimen belongs (See Section 2.4). The third character stands for concentric, C, and eccentric, E, specimens. The first number represents the stress intensity on the specimen as a percent of the short time strength at the time of loading. The possible next character (A through E) distinguishes the specimens with the same intensity. If the specimen is tested at the age of 70 days instead of 56 days, the age appears in parentheses.

The stress is shown as the ratio of the ultimate strength of the specimen. The relationships between normalized stress and longitudinal, transverse, and volumetric strains are shown. The strain results are based on data from electrical resistance strain gages.

The volumetric strain is calculated based on the small strain theory. Based on small strain theory, volumetric strain is equal to the longitudinal strain plus twice the transverse strain (assuming a positive sign for compressive strain and a negative sign for tensile strain).

H-4.2 Discussion of Results

The relations between normalized stress, as the percentage of the ultimate, and volumetric strain are summarized in Figures H-4.2.A through D for series LH, UH, LU, and UU, respectively.

The critical stress, as the percentage of the ultimate short term monotonic compressive strength, is presented in Tables H-4.2.A through D for LH, UH, LU, and UU series, respectively. The critical stress is defined as the stress level at which the volumetric strain begins to increase instead of decreasing. The critical stress is assumed to be 100 percent if the volumetric strain continues to increase up to failure.

The average critical stress is 94, 98, 93, and 100 percent for LH, UH, LU, and UU series, respectively. The overall average critical stress is above 95 percent of the ultimate. As it was discussed in Chapter 4 and Appendix F, the sustained compressive strength of high performance concrete is 70% to 75%, 75% to 80%, 85% to 90%, and 85% to 90% of the ultimate for LH, UH, LU, and UU series, respectively. As can be seen, defining the discontinuity or critical stress based on zero rate of change of slope of the volumetric strain - stress curves does not predict the long term sustained compressive strength of these high performance concretes.

As Shah et al[55] observed, under monotonic compressive stress, the volume of rock specimens continues to decrease except at the very end when a slight expansion occurs. High performance concretes studied in this experimental work showed behavior very similar to rock specimens. This may be due to very strong paste which is sometimes even stronger than the rock that is the origin of the coarse aggregate. Due to presence of the strong rich paste, the high strength, high performance concrete does not show its composite nonhomogeneous characteristics in a short term volumetric strain study.

Based on the current volumetric strain study and the study by Shah et al[55], it can be concluded that the short term behavior of high strength high performance concrete under compressive stresses should be similar to rock behavior; while its long term behavior under compressive stresses is similar to conventional concrete. It should be also mentioned that the long term sustained compressive strength of silica fume ultra high strength high performance concrete is higher than the values for conventional concrete (See Chapter 4 and Appendix F).

H-5 Poisson's Ratio Study of High Performance Concrete

H-5.1 Test Results

The experimental results of the specimens tested monotonically and concentrically are presented in Figures H-5.1.A through D for LH, UH, LU, and UU series, respectively. Each specimen is represented by an abbreviation as explained in section H-4.1.

The stress is shown as the ratio of the ultimate strength of the specimen. The relation between normalized stress and Poisson's ratio is shown. The strain results are based on data from electrical resistance strain gages. Details of experimental program are presented in Section 2.6.6.

The Poisson's ratio is calculated as the ratio of the transverse strain to the longitudinal strain at each stress level.

H-5.2 Discussion of Results

The Poisson's ratio value of most specimens never did reach 0.50. As a result, the criteria of defining critical stress as the stage at which Poisson's ratio is equal to 0.50, suggested by Dhir et al[57], does not appear to be valid for high performance concrete.

Shah et al[55] defined the initiation stress as the stress level above which the Poisson's ratio continuously and significantly increases. Such a state of stress can be observed for LH series at stresses of 65 to 97 percent of the ultimate. Shah et al[55] observed slight and continuous increase in values of Poisson's ratio of rock specimens. The Poisson's ratio of UH, LU, and UU series increase slightly and continuously like those rock specimens tested by Shah et al[55]. Shah et al[55] observed slight and continuous increase in values of Poisson's ratio of rock specimens.

As the result of current study of Poisson's ratio, it can be concluded that discontinuity, initiation stress, and critical stress, as defined in literature for conventional concrete, are not compatible with the behavior of high performance concrete and cannot to be used for predicting the long term sustained compressive strength of high performance concrete. It can also be concluded that the short term behavior of high performance concrete (especially UH, LU, and UU series) is more similar to short term behavior of rocks than conventional concrete; but as can be concluded from Chapter 4 and Appendix F, the long term behavior of high performance concrete is dominated by its nonhomogeneous composite structure, the kind of rocks in the aggregates (especially the coarse aggregate) and the creep behavior of the paste and is more similar to conventional concrete than to rock.

H-6 Conclusions

Based on the results of the current study, presented in Chapter 4, Appendix F, this appendix, and previous studies mentioned in the literature, the following conclusions can be drawn for strain behavior of high performance concrete and prediction of sustained compressive strength of high performance concrete with short term studies:

1. Due to the unstable and violent uncontrollable failure of high strength high performance concrete specimens after the peak load, the true ultimate strength of high strength high performance concrete cannot be predicted from the log stress - log strain plots of concrete specimens tested concentrically and monotonically with a constant rate of load increase as suggested by Desayi et al[60].

2. The ascending branch of the short - time stress - strain curves have a steeper slope and are more linear over a greater range as the compressive strength of concrete increases.

3. The short - time stress - strain curves deviated from straight lines at about 65 to 70, 75 to 80, above 85, and above 85 percent of the ultimate stress for LH, UH, UU, and LU series, respectively. These can be considered as the approximate start of unstable self propagating crack development in the system.

4. The stress - strain curve of high performance concrete specimens, tested monotonically under compressive stresses with the same test condition as the specimens tested under long term sustained compressive stresses (similar to curing conditions, bearing blocks, end preparation, and specimen sizes), can be used to define the discontinuity point as defined by Newman et al[59].

5. The point of deviation of the stress - strain curves of high performance concrete specimens tested monotonically not only represents the discontinuity point but also represents the critical stress level as it is defined in literature for predicting the long term sustained compressive strength of high performance concrete. As a result, it can be concluded that if the specimens have the same test parameters as of those tested under sustained compressive stresses, the deviation of stress - strain curve from straight line can be an approximate estimate of the long term sustained compressive strength of high performance concrete.

6. The volumetric strain behavior of high strength high performance concrete specimens are more similar to that of rock specimens behavior than to conventional concrete specimens; but their long term behavior under sustained compressive stresses is more similar to conventional concrete. As a result, the volumetric strains in short time tests of high strength high performance concrete cannot be used for predicting its long term sustained compressive strength.

7. The stress - Poisson's ratio relationship of high performance concrete specimens is more similar to rock specimens than to conventional concrete specimens. The variation in the Poisson's ratio of high performance concrete does not give any proper indication of

discontinuity, initiation stress, and critical stress. Poisson's ratio equal to 0.50, as it was suggested by Dhir et al[57], cannot represent the level of critical stress. As the result, a study of Poisson's ratio of high performance concrete cannot predict the long term sustained compressive strength of high performance concrete.

8. As the overall result, the short term behavior of high performance concrete is similar to rock behavior but its long term behavior is more similar to conventional concrete. The effect of composite nonhomogeneous structure of high performance concrete, creep of the paste, and the effect of rock in aggregates, especially coarse aggregates show their dominant effects with time.

Table H-4.2.A - Critical Stress Results (LH Series)

Specimen	Critical Stress (Percent)	Compressive Strength (MPa)
LHC100A	99	65.5
LHC100B	72	64.1
LHC100C	92	65.9
LHC100D	100	65.8
LHC100E	96	66.0
LHC100A(70)	100	66.7
LHC100B(70)	98	66.2
LHC100C(70)	98	65.1

Table H-4.2.B - Critical Stress Results (UH Series)

Specimen	Critical Stress (Percent)	Compressive Strength (MPa)
UHC100A	97	97.5
UHC100B	100	90.7
UHC100C	99	95.9
UHC100D	94	97.9
UHC100E	100	94.2

Table H-4.2.C - Critical Stress Results (LU Series)

Specimen	Critical Stress (Percent)	Compressive Strength (MPa)
LUC100A	89	103.5
LUC100B	87	102.4
LUC100C	98	105.1
LUC100D	96	106.2
LUC100E	93	106.5

Table H-4.2.D - Critical Stress Results (UU Series)

Specimen	Critical Stress (Percent)	Compressive Strength (MPa)
UUC100A	100	115.5
UUC100B	100	125.0
UUC100C	100	121.6
UUC100D	100	119.7
UUC100E	100	120.6

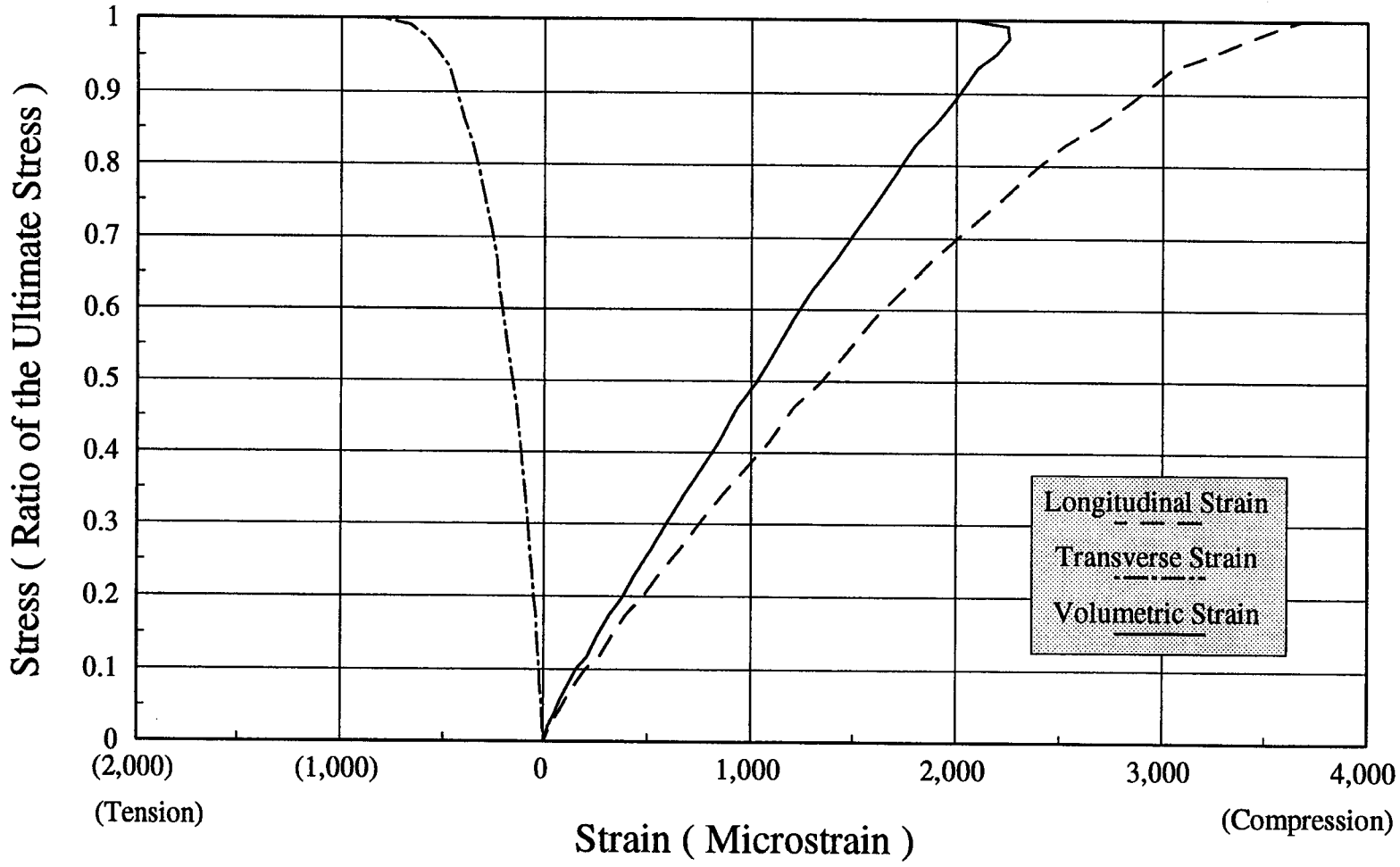

Figure H-4.1.A - Stress - Strain Relationships - LHC100A Specimen

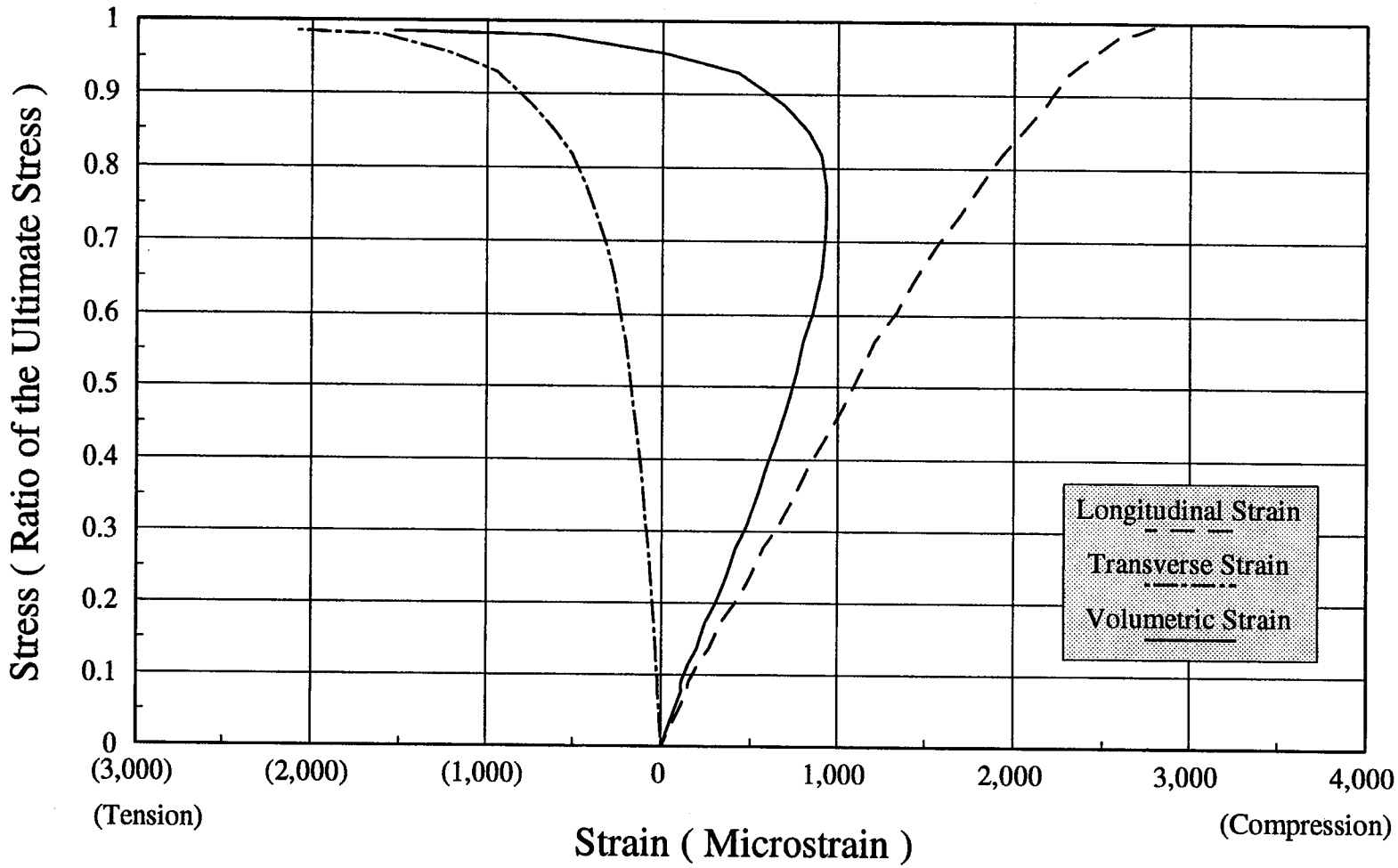

Figure H-4.1.B - Stress - Strain Relationships - LHC100B Specimen

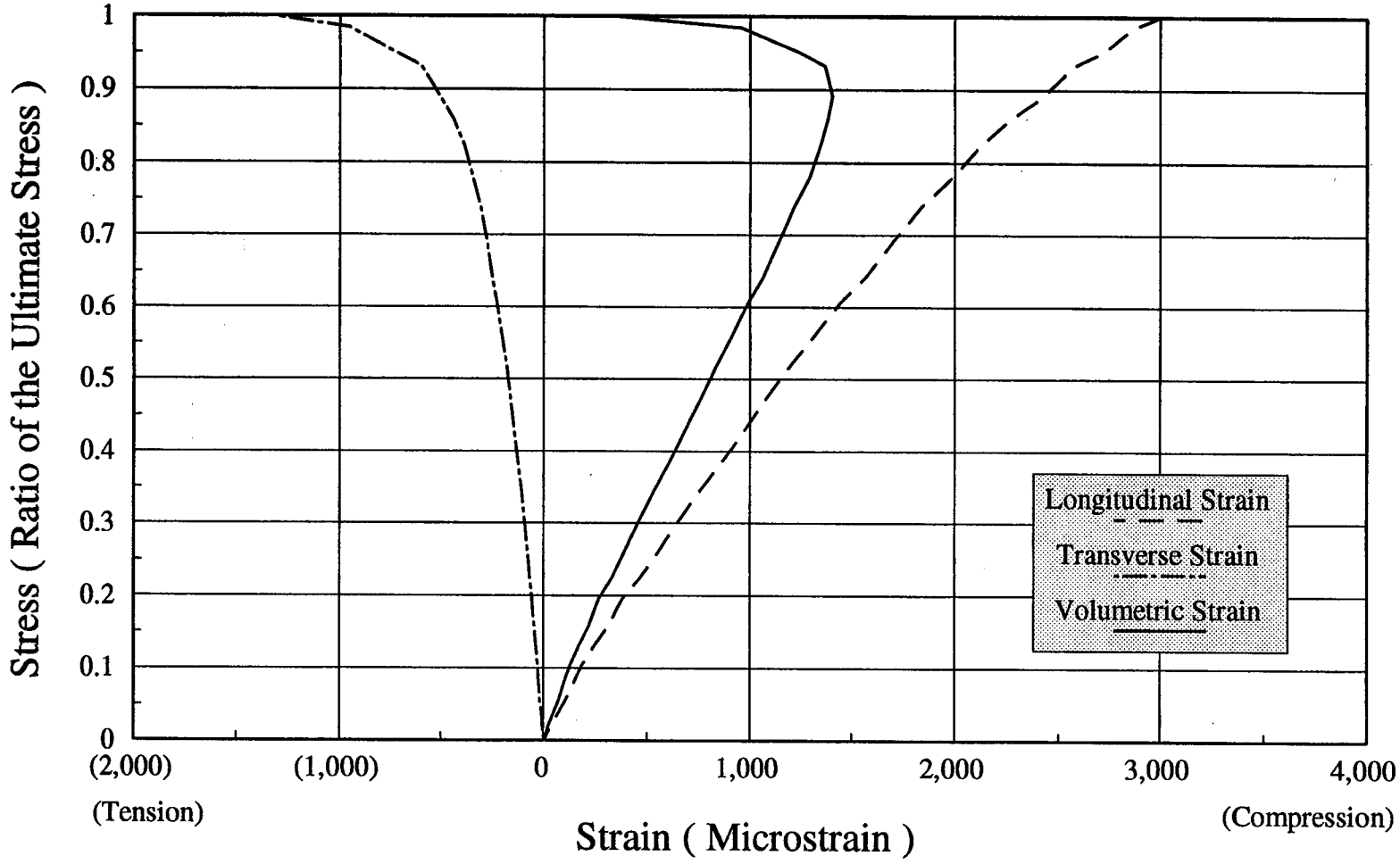

Figure H-4.1.C - Stress - Strain Relationships - LHC100C Specimen

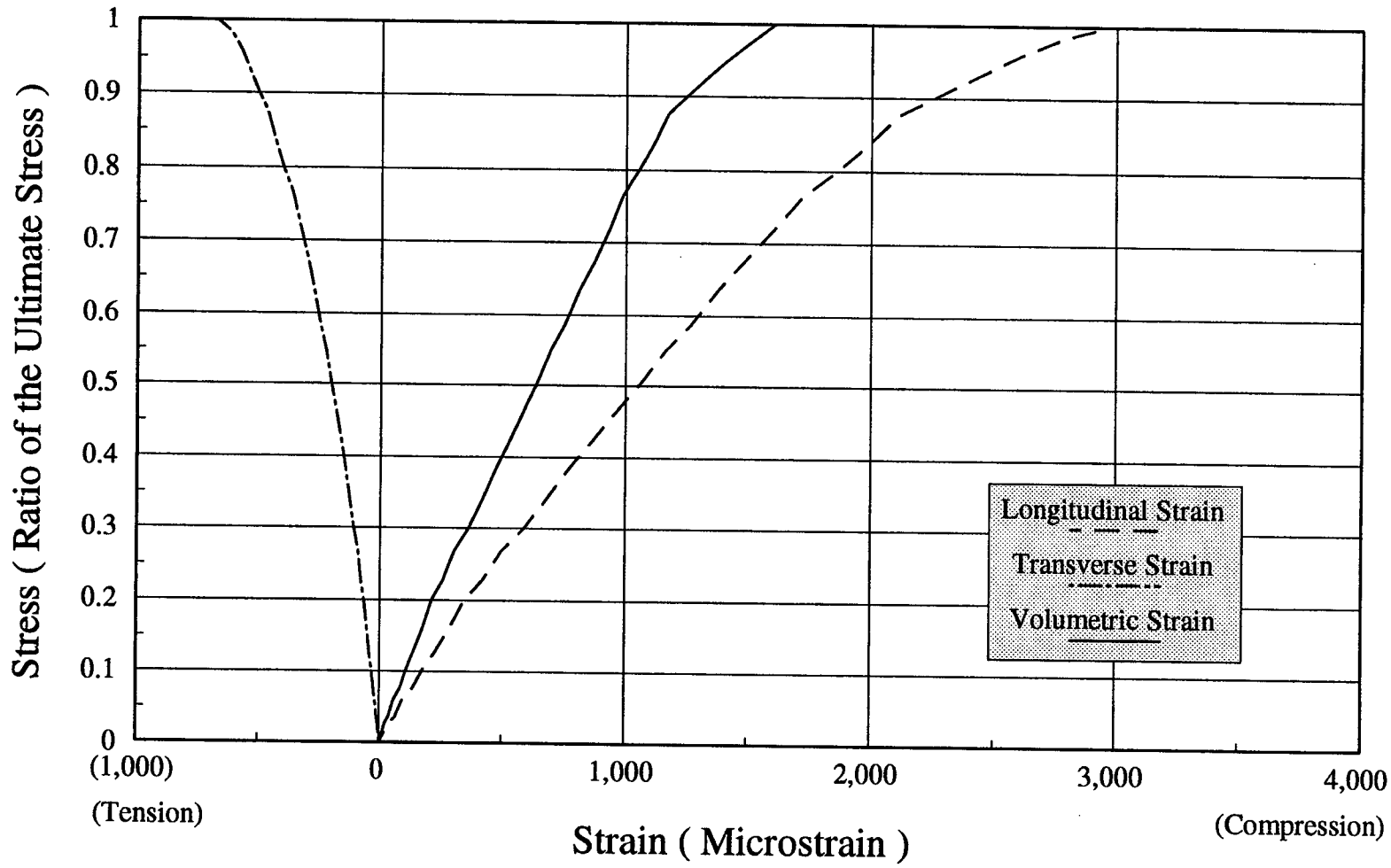

Figure H-4.1.D - Stress - Strain Relationships - LHC100D Specimen

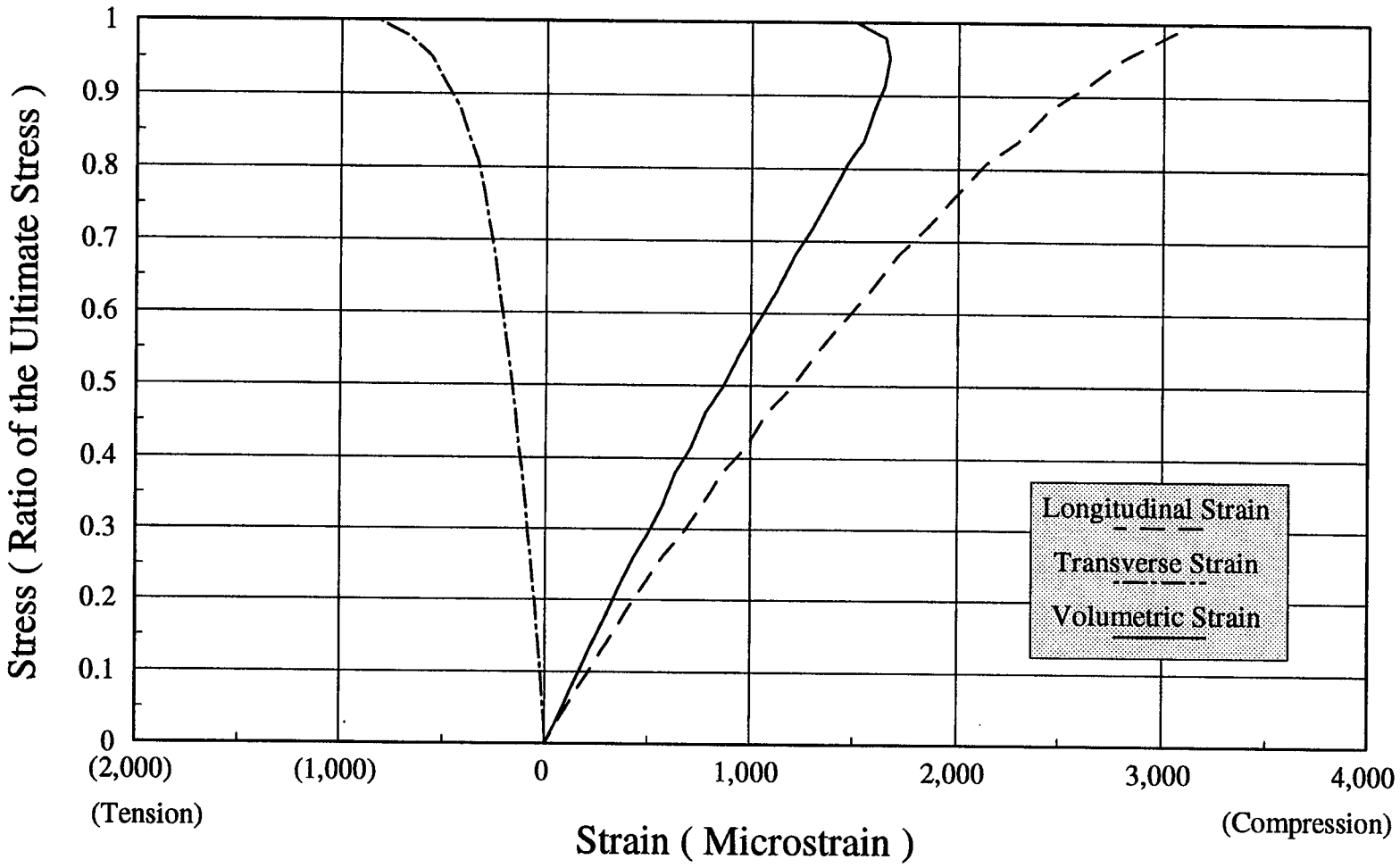

Figure H-4.1.E - Stress - Strain Relationships - LHC100E Specimen

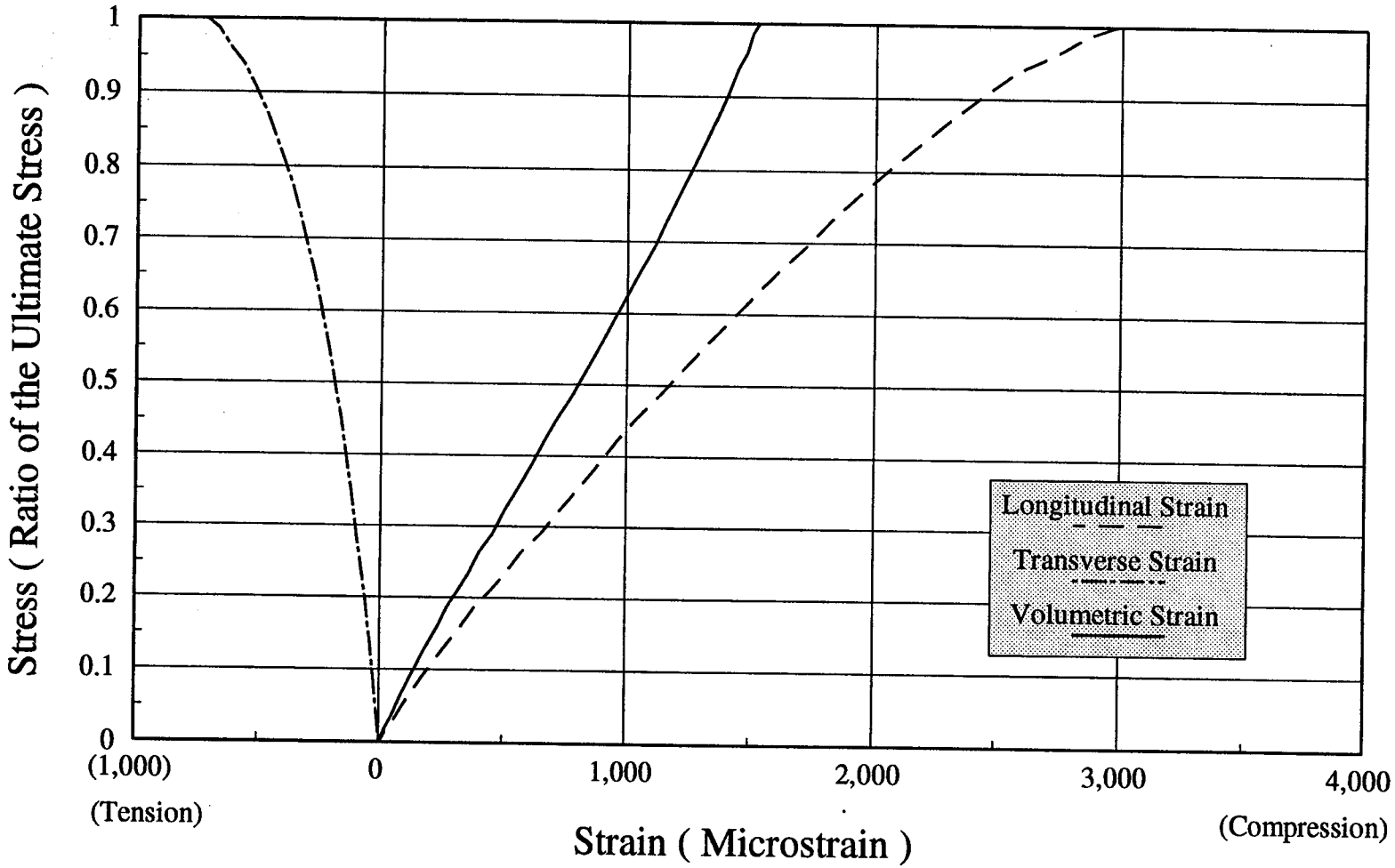

Figure H-4.1.F - Stress - Strain Relationships - LHC100A(70) Specimen

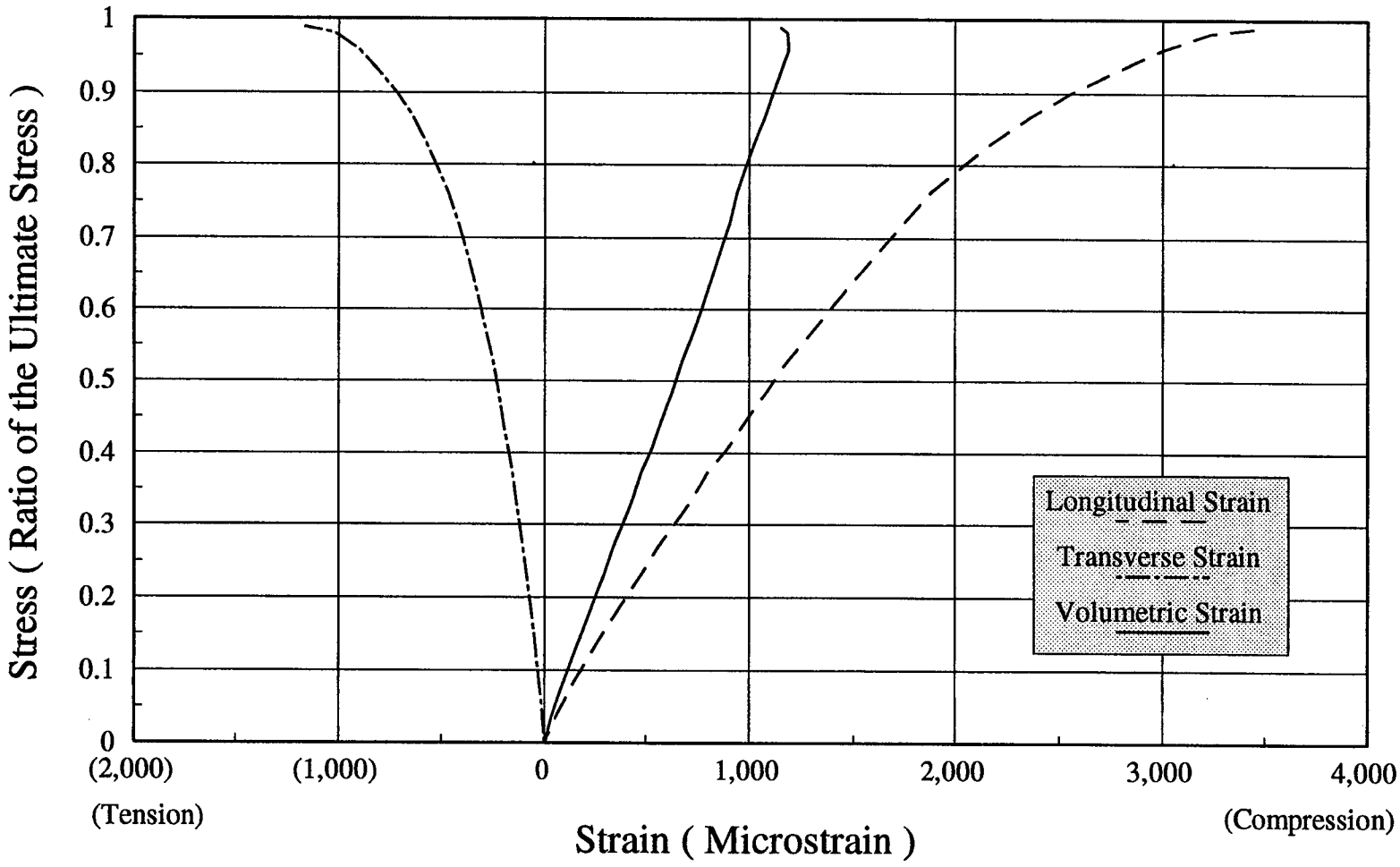

Figure H-4.1.G - Stress - Strain Relationships - LHC100B(70) Specimen

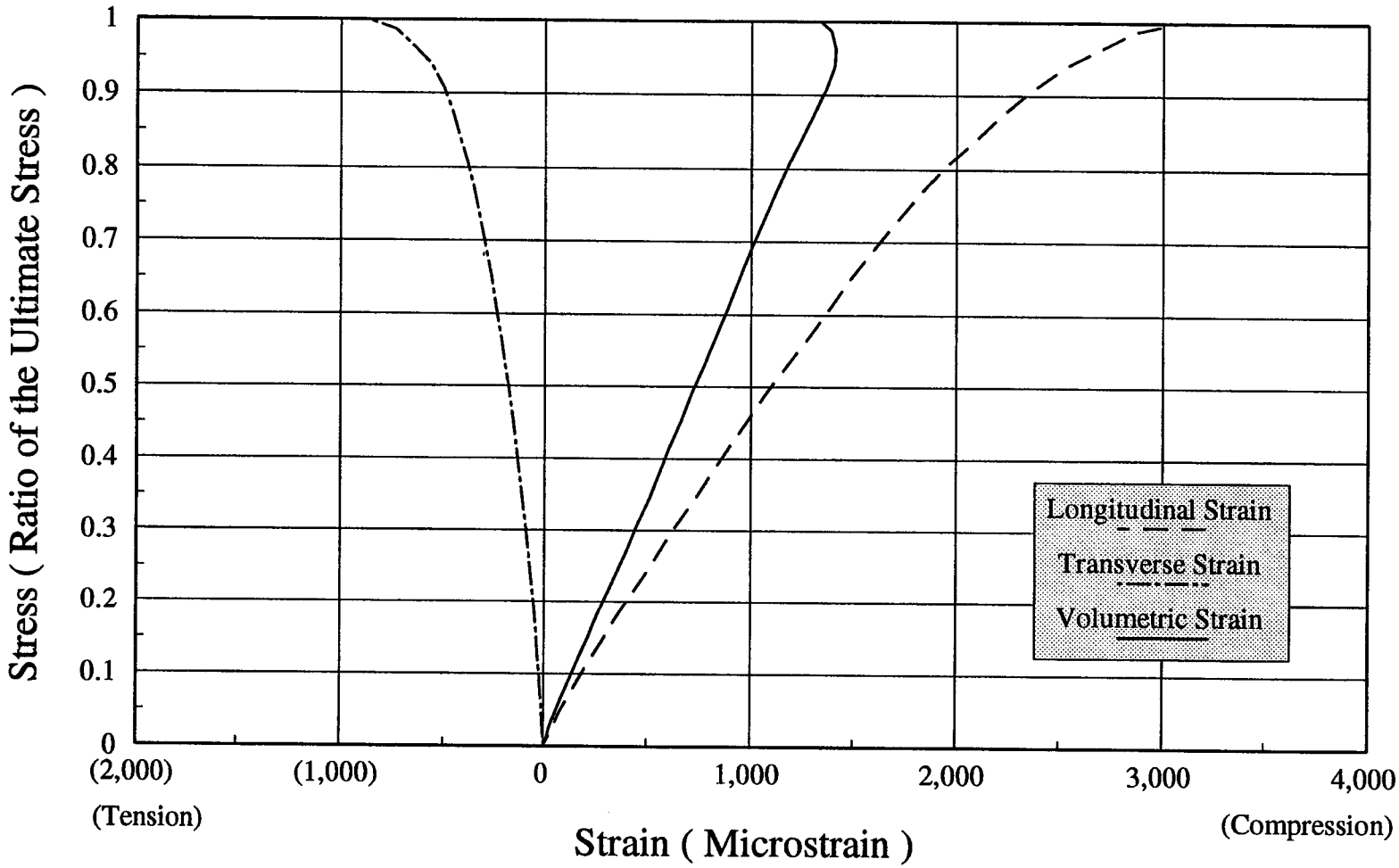

Figure H-4.1.H - Stress - Strain Relationships - LHC100C(70) Specimen

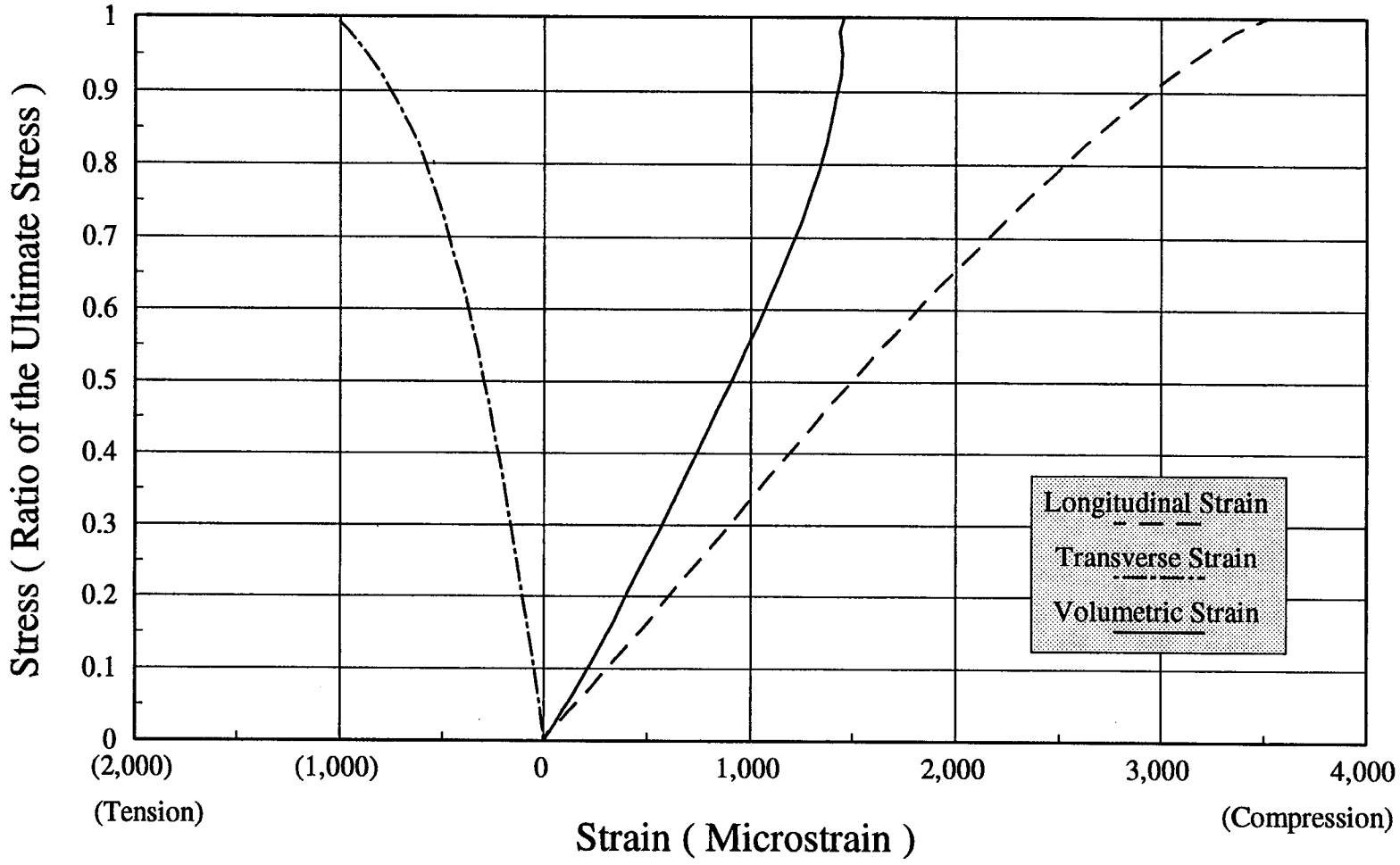

Figure H-4.1.I - Stress - Strain Relationships - UHC100A Specimen

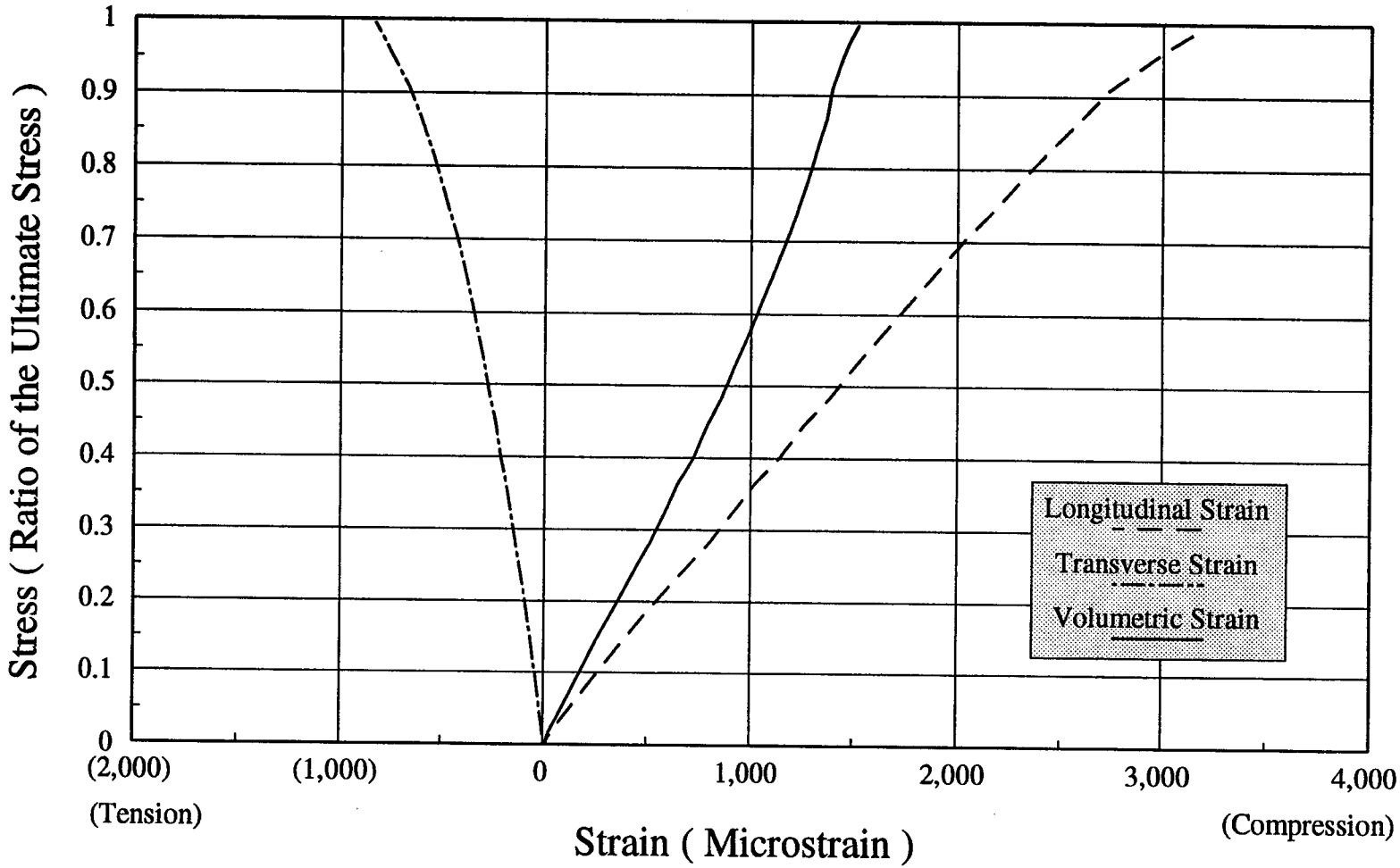

Figure H-4.1.J - Stress - Strain Relationships - UHC100B Specimen

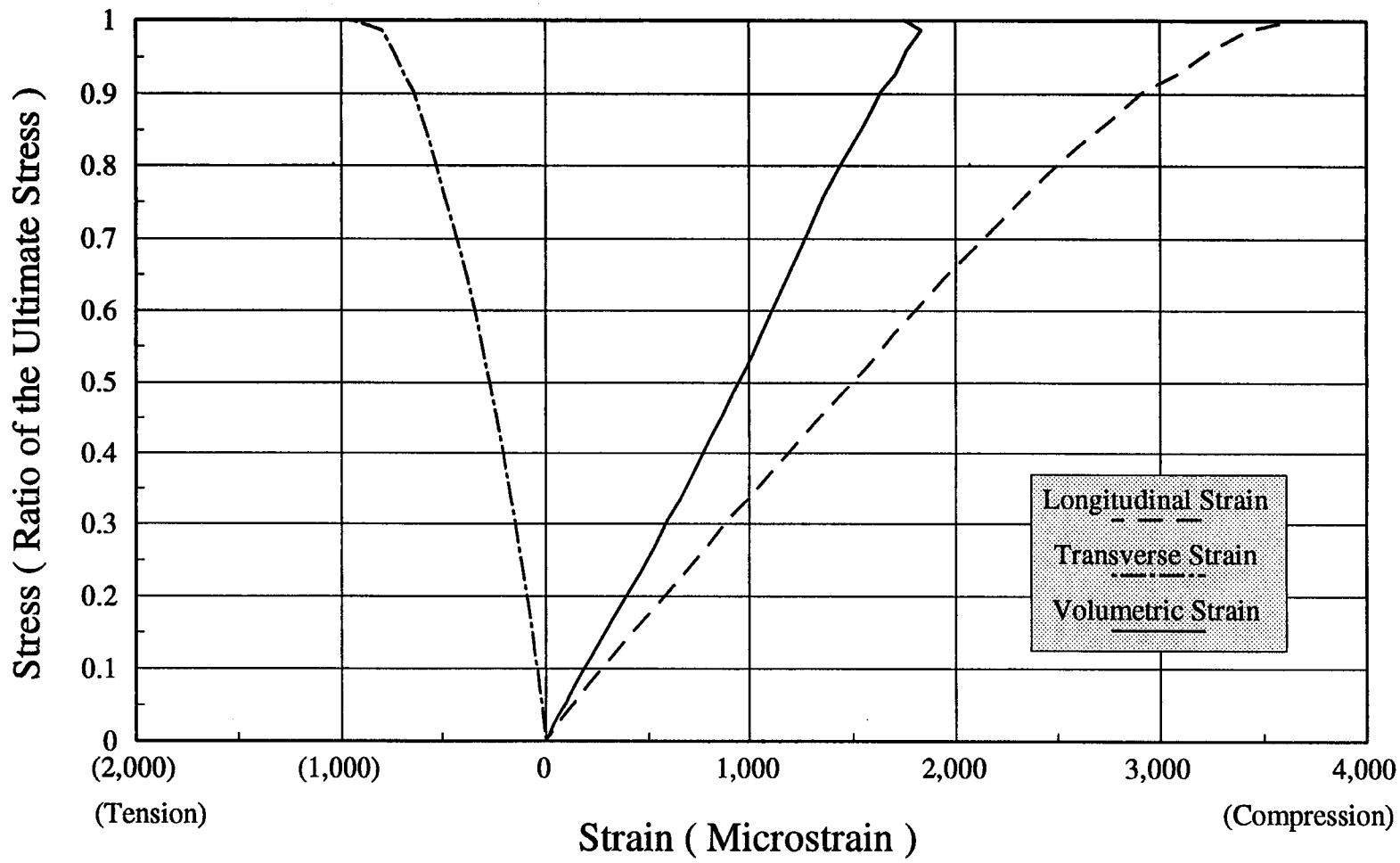

Figure H-4.1.K - Stress - Strain Relationships - UHC100C Specimen

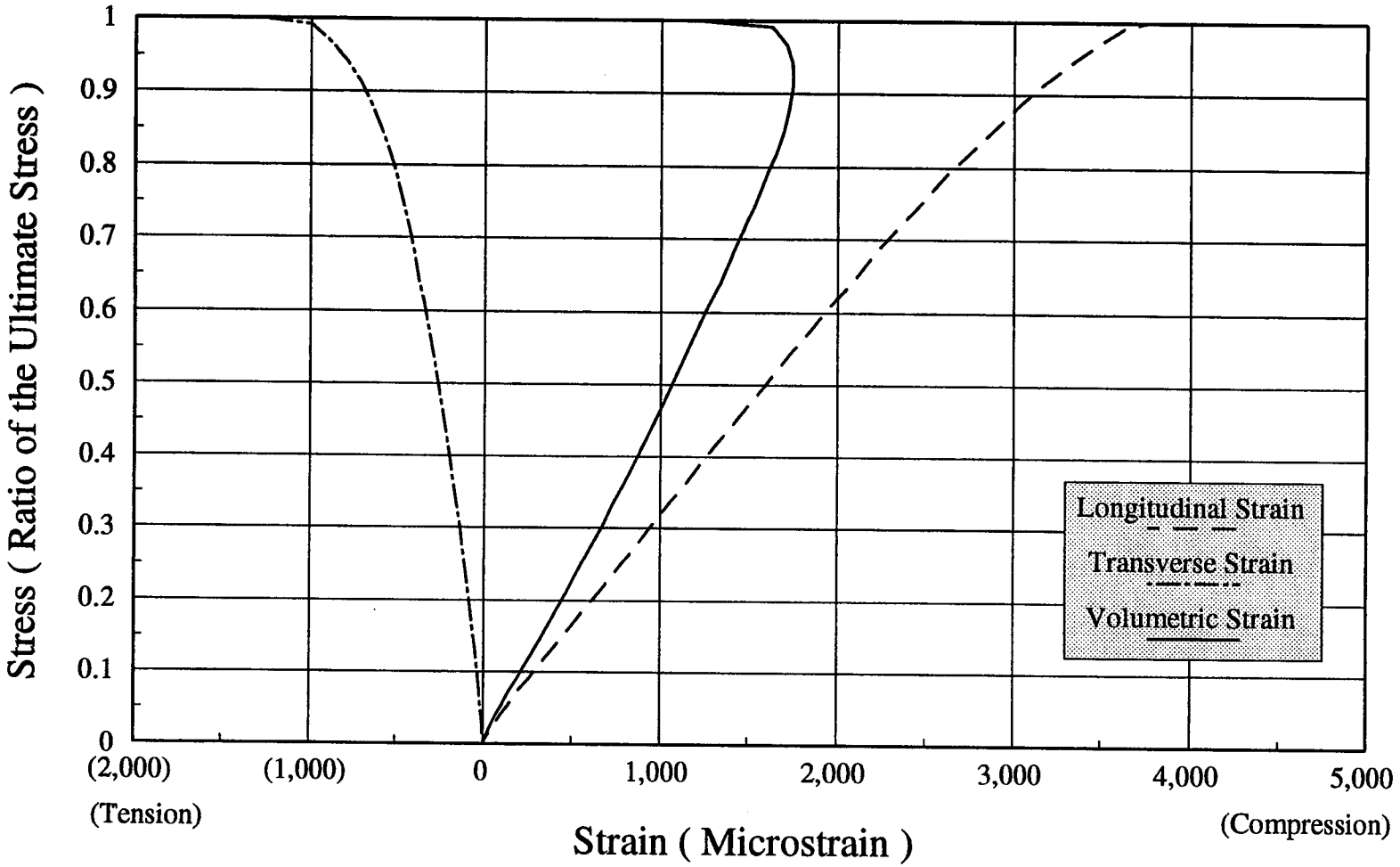

Figure H-4.1.L - Stress - Strain Relationships - UHC100D Specimen

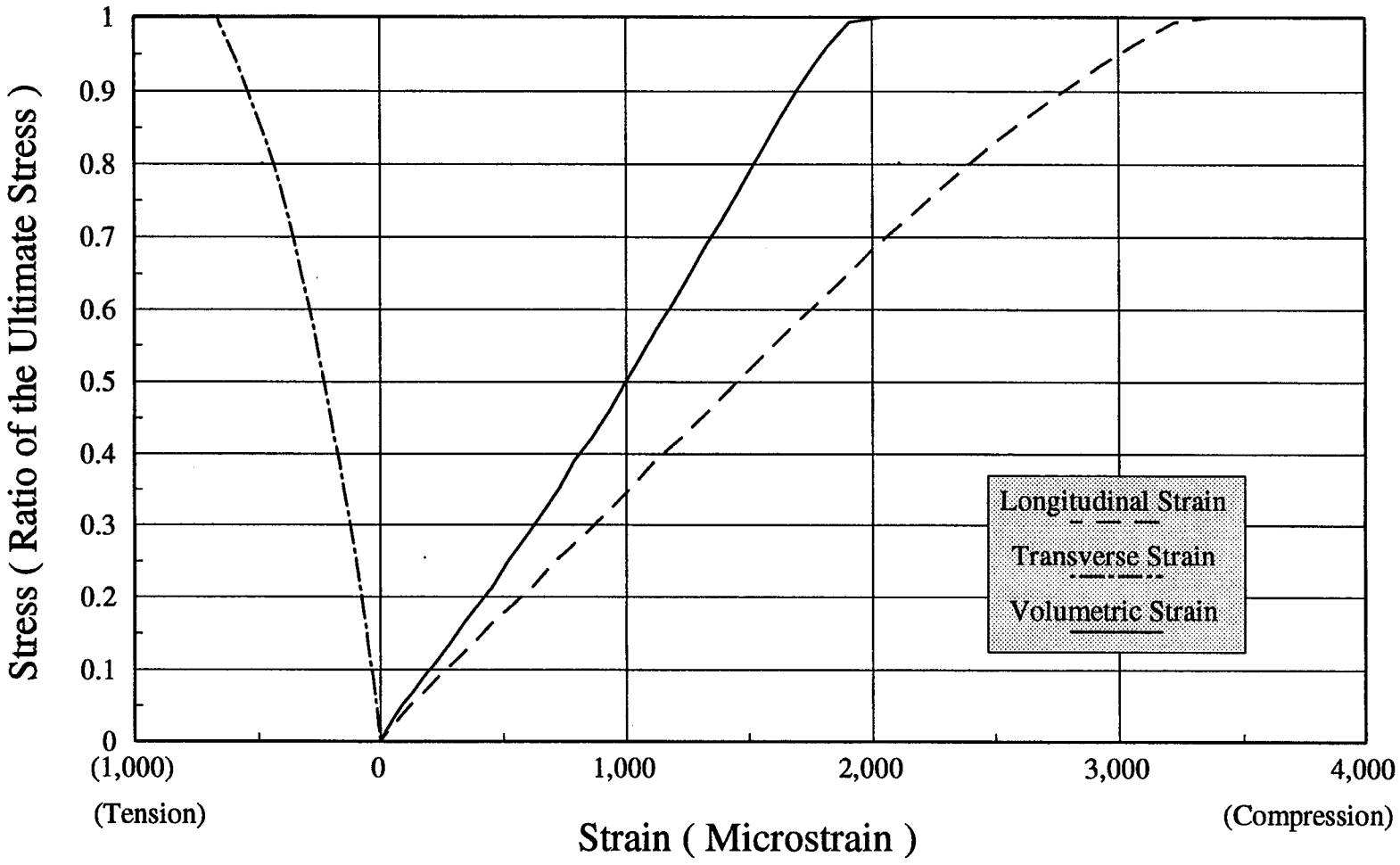

Figure H-4.1.M - Stress - Strain Relationships - UHC100E Specimen

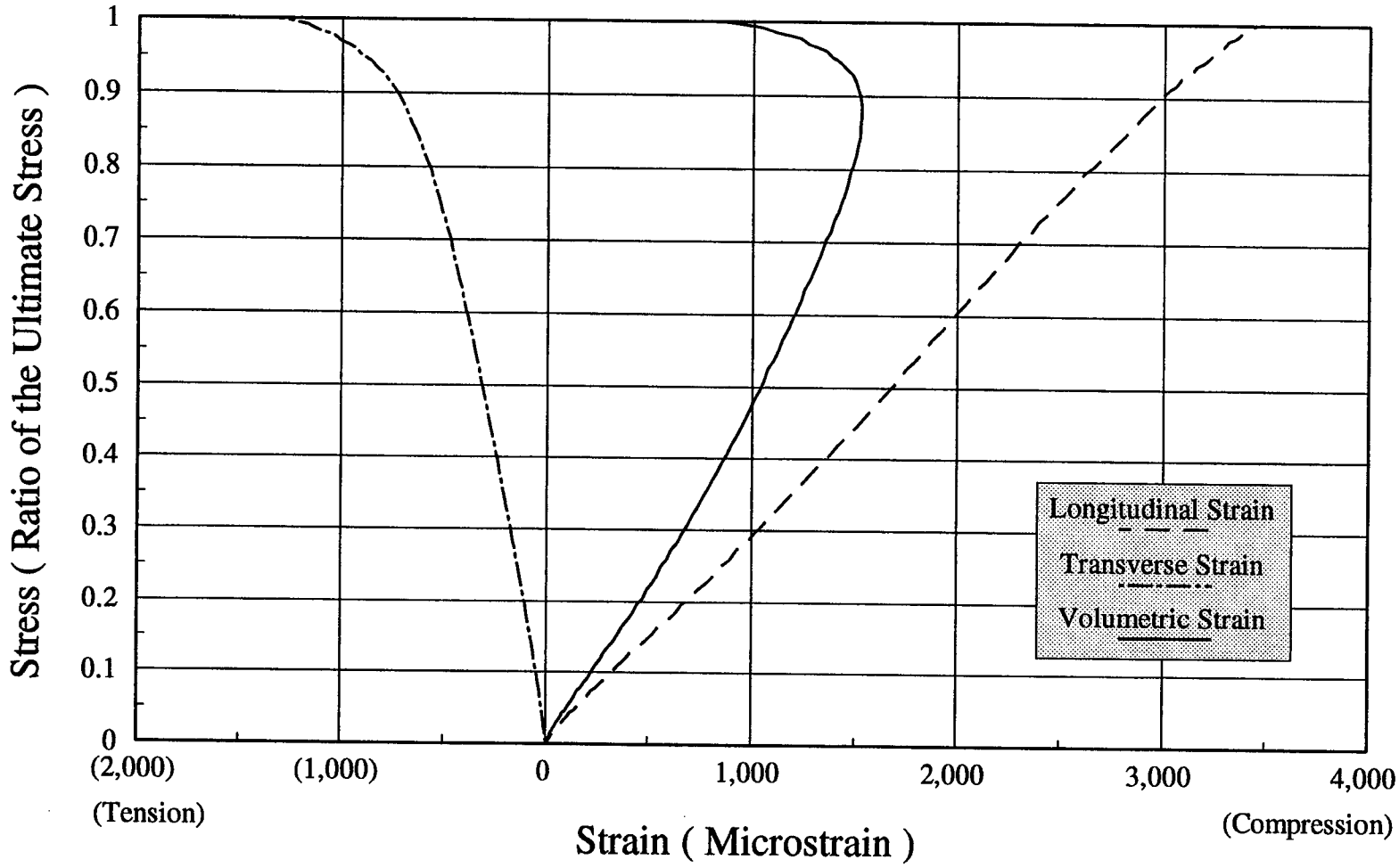

Figure H-4.1.N - Stress - Strain Relationships - LUC100A Specimen

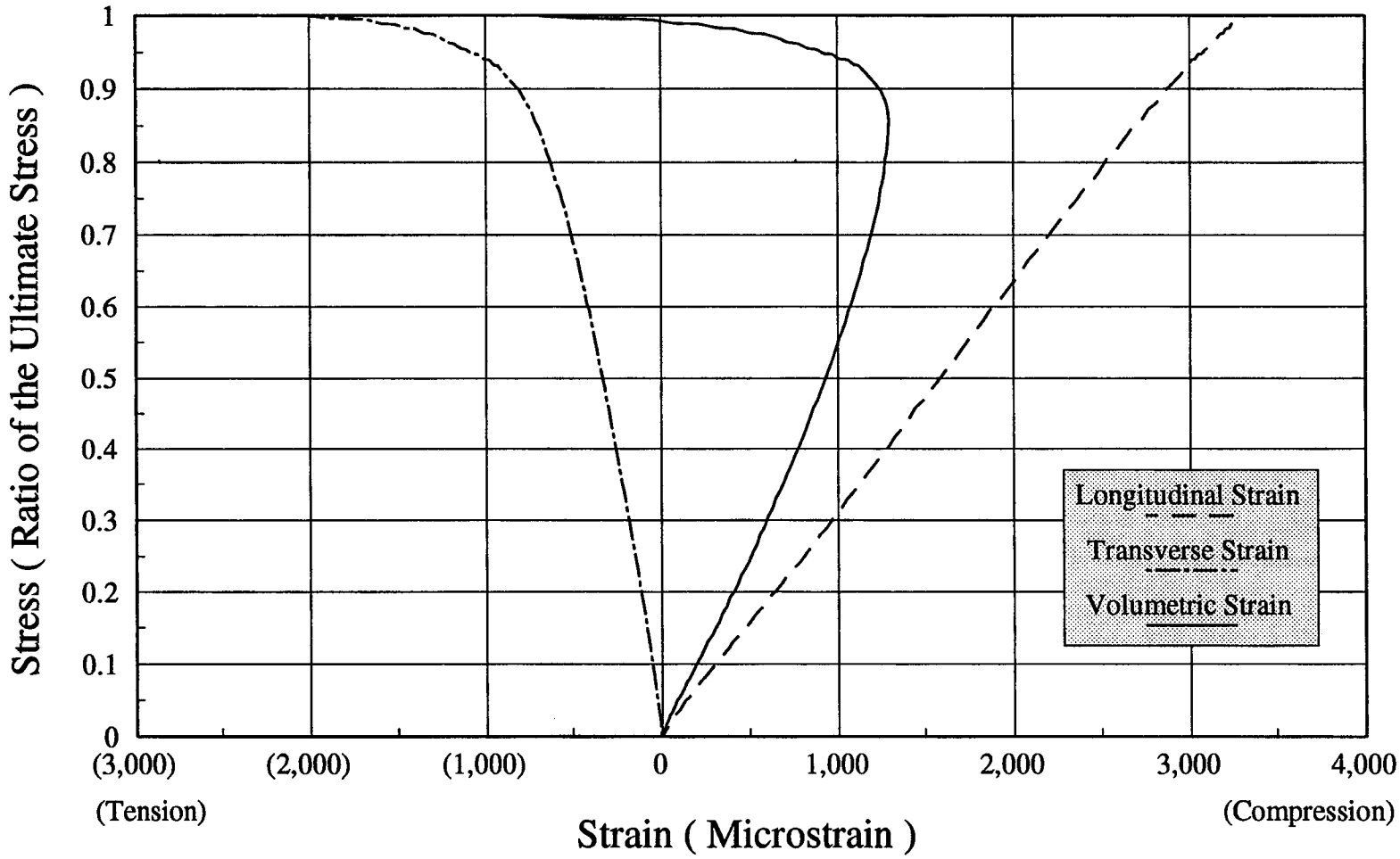

Figure H-4.1.O - Stress - Strain Relationships - LUC100B Specimen

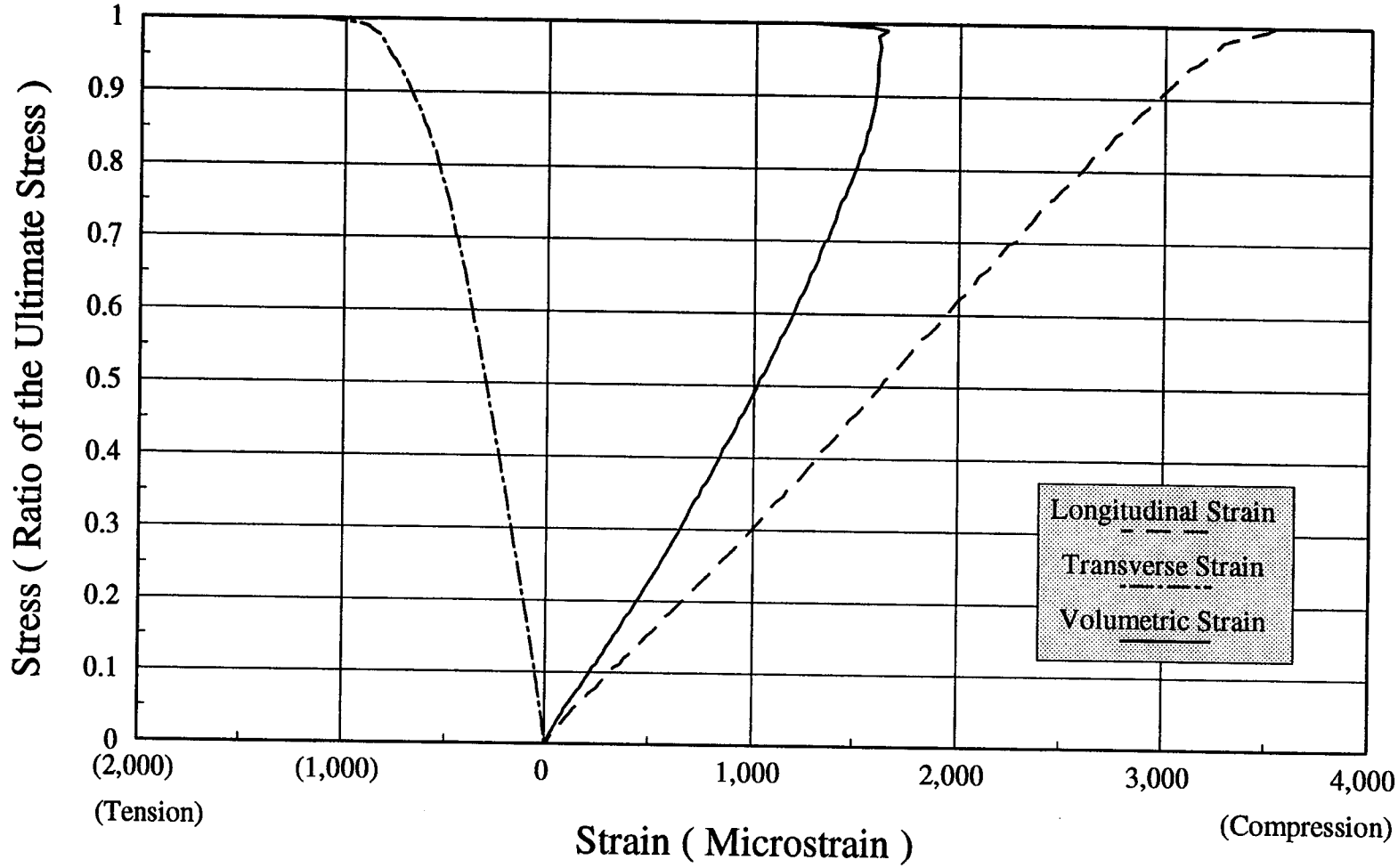

Figure H-4.1.P - Stress - Strain Relationships - LUC100C Specimen

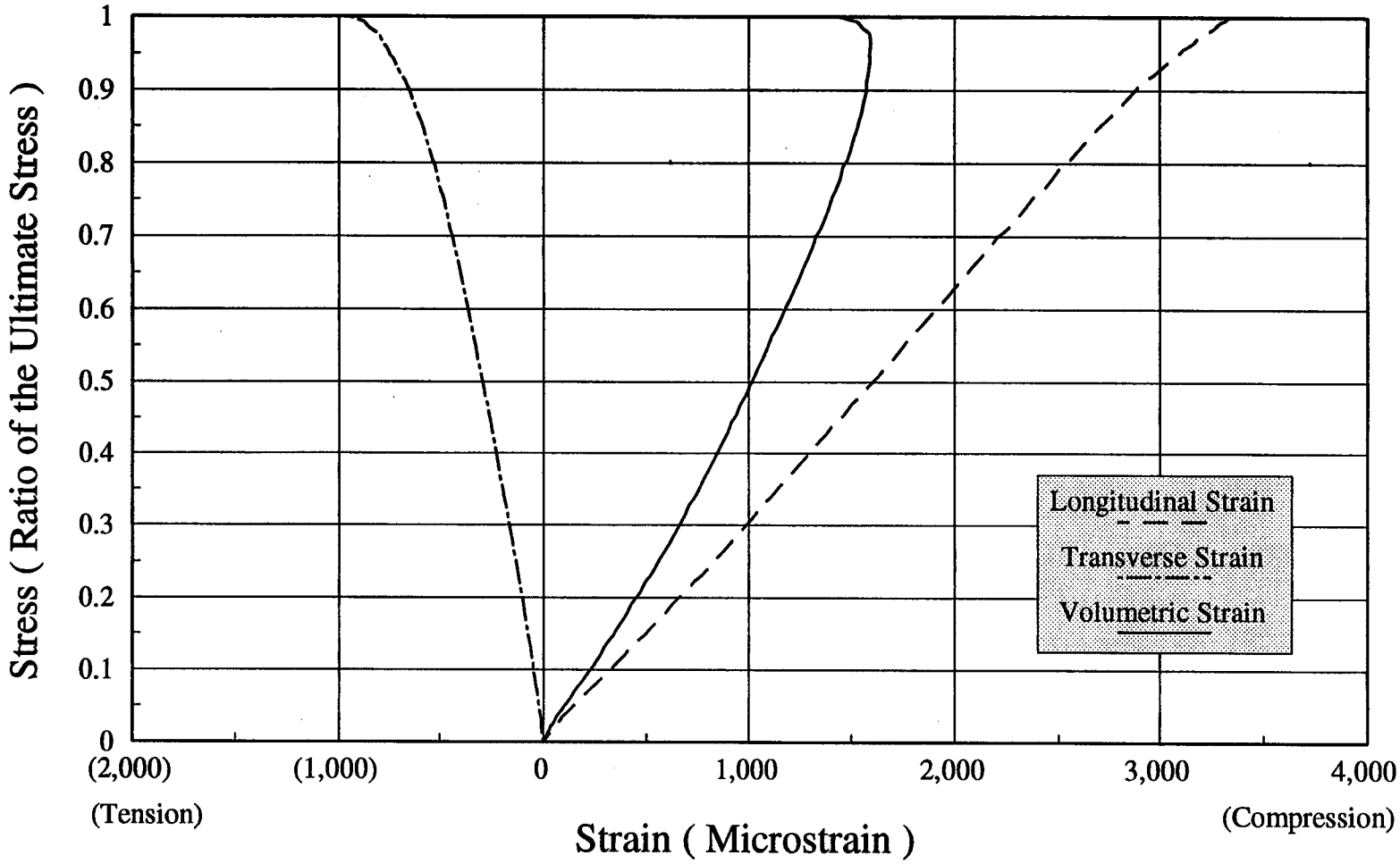

Figure H-4.1.Q - Stress - Strain Relationships - LUC100D Specimen

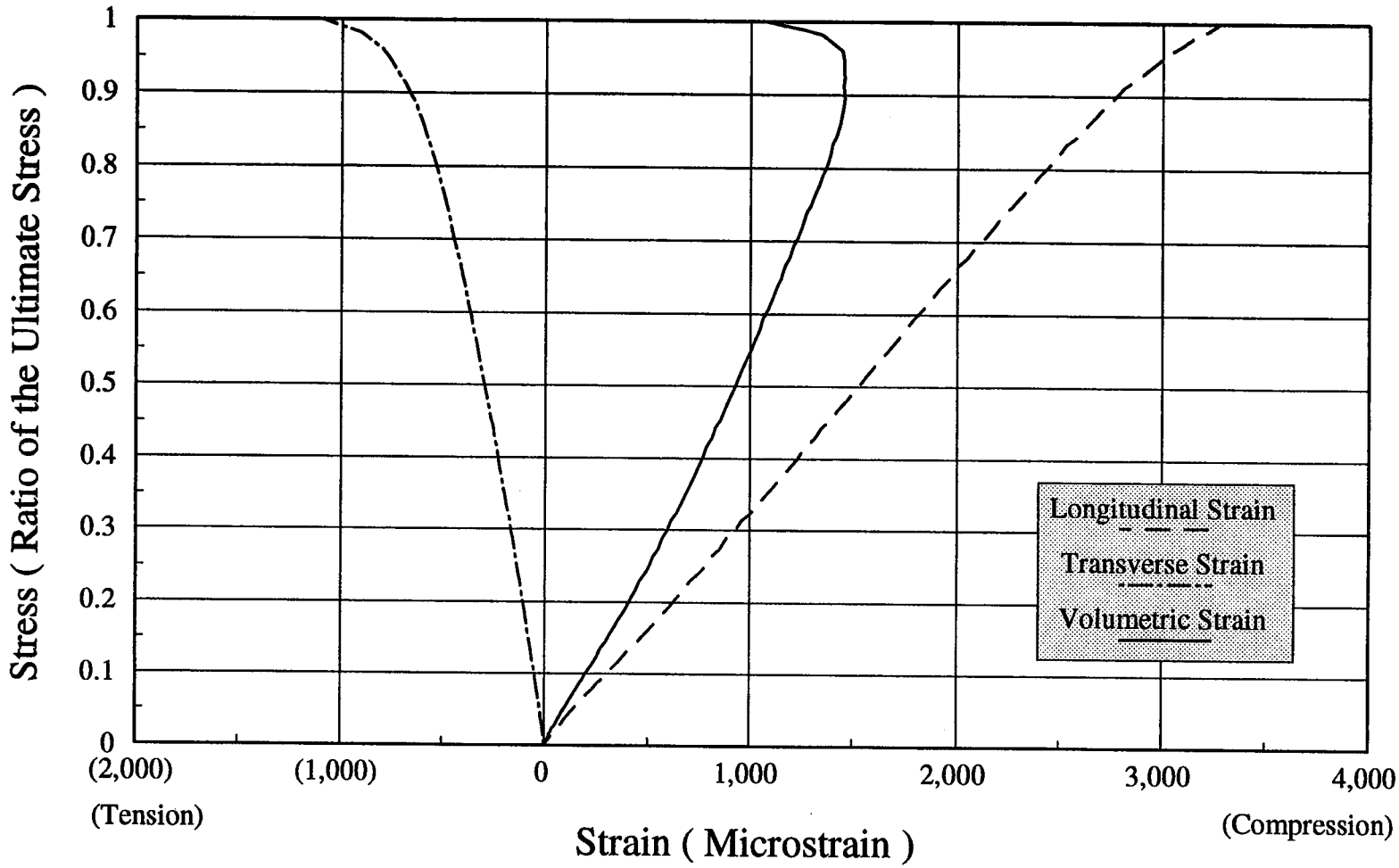

Figure H-4.1.R - Stress - Strain Relationships - LUC100E Specimen

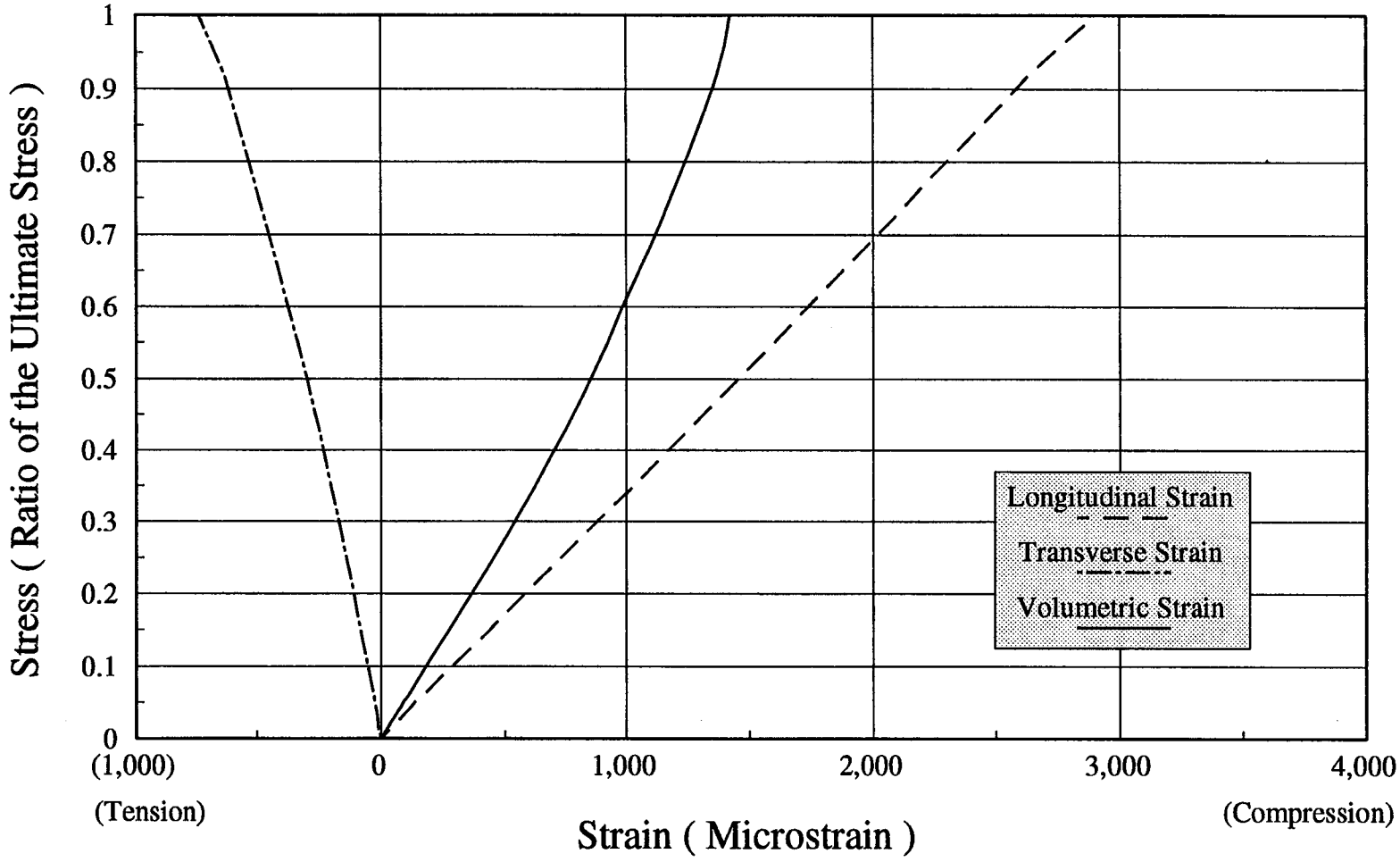

Figure H-4.1.S - Stress - Strain Relationships - UUC100A Specimen

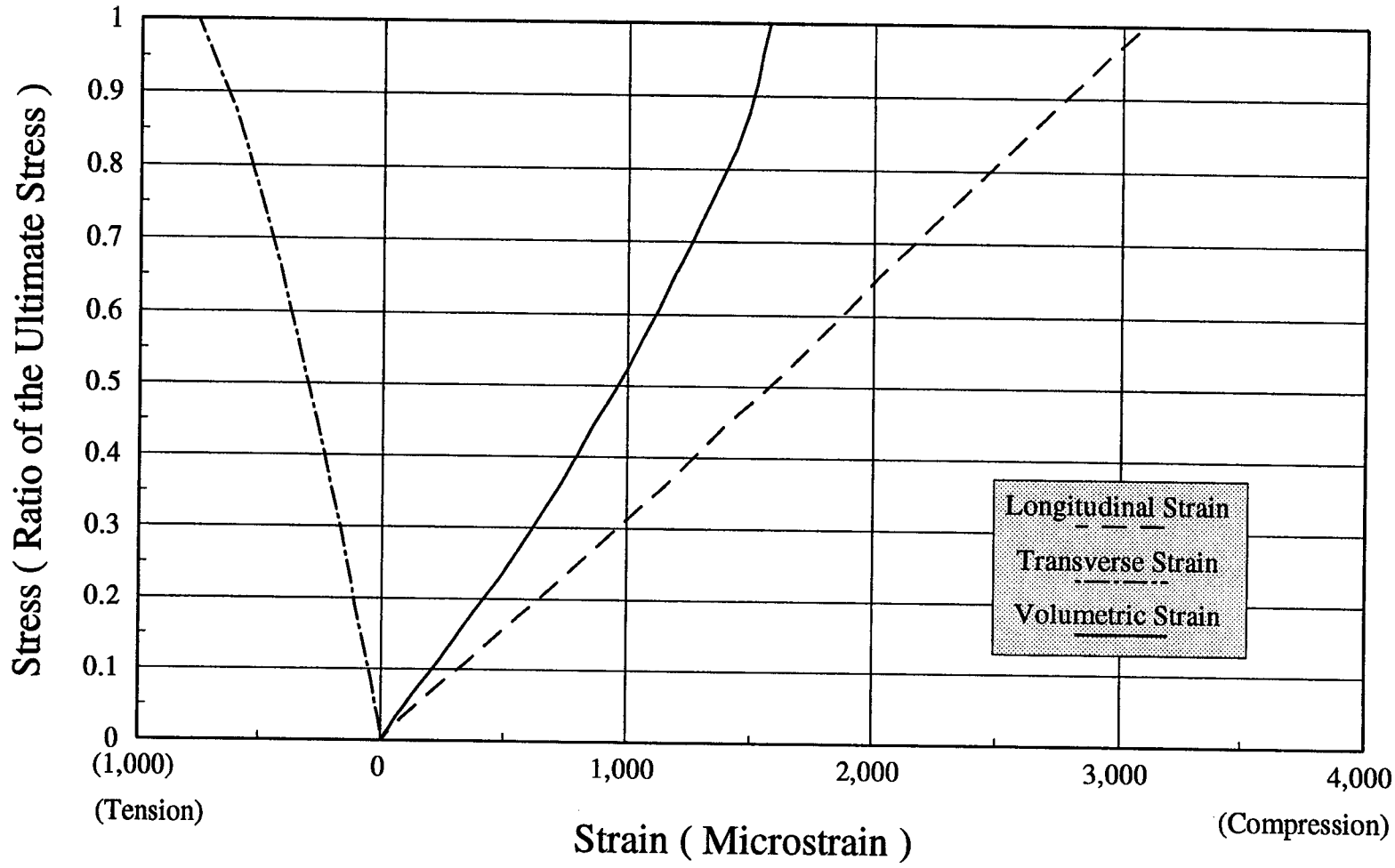

Figure H-4.1.T - Stress - Strain Relationships - UUC100B Specimen

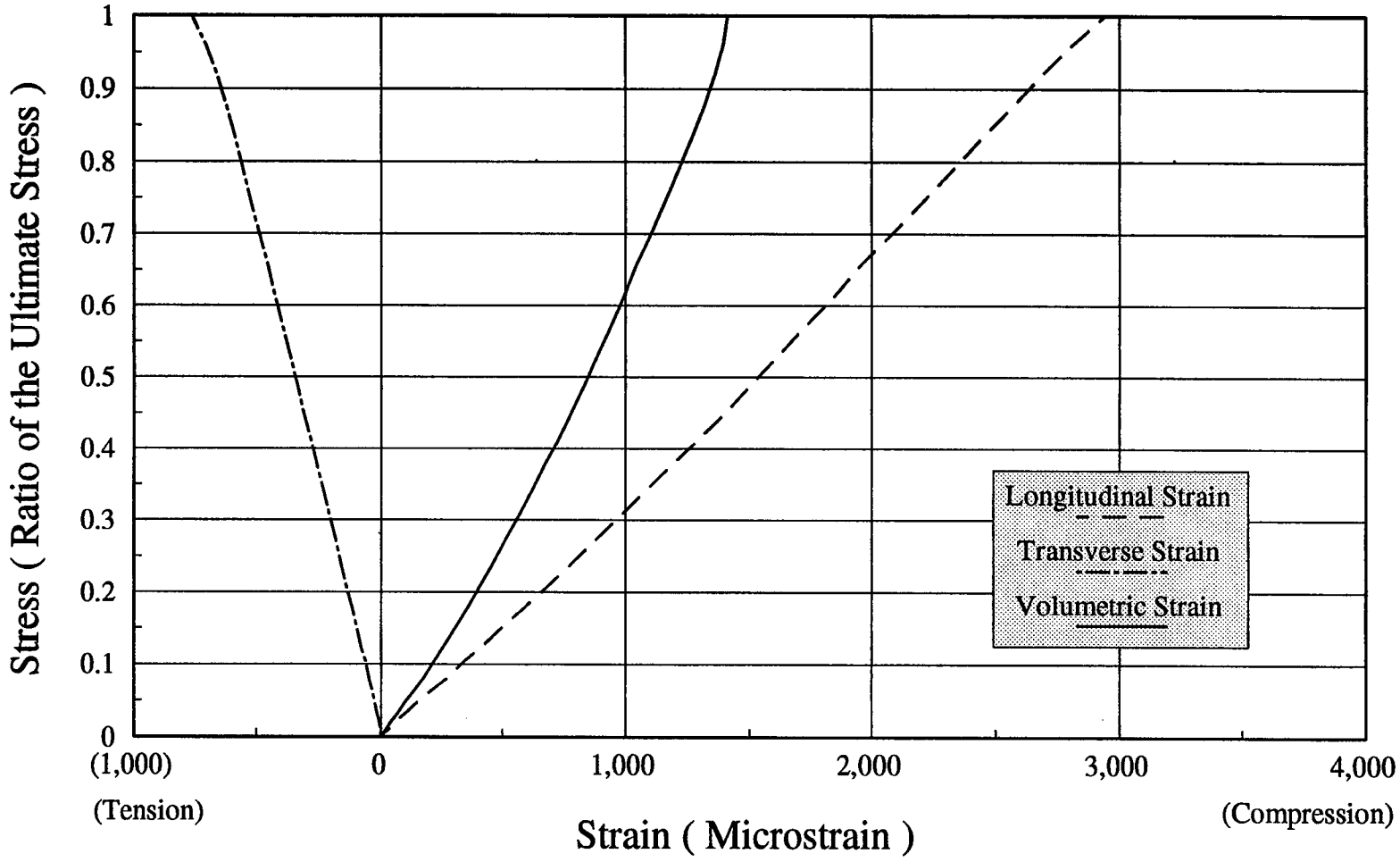

Figure H-4.1.U - Stress - Strain Relationships - UUC100C Specimen

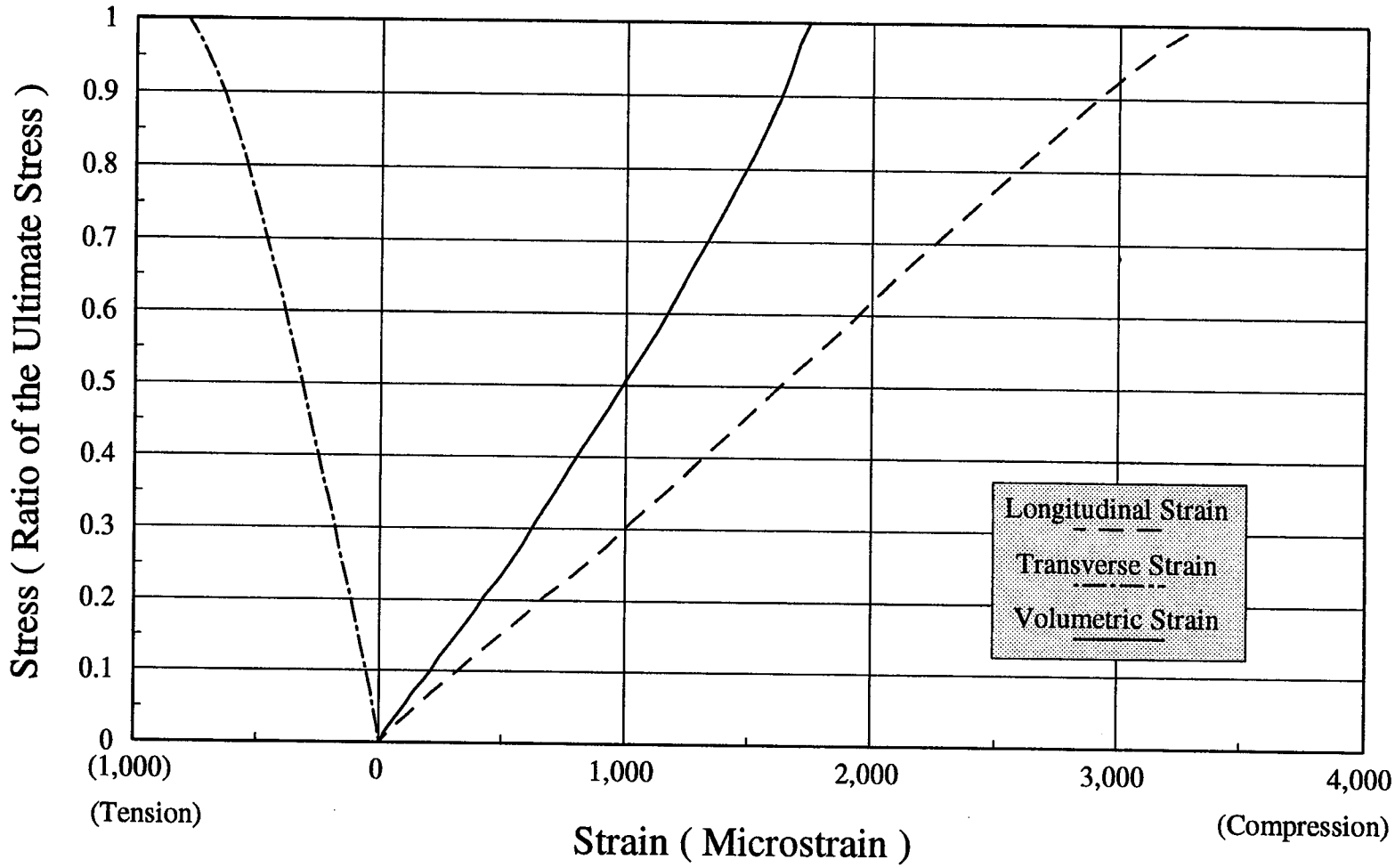

Figure H-4.1.V - Stress - Strain Relationships - UUC100D Specimen

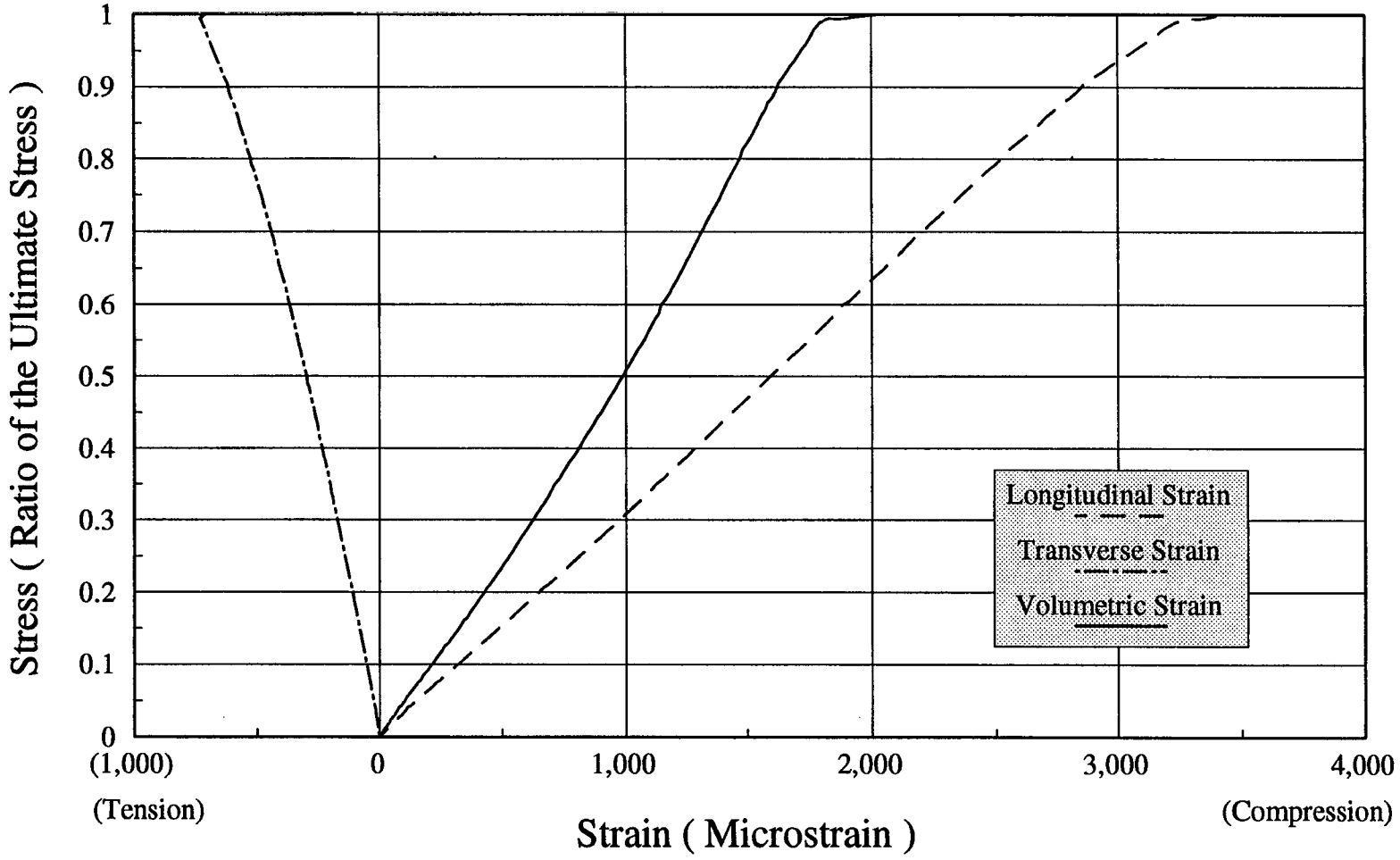

Figure H-4.1.W - Stress - Strain Relationships - UUC100E Specimen

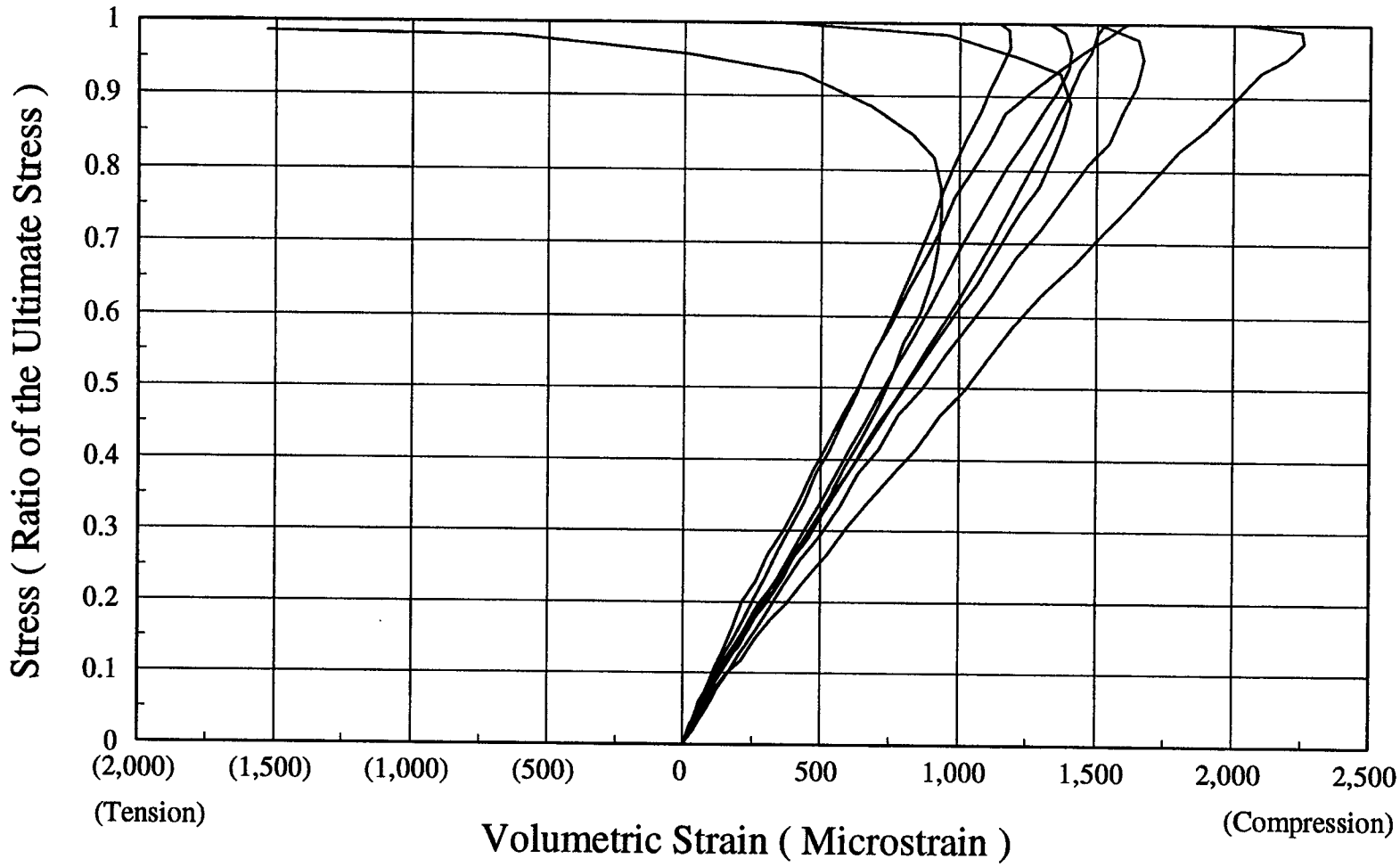

Figure H-4.2.A - Summary of Volumetric Strain Study - LH Series

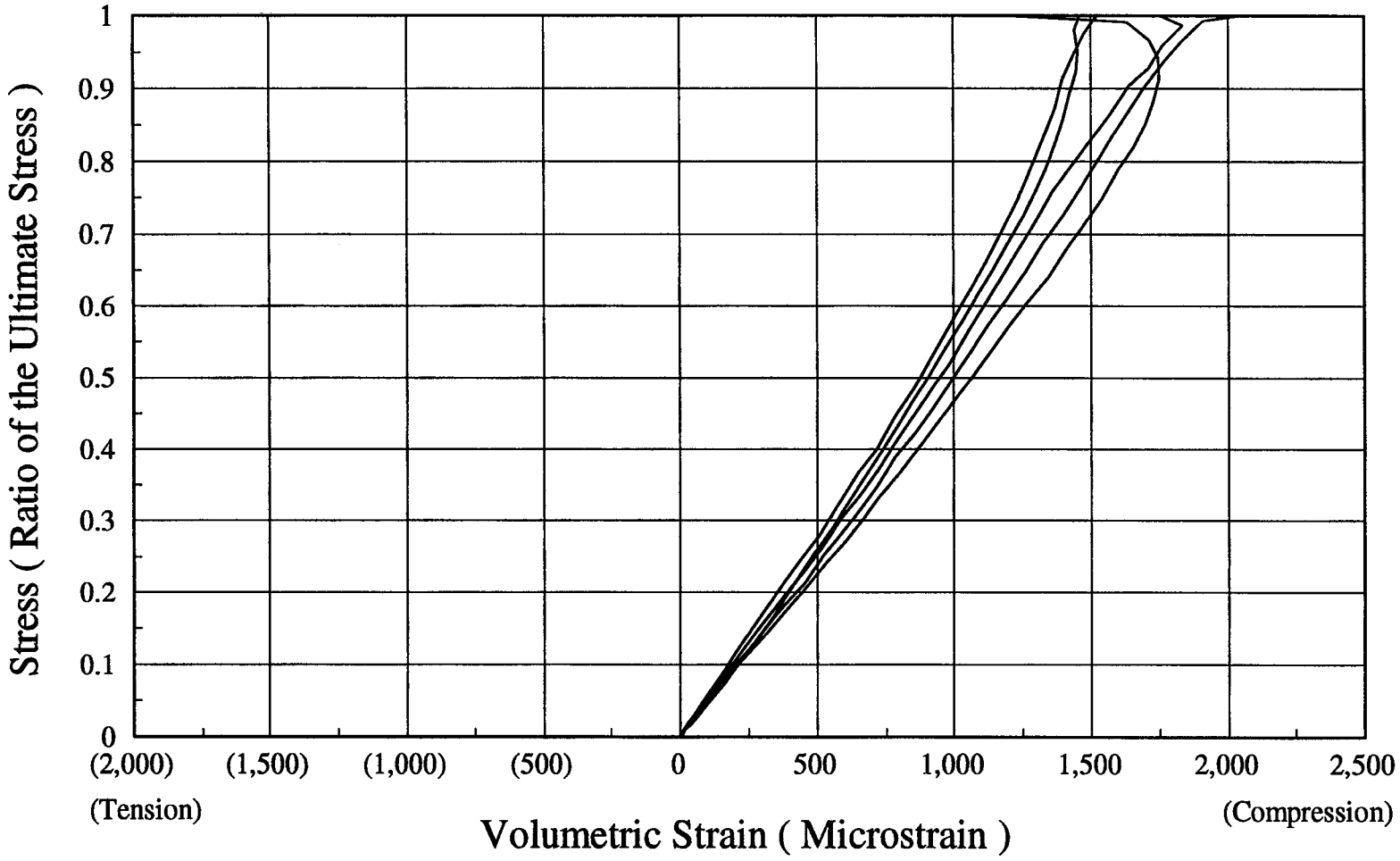

Figure H-4.2.B - Summary of Volumetric Strain Study - UH Series

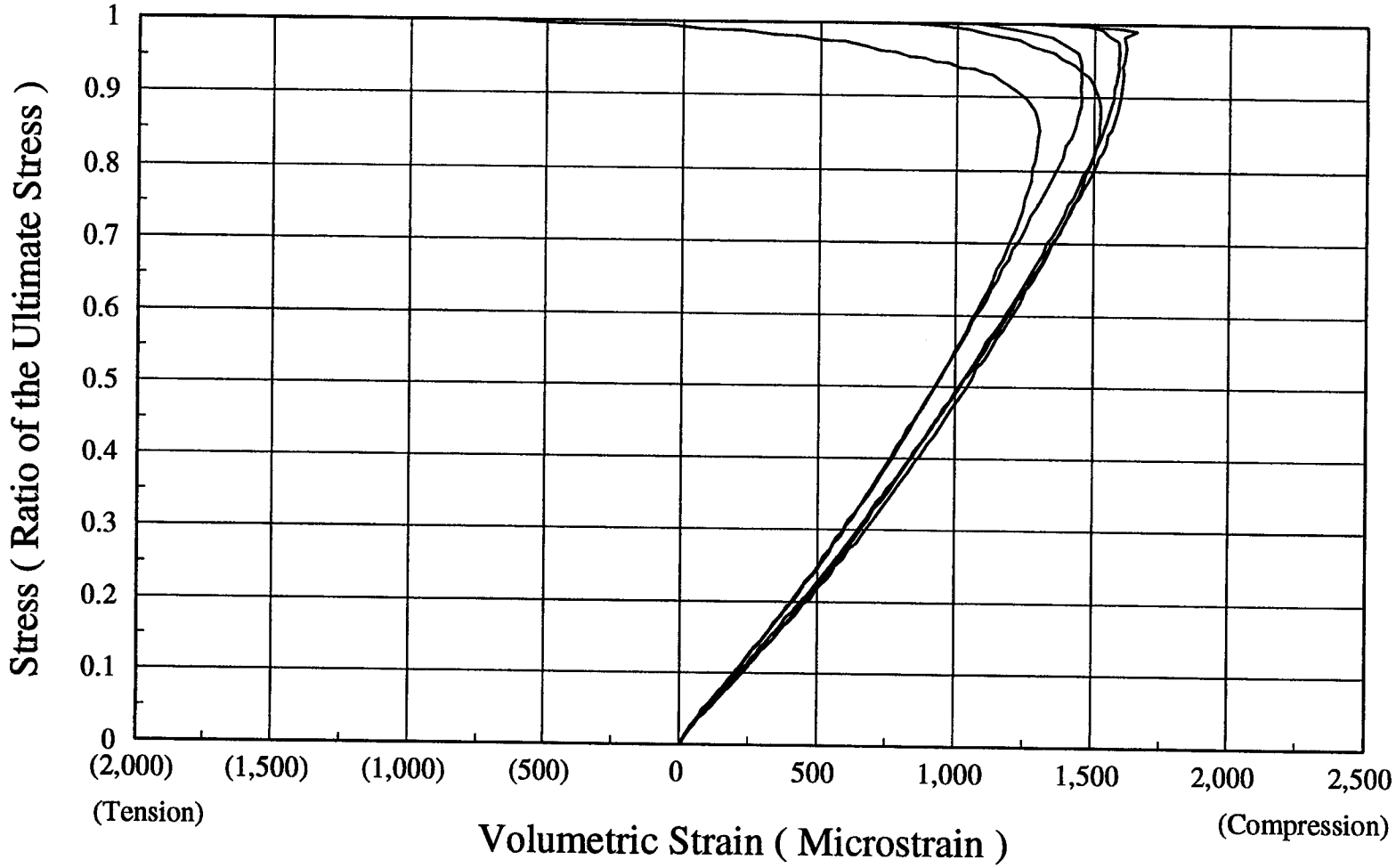

Figure H-4.2.C - Summary of Volumetric Strain Study - LU Series

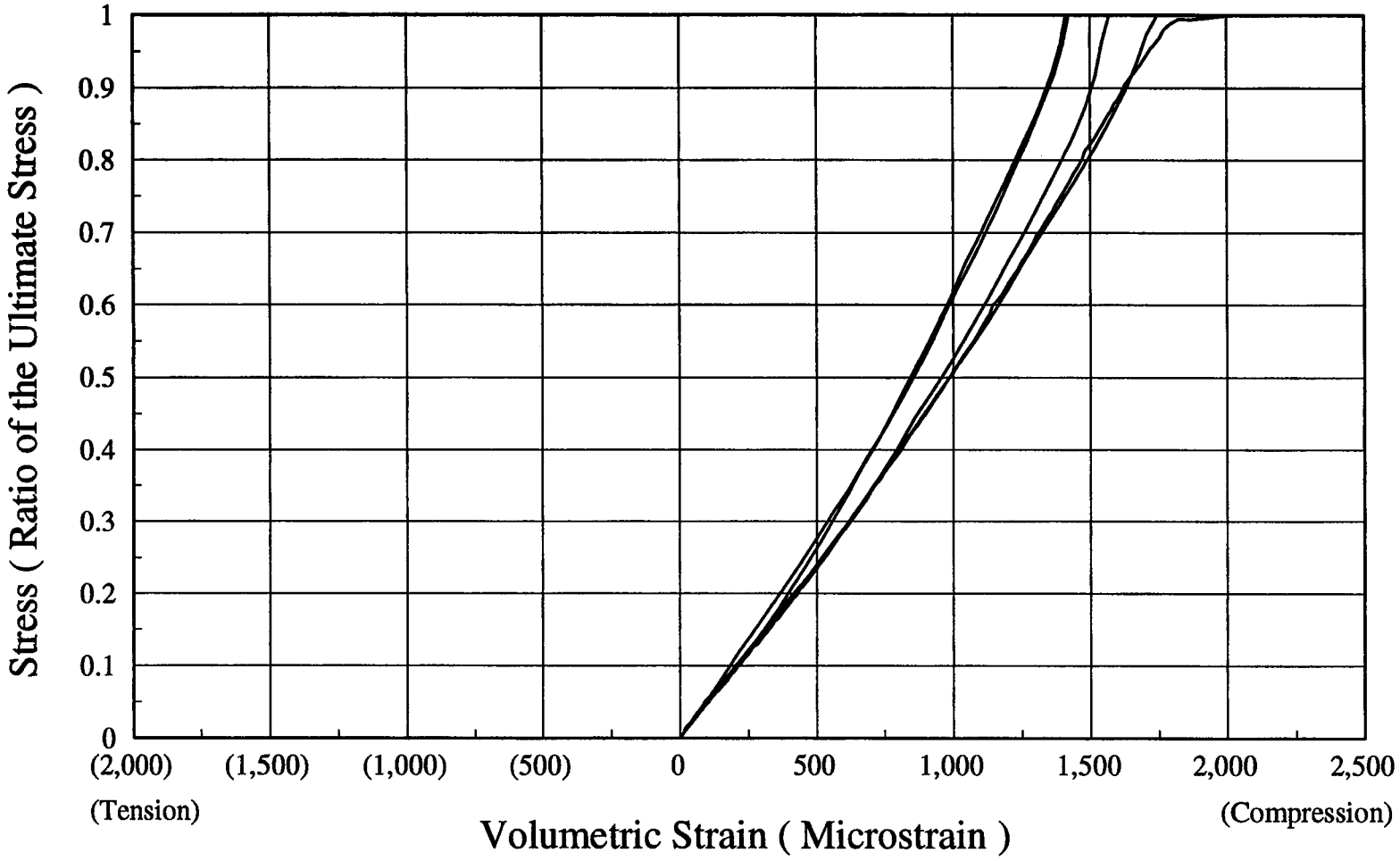

Figure H-4.2.D - Summary of Volumetric Strain Study - UU Series

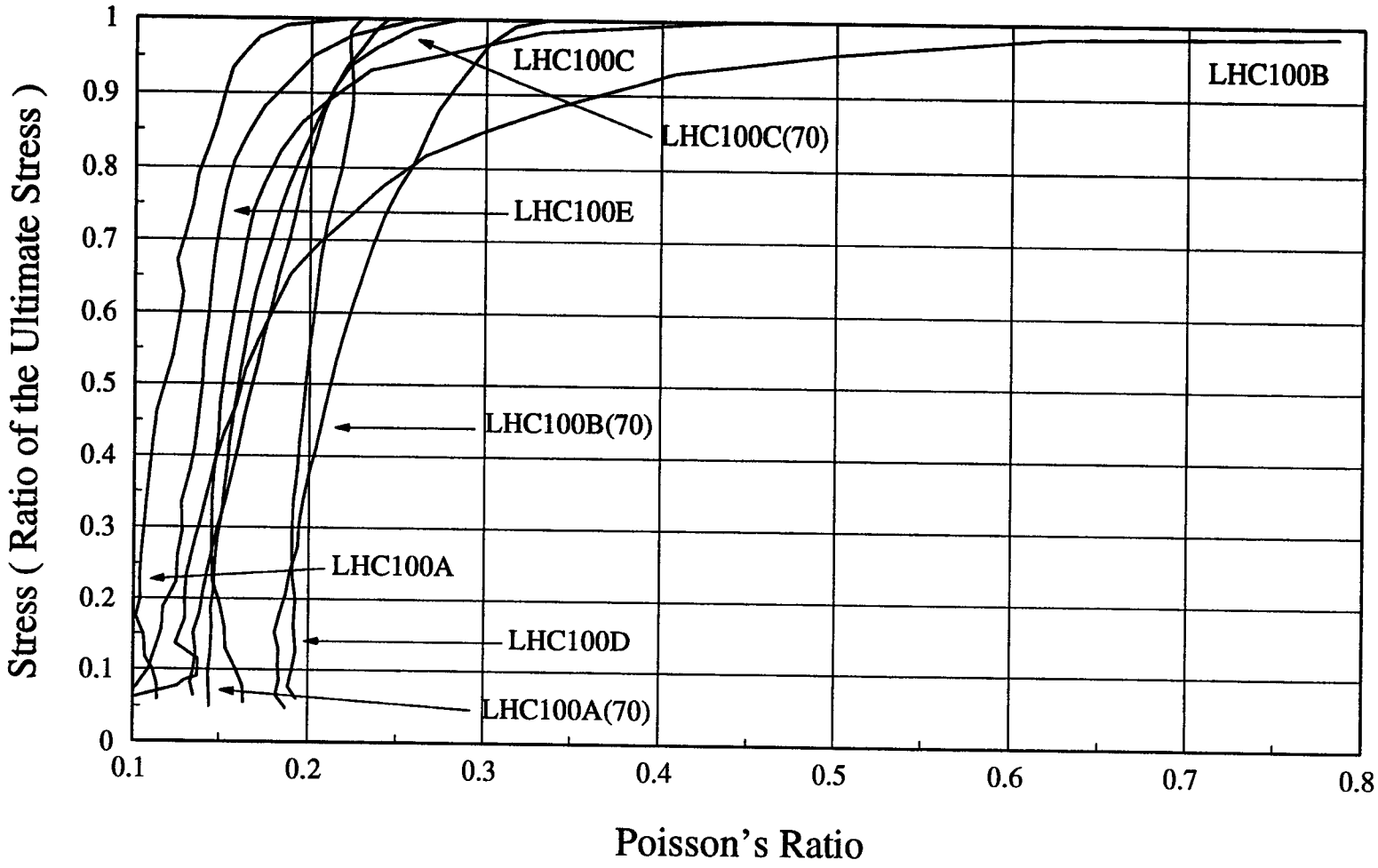

Figure H-5.1.A - Poisson's Ratio Study - LH Series

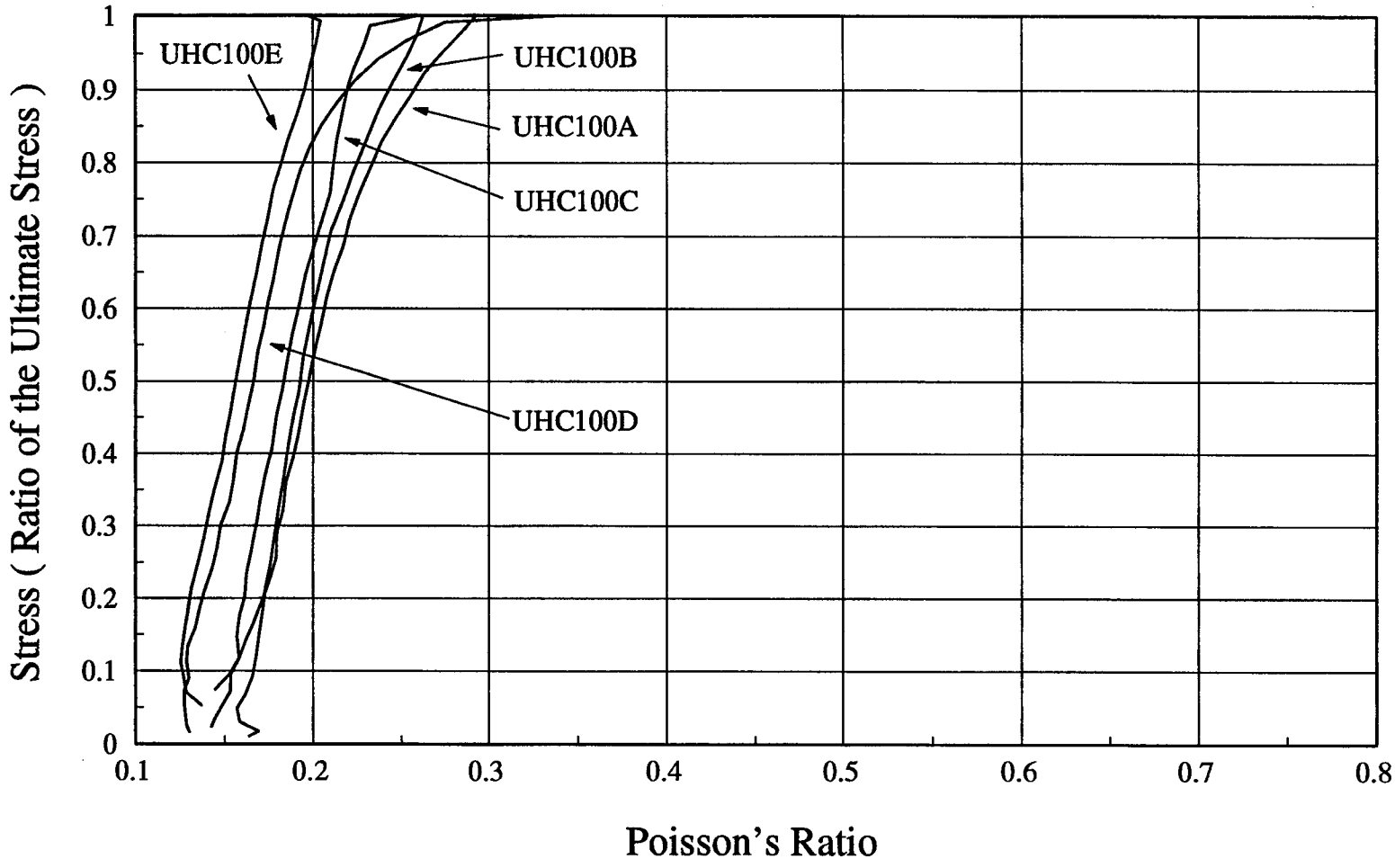

Figure H-5.1.B - Poisson's Ratio Study - UH Series

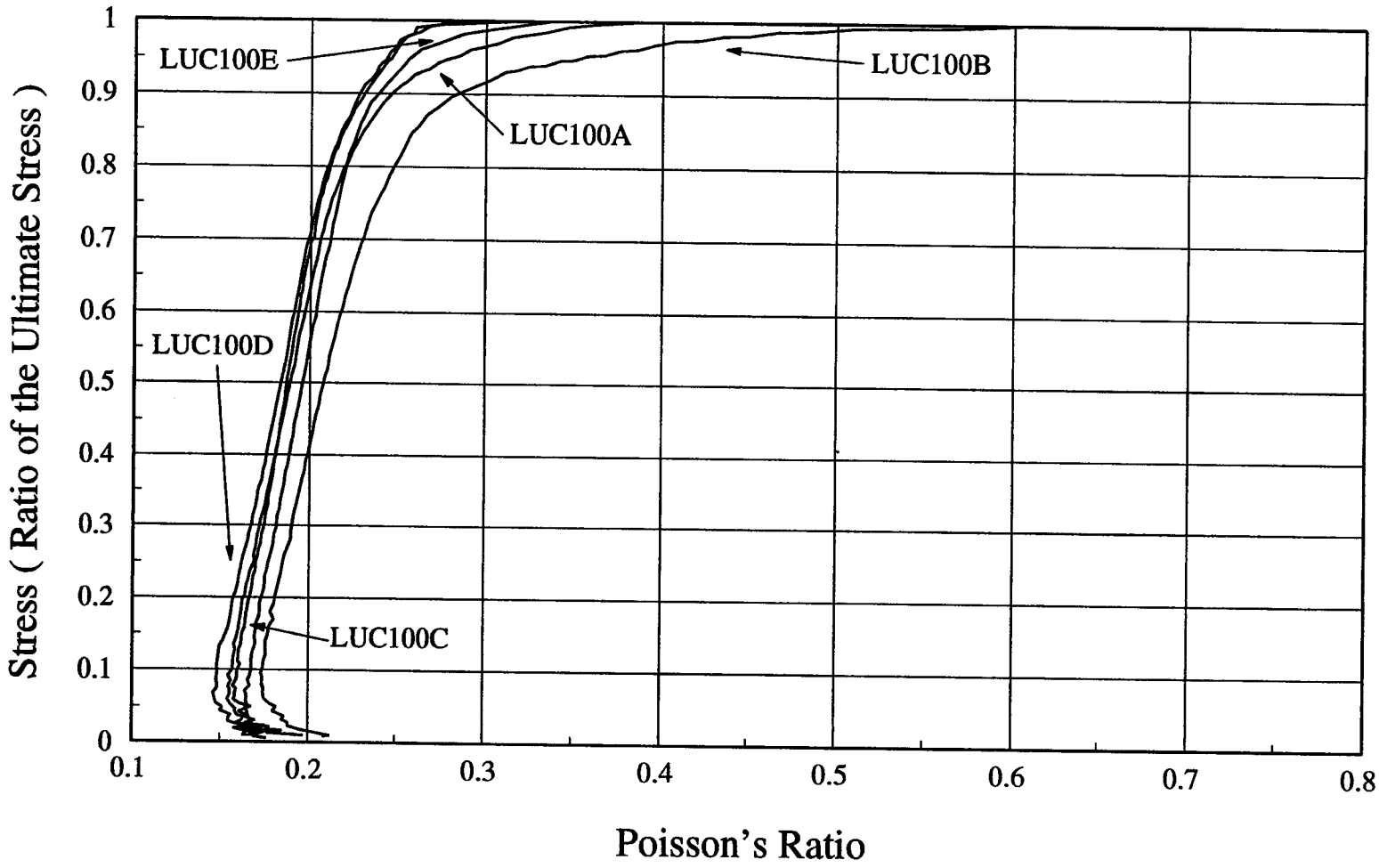

Figure H-5.1.C - Poisson's Ratio Study - LU Series

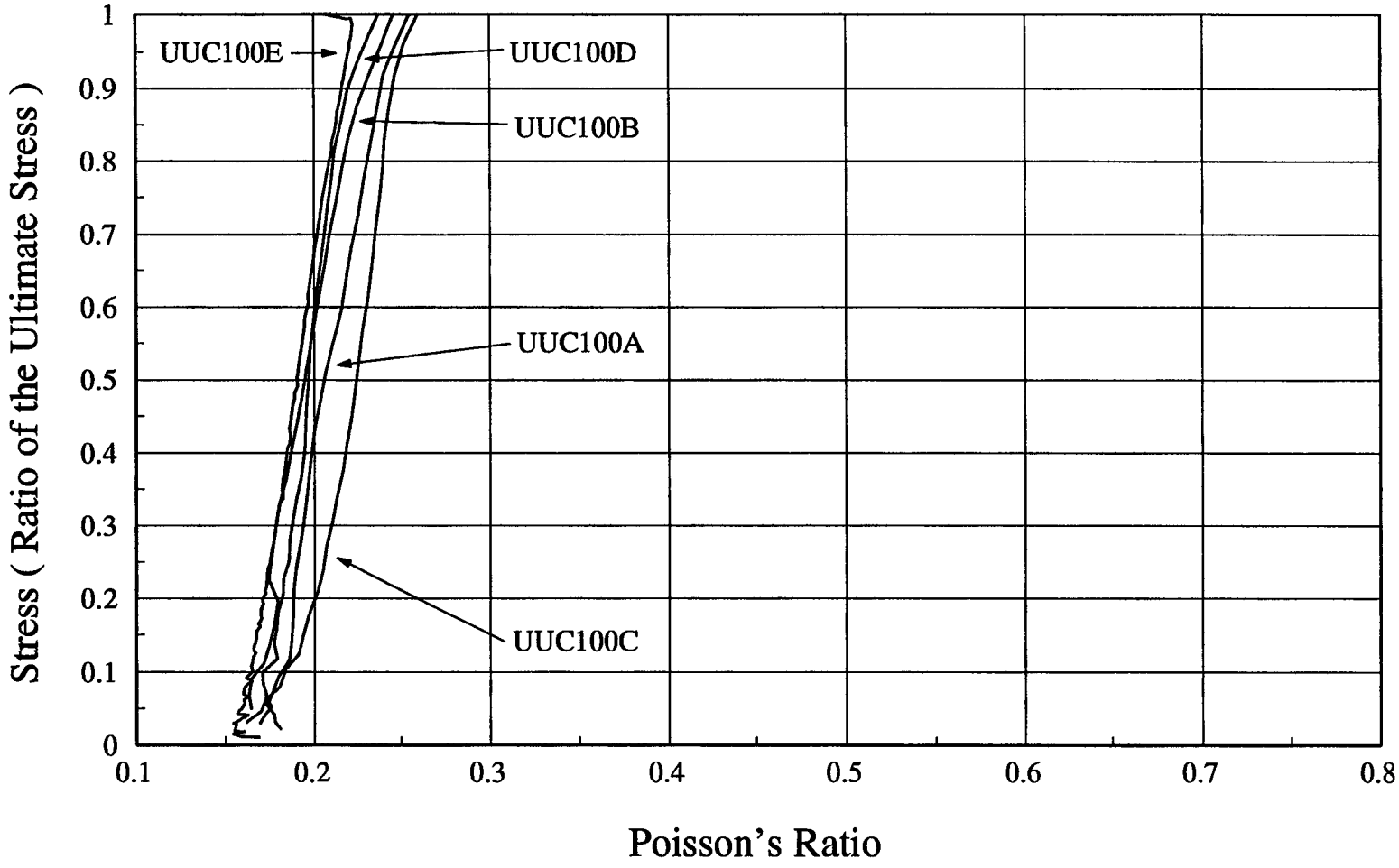

Figure H-5.1.D - Poisson's Ratio Study - UU Series

Appendix I. Details of Concrete Cylinder Tests

The details of concrete cylinder tests are presented in Tables I-3.2.2.A through C, I-3.3.2.A through C, I-3.4.2.A through C, and I-4.3.A through C for those test results reported in sections 3.2.2, 3.3.2, 3.4.2, and 4.3, respectively. For those test results reported in sections E-3.2, E-3.3, E-3.4, and F-4.3, the details of concrete cylinder tests are also presented in Tables I-E-3.2, I-E-3.3, I-E-3.4, and I-F-4.3, respectively. The reported results in this appendix are the compressive strength of individual specimens tested.

Table I-3.2.2.A - Compressive Strength Gain with Time (LH Series)

Concrete Series	Age (Days)	Compressive Strength (MPa)					
		S_1	S_2	S_3	S_4	S_5	Mean
LH2	1	24.2	22.9	24.9	-	-	24.0
LH2	3	37.2	37.8	-	-	-	37.5
LH2	7	43.9	43.6	-	-	-	43.8
LH2	28	50.5	52.5	-	-	-	51.5
LH2	56	56.1	56.0	-	-	-	56.1
LH2	91	58.6	57.7	-	-	-	58.2
LH2	147	58.0	61.0	55.8	-	-	58.3
LH4	1	24.6	24.4	-	-	-	24.5
LH4	3	38.8	40.5	-	-	-	39.7
LH4	7	43.5	43.2	-	-	-	43.4
LH4	28	52.9	49.4	50.6	-	-	51.0
LH4	56	55.1	53.8	57.8	54.2	55.7	55.3
LH4	91	57.9	55.9	-	-	-	56.9
LH4	147	57.7	56.3	52.1	-	-	55.4

Table I-3.2.2.B - Compressive Strength Gain with Time (UH Series)

Concrete Series	Age (Days)	Compressive Strength (MPa)					
		S_1	S_2	S_3	S_4	S_5	Mean
UH2	1	56.7	54.5	-	-	-	55.6
UH2	3	58.3	56.6	-	-	-	57.5
UH2	7	62.4	61.7	-	-	-	62.1
UH2	28	66.8	71.8	73.8	-	-	70.8
UH2	56	75.7	75.6	-	-	-	75.7
UH2	91	74.3	82.2	80.3	-	-	78.9
UH2	147	78.2	81.3	-	-	-	79.8
UH4	1	54.4	53.8	-	-	-	54.1
UH4	3	56.3	54.0	-	-	-	55.2
UH4	7	58.7	59.7	-	-	-	59.2
UH4	28	68.6	69.8	-	-	-	69.2
UH4	56	71.1	71.7	69.3	73.9	71.6	71.5
UH4	91	72.0	73.0	-	-	-	72.5
UH4	147	78.1	72.7	75.1	-	-	75.3

Table I-3.2.2.C - Compressive Strength Gain with Time (UU Series)

Concrete Series	Age (Days)	Compressive Strength (MPa)					
		S_1	S_2	S_3	S_4	S_5	Mean
UU2	1	53.7	58.6	53.5	-	-	55.3
UU2	3	69.7	66.3	64.7	-	-	66.9
UU2	7	76.0	68.7	74.6	-	-	73.1
UU2	28	97.1	93.5	-	-	-	95.3
UU2	56	95.8	95.4	-	-	-	95.6
UU2	91	98.8	98.2	-	-	-	98.5
UU2	147	98.2	98.4	97.9	-	-	98.2
UU4	1	56.6	57.0	-	-	-	56.8
UU4	3	66.4	61.8	64.0	-	-	64.1
UU4	7	75.9	74.1	-	-	-	75.0
UU4	28	97.6	101.6	-	-	-	99.6
UU4	56	97.2	104.0	98.3	106.9	108.2	102.9
UU4	91	101.1	112.9	110.3	-	-	108.1
UU4	147	115.2	116.6	-	-	-	115.9

Table I-3.3.2.A - Effect of Type of Cement on the Compressive Strength Gain (LH Series)

Concrete Series	Age (Days)	Compressive Strength (MPa)					
		S_1	S_2	S_3	S_4	S_5	Mean
LH2	1	24.2	22.9	24.9	-	-	24.0
LH2	3	37.2	37.8	-	-	-	37.5
LH2	7	43.9	43.6	-	-	-	43.8
LH2	28	50.5	52.5	-	-	-	51.5
LH2	56	56.1	56.0	-	-	-	56.1
LH2	91	58.6	57.7	-	-	-	58.2
LH2	147	58.0	61.0	55.8	-	-	58.3
LH3	1	39.3	39.3	-	-	-	39.3
LH3	3	49.0	47.8	-	-	-	48.4
LH3	7	50.2	51.7	-	-	-	51.0
LH3	28	63.8	59.5	62.4	-	-	61.9
LH3	56	64.8	65.3	-	-	-	65.1
LH3	91	68.0	63.3	-	-	-	65.7
LH3	147	68.2	68.4	-	-	-	68.3

Table I-3.3.2.B - Effect of Type of Cement on the Compressive Strength Gain (UH Series)

Concrete Series	Age (Days)	Compressive Strength (MPa)					
		S_1	S_2	S_3	S_4	S_5	Mean
UH2	1	56.7	54.5	-	-	-	55.6
UH2	3	58.3	56.6	-	-	-	57.5
UH2	7	62.4	61.7	-	-	-	62.1
UH2	28	66.8	71.8	73.8	-	-	70.8
UH2	56	75.7	75.6	-	-	-	75.7
UH2	91	74.3	82.2	80.3	-	-	78.9
UH2	147	78.2	81.3	-	-	-	79.8
UH3	1	62.0	60.0	-	-	-	61.0
UH3	3	65.0	64.9	-	-	-	65.0
UH3	7	70.7	75.8	69.0	-	-	71.8
UH3	28	75.4	78.5	-	-	-	77.0
UH3	56	88.0	86.1	-	-	-	87.1
UH3	91	88.9	85.5	-	-	-	87.2
UH3	147	83.9	85.9	-	-	-	84.9
UH3	273	91.6	88.7	-	-	-	90.2

Table I-3.3.2.C - Effect of Type of Cement on the Compressive Strength Gain (UU Series)

Concrete Series	Age (Days)	Compressive Strength (MPa)					
		S_1	S_2	S_3	S_4	S_5	Mean
UU2	1	53.7	58.6	53.5	-	-	55.3
UU2	3	69.7	66.3	64.7	-	-	66.9
UU2	7	76.0	68.7	74.6	-	-	73.1
UU2	28	97.1	93.5	-	-	-	95.3
UU2	56	95.8	95.4	-	-	-	95.6
UU2	91	98.8	98.2	-	-	-	98.5
UU2	147	98.2	98.4	97.9	-	-	98.2
UU3	1	61.8	59.6	-	-	-	60.7
UU3	3	69.1	65.6	66.0	-	-	66.9
UU3	7	78.2	73.6	76.2	-	-	76.0
UU3	28	83.4	84.9	-	-	-	84.2
UU3	56	86.8	99.2	93.0	-	-	93.0
UU3	91	91.7	99.0	93.8	-	-	94.8
UU3	147	89.4	106.0	86.3	-	-	93.9

Table I-3.4.2.A - Effect of Drying on the Compressive Strength Gain (LH4 Series)

Age (Days)	Curing Condition	Compressive Strength (MPa)					
		S_1	S_2	S_3	S_4	S_5	Mean
1	Continuously Moist	24.6	24.4	-	-	-	24.5
3	Continuously Moist	38.8	40.5	-	-	-	39.7
7	Continuously Moist	43.5	43.2	-	-	-	43.4
28	Continuously Moist	52.9	49.4	50.6	-	-	51.0
28	3 Weeks Moist	58.5	55.8	-	-	-	57.2
56	Continuously Moist	55.1	53.8	57.8	54.2	55.7	55.3
56	3 Weeks Moist	65.2	66.7	-	-	-	66.0
56	7 Weeks Moist	66.9	63.5	61.8	-	-	64.1
91	Continuously Moist	57.9	55.9	-	-	-	56.9
91	3 Weeks Moist	66.5	67.3	-	-	-	66.9
91	7 Weeks Moist	66.6	68.0	-	-	-	67.3
147	Continuously Moist	52.1	57.7	56.3	-	-	55.4
147	3 Weeks Moist	68.2	66.1	-	-	-	67.2
147	7 Weeks Moist	70.5	69.1	-	-	-	69.8

Table I-3.4.2.B - Effect of Drying on the Compressive Strength Gain (UH4 Series)

Age (Days)	Curing Condition	Compressive Strength (MPa)					
		S_1	S_2	S_3	S_4	S_5	Mean
1	Continuously Moist	54.4	53.8	-	-	-	54.1
3	Continuously Moist	56.3	54.0	-	-	-	55.2
7	Continuously Moist	58.7	59.7	-	-	-	59.2
28	Continuously Moist	68.6	69.8	-	-	-	69.2
28	3 Weeks Moist	79.9	81.6	-	-	-	80.8
56	Continuously Moist	71.1	71.7	69.3	73.9	71.6	71.5
56	3 Weeks Moist	87.4	89.7	-	-	-	88.6
56	7 Weeks Moist	87.8	84.0	-	-	-	85.9
91	Continuously Moist	72.0	73.0	-	-	-	72.5
91	3 Weeks Moist	88.1	89.9	-	-	-	89.0
91	7 Weeks Moist	86.0	88.5	-	-	-	87.3
147	Continuously Moist	78.1	72.7	75.1	-	-	75.3
147	3 Weeks Moist	96.1	91.7	93.1	-	-	93.6
147	7 Weeks Moist	92.1	94.0	-	-	-	93.1

Table I-3.4.2.C - Effect of Drying on the Compressive Strength Gain (UU4 Series)

Age (Days)	Curing Condition	Compressive Strength (MPa)					
		S_1	S_2	S_3	S_4	S_5	Mean
1	Continuously Moist	56.6	57.0	-	-	-	56.8
3	Continuously Moist	66.4	61.8	64.0	-	-	64.1
7	Continuously Moist	75.9	74.1	-	-	-	75.0
28	Continuously Moist	97.6	101.6	-	-	-	99.6
28	3 Weeks Moist	107.3	111.6	-	-	-	109.5
56	Continuously Moist	97.2	104.0	98.3	106.9	108.2	102.9
56	3 Weeks Moist	119.5	119.8	117.4	-	-	118.9
56	7 Weeks Moist	105.2	110.0	116.6	-	-	110.6
91	Continuously Moist	101.1	112.9	110.3	-	-	108.1
91	3 Weeks Moist	127.3	108.6	122.4	-	-	119.4
91	7 Weeks Moist	120.0	134.7	127.4	-	-	127.4
147	Continuously Moist	115.2	116.6	-	-	-	115.9
147	3 Weeks Moist	125.5	121.9	-	-	-	123.7
147	7 Weeks Moist	135.8	134.9	-	-	-	135.4

Table I-4.3.A - Compressive Strength History (LH1 Series)

Age (Days)	Compressive Strength (MPa)					
	S_1	S_2	S_3	S_4	S_5	Mean
1	28.1	26.5	27.8	-	-	27.5
3	38.4	38.2	-	-	-	38.3
7	43.0	42.2	-	-	-	42.6
28	58.3	56.6	-	-	-	57.5
56	65.5	64.1	65.9	65.8	66.0	65.5
70	66.7	66.2	65.1	-	-	66.0
156	67.3	70.5	69.7	-	-	69.2

Table I-4.3.B - Compressive Strength History (UH1 Series)

Age (Days)	Compressive Strength (MPa)					
	S_1	S_2	S_3	S_4	S_5	Mean
1	49.2	50.2	-	-	-	49.7
3	59.7	59.3	-	-	-	59.5
7	65.6	65.8	-	-	-	65.7
28	85.2	83.7	-	-	-	84.5
56	97.5	90.9	95.9	97.9	94.2	95.3
147	102.7	99.4	103.3	-	-	101.8

Table I-4.3.C - Compressive Strength History (UU1 Series)

Age (Days)	Compressive Strength (MPa)					
	S_1	S_2	S_3	S_4	S_5	Mean
1	60.7	58.2	61.8	-	-	60.2
3	72.8	70.2	-	-	-	71.5
7	80.7	79.3	-	-	-	80.0
28	112.3	111.4	110.6	-	-	111.4
56	115.5	125.0	121.6	119.7	120.6	120.5
70	120.5	118.0	120.8	-	-	119.8
154	136.8	139.4	133.1	-	-	136.4

Table I-E-3.2 - Compressive Strength Gain with Time (LU Series)

Concrete Series	Age (Days)	Compressive Strength (MPa)					
		S_1	S_2	S_3	S_4	S_5	Mean
LU2	1	32.8	32.6	-	-	-	32.7
LU2	3	54.9	53.0	-	-	-	54.0
LU2	7	69.5	71.7	-	-	-	70.6
LU2	28	89.1	90.9	-	-	-	90.0
LU2	56	98.8	94.1	-	-	-	96.5
LU2	91	104.1	105.3	-	-	-	104.7
LU2	147	103.6	106.1	-	-	-	104.9
LU4	1	32.3	31.4	-	-	-	31.9
LU4	3	54.5	53.5	-	-	-	54.0
LU4	7	70.0	67.5	-	-	-	68.8
LU4	28	87.9	87.4	-	-	-	87.7
LU4	56	98.8	95.9	93.8	98.2	89.8	95.3
LU4	91	105.4	101.4	-	-	-	103.4
LU4	147	101.9	105.5	-	-	-	103.7

Table I-E-3.3 - Effect of Type of Cement on the Compressive Strength Gain (LU Series)

Concrete Series	Age (Days)	Compressive Strength (MPa)					
		S_1	S_2	S_3	S_4	S_5	Mean
LU2	1	32.8	32.6	-	-	-	32.7
LU2	3	54.9	53.0	-	-	-	54.0
LU2	7	69.5	71.7	-	-	-	70.6
LU2	28	89.1	90.9	-	-	-	90.0
LU2	56	98.8	94.1	-	-	-	96.5
LU2	91	104.1	105.3	-	-	-	104.7
LU2	147	103.6	106.1	-	-	-	104.9
LU3	1	55.3	55.6	-	-	-	55.5
LU3	3	65.6	67.4	-	-	-	66.5
LU3	7	79.7	79.5	-	-	-	79.6
LU3	28	95.1	94.0	-	-	-	94.6
LU3	56	99.9	100.3	-	-	-	100.1
LU3	91	104.7	103.9	-	-	-	104.3
LU3	147	103.4	107.3	-	-	-	105.4

Table I-E-3.4 - Effect of Drying on the Compressive Strength Gain (LU4 Series)

Age (Days)	Curing Condition	Compressive Strength (MPa)					
		S_1	S_2	S_3	S_4	S_5	Mean
1	Continuously Moist	32.3	31.4	-	-	-	31.9
3	Continuously Moist	54.5	53.5	-	-	-	54.0
7	Continuously Moist	70.0	67.5	-	-	-	68.8
28	Continuously Moist	87.9	87.4	-	-	-	87.7
28	3 Weeks Moist	94.0	98.5	-	-	-	96.3
56	Continuously Moist	98.8	95.9	93.8	98.2	89.8	95.3
56	3 Weeks Moist	107.5	104.7	-	-	-	106.1
56	7 Weeks Moist	106.4	102.5	-	-	-	104.5
91	Continuously Moist	105.4	101.4	-	-	-	103.4
91	3 Weeks Moist	108.5	108.1	-	-	-	108.3
91	7 Weeks Moist	113.7	112.9	-	-	-	113.3
147	Continuously Moist	101.9	105.5	-	-	-	103.3
147	3 Weeks Moist	112.9	116.7	-	-	-	114.8
147	7 Weeks Moist	112.9	118.7	-	-	-	115.8

Table I-F-4.3 - Compressive Strength History (LU1 Series)

Age (Days)	Compressive Strength (MPa)					
	S_1	S_2	S_3	S_4	S_5	Mean
1	31.7	32.5	-	-	-	32.1
3	54.5	55.3	-	-	-	54.9
7	68.7	67.6	-	-	-	68.2
28	94.8	94.0	-	-	-	94.4
56	103.5	102.4	105.1	106.2	106.5	104.7
154	113.3	113.1	110.5	-	-	112.3

Recent Structural Engineering Reports

Department of Civil Engineering

University of Alberta

173. *Slenderness Effects in Eccentrically Loaded Masonry Walls* by Muqtadir, Mohammad A., Warwaruk, J. and Hatzinikolas, M.A., June 1991.

174. *Bond Model For Strength of Slab-Column Joints* by S.D.B. Alexander and Sidney H. Simmonds, June 1991.

175. *Modelling and Design of Unbraced Reinforced Concrete Frames* by Yehia K. Elezaby and Sidney H. Simmonds, February 1992.

176. *Strength and Stability of Reinforced Concrete Plates Under Combined Inplane and Lateral Loads* by Mashhour G. Ghoneim and James G. MacGregor, February 1992.

177. *A Field Study of Fastener Tension in High-Strength Bolts* by G.L. Kulak and K. H Obaia, April 1992.

178. *Flexural Behaviour of Concrete-Filled Hollow Structural Sections* by Yue Qing Lu and D.J. Laurie Kennedy, April 1992.

179. *Finite Element Analysis of Distributed Discrete Concrete Cracking* by Budan Yao and D.W. Murray, May 1992.

180. *Finite Element Analysis of Composite Ice Resisting Walls* by R.A. Link and A.E. Elwi, June 1992.

181. *Numerical Analysis of Buried Pipelines* by Zhilong Zhou and David W. Murray, January 1993.

182. *Shear Connected Cavity Walls Under Vertical Loads* by A. Goyal, M.A. Hatzinikolas and J. Warwaruk, January 1993.

183. *Frame Methods for Analysis of Two-Way Slabs* by M. Mulenga and S.H. Simmonds, January 1993.

184. *Evaluation of Design Procedures for Torsion in Reinforced and Prestressed Concrete* by Mashour G. Ghoneim and J.G. MacGregor, February 1993.

185. *Distortional Buckling of Steel Beams* by Hesham S. Essa and D.J. Laurie Kennedy, April 1993.

186. *Effect of Size on Flexural Behaviour of High Strength Concrete Beams* by N. Alca and J.G. MacGregor, May 1993.

187. *Shear Lag in Bolted Single and Double Angle Tension Members* by Yue Wu and Geoffrey L. Kulak, June 1993.

188. *A Shear-Friction Truss Model for Reinforced Concrete Beams Subjected to Shear* by S.A. Chen and J.G. MacGregor, June 1993.

189. *An Investigation of Hoist-Induced Dynamic Loads* by Douglas A. Barrett and Terry M. Hrudey, July 1993.

190. *Analysis and Design of Fabricated Steel Structures for Fatigue: A Primer for Civil Engineers* by Geoffrey L. Kulak and Ian F.C. Smith, July 1993.

191. *Cyclic Behavior of Steel Gusset Plate Connections* by Jeffrey S. Rabinovitch and J.J. Roger Cheng, August 1993.

192. *Bending Strength of Longitudinally Stiffened Steel Cylinders* by Qishi Chen, Alla E. Elwi and Geoffrey L. Kulak, August 1993.

193. *Web Behaviour in Wood Composite Box Beams* by E. Thomas Lewicke, J.J. Roger Cheng and Lars Bach, August 1993.

194. *Experimental Investigation of the Compressive Behavior of Gusset Plate Connections* by Michael C.H. Yam and J.J. Roger Cheng, September 1993.

195. *Some Behavioural Aspects of Composite Trusses* by Berhanu Woldegiorgis and D.J. Laurie Kennedy, January 1994.

196. *Flexural Behavior of High Strength Concrete Columns* by Hisham H.H. Ibrahim and James G. MacGregor, March 1994.

197. *Prediction of Wrinkling Behavior of Girth-Welded Line Pipe* by L.T. Souza, A.E. Elwi, and D.W. Murray, April 1994.

198. *Assessment of Concrete Strength in Existing Structures* by F. Michael Bartlett and J.G. MacGregor, May 1994.

199. *The Flexural Creep Behavior of OSB Panels Under Various Climatic Conditions* by Naiwen Zhao, J.J. Roger Cheng, and Lars Bach, June 1994.

200. *High Performance Concrete Under High Sustained Compressive Stresses* by S. Iravani and J.G. MacGregor, June 1994.